Structure Elucidation of Bioactive Marine Natural Products using Modern Methods of Spectroscopy

(Strukturaufklärung bioaktiver mariner Naturstoffe mit modernen Methoden der Spektroskopie)

Inaugural-Dissertation

zur

Erlangung des Doktorgrades

der Mathematisch-Naturwissenschaftlichen Fakultät der

Heinrich-Heine-Universität Düsseldorf

vorgelegt

von

Mohamed A.A. Ashour

Aus El-Sharkiya, Ägypten

Düsseldorf, 2006

Gedruckt mit Genehmigung der Mathematisch-Naturwissenschaftlichen Fakultät
der Heinrich-Heine-Universität Düsseldorf

Eingereicht am : 04.12.2006

Referent : Prof. Dr. Peter Proksch

Koreferent : Dr. Rainer Ebel, Juniorprofessor

Erklärung

Hiermit erkläre ich ehrenwörtlichen, daß ich die vorliegende dissertation „Strukturaufklärung bioaktiver mariner Naturstoffe mit modernen Methoden der Spektroskopie“ selbständig angefretigt und keine anderen als die angegebenen Quellen und Hilfsmittel benutzt habe. Ich habe diese Dissertation in gleicher oder ähnlicher Form in Keinem anderen Prüfungsverfahren vorgelegt. Außerdem erkläre ich, daß ich bisher noch keine weiteren akademischen Grade erworben oder zu erworben versucht habe.

Düsseldorf, 04.12.2006

Mohamed A.A. Ashour

In the name of Allah, the Compassionate, the Merciful.

Recite! (or read!) in the name of your Lord who created (1) Created man from clots of blood (2) Recite!, your Lord is the most Gracious (3) Who taught by the pen (4) Taught the man what he knew not (5).

(***The first verses of the holy Qur'an that came dwon from the sky***)

To the Almighty God "ALLAH" who has granted me all these graces to fulfil this work and who supported me and blessed me by His power and His mercy in all my life. To Him I extend my heartfelt thanks.

Acknowledgements

Many institutions and individuals were responsible for the crystallisation of this humble work, whose associations and encouragement have contributed to the accomplishment of the present thesis, and I would like to pay tribute to all of them.

I specially wish to express my sincere thanks and gratitude to Prof. Dr. **Peter Proksch**, chairman of the Department of Pharmaceutical Biology and Biotechnology, Heinrich-Heine University, Düsseldorf, for his kindness, admirable supervision, direct guidance, generous considerations and valuable support during my study in his group.

I would also like to express my deep thanks to my sincere teacher Dr. **RuAngelie Edrada** for her guidance, fruitful discussions, constructive advises, NMR courses and particularly for sharing her expertise in NMR data interpretation and revision of this thesis.

I would also wish to thank **J. Prof. Rainer Ebel**, of the same department for his direct guidance, valuable comments and suggestions and specially for sharing his expertise in both NMR spectroscopy and mass spectrometry.

I am deeply indebted to Dr. **Victor Wray** (Gesellschaft für Biotechnologische Forschung, Braunschweig), for the measurement of the NMR spectra, HRMS, and his vital comments in the structure elucidation of the isolated compounds.

I am grateful to Dr**. R. van Soest** (Zoological Museum, University of Amsterdam) for the identification of the sponge materials.

I am thankful to both Dr. **Steube** of DSMZ (Deutsche Sammlung von Mikroorganismen und Zellkulturen) and Prof. Dr**. W.E.G. Müller** (Universität Mainz,Germany) for the cytotoxicity tests.

My deep thanks are also to PD Dr.**Wim Wätjen** Institut für Toxikologie, Heinrich-Heine-Universiät Düsseldorf, Universitätsstr. 1, Geb. 22.21, 40225 Düsseldorf, Germany

I am thankful to Dr. **Thomas Schmidt** (HHU Düsseldorf) for his kind help in the measurement of some compounds at the GC machine.

I would also like to express my gratefulness to Dr. **Peter Tomme**s, Dr. **U. Matthiesen** (HHU Düsseldorf) for the measurement of EIMS, FABMS and high resolution ms data.

I am very thankful to **AnagnosTec** [Gesellschaft für Analytische Biochemie und Diagnostik mbH im Biotechnologiepark, TGZ II , D-14943 Luckenwalde, Berlin] for peptide sequancing by MALDI-TOF-PSD.

I am thankful to the Egyptian Ministry of Higher Education, Missions Office for providing the financial support for my study in Germany.

My deep thanks are to my friends, Dr. **Mustafa abdelgawwad** and Dr. **Ihab El-khayat** for their kind friendship, valuable help, encouragement and co-operation during the first monthes of my stay in Germany.

My deep thanks are also to my new and old colleagues at the Department of Pharmaceutical Biology and Biotechnology, Düsseldorf, Amal Hassan (Egypt), Arnulf Diesel (Germany), his wife Ine Inderiani (Indonesia), Clécia Freitas (Brasil). Dr. Yasman (Indonesia), Dr. Franka (Germany), Dr. Carsten (Germany), Dr. Hefni (Indonesia), Dr. Sabrin (Egypt), Dr. Gamal (Egypt), Dr. Bärbel (Germany), Dr. Tu (Vietnam), Dr. Yosi (Indonesia), Dr. Haofu (China), Dr Suwigarn (Thailand), Abdessamad (Morocco), Nadine (Germany), Mirko (Germany), Frank (Germany), Julia (Germany), Sofia (Sweeden), Idi (Indonesia), Yodi (Indonesia), Triana (Indonesia), Yao (China) and all the others for their help, friendship and for the good working atmosphere.

My special thanks to my colleague **Annika Putz** for his help in the revision of the German summary in my thesis.

My deep thanks to **Mareike, Katrin** and Mrs **Schlag** for their kindness and for always providing me with the materials and glassware which I needed in my work.

I would also like to express my gratefulness to my supervisors for my Master thesis, Prof. Dr. **Hassan Ammar,** Prof. Dr. **Taha Khalifa** and Ass.Prof. Dr. **Samir Al-Donditi** and also to Prof. Dr. **Hazem kadry** and all staff members and colleagues of the Department of Pharmacognosy, Faculty of Pharmacy, al-Azhar University (Boys), Nasr City, Cairo for providing me the basic science and for their motivations, recommendations and for teaching me very precious knowledge about Pharmacognosy and Phytochemistry offering me such a kind of opportunity to study in Germany and their continuous encouragement and kind advises.

*My special thanks for my wife **Dr. Hasnaa Abouseif** for her vast understanding, everlasting, moral support and contineous encouragement and also for my children **Yasmin Ashour** and **Ahmed Ashour** who could relieve any kind of tirdness by their lovely smiles and nice atmosphere at home.*

Table of contents

4.1- Isolation, characterisation, structure elucidation, and biological evaluation of

Zusammenfassung

Moderne Techniken und überlegene Werkzeuge haben die Arbeit von Naturstoff-Chemikern erleichtert und ermöglichen im Vergleich zu älteren Methoden eine beträchtlich schnellere Entdeckung, Isolierung und Strukturaufklärung von bioaktiven Naturstoffen. Naturstoffe besitzen oft neue oder ungewöhnliche strukturelle Eigenschaften und / oder viel versprechende biologische Aktivität. Die Anwendung neuer Methoden reduziert Zeit, Aufwand und Kosten der Entdeckung bioaktiver Naturstoffdrogen. In dieser Studie wurde oben genanntes Ziel mit Hilfe von modernen Techniken wie NMR, MS und HPLC Systemen als effiziente Werkzeuge verfolgt. Das in dieser Studie verwendete biologische Material umfasst sechs marine Invertebraten, die vier verschiedenen geographischen Standorten entstammen. Insgesamt wurden 40 Substanzen in reiner Form gewonnen und deren Struktur aufgeklärt. Einige von diesen zeigten sehr viel versprechende biologische Aktivität und stellen somit potentielle Kandidaten für die Entwicklung zukünftiger Naturstoffdrogen dar.

1. *Elysia rufescens*

Der Mollusk *Elysia rufescens* (Sacoglossa) wurde beim schwarzen Punkt „Kahala“ auf der Oahu Insel (Hawaii) gesammelt. Aus Extrakten dieser Tiere konnten neben fünf bekannten Kahalaliden (Kahalalid B, C, D, E und F) β-Sitosterol und ein bislang als Fabaceen-Sekundärmetabolit bekannter N,N-Dimethyltryptophanmethylester gewonnen werden.

2. *Elysia grandifolia*

Der Mollusk *Elysia grandifolia* (Sacoglossa) wurde im Golf von Mannar und Palk Bay (Rameswaram, Indien) gesammelt. Im LCMS-Spektrum des methanolischen Rohextrakts zeigten sich neben den Peaks der Kahalalide B, C, D, E, F, G, J, K, und O auch zwei neue Peaks ähnlich den Kahalaliden R und S. Im Fokus des Isolationsprozesses standen diese neuen Substanzen. Zusätzlich zu diesen konnten noch zwei bereits bekannte Kahalalide isoliert werden (Kahalalid D und F).

3. *Pachychalina* sp.

Der unbekannte Schwamm *Pachychalina* sp. stammte aus Pulau, Baranglompo (Indonesien). Im methanolischen Rohextrakt fanden sich sowohl zwei 5α, 8α-Epidioxysteroide als auch das bereits bekannte 8-Hydroxy-4-quinolon, welches als Bestandteil der Tinte des Riesen-Oktopus *Octopus dofleini martini* beschrieben wurde.

4. *Petrosia nigricans*

Der Schwamm *Petrosia nigricans* wurde in Baranglompo (Indonesien) gesammelt. Der methanolische Extrakt wurde intensiv untersucht, es konnten insgesamt 17 Substanzen isoliert werden. Davon waren zehn bereits bekannte Naturstoffe, zwei neue Cerebroside, ein bis-Indolderivat und vier neue Oxopurinderivate.

5. *Callyspongia biru*

Proben des Schwammes *Callyspongia biru* stammten aus Taka Bako (Indonesien). Aus dem methanolischen Rohextrakt konnten die fünf bekannten Substanzen Indol-3-carbaldehyd, Indol-3-essigsäure, p-Hydroxyphenylessigsäure, p-Hydroxyphenylessigsäuremethylester und 2`-Deoxythymidin gewonnen werden.

6. *Hyrtios erectus*

Individuen des Schwammes *Hyrtios erectus* wurden bei El-Quesir im Roten Meer (Ägypten) gesammelt. Im methanolischen Rohextrakt befanden sich neun Substanzen, darunter ein Epidioxycholesterolderivat, drei Sesterterpene vom Scalaran-Typ, vier bekannte Indolderivate und ein neues 5-Hydroxyindolderivat.

I. Introduction

1.1- The significance of the study:

Although effective drugs for many diseases that afflict mankind have been discovered, many health problems remain untreatable. These problems include various types of cancer; viral infections such as HIV and viral hepatitis, particularly types related to hepatitis C viral infections; severe fungal infections, especially in immunocompromised patients; cardiovascular diseases, and inflammatory and allergic disorders (Gullo, 1994). Only, approximately, one third of all diseases can be treated efficiently (Müller *et al*. 2000). Therefore the search for novel therapeutic agents continues, and the need still remains to uncover the initial structural lead that interacts with therapeutic targets. Natural products give a good chance for the discovering of an effective medication of the remaining untreatable diseases either, by direct therapeutic effect, after semisynthetic modification or by new synthesis of chemicals based on the natural product models (Cragg *et al*. 1997). The discovery of natural products with therapeutic potential is affected by many factors comprising all steps of extraction, isolation, characterisation, structural elucidation, and biological evaluations. In the last few years these methods were highly advanced in order to save time, and economy of isolation process, discover, and ensure the proper biological activity of natural products. Now, using this technological evolution, one is sometimes able to extract, isolate, and elucidate the natural product in only one day (Steinbeck 2004). This work deals with natural products and covers many aspects in which they are included.

1.2- Natural Products

Natural products have inspired chemists and physicians for millenia. Their rich structural diversity and complexity has prompted synthetic chemists to produce them in the laboratory, often with therapeutic applications in mind, and many drugs used today are natural products or natural product derived. Recent years have seen considerable advances in our understanding of natural product biosynthesis coupled with improvements in approaches for natural product isolation, characterization and synthesis; these could be opening the door to a new era in the investigation of natural products in academia and industry (Clardy & Walsh, 2004). Nature has continuously provided mankind with a broad and structurally diverse array of pharmacologically active compounds that have proved to be indispensible for the cure of

deadly diseases or as lead structures for novel pharmaceuticals (Newmann *et al*, 2000a). In the present drug discovery programs, compounds derived from natural products account for more than 40% of the newly registered drugs (Cragg, *et al*, 1997)

The discovery of antibiotics gave the study of natural products a great boost in microbiology departments and ensured that natural products remained central to growing pharmaceutical companies (Firn & Jones 2003).

1.2.1- Definitions of „*Natural products*“:

Most scientists define the *natural products* as chemical substances that are made by organisms and are not active participants in primary metabolism. In other words they are chemicals that are usually found in few families or species and which do not seem to serve a purpose in minute-to-minute activities of the cells. Indeed another term used for *natural product* is the term *secondary metabolite* or *secondary product*. The term *secondary products* or *secondary metabolites* is widely used now to distinguish this type from the other one „ *primary metabolites*“. (Firn 2004)

Bennett (1995) mentioned five different definitions for the term *secondary metabolism* :

- secondary metabolites are those metabolites which are often produced in a phase subsequent to growth, have no function in growth (although they have survival function), are produced by certain restricted taxonomic groups of microorganisms, have unusual chemical structures, and are often formed as mixtures of closely related members of a chemical family. (Martin & Demain 1978)
- the simplest definition of secondary products is that they are not generally included in standard metabolic charts (Davies, 1985)
- A metabolic intermediate or product, found as a differentiation product in restricted taxonomic groups, not essential to growth and the life of the producing organism, and biosynthesized from one or more general metabolites by a wider variety of pathways than available in general metabolism. (Bennett& Bentley, 1989).
- Secondary metabolites are not essential for growth and tend to be strain specific.They have a wide range of chemical structures and biological activities. They are derived by unique biosynthetic pathways from primary metabolites and intermediates (Vining,1992)

- Secondary metabolism includes biochemical pathways that are not necessary for growth or reproduction of an organism, but which can be demonstrated genetically, physiologically or biochemically (Hunter 1992).

1.2.2- Primary and secondary metabolism :

Primary metabolism refers to the processes producing the carboxylic acids of krebs cycle, α-amino acids, carbohydrates, fats, proteins and nucleic acids, all are essential for the survival and well-being of the organism. All organisms possess the same metabolic pathways by which these compounds are synthesized and utilized. Secondary metabolites on the other hand, are non essential to life but contribute to the species´fitness for survival (Torssell 1997).

Other descriptions of primary metabolism refer to all biochemical processes for the normal anabolic and catabolic pathways which result in assimilation, respiration, transport, and differentiation. Primary metabolism shared by all cells are virtually identical in most living organisms in order for production of extremly similar molecules giving the same biological function. The secondary products, having no role in the basic life process, are produced by pathways derived from primary metabolic routes. Secondary metabolite products accounting for the plant colours, flavours and smells, are source of fine chemicals, such as drugs, insectisides, dyes, flavours, and fragrances, and phyto-medicines found in medicinal plants. The concept of secondary metabolism was first introduced by Kössel,1891, (Haslam,1986; Seigler,1998; Turner, 1971).

1.2.3- The role of secondary metabolite in the producing organism

„ *to every thing there is a season*“

In certain scientific circles it is something of a sport to theorize about function, often with the intent of finding one overriding axiom true for all secondary metabolism. Speculations range from the notion that they are waste products or laboratory artefacts, to the concept that they are neutral participants in an evolutionary game, to ideas of chemical weaponry and signalling, through a number of other creative notions. (Bennett, 1995).

A) Waste product hypothesis

The role of the secondary metabolites has been rather ambiguous, and initially they were thought to be just waste materials. The relatively large number and amount of secondary metabolites observed in nature and the notion that these compounds arose from´´errors´´ in primary metabolisms in plants, led to the idea that secondary compounds arise and

accumulate as „waste-products“. However, considering their non-motile nature and the lack of sophosticated immune system, plants have developed their own defense system against pathogens and predators, and systems to lure motile creatures, for fertilisation and dissemination (Luckner, 1990; Seigler, 1998)

B) **The overflow or excess of the primary metbolism hypothesis**:

In instance of unbalanced growth, secondary metabolites have been envisioned by some as shunt metabolites produced in order to reduce abnormal concentration of normal cellular constituents. The synthesis of enzymes designed to carry out secondary metabolism permits primary metabolic enzymes to continue to function until such time as circumstances are propitious for renewed metabolic activity and growth. This could be linked to the depletion of nutrients such as phosphorous or nitrogen (Bu´Lock, 1980; Haslam, 1986).

C) **The increased fitness hypothesis**:

This hypothesis is based on the fact that many natural products trigger very specific physiological responses in other organisms and in many cases remarkably bind to its complementary receptors. In other words, natural products may aid an organism´s survival in the absence of an immune system. This supports the hypothesis that secondary metabolites increase the fitness of the individuals that possess them and that those individuals have been favoured by the process of natural selection. Secondary metabolites have an important ecological role in the interaction with the environment, and are like the communication interface between a plant and its friends and enemies in the environment, (Harborne, 1986; Rosenthal and Janzen,1979; Swain, 1977; Torssell,1997).

D) **Secondary metabolism is a defense system** :

Some scientists refer the production of the secondary metabolits to be a potent chemical defense system against herbivorous, deterrants, pathogens….etc. The immobility of plants in diverse and changing physical environment, along with the danger of attack by herbivores and pathogens, has led to the development of numerous chemical and biochemical adaptations for protection and defense (Knox and Dodge 1985, Harborne 1988), plants for example can produce higly toxic compounds or compounds mimicking substances normally produced by a herbivore, for example growth hormones or phermones.

It may be sufficient for the plant to produce compounds that are unpleasant, odorous, or distasteful, or that possess digestibility reducing properties, i.e. compounds that decrease the uptake of nutrients, thus preventing over-browsing of the plant. One example of a compound with strong antifeedant activity against numerous insects is azadirachtin (**1**), produced by the indian neem tree (*Azadirachta indica*). The tree has been used for centuries

to protect other plants and clothes from insects. The structure of the active compound is very complex and not proven until 1985. Due to its potency and selectivity against insects this compound has been commercialized as antifeedent (Bratt, 2000).

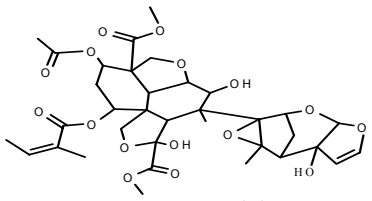

(**1**)

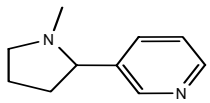

(**2**)

Indeed many plants do not keep permanent stores of their defense compounds, but manufacture them in response to predation. One example is the tobacco plant (*Nicotiana sylvestris*) that produces nicotine (**2**), a compound that deters a wide variety of herbivores. The level of nicotine produced by the plant is regulated by the extent to which it is being attacked by herbivores and the wild tobacco plant can increase the amount of nicotine produced by 3-4 times as response to an attack.(Mann, 1994).

E) The screening hypothesis :

This hypothesis was introduced by Richard D. Firn & Clive G. Jones [(Firn and Jones 1996, 1998, 1999, 2000, &2003), (Jones and Firn 1991), (Firn , 2003 and 2004)]

The hypothesis is composed of two parts.

1. *The identification of a fundamental constraint that must be a very significant factor in the evolution of secondary metabolism.*

Potent, specific biological activity is a rare property for a molecule to possess – that is why large screening programmes are needed to find useful biological activity. The low frequency of potent, specific biological activity is a consequence of the specificity of ligand/binding site interactions. Some organisms can increase their fitness by making and exploiting biological active molecules. However, the low frequency of evolving new molecules places severe constraints on the evolution of the biochemical pathways leading to such products.

2. *A proposal as to how secondary metabolism might have evolved with such a constraint including a prediction as to the metabolic traits that would be expected to minimize the effects of these constraints*

How do organisms generate sufficient chemical diversity to enhance their chances of finding the rare beneficial chemical? How do organisms retain the capacity to generate so much chemical diversity when indivdual compounds or pathways become redundant***?. The Screening Hypothesis*** proposes that certain metabolic traits (matrix pathways, non-enzymic

transformations, branched pathways, shared pathways and enzymes with a broad substrate tolerance) would all help increase generation and retention of chemical diversity and evolution of secondary metabolism.

Some consequences of this hypothesis:

- One should not expect all naturally made chemicals to have a role in the organisms that make them. Many will have no role and will never have had any role in the organisms in which they are found. Many chemicals will simply have been made because the metabolic machinery cabable of their production has a benefit for the producer. If only one product that those pathways can produce has a beneficial biological activity, the pathways will be sustained if the costs of possessing that capacity is sustainable.
- One should not assume that some biological activity found in a screening trial conducted by humans has any significance to the role of the chemical in the organism that produces it. If organisms are producing chemical diversity they must inevitably produce chemicals with structures that will possess fortuitous biological activity in non-target organisms.
- The metabolic traits predicted by the ***screening hypothesis*** will sometimes make it hard to precisely genitically manipulate secondary product pathways. For example, it is proposed that in order to enhance the production and retention of chemical diversity, many enzymes involved in secondary product biosynthesis will have low substrate specificity. Consequently, if a new enzyme is introduced into an organism to cause the production of a new secondary product, there is high probability that existing enzymes in the transformed organism will further elaborate the new product to produce more novel diversity.
- Some of the metabolic traits predicted (for example low substrate specificity) might be exploited in biotransformation and bioremedation studies.
- The flux of carbon through secondary metabolite pathways must have been very large throughout the period of life on earth. The metabolic traits predicted by the screening hypothesis may have played a part in encouraging the catabolism of this huge amount of chemical diversity. The world has never been a clean place chemically hence organisms must have the capacity to survive and thrive in the presence of chemical diversity. Most synthetic chemicals released into the environment in small amounts will find enzymes that can transform them.

1.2.4- The secondary metabolite pathways:

Secondary metabolites are produced through other metabolic pathways than that of primary metabolites. These pathways are more characteristic for the particular family or genus and are related to the mechanism of evolution of species. In the fact, the specific constituents in a certain species have been used to help with systemic determination, groups of secondary metabolites being used as markers for botanical classification (chemotaxonomy) (Torssell,1997) .

The differentiation between primary and secondary metabolism is not clear and the two types are linked together because primary metabolism provides the small molecules that are the starting materials of the secondary metabolic pathways (Figure 1.1).

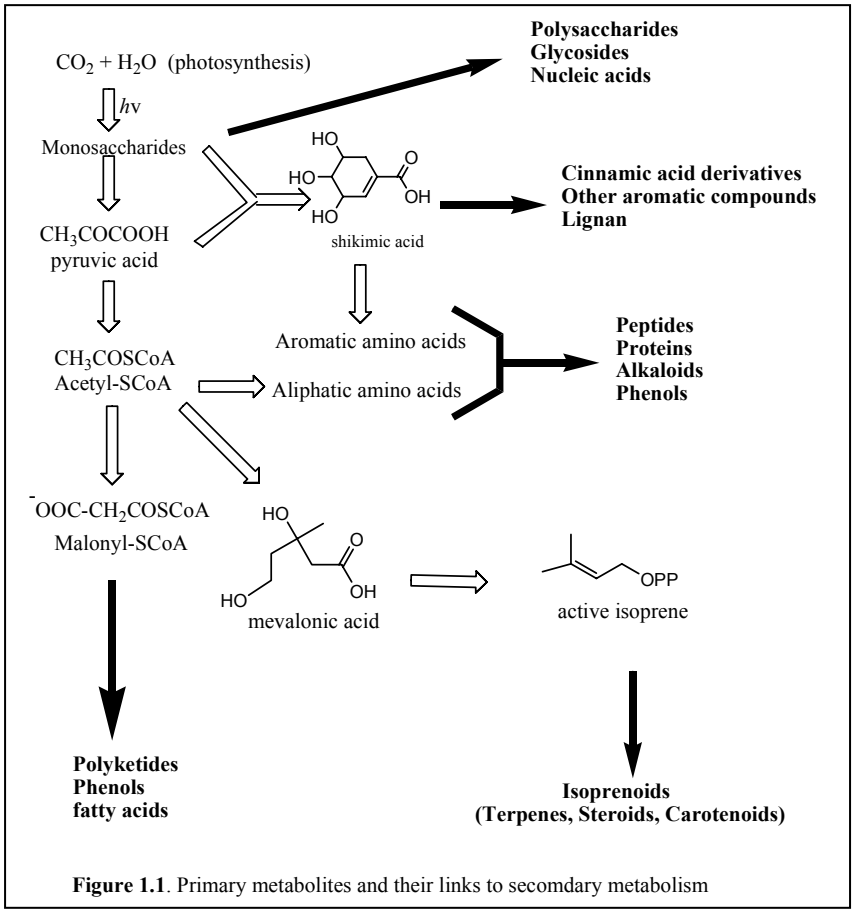

Figure 1.1. Primary metabolites and their links to secomdary metabolism

1.2.5- The chemical diversity of the secondary metbolites:

"Organic chemistry just now is enough to drive one mad. it gives the impression of a primeval tropical forest, full of the most remarkable things, a monstrous and boundless thicket, with no way to escape, into which one may well dread to enter." (Wöhler in a letter written to Berzelius in 1835).

When Wöhler wrote those words he was expressing his despair at the emerging complexity of the composition of natural products. Yet within a few decades, this complexity was tamed by the Kekule` theory of structure. Increasingly, confident chemists took up the challenge of determining the structures of ever more complicated natural products. There are more than 5oo,ooo secondary chemical products already estimated in plants alone. The majority of natural products described in plants are made by a relatively small number of key pathways and the structural diversity is therefore largely a consequence of diversity of product within these few broad groups of chemical clases of natural products (Firn & Jones,1996).

„It is widely accepted that the mutation of a gene coding for an enzyme will result in various outcomes“. (Firn 2004)

This concept leads to :

1) The enzyme activity will be unaltered (the most likely scenario).
2) The kinetic properties of the enzyme will be changed, usually in a detrimental way.
3) The enzyme will change its substrate specificity.
4) Sites necessary for the allosteric control of the enzyme will be altered.

It is not widely believed that a mutation of the gene coding for an enzyme will change the type of transformation carried out. Thus most biochemical inventivness will arise from existing catalytic functions being applied to new substrates rather than new types of transformations being applied to the original substrate. Such biochemical inventivness requires that multiple copies of a gene must exist if the gene being mutated codes for enzyme that is involved in primary metabolism, otherwise a loss of an essential part of primary metabolism would result (Firn & Jones,1996)

Some simple scenarios to illustrate the constraints that might have operated during the evolution of natural product pathways. (Firn 2004)

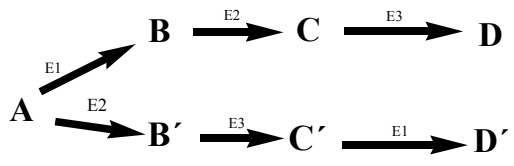

Fig. 1.2 : relaxed substrate specificity facilitates the generation and retention of chemichal diversity. such predictable characteristics have been found in "secondary metabolism"-carotenoids, phenylpropanoids, terpenoids, etc..

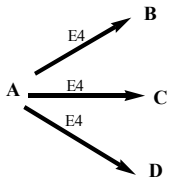

Fig .1 3 single product converted to multiple products by one enzyme.

In (figure 1.2) there is a diagram showing how 3 enzymes (E1-3) convert A to D. Now if the substrate specificity is relaxed the order in which the substrates are converted in unimportant pathway, hence the 3 enzymes will generate 6 products not 3. So this helps **generate** diversity. Furthermore, if D increases the fitness of the producer then B′,C′ and D′ may still get made even though they play no role currently- this helps **retain** chemical diversity.

This phenomenon is evident in the present study where, Kahalalide F, the major depsipeptide in a saccoglossan molluscs *Elysia* sp. has antipredatory effect against fish predators, its biosynthesis was accompanied with the production of other depsipeptides, that have no antipredatory effects.

Another example, (figure 1.3) illustrates another proposal where one enzyme produces multiple products instead of the usual single one. Again this helps generate and retain chemical diversity.

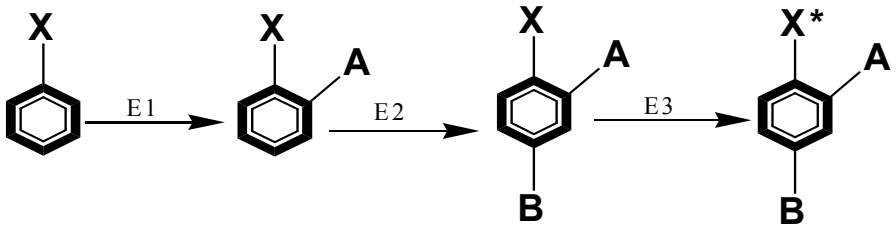

Fig. 1.4. hypothetical pathway. illustrated three enzymes of very strict substrate spicificity , resulting in production of only three products.

The third example (figure 1.4) of illustrating this principle is to consider a hypothetical pathway which has three enzymes leading from a precursor. If the enzymes have a very strict (narrow) substrate specificity then only three products will be formed.

However if the enzymes have a broad substrate tolerence it is possible that they could each carry out their own little piece of biochemistry on a selected part of any molecule irrespective of the whole structure of the molecule. Theoretically, many more structures could be generated using just these three enzymes as shown in (figure 1.5).

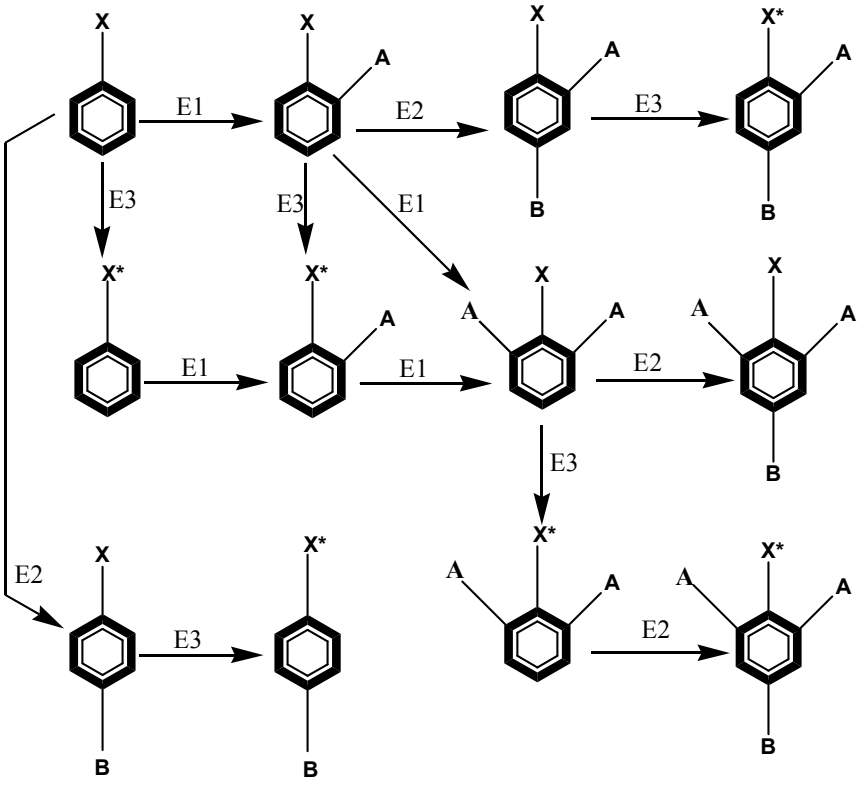

Fig. (1.5) many structures generates from the hypothetical pathway in which enzymes have a broad substrate tolerance

1.3- The biological activity of natural products.

1.3.1- The history of biological benefits of natural products

Man has used natural products since the down of time as remidies for diseases, spices, narcotics, dyes, and poison for warfare and hunting. Most of these compounds were used in their crude forms and active components were mostly not isolated until the nineteenth century. Morphine (**3)**, first isolated from opium (*Papaver somniferum* and *P. setigrum*) in 1803 is a well-known example. It is one of the powerful analgesics known, and also possesses strong narcotic effects (Mann, 1987).

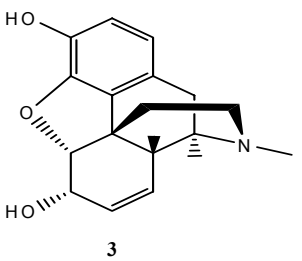

3

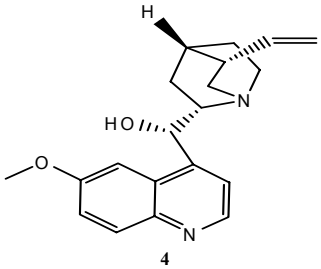

4

Another example is quinine (**4)** an anti-malaria agent isolated from the *Cinchona* tree as early as in the seventeenth century (Mann 1987). Of course there was a widely held view in the 19th century that God had created all organisms for man`s benefit. Hence many considered that the chemicals other organisms contained were for human use. Such views would have influenced the thoughts of some scientists (Firn and jones 2003, Firn 2004).

Before the 19th century, the only real interest in natural products came from herbalists and physicians. They were interested in the fact that plants (and sometimes fungi) contained substances that were thought to be useful in treating patients. For some considerable time, botanists had been sent from the United Kingdom, and many other countries, to scout the world for new, exotic plants, and the number of species that were accessible to herbalists and physicians increased. By the 19th century chemistry had began to ask questions about the nature of substances and there was a growing scientific interest in the natural products however this interest was still biased towards their use by humans rather than their role in the organisms that made them. (Firn 2004)

1.3.2- The importance of biological activity testing of the isolated natural products:

The fact that microbially-derived antibiotics found by screening make up most of a $16.5 billion *per annum* antimicrobial pharmaceutical sales (Nisbet 1992), explains why so many large antibiotic screening programmes have been conducted during the last half century (Firn 2004).

This antimicrobial screening of the isolated natural products represents only one of many lines of biological activity testing that made in order to overcome the most recently encountered problematic diseases for example, viral hepatitis, AIDS, cancers, autoimmune diseases, parasites,etc.

The biological activity testing should also expand to comprise most toxicological studies in order to show the most advantages together with the disadvantages of the given total extract or the purified natural product. At the end of these biological and toxicological studies we can decide whether the given product is usefull or not.

This problematic equation (effective, cheap, of wide safty margin, and widely available natural product drugs) is not easy to be accomplished. For example :

(i) 400,000 microbial cultures were assayed over a 10 year period and only three utilisable compounds were found (Fleming *et al*. 1982, Nelson 1961)

(ii) 21,830 isolates screened in one year to give 2 possible compounds (Woodruff et al 1979).

(iii) 10,000 Microorganisms gave only one clinically effective agent (Woodruff and MacDaniel 1958).

Those sceptical of such evidence leads man to ask, **Is biological activity a rare property for a natural product to possess?** in another word, **Is it true that, the majority of secondary metabolites have no biological benefits?**

A meaningful answer requires a definition of the term ***BIOLOGICAL ACTIVITY***.

At a time when natural products were mainly of interest only to herbalists, the father of modern toxicology, Paracelsus (1493-1541) astutely observed that whether one thought of a substance as a poison or not depend entirely on the dose that was adminstered. it is therefore obvious that a discussion of the biological activity of any compound is meaningless unless some comparative standard is adopted with regards to the dose. The problem is especially acute when the biological activity is evaluated on the basis of an adverse effect on an organism, because a sufficient dose of many substances will have an adverse effect on virtually any organism (Rodricks 1992).

For purposes of this discussion it seems sensible that the only realistic bases for judging the biological activity of a substance is whether the compound would have a significant effect at a dose that a recipient organism would receive. A biological activity that is found when the compound is applied to test organisms at unrealistic concentrations cannot sensibly be regarded as meaningful. The importance of these considerations can be illustrated by considering model dose-response curves for three hypothetical substances C1, C2, and C3 (Fig. 1.6). It is appearent that all three substances can be regarded as showing biological activity in that all saturate the response when applied at high concentrations ($>10^{-5}$ M). However, suppose that each substance occures in an organism at a concentration of 10^{-8} M. In that case, only compound C1 can be considered to possess meaningful biological activity. Compounds C2 and C3 show no significant activity at their endogenous concentrations and would therefore confer no selective advantage to the organism [Firn and Jones 1996] .

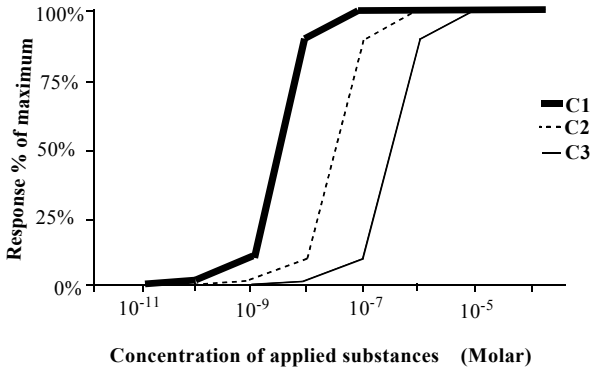

Fig. 1.6 „the dose makes the poison". The dose response curves of three hypothetical substances C1,C2 and C3 illustrate that whether or not a substance is considered to be biologically active depends on the dose being considered . (firn &Jones 1996)

The law of mass action explains why substances C2 and C3 are actively bound to the protein binding sites producing their effect at high concentrations and inactive at low concentrations.

$$\text{Chemical} + \text{Protein} \underset{\text{Kd}}{\overset{\text{Ka}}{\rightleftharpoons}} \text{Chemical protein complex}$$

Where: Ka = rate of association

Kd = rate of dissociation

The rate of association and the rate of dissociation are properties of the particular protein and molecule combination if the former is larger than the latter, there is a high chance of the protein having a molecule bound to it at any moment (the ratio of the two rate constants is used to assess the strength of any binding process). The law of mass action tells us that the equilibrium will be driven to the right as the concentration of the molecule increases. Consequently there is a much greater probability of finding an interaction between any chemical and any protein if you test the chemical at high concentration than that at low concentration. This relationship is also helpful when assessing the safety margin of a tested compound.

Also, it is obvious that the wider the range of organisms for which biological activity of a compound is assessed, the greater the chance that some effect will be found, and also it must be borne in mind that the selective pressures that operate on any individual within a population at any one time will be quite specific and only a limited range of

opportunities will be available where chemical interactions can be beneficially used.[Firn and Jones 1996] .

Firn and Jones 1996, mentioned some limitations that affect the biological activity studies of the secondary metabolites and consequently minimize the chance of detecting highly biologically active compounds, specially for commercial use, for example:

- The high selectivity required for a biologically active substance means that many active compounds will be rejected at an early stage because of lack of specificity.
- Some active compounds are unstable and are either lost during isolation or are unsuitable for use .
- Some compounds are too difficult to synthesise or extract from cultures and are never developed.
- Some compounds have already been isolated (and possibly patented before).
- The type of biological activity found is not meaningful in terms of the particular usage sought.
- The screening process is inappropriate.
- Some forms of biological activity are dependent on the presence of other compounds (synergists) which are lost during the purification processes before the substance is bioassayed.

Each of the above reasons could be valid in some circumstances but even taken together they only partially account for the fact that screening natural products has produced relatively few biologically active compounds with high selective functions.

Although there are several limitations that minimize the chance of detecting the biologically active natural product, there are many active natural products that extensively affect the different forms of our life and can be beneficially used as nutritional supplements , dyes, insecticides and also there are many natural products that are already used for treatment of many diseases that counteract our healthy life.

1.3.3- Approaches to the discovery of biologically active natural products:

In general, drug discovery strategies can be trivially separated into three categories:

1. Chemically driven, finding biological activities for purified compounds.
2. Biologically driven, bioassay-guided approach beginning with crude extracts.
3. Combination of chemically and biologically driven approaches (vide infra).

For marine-derived drug discovery, strategies may involve one or more of the following elements:

1. In vivo screens
2. Mechanism-based screens
3. Functional, whole cell, or tissue-based assays
4. On-site assays versus post collection assays
5. „Dereplication," via biological profiles or chemical profiles, e.g., thin layer chromatography (TLC), nuclear magnetic resonance (NMR), and high pressure liquid chromatography (HPLC), (McConnell *et al.* 1994)

Beginning in the 1970´s through today, the majority of the academic-based research efforts have become essentially „biologically driven" i.e., the object of the search has shifted to discover natural products with biological activity. The biological activities include exploring their potential as agrochemicals (Crawley 1988) and pharmaceuticals, as well as their possible chemical ecological roles (Bakus et al. 1986; Hay and Fenical 1988)

Drug discovery in industry has evolved to the use of specific assays with target receptors and enzymes involved in the pathogenesis of disease rather than cellular or tissue assays (Johnson and Hertzberg 1989), and has benefitted immensely from breakthroughs in receptor technology (Hall 1989; Reuben and wittcoff 1989). These assays reflect new opportunities due to the recent identification of previously unrecognized biomolecular targets for therapy (Larson and Fischer 1989). More specifically, this approach for most disease areas is characterized in industry by:

1. Essentially exclusive reliance on biological activity of crude extracts in numerous target-specific assays, i.e., enzyme assays and receptor-binding assays, for selection of crude extracts and bioassay-guided fractionation of the crude extracts (prioritization criteria emphasize selectivity and potency).
2. High volume, automated screening, i.e., thousands of samples per year for smaller companies and thousands per week for larger companies.
3. The use of „functional" or whole-cell assays to confirm activity in a particular disease state and to further prioritize samples for fractionation.
4. The use of gentically engineered microorganisms, enzymes, and receptors.

Because of low correlation between cytotoxity and antitumor activity, a number of programs have utilized *in vivo* tumor models directly for drug discovery (Johnson and Hertzberg 1989). From 1958 through 1985, NCI used in vivo L1210 and P-388 murine

leukemia assays as primary screens (Suffness *et al*. 1989; Boyd *et al*. 1988) and was successful primarily in identifying compounds possessing clinical activity against leukemias and lymphomas. Unfortunately, they were not very successful in finding compounds active against slow growing tumours in humans. Further, these *in vivo* assays were expensive, time consuming, and relatively insensitive (Suffness *et al*. 1989). In other disease areas it was shown that activity in *in vitro* antiviral assays does not translate well to *in vivo* activity, e.g., using *Herpes simplex.* In contrast, reasonable correlations exist between *in vitro* and *in vivo* antifungal activity, e. g., using *Candida albicans*.(McConnell *et al*., 1994)

Chemically and biologically driven approaches can be combined. The combination means that selecting extracts for chemical fractionation based on the biological activity profile of the crude extract. However, instead of using a bioassay-guided approach to purify the compounds responsible for the activity of the extract, NMR and some chromatographic techniques are used to isolate the chemically most interesting substances. Ideally the structurally unusual or novel compounds are also responsible for the activity of the extract. This approach works well when the active compounds are present in high concentration and the assay turnaround time is longer than a couple of weeks. This approach is indeed productive with respect to isolating numerous new compounds, at least some of which usually express some of the activity observed for the crude extract, but is obviously not the best method to identify the most active compounds if they are present in low concentrations (McConnell et al., 1994).

1.4- The strategies and approaches that influence the extraction, isolation and purification of natural products.

Unlike the medicinal chemist, who usually concentrates on a series of compounds of similar chemical and physical properties and hence is able to master the limited number of separation techniques applicable to the specific chemotype, the natural product chemist must be prepared to deal with molecules of the whole spectrum of bioactive metabolites. These can vary in hydro- and lipophilicity, charge, solubility, and size (McAlpine and Hochlowski1994). In general, the more hydrophilic metabolites may be candidates for ion exchange chromatography, reversed phase silica gel chromtography, or size exclusion chromatography on polysaccharide resins. The more lipophilic metabolites can be further purified by chromatography on normal phase silica gel, florisil, alumina, or lipophilic size exclusion resins such as sephadex LH-20. They may be also candidates for a variety of high-speed

countercurrent techniques or chromatography on polyresins (McAlpine and Hochlowski 1994). Natural product chemistry is one of the oldest branches of the chemical sciences, its origin dating back to the first decades of the 19th century, or even earlier. Presently after almost 200 years of study, this is still vibrant and evolving. What are the reasons for this continuous and continuing interest? Possible answers would have to include the challenges offered by the detection, isolation and purification procedures; by the permanently improving methods of structure elucidation; and by the complexities of the biogenetic pathways leading to these compounds (Shamma 1989).

The modern highly specific and sensitive screens to detect bioactive molecules have become available and as researchers have looked at ways to concentrate extracts for primary screening, novel metabolites have been discovered from fermentations in which they were produced in levels as low as 1μg/l. (McAlpine and Hochlowski1994). High performance liquid chromatography (HPLC) including both normal and reversed phases (RP) is now a well-developed and widely used technique for separation of complex mixtures (Exarchou, *et al,* 2005). All parts of the process leading to an elucidated structure have experienced an immense speed-up in the past fifty years. Separation technology, analytical and spectroscopic methods have improved steadily and with good fortune, a chemist might be able to go from a crude extract to a full set of 2D NMR spectra in one day (Steinbeck 2004).

The traditional way of studying natural products includes fractionation of a crude mixture or extract, separation and isolation of the individual components using liquid chromatography and structure elucidation using various spectroscopic methods (UV, IR, NMR, MS). (Exarchou, *et al*, 2005). It is therefore of great importance to be able to gain information about extract constituents before investment in the preparative isolation process (Lambert, *et al*, 2005).

The chemical components of a biological source are isolated one by one, by chromatography of the respective extracts, and then their structures are elucidated, such a complete analytical screening is, unfortunately very time-consuming and material-intensive, since it is a major effort – and a waste of resources – to isolate all of the compounds in a pure form, even the known ones. Furthermore, to obtain the required milligram quantities of the sometimes rare biological source – and of expensive adsorbents and eluents, and thirdly, unstable compounds will decompose already during the preparative separation and thus escape the analysis (Bringmann and Lang 2003). A solution of this problem is coupling of the two steps, the isolation and the structural elucidation, by combining them online. This may help with the facile acquisition of metabolic profiles, for deciding which of the extracts to be

analyzed should have the highest priority, for avoiding a tedious isolation of known compounds, and for checking whether a compound preparatively isolated is genuine natural product or possibly an artifact (Bringmann and Lang 2003).

In order to discover new bioactive compounds from their biological sources, which could become new leads or new drugs, extracts should be submitted at the same time to a chemical screening and to various biological or pharmacological targets. The chemical screening or metabolite profiling is aimed at distinguishing between already known compounds (dereplication) and new molecules directly in crude extracts. Thus, the tedious isolation of known compounds can be avoided and a targeted isolation of constituents presenting novel or unusual spectroscopic features can be undertaken. (Wolfender, *et al* 2005)

Metabolite profiling in crude extracts is not an easy task to perform since natural products display a very important structural diversity. For each compound the order of the atoms and stereochemical orientations have to be elucidated *de novo* in a complex manner and the compounds can not simply be sequenced as it is the case for genes or proteins. Consequently a single analytical technique does not exist, which is capable of profiling all secondary metabolites in the biological source. The dereplication procedure strongly relies mainly on hyphenated techniques coupled to HPLC such as LC-UV-photodiode array detection (LC/UV-DAD), LC-mass spectroscopy (LC-MS, LC-MS-MS) and LC-NMR which has been successfully and practically achieved in the last decade. (Wolfender, et al 2005, and Exarchou, *et al*, 2005). A common step in the purification and analysis of chemicals of unknown structure is the separation of the individual components from a chemical or biological mixture. Chromatographic separation techniques have been coupled with large number of detection methods, including ultraviolet-optical spectroscopy, Raman spectroscopy, mass spectrometry, conductivity measurements and NMR spectroscopy. Each technique can be characterised in terms of easy implementation, intrinsic sensitivity, structural information produced, and non destructive nature (Webb , 2005).

The combination of LC-UV and LC-MS information can be helpful in a first step of dereplication, especially when this information is combined with taxonomical considerations for cross search in natural product databases. This approach is, however, limited by the unavailability of general LC-MS and LC-MS-MS databases. For the on-line *de novo* structure determination of natural products, LC-NMR (see figures 1.7 and 1.8) plays a key role and allows the recording of precious complementary on-line structure information when LC-UV-MS data are often insufficient for unambiguous peak identification. (Wolfender, *et al* 2005).

The online technique of liquid chromatography coupled with solid-phase extraction and NMR (LC-SPE-NMR) has recently been used to analyze mixtures originating from natural product extracts, drug metabolites, and pharmaceutical impurities. The growing use of this technique results largely from the capability of on-line LC-SPE to isolate, enrich and allow NMR analysis of an individual analyte present in a complex micture (Xu and Alexander , 2005).

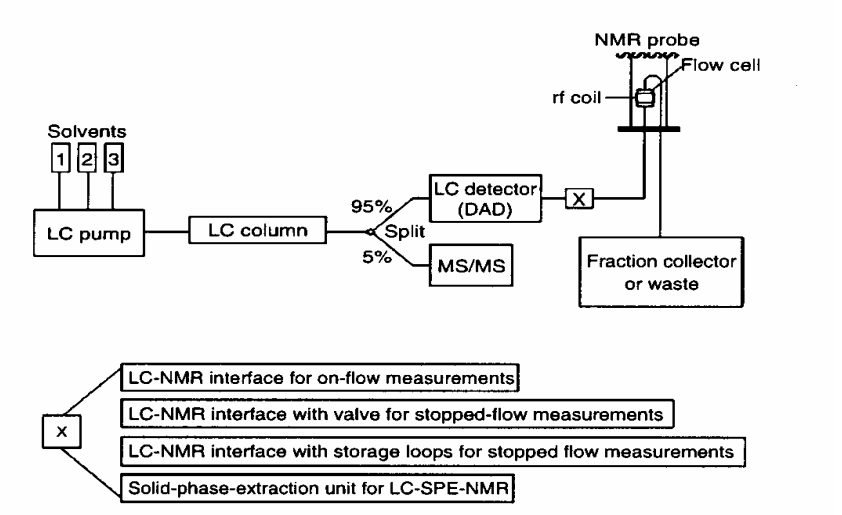

Fig. (1.7) Various LC-NMR modes and their applications in natural product analysis (Exarchou, *et al*, 2005)

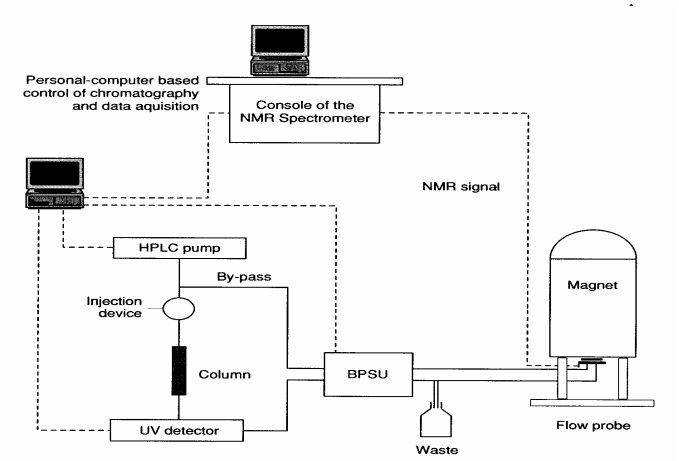

Fig. (1.8) Schematic diagram of the experimental set-up used for HPLC-NMR coupling; BPSU= Brucker peak sampler unit; (⎯) capillary junctions; (-----) electric junctions. (Albert, 2002)

Other isolation strategies are focused on the biological activities of the constituents of the given biological source through what is called „bioactivity-guided isolation“ , where the isolation steps will continue only with regard to the bioactve fractions and subfractions of the

biological mixture or extract until the isolation of the bioactive pure compound (Gunatilaka et al , 1994)

An example for bioactivity-guided isolation for natural product-based anticancer agents is demonstrated in figure 1.9, where the bioactive compounds and their analogues have been subjected to cytotoxicity assays with a view to selecting candidates for further development as anticancer agents.

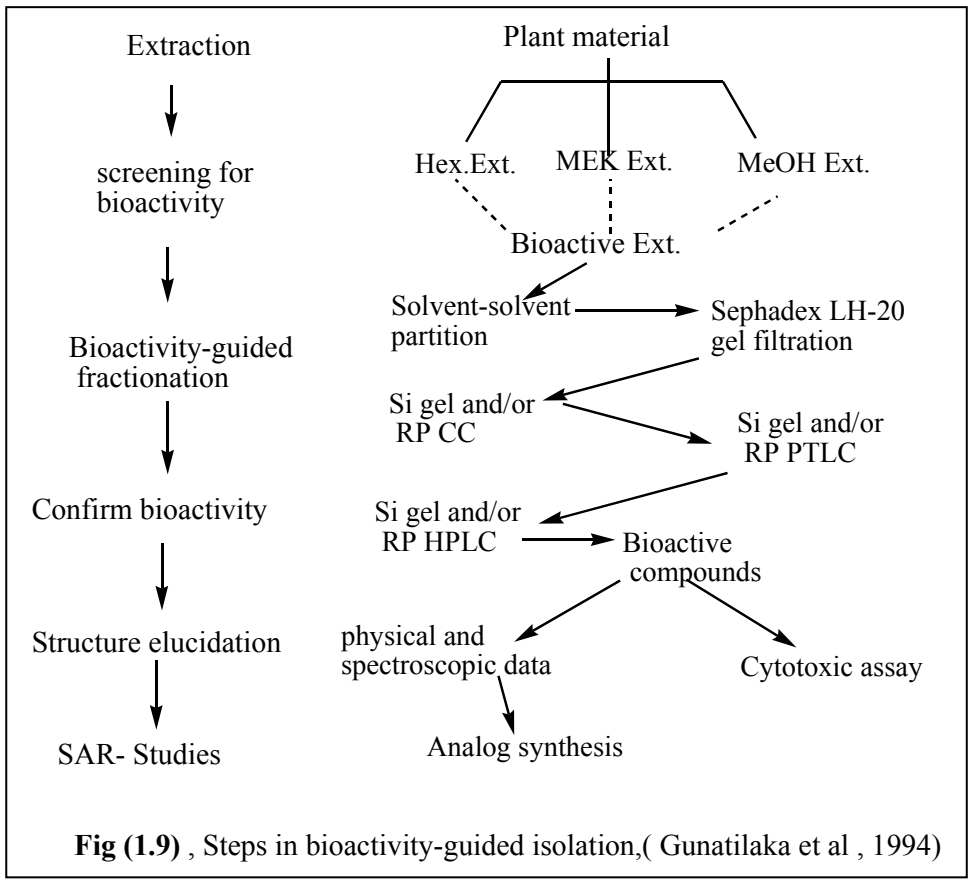

Fig (1.9) , Steps in bioactivity-guided isolation,(Gunatilaka et al , 1994)

With few exceptions, intense and systematic bioassay-guided studies of extract and compounds from marine organisms by academic, government, and industerial research groups using clinically relevant assay to discover naturally occuring substances with therapeutic potential have only been underway for less than 10 years. Because of the tremendous advances in understanding of the biology of certain diseases and the concomitant explosion of new assays, researchers are now in a position to explore fully the potential of natural products. These biological advances highly complement the devlopment of new chemical technology, i.e., new separation and structure elucidation techniques. (McConnell *et al.*, 1994).

1.5- The structural elucidation of the natural products:

Tens of thousands of new compounds have to be synthesized or extracted from natural sources in order to discover a potential drug. Despite the use of rational drug design techniques, economic success mainly depends on the number of new candidates available for activity tests. Consequently, research groups have begun to introduce new automation procedures such as synthesis robots and combinatorial chemistry. These enhancements on the production side are only part of the whole task. Additional efforts in the subsequent structure elucidation process are also vital in order to avoid bottlenecks (Neudert and Penk 1996). In natural product drug discovery programs, the major bottleneck has always been structure elucidation (Jaspars 1999). Conventional approaches to the structure elucidation of organic compounds are based on the use of spectroscopic data from different sources. The spectroscopist´s task is to interpret the spectra and to derive structure proposals. The efficiency of this process depends mainly on his or her knowledge of structure-spectrum correlations, acquired in the course of everyday work (Neudert and Penk 1996).

The usual spectroscopic methods that used in the structural elucidation of natural product chemistry includes UV, IR, NMR, and MS (Exarchou, *et al*, 2005). Recently, the 3D structural determination was available through X-ray spectroscopy even if no other additional spectral informations exist. An X-ray crystal structure determination is the ultimate analysis. No other analytical technique currently available can deliver such complete and unambiguous information about the nature of the substance being investigated, but this technique has some limitations :

- Good single crystals are required, and these are sometimes difficult or impossible to obtain without considerable effort.
- Decomposition of the compound during crystallisation attempts can be a difficulty with reactive compounds.
- The analysis is done on a single crystal, which may not be representative of the bulk material.
- The conformational results apply to the solid state and may be different to the molecular conformations present in solution, which is where most reactions take place.

The modern and highly advanced technology applied in NMR spectroscopy and mass spectrometry provide unequivocal structural information for the individually isolated compounds (Exarchou, *et al*, 2005).

1.5.1- Mass spectrometry :

Mass spectrometry (MS) has been appropriately used for analysis of molar masses of molecules for the past 50 years (Burlingame,1992). MS remains the method of choice for determining molecular formulas and identifying known substances. Where applicable, depending largely upon volatility and fragmentation patterns, MS can be a very powerful tool, as has been demonstrated in the analysis and sequencing of peptides and carbohydrates. In parallel with development of NMR, the field has benefited greatly from studies of peptides and proteins where the problem of volatility has been paramount (Hensens 1994).

The application of MS to large biomolecules and synthetic polymers has been limited due to low volatility and thermal instability of these materials. These problems have been overcome to a great extent through the development of soft ionization techniques such as chemical ionization (CI), (Silverstein, *et al* ,1991, and Cotter, 1980) , secondary-ion mass spectrometry (SIMS) (Silverstein, *et al* ,1991, Cotter, 1980 and Bletsos *et al*, 1991), field desorption (FD) (Silverstein, *et al* ,1991, and Cotter, 1980), fast atom bombardment (FAB), (Silverstein, *et al* ,1991, and Cotter, 1980), electrospray ionization (ESI) (Fenn J. B.2003, and Ashcroft, A. E., 1997) and matrix asssted laser desorption ionization mass spectrometry (MALDI), (Karas, *et al*, 1988, Karas, and Hillenkamp, 1991, and Tanaka, K., 2003).

Mass spectrometry (fig. 1.10) is an analytical technique that can provide both qualitative (structure) and quantitative (molecular mass or concentration) information on analyte molecules after their conversion to ions. The molecules of interest are first introduced into the ionization source of the mass spectrometer, where they are first ionized to acquire positive or negative charges. The ions then travel through the mass analyser and arrive at diffferent parts of the detector according to their mass (m)-to-charge(z) ratio (m/z). After the ions make contact with the detector, usable signals are generated and recorded by a computer system. The computer displays the signals graphically as a mass spectrum showing the relative abundance of the signals according to their m/z ratio (Ho, *et al* , 2003).

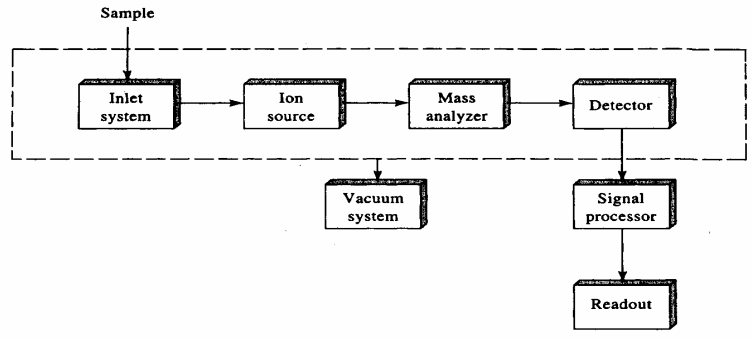

Fig (1.10) a simple Mass spectrometer diagram

The analyser and detector of the mass spectrometer, and often the ionisation source too, are maintained under high vacuum to give the ions a reasonable chance of travelling from one end of the instrument to the other without any hindrance from air molecules. The entire operation of the mass spectrometer, and often the sample introduction process also, is under complete data system control on modern mass spectrometers. (Ashcroft, A. E., 1997)

Methods of sample ionization:

The choice of ionization methods depends on the nature of the sample and type of information required from the analysis. so-called "soft ionization" methods such as field desorption and electrospray ionization tend to produce mass spectra with little or no fragmentation content whereas "hard ionization" methods such as electron ionization (EI) which are also refered to as electron impact ionization tend to produce mass spectra with large amount of fragments or daughter ion peaks. There are several methods that are used effectively to provide ionization in the currently available mass spectrometrs. In most ionization methods there are the possibility of creating both positively and negatively charged sample ions, depending on the proton affinity of the sample. Before embarking on an analysis the user must decide whether to detect the positively or negatively charged ions (Ashcroft, A. E., 1997).

Collision Induced dissociation (CID):

Collision induced dissociation (CID) sometimes also called collisionally activated decomposition (CAD) is one of the most common fragmentation procedures that is applied in biopolymer (e.g. peptides or polysaccharides) sequencing, structural elucidation, and analyte identification through finger-printing. The precursor ion enters the collision cell containing a high pressure of energised, chemically inert collision gas (e.g. Ar, He, N_2, CO_2 etc.) The precursor ions undergo repeated collisions with the collision gas, building up potential energy in the molecule, until eventually the fragmentation threshold is reached and product ions are formed, see figure (1.11). The types of fragmentaion that occur vary considerably with the type of product ion and amount of energy involved. At lower energies (close to the threshold), fragmentation reactions are often limited to neutral losses (H_2O, MeOH, CO, CO_2, MeCN etc.) depending on the nature of the precursor ion. These neutral loses are often not cosidered structurally significant, although they can be used to obtain information about functional groups. At higher energies, retro-synthetic type reactions are often observed. These are much more structurally significant, and often result in cleavage of the molecule at characteristic positions.

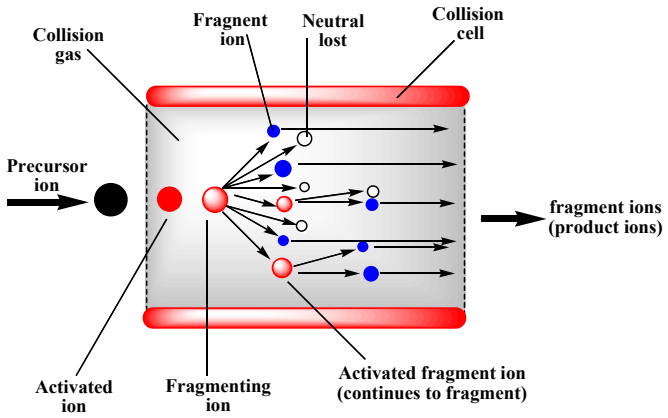

Fig (1.11). A Schematic diagram of CID fragmentation

If the energy is too high, C-C bond cleavage can occur leading to uncontrolled fragmentation; this should be avoided. Usually it is best to work at around the fragmentation threshold, or just above, to maintain most control over the fragmentation processes. Ion-trap and FT-MS instruments allow for the most control over CID, but also tend to produce less energetic reactions. Triple quadrupole and Q-TOF instruments tend to produce more energetic CID with more fragmentation, but less operator control. Ion-trap and FT-MS allow multistage fragmentation experiments to be conducted through, which is essential for structural elucidation studies (Ojima et al 2005 and Gates, 2005b).

1.5.2- Nuclear magnetic resonance spectroscopy of Natural Products (NMR):

Structural elucidation in general involves determining an extended sequence of bond connectivities. Natural product chemists have to build up a structure from scratch in a logical manner as they require some biogenetic knowledge and chemical intuition. Indeed they have to be quite successful in solving structures where initially they had no idea what class of compound was involved (Rycroft 1988)

Advances in radio frequency and probe technology, in the application of higher magnetic fields and the ever expanding repertoire of pulse sequences in one-dimentional (1D) and two-dimensional (2D) NMR and in the biological area of three-dimensional (3D) NMR and even four-dimensional (4D) NMR, will inevitably be passed down to the structural organic chemist to allow the resolution of more complex structural problems on increasingly

smaller sample quantities. This non destructive methodology contrasts sharply with chemical degradation studies that so typically have dominated natural product structure determination in the not too distant past (Hensens 1994). The most of the recent advanced NMR techniques will be disscussed, briefely, through the following structural elucidation strategies:

1.5.2.1- The most applied structral elucidation strategy depends largely on NMR and MS modern techniques:

1) ***the establishment of the molecular formula***: the determination of the molecular formula is critical in the structure determination process of natural product. MS remains the method of choice for determining molecular formulas and identifying known substances (Hensens 1994). Depending on the particular instrumentation available, the accuracy of these methods does not always define an emperical formula uniquely but provides a range of formulas especially in the molecular weight range above 500 Dalton (Da). increasing number of examples have recently appeared in the litrature where determining emperical formulas of natural products with molecular wieght 500 Da or more have required an interplay between MS and NMR methods.
2) ***Determination of carbon count of the molecule***: a proton–decoupled ^{13}C spectrum can in principle provide a reliable carbon count of the molecule. However, depending on carbon spin-lattice relaxation times, the flip angle (pulse width) and the acquisition time employed, quaternary carbons can sometimes appear as week signals that may not be readily distinguished from impurity peaks that are present. In this case, changing the solvent pH, temperature, and/or parameter selection may be helpful. Demonstrating its long-range connectivity to an assigned proton usually ensures that a quaternary carbon belongs to molecule. It should be taken in mind that the No. of ^{13}C resonances in the molecule does not immediately infer the correct carbon count and degeneracy in chemical shift position is often the reason this drowback may be largely overcome by remeasurment in different solvents. In other cases the degeneracy may be associated with a symmetry feature of the molecule such as monomeric versus dimeric forms or overlaping of more than one carbon peaks.
3) ***Determination of the proton count***: The next step in the strategy is the determination of the proton count, several methods are currently available to determine carbon multiplicities and consequently the carbon-bound proton count. for example the *J*-modulated attached-proton-test (APT), and the more preferred one „distortionless

enhancement by polarization transfer“ (DEPT). DEPT is more preferred for various reasons, it has reduced dependence on *J*, is not very sensitive to misset pulses or in homogeneities in the rf, has definit sensitivity advantages, require less amount based on the availabe aparatus. The solvent peak is effectively suppressed in all spectra, which may thus advantageously detect nonquaternary carbons obscured by the solvent peak. Having established the No. of carbon-bound protons in the molecule, it remains to determine the No. of active protons, which is usually less straightforward. Deuterium (^{2}H) exchange experiments are often used. As far as MS methods are concerned for the determination of the No. of active protons in a molecule, the formation of trimethylsilyl (TMS) ethers and esters have enjoyed great popularity. MS data for the derivatives are compared with that of the corresponding deuterated d_9-TMS derivatives.

4) ***Determination of the No. of possible empirical formulas***: With the molecular weight, ^{1}H and ^{13}C counts in hand, severe restrictions are now placed on the No. of possible empirical formulas for a given molecule. This is particularly the case if some knowledge of elements present has been obtained from either a combustion analysis or by inference from NMR data. The HRMS data can only be regarded as consistent with the calculated empirical formula as distinct from rigorously establishing it. This should be kept in mind because journals such as the *Journal of the American Chemical Society* and *Journal of Organic Chemistry*, for example, set widely varying, acceptable limits in 1991 of ± 3 and ± 13 mmu, respectively for mol.weights up to 500 and ± 6 and ± 16 mmu respectively, for molecular weights 500 to 1000.
5) ***Determination of partial structures***: This can be established from the ^{1}H-^{1}H connectivity data, obtained from conventional double irradiation or 2D-COSY-Type experiments. Included in the development of partial fragments is usually some knowledge of preliminary ^{13}C NMR data as well as one-bond ^{1}H-^{13}C correlations. One-bond ^{1}H-^{13}C techniques, which by definition are limited to nonquaternary carbons, provide little connectivity data unless used in conjunction with long-range ^{1}H-^{13}C data where such ^{13}C NMR assignments are essential. The most important information the 2D ^{1}H-^{13}C correlation experiment offers is that can provide a clear distinction between methine and methylene proton positions in crowded regions of a ^{1}H NMR spectrum. This information cannot always be unambiguously obtained from COSY-type experiments and when attempted, is solely inferred from the No. and size of the couplings involved, a process that is not unambiguous and difficult in situations where there is significant overlap.

5a) H-H connectivities: this may be established from the basic correlation spectroscopy (COSY) experiment, double-quantum filtered COSY (DQF-COSY), the complementary relayed COSY (RCOSY), and homonuclear Hartman-Hahn spectroscopy (HOHAHA) or total correlation spectroscopy (TOCSY) experiments.

5b) ^{1}H-^{13}C one-bond connectivities: The 2D-heteronuclear correlation (HETCOR) experiment, which correlates a ^{13}C nucleus with its attached protons or the more preferred and more sensetive experiment, ^{1}H-detected heteronuclear multiple quantum coherence experiment, (HMQC) or Hetero nuclear single quantum coherence (HSQC) are applicable in this stage of the strategy.

6) ***Determination of the total Structure***: this stage of the strategy can be performed by NMR experiments that are used to bridge isolated spin systems in natural product compound. For example :

6a) ^{1}H-^{1}H through space correlations: this correlations can be obtained from *J*-coupled methods e.g. long range correlations in the COSY experiment (LOCOSY), or from dipolar coupled methods e.g. 1D- (NOE) or 2D- (NOESY) nuclear overhauser effect or Rotating frame NOESY, (ROESY) which give indications of distance-dependent „through space" dipolar interactions. 1D- or 2D NOE experiment can give valuable informations not only about the sequence and attachment of the separated partial structures but also about the stereochemical/conformational informations.

6b) ^{1}H-^{13}C long range connectivities: powerful as this widely applicable methodology of ^{13}C-detected and especially ^{1}H-detected ^{1}H-^{13}C long range correlation experiments has become, it nevertheless has its shortcomings. By implication, this technique depends on each carbon being strategically located usually 2- or 3-bonds away from a proton in the molecule. Many NMR experiments may be used in this stage e.g. long range version of the HETCOR experiment (LR-HETCOR) or correlation via long range coupling (COLOC) which are 2D- ^{13}C-detected ^{13}C-^{1}H long range correlation experiments. But the more applicable and widely used experiment is heteronuclear multiple bond correlation (HMBC), which inverse ^{1}H-^{13}C long range coupling through ^{1}H-detected ^{1}H-^{13}C long range correlation experiment. Because of the extreme usefulness of the HMBC experiment, it is highly recommended that for optimal results, several experiments be run under different experimental conditions (e.g., solvent or temperature), optimized for different couplings and that these experimental conditions be reported.

1.5.2.2- The Computer-Assisted Structural elucidation strategy (CASE):

The most time-consuming process, that of assembling structures using the substructure information extracted from the spectra can be performed by computers (Neudert and Penk 1996). The ideal of computer assisted structure elucidation (CASE) is to generate, exhaustively and without redundancy, all possible structures that are consistent with a particular set of spectroscopic data. The aim is to achieve this goal with the minimum amount of human intervention to overcome the major bottleneck in the natural product drug discovery (Jaspars 1999).

Some approaches without resorting to 2D NMR data, have been tried using ^{13}C NMR data alone. One example of this type of system is Richert´s Specsolv (Will et al. 1996), which is a new module of the NMR database SpecInfo. SpecInfo has used data from thousands of compounds to calculate typical chemical shifts for a carbon with a particular set of neighbours (a substructure). SpecSolv allows the user to enter the ^{13}C NMR spectrum of the unknown , without having to give the molecular formula, and structures matching these chemical shifts are returned. For 80% all compounds containing only C,H,N,O,S,P and halogens, the correct structure is derived. The program relies on a subspectrum search, which is then translated to a collection of substructures. The substructures are assembled to give the greatest degree of overlap, and the ^{13}C chemical shift is calculated for each generated structure. The structure which gives the correct ^{13}C NMR spectrum is returned to the user as the most likely candidate structure. With „exotic unknowns“ such as complex natural products no final structure can be proposed by SpecSolv due to the lack of spectral matches. In addition, two carbons with the same neighbouring groups, but in different conformations may have very different chemical shifts, and this may confound the subspectrum search. Although ^{13}C shift based programs are likely to find great utility in a synthetic laboratory with a high turnover of compounds, it is unlikely to fulfil the ideal of CASE (Jaspars 1999).

Another approach to CASE, which does incorporate the use of 2D NMR data, is to compose a new NMR pulse sequence which enables the direct determination of proton spin systems in a molecule (Eggenberger and Bodenhausen 1989).The generation of proton spin systems is also possible using a graph theoretical method which determines a C-C connectivity matrix for protonated carbons by the direct determination of the matrix product of ^{1}H-^{1}H COSY and ^{1}H-^{13}C COSY (1bond) spectra. These last two methods are useful in generating spin systems only, but they do not allow the generation of complete structures without the use of further long range data. This goal can be achieved through the application

of CASE programs which are able to use routinely available 2D NMR data (e.g. ^{1}H-^{1}H COSY, HMQC or HSQC, HMBC, NOESY and INADEQUATE) (Jaspars 1999).

The human thought process:

It is important to appreciate firstly, how a spectroscopist will elucidate a structure from spectroscopic data. The process is summerized in Fig. (1.12). Normally the molecular formula is derived from a combination of ^{13}C NMR, DEPT and MS data. Using IR, UV and ^{13}C NMR the functional groups can be proposed, and ^{1}H NMR coupling data or 2D NMR correlations are used to assemble substructures. These are then combined into „working structures“ which are possible combination of the substructures. These are then checked for consistency with the 2D NMR data and MS fragmentations etc. The ^{13}C chemical shifts of the surviving structure(s) are then compared with litrature, database or predicted values to confirm the 2D structure of the molecule. To determine the relative stereochemistry of the molecule, ^{1}H coupling constant (*J*) and NOE data are used. The absolute streochemistry can then be determind by a variety of methods such as optical rotatory dispersion-circular dichroism (ORD-CD), derivatisation or degradation. It is important, as early as possible, to know whether the unknown compound has previously been described, a process known as **dereplication,** which can be performed using a combination of molecular formula, substructures and chemical/structural databases (Corely and Dorley 1994).

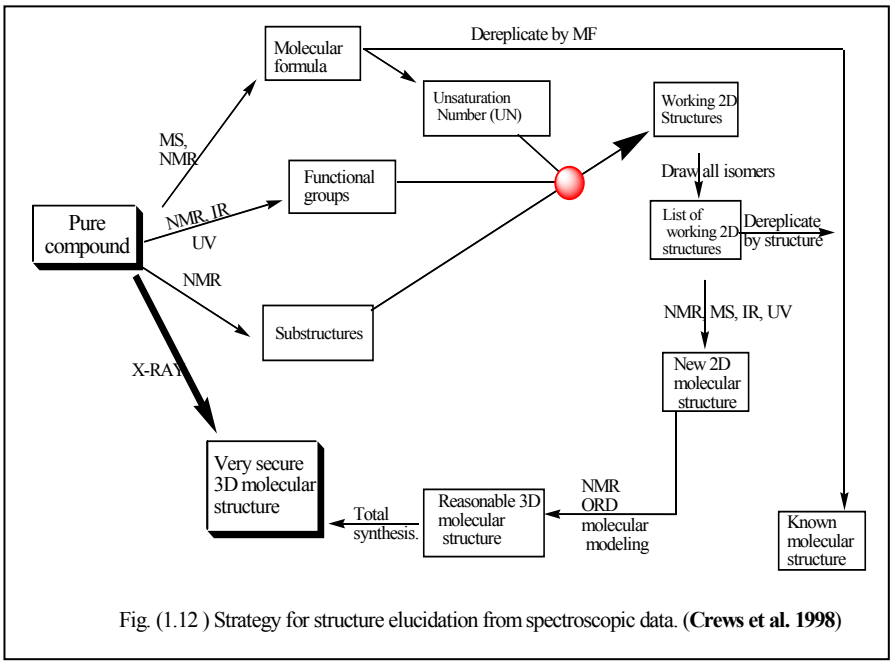

Fig. (1.12) Strategy for structure elucidation from spectroscopic data. (**Crews et al. 1998**)

Once it has been established that the compound in question has not been reported before, the process of structure elucidation as depicted in Fig (1.12) can begin (Jaspars 1999).

Two common strategies are employed when elucidating organic structures, one involving C-C correlations from a 2D INADEQUATE spectrum, the other using C-C connectivities inferred from C-H data. The INADEQUATE strategy is summarised in Fig. (1.13a). The main problem of this approach is the inherent insensitivity of the INADEQUATE experiment, which dictates that a large amount of sample is needed, which may be not available in some cases, and that it must be (if available) soluble in a small amount of solvents (Jaspars 1999).

The alternative strategy involves the use of more 2D NMR experiments, but these can be obtained in a reasonable time using inverse detected techniques on a multimilligram sample. This strategy is outlined in Fig. (1.13b) (Jaspars 1999).

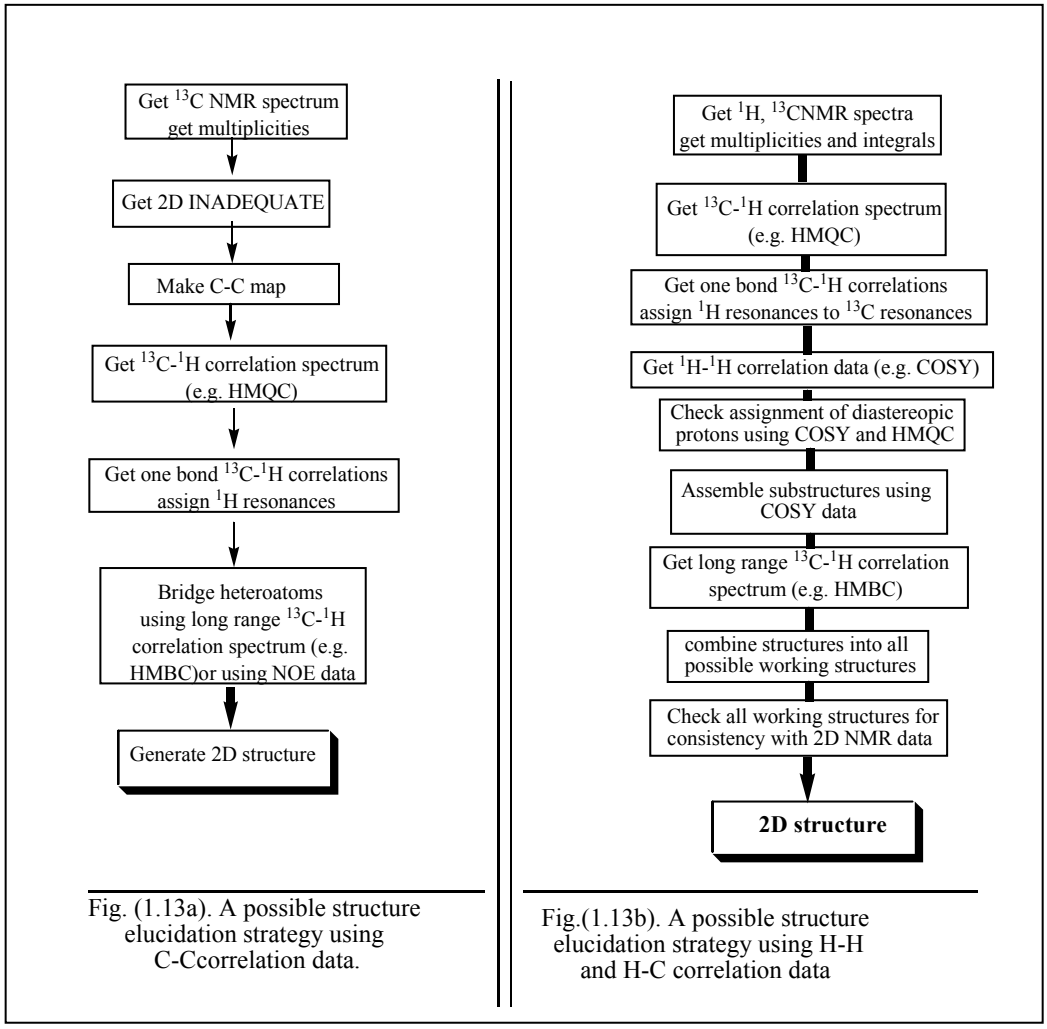

Fig. (1.13a). A possible structure elucidation strategy using C-Ccorrelation data.

Fig.(1.13b). A possible structure elucidation strategy using H-H and H-C correlation data

Structure of the CASE Program:

The CASE system is composed of several steps (Fig.1.14) (Jaspars 1999).

1- The first step is the input of the spectra, or „**peak-picking**“, to convert the data into a more computer digestible form. This can rely on the skill of a spectroscopist who

translates the cross peaks of a 2D spectrum into correlations, or ideally on a sophisticated peak picking program.

2- The next step is to produce a list of possible components (*e.g.* CH_3, CH_2-O etc.) present in the molecule. Generated substructures can be checked during the process of structure generation (**Prospective checking**) or after all complete structures have been generated (**retrospective checking**). Clearly, prospective checking will be faster, as those substructures that are not consistent with the 2D NMR data are removed from the structure generation process. In the case of retrospective checking a combinatorial explosion occurs for exhaustive structure generation, even for molecules of a moderate size. These generated components are fed into the most important part of the program, the structure generator.

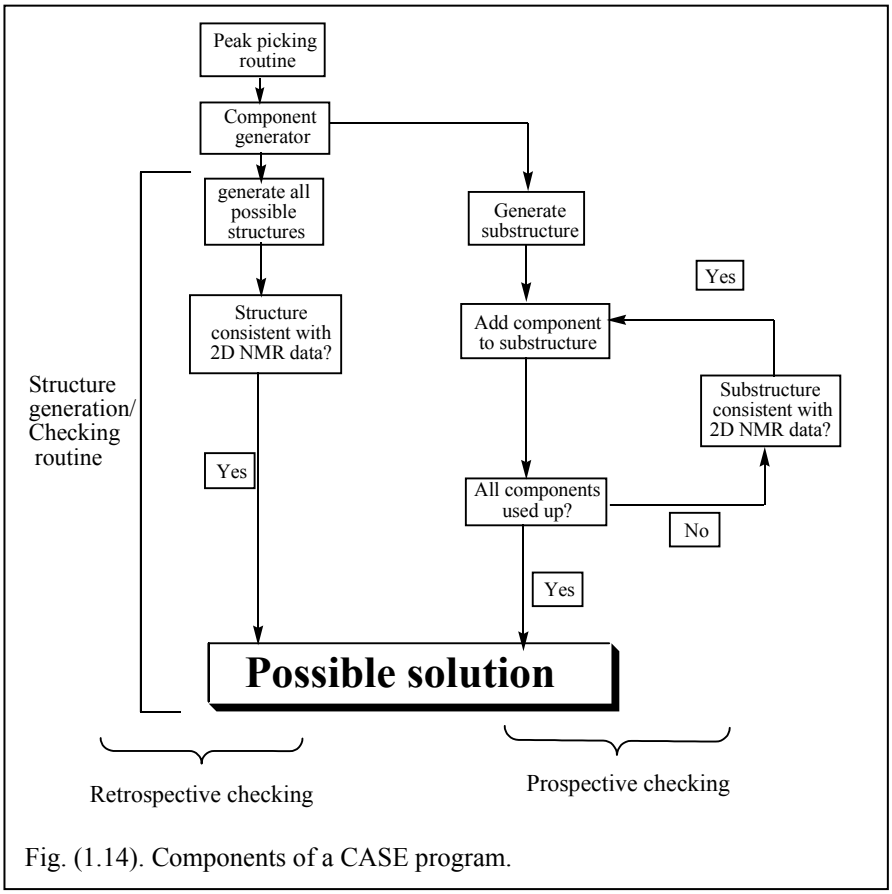

Fig. (1.14). Components of a CASE program.

3- The next part is „the structure generator“ which will use the components that are generated by one of the methods mentioned above to generate exhaustive list of all possible structures without redundancy, and without missing out any plausible structures. The structure generator is the part of the CASE program that will take the greatest amount of CPU time, and this is also where the greatest time savings can be made by the use of efficient algorithms.

4- The generated structures are checked for consistency with the 2D NMR data. An innovative feature to determine whether the structure generator is heading in the right direction is by checking the rate at which 2D NMR constraints are being satisfied. In general as the generation extends towards the correct structure, the number of constraints satisfied should increase. As long as this rate of constraint satisfaction is above a predetermined value, the structure generation continues, if it falls below this level generation using this particular substructure is discontinued. This is a very powerful way to direct the structure generation process, and greatly reduces the time taken to achieve a plausible solution.

5- Determination of stereochemistry: For large molecules the determination of three dimensional structure is performed by using a combination of molecular modelling and constraints derived from NOE data as well as coupling constant information (Evans, 1995). The absolute stereochemistry will still need to be determined by the use of degenerative methods, auxiliary reagents, or optical rotatory dispersion-circular dichroism (ORD-CD) (Jaspars 1999).

Currently, the modification of CASE systems is continued to overcome as great as possible, the above encountered problems including the CASE programs, structure generators, and the database projects, in order to make the CASE more applicable.

Interaction between a spectroscopist and the CASE system will remain important in order to generate the correct structure rapidly. Therefore CASE will complement the skills of the spectroscopist, not replace them. The use of CASE system is likely to increase in the near future, and this will enable the bottleneck so often caused by structure elucidation to be removed from the natural product drug discovery process (Jaspars 1999).

1.6- Marine Natural Products

1.6.1- Marine organisms are rich biological sources for bioactive natural product discovery:

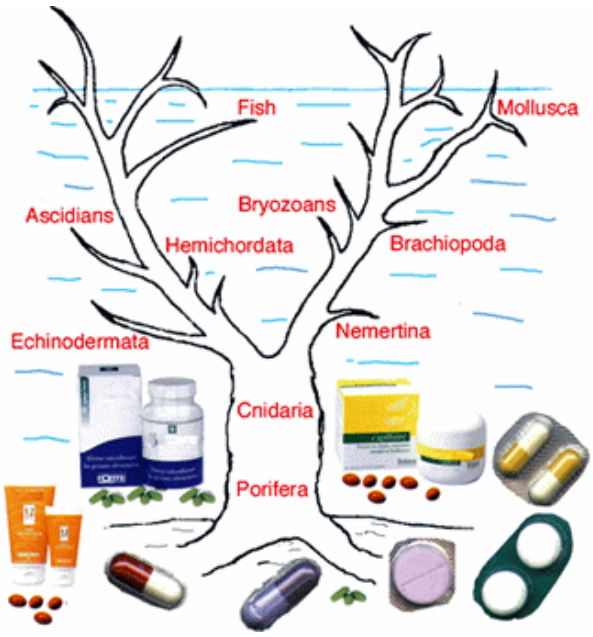

Picture from : **Marine Pharmacology**: Potentialities in the Treatment of Infectious Diseases, Osteoporosis and Alzheimer's Disease. (Bourguet-kondracki and Kornprobst, 2005)

Selection of marine organisms as biological materials in this work was largely attributed to the tremendous level of worldwide interest in marine natural products with therapeutic potential in industry, academia, and government research labs (McConnell *et al*., 1994, Proksch *et al* 2002). Marine natural products chemistry is essentially a child of the 1970´s that developed rapidly during the 1980´s and matured in the last decade (Faulkner, 2000a). By 1975 there were already three parallel tracks in marine natural products chemistry: marine toxins, marine biomedicinals and marine chemical ecology. It is the integration of the three fields of study that has given marine natural products chemistry its unique character and vigour . Marine organisms have provided a seemingly endless parade of novel structures. New carbon skeletons were discovered and several functional groups are uniquely or predominantly marine (Faulkner 2000a).

The first natural products isolated from marine organisms that proved to be valuable lead structures for the development of new pharmaceuticals were the unusual nucleosides

spongouridine and spongothymidine from the caribbean sponge [*Cryptotethia crypta,* Tethydae, (Bregmann and Feeney 1951)] which served as models for the development of adenine arabinoside (ARA-A), (Vidarabin, Thilo), for treatment of Herpes simplex infection and cytosine arabinoside (ARA-C), (Cytarabin, Alexan, Udicil), for the treatment of leukemia respectively (Ireland et al 1993). The discovery of sizeable quantities of prostaglandins, which had been discovered as important mediators involved in inflammatory disease, fever and pain in the gorgonian *Plexaura homomalla* by Weinheimer and Spraggnis in 1969 is considered as the take-off point of systematic investigation of marine environments as sources of novel biologically active componds (Newman, *et al*., 2000a; Proksch *et al*., 2002).

1.6.2- Marine natural products:

Marine natural products with their unique structural features and pronounced biological activities continue to produce lead structures in the search for new drugs from nature. Invertebrates such as sponges, tunicates, shell-less mollusks and others that are either sessile or slow moving and mostly lack morphological defense structures have so far provided the largest number of marine-derived secondary constituents including some of the most interesting drug candidates (Proksch *et al*. 2003)

It is clear that marine natural products chemistry has had a major impact over the past 30 years, and man can not predict what will happen in the next few years (Faulkner 2000a). Faulkner 2000a, predict a great impact of chemical and biological researches including genetic engineering concerning different forms of marine living forms ranging from marine invertebrates to the marine-derived microorganisms. Faulkner also expects that, in the near future we able to transfer biosynthetic genes from one marine organism to another and imagine the marine natural product chemist of 2025 still involved in structural elucidation, but considerable effort to the genetic engineering required to produce unique metabolites by fermentation of genetically modified microbes. This will accomplish the goal of having the marine organisms provide the inspiration for new compounds while avoiding their excessive harvesting.

The sponges are the source of the greatest diversity of marine natural products. About one-third of all marine natural products have been isolated from sponges, which make them currently the most popular source of novel compounds (Whitehead, 1999). The marine sponges are considered not only as a very important source of new natural products but also a

source for bioactive compounds. These compounds are interesting candidates for new drugs, primarily in the area of cancer, anti-inflammatory and analgesic (Proksch *et al*, 2002).

1.6.3- The biological evaluation of marine natural products

Marine organisms have provided a large proportion of the bioactive natural products reported over the last 20 years, but non of these compounds have reached the pharmaceutical marketplace (Faulkner 2000b).

Now, marine natural products are already available in the market as effective drugs. Ziconotide (*Prialt*) which is a 25-aminoacid peptide isolated from the venom of the marine snail *Conus magus* is now available in the market as a potent analgesic for severe chronic pain, its analgesic effect is comparable to the opioid analgesics (e.g. Morphine) but its mode of action not includes binding to the opioid receptors and its actions are not blocked by opioid antagonists. Ziconotide has a unique mechanism of action, binding to N-type calcium channels on nerves in the spinal cord and blocking their ability to transmit pain signals to the brain. Unlike the opioid analgesics, it doesn't cause tolerance or addiction (Hussar 2006).

However, several marine-derived compounds have generated considerable interest scientifically, commercially, and from public and health point of view, these include prostaglandins, palytoxin, ciguatoxin. Further, because of their unique and potent biological activities, several marine-derived compounds have already found use as biological probes or biochemical tools and are sold commercially, e.g., palytoxin, brevetoxins, ocadaic, tetrodotoxin, saxitoxin, calyculin A, manoalide, and kainic acid (McConnell *et al*., 1994). Several marine derived natural products have a significant biological activity and many of them, are currently, in different phases of clinical trials as drug candidates. Some of these bioactive marine-derived natural products will be mentioned below.

Approximately, half of all marine natural products papers report bioactivity data for new compounds (Faulkner 2000b). Significant number of marine-drived natural products have been entered into antitumor preclinical or clinical trials since the early 1980s (Newmann and Cragg 2004).

Table 1.2 Status of marine-derived natural products in clinical and preclinical anticancer trials*

Name	Source	Status	comment
Didemnin B	*Tridemnum solidum*	Phase II	Dropped middle 90s (very toxic)
Dolastatin 10	*Dolabella auricularia*	Phase I/II	

Giroline	*Pseudaxinyssa cantharella*	Phase I	Discontinued (hypertension)
Bengamide derivative	*Jaspis sp.*	Phase I	Licensed to Novartis, Met-AP1 inhibitor, withdrawn 2002
Cryptophycins (also arenastatin)	*Nostoc sp.& Dysidea arenaria*	Phase I	Licensed to Lilly, but withdrawn 2002.
Bryostatin 1	*Bugula neritina*	Phase II	
TZT-1027	Synthetic dolastatin	Phase II	also known as auristatin PE and soblidotin
Cematodin	Synthetic dolastatin 15	Phase I/II	
ILX 651, synthetadin	Synthetic dolastatin 15	Phase I/II	
Ecteinascidin 743	*Ecteinascidia turbinata*	Phase II/III	
Aplidine	*Aplidium albicans*	Phase II	Dehydrodidemnin B, made by total synthesis
E7389	*Lissodendoryx sp.*	Phase I	Synthetic halichondrin B derivative
Discodermolide	*Discodermia dissoluta*	Phase I	
Kahalalide F	*Elysia rufescens / Bryopsis sp.*	Phase II	Licensed to PharmaMar, (isolated also from *E. grandifolia* together with very similar analogues as bioactive depsipeptides in the present work.)
ES-285 (spisulosine)	*Spisula polynyma*	Phase I	*Rho*-GTP inhibitor
HTI-286 (hemiasterlin derivative)	*Cymbastella sp.*	Phase II	Synthetic derivative, licensed to Wyeth.
KRN-7000	*Agelas mauritianus*	Phase I	
Squalamine	*Squalus acanthias*	Phase II	also has antiangiogenic activity.
Æ-941(Neovastat)	shark	Phase II/III	Defined mixture of <500 kDa from cartilage, also has antiangiogenic activity.
NVP-LAQ824	Synthetic	Phase I	Derived from Psammaplin trichostatin, and trapoxin structures.
LU103793	*Dolabella auricularia*	Phase II	Semisynthetic pseudopterosin
Laulimalide	*Cacospongia mycofijiensis*	preclinical	synthesized by a variety of investigators
Curacin A	*Lyngbya majuscula*	preclinical	synthesized
Vitilevuamide	*Didemnum cucliferum & Polysyncraton lithostrotum*	preclinical	
Diazonamide	*Diazona angulata*	preclinical	synthesized and new structure elucidated.
Eleutherobin	*Eleutherobia sp.*	preclinical	synthesized and also derivatized, can be produced by aquaculture
Sarcodictyin synthetic derivatives.	*Sarcodictyon roseum*	preclinical	

Peloruside A	*Mycale hentscheli*	preclinical	
Salicylhalimides A	*Haliclona sp.*	preclinical	first marine Vo-ATPase inhibitor, synthesized.
Thiocoraline	*Micromonospora marina*	preclinical	DNA polymerase α inhibitor
Ascididemnin		preclinical	Reductive DNA-cleavage agents
Variolins	*Kirkpatrickia variolosa*	preclinical	Cdk inhibitors
Dictyodendrins	*Dictyodendrilla verongiformis*	preclinical	Telomerase inhibitors

(*Reported from Proksch *et al.*2002 and Newmann and Cragg 2004)

There are other marine-derived natural products showing vast pharmacological activities, many of them are currently evaluated as drug candidates and entered clinical trials. Table (1.3) shows other marine-derived natural products that are, currently, in clinical trials for non antitumour therapeutic activities.

Table 1.3. Status of marine-derived natural products in clinical and preclinical trials* other than antitumors.

Name	**Source**	**Status (disease)**	**comment**
GTS-21 (aka DMBX)	*Amphiporeus lactifloreus*	Phase I (Alzheimer´s / schizophrinia)	Modification of a worm toxin : contignasterol 8 IZP-94,005
Manoalide	*Luffariaella variabilis*	Phase II (antipsoriatic)	discontinued (formulation problems)
IPL-576,092 (aka HMR-4011A)	*Petrosia contignata*	Phase II (antiasthmatic)	licensed to Aventis
IPL-512,602	derivative of IPL-576092	Phase II (antiasthmatic)	licensed to Aventis
IPL-550,260	derivative of IPL-576092	Phase I (antiasthmatic)	licensed to Aventis
Ziconotide (aka Prialt)	*Conus magus*	Phase III (neuropathic pain)	Licensed by Elan to Warner Lambert (**it is on the market now**)
CGX-1160	*Conus geographus*	Phase I (pain)	Contulakin G
CGX-1007	*Conus geographus*	Phase I (pain & epilepsy)	Conantokin G; discontinued
AMM336	*Conus catus*	Preclinical (pain)	ω-conotoxin CVID
χ-conotoxin	*Conus sp.*	Preclinical (pain)	Conotoxin MR1A/B
CGX-1063	Thr10-contulakin G	Preclinical (pain)	Modified toxin
ACV1	*Conus victoriae*	Preclinical (pain)	A-conotoxin Vc1.1
Methopterosin	*Pseudopterogorgia elisabethae*	Phase I (inflamation / wound)	Semisynthetic pseudopterosin derivative

(*Reported from Proksch *et al*.2002 and Newmann and Cragg 2004)

Although during 2000 no new marine natural product was approved for patient care by the U.S. Food and Drug Administration (FDA), during 2000 preclinical pharmacologic research with marine chemicals continued to proceed at a very active pace, involving both natural product chemists and pharmacologists from foreign countries and the United States (Mayer and Hamann 2004)

In order to reflect the worldwide interest towards the marine derived natural products as drug candidates, Mayer and Hamann 2004 reported a review for preclinical trials involving pharmacological and toxicological studies for some bioactive marine natural products that are published during only one year (2000), 35 marine natural products reported as antibacterial, anticoagulant, antifungal, antimalarial, antiplatelet, antituberculosis, antiviral and 20 marine natural products having antiinflammatory, immunosuppressant, cardiovascular activity, and compounds affecting nervous systems. Some of this report is presented in Tables (1.4 and 1.5 respectively.)

Table 1.4. Marine compounds with antibacterial, anticoagulant, antifungal, antimalarial, antiplatelet, antituberculosis, and antiviral activities, that are reported in one year (2000) as drug leads in preclinical trials.

Drug class	Compound/organism	Chemistry	Pharmacologic activity	Molecular mechanism of action (MMOA)
Antibacterial	Acetylenic acids/sponge	Fatty acid	Gram-positive and nigative inhibition	Undetermined
Antibacterial	Discorhabdin R /sponge	Alkaloid	Gram-positive and nigative inhibition	Undetermined
Anticoagulant	Fucoidan/alga	Sulfated polysaccharide	Inhibition of microvascular thrombus	No effect on P- and L-selectin
Anticoagulant	Proteoglycan/alga	Polysaccharide	Anticoagulant	Inhibition of thrombin and potentiation of antithrombin III
Anticoagulant	Sulfated D-galactan/alga	Sulfated Polysaccharide	Anticoagulant	Inhibition of thrombin and factor Xa
Antifungal	Lyngbyabellin B/bacterium	Depsipeptide	*C. albicans* inhibition	undetermined
Antifungal	Naamine D/sponge	Alkaloid	*C. neoformans* inhibition	Nitric oxide

				inhibition
Antimalarial	Ascosalipyrrolidin 1A/fungus	Polyketide	*P. falciparum* inhibition	$p56^{lck}$ tyrosine
Antimalarial	Homofascaplysin A & fascaplysin/sponge	Sesterterpene	*P. falciparum* inhibition	Undetermined
Antimalarial	Manzamine A/sponge	Alkaloid	In vivo *P. berghei* inhibition	Undetermined
Antiplatelet	Eryloside F/sponge	Sterol glycoside	Platelet aggregation inhibition	Thrombin receptor antagonist
Anti-tuberculosis	Axisonitrile-3/sponge	Sesquiterpene	*M. tuberculosis* inhibition	Undetermined
Anti-tuberculosis	Elisapterosin B/soft coral	Diterpene	*M. tuberculosis* inhibition	Undetermined
Antiviral	Cyclodidemniserinol trisulfate/ascidian	Polyketide	In vitro HIV infection inhibition	HIV-1 integrase inhibition
Antiviral	Dragmacidin F/sponge	Alkaloid	In vitro HSV-1 and HIV-1 inhibition	Undetermined
Antiviral	Lobohedleolide, 17-dimethylamino/soft coral	Diterpene	In vitro HIV infection inhibition	Undetermined
Antiviral	Mololipids /sponge	Alkaloid	In vitro HIV-1 infection inhibition	Undetermined

Table.1-5. Marine compounds with anti-inflammatory and immunosuppressant effects and others affecting cardiovascular and nervous system that reported in one year (2000) as drug candidates in preclinical trials.

Drug class	**Compound/organism**	**chemistry**	**Pharmacologic activity**	**Molecular mechanism of action (MMOA)**
Anti-inflammatory	Cavernolide /coral	Terpene	In vitroTNF-α, NO and PGE_2 inhibition	$sPLA_2$, iNOS and COX_2 inhibition
Anti-inflammatory	Contignasterol/ sponge	sterol	In vivo allergen-induced plasma protein exudation inhibition	Undetermined
Anti-inflammatory	Cyclolinteinone/sponge	Sesterterpene	In vitro NO and PGE_2 inhibition	NF-kB binding, iNOS and COX_2 expresion inhibition
Anti-inflammatory	Oxepinamide A/fungus	Alkaloid	In vivo neurogenic inflammation assay	Undetermined
Anti-inflammatory	Sterol/alga	Sterol glycoside	In vivo inflammation assay	Undetermined

Cardiovascular	Docosahexanoic acid/fish	Fatty acid	In vivo vascular reactivity assays and in vitro biochemical assays	Undetermined
Immuno-suppressant	Theonellapeptolides/ sponge	peptide	In vitro mixed lymphocyte reaction assay	Undetermined
Nervous system	Conantokin G, T/snail	Peptide	In vivo parkinson´s disease model	Alteration of striatal efferent neurons function
Nervous system	Conantokin-G/snail	Peptide	In vivo block of dopamine-enhancing drug methamphetamine	NMDA receptor antagonism
Nervous system	Conantokin-G/snail	Peptide	In vitro neuronal and oocyte whole-cell electrophysiology	Competitive antagonist of NR2B NMDA receptors
Nervous system	Conantokin-G/snail	Peptide	In vivo and in vitro neuroprotective assays	Decrease Ca^{++} response to NMDA
Nervous system	Conantokin-R/snail	Peptide	In vitro NMDA receptor antagonist and in vivo anticonvulsant assays	NR2 NMDA receptor selectivity
Nervous system	Conantokin-R/snail	Peptide	In vitro binding assays	Disulfide loop not essential for receptor and cation binding.

1.7- Aim of the work:

The present work is focused on some of the modern methods that currently included in the recent discovery of natural products with therapeutic potentials. This study deals with the modern technical applications ranging from the use of various types of HPLC, the use of hyphenated analytical techniques during the isolation procedures (e.g. HPLC/UV, HPLC/MS, HPLC/MS/MS, GC/MS), new methods of chemical modification and different techniques in molecular weight determination during the structural elucidation, different methods of NMR spectral analysis and bioactivity guided isolation.

In the present study, the isolation of some new natural product is guided by dereplication procedure using hyphenated techniques coupled to HPLC such as LC-mass spectroscopy (LC-MS, LC-MS-MS). Some soft bodied marine organisms are included in this study as they are attractive biological materials that, attract worlwide interest of natural product chemists and pharmacologists.

II. Materials and Methods

2.1 Animal materials

All biological materials included in this work are marine animals, and collected from four different geographical zones and including 2 saccoglussan mollusks, *Elysia rufescens* which was collected from the black point Kahala, in the Pacific Ocean (Hawaii), and *Elysia grandifolia* which was collected from the Indian Ocean (India), and 4 sponges, unidentified *Pachychalina sp*., *Petrosia nigricans*, and *Callyspongia biru* which were collected from the Pacific Ocean (Indonesia), in addition to *Hyrtios erectus* which was collected from the Red Sea (Egypt).

2.1.1 Sacoglossan mollusks from the genus *Elysia :*

Genus *Elysia* belongs to the herbivorous marine mollusks, sacoglossans, with the ability to sequester from their algal diet functioning chloroplasts, which then may participate in the biosynthesis of secondary metabolites. (Hamann and Scheuer 1993)

2.1.1.1. *Elysia rufescens*

Elysia rufescens Pease, 1871

Order: Sacoglossa

Superfamily: Elysioidae

Family: Elysiidae

Elysia rufescens : "Length: 11 mm up to 60 mm; parapodial height: 3 mm. Parapodia is low but erect, with two or three undulations; rhinophores are long, slender and directed anteriorly. The pericardial prominence is a white sac at the anterior end of the parapodia. The color is dark red maculated with spots of creamy green which impart a reticulated appearance to the animal. The parapodial margine is orange, while the rhinophores are dark red in color tipped with purple". (Kay, E.A. 1979; Pease, W.H. 1871; Rudman, W.B., 1999). *Elysia rufescens* was collected and provided by D. Horgen (University of Hawaii at Manoa) from Black point, Kahala, Oahu Island in Hawaii, dried and sent as coarse powder to our Laboratory in April 2003.

2.1.1.2- *Elysia grandifolia*

Elysia grandifolia Kelaart, 1858

Order: Sacoglossan

Superfamily: Elysioidea

Family: Elysiidae

The mollusc *E. grandifolia* (17 molluscs ; 77 g wet wt) which were observed to be feeding on the algae *Bryopsis plumosa* (Hudson), were collected by snorkeling from the Gulf of Mannar and Palk Bay, Rameswaram, India (9°15' N; 79°15'E) at 1 to 2 meter depth in May, 2003, immediately preserved in methanol and kept frozen until extraction work. The animal was 10 cm in length and had a translucent green color with a large parapodial margin. The parodial margin had a very thin, black line, and a submarginal yellow or orange band.

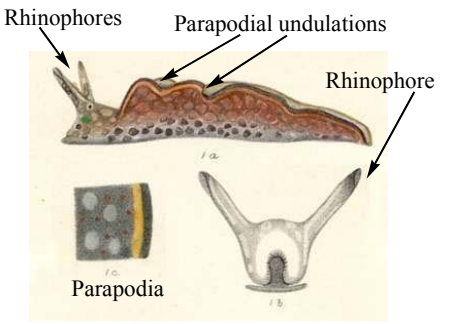

Figure (2.1) *Elysia* sp

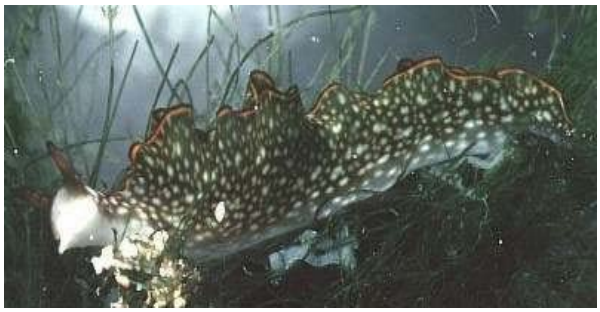

Fig. (2.2) *Elysia rufescens* 60mm, on *Bryopsis pennata* (algal diet)

Fig. (2.3) *Elysia rufescens*

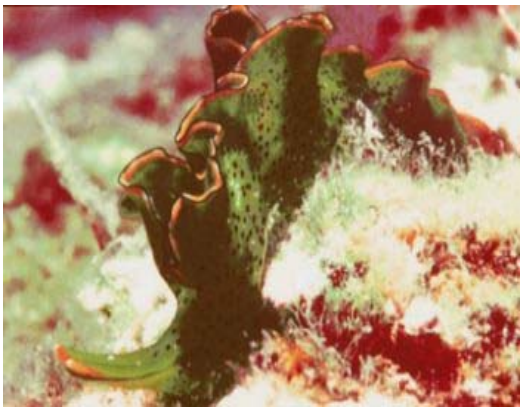

Figure (2.4) *Elysia ornata*

Fig. (2.5) *Elysia grandifolia*

There was no white line between the orange and yellow bands (distinct. from *E. ornata*). The tip of the rhinophores had a similar color as its orange bands. The body is covered with numerous black and white dots. It had a long renopericardial ridge with 7 pairs of dorsal vessels as described by Eliot (1906). The figure of the teeth showed blunt tips and rather broad, denticulate blades as reported by O'Donoughe (1932) for specimens from the Gulf of Mannar. The sacoglossan was identified by Dr. Kathe Rose Jensen, National Natural History Museum, Copenhagen. Voucher specimens (EG-TMMP-3) were deposited in the Centre for Marine Diversity, University of Kerala, India. Jensen (1992) reported that *E. grandifolia* feeds on *Bryopsis* in both the Caribbean and the Indo West Pacific. (Jensen, 1992 & Rudman, 1999). It is very similar in colour to *Elysia ornata*. It is possibly the same species, Rudmann 2001 thought that, there are probably good grounds for considering it distinct. It grows to a very large size, 10 cm or more. He suspect that *Elysia ornata* and *E. grandifolia* are part of a group of similarly coloured species which need closer examination. (Rudman, 2001 & Kelaart, 1858).

2.1.2- The sponges

"**Sponge**" is the common name for the Poriferae, who are members of the phylum Porifera. It is named for the pores with which every sponge is covered, 'porifera' meaning 'pore bearer'. Sponges come in an incredible variety of colours and an amazing array of shapes. They probably achieved their greatest diversity during the Cretaceous period and between 5000 and 10000 species live today. They are the simplest form of the multicellular organisms and all are aquatic, benthic organisms. Most are marine, with only 150 fresh water species known today. They are known to be present in all seas and in several lakes.

Sponges are divided into three distinct groups, as follows:

Hexactinellida, or glass sponges. These are characterized by siliceous spicules consisting of six rays intersecting at right angles.

Demospongia. This is by far the most diverse sponge group, although they are not well represented in the fossil record, as they do not possess skeletons that would easily fossilize. Demosponge skeletons are composed of 'spongin' fibres and/or siliceous spicules. Demosponges take on a variety of growth forms from encrusting sheets living beneath stones to branching stalks upright in the water column. They tend to be large and only exhibit the more complex 'leucon' grade of organization.

Calcarea. Members of the group Calcarea, the calcareous sponges, are the only sponges that possess spicules composed of calcium carbonate.

Morphology:

Sponges have a cellular grade of organization, lack symmetry, and unlike all other marine invertebrates, they do not possess any structures that can be considered true tissues or organs. Sponges do not have stomachs , kidneys. They do not have nerve or muscle cells. The body of a sponge is hollow, and it is composed of a simple aggregation of cells, between which there is little nervous coordination. However, these cells perform a variety of bodily functions and appear to be more independent of each other than are the cells of other animals. This gelatinous matrix is supported by an internal skeleton of spicules of silica, calcium carbonate, or fibrous protein known as 'spongin'. The sponge's body encloses a vast network of chambers and canals that connect to the open pores on their surface. The porous nature of the sponges makes them ideally suited for habitation by opportunistic crustaceans, various worms, etc. in addition to these macro-organisms, bacteria, fungi, blue-green algae and dinoflagellates are also observed in many species. Many of the most common types of cells are described below.

Pinacocytes

These cells are the "skin cells" of sponges. They line the exterior of the sponge body wall. They are thin, leathery and tightly packed together.

Choanocytes

These distinctive cells line the interior body walls of sponges. These cells have a central flagellum that is surrounded by a collar of microvilli. It is their striking resemblance to the single-celled protists called choanoflagellates that make many scientists believe that choanoflagellates are the sister group to the animals Choanocytes. Their flagella beat to create the active pumping of water through the sponge, while the collars of the choanocytes are the primary areas that nutrients are absorbed into the sponge. Furthermore, in some sponges the choanoflagellates develop into gametes.

Mesenchyme

Between the two layers is a thin space called mesenchyme or mesohyl. The mesenchyme consists of a proteinaceous matrix, some cells, and spicules.

Archaeocytes

Archaeocytes are very important to the functioning of a sponge. These cells are totipotent, which means that they can change into all other types of sponge cells. Archaeocytes

ingest and digest food caught by the choanocyte collars and transport nutrients to the other cells of the sponge. In some sponges, archaeocytes develop into gametes.

Sclerocytes

The secretion of spicules is carried out by sclerocytes. Other cells, called spongocytes, secrete the spongin skeletat fibres when those are present.

Myocytes and Porocytes

Poriferans do not have any muscle cells, so their movement is rather limited. However, some poriferan cells can contract in a similar fashion as muscle cells. Myocytes and porocytes which surround canal openings and pores can contract to regulate flow through the sponge.

Taxonomic classification

The Porifera are sometimes placed into the Subkingdom Parazoa of Animalia, while all the other animals are in the Metazoa. As described above, they are divided into three distinct groups, the Hexactinellida (glass sponges), the Demospongia, and the Calcarea (calcareous sponges). The classification of sponges once relied on the characters of the spicules and the fibres, since the outer shape and the colour vary with the habitat. However, the classification is now more complex. The following extract, from the systematics page of the excellent Berkeley University description of Sponges [http.//www.ucmp.berkeley.edu/porifera/porifera.html.] explains the development of the current taxonomic classification of sponges.

At one time, a diagnostic feature of the Porifera was the presence of spicules. As a result, certain fossil groups whose organization was consistent with that of living sponges were not placed within the phylum Porifera. In particular, groups with a solid calcareous skeleton such as the Archaeocyatha, chaetetids, sphinctozoans, stromatoporoids, and receptaculids were problematic. A great deal of insight into the phylogenetic affinities of these groups was gained with the discovery of more than 15 extant species of sponges having a solid calcareous skeleton. These species are diverse in form, and would be classified with the chaetetids, sphinctozoans and stromatoporoids if found as fossils. However, with the living material in hand, histological, cytological, and larval characteristics can be observed. This information suggests that these 15 species can readily be placed within the Calcarea and the Demospongia. This radically changes our view of poriferan phylogeny.

It is widely accepted among poriferan biologists that the Calcarea and the Demospongia are more closely related to each other than either is to the Hexactinellida. With the discovery of living chaetetids, stromatoporoids, and sphinctozoans, a fourth class was erected for these so-called sclerosponges. However, the Sclerospongia is not a natural monophyletic grouping and is thus being abandoned. The abundant fossil chaetetids, stromatoporoids, and sphinctozoans are probably part of the classes Demospongia and Calcarea, though some uncertainty still

remains. The Archaeocyatha pose a special case. No living representative of this group has been discovered. Their organization is consistent with that of living sponges. The one phylogenetic analysis (carried out by Reitner) that included archaeocyaths with other sponges, grouped them as sisters to the demosponges. Therefore, although the taxonomic term Archaeocyatha is often accorded phylum status it is likely a sub-clade of the phylum Porifera, thereby violating the ranking system. (www.bbm.me.uk/portsdown/PH_321_sponge.htm, Pechenik 2000, Barnes 1986, Goerge and Goerge, 1979, Gerwick and Bernart 1992, Pearse *et al.* 1987, and Hooper and van Soest 2002)

2.1.2.1- *Pachychalina sp.*

The sponge *Pachychalina sp.* (Phylum: Porifera, Class: Demospongia, order: Haploscleridea, suborder: Haplosclerina family: Niphatidae) is columnar, clavate, subcylindrical growth forms, having a well-developed aquiferous system with large canals rendering the texture highly compresible. Numerous small rounded auiferous openings not clearly differentiated into oscules or pores. The whole skeleton is rather confused, with the choanosomal skeleton irregular, diffuse, and occuring as a radially plumose network of primary, ramified, multispicular fibers, irregularly connected by no proper secondary multispicular fibers and no visible spongin. The outer surface is light rose in colour, the inner side is white to faint yellow, the growing branches are finger-like branches. It was collected in Pulau Baranglompo (Indonesia) at depth of 27 ft. (25. 07. 1997). A voucher specimen has been deposited in the Zoological Museum Amsterdam under registration number ZMA POR17545

2.1.2.2- *Petrosia nigricans*

The sponge *Petrosia nigricans* Lindgren, 1897 (Phylum: Porifera, class: Demospongia, order: Haplosclerida, suborder: Petrosina, family: Pterosiidae) is a massive sponge, irrigularly globular, with a large base that produces several fused lobes. Aquiferous system with a terminal deep aquiferous cavity connected with a unique volcano-shaped osculumat the end of the lobes. Surface smooth, fine, compact, covered by a fine ectosomal layer, hispid to the touch. Texture hard, firm. The collected specimens are brown, hard, rag-like, the outer surface is rough sometimes with long fistulae, the inner side is white to faint yellow. The specimen shows small krabs introduced their heads into the osculum of the sponges. It was collected in Pulau Baranglompo (Indonesia) at depth of 30 ft. (25. 07. 1997). A voucher specimens has been deposited in the Zoological Museum Amsterdam under registration numbers ZMA POR17546 and ZMA POR17713

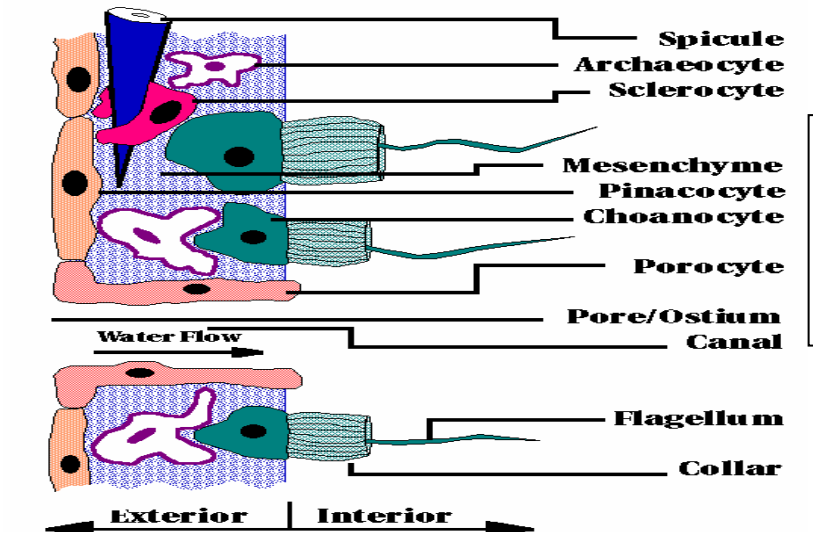

Fig (2.6) Microscopic view of a Poriferan wall (www.ucmp.berkeley.edu/porifera/pororg.html)

Figure (2.7) ***Pachychalina sp.***

Figure (2.8), ***Callyspongia biru***

Figure (2.9), ***Petrosia nigricans***

Figure (2.10), ***Hyrtios erectus***

2.1.2.3- *Callyspongia biru*

The sponge *Callyspongia biru.* (Phylum: Porifera, Class: Demospongia, order: Haploscleridea, suborder: Haplosclerina family: Callyspongiidae) is lobate repent encrusting to massive or short anastomosed upright tubes with apical oscule. Surface smooth. Single ectosomal non-hispid, layer and regular size of single, rounded to polygonal mesh. Choanosomal a well- developed network with rectangular empty mesh, primary choanosomal fibers multispicular, non-fasciculated, non ramified, spongin sheath well-defined. The specimens are blue, soft , finger-like branched sponge. the inner side is white to faint yellow. It was collected in Taka Bako (Indonesia) at depth of 30 ft. (31. 07. 1997). A voucher specimen has been deposited in the Zoological Museum Amsterdam under registration number ZMA POR18290

2.1.2.4- *Hyrtios erectus*

The sponge *Hyrtios erectus.* Keller (Phylum Porifera, class Demospongia, order Dictyoceratida, family Thorectidae) is cake shaped, with protruding lobes forming large erect rounded digits, occasionally branched, with a rounded apex. The consistency is very spongy and difficult to tear. It is very distinctive black, was collected from a depth of 15-20 m from El Quseir, 120 km south of Hurghada, Egypt, in the Red Sea, on January 22, 2005. The color in life is deep greenish black, the interior slightly lighter black to brown. The texture is incompressible, and the sponge easily snapped in half as the sponge fibers are packed solidly with sand grains. The surface is regularly conulose and quite spiky to the touch. black, hard, rag-like. A voucher specimen has been deposited in the Zoological Museum Amsterdam under registration number ZMA POR18348.

2.2 Chemicals used

2.2.1. General laboratory chemicals

Agar-Agar	Merck
Anisaldehyde (4-methoxybenzaldehyde)	Merck
(-)-2- butanol	Merck
Dimethylsulfoxide	Merck
Formaldehyde	Merck
Hexamethyldisilazane	Merck
Chlorotrimethylsilane	Merck
Hydrochloric acid	Merck
Potassium hydroxide	Merck

Pyridine	Merck
Concentrated sulphuric acid	Merck
Trifloroacetic acid (TFA)	Merck
Concentrated amonia solution	Merck
D-Glucose	Sigma
L-Glucose	Sigma
D-Galactose	Sigma
L-Galactose	Sigma
Acetic anhydride .	Merck
Ortho-phosphoric acid 85% (p.a.)	Merck
N-(5-fluoro-2,4-dinitrophenyl)-L-alaninamide.	Merck
Aminoacids standards.	Merck
Sodium bicarbonate	Merck

2.2.2. Solvents

Acetone

Acetonitrile

Dichloromethane

Ethanol

Ethyl acetate

Hexane

Methanol

Butanol

The solvents were purchased from the institute of chemistry, university of Düsseldorf. They were distilled before using and special grade were used for spectroscopic measurements.

2.3. Equipments used

Balances	: Mettler 200
	: Mettler AT 250
	: Mettler PE 1600
	: Sartorious RC210P
Centrifuge	: Kendro D-37520 osterde
Fraction collector	: ISCO Cygnet

Freeze dryer	: LYOVAC GT2; Pump TRIVAC D10E
Hot plate	: Camag
Syringe	: Hamilton 1701 RSN
Mill	: Molinex 354
Magnetic stirrer	: Variomag Multipoint HP
Mixer	: Braun
PH-Electrode	: Inolab
	: Behrotest PH 10-Set
Rotary evaporator	: Büchi Rotavap RE 111; Buchi Rotavap R -200
Drying Ovens	: Heraeus T 5050
Sonicator	: Bandelin Sonorex RK 102
UV Lamp	: Camag (254 and 366)
Vacuum Exicator	: Solvent speed vac SPD 111V

2.3.1. Hyphenated HPLC equipments

I. Dionex Analytical HPLC (LC/UV) :

HPLC program	: Chromeleon Ver 6.3
Pump	: Dionex P580A LPG
Detector	: Dionex, Photoiode Array Detector UVD 340S
Autosampler	: ASI-100T
Column Thermostat:	: STH 585

Mobile Solvents:

Methanol LiChrosolv HPLC	Merck
ortho-phosphoric acid 0.15 %, pH 2.0 (prepared from	
ortho-phosphoric acid 85% p.a.)	Merck
Nanopure water	Barnstead

II. Semi-preparative HPLC (LC/UV) :

Pump:	: Gynkotek, M40
HPLC program:	: Gynkosoft (V. 5.4)
Detector:	: Gynkotek, Photoiode Array Detector UVD 340
Autosampler:	: Gynkotek Autosampler GINA 50
Printer:	: NEC P60

Mobile Solvents:

Methanol LiChrosolv HPLC Merck
Nanopure water Barnstead

III. Analytical HPLC (LC /UV/ MS hyphenated system) :

MS spectrometer : Finnigan LC Q-DECA
HPLC system (Pump,
Detector and autosampler) : Agilent 1100 series

Column Knauer (125mm L, 2 mm ID), prepacked with Eurosphere- 100 C-18 (5 µm) and with integrated pre-column.

Mobile Solvents:

Acetonitrile or Methanol LiChrosolv HPLC Merck
ortho-phosphoric acid 0.15 %, pH 2.0 (prepared from
ortho-phosphoric acid 85% p.a.) Merck
Nanopure water Barnstead

LC /ESI-MS was carried out using a Finnigan QDECA-7000 mass spectrometry connected to a UV detector. The sample is dissolved in methanol and injected to HPLC/ESI-MS hyphenated system. HPLC was run on a Eurospher C-18 reversed phase column. The mass spectra were generated on a dual octopole ion trap mass spectrometer operated in positive and negative ion modes and fitted with an atmospheric pressure electrospray-ionization sample introduction device. Fragmentation experiments were performed by automatic MS technique.

2.4. Chromatographic methods

2.4.1. Thin layer chromatography (TLC)

Pre-coated TLC Alu Plates (Silica gel 60 F254, Layer thickness 0.2 mm) Merck
Pre-coated TLC glass Plates (RP-18, F254 S, Layer thickness 0.25 mm) Merck
Preparative TLC glass plate (Silica gel G 60, Merck
spread on a clean glass sheets and activated in oven at 120 °C 5 Hours)

The compounds were monitored by the UV absorbance at 254 and 366 nm or by spraying with Anisaldehyde reagent , Methanol-sulphouric acid, Dragendorf´s spray reagents.

Anisaldehyde /H_2SO_4 spray reagent (DAB10)

Anisaldehyde :5 parts

Glacial Acetic Acid : 100 Parts
Methanol : 85 parts
Conc. H_2SO4 : 5 parts (added slowly)

The solution was stored in amber-coloured bottles and kept refrigerated until use. TLC was used for the fractions and for the pure compounds to identify the fractions and determine the purity of the isolated compounds. After spraying, the TLC plates were heated at 110 °C in order to monitor the UV-undetected sample components.

2.4.2. Vacuum liquid chromatography

Vacuum liquid chromatography (VLC) is a useful method as rapid and initial fractionation procedure for a crude extracts or large amounts of fractions. The apparatus consists of a sintered glass büchner filter funnels with different lengthes and internal diameters suitable for different sample quantities. Fractions are collected in Erlenmeyer flasks. Silica gel 60 was packed to a hard cake at a height of 5-10 cm under applied vacuum. The sample used was mixed with a small amount of silica gel using a volatile solvent. The resulting sample mixture was then packed onto the top of the column. Step gradient elution with non-polar solvent (hexane) then increasing the amount of the polar solvent (EtOAc, MeOH) is added to each successive fraction. The flow is produced by vacuum and the column is allowed to run dry after each fraction was collected.

2.4.3. Column chromatography

Fractions obtained from VLC were subjected to series of chromatographic columns using different stationary phases and solvent systems according to the chemical nature and quantity of the fraction components.

The following separation systems were used :

a) Normal phase chromatography uses a polar stationary phase, typically silica gel in conjunction with a non-polar mobile phase (n-Hexane, EtOAc, CH_2Cl_2,..etc). thus hydrophobic compounds elute more quickly than do hydrophilic compounds.
b) Reversed phase (RP) chromatography uses a non polar stationary phase and a polar mobile pase (water, methanol). The stationary phase consists of silica packed with n-alkyl chains covalently bound. For instance, C-18 signifies an octadecyl ligand in the silica matrix. The more hydrophobic the ligand on the matrix, the greater the tendency of the stationary phase to elute the hydrophilic components of the sample and retain the hydrophobic ones.

c) Size exclusion chromatography involves separations based on molecular size of the sample components. The stationary phase consists of porous beads. The larger compounds will be excluded from the interior of the bead and thus will elute first. The smaller compounds will be allowed to enter the beads and elute according to their ability to exit from the small sized pores they were internalised through.

2.4.4. Semi-preparative HPLC

Semi-preparative HPLC (Merck-HPLC apparatus, using MERCK HITACHI pump L-7100 and MERCK HITACHI UV Detector L-7400, Hitachi,Ltd. Tokyo Japan,) was used for the purification of relatively pure compounds obtained from fractions eluted by column chromatography or in some cases used to separate very closely related compounds (see figure 2.11). Each injection was in concentration of 3 mg of the dried fraction dissolved in 1 ml of solvent system. The injection volume up to 1 ml was injected into the column and the flow rate was 5 ml/min. The eluted peaks were detected by online UV detector involved in the apparatus.

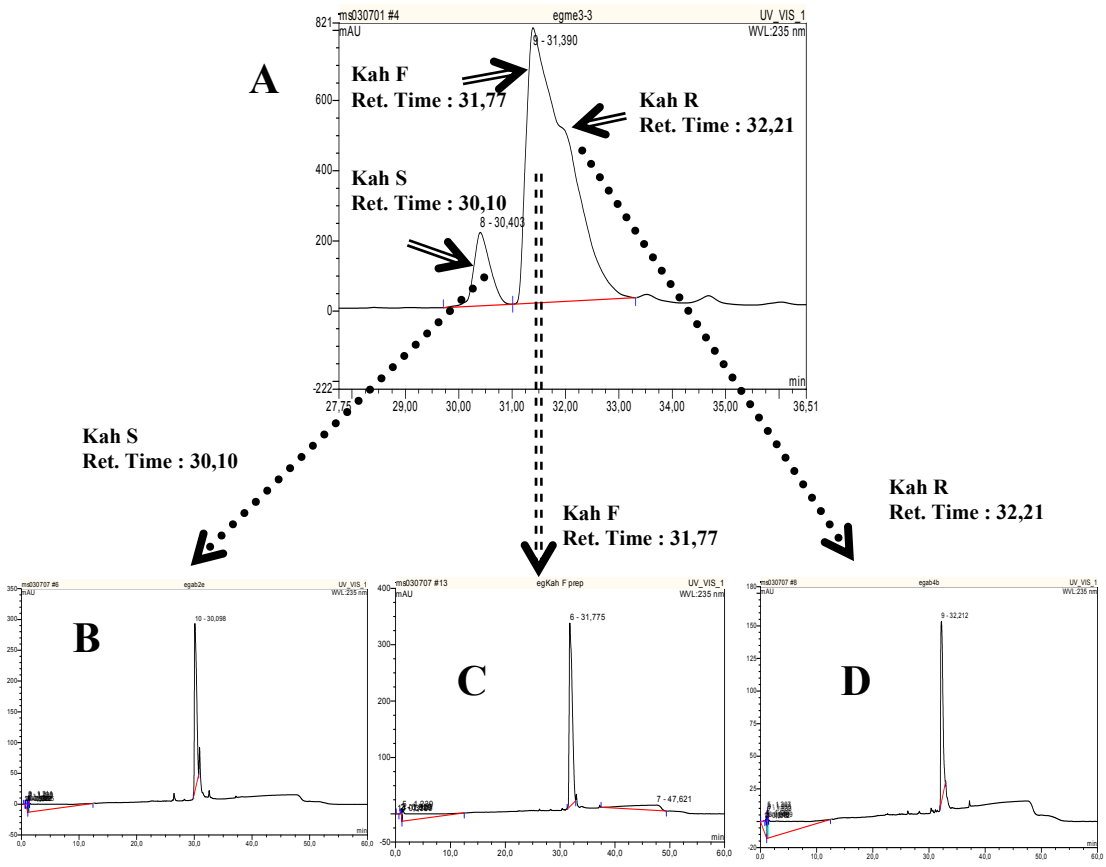

Figure (2.11) HPLC chromatogram A, shows sub-fraction of *E. grandifolia*–methanol extract containing three closely related peptides , their retention times are very close to each others. Chromatograms B, C, and D shows the pure compounds Kahalalide S, F, and R respectively after successful separation using preparative HPLC.

For separation of the above mentioned peptides (kahalalide S, F, and R), the separation was carried out by using Methanol : H_2O gradient elution; [solvent A: nanopure H_2O 100%, solvent B: MeOH 100%, the gradient commenced with 50% solvent B to 100% in 20 min then the mobile phase was stabilised at 100% MeOH for 10 min, then MeOH-percentage was decreased until 50 % for an additional 5 min], at a flow rate of 5 ml/min through a C-18 reversed phase column to yield three well-separated peaks of Kahalalide S (8 mg), F (103mg), and R (20 mg) at retention times 17, 19, and 20 min. respectively. The semi-preparative RP-columns were (300 x 8mm) pre-filled with Eurospher-100 , C-18 reversed phase silica gel beds.

2.4.5. Analytical HPLC

Analytical HPLC was used to identify the UV-absorbable compounds in the isolated fractions or to evaluate the pure componds. The plotting of the peaks was guided by UV-VIS photodiode array detector operating in four different wave lengthes 235, 254, 280 and 340 nm. The solvent gradients used started with 10:90 [MeOH 100 % : nanopure H_2O (adjusted to pH 2 with *o*-phosphoric acid)] , the commencing methanol ratio was equilibrated for 5 min at 10 % , then gradiently increased up to 100% after 35 min., then washing with 100 % MeOH for additional 10 min. In some cases, special programs were applied using the same solvent systems but in different ratios according to the chemical nature and the relative retention times of the compounds being analysed. The flow rate of the mobile phase was at 1 ml / min. The analytical HPLC column was a reversed phase column, thus eluting the polar compounds firstly, then the relatively nonpolar compounds.

Role of *ortho*-phosphoric acid in the analytical HPLC process:

o-phosphoric acid gives a good compound-separation, allowing the UV-detector to impart sharp peaks, but it has some disadvantages that, in some cases of poly-nitrogenous compounds (e.g. Purine derivatives, nucleotides and other similar small biologically active metabolites), the presence of acid makes the nitrogenous compounds highly protonated (in other word, highly polar according to the affinity of that compounds to accept protons), which in turn elute the compounds very rapidly and in some cases can not be detected with the UV-detector). This problem prompted some analytical chemists (e.g. Nordström 2004) to derivatise such basic compounds to be more hydrophobic and consequently improve their retentions on reversed phase materials and enhance their ESI response. The following example will explain the effect of *ortho*-phosphoric acid in masking of the peaks for the nitroginous compounds during HPLC analysis.

Detection and isolation of new purine derivatives in sub-fractions of EtOAc-Fraction of *Petrosia nigricans:*

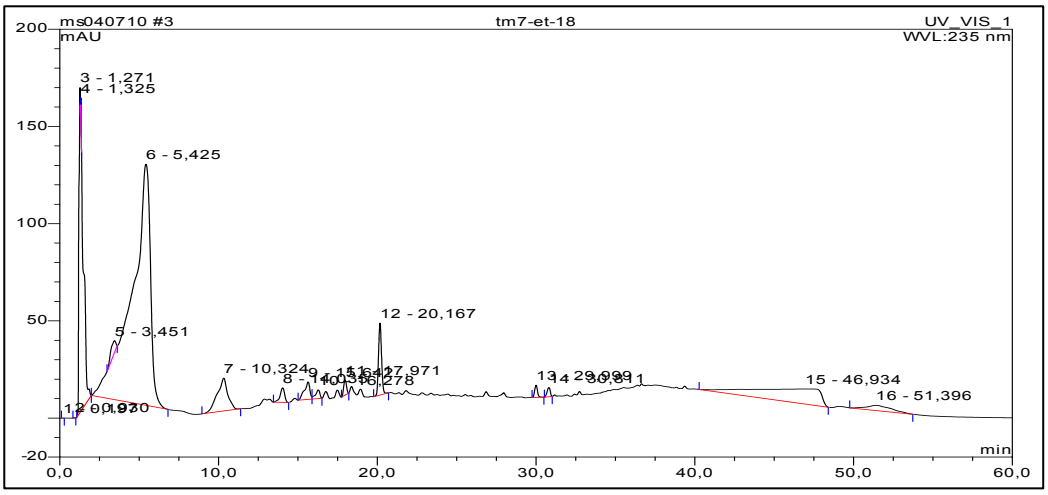

Fig (2.12) HPLC chromatogram of EtOAc subfraction (Et-18) of Petrosia nigricans, pH 2 nanopure water was maintained by phosphoric acid.

From the experiment (figure2.13), it is noted that, in case of acidified water, low concentrated sample showed nothing and the test purine peak was completely undetected, while in more concentrated sample the corresponding peak was broad with low resolution, and short retention time. On the other hand, the chromatograms that plotted during the measurment in which the neutral nanopure water was applied, showed a purine peak with high resolution, good peak-sharpness, longer retention times, and more descriptive. It is noted also the resulting UV-spectra were varied according to pH value of the mobile phase, and the compounds of the same chromophoric functions give the same UV spectra.

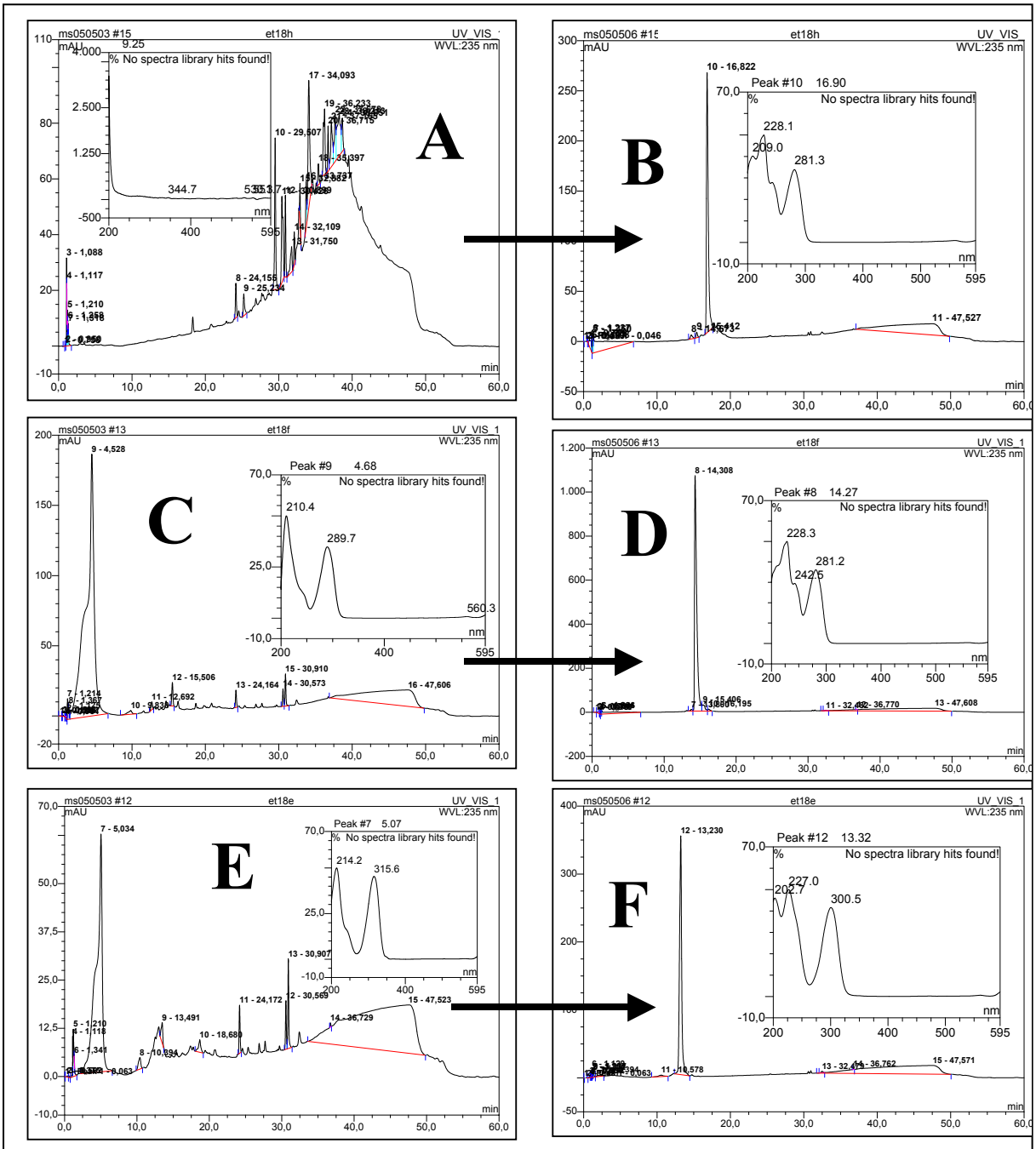

Figure (2.13) shows three HPLC chromatograms A, C & E of three pure new purine derivatives isolated from *Petrosia nigricans* subfraction Et-18, measured in HPLC using standard mobile phase that composed of methanol 100 % and acidified water pH 2 using phosphoric acid. The peak resolution in HPLC chromatograms was improved when the same samples were chromatographed again using the same mobile phase and the same gradient program under the same condition, but the difference was only the use of neutral water instead of pH 2 water, where chromatograms B, D & F, respectively were obtained.

2.4.6. Flash chromatography

Flash chromatography was used for rapid isolation of compounds. A silica gel 60 GF_{254} pre-packed column was used and the sample was dissolved in a small volume of the initial solvent used. The resulting mixture was then packed onto the top of the column using special syringe. The flow rate was maintained by an air pump and 5 ml fractions were collected and monitored by TLC.

2.4.6. Gas Chromatography :

Gas chromatography (GC) was used to determine the nature of the absolute stereochemistry of sugar units (D or L forms). The sugar fraction of the test sample was injected in the GC after hydrolysis and derivatisation using a special program. The samples were analysed by comparison of the retention times with those observed for the authentic samples.

2.5. Procedures of the isolations of the secondary metabolites:

2.5.1. Isolation of secondary metabolites from *Elysia rufescens*

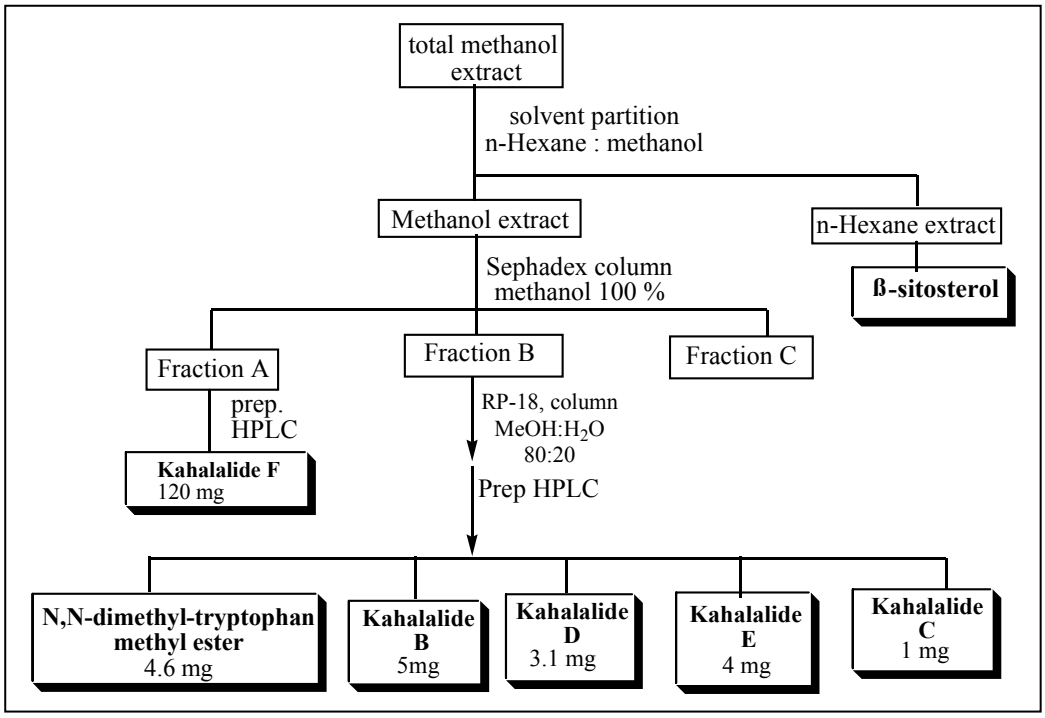

2.5.2. Isolation of secondary metabolites from *Elysia grandifolia*

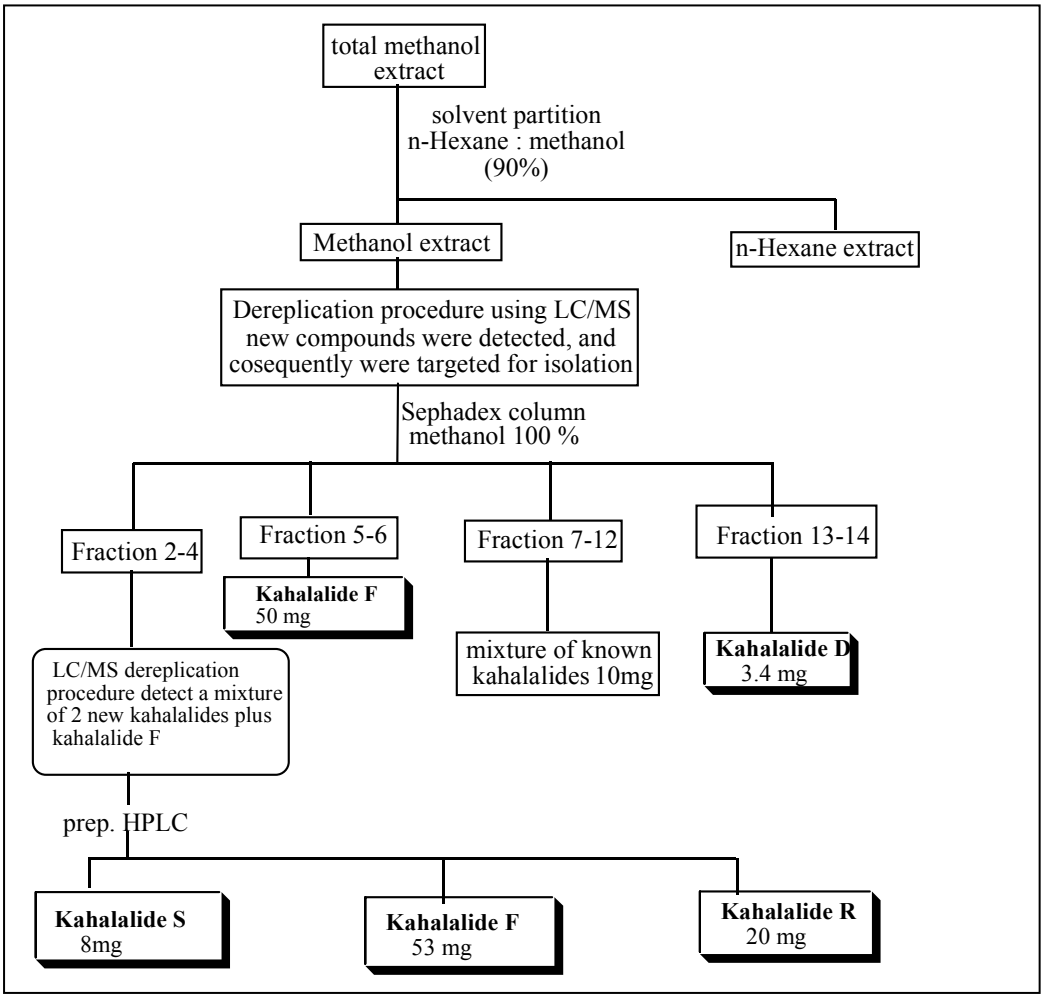

2.5.3. Isolation of secondary metabolites from *Pachychalina sp.*

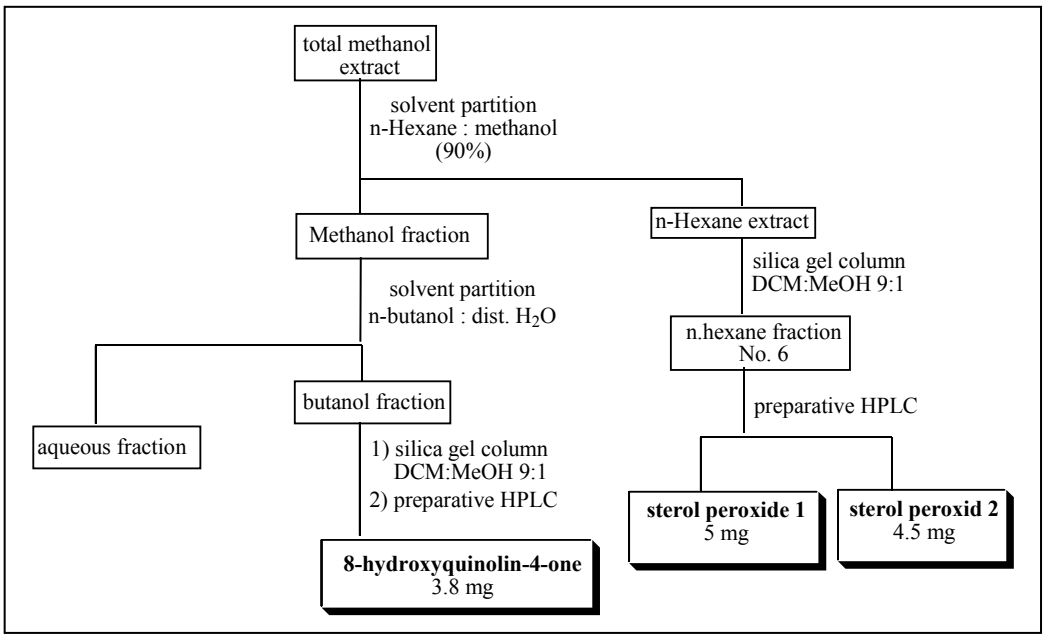

2.5.4. Isolation of secondary metabolites from *Callyspongia biru*

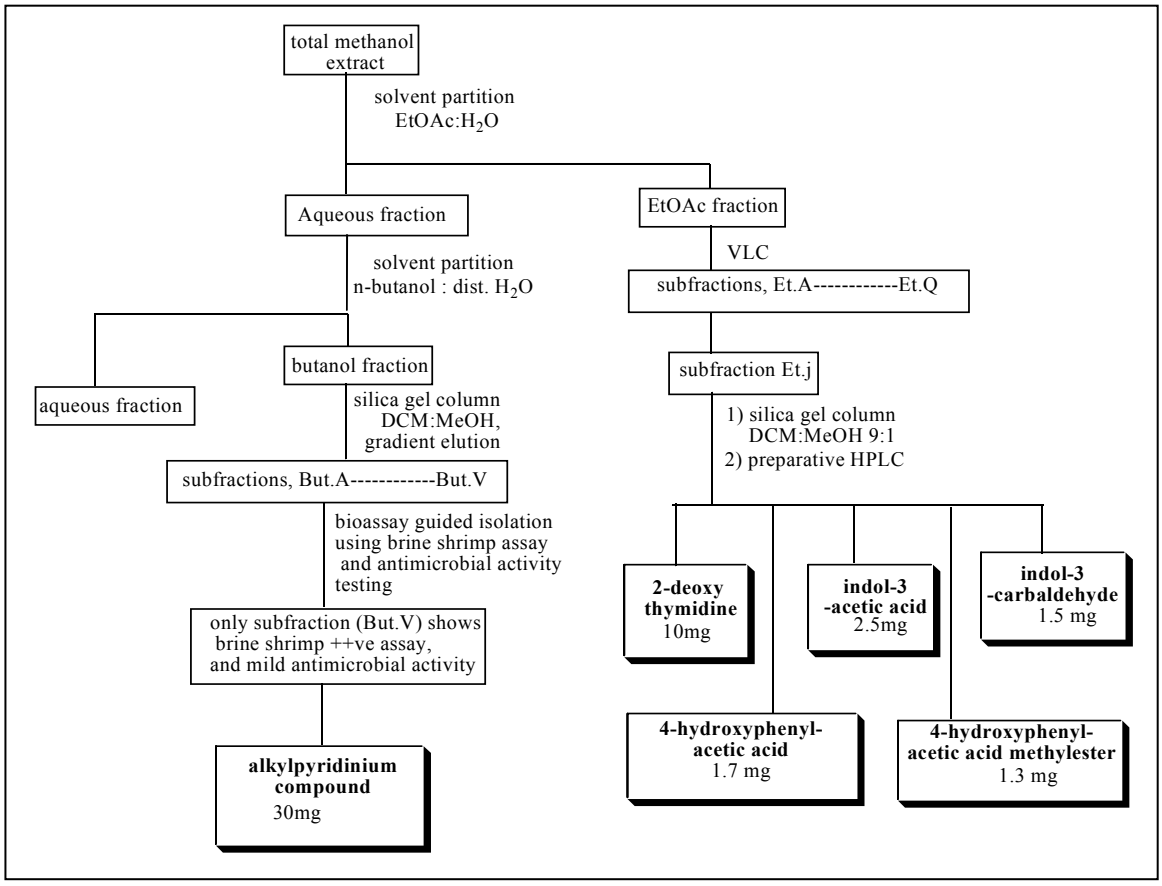

2.5.5. Isolation of secondary metabolites from *Hyrtios erectus*

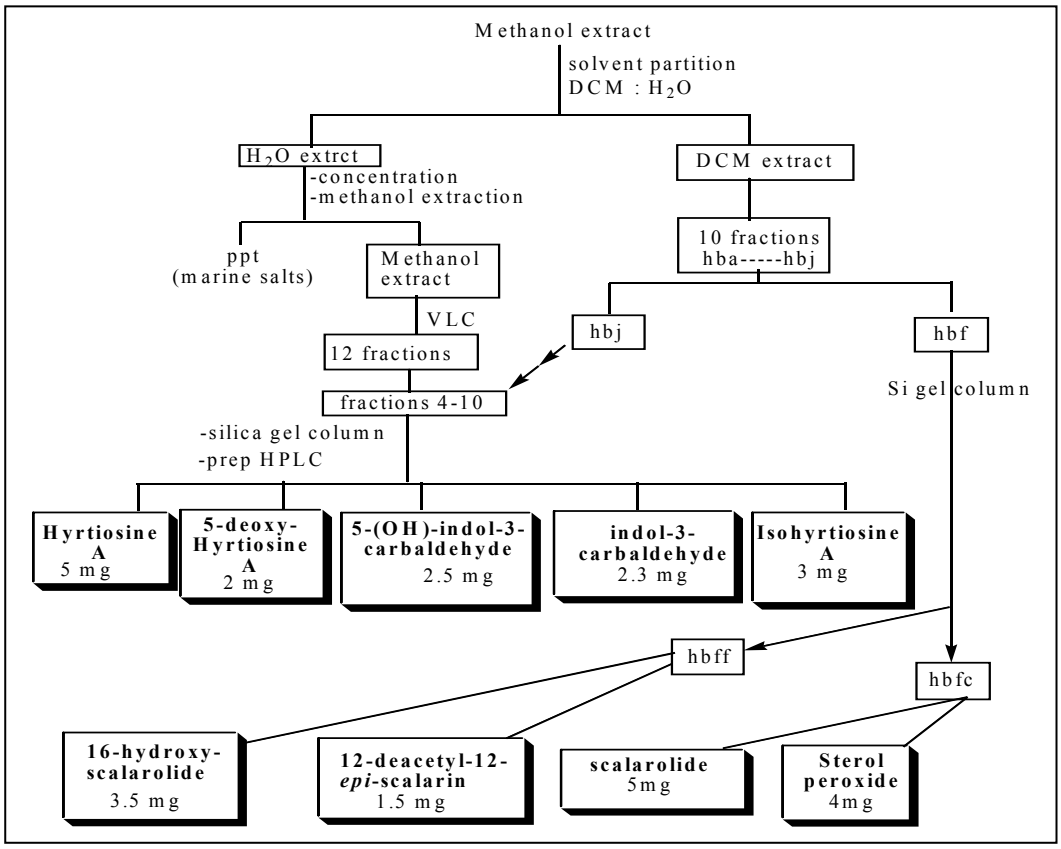

2.5.6. Isolation of secondary metabolites from *Petrosia nigricans*

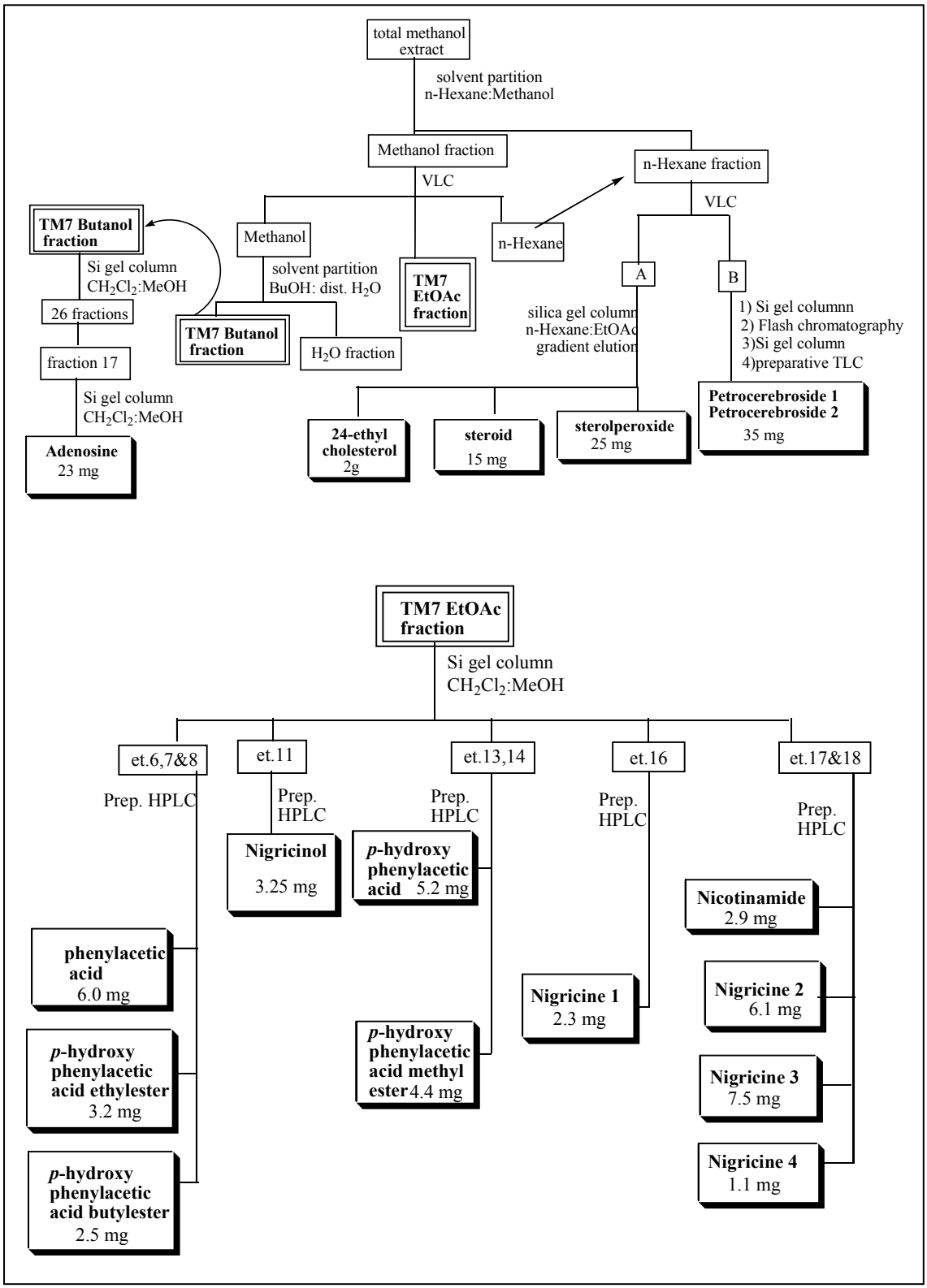

2.6. Structure elucidation of the isolated compounds

2.6.1. Mass spectrometry (MS)

2.6.1.1. Low resolution MS:

Low resolution mass spectra were measured by ESI, EI, MALDI, and FAB-MS on a Finnigan MAT 8430 mass spectrometer. Measurements were done in Institute für Pharmazeutische Biologie and Institute für Anorganische und Strukturchemie, Heinrich-Heine University, Düsseldorf.

2.6.1.2. HRMS (High resolution mass spectra):

High resolution mass spectra were determined on a micromass Q-Tof 2 mass spectrometer.

2.6.1.3. LC/ESI-MS (liquid chromatography/Electrospray ionization mass spectrometry):

LC/ESI-MS was carried out using a Finnigan LC QDECA mass spectrometer connected to a UV detector. The samples were dissolved in methanol and injected into HPLC/ESI-MS set-up. HPLC was run on a Nucleosil C-18 reversed-phase column. Measurements were done at Institute für Pharmazeutische Biologie, Heinrich-Heine University, Düsseldorf. Standard mobile phase system was applied, which was composed of 10:90 Acetonitrile:nanopure H_2O (0.1% HCOOH) – 100 % acetonitrile in 35 minutes in gradient elution system.

Electrospray ionization Mass spectrometer (ESI-MS) :

Electrospray ionization (ESI) is a gentle method of the atmospheric pressure ionization (API) technique and is well-suited to the analysis of polar molecules ranging from less than 100 Da to more than 100,000 Da in molecular weight. ESI –MS has been shown to be a successful and popular tool for the analysis of noncovalently bound protein macromolecules, (Ashcroft, A. E., 2005).

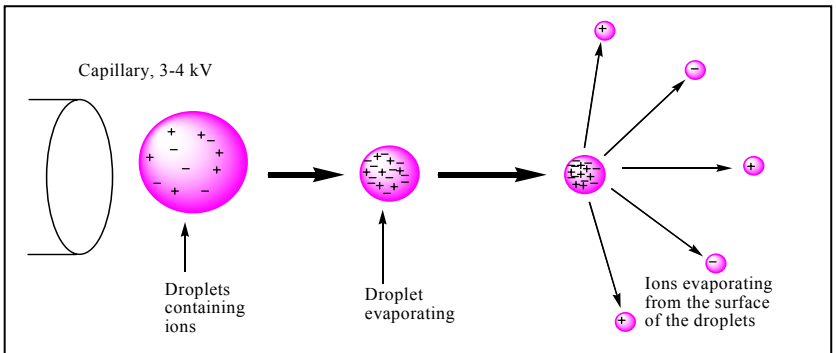

Fig (2.14) The electrospray ionization (ESI) process

The mechanism of electrospray ionization spectrometer

The sample is dissolved in a polar, volatile solvent and pumped through a narrow, stainless steel capillary (75-150 μm i.d.) at a flow rate of between 1μl/min and 1 mL/min. A high voltage of 3-4 Kv is applied to the tip of the capillary, which is situated within the ionization source of the mass spectrometer, and as a consequence of this strong electric field, the sample emerging from the tip is dispersed into an aerosol of highly charged droplets, a process that is aided by a co-axially introduced nebulising gas flowing around the outside of the capillary. This gas, usually nitrogen, helps to direct the spray emerging from the capillary tip towards the mass spectrometer. The charged droplets diminsh in size by solvent evaporation (see figure 2.14), assisted by a warm flow of nitrogen known as the drying gas which passes across the front of the ionization source. Eventually charged sample ions, free from solvent, are released from the droplets, some of which pass through a sampling cone or orifice into an intermediate vacuum region, and from there through a small aperture into the analyser of the mass spectrometer, which is held under high vacuum. The lens voltages are optimized individually for each sample (Ashcroft, A. E., 2005).

The ESI-MS was modified by John Fenn, 1987. Fenn´s modifications include the replacement of the simple orifice into the vacuum system by glass capillary tube (see fig. 2.15). That glass tube was metallized at each end to provide an electrical contact. The inlet end of the capillary would be maintained at the required potential below ground so the ions entering the tube would be in a potential well. The fairly high-velocity flow of bath gas through the glass (dielectric) tube into the vacuum system could drag the ions out of that potential well up to whatever potential might be desired at the metallized exit end of that tube. Indeed, the gas flow could raise the ions to an exit potential of several tens of kV, sufficient to inject the ions into the analyzer. At the same time all exposed external parts and surfaces of the instrument could be maintained at ground potential, thereby posing no hazard to an operator. Thus, Fenn`s modification brought the proteins and biomacromolecules to fly, or as John Fenn himself said, to give "wings to molecular elephants" (Fenn 2003).

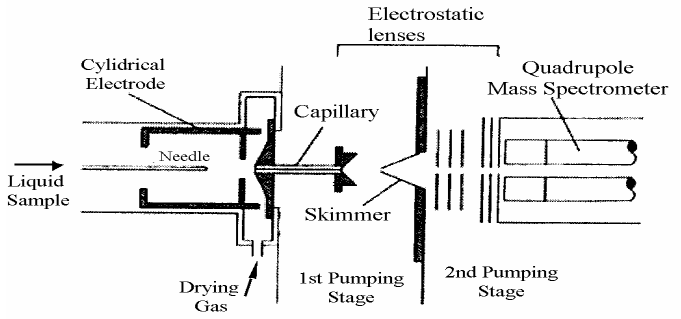

Fig. (2.15) Fenn´s modification of ESI-MS

2.6.1.4. MALDI-TOF-PSD-MS

Post source decay mass spectrum was obtained using Matrix-assisted laser desorption/ionization technique coupled to Time-of-Flight mass analyser. This PSD-MS is the method of choice for sequence determination of the amino acids of isolated depsipeptides (or peptides). MALDI-TOF-PSD spectra were obtained on a Perspective Biosystems Voyager-DE PRO MALDI-TOF mass spectrometer and Bruker Esquire 2000 LC-MS system equipped with an electrospray source. Sample application for MALDI-TOF-PSD MS was carried out directly on sample plates with a mixture of 1µL of matrix (saturated 2,5- dihydroxybenzoic acid in 50 % acetonitrile, 0.3%TFA) and 1µL of a 50% MeOH solution containing about 0.2µg of the sample.

The analysis was measured through **AnagnosTec** (Gesellschaft für Analytische Biochemie und Diagnostik mbH im Biotechnologiepark, TGZ II , D-14943 Luckenwalde, Berlin). Post source decomposition mass spectrum was recorded as peaks corresponding to molecular weight $[M^+]$, $[M^+]$ - 1 mole amino acid, $[M^+]$ - 2 moles, $[M^+]$ - 3 moles, and so on., where the decomposition was predominantly at the amide (peptide) bonds (i.e. retro-biosynthetic decomposition). The data collection was assisted automatically by specific computer program, plotted and interpretted using a computer program. This method has an advantage, that the cyclic peptide can be measured directly without linearisation or decyclisation and it also needs no terminal NH_2 group.

Matrix-assisted laser desorption ionization (MALDI)

The use of Laser desorption/ionisation-mass spectrometry (LDI-MS) was limited to compounds that could be vaporised without being decomposed, since the laser light is absorbed directly into the analyte, the molecular bonds may be broken owing to the increased internal energy. In other words, there is an increased risk that measurement would occur in the decomposed state. This method was usually inadequate for compounds exceeding 1000 Dalton (Da) and ionization of compounds having a molecular weight exceeding 10000 Da was considered by chemists at that time to be impossible (Tanaka, 2003).

In 1987, Koichi Tanaka, proposed the application of suitable matrix (glycerin) together with a good laser light absorpable material, UFMP, (Ultrafine metal powder). The mixing of this combination with the sample allowed to provide an efficiently enough heating and release of solid sample from its crystalline state to dissolve in the liquid, thereby assisting ionization (see figure 2.16). Thus, he was able to measure an ion cluster having a mass number exceeding 100, 000 Da (Tanaka, 2003).

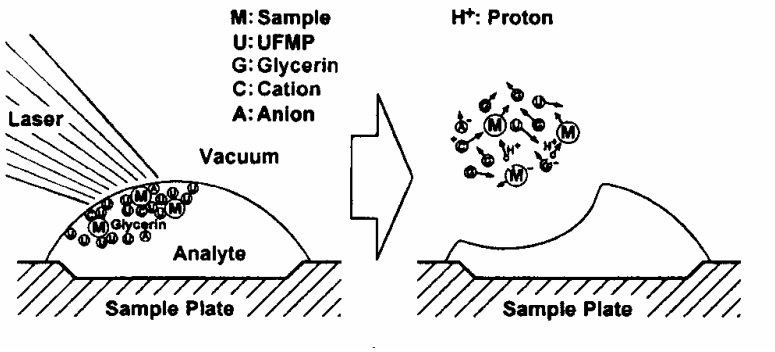

Fig (2.16) Desorption/ionization of macromolecules by using the UFMP-glycerin mixed matrix.

The mechanism of MALDI spectrometer:

The mechanism of MALDI is believed to consist of three basic steps (Gates, P., 2005a):

(i) Formation of a *solid solution*: it is essential for the matrix to be in access thus leading to the analyte molecules being completely separated from each other. This eases the formation of the homogenous *solid solution* required to produce a stable desorption of the analyte.

(ii) *Matrix extraction*: the laser beam is focused onto the surface of the matrix-analyte solid solution. The chromophore of the matrix couples with the laser frequency causing rapid vibrational excitation, bringing about localised disintegration of the solid soltuion. The clusters ejected from the surface consists of analyte molecules surrounded by matrix and salt ions. The matrix molecules evaporate away from the clusters to leave the free analyte in the gas-phase.

(iii) *Analyte Ionization* : The photo-excited matrix molecules are stabilised through proton transfer to the analyte. Cation attatchment to the analyte is also encouraged during this process. It is in this way that the characteristic $[M+X]^+$ (X= H, Na, K etc.) analyte ions are formed. This ionization reactions take place in the desorbed matrix-analyte could just above the surface. The ions are then extracted into the mass spectrometer for analysis (see figure 2.17).

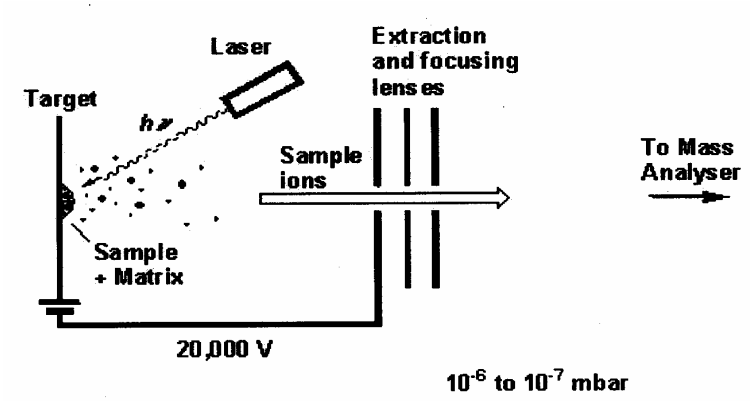

Fig. (2.17) Schematic diagram of matrix-assisted laser desorption ionization mechanism

Matrix-assisted laser desorption/ionisation - time-of-flight mass spectrometer (MALDI-TOF MS):

It is a relatively new mass spectrometer in which matrix assisted laser desorption/ionization procedure was applied together with the efficient mass detector, Time-of-Flight (TOF) detector which is available in two modes, linear and refractory modes (Fig 2.18).

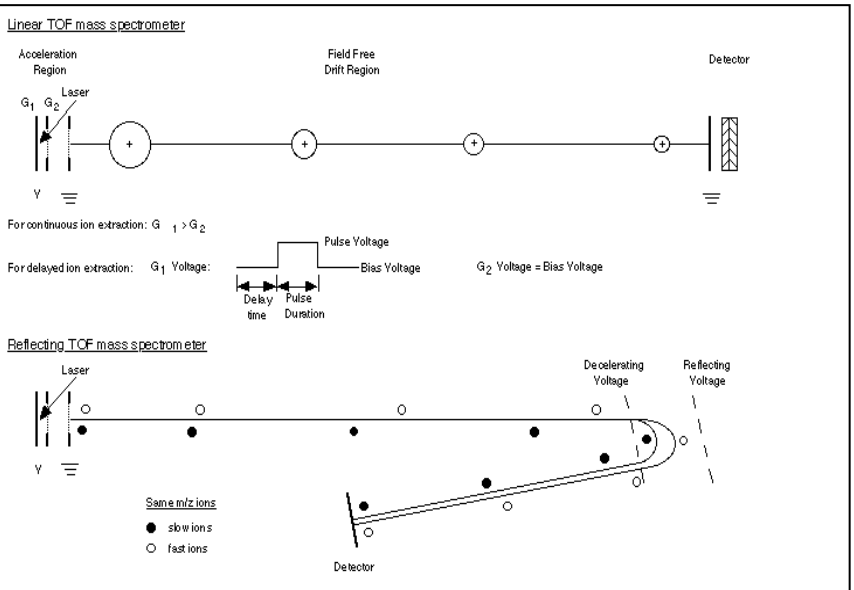

Fig. (2.18) basic components of a linear (upper) and reflecting (lower) TOF mass spectrometer.

Matrix-assisted laser desorption/ionisation-time-of-flight in source decompostion mass spectrometer (MALDI-TOF-ISD MS):

A recent extension of the MALDI in source design dramatically increased the ion resolution and mass accuracy. The technique was dubbed "time lag focusing" (TLF), "delayed extraction" (DE) or "pulsed ion extraction" (PIE). After desorption/ionization, the ions are kept in the ion source under field-free conditions for a short period of time, like 100-400 ns, before they are extracted with a high electrical field and accelerated towards the detector. During the brief time between ion desorption and the extraction pulse, analyte ions can undergo prompt fragmentaion within the ion source (in source decompostion, ISD). Many reports of this phenomenon were published in which linear TOF instruments were incorporated to provide a protein sequencing. Because the fragmentation occurs in the source, product ions experience some of the effects of pulsed ion extraction, but due to the higher laser power required to induce fragmentation it is very difficult to obtain high resolution and mass accuracy for product ions in linear mode. Suckau and Cornett 1998, presented results from ISD measurements made using an instrument with ion reflector, which provided isotopic resolution for product ions up to several thousand Da. (Suckau and Cornett 1998).

Matrix-assisted laser desorption/ionisation-time-of-flight post source decay mass spectrometer (MALDI-TOF-PSD MS):

PSD analysis is an extention of MALDI/MS that allows one to observe and identify structurally informative fragment ions from decay taking place in the field free region after leaving the ion source (Spengler, 1997). Mass spectrometric analysis of product ions from post source decay of precursor ions that were formed by matrix-assisted laser desorption ionization (MALDI-PSD) has evolved into a powerful method for primary structure analysis of biopolymers. Especially in the field of peptide sequencing, MALDI-PSD has been widely applied, mainly because of its high sesitivity for prepared sample amounts in the range 30-100 fmol and because of its high tolerance of sample impurities and sample inhomogenity (Spengler, 1997).

It was first concluded that ions formed by MALDI must be extremely stable and internally cool and that MALDI is therefore a very soft ionization technique (i.e. provide highly stable molecular ion or provide no fragment ions), the main reason for this assumption was that these large biopolymers could be desorbed and ionized intact (which was impossible with

other ionization techniques) and these molecular ions had obviously survived hundreds of microseconds during their flight through the instrument until detection (Spengler, 1997).

More recently, fragment ions, which are produced after leaving the ion source during the flight in the field-free region were used for peptide sequencing, (see figure 2.19). These ions are called "Post-source decay" or PSD ions and can be observed in instruments equipped with an ion reflector. In contrast to classical Edman sequencing, PSD-sequence determinations are possible even from complex mixtures like proteolytic digests if a gated electrostatic ion selector is used (Suckau and Cornett 1998).

Mechanism of MALDI-PSD:

With reflector TOF-MS, it is in theory possible to obtain structural information on a selected quasimolecular ion by mass analysis of daughter ions issued from in-flight fragmentation of the parent ion. Intact molecular ions leaving the ion source and having acquired sufficient internal energy during the desorption process (photoactivation, low energy collisions,) can release this energy by undergoing fragmentation while traveling the first field-free drift path of the instrument called post-source-decay or (PSD). The fragment ions have the same velocity as their precursor ions but have different energy as a function of their mass. Fragment ions are then discriminated as a function of their kinetic energy (thus their mass) by the time dispersions induced by the electrostatic reflector. Large fragment ions (with higher keinetic energy) will penetrate deeper into the reflectorn than smaller fragment ions and will appear at later time on the resulting reflectron time-of-flight spectrum (Chaurand et al ,1999). An important feature of MALDI-PSD instrument is their MS/MS capability, allowing one to preselect a certain precursor ion in a mixture of multiple components. Precursor selection is done by electrostatic "beam blanking" or "ion gating".

All ions passing the beam blanking device are deflected off the ion detector except a certain mass window which is transmitted without deflection. Deflection is performed by a fast high voltage drop applied to the device which typically built of small plates, wires or strips. Positioning of the ion gate within the flight path is always a compromise between position-dependent dispersion of precursor ions of different masses and high transmission for (low energy) PSD ions already formed at the position of the ion gate (Spengler, 1997).

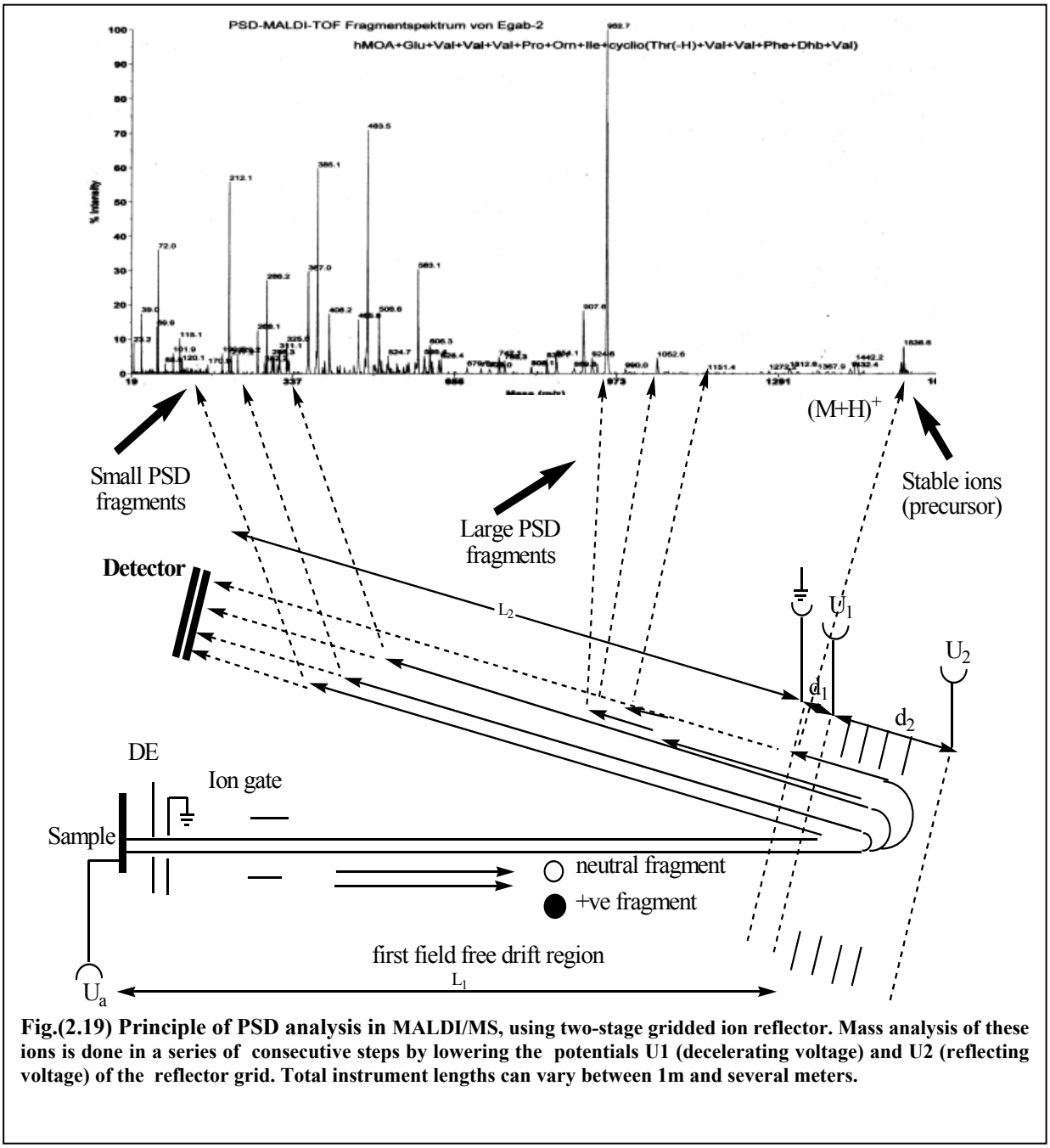

Fig.(2.19) Principle of PSD analysis in MALDI/MS, using two-stage gridded ion reflector. Mass analysis of these ions is done in a series of consecutive steps by lowering the potentials U1 (decelerating voltage) and U2 (reflecting voltage) of the reflector grid. Total instrument lengths can vary between 1m and several meters.

2.6.1.5. GC/MS (hyphenated Gas chromatography /Mass spectrometry):

GC/MS is a combination of two microanalytical techniques: a separation technique, GC, and an identification technique, MS. GC/MS combination overcomes certain deficiencies or limitations caused by using each technique individually and gives a two-diminsional identification consisting of both GC retention time and a mass spectrum for each component of the mixture. This combination has several advantages. First, it can separate the components of a complex mixture so that mass spectra of individual compounds can be obtained for qualitative

purposes, second , it can provide a quantitative information on these same compounds. GC/MS can provide complete mass spectrum for as little as 1 pmol of an analyte. It gives direct evidence for the molecular weight and the characteristic fragmentation pattern or chemical fingerprint that can be used as the bases for identification. GC/MS is limited to the analysis of those compounds that can be made volatile without thermal decomposition.

GC/MS consists essentially of three components: the gas chromatograph, the mass spectrometer and the data system. The sample was dissolved in a volatile solvent (methanol, n-hexane or EtOAc) and injected manually (10µl) in the GC/MS set-up working in the EI-MS mode. The sample which eluted from the GC-column, was divided -in the same time- into two parts, one of them passed through GC-detector (electron capture detector, ECD), and another part passed through the EI-MS detector involved in the system. GC chromatograms were obtained as quantitative peak intensities plotted versus retention times. EI-MS of each peak was recorded depending on the retention times of each compond.

2.6.2. Nuclear magnetic resonance spectroscopy (NMR)

NMR measurements were done at the Institut für Anorganische Chemie und Makromolekulare Chemie of Heinrich-Heine University, Düsseldorf. ID and 2D, ^{1}H and ^{13}C-NMR spectra were recorded at 300º K on Bruker DPX 300, ARX 400, 500 or GBF 600 NMR spectrometers. All 1D and 2D spectra were obtained using the standard Bruker software. The samples were dissolved in deuterated solvents (DMSO-d_6, $CDCl_3$, CD_3OD, Pyridine-d_5), the choice of the solvent depends mostly on the solubility of the compound. Residual solvent signals of (CD_3OD at 3.3 ppm ,^{1}H, and 49.0 ppm,^{13}C), ($CDCl_3$ at 7.26 ppm and 77.0 ppm), (DMSO-d_6 at 2.49 ppm and 39.5 ppm) were considered as internal reference signal for calibration. The observed chemical shift values (δ) were given in ppm. and the coupling constant (*J*) in Hz.

2.6.3. The optical activity

Optically active compounds are compounds which have at least one chiral carbon. Optically active compounds can rotate the plane polarized light. Optical rotation was determined on a Perkin-Elmer-241 MC Polarimeter. The substance was stored in a 0.5 ml cuvette with 0.1 dm length. the angle of rotation was measured at a wavelength of 546 and 579 nm of a mercury vapour lamp at room temperature (25°C). The specific optical rotation was calculated using the equation:

$$[\alpha]_D^{20} = \frac{[\alpha]_{579} \text{ x } 3.199}{4.199 - \frac{[\alpha]_{579}}{[\alpha]_{546}}}$$

Where $[\alpha]^{20}_D$ = the specific rotation at the wavelength of the sodium D-line, 589 nm, at a temperature of 20ºC.

$[\alpha]_{579}$ and $[\alpha]_{546}$ = the optical rotation at the wavelength 579 and 546 nm respectively, calculated using the formula:

$$[\alpha]_\lambda = \frac{100 \text{ x } \alpha}{I \text{ x } C}$$

Where:

α = the measured angle of the rotation in degrees

I = the length in dm of the polarimeter tube,

C = the concentration of the substance expressed in g/100 ml of the solution.

2.6.4 Special procedures:

2.6.4.1 LC/MS dereplication procedure for targeting new kahalalides of *Elysia grandifolia*

Total methanol extract of *E. grandifolia* was subjected to ESI-MS analysis using LC/MS set-up available in the Institut für Pharmazeutische Biologie, Heinrich-Heine University, Düsseldorf. ESI-MS spectrum (Fig 2.20 & 2.21) detects many positive molecular ion peaks, 879.8, 914.9, 596.7, 1478.8, 1494.3, and 1240.0, of known kahalalides, kahalalide B, kahalalide C, kahalalide D, kahalalide F, kahalalide G and kahalalide J, respectively, that have been found and were previously reported from *E. rufescens* extract.

Indeed , it shows two minor new kahalalides (based on mol. wt.) close to the major one (kahalalide F). The corresponding molecular ion peaks of both peptides appeard in both sides left and right to the corresponding peak of the major peptide. The mol.wt. of the first one, kahalalide S (M+1= 1536.6), was 58 mass units more than kahalalide F and slightly more polar, and the other, kahalalide R (M+1= 1520.5), was 16 mass unit (which equal to one oxygen atom) less than the first new one, and slightly less polar than kahalalide F (Fig. 2.11)

Both new kahalalides were targeted for isolation based on the obtained data including the molecular weight and the HPLC retention times, where the total methanol extract was chromatographed by gel filtration, to separate as pure as possible the targeted peptides. Complete isolation and purification was carried out by semi-preparative HPLC.

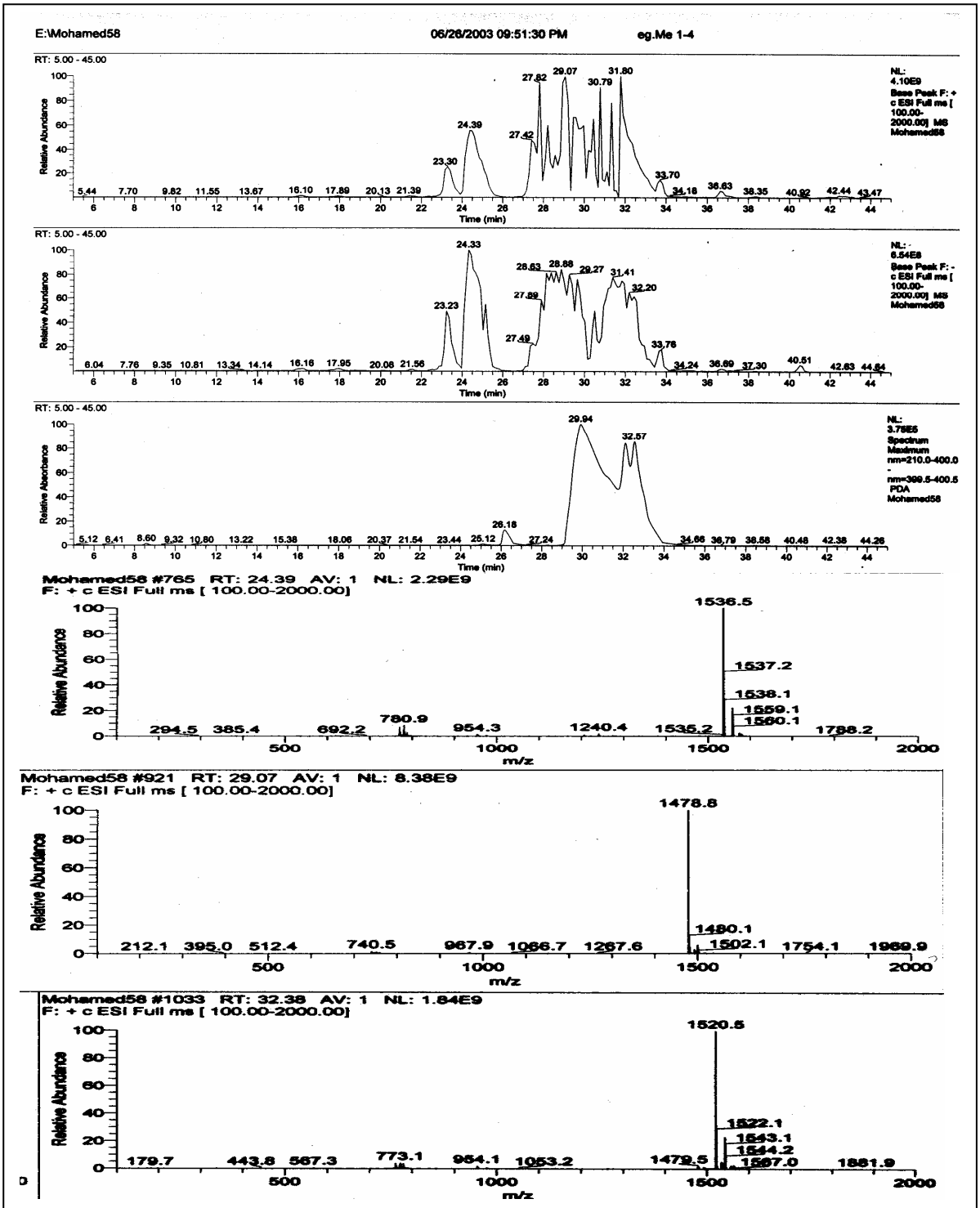

Figure (2.20) ESI-MS survey for the methanol extract of *Elysia grandifolia* detect 2 new depsipeptides, kah.S [m/z 1536.5 $(M+H)]^+$ and kah. R [m/z 1520.5 $(M+H)]^+$ in addition to the known kah. F [m/z 1478.8 $(M+H)]^+$.

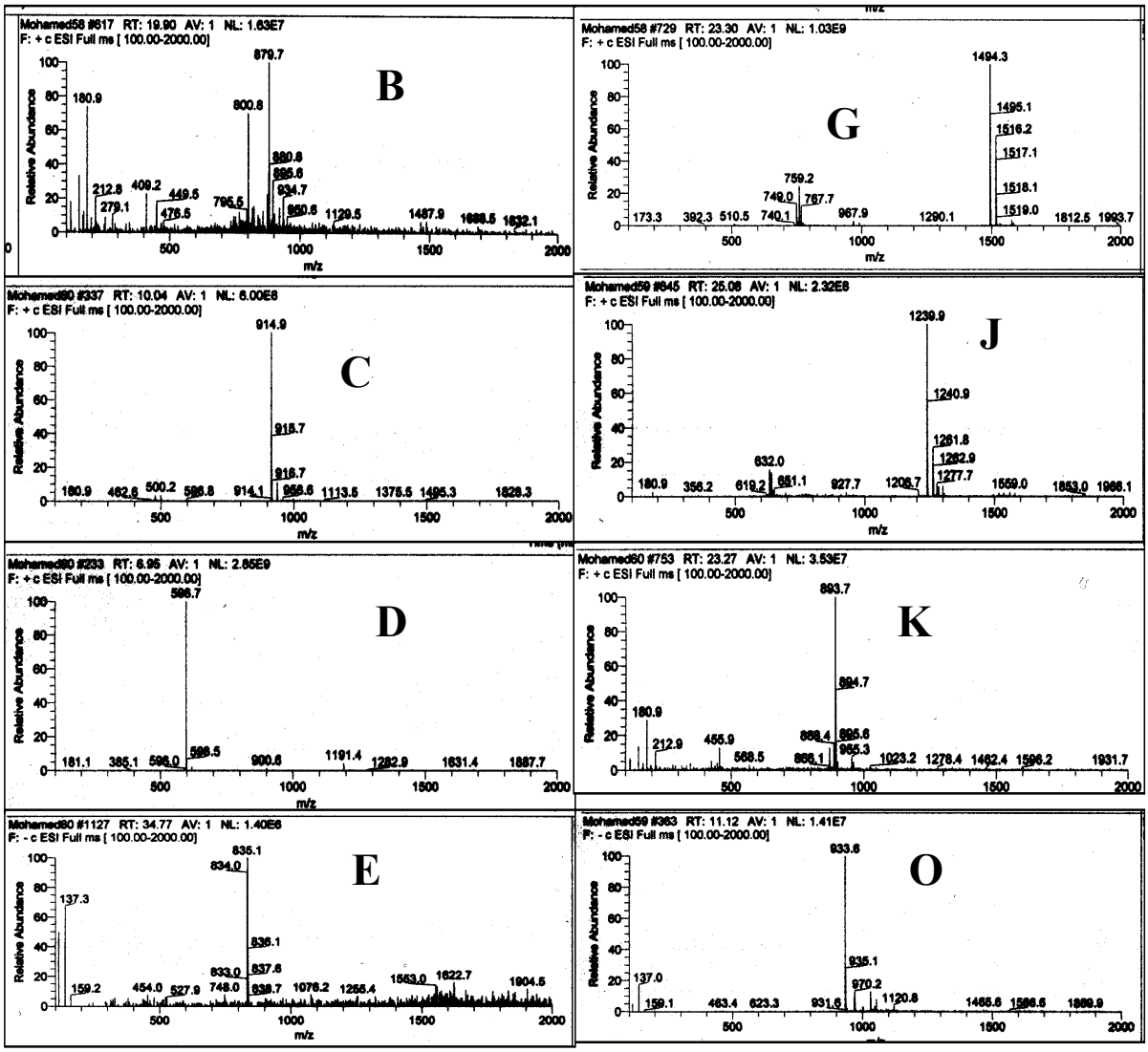

Fig (2.21): ESI-MS survey for the methanol extract of *Elysia grandifolia* detect many of known depsipeptides. (Kahalalides B, C, D, E, G, J, K, O).

2.6.4.2. Determination of amino acid diastereoisomers of isolated kahalalides :

Marfey reagent N-(5-flouro-2,4-dinitrophenyl)-L-alanine amide (FDAA) was used to prepare diastereoisomers of amino acid derivatives. This diastereoisomers can be very useful in quantitative determination of D- and L- amino acids in protein hydrolysates by HPLC analysis. The L- amino acid derivatives were eluted more rapidly than the D-isomers due to the strong intramolecular hydrogen bonding (more hydrophobic) in the latter diastereoisomers (Marfey,

1984). Marfey´s procedure was applied for the isolated kahalalides after complete acid hydrolysis.

Each peptide (0.1 mg) was hydrolysed by heating in a sealed vial with 6N HCl (2 ml) until complete hydrolysis and liberation of free amino acids. The hydrolysate was cooled, dried and dissolved in 0.5 ml of 1 % acetone solution of N-(5-fluoro-2,4-dinitrophenyl)L-alaninamide [FDAA], followed by 20 µmol of $NaHCO_3$, the contents were mixed and heated over a hot plate at 40 °C for 1 hour with frequent mixing, and after cooling, a 20 µmol HCl was added, and the mixture was filled to a volume of 1 ml by addition of MeOH. Amino acid standards were individually derivatised in the same manner using 2.5 µmol amino acid standard to react with 3.6 µmol FDAA to obtain the amino acid-DAA derivative.

The obtained derivatives were centrifuged and the supernatants were injected in the HPLC/MS spectrometer, the elution time was 1 hour for each peptide-hydrolysate-DAA derivative. Standard amino acid-DAA derivatives were used in order to determine the molecular weight (MW) and the retention time (RT) of each amino acid unit. After comparison of the MW and RT of the hydrolysate derivatives with that of derivatised standards, diastereoisomers were detected in each peptide hydrolysate. The test was repeated again using the same procedure by co-chromatography (peak enrichment technique) to confirm this determination. The derivatised standards were added separately to the derivatised hydrolysate of each kahalalide and run again under the same condition in HPLC-MS spectrometer, to show what diastereoisomer-standard peak will be enriched or completely overlap the unknown peak of the hydrolysate derivatives. Complete overlapping means complete stereosimilarity between standard amino acid and the corresponding amino acid in the hydrolysate.

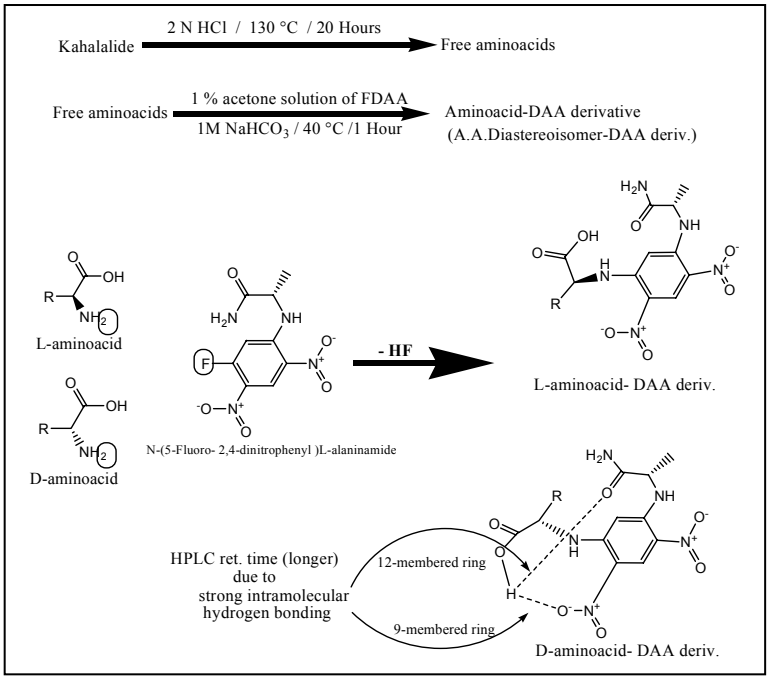

The following reaction products were detected in the new kahalalide hydrolysates (kahalalide R and kahalalide S) using LC/MS analysis:

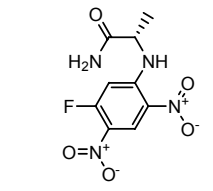

N-(2,4-dinitro-5-fluoro-phenyl)-L-alaninamide

$C_9H_9FN_4O_5$
Exact Mass: 272,06
Mol. Wt.: 272,19
(**FDAA**)

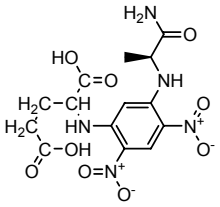

$C_{14}H_{17}N_5O_9$
Exact Mass: 399,10
Mol. Wt.: 399,31
DAA- glutamic acid

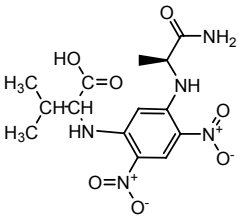

DAA- valine

$C_{14}H_{19}N_5O_7$
Exact Mass: 369,13
Mol. Wt.: 369,33

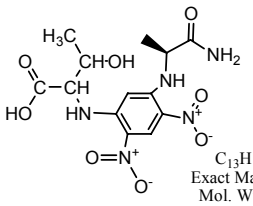

$C_{13}H_{17}N_5O_8$
Exact Mass: 371,11
Mol. Wt.: 371,30
DAA-threonine

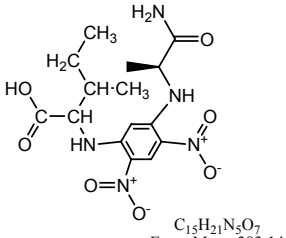

$C_{15}H_{21}N_5O_7$
Exact Mass: 383,14
Mol. Wt.: 383,36
DAA- Isoleucine

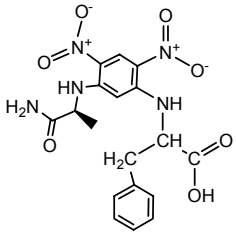

$C_{18}H_{19}N_5O_7$
Exact Mass: 417,13
Mol. Wt.: 417,37
DAA-phe.ala.

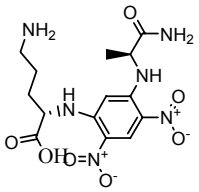

$C_{14}H_{20}N_6O_7$
Exact Mass: 384,14
Mol. Wt.: 384,34
DAA-ornithine

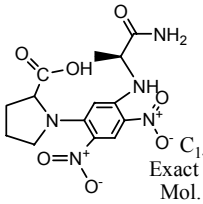

$C_{14}H_{17}N_5O_7$
Exact Mass: 367,11
Mol. Wt.: 367,31
DAA-proline

2.6.4.3. Acid hydrolysis and GC analysis :

Petrosia cerebrosides (2.0 mg) were hydrolysed by treatment with 3N HCl and stirred at 80 °C for about 5h. The solution was concentrated using N_2**.** The residue was re-dissolved in (-)-2-butanol (0.5 mL) and one drop of triflouroacetic acid. The solution was transferred to an ampoule, sealed and heated at 130 °C in an oven overnight until complete butanolysis. The solution was concentrated to dryness in a vacuum evaporator and then connected to the freeze dryer overnight until complete dryness. The residue was then treated with hexamethyldisilazane-chlorotrimethylsilane-pyridine (0.1 mL, 1:1:5) for 30 min at room temperature. The solution was then centrifuged and the supernatant (1µL) was analysed by GC on HP-5 column. The injection port and detector temperatures were 200 °C and 220 °C, respectively. The temperature gradient was programmed as linear increase from 135 °C to 200 °C at 1 °C/min. Four peaks of hydrolysate were detected at 37.21, 39.91, 41.98, 42.95 minutes, which was in agreement with the four peaks obtained for authentic D-galactose at 37.49, 40.15, 42.43, 43.32 minutes treated simultaneously in the same manner, [Leontein, et al.1977 and Gerrit, et al., 1977].

2.7. Bioassays

2.7.1. Antimicrobial activity

Microorganisms

The crude extracts and the pure compounds were tested for activity against the following standard strains: gram positive bacteria *Bacillus subtilis* **DSM2109**, Staphylococcus aureus **ATCC 25923** and gram negative bacteria *Escherichia coli* **DSM10290**; the yeast *Sacharomyces cerevisiae* **DSM1333** and two fungal strains *Cladosporium herbarum* **DSM62121** and *C. cucumerinum* **DSM62122**.

Culture preparation

The agar diffusion assay was performed according to the Bauer-Kirby-Test (DIN 58940, Bauer *et al*, 1966). Prior to testing, a few colonies (3 to 10) of the organism to be tested, were subcultured in 4 ml of tryptose-soy broth (Sigma, FRG) and incubated for 2 to 5 h to produce a bacterial suspension of moderate cloudiness. The suspension was diluted with sterile saline solution to a density visually equivalent to that of a $BaSO_4$ standards. The standards were prepared by adding 0.5 ml of 1 % $BaCL_2$ to 99.5 ml of 1% H_2SO_4 (0.36 N). The prepared bacterial broth is inoculated onto Müller-Hinton-Agar plates (Difco, USA) and dispersed by means of sterile beads.

Agar diffusion assay

For screening, aliquots of the test solution were applied to sterile filter-paper discs (5 mm diameter, Oxoid Ltd) using a final disc loading concentration of 500 µg for the crude extract and 50 and 100 µg for the pure compounds. The impregnated discs were placed on agar plates previously seeded with the selected test organisms, along with discs containing solvent blanks. The plates were incubated at 37°C for 24 hr. and anti-microbial activity was recorded as the clear zones of inhibition surrounding the discs. The diameter was measured in mm.

2.7.2 Bioactivity guided isolation using brine shrimp lethality test:

This technique is an *in vivo* lethality test involving the whole body of a tiny crustacean, the brine shrimp, *Artemia salina* Leach. It has been previously utilised in various bioassay systems including the analysis of pesticide residues, mycotoxins, stream pollutants, anaesthetics, dinoflagellate toxins, morphine-like compounds, toxic oil dispersants, carcinogenic phorbol esters and toxicants in marine environments (Mayer, *et al*., 1982).

This test takes into account the basic premise that pharmacology is simply toxicology at a lower dose, and that toxic substances might indeed elicit, at a lower nontoxic dose, interesting pharmacological effects. The procedure determines LC_{50} values in µg/mL of active compounds and extracts in the brine medium.

Sample preparation

Crude extract, butanol fraction, EtOAc fraction, and all butanol sub-fractions of *Callyspongia biru* were subjected to the brine shrimp lethality test. The test samples were dissolved in a suitable organic solvent and the appropriate amount was transferred to 10 mL sample vials. Bioassay was done on 1.0 & 0.5 mg test samples. The samples were then dried under nitrogen and redissolved in 20 µl DMSO. Negative control vials contain the same amount of DMSO were also prepared.

Hatching the eggs

Brine shrimp eggs (Dohse, Aquaristik GmbH, Bonn, Germany) were hatched in a small tank filled with artificial sea water which was prepared with a commercial salt mixture (33 g, Sera Sea-Salt, Aquaristik GmbH, Bonn, Germany) and distilled water (1000 mL). The eggs hatched and became ready for the bioassay after 48 hours. Twenty nauplii were taken out by pipette (counted macroscopically in the stem of the pipette against a lighted background) and transferred into each test sample vial. Artificial sea water was added to render the volume 5 mL and the vials were maintained under illumination. Survivors were counted, with the aid of a magnifying glass after 24 hours and the mortality at each dose and control were determined. The LC_{50} values were determined using the probit analysis method. The LD_{50} was derived from the best fit line obtained by linear regression analysis.

Results

The most active fraction was butanol subfraction (But V) the last fraction eluted from the silica gel column of the butanol fraction of the sponge. Where it shows 80 % and 100 % lethality effects at concentrations of 0.5 mg and 1.0 mg respectively. Therefore the isolation was continued for this fraction where alkylpyridinium compound was isolated from this fraction.

2.7.4. Cytotoxicity test

Cytotoxicity Assay

Antiproliferative activity was examined against several cell lines, which included MCF-7, PC12, HeLa, L1578Y and H4IIE, and was determined by an MTT assay as described earlier (Kreuter et al 1992, Mosmann 1983).

Cell cultures

L5178Y mouse lymphoma cells were grown in Eagle's minimal essential medium supplement with 10% horse serum in roller tube culture. H4IIE-cell line was grown in a DMEM-medium with 10% fetal bovine serum, while HELA, PC12, and MCF-7 cells were grown in RPMI 1640 medium supplemented with non-essential amino acids, sodium pyruvate, 10 µg/mL insulin and 10% fetal bovine serum. The cell culture media contained 100 units/mL penicillin and 100 µg/mL streptomycin and were changed twice per week. The cells were maintained in a humidified atmosphere at 37°C with 5% CO_2.

Determination of cytotoxicity *(MTT colorimetric assay)*

MCF-7 cells, PC12, HeLa, L1578Y, and H4IIE were plated on 96-multiwell plates with 50.000 cells/well. The cells were allowed to attach for 24 h and then treated with different concentrations of kahalalides for 24 h. After this treatment the medium was changed and the cells were incubated for 3 h under cell culture conditions with 20 µg/ml MTT (3-(4,5-dimethyl-2-thiazolyl)-2,5-diphenyl-2H-tetrazolium bromide). The conversion of the tetrazolium salt MTT to a colored formazan by mitochondrial dehydrogenases was determined as a marker of cell viability according to Mosman 1983 (Kreuter et al 1992, Mosmann 1983). After this incubation the cells were fixed on the plate with an aqueous solution containing 1% formaldehyde and 1% calcium chloride and then lysed with 95% isopropanol-5% formic acid. The concentration of reduced MTT as a marker for cell viability was measured photometrically at 560 nm.

III. Results

3-1 **Natural Products from *Elysia rufescens*:**

Sacoglossan molluscs of the genus *Elysia* have been intensively investigated for their biologically active natural products which include diterpenoids (Paul and Van Alstyne 1988), polypropionates (Gavagnin, *et al* 1994, Cueto *et al* 2005), and depsipeptides (Hamann and Scheuer 1993, Hamann *et al* 1996, Goetz *et al* 1997, Horgen *et al* 2000). *Elysia*-derived natural products show significant biological and pharmacological activities. The diterpenoids were reported to be active against anti-HIV opportunistic infections as well as against *Herpes simplex* type II (HSV II) (Paul and Van Alstyne 1988). The polypropionates exhibited ichthyotoxicity (Gavagnin, *et al* 1994, Cueto *et al* 2005), while the depsipeptides were shown to have fish deterrent activity and are used as a chemical defence by the sacoglossan (Becerro *et al* 2001). The peptide derivatives which carry the trivial name kahalalides, were further described to have anti-malarial, anti-cancer, anti-psoriatic, anti-tuberculosis, and anti-fungal activities (Hamann and Scheuer 1993, Hamann *et al* 1996, Goetz *et al* 1997, Horgen *et al* 2000, Bourel-Bonnet *et al*. 2005, El-Sayed *et al* 2000). The name kahalalide, was derived from the mollusc's collection site, at Black Point near the shores of Kahala District of the Oahu Island in Hawaii. Kahalalides have been isolated from the sacoglossans *E. rufescens* (Hamann and Scheuer 1993, Hamann *et al* 1996, Goetz *et al* 1997), *E. ornata* (Horgen *et al* 2000) (Plakobranchidae) as well as from their green algal diet, *Bryopsis* sp. (Bryopsidaceae) (Hamann and Scheuer 1993, Hamann *et al* 1996, Goetz *et al* 1997, Horgen *et al* 2000). The green algal diet, *Bryopsis* sp., has been found to yield kahalalides A, B, F, G, K, P and Q. (Hamann and Scheuer 1993, Hamann *et al* 1996, Goetz *et al* 1997, Horgen *et al* 2000, Kan *et al* 1999, Dmitrenok et al 2006). The kahalalide peptides consist of 3 to 13 amino acid units, ranging from a C_{31} tripeptide to a C_{75} tridecapeptide, with cyclic and linear components, the latter terminating in a saturated fatty acid moiety. Ten of these derivatives are cyclic depsipeptides, kahalalides A to F, K, O, P and Q, while three analogues, kahalalides G, H, and J are linear peptides. Kahalalide F and its linear analogue kahalalide G are the only congeners that feature the atypical amino acid, *Z*-dehydroaminobutyric acid (*Z*-Dhb).

Due to their biological importance, kahalalides A, B, and F have been chemically synthesized. (López-Maciá *et al* 2001a, López-Maciá *et al* 2001b, Bourel-Bonnet *et al*. 2005). To date, kahalalide F is the only derivative reported to have significant activity towards solid tumor cell lines, including human colon and lung cancers, and against some of

pathogenic microorganisms that cause opportunistic infections in HIV/AIDS patients (Hamann and Scheuer 1993). Kahalalide F displays both *in vitro* and *in vivo* anti-tumor activity in various solid tumor models, which include colon, breast, non-small cell lung, and in particular prostate carcinoma. *In vitro* anti-proliferative studies showed activity among certain prostate cancer cell lines (PC-3, DU-145, T-10, DHM, and RB), but no activity was found against the hormone-sensitive LnCAP (prostate cancer) cell line. *In vivo* models also confirmed selectivity and sensitivity of the prostate tumor xenograft derived from hormone-independent prostate cancer cell lines, PC-3 and DU-145. Furthermore, *in vitro* evaluation exhibited that this activity is selective but not restricted to prostate tumor cells (Rademaker-Lakhai *et al* 2005). It has also been revealed that kahalalide F induces cell death via oncosis preferentially in the tumor cell (Suarez *et al* 2003). Kahalalide F has attracted most attention and has been the subject of a patent application. Its mode of action and preclinical toxicity has also been studied (García-Rocha *et al* 1996, Sewell *et al* 2005, Janmaat *et al* 2005, Suarez *et al* 2003) and the compound is currently in phase II clinical trial as a potential anticancer agent (Brown *et al* 2002, Ciruelos *et al* 2002, Rademaker-Lakhai *et al* 2005).

Chemical investigantion of methanol extract of *Elysia rufescens* led to the isolation of five known kahalalides in addition to β-sitosterol and N,N-dimethyltryptophan methyl ester

3.1.1- Kahalalide F (1, Known compound)

Kahalalide F was isolated as a white amorphous powder, with $[\alpha]_D$ of – 5° (*c* 0.35 MeOH). It has UV absorbance at λ_{max} 203 nm. FAB-MS showed pseudomolecular ion peak *m/z* 1478 $[M+1]^+$ and 1500 $[M+Na]^+$, suggesting the molecular formula $C_{75}H_{124}N_{14}O_{16}$. The molecular weight of **1** was also confirmed by ESI-MS, and MALDI-TOF-MS. The ^{1}HNMR spectrum of kahalalide F revealed 14 deshielded amide N*H* resonances in the lower field region, ranging from 6.76 ppm to 9.69 ppm, suggesting the peptidic nature of the compound. One N*H* proton, a sharp singlet at δ 9.69, indicated an α,β-unsaturated amino acid, a broad 2H singlet at δ 7.69 was shown by a cosy experiment to be the terminal NH_2 of ornithine. Compound **1** was ninhydrin-positive, thus supporting the presence of the free amino group of ornithine. The remaining 11 N*H* protons were doublets; those that are part of the ring are sharp, while the N*H* protons of the linear portion of the molecule are splitted and broad due to several conformations of the molecule. COSY spectrum showed 14 different spin systems, that were also confirmed by TOCSY spectrum, 12 spin systems possessing deshielded amide

N*H* resonances at δ 6.76 Val-1 N*H*, δ 9.69 Dhb N*H*, δ 8.79 Phe N*H*, δ 7.62 Val-2 N*H*, δ 8.82 Ile-1 N*H*, δ 8.56 Thr-1 N*H*, δ 7.90 Ile-2 N*H*, δ 7.95 Orn N*H*, δ 8.10 Val-3 N*H*, δ 7.57 Val-4 N*H*, δ 7.82 Thr-2 N*H*, δ 7.88 Val-5 N*H* (Abbreviations used for amino acids and the designations of peptides follow the rules of the IUPAC-IUB Commission of Biochemical Nomenclature in: *J. Biol. Chem.* 1972, *247*, 977-983)**.** The other 2 spin systems show no correlations to amide N*H* protons, they were assigned to proline and to the aliphatic acid, 5-methylhexanoic acid. Each N*H* proton showed COSY correlation to the next α –proton, then to the β-proton, then to γ- and δ-proton resonances. The COSY spectrum revealed the presence of one proline spin system, [δ 4.36 (dd, *J*= 9.1, 6.6 Hz, H-α), 2.03,1.97 (m,m, 2*H*-β), 1.86 (m, 2*H*- γ) and δ 3.76, 3.52 (m,m, 2*H*- δ)]. The presence of 5-methylhexanoic acid (5-MeHex) was indicated by the 2D NMR data, sequential COSY correlations were observed between the α-methylene signals at δ 2.13 and the subsequent methylenes at δ 1.47 (m, 2*H*-3), 1.11 (m, 2*H*-4) followed by aliphatic methine proton at δ 1.47 (m, *H*-5) and two methyl groups at δ 0.82 (d, *J* = 7.1 Hz) and 0.82 (d, *J* = 7.0 Hz). As shown by the broad N*H* signals for the linear part of compound **1**, a second regio-isomer of the aliphatic acid was detected from the COSY spectrum as exhibited by the signals at δ 2.2 (m, 2*H*-2), δ 1.6 (m, 2*H*-3), δ 1.14 (m, 2*H*-4), δ 1.35 (m, *H*-5) and two methyl groups at δ 0.80 (d, *J* = 6.9 Hz, CH_3 -6) and 0.80 (d, *J* = 7.0 Hz, CH_3-7). TOCSY experiment showed an uncommon spin system which was assigned as dehydroaminobutyric acid (Dhb) at 9.69 (s, N*H*), 6.34 (q, *J* =7.0Hz, 1*H*), 1.26 (d, *J* =7.5Hz, CH_3). The ROESY correlation between N*H* and CH_3 protons indicated a *Z* stereochemistry of this uncommon amino acid. This uncommon amino acid was reported as a constituent of peptides isolated from the terrestrial blue-green alga (Moore *et al* 1989), and from an herbivorous marine mollusk (Pettit *et al* 1989). The ester linkage of the ring part of the compound was confirmed by HMBC correlation between the β-Proton (shifted downfield at δ 4.96) of threonine and the carbonyl at δ 164.4 of valine-1.

^{13}C NMR and DEPT spectra displayed signals for 75 carbons including 14 carbonyls at δ 169.5 , 164.4, 171.3, 172.9, 170.0, 169.7, 170.6, 173.0, 172.6, 171.3, 169.8, 169.0, 172.2, and 173.8 of val-1, Dhb, Phe, Val-2, Ile-1, Thr-1, Ile-2, Orn, Pro, Val-3, Val-4, Thr-2, Val-5, and 5-MeHex, respectively. In addition to 6 sp^2 methines and 2 sp^2 quaternary carbones, 18 methyl signals, 12 methylenes and 22 sp^3 methines including 12 α-methines and two oxygenated β methines one of them is more deshielded at δ 69.98 for Thr-1 indicating the ester linkage to Val-1, and another at 67.4 ppm for Thr-2 as mentioned in table 3.1.2.

HMBC and ROESY experiments established the connectivity of the amino acids. The 5-MeHex—Val-5—Thr-2—Val-4—Val-3 connectivity could be established by HMBC

correlations between N*H* signals of Val-5, Thr-2, Val-4 and Val-3 at δ 7.88, 7.82, 7.57 and 8.10 respectively, to the vicinal carbonyls of 5-MeHex, Val-5, Thr-2, and Val-4 at δ 173.8, 172.2, 169.0, and 169.8, respectively. Connections of the amino acids Thr-1—Ile-2—Orn—Pro were determined through HMBC correlations of the N*H* signals at 8.56, 7.90, 7.95 ppm to the vicinal carbonyls at 170.6, 173.0, 172.6 ppm, respectively. The connectivity of Pro to Val-3 was established through the HMBC correlation between δ-proton of Pro at δ 3.52 and the carbonyl of Val-3 at δ 171.3, and through the ROESY correlation between δ-protons of Pro at δ 3.76, 3.52 and the α-proton of Val-3 at δ 4.26. The cyclo [Val-1—Dhb—Phe—Val-2—Ile-1—Thr-1] linkage was deduced through HMBC correlations of NH signals at 6.76, 9.69, 8.79, 7.62, 8.82 ppm to the vicinal carbonyls 164.4, 171.3, 172.9, 170.0, 169.7 ppm respectively, while the connectivity of Val-1 to Thr-1 was confirmed by an HMBC correlation between the β-proton at δ 4.96 of Thr-1 and the carboxyl at δ 169.5 of Val-1, and also the ROESY correlation between the β-proton at δ 4.96 of Thr-1 and the α-proton of Val-1 at 3.86 ppm.

The deduced data of compound **1** as obtained by NMR were further confirmed by ESI-MS/MS experiment, MALDI-TOF-PSD MS (matrix –assisted laser desorption/ionisation – time-of-flight – post source decay mass spectrometry) and by Marfey´s analysis. The reflectron mode MALDI-TOF mass spectrum performed with delayed extraction (DE) showed a positive ion signal at *m/z* 1499.92 which was identified as sodium-ion associated monoisotopic peak $[M+Na]^+$ of compound **1**, and showed also a positive ion signal at *m/z* 1515.9, $[M+K]^+$ and at *m/z* 1478.5, $[M+1]^+$.

MALDI-TOF-PSD spectrum confirmed the sequence of the depsipeptide, kahalalide F, as shown in table (3.1.3). Similar results were obtained from tandem ESI-MS/MS spectrum, where the positive protonated fragment ion peaks were evident at *m/z* 1266.7, 1165.7, 1066.6, 967.8, 836.0, 756.8 , 642.7 and 443.5 corresponding to $[M+1]^+$-[5-MeHex-Val-5], $[M+1]^+$ -[5-MeHex- Val-5- Thr-2], $[M+1]^+$ -[5-MeHex- Val-5- Thr-2- Val-4], $[M+1]^+$-[5-MeHex- Val-5- Thr-2- Val-4- Val-3], [(5-MeHex- Val-5- Thr-2- Val-4- Val-3-Pro- Orn-Ile-2)+1]$^+$, [cyclo (Val-1- Dhb- Phe- Val-2- Ile-1- Thr-1) + Ile-2+1]$^+$, [cyclo (Val-1-Dhb- Phe- Val-2- Ile-1- Thr-1) +1]$^+$ and [(Dhb- Phe- Val-2- Ile) +1]$^+$, respectively.

The stereochemistry of the amino acids were determined using Marfey analysis (Marfey, 1984), and the experiment resulted in the presence of D-Pro, L-Orn , D-*a*Ile, L-*a*Thr, D-*a*Thr, D-Val, L-Val, and L-Phe. The NMR data, amino acid sequences, and stereochemistry of compound **1** were identical to those of kahalalide F (Hamann and Scheuer 1993).

3.1.1- Kahalalide F (1, Known compound)

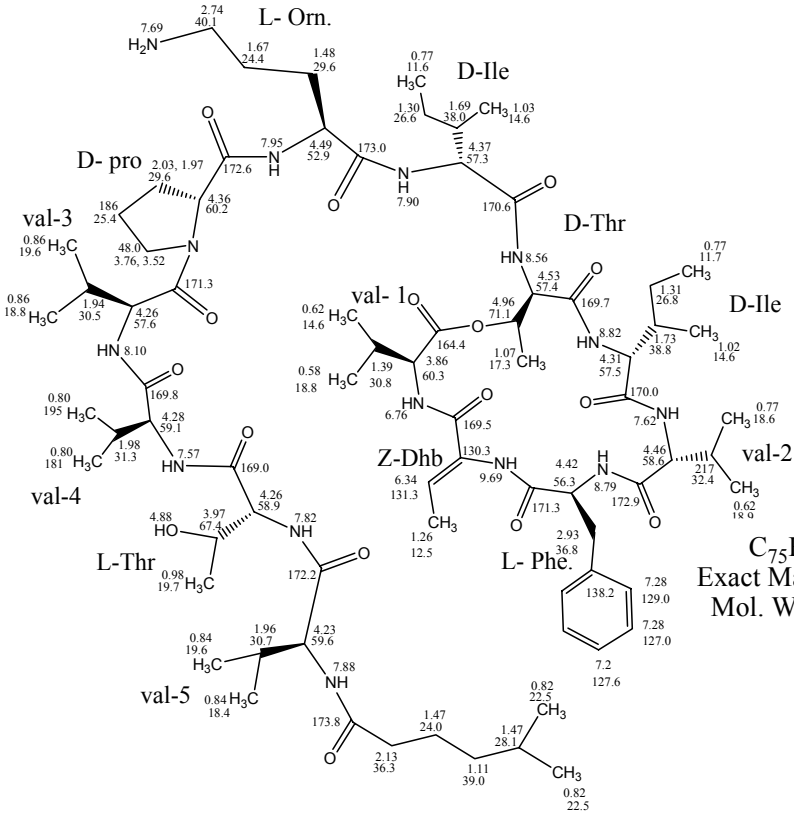

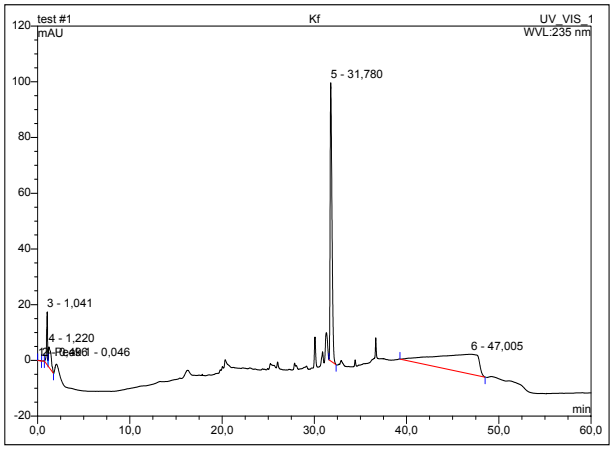

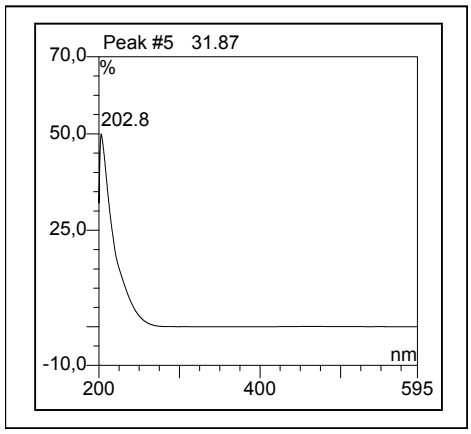

Fig. (3.1.1): chemical structure with NMR values (up), HPLC chromatogram (down left and UV spectrum (down right) of compound 1, kahalalide F

Yield : 120 mg

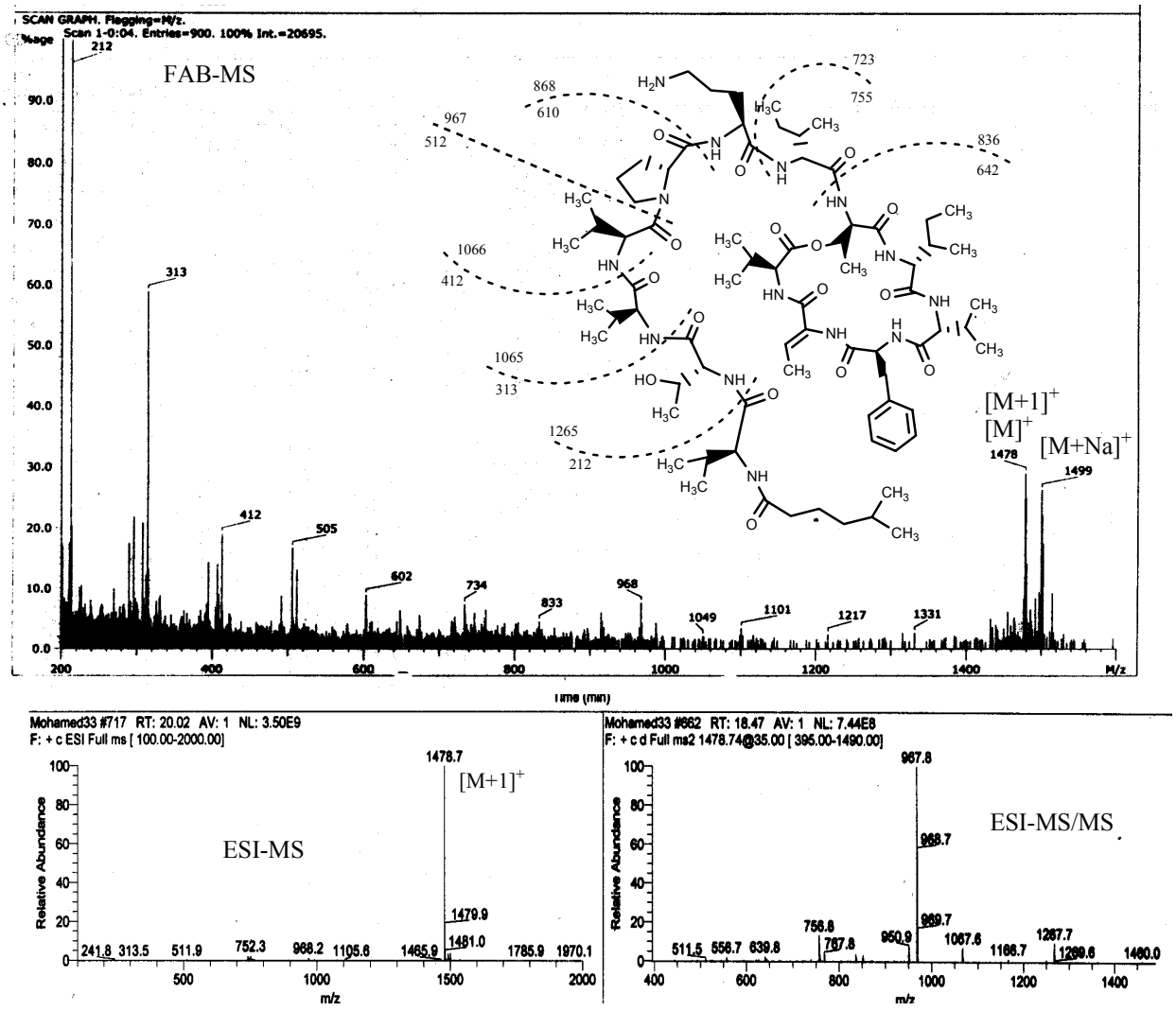

Fig.(3.1.2) : FAB-MS , ESI-MS and ESI-MS/MS of compound 1

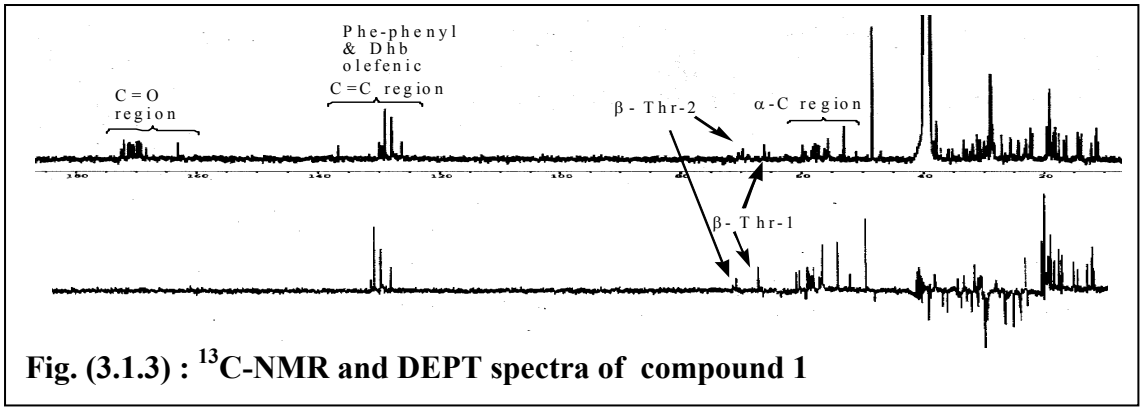

Fig. (3.1.3) : ^{13}C-NMR and DEPT spectra of compound 1

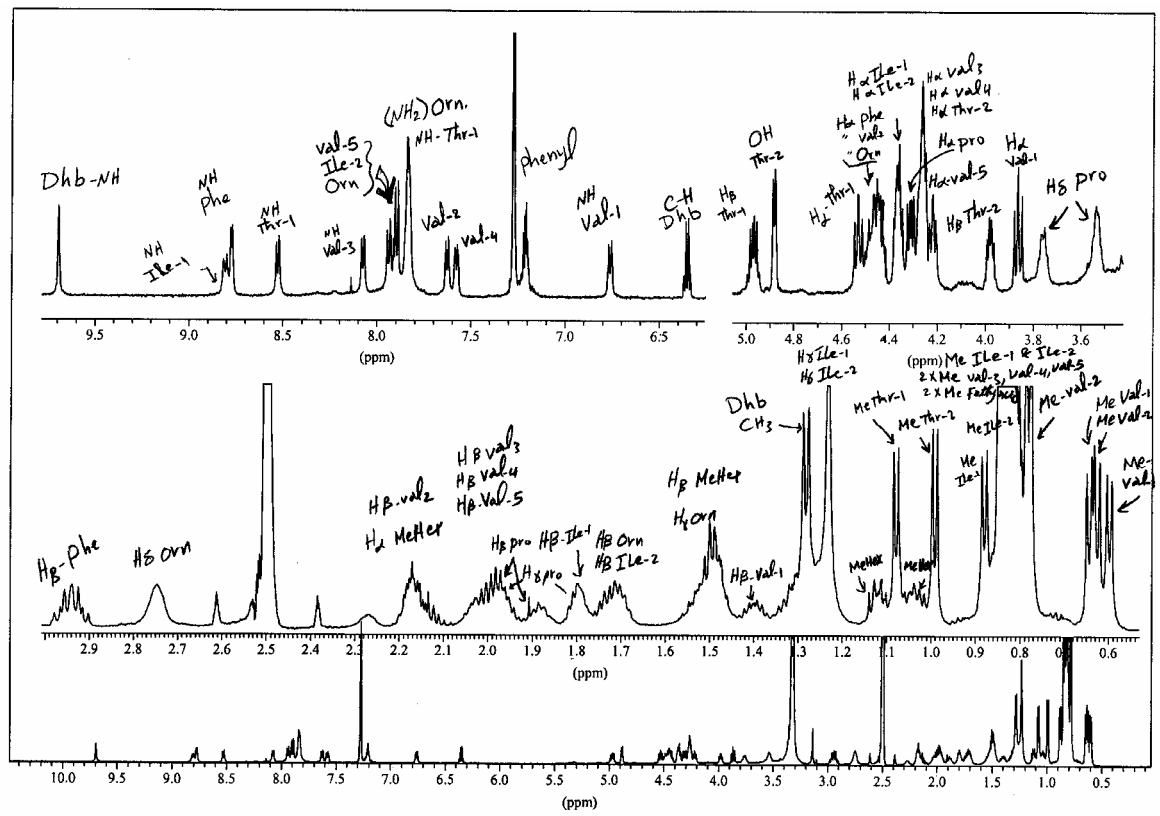

Fig. (3.1.4) : different reigons of ^{1}HNMR spectrum of compound 1

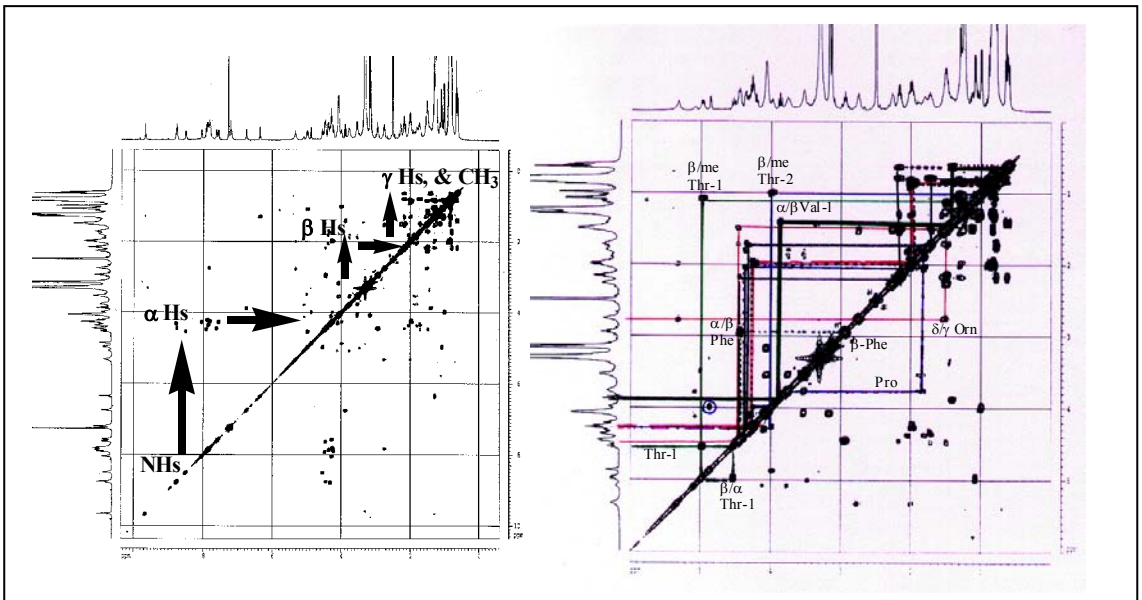

Fig. (3.1.5) : Total COSY (left), part of COSY (right) spectra of compound 1

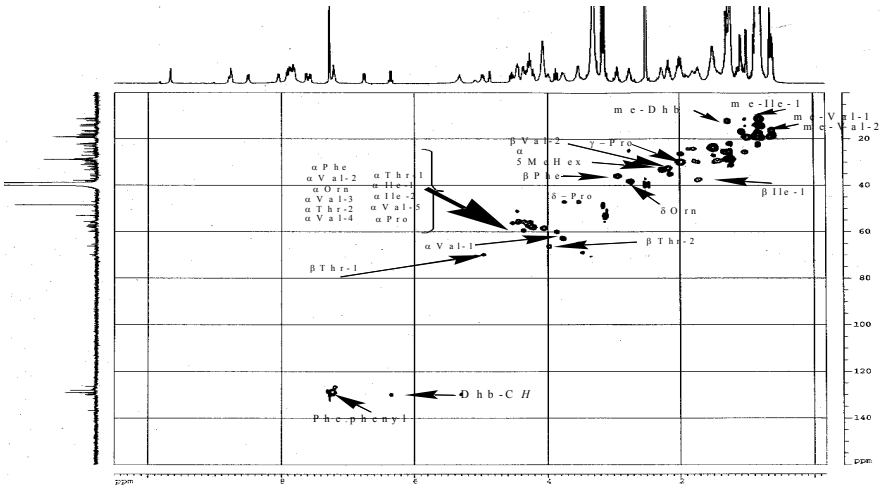

Fig. (3.1.6) : Total HMQC spectrum of compound 1

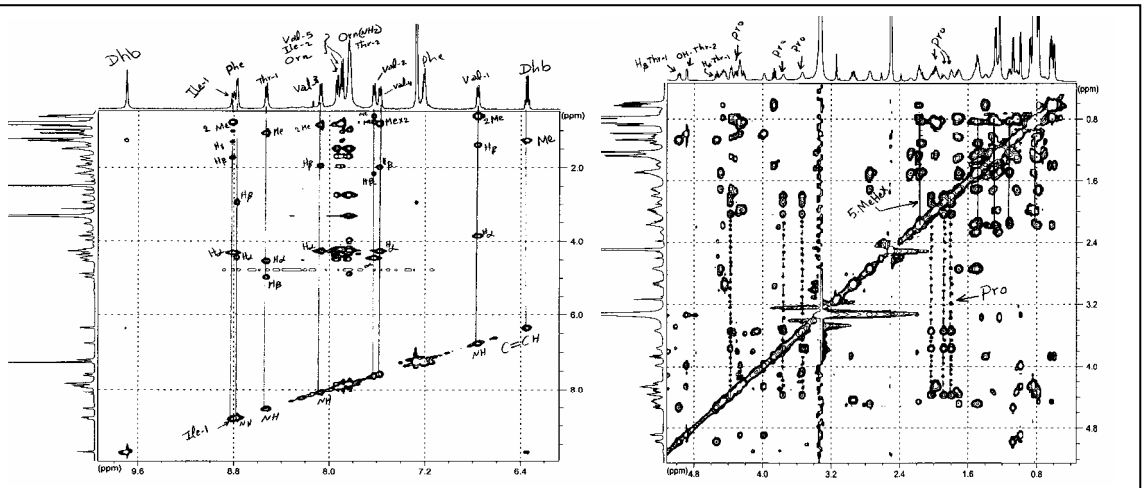

Fig.(3.1.7) : NH-detected spin systems (left), Proline and 5-MeHex (right) spin systems from partial TOCSY spectrum of compound 1

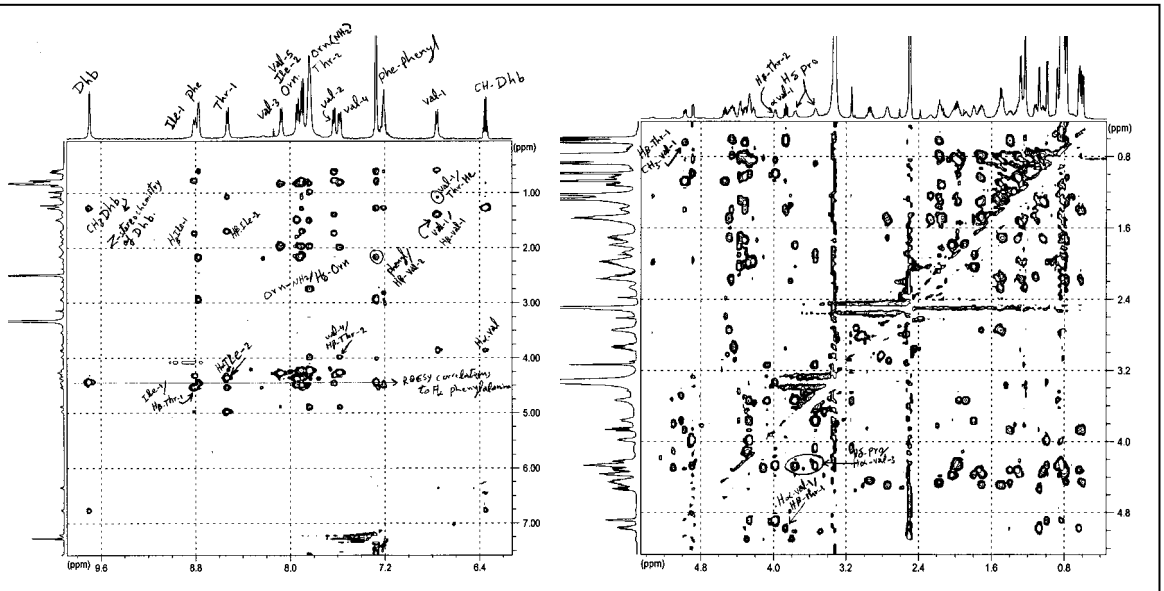

Fig.(3.1.8) : NH-detected ROESY correlations (left), upfield part of ROESY spectrum (right) of compound 1

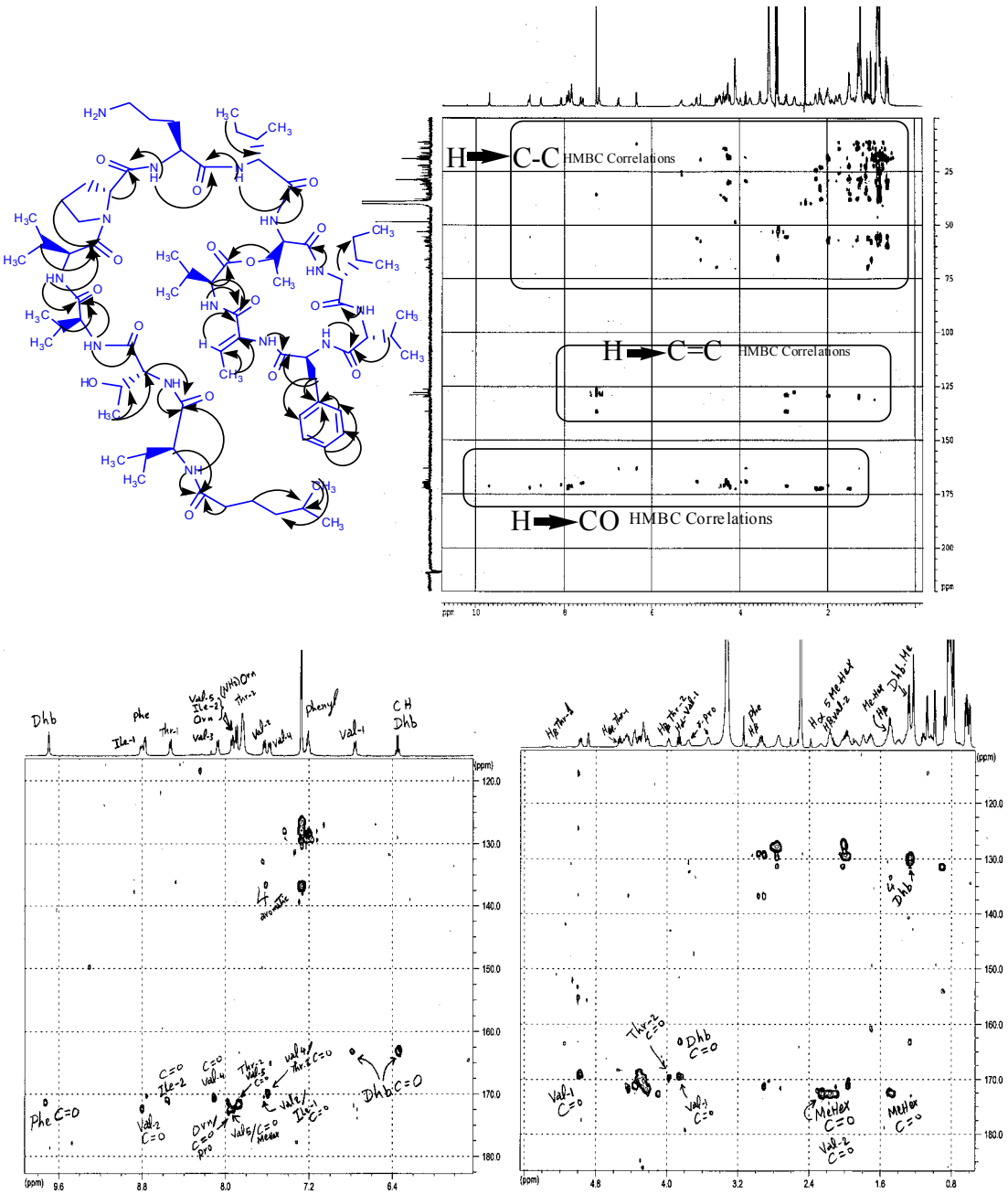

Fig.(3.1.9) : Total HMBC spectrum showing different H-detected HMBC correlations (up), NH-detected correlations to C=O (down left), and aliphatic protons–detected HMBC correlations to C=O (down right) of compound 1.

Table (3.1.1) Marfey´s analysis results of kahalalide F hydrolysates :

Amino acid-DAA deriv.	D.Ile	L.Phe	L. Val	D. Val	D.Pro	L.Thr	D.Thr	L. Orn*
MW (+ve mode)	384.0	418.0	370.0	370.0	368.1	372.0	372.0	385.1
MW (-ve mode)	382.4	416.5	368.3	368.3	366.3	370.3	370.3	383.5
Ret.time in minutes	24.53	22.98	20.97	22.77	18.68	15.93	16.60	13.44 & 14.14

* It was detected that L-ornithine isomer has two different retention times, because ornithine contains α- and δ- reactive amino groups which could both react with FDAA producing two ESI-MS-detectable products as shown in figure 3.1.12.

Table (3.1.2) : ^{1}H and ^{13}C NMR data of compound 1 in DMSO-d_6

Amino acid	No.	^{13}C,PPM	^{1}H,PPM	multiplicity	Amino acid	No.	^{13}C,PPM	^{1}H,PPM	multiplicity
Val-1	1	169.5	(NH) 6.76	(d, J=9.0Hz)	**Pro**	1	172.6	-	-
	2	60.3	3.86	(t,J= 9.0 Hz)					(dd,J= 9.1,
	3	30.8	1.39	(m)		2	60.2	4.36	6.6 Hz)
	4	14.6	0.62	(d, J=7.0Hz)		3	29.6	2.03,1.97	(m,m)
	5	18.8	0.58	(d, J=6.0Hz)		4	25.4	1.86	(m)
						5	48.0	3.76,3.52	(m,m)
Dhb	1	164.4	(NH) 9.69	(s)	**Val-3**	1	171.3	(NH) 8.10	(d, J=8.5Hz)
	2	130.3	-	-		2	57.6	4.26	(m)
	3	131.3	6.34	(q, J=7.0Hz)		3	30.5	1.94	(m)
	4	12.50	1.26	(d,J=7.5Hz)		4	19.6	0.86	(m)
						5	18.8	0.86	(m)
Phe.	1	171.3	(NH) 8.79	(d, J=5.5Hz)	**Val-4**	1	169.8	(NH) 7.57	(d, J=8.5Hz)
	2	56.3	4.42	(q, J=6.5Hz)		2	59.1	4.28	(m)
	3	36.8	2.93	(m)		3	31.3	1.98	(m)
	4	138.2	-	-		4	19.5	0.80	(m)
	5,5`	129.0	7.28	(m)		5	18.1	0.80	(m)
	6,6`	127.0	7.28	(m)					
	7	127.6	7.2	(m)					
Val-2	1	172.9	(NH) 7.62	(d, J=8.5Hz)	**Thr-2**	1	169.0	(NH) 7.82	(d, J=8.0Hz)
	2	58.6	4.46	(m)		2	58.9	4.26	(m)
	3	32.4	2.17	(m)		3	67.4	3.97	(m)
	4	18.9	0.62	(d, J=7.0Hz)		4	19.7	0.98	(d,J=6.5Hz)
	5	18.6	0.77	(d, J=6.5Hz)		-	-	(OH) ,4.88	(d,J=5.0Hz)
Ile-1	1	170.0	(NH) 8.82	(d, J=10.0Hz)	**Val-5**	1	172.2	(NH) 7.88	(d, J=7.5Hz)
	2	57.5	4.31	(m)				2^{nd}conf. (	(d, J=7.5Hz)
	3	38.8	1.73	(m)		2	59.6	7.85)	(m)
	4	26.8	1.31	(m)		3	30.7	4.23	(m)
	5	14.6	1.02	(t, J= 7.6 Hz)		4	19.6	1.96	(m)
	6	11.7	0.77	(d)		5	18.4	0.84	(m)
								0.84	
Thr-1	1	169.7	(NH) 8.56	(d, J=8.0Hz)	**5-Me-Hex. 1st conf**	1	173.8	-	-
	2	57.4	4.53	(t, J=7.8Hz)		2	36.3	2.13	(m)
	3	71.1	4.96	(m)		3	24.0	1.47	(m)
	4	17.3	1.07	(d,J=6.5Hz)		4	39.0	1.11	(m)
						5	28.1	1.47	(m)
						6	22.5	0.82	(m)
						7	22.5	0.82	(m)
Ile-2	1	170.6	(NH) 7.90	(d, J=8.2.0Hz)	**5-Me-Hex.**	1	174.1	-	-
	2	57.3	4.37	(m)		2	33.9	2.2	(m)
	3	38.0	1.69	(m)		3	32.8	1.6	(m)
	4	26.6	1.30	(m)	**2st conf.**	4	38.8	1.14	(m)
	5	14.8	1.03	(t, J= 6.5 Hz)		5	29.5	1.35	(m)
	6	11.6	0.77	(d)		6	19.5	0.80	(m)
Orn.	1	173.0	(NH) 7.95	(d, J=8.50Hz)		7	11.5	0.80	(m)
	2	52.9	4.49	(m)					
	3	29.6	1.48	(m)					
	4	24.4	1.67	(m)					
	5	40.1	2.74	(m)					
	-	-	(NH_2),7.69	b.singlet					

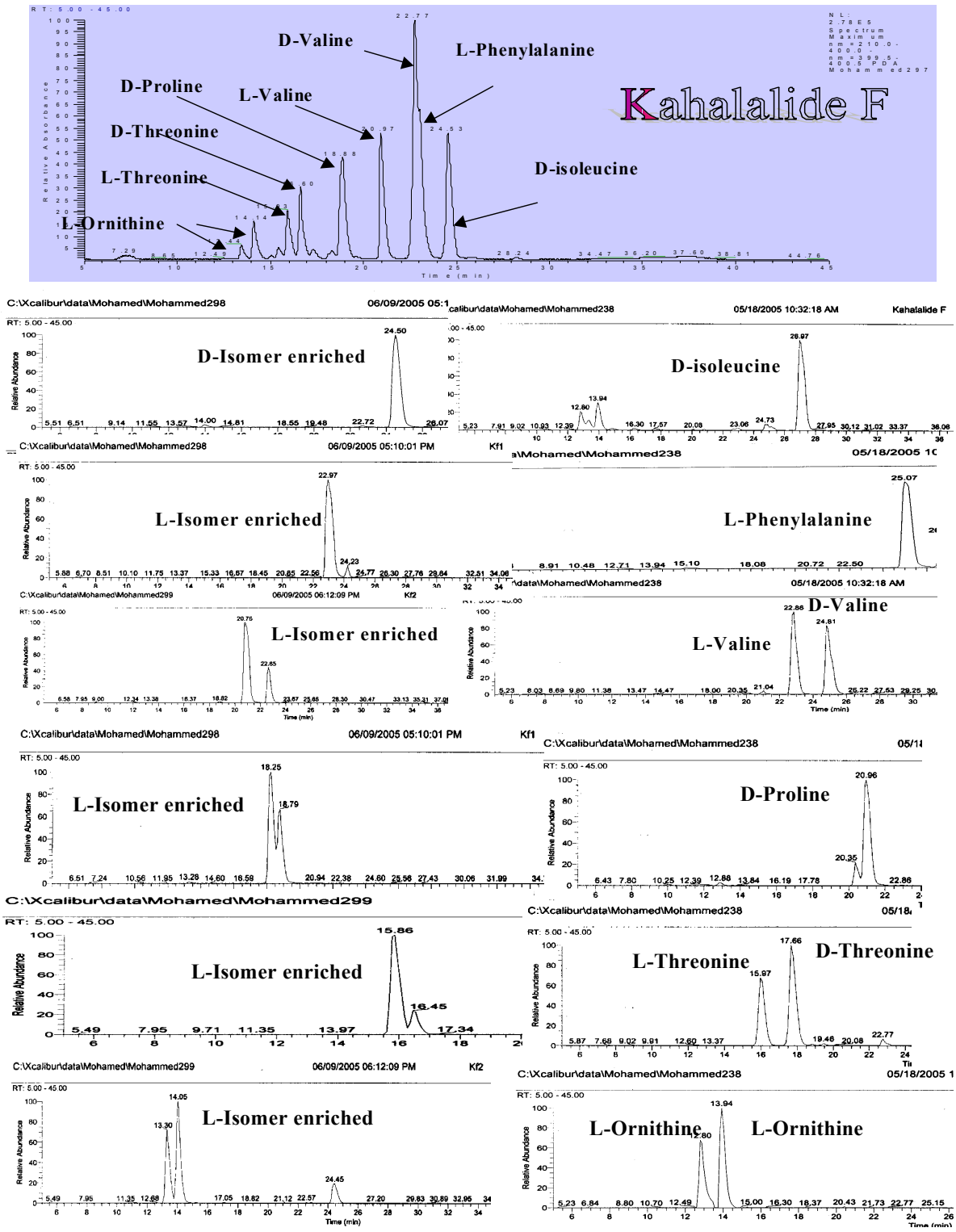

Fig (3.1.10): Marfey´s analysis results of kahalalide F-amino acids (up), ESI-MS chromatogram showing base peak search for each individual amino acid (chromatograms right) and their peak enriched analysis (opposite chromatograms left) for D-Ile, L-Phe, L-Val& D-Val, D-Pro, D- Thr &L-Thr, and L-Orn.

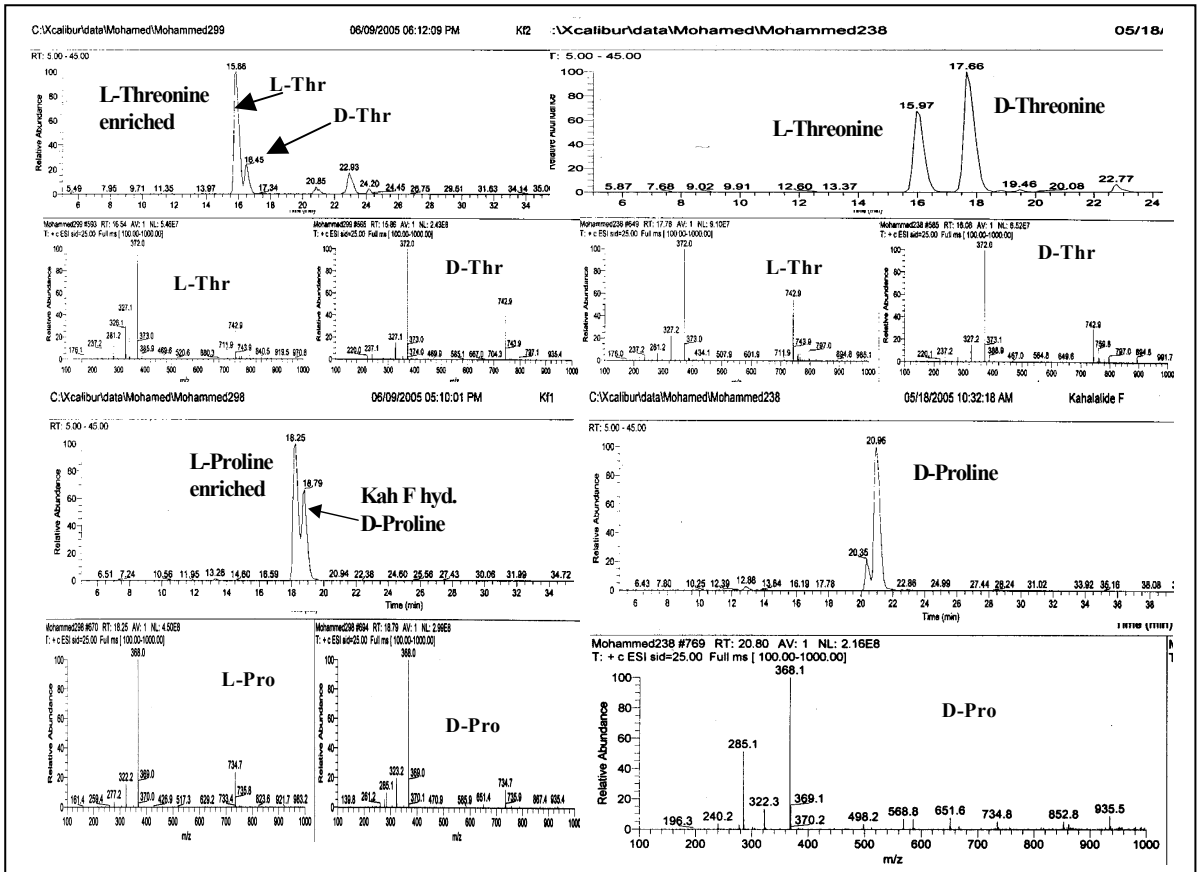

Fig (3.1.11): Compound 1–hydrolysate ESI-MS (+ve) : comparison of D-Thr and D-Pro [right] against enriched L isomers [left], the retention time was not always constant. Therefore, the peak enrichment technique was applied to unambiguously confirm the stereochemistry of each amino acid.

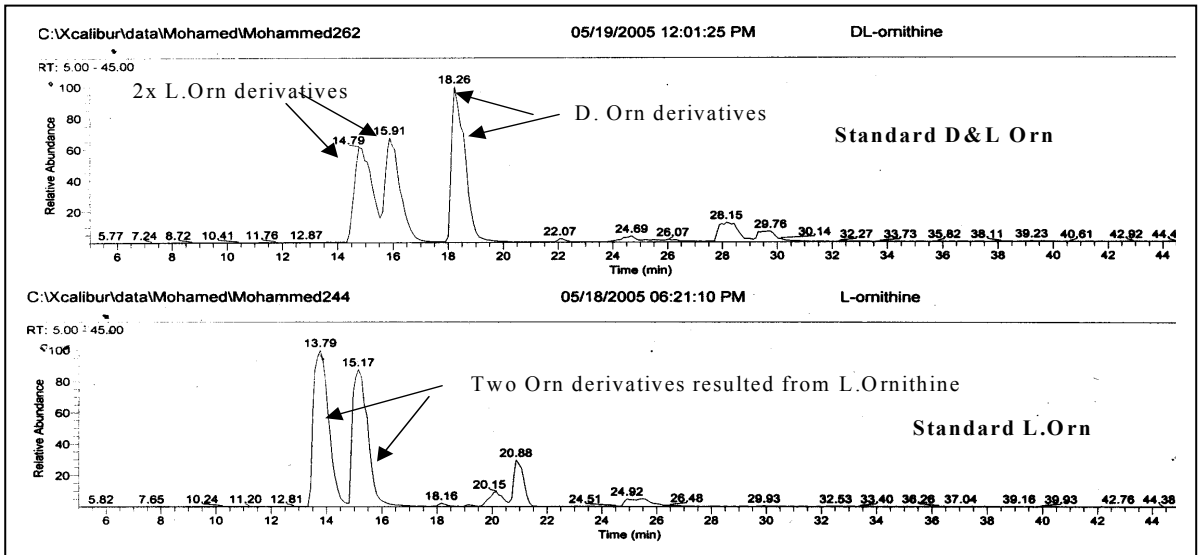

Fig (3.1.12) : Standard L.Orn vs DL.Orn. , showing two possible products for each stereoisomer.

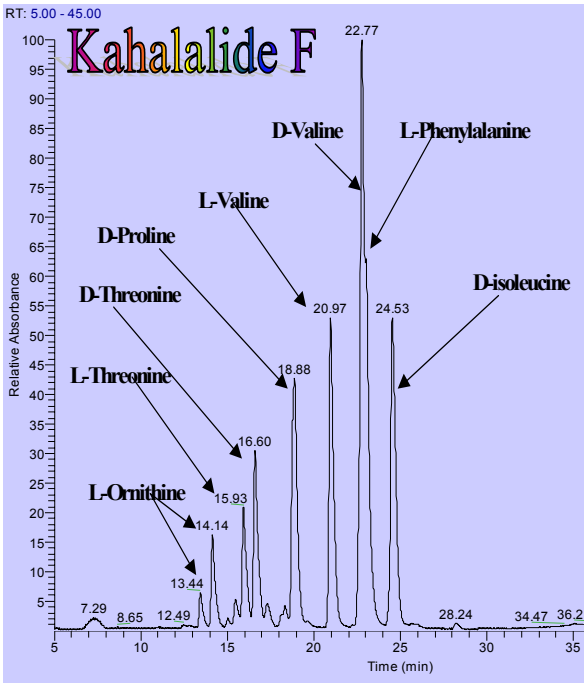

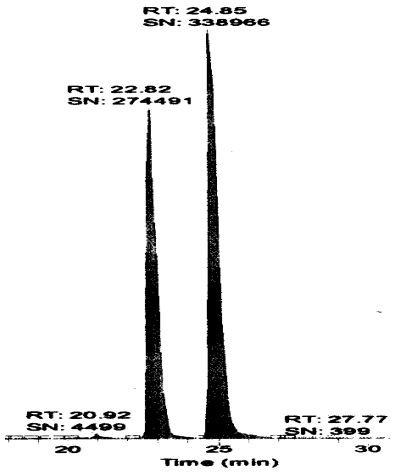

Fig (3.1.13) : relative peak area of D-Val (right) to the L-Val (left) of compound 1 [ratio = 3:2]

Fig.(3.1.14) The stereochemical profile of Amino acid units of compound 1

Table (3.1.3): The calculated mass fragments from MALDI-TOF-PSD-MS of compound 1 and sequence determination.

MHex	Val	Thr	Val	Val	Pro	Orn	Ile	Thr(-H)	Ile	Val	Phe	Dhb	Val	M+H	M-CO+H
113,10	99,07	101,05	99,07	99,07	97,05	114,08	113,08	100,04	113,08	99,07	147,07	83,04	99,07	1477,94	1449,94
MHex	Val	Thr	Val	Val	Pro	Orn	Ile	Thr(-H)	Ile	Val	Phe	Dhb	Val	1477,9	1449,9
	Val	Thr	Val	Val	Pro	Orn	Ile	Thr(-H)	Ile	Val	Phe	Dhb	Val	1364,8	1336,8
		Thr	Val	Val	Pro	Orn	Ile	Thr(-H)	Ile	Val	Phe	Dhb	Val	1265,8	1237,8
			Val	Val	Pro	Orn	Ile	Thr(-H)	Ile	Val	Phe	Dhb	Val	1164,7	1136,7
				Val	Pro	Orn	Ile	Thr(-H)	Ile	Val	Phe	Dhb	Val	1065,7	1037,7
					Pro	Orn	Ile	Thr(-H)	Ile	Val	Phe	Dhb	Val	966,6	938,6
						Orn	Ile	Thr(-H)	Ile	Val	Phe	Dhb	Val	869,5	841,5
MHex	Val	Thr	Val	Val	Pro	Orn	Ile							836,6	808,6
							Ile	Thr(-H)	Ile	Val	Phe	Dhb	Val	755,5	727,5
MHex	Val	Thr	Val	Val	Pro	Orn								723,5	695,5
								Thr(-H)	Ile	Val	Phe	Dhb	Val	642,4	614,4
MHex	Val	Thr	Val	Val	Pro									609,4	581,4
									Ile	Val	Phe	Dhb	Val	542,3	514,3
MHex	Val	Thr	Val	Val										512,4	484,4
									Ile	Val	Phe	Dhb		443,3	415,3
					Pro	Orn	Ile	Thr(-H)						425,3	397,3
MHex	Val	Thr	Val											413,3	385,3
	Val	Thr	Val	Val										399,3	371,3
										Val	Phe	Dhb		330,2	302,2
					Pro	Orn	Ile							325,2	297,2
					Pro	Orn	Ile							325,2	297,2
MHex	Val	Thr												314,2	286,2
	Val	Thr	Val											300,2	272,2
										Val	Phe			247,1	219,1
											Phe	Dhb		231,1	203,1
MHex	Val													213,2	185,2
									Ile	Val				213,2	185,2
					Pro	Orn								212,1	184,1
	Val	Thr												201,1	173,1
		Thr	Val											201,1	173,1
								Thr(-H)					Val	200,1	172,1
			Val	Val										199,1	171,1
												Dhb	Val	183,1	155,1
											Phe			148,1	120,1
						Orn								115,1	87,1
MHex														114,1	86,1
	Val													100,1	72,1

3.1.2- **Kahalalide E (2, Known compound)**

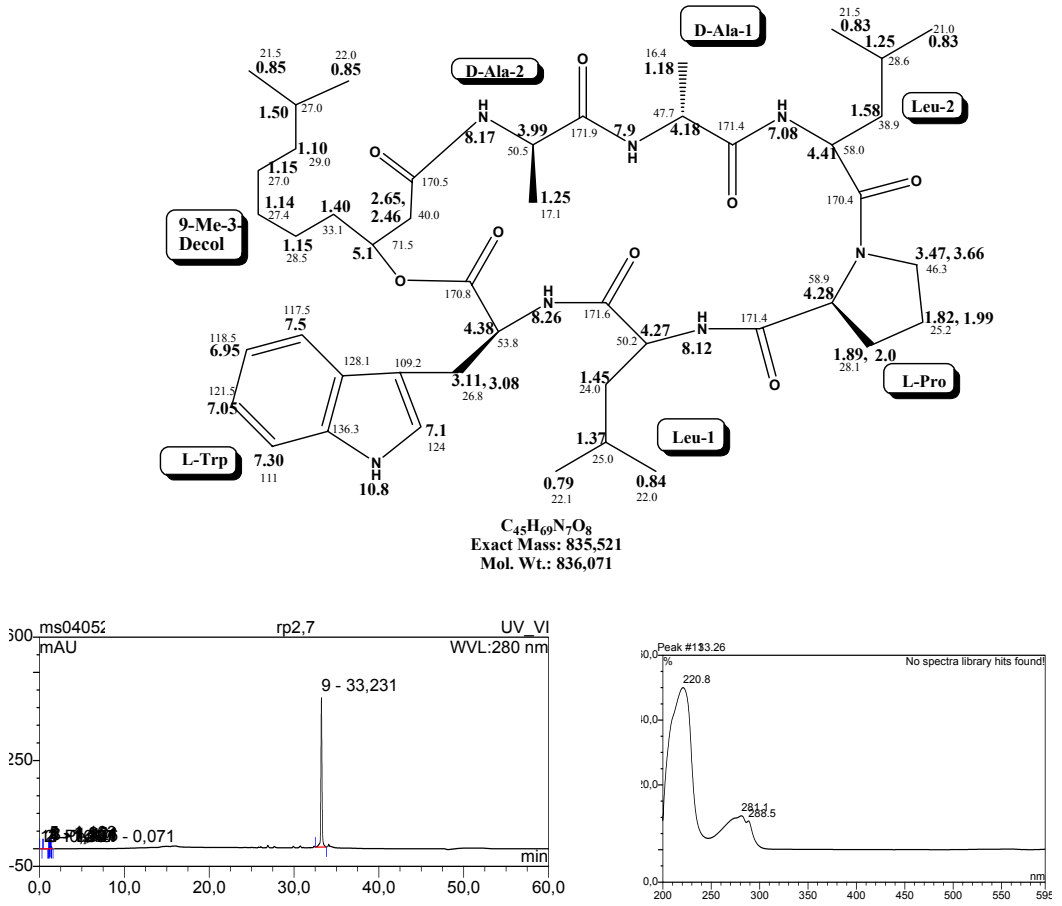

Fig (3.1.15): chemical structure of compound 2 with δ_C and δ_H values (up), HPLC-chromatogram (down left) and UV-spectrum (down right).

Yield : 4 mg

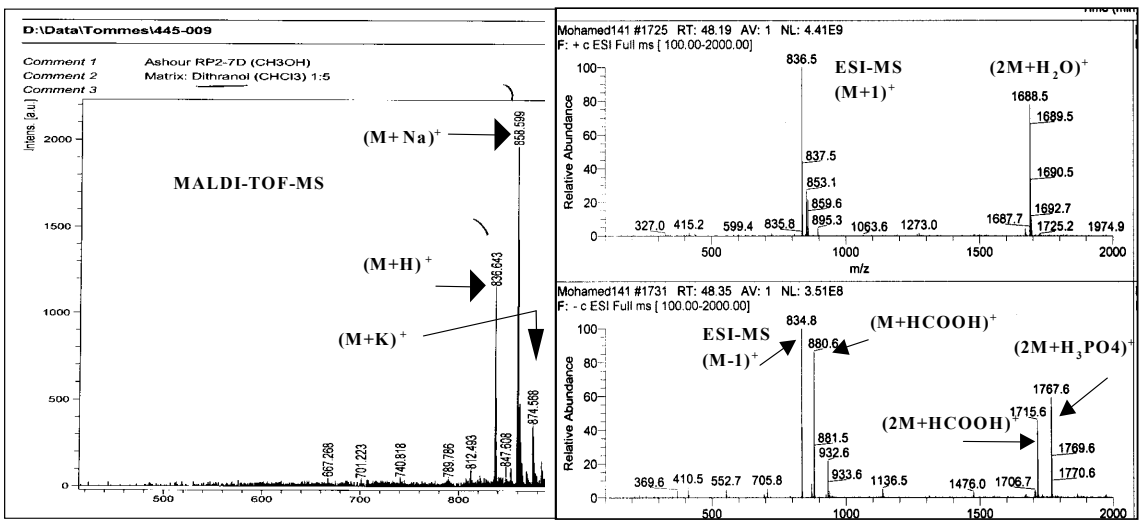

Fig.(3.1.16) : MALDI-TOF-MS and ESI-MS of compound 2

Kahalalide E was isolated as a white amorphous powder, with $[\alpha]_D$ of + 5° (*c* 0.25 MeOH). It has UV absorbance at λ_{max} 221, 281, 288 nm. MALDI-TOF-MS showed pseudomolecular ion peak at *m/z* 858.57 $[M+Na]^+$ and 874.55 $[M+K]^+$ and 836.65$[M+1]^+$ suggesting the molecular formula $C_{45}H_{69}N_7O_8$. The molecular weight of **2** was also confirmed by ESI-MS, and MALDI-TOF-PSD-MS. The ^{1}HNMR spectrum of **2** showed 5 deshielded amide-N*H* resonances in the lower field region, at 7.08, 7.90, 8.12, 8.17 and 8.26 ppm, suggesting the peptidic nature of the compound. In addition to the most downfield N*H* proton which is a sharp singlet at δ 10.8, an ABCD aromatic spin system as resembled by resonances at 7.50, 6.95, 7.05 and 7.3 ppm was observed and suggested the presence of tryptophane, Trp. COSY spectrum together with TOCSY experiment indicated 5 spin systems commencing from the above mentioned five N*H*-resonances, in addition to the characteristic indole spin system of Trp. TOCSY spectrum showed also the presence of characteristic proline spin system (H_α 4.28, H_β 1.89 & 2.00, H_γ 1.83 & 1.99 and H_δ 3.47 & 3.66 ppm) and β-hydroxy aliphatic acid, 9-methyl-3-hydroxydecanoic acid (9-Me-3-Decol) [(H-2) at δ 2.65 & 2.46, (H-3) at δ 5.1, (H-4) at δ 1.40, (H-5) at δ 1.15, (H-6) at δ 1.14, (H-7) at δ 1.15, (H-8) at δ 1.10, (H-9) at δ 1.15 and two methyls at δ 0.85 and 0.85 ppm].

^{13}C NMR spectra displayed signals for 45 carbons including 7 carbonyls at δ 170.8, 171.6, 171.4, 170.4, 171.4, 171.9, 170.5 of Trp, Leu-1, Pro, Leu-2, Ala-1, Ala-2 and 9-Me-3-Decol, respectively, in addition to 8 aromatic carbons, 6 α-*C*H, one downfield aliphatic methine carbone at 71.5 (C-3 of 9-Me-3-Decol), 3 highfield methines,12 CH_2 and 8 methyls as mentioned in table 3.1.5.

HMBC and NOESY experiments established the connectivity of the individual spin systems. *H*-2 of indole at 7.1 ppm showed HMBC correlation to C-3, C-3a, C-7 and C-7a at δ 109.2, 128.1 111.0 and 136.3 respectively. The connectivity of Trp to Leu-1 was evident through HMBC correlation between Trp-N*H* at δ 8.26 to the vicinal carbonyl of Leu-1 at 171.6 ppm. The sequence for Ala-1-Ala-2-9-Me-3-Decol was established also by HMBC correlations of N*H* resonances at δ 7.90 and 8.17 to vicinal carbonyls at δ 171.9 and 170.5, respectively. Connection of 9-Me-3-Decol to Trp was established through HMBC correlation of H_β-9-Me-3-Decol to carboxyl at 170.8. Although there are no evident HMBC correlations between Leu-2-N*H* and the vicinal carbonyl of Ala-1, due to peak broadness, the connection of Leu-2 to Ala-1 was determined by the HMBC correlation at δ 4.41 (H_α, Leu-2) to Ala-1 carbonyl at 171.4. HMBC experiment showed a correlation between H_α Pro at δ 4.28 and Leu-2 carbonyl at 170.4 ppm. The connectivity of Leu-1 to Pro was established through the NOE between Leu-1 N*H* at 8.12 and H_α-Pro 4.28 ppm. Also, the connection of the amino

acids of Pro- Leu-2 was confirmed by NOE between δ-protons Pro at 3.47, 3.66 ppm and H_α of Leu-2 at δ 4.41. NOESY experiment showed also a through space correlation between Ala-1 N*H* at 7.9 ppm to Ala-2 N*H* at δ 8.17, while Ala-2 N*H* showed a through space correlation to H_β of 9-Me-3-Decol at 2.65 and 2.46. In addition, further NOEs were observed between the downfield H_β of 9-Me-3-Decol at 5.1 ppm and H_α of Trp 4.38 ppm. The NMR data of compound **2** were identical to those of kahalalide E (Hamann *et al* 1996).

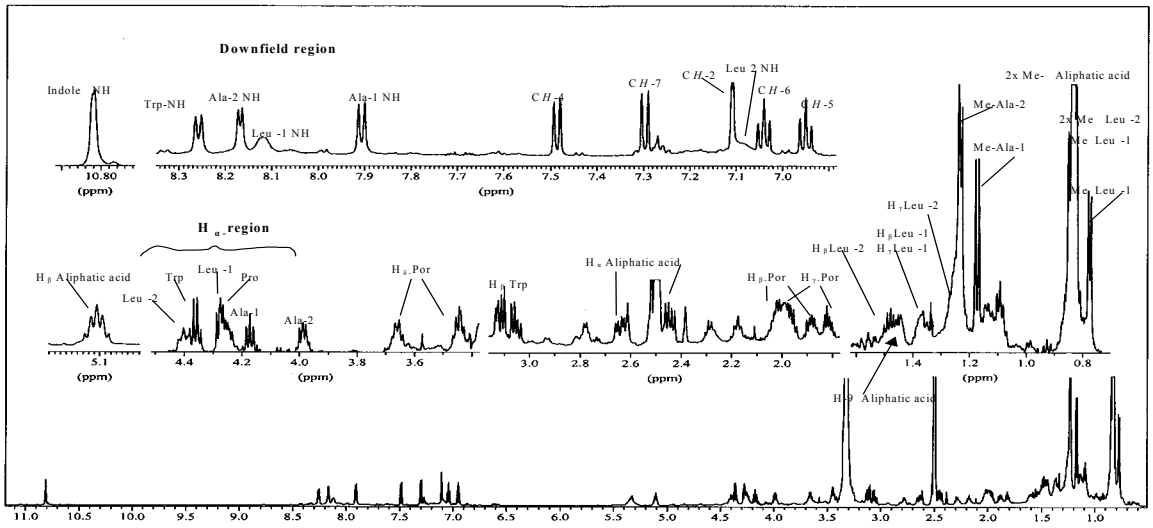

Fig (3.1.17): ^{1}H NMR spectrum.

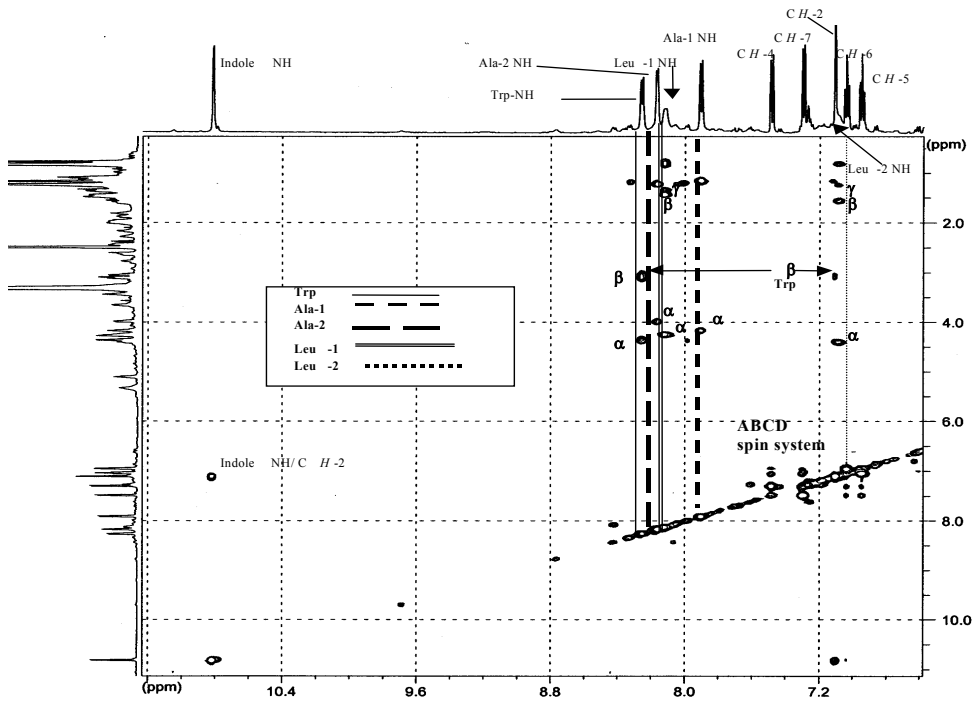

Fig (3.1.18): parts of TOCSY Spectrum of Compound 2 showing NH-detected spin system .

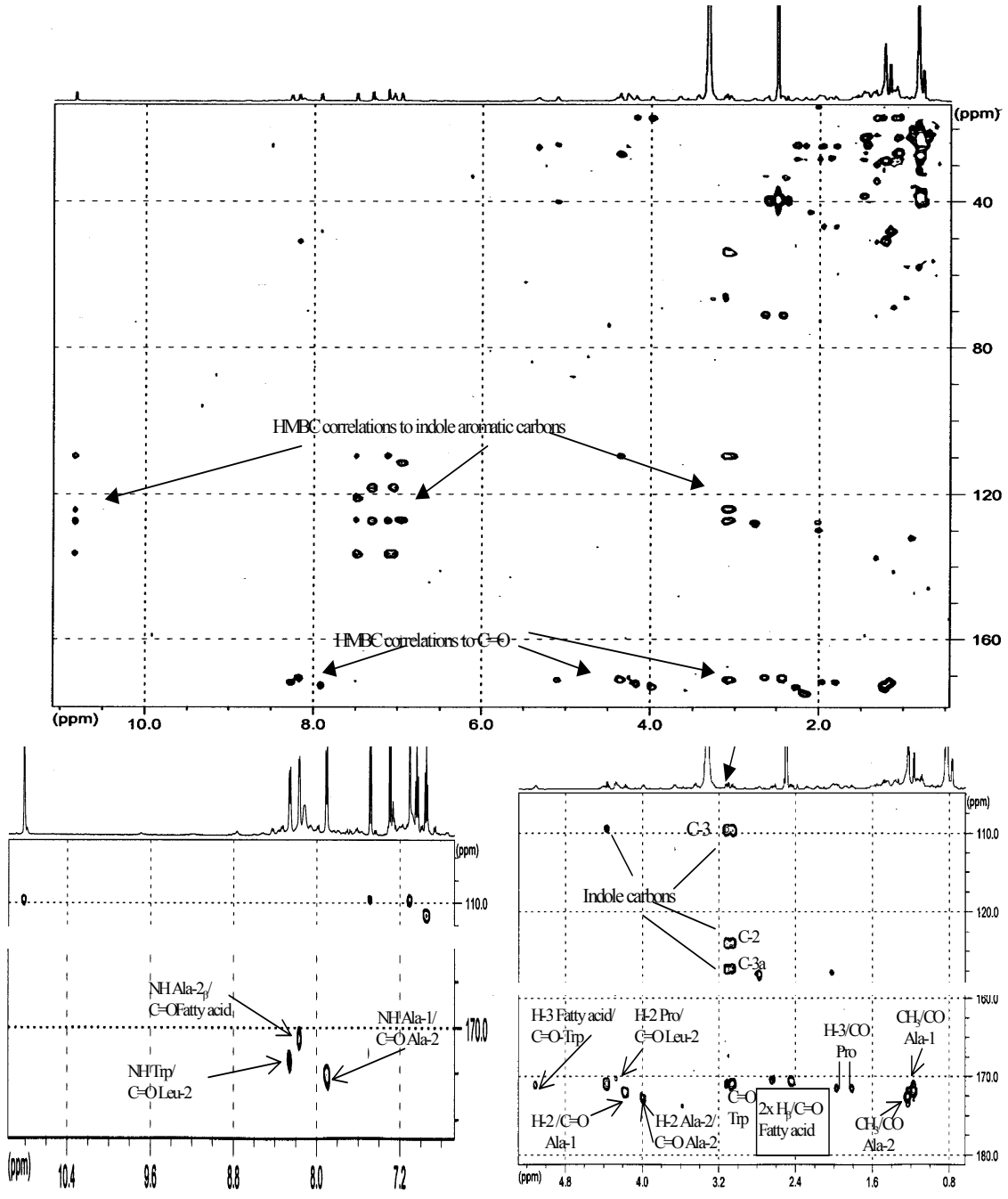

Fig (3.1.19): Total HMBC spectrum of compound 2 (up), different parts (down) showing important HMBC correlations

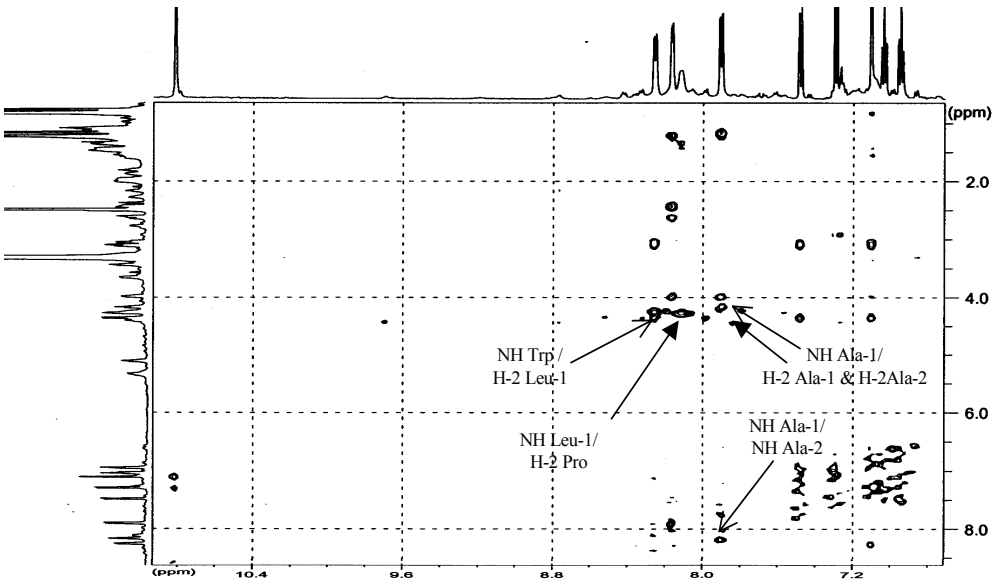

Fig (3.1.20) : NH-detected NOESY correlations.

Deduced data of compound **2** obtained by NMR were confirmed by ESI-MS/MS experiment and MALDI-TOF-PSD MS.

MALDI-TOF – PSD spectrum confirmed the sequence of a depsipeptide, kahalalide E, as shown in table (3.1.4). Similar results were obtained from tandem ESI-MS/MS spectrum, where the positive protonated fragment ion peaks were evident at *m/z* 808.4, 765.2, 650.1, 599.1, 581.3, 537.1, 464.7, 440.0, 415.1, 395.1, 326.9, 308.9, 282.1 corresponding to $[M+1-CO]^+$, $[M-Ala]^+$, $[M+1-Trp]^+$, $[M+1-(Leu+pro+CO)]^+$, $[M+1-(Ala+9\text{-}Me\text{-}3\text{-}Decol)]^+$, $[M+1-(Leu+Trp)]^+$, $[M+1-(Trp+9\text{-}Me\text{-}3\text{-}Decol)]^+$, $[9\text{-}Me\text{-}3\text{-}Decol+Ala+Ala+Leu+1]^+$, $[Trp+9\text{-}Me\text{-}3\text{-}Decol+Ala+1\text{-}(CO)]^+$, $[Ala+Leu+Pro+Leu+1]^+$, $[9\text{-}Me\text{-}3\text{-}Decol+Ala+Ala+1]^+$, $[Ala+Leu+Pro+CO+1]^+$, and $[Ala+Leu+Pro+1]^+$ respectively.

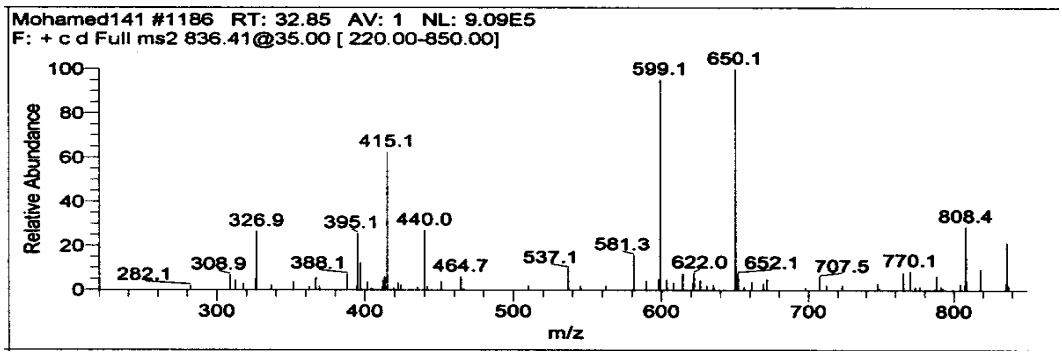

Fig (3.1.21) ESI-MS/MS spectrum of compound 2.

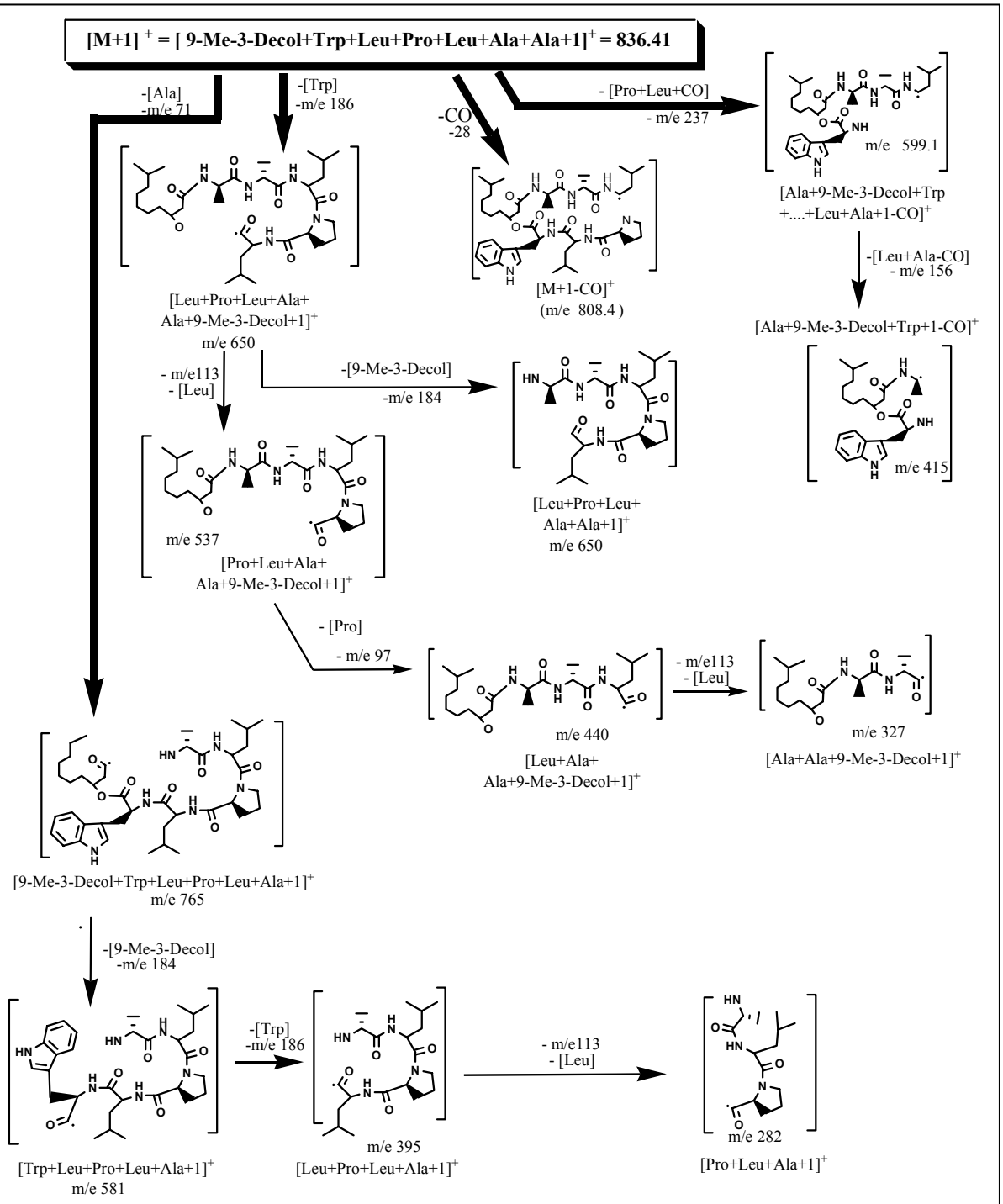

Fig (3.1.22) Possible fragmentation pattern and amino acids-sequencing of compound 2 by interpretation of Tandem ESI-MS spectrum.

Table (3.1.4): The calculated mass fragments from MALDI-TOF-PSD-MS of compound 2

	Leu	Pro	Leu	Ala	Ala	X	Trp	M+H	M-CO+H
Masse	113,084	97,053	113,084	71,037	71,037	184,146	186,079	836,5278	808,5278
Fragmente		Pro	Leu	Ala	Ala	X	Trp	723,4438	695,4438
	Leu	Pro	Leu	Ala	Ala	X		650,4488	622,4539
	Leu		Leu	Ala	Ala	X	Trp	739,4748	711,4799
	Leu	Pro		Ala	Ala	X	Trp	723,4438	695,4489
	Leu	Pro	Leu	Ala	Ala		Trp	652,3818	624,3869
		Pro	Leu	Ala	Ala	X		537,3648	509,3699
	Leu	Pro	Leu		Ala	X	Trp	765,4830	737,4881
			Leu	Ala	Ala	X	Trp	626,3908	598,3959
	Leu	Pro	Leu	Ala	Ala			466,3028	438,3079
	Leu			Ala	Ala	X	Trp	626,3908	598,3959
			Leu	Ala	Ala	X		440,3118	412,3169
		Pro	Leu	Ala	Ala			353,2188	325,2239
	Leu	Pro			Ala	X	Trp	652,4068	624,4119
				Ala	Ala	X	Trp	513,3068	485,3119
	Leu	Pro	Leu	Ala		X	Trp	765,4908	737,4959
				Ala	Ala	X		327,2278	299,2329
			Leu	Ala	Ala			256,1658	228,1709
	Leu	Pro	Leu	Ala			Trp	581,3448	553,3499
	Leu				Ala	X	Trp	555,3538	527,3538
	Leu	Pro	Leu	Ala			Trp	581,3448	553,3448
					Ala	X	Trp	442,2698	414,2698
	Leu	Pro	Leu			X	Trp	694,4538	666,4538
	Leu	Pro	Leu	Ala				395,2658	367,2658
				Ala	Ala			143,0818	115,0818
					Ala	X		256,1908	228,1908
		Pro	Leu	Ala				282,1818	254,1818
	Leu	Pro				X	Trp	581,3698	553,3698
	Leu	Pro	Leu				Trp	510,3078	482,3078
	Leu	Pro	Leu					324,2288	296,2288
			Leu	Ala				185,1288	157,1288
	Leu					X	Trp	484,3168	456,3168
	Leu	Pro					Trp	397,2238	369,2238
		Pro	Leu					211,1448	183,1448
						X	Trp	371,2328	343,2328
	Leu	Pro						211,1448	183,1448
				Ala				72,0448	44,0448
	Leu						Trp	300,1708	272,1708
					Ala			-106,9630	
			Leu					114,0918	86,0918
						X		185,1538	157,1538
		Pro						98,0608	70,0608
							Trp	187,0868	159,0868

X = 9-Me-3-hydroxy Decanoic acid [9-Me-3-Decol]

Table (3.1.5) : ^{1}H and ^{13}C NMR data of compound 2 in DMSO-d_6

Amino acid	Carbon	^{13}C NMR ppm, Mult	1H NMR, ppm	Multiplicity , *J*= Hz
Tryptophan	1	170.8, s	NH,8:26	d, *J*=7.7
	2	53.8, d	4.38	q, *J*=7.4
	3	26.8, t	3.11; 3.08	m; dd, *J*=14.7, 8.1
	4	109.2, s		
	5	124.0, d	7.1; NH,10.80	s; s
	6	136.3, s		
	7	128.1, s		
	8	117.5, d	7.50	d, *J*=8.1
	9	118.5, d	6.95	dt, *J*=7.0, 0.7
	10	121.5, d	7.05	dt, *J*=7.0, 1.1
	11	111.0, d	7.30	d, *J*=8.1
Leucine-1	1	171.6, s	NH, 8.12	br d
	2	50.2, d	4.27	m
	3	24.0, t	1.37	m
	4	25.0, d	1.45	m
	5	22.0, q	0.84	m
	6	22.1, q	0.79	d, *J*= 5.9
Proline	1	171.4, s		
	2	58.9, d	4.28	m
	3	28.1, t	2.00; 1.89	m; m
	4	25.2, t	1.99; 1.83	m; m
	5	46.3, t	3.66; 3.47	m; m
Leucine-2	1	170.4, s	NH, 7.08	br d
	2	58.0, d	4.41	m
	3	38.9, t	1.58	m; m
	4	28.6, d	1.25	m
	5	21.0, q	0.83	m
	6	21.5, q	0.83	m
Alanine-1	1	171.4, s	NH, 7.90	d, *J*= 7.7
	2	47.7, d	4.18	p, *J*= 7.3
	3	16.4, q	1.18	d, *J*= 7.0
Alanine-2	1	171.9, s	NH, 8.17	d, *J*= 5.6
	2	50.5, d	3.99	p, *J*= 6.3
	3	17.1, q	1.25	d, *J*= 7.4
9-Me-3-Decol	1	170.5, s		
	2	40.0, t	2.65; 2.46	dd, *J*= 14.7, 5.6; dd, *J*= 14.7, 7.0
	3	71.5, d	5.10	p, 6.3
	4	33.1, t	1.40	m
	5	28.5, t	1.15	m; m
	6	27.4, t	1.14	m
	7	27.0, t	1.15	m
	8	29.0, t	1.10	m
	9	27.0, d	1.50	m
	10	22.1, q	0.85	d, *J*= 6.7
	11	22.1, q	0.85	d, *J*= 6.7

3.1.3- **Kahalalide D (3, Known compound)**

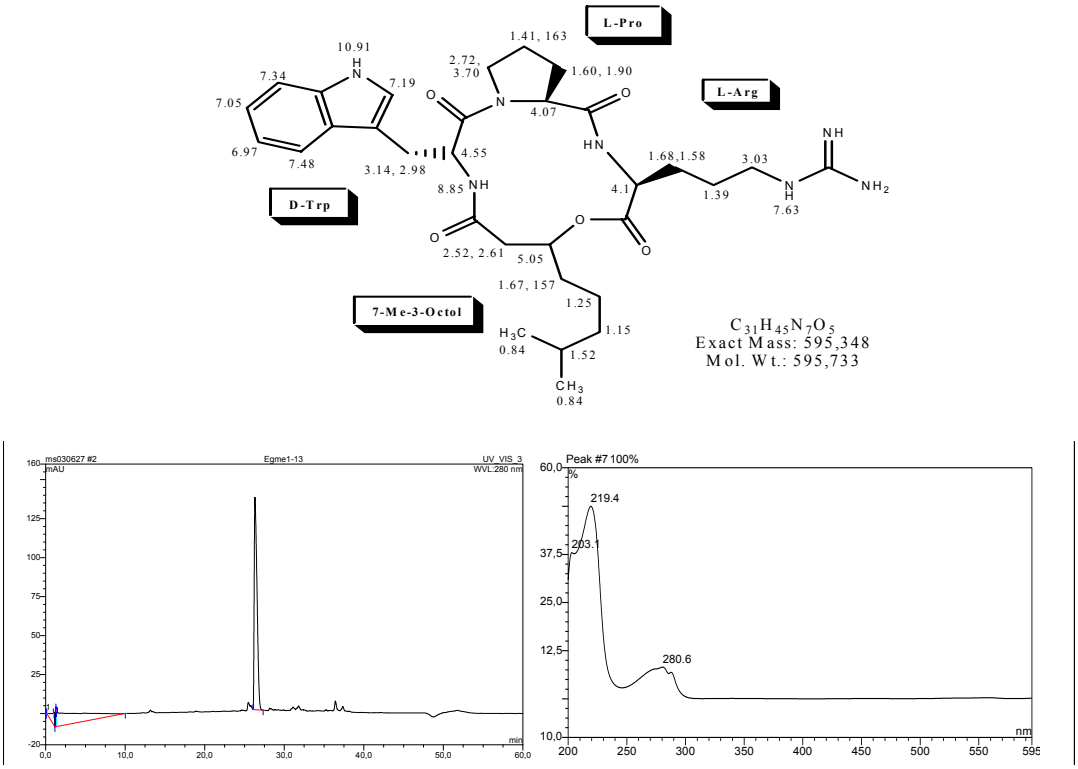

Fig (3.1.23): chemical structure of compound 3 showing δ_H values (up) and HPLC chromatogram (down left) and UV spectrum (down right).

Yield : 3.1 mg

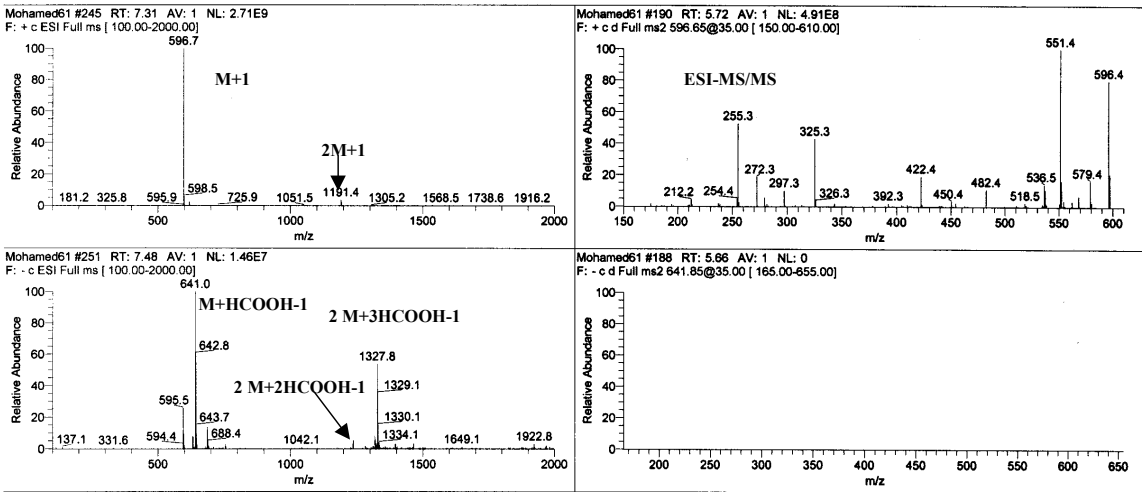

Fig.(3.1.24) : ESI-MS and ESI-MS/ MS spectra of compound 3

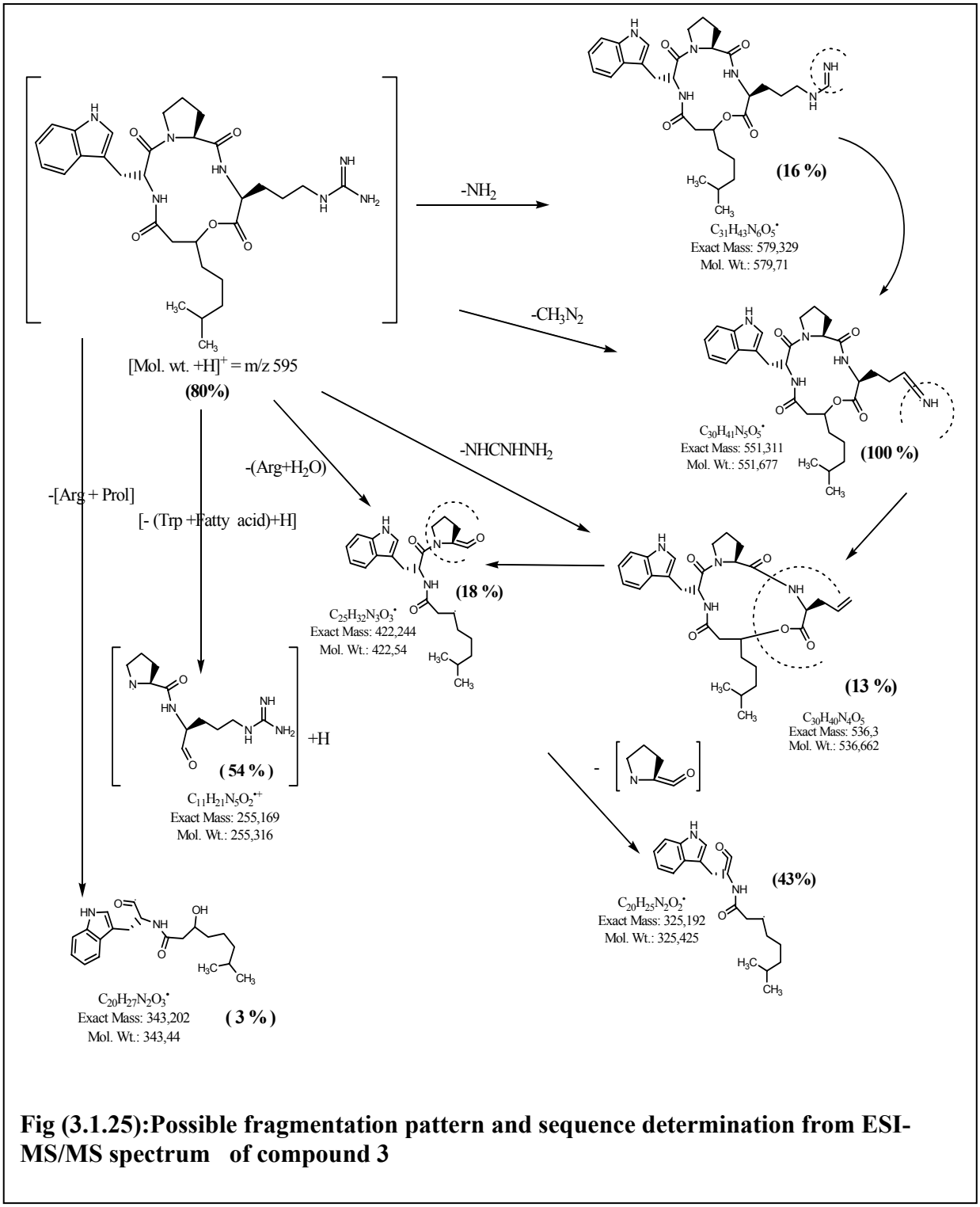

Fig (3.1.25):Possible fragmentation pattern and sequence determination from ESI-MS/MS spectrum of compound 3

Kahalalide D was isolated as a white amorphous powder, with $[\alpha]_D$ of - 40° (*c* 0.25 MeOH). It has UV absorbance at λ_{max} 203, 219, 280 nm. Positive ESI-MS showed pseudomolecular ion peak *m/z* 596.7 $[M+1]^+$ and 1191.0 $[2\ M+1]^+$ and negative ESI-MS showed pseudomolecular ion peak at m/z 641.0 $[M+HCOOH-1]^-$ and 1327.8 $[2M+3HCOOH-1]^-$ suggesting the molecular formula $C_{31}H_{45}N_7O_5$. The molecular weight and the sequence

determination of **3** was confirmed by ESI-MS/MS fragmentation pattern as shown in figure 3.1.25. The ^{1}HNMR spectrum of **3** showed characteristic proton resonances that belongs to the simplest known kahalalide, which is kahalalide D. Compound **3** is made up of three amino acids consisting of tryptophane (Trp), proline (Pro), and arginine (Arg) plus one aliphatic acid [7-Me-3-Hydroxy-Octanoic acid]. ^{1}HNMR showed **2** deshielded amide-N*H* resonances in the lower field region, at 6.78 (d, *J* = 5.68 Hz, Arg-N*H*) and 8.85(d, *J* = 6.9 Hz, Trp-N*H*) in addition to downfield proton resonance at 7.63 (br t, *J* = 5.63 Hz, Arg-N*H*) and a characteristic indole protons of Trp resonating at 6.97 (t, *J* = 7.4 Hz, Trp-C*H*-10), 7.05 (t, *J* = 7.3 Hz, Trp-C*H*-9), 7.34 (d, *J* = 8.2 Hz, Trp-C*H*-9), 7.48 (t, *J* = 8.2 Hz, Trp-C*H*-11), 7.19 (d, *J* = 2.3 Hz, Trp-C*H*-5) and a downfield resonance at 10.91 (d, *J* = 1.2 Hz) for an indol-N*H*. TOCSY experiment and COSY spectrum showed the rest of arginine-proton resonances as mentioned in table 3.1.6. ^{1}HNMR showed a characteristic proline spin system at δ 4.07 (dd, *J* = 8.6, 4.3 Hz, *H*-2), 1.60, 1.90 (m,m, *H*-3),1.41, 1.63 (m,m, *H*-4), 3.70, 2.72 (m,m, *H*-5) which was also confirmed by COSY and TOCSY experiments. The aliphatic acid of **3** was assigned to be 7Me-3-Octol from the COSY and TOCSY spectra of compound **3** at δ 2.52, 2.61 (dd, *J* = 15.2, 4.95 Hz, H-2a and dd, *J* = m, *H*-2b), 1.67,157 (m,m, *H*-4), 1.25 (m, *H*-5), 1.15 (m, *H*-6), 1.52 (m, *H*-7), the presence of downfield proton resonance at δ 5.05 (m) indicated the presence of an oxygenated methine group of the fatty acid (H-3) where its position was established by direct COSY correlations to *H*-2. As are most of fatty acid moieties of known depsipeptides, compound **3**-fatty acid is an iso-acid showing a two methyl-proton resonances at δ 0.84 and 0.84 (d, *J* 6.3 Hz, *H*-8 and *H*-9). The presence of a guanidine group was established through ESI-MS/MS fragmentation where the presence of molecular ion fragments at 579.3 [M - NH2, (16 %)], 551.3 [M - $NHCHNH_2$, (100 %)] and 536.5 [M – guanidine (14 %)] confirmed the presence of guanidine group. The connection of a different spin systems was confirmed by ROESY and ESI-MS/MS fragmentation data. ROESY spectrum showed a NOEs between (N*H*-Trp) at δ 8.85 ppm to Hα of 7Me-3-Octol and Hα-Pro at δ 2.52, 2.61 and 4.07ppm, respectively. H-3 of the fatty acid at δ 5.05 showed an NOE to Arg N*H* at δ 6.78, while Arg-NH at 6.78 showed an NOE to proline-H_α at 4.07, and additional correlations to Trp-NH and H_α of the fatty acid moiety. ROESY, COSY and TOCSY correlations as well as ^{1}HNMR data are identical to those of kahalalide D (Hamann *et al* 1996).

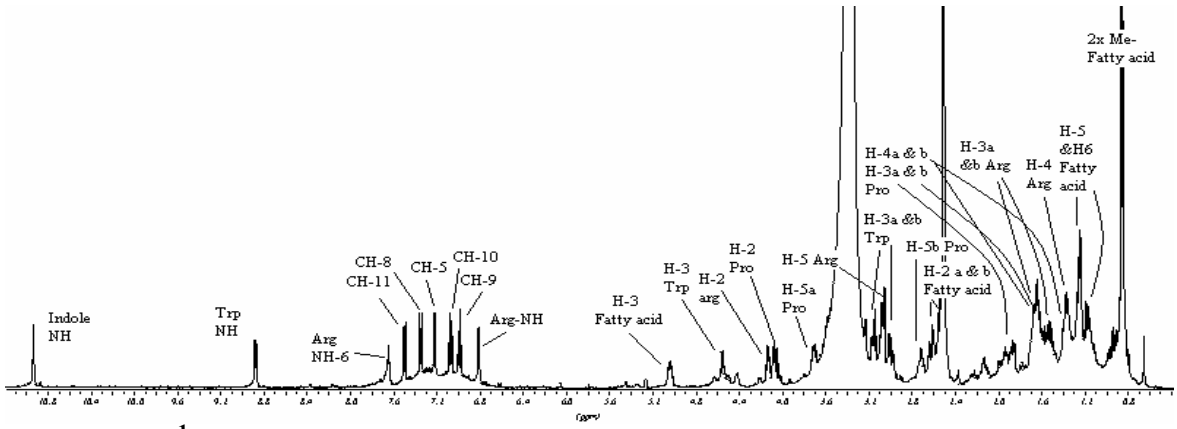

Fig (3.1.26): ^{1}H NMR spectrum of compound 3

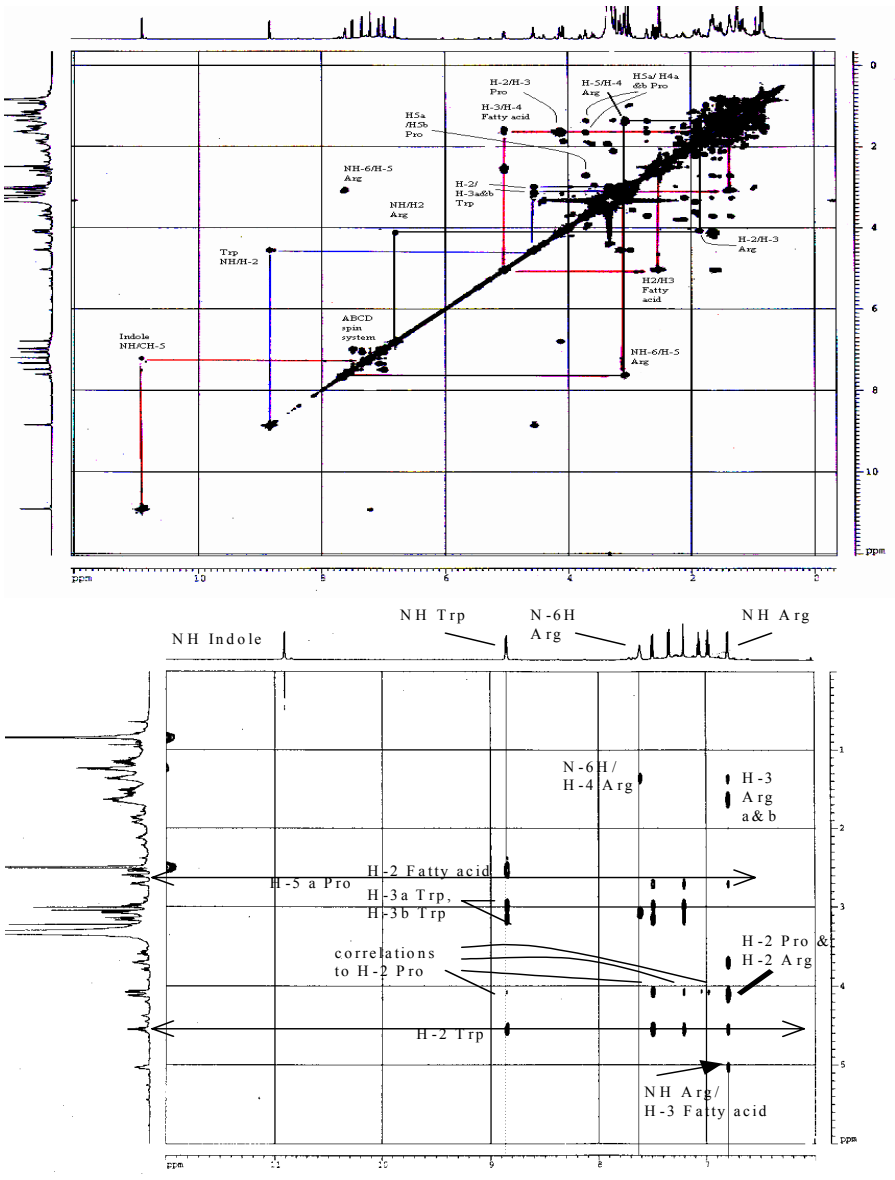

Fig (3.1.27): Total COSY spectrum (up) showing different spin systems and NH-detected ROESY correlations (down) of compound 3

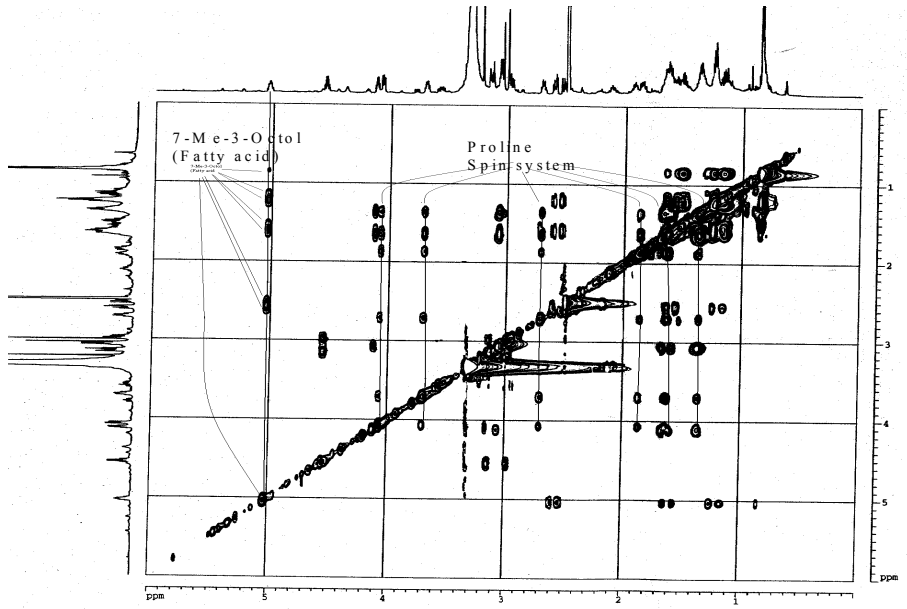

Fig (3.1.28): Total TOCSY spectrum (up), and part of TOCSY spectrum showing proline and Fatty acid spin systems of compound 3 (down).

Table (3.1.6): NMR data of compound 3 in DMSO-d_6

Amino acid	Carbon	1H NMR, ppm	Multiplicity , J= Hz	ROESY correlations
Tryptophan	1	(NH) 8.85	d, *J*=6.9	Pro H-2; F.A H-2
	2	4.55	q, *J*=7.4	Trp H-3, H-5
	3	3.14; 2.98	m; dd, *J*=14.7, 7.1	Trp H-5
	5	7.19	d, *J*=1.9	indole NH, Trp H-2, H-8, H-11; Pro H-5
		(NH) 10.91	d, *J*=1.3	Trp H-5;
	8	7.34	d, *J*=8.2	
	9	7.05	t, *J*=7.6	
	10	6.97	t, *J*=7.3	
	11	7.48	d, *J*=8.2	
Proline	2	4.07	m	Arg NH, Trp NH
	3	1.60; 1.90	m; m	
	4	1.41; 1.63	m; m	
	5	3.70; 2.72	m; m	
Arginine	1	NH, 6.78	d, *J*=5.68	Arg H-3a &b, NH-6; Pro H-2; Trp H-2; F.a H-3
	2	4.1	m	
	3	1.68;158	m	
	4	1.39	m	
	5	1.03	m	
	6	7.63	br t, *J*= 5.6	
9-Me-3-Decol (F.A)	2	2.52; 2.61	dd, *J*= 14.7, 5.6; dd, *J*= 14.7, 7.0	F.A H-3; Trp NH;
	3	5.05	p, 6.3	Arg NH
	4	1.57;167	m; m	
	5	1.25	m; m	
	6	1.15	m	
	7	1.52	m	
	8	0.84	d, *J*= 6.3	
	9	0.84	d, *J*= 6.3	

3.1.4- **Kahalalide B (4, Known compound)**

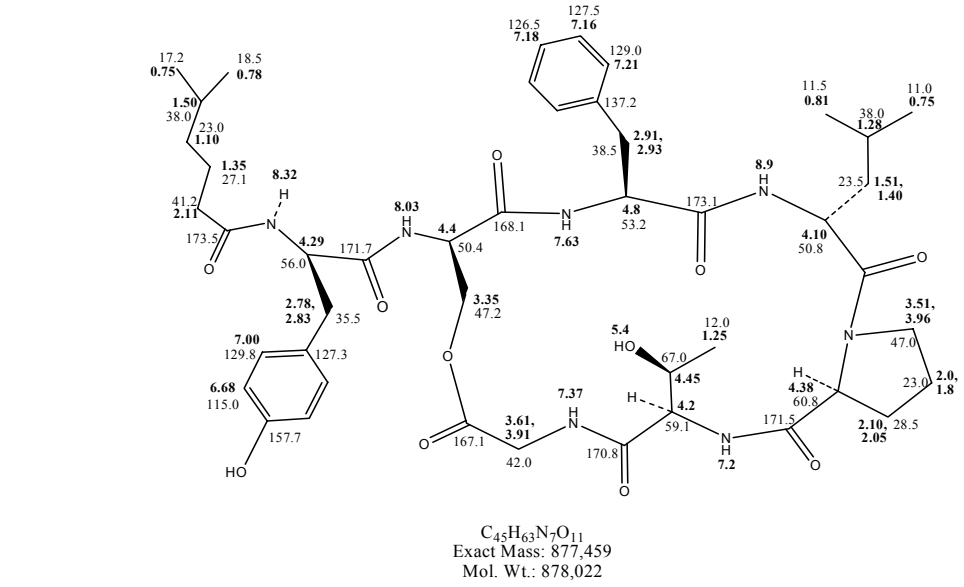

$C_{45}H_{63}N_7O_{11}$
Exact Mass: 877,459
Mol. Wt.: 878,022

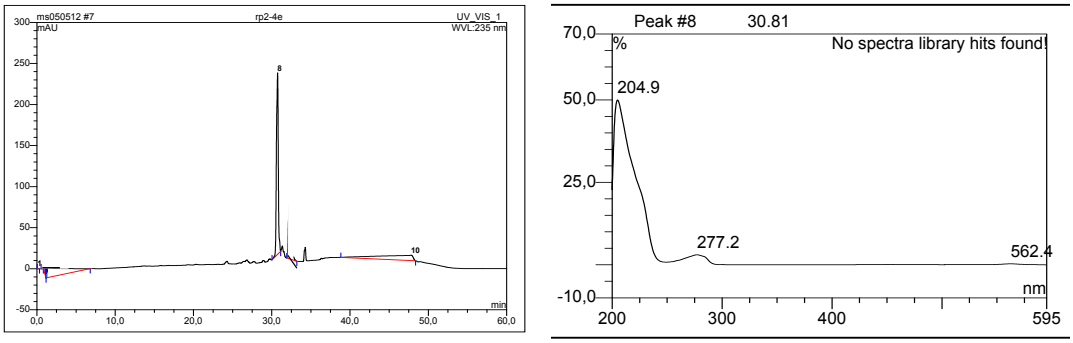

Fig (29) : compound 4 (Kahalalide B)

Yield : 5 mg

Kahalalide B was isolated as a white amorphous powder, with $[\alpha]^{20}_{D}$ of + 35° (*c* 0.25 MeOH). It has UV absorbance at λ_{max} 205, 228sh, 277 nm. ESI-MS showed positive pseudomolecular ion peak *m/z* 878.8 $[M+1]^+$ and 895.6 $[M+H_2O]^+$, 1774.9 $[2M+H_2O]^+$ and 1755.8$[2M+1]^+$ and negative pseudomolecular ion peak *m/z* 913.1 $[M+HCOOH-1]^-$, 975 $[M+H_3PO_4-1]^-$, suggesting the molecular formula $C_{45}H_{63}N_7O_{11}$. The ^{1}HNMR spectrum of **4** showed 6 deshielded amide-N*H* resonances in the lower field region, at δ 8.90 (d, *J*= 0.9 Hz), 8.32 (d, *J*= 5.4 Hz), 8.03 (d, *J*= 9.6 Hz), 7.63 (d, *J*= 9.4 Hz), 7.37 (t, *J*= 6.2 Hz), and 7.20 (d, *J*= 7.3 Hz) of Leu, Tyr, Ser, Phe, Gly, and Thr, respectively, suggesting the peptidic nature of the compound. COSY spectrum together with TOCSY experiment indicated 6 spin systems

commencing from the above mentioned 6 N*H* resonances as mentioned in table 3.1.8, in addition to the characteristic proton resonances of *p*-disubstituted benzene ring (the rest of Tyrosine protons) at δ 6.68 (d, *J*= 8.2 Hz) and 7.0 (d, *J*=8.2 Hz) and proton resonance cluster at δ 7.16-7.21 (5 aromatic proton of phenylalanine). COSY and TOCSY spectra revealed the presence of two more spin systems which were assigned to proline and 5-methyl hexanoic acid (see table 3.1.8). As in the case of kahalalide F, kahalalide B showed a second regio-isomer of 5MeHex. ^{13}C chemical shifts were extracted from HMQC and HMBC spectra as mentioned in table 3.1.8.

HMBC and ROESY experiments established the connectivity of the individual spin systems. The N*H*s of Thr, Gly, Ser, Phe, and Leu at δ 7.20, 7.37, 4.4, 7.63 and 8.90, respectively showed a ROESY correlation to Pro *H*-2, Thr *H*-2, Phe N*H*, Ser *H*-2 and Phe *H*-2, at δ 4.38, 4.2,7.63, 4.4 and 4.8, respectively, thus the connections of the amino acids Thr-Gly-Ser-Phe-Leu were determined. The connectivity of Leu to Pro was established by ROESY through NOEs between Leu *H*-2 at 4.1 ppm and Pro *H*-5 at 3.51 ppm. Furthermore, the sequence [5MeHex-Tyr-Ser] was established through NOEs between Tyr N*H* and Tyr *H*-2 at 8.32 and 4.29, respectively to *H*-2 of 5MeHex and Ser N*H* *at* δ 2.11, and 8.03, respectively.

Again Ser-Gly connectivity through the ester bond between the terminal C-3 of Ser and the carboxyl of Gly was confirmed by HMBC correlation of Ser H-3 at δ 3.35 to the carboxyl at 167.1 ppm. The above deduced connectivities of the different amino acids were confirmed through additional HMBC correlations. N*H*s of Leu, Tyr, Ser, Phe, Gly, and Thr showed HMBC correlations to vicinal carbonyls at 173.1, 173.5, 171.7, 168.1, 170.8, 171.5 of Phe, 5MeHex, Tyr, Ser, Thr, and Pro respectively. ROESY, COSY, TOCSY and HMBC as well as ^{1}HNMR and ^{13}C NMR data are identical to those of kahalalide B (Hamann *et al* 1996).

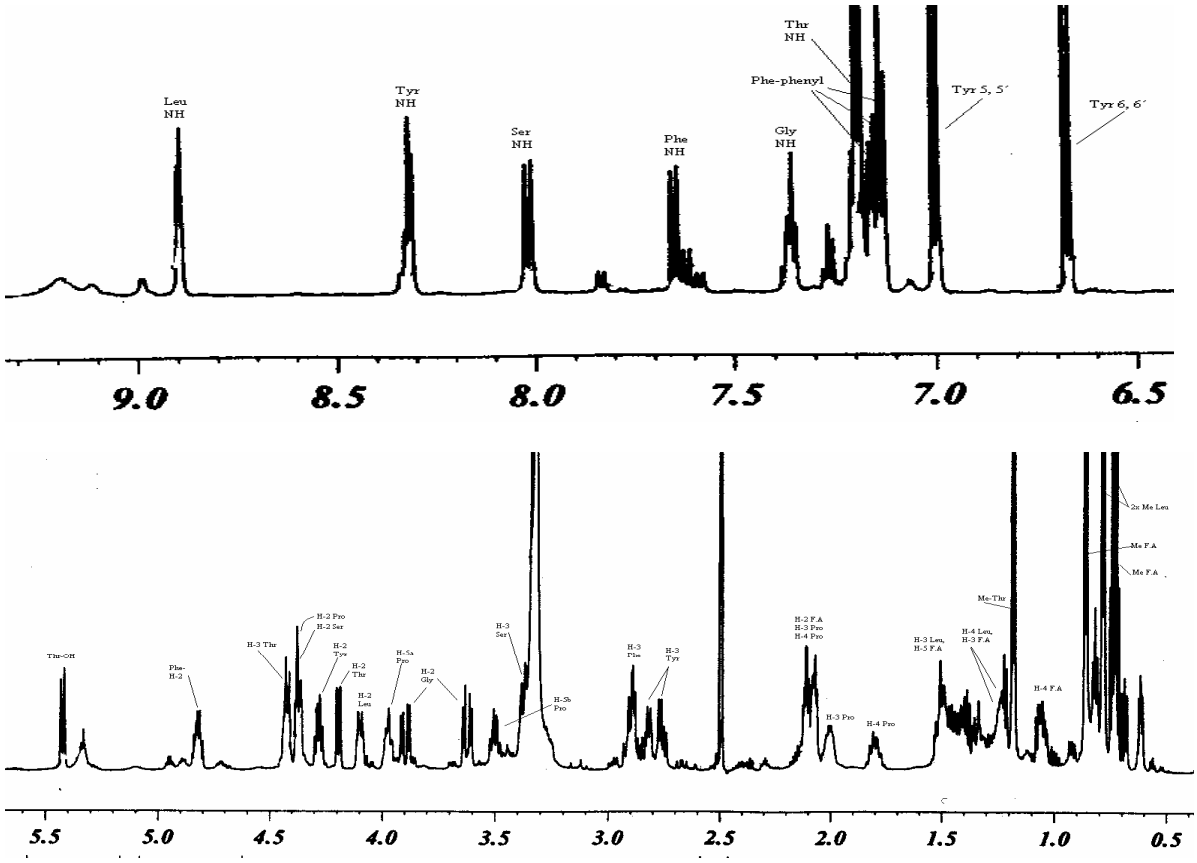

Fig (3.1.30): ^{1}H NMR spectrum, NHs and aromatic region (up), and α-protons and higher field region (down)

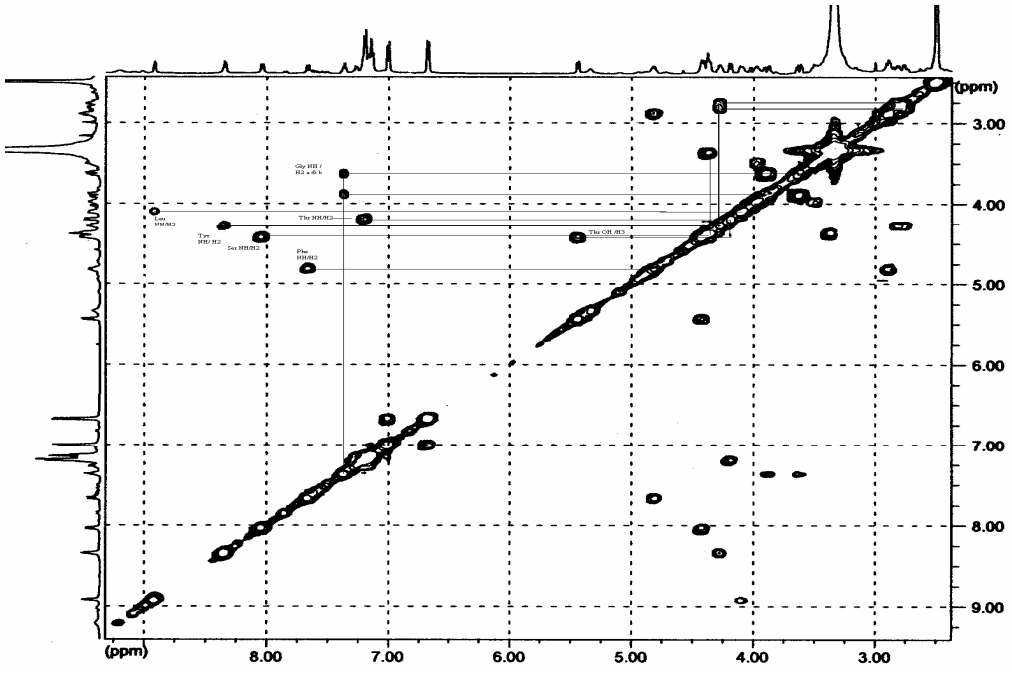

Fig (3.1.31) : Part of COSY spectrum of compound 4, showing Lower field part

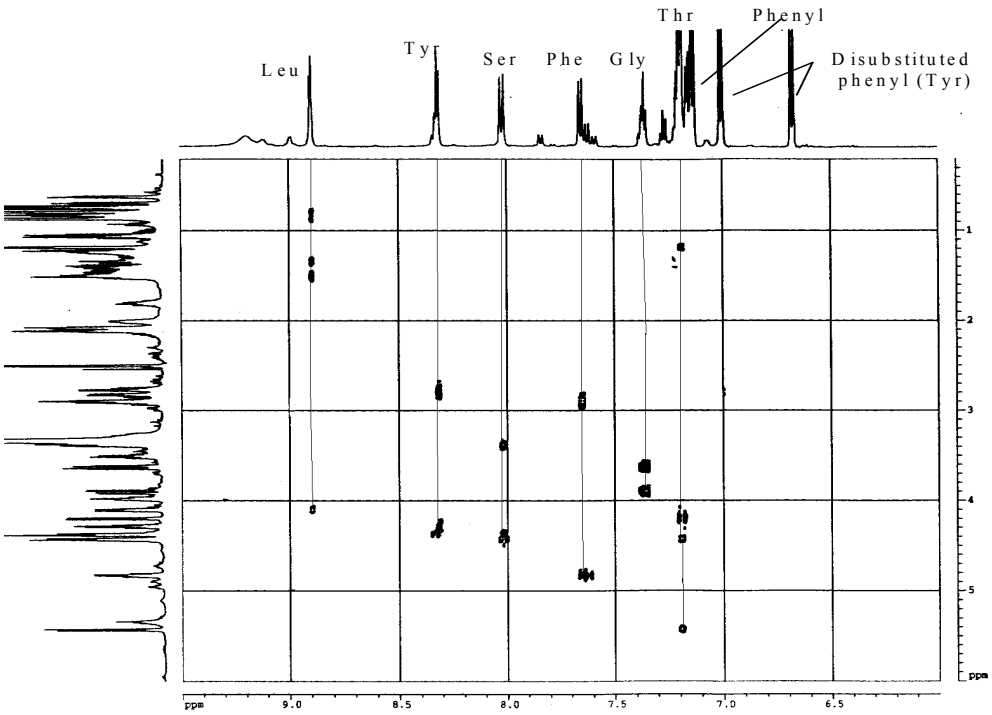

Figure (3.1.32): Parts of TOCSY spectrum , NH-detected spin systems (up).

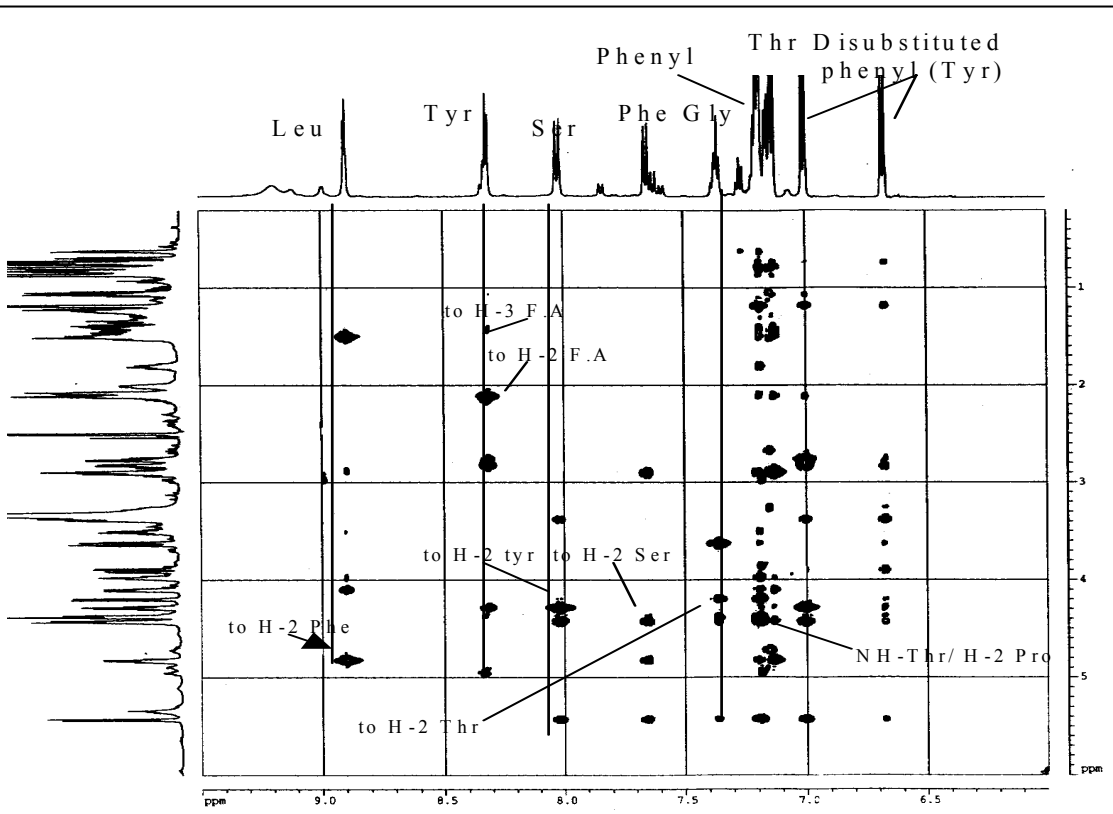

fig (3.1.33): Parts of ROESY spectrum of compound 4, N*H*/N*H* correlation (up-left), higher field region (up-right) and N*H*/ aliphatic proton correlations (down)

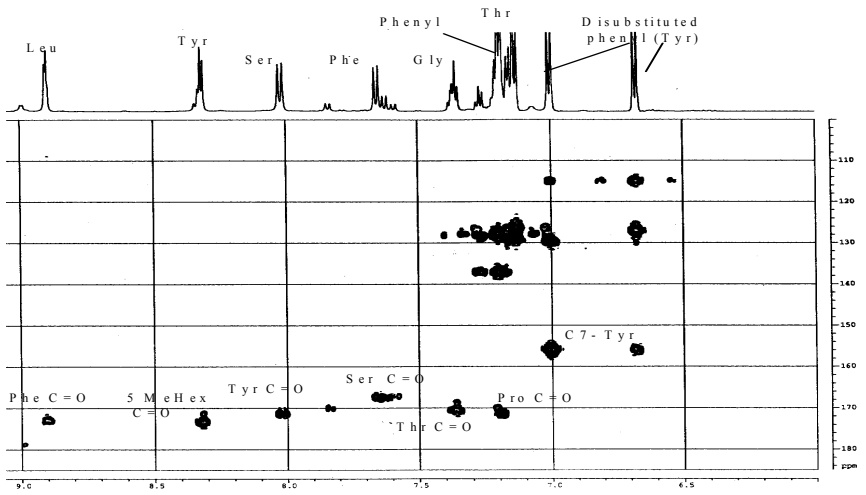

Fig (3.1.34): Part of HMBC spectrum of compound 4 showing NH-detected correlations to vicinal carbonyls.

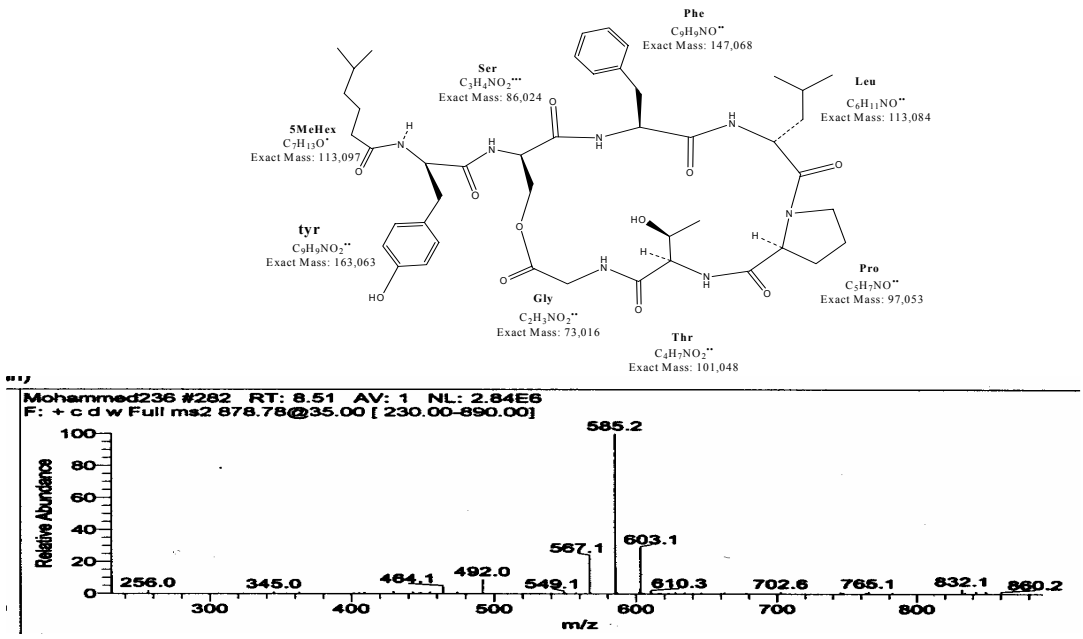

Fig (3.1.35): ESI-MS/MS of compound 4

Table (3.1.7) ESI-MS/MS Fragment ions of compound 4 and sequence determination

Ion composition	*m/z*
M-[C_2H_5OH (Thr side chain)]+1	832.1
M-[Fatty acid] +1	765.1
M-[Fatty acid + C_2H_5OH+ H_2O] +1	702.6
M-[Fatty acid + Tyr] +1	603.1
M-[Fatty acid + Tyr + H_2O] +1	585.2
M-[Fatty acid + Tyr +2 H_2O] +1	567.1
Tyr + Ser + Phe + Leu –[H_2O] + 1	492.0
Tyr + Ser + Phe + Leu –[H_2O + C=O] + 1	464.1
Ser + Phe + Leu –[H_2] + 1	345.0
Pro + Thr + Gly +1	256.0

Table (3.1.8) : ^{1}H and ^{13}C NMR data of compound 4 in DMSO-d_6

Amino acid	Carbon	^{13}C NMR ppm, Mult	1H NMR, ppm	Multiplicity, J= Hz
Gly	1	167.1 s	(NH) 7.37	t, *J*= 6.2
	2	42.0 t	3.61 &3.91	dd, *J*= 17.4, 5.4; dd *J*=17.6, 5.9
Thr	1	170.8 s	(NH) 7.20	d, *J*= 7.3
	2	59.1 d	4.2	dd, *J*= 8.8, 1.0
	3	67.5 d	4.45	m
	OH		5.4	d, *J*= 9.2
	4	12.0q	1.25	d, *J*= 7.3
Pro	1	171.5 s		
	2	60.8 d	4.38	m
	3	28.5 t	2.10, 2.05	m,m
	4	23.0 t	1.80, 2.00	m,m
	5	47.0 t	3.51, 3.96	dd, *J*= 16.7, 8.8; dd, *J*= 6.5, 9.5
Leu	1	172.5	(NH) 8.90	d, *J*= 0.9
	2	50.8 d	4.1	m
	3	23.5 t	1.4 , 1.51	m,m
	4	38.0 d	1.28	m
	5	11.0 q	0.75	d, *J*= 7.1
	6	11.5 q	0.81	d, *J*= 7.1
Phe	1	173.1 s	(NH) 7.63	d, *J*= 9.4
	2	53.2 d	4.8	dd, *J*= 15.5, 8.8
	3	38.5 t	2.91, 2.93	m;m
	4	137.2 s		
	5,5´	129.0 d	7.21	m
	6,6´	127.5 d	7.16	m
	7	126.5 d	7.18	m
Ser	1	168.1 s	(NH) 8.03	d, *J*= 9.6
	2	50.4 d	4.4	m
	3	47.2 t	3.35	m
Tyr	1	171.7 s	(NH) 8.32	d, *J*= 5.4
	2	56.0 d	4.29	dd, *J*= 13.3,7.3
	3	35.5 t	2.78 , 2.83	dd, *J*= 14.1, 8.5; dd *J*=14.8, 7.2
	4	127.3 s		
	5,5´	129.8 d	7.0 0	d, *J*=8.2
	6,6´	115.0 d	6.68	d, *J*= 8.2
	7	157.7 s		
5-MeHex	1	173.5 s		
	2	41.2 t	2.11	t, *J*= 7.2Hz
	3	27.1 t	1.35	m
	4	23.0 t	1.10	m
	5	38.0 d	1.5	m
	6	11.5 q	0.75	d, J= 6.9
	7	12.0 q	0.78	d, J=6.9 H-7

3.1.5- Kahalalide C (5, known compound)

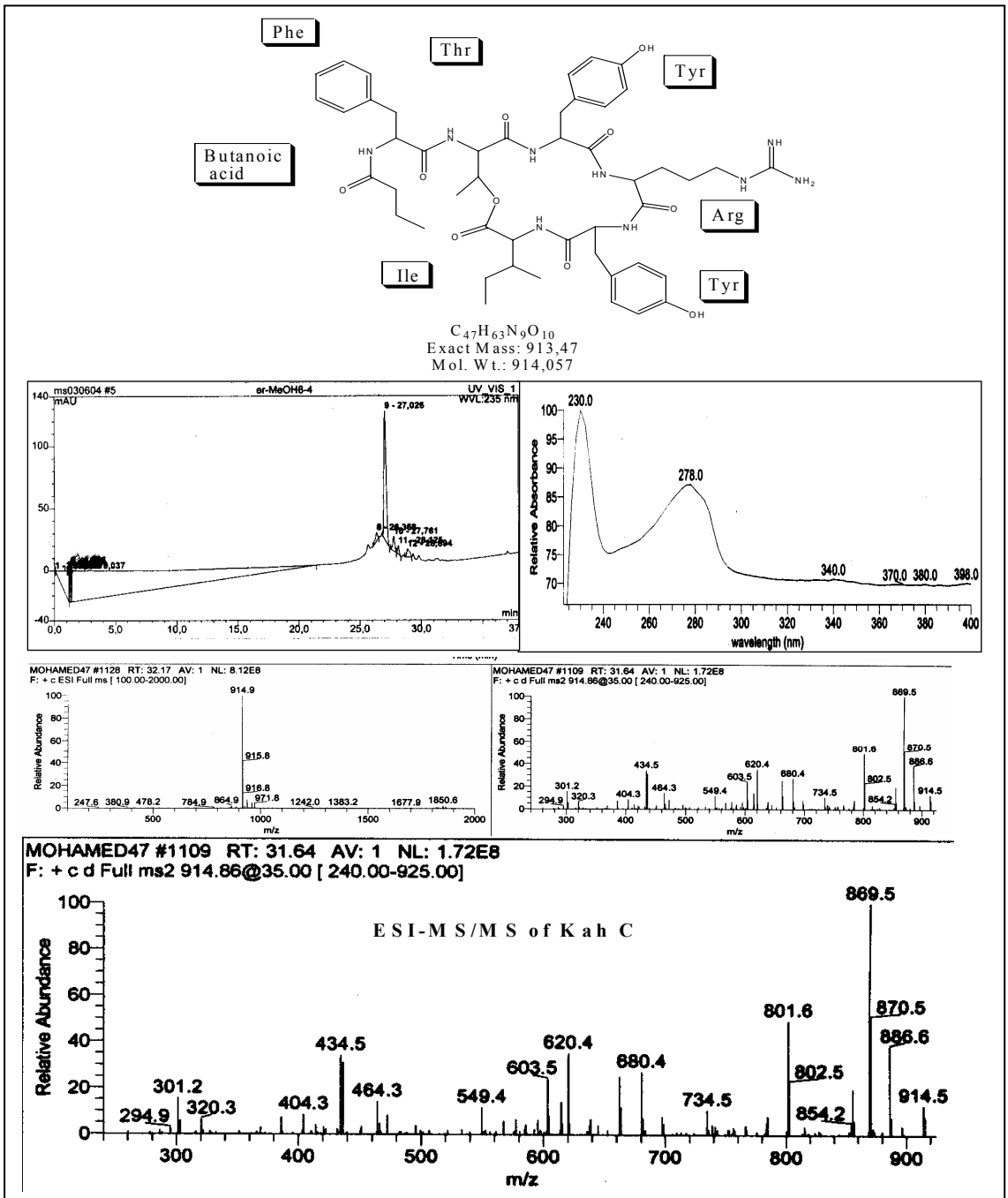

Fig(3.1.36):Compound 5 (kahalalide C).

Yield : 1 mg

Kahalalide C was isolated as a white amorphous powder, with $[\alpha]_D$ of + 40° (*c* 0.11 MeOH). It has UV absorbance at λ_{max} 230, 278 nm. ESI-MS showed pseudomolecular ion peak *m/z* 914 $[M+1]^+$ and 937 $[M+Na]^+$, 953 $[M+K]^+$ and 971$[M+K+H_2O]^+$ and

pseudomolecular ion peak *m/z* 913.1 $[M-1]^-$, 1827 $[2M-1]^-$. MALDI-TOF-MS showed positive pseudomolecular ion peak at *m/z* 914 $[M+1]^+$ and 937 $[M+Na]^+$, suggesting the molecular formula $C_{47}H_{63}N_9O_{10}$. The indivdual amino acids and the sequence were established through interpretation of both ESI-MS/MS [see figure 3.1.36 and table 3.1.9] and MALDI-TOF-PSD [see figure 3.1.38 and table 3.1.10]. This kahalalide was previously isolated from the same mollusc (*E. rufescens*) which was collected from the same geographical zone (Hamann *et al* 1996).

Table (3.1.9) ESI-MS/MS Fragment ions of compound 5 and sequence determination

Ion composition	*m/z*
M-[OH] +1	897
M-[C=O] +1	886.4
M-[C_2H_5OH (Thr side chain)]+1	869.4
M-[guanidine] +1	855.5
M-[Ile] +1	801.3
M-[Ile + H_2O] +1	783.2
M-[Tyr] + 1	752.3
M-[Phe + Fatty acid] + 1	697.3
M-[Phe + Fatty acid + OH] + 1	680.3
M-[Phe + Fatty acid + OH + OH] + 1	662.4
M-[Ile + Tyr + H_2O] + 1	620.2
M-[Ile + Tyr + H_2O + NH_3] + 1	603.3
[Arg + Tyr + Thr + Phe - H_2O] +1	549.4
[Tyr + Thr + Phe + Fatty acid - H_2O] +1	463.9
Tyr + Thr + Phe + Fatty acid – [C=O + OH]	436.0
[Tyr + Thr + Phe + Fatty acid – (C=O+H_2O)] +1	434.2
Arg + Tyr + Ile –[C=O]	404.1
[Arg + Tyr + Thr –(NH_2 + OH)] +1	386.0
[Arg + Tyr] +1	320.7
[Arg + Tyr –(OH)] +1 //also // [Thr + Phe + Fatty acid – (OH)] + 1	302.9

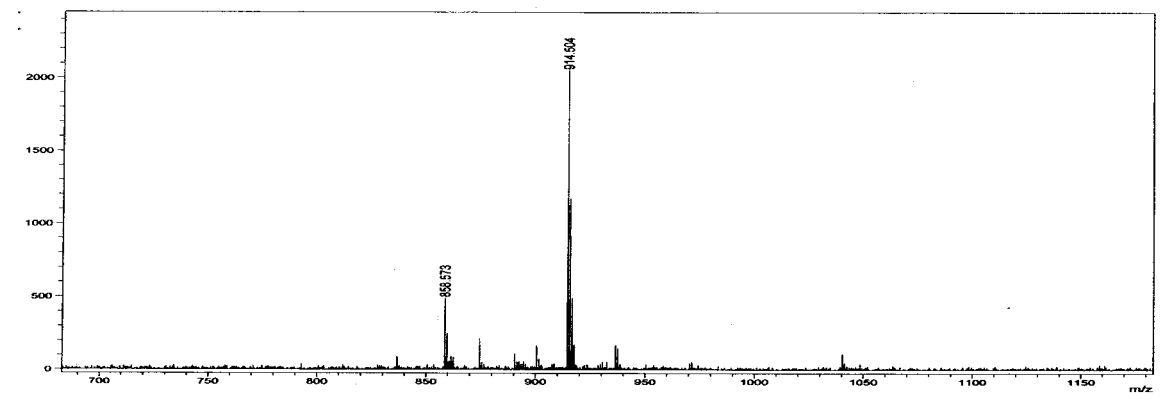

Fig (3.1.37): MALDI-TOF-MS of compound 5

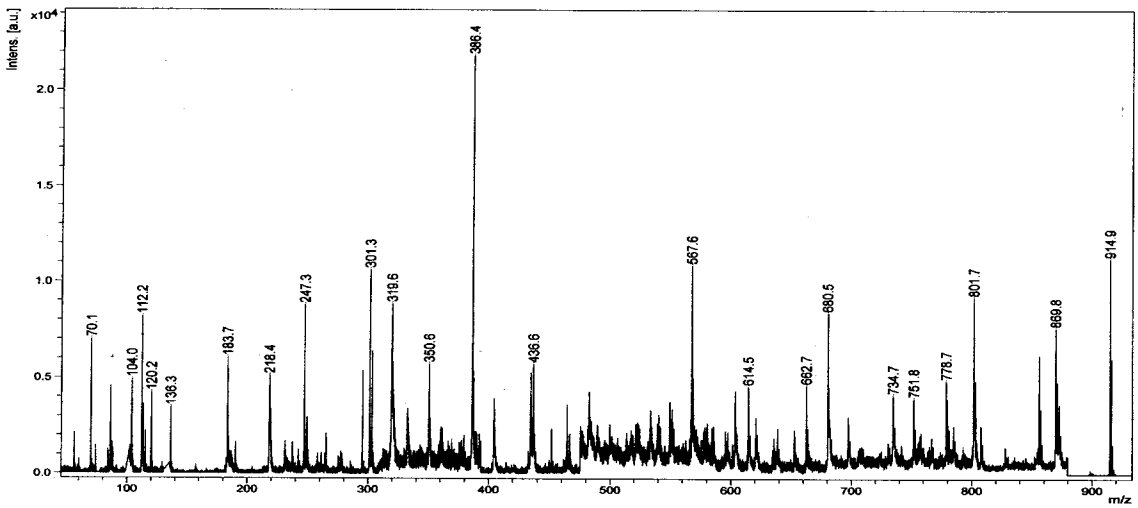

Fig (3.1.38): MALDI-TOF-PSD-MS of compound 5

Table (3.1.10) MALDI-TOF-PSD Fragment ions of compound 5 and sequence determination

Ion composition	*m/z*
M-[C_2H_5OH (Thr side chain)]+1	869.8
M-[guanidine] +1	855.4
M-[Ile] +1	801.7
M-[Ile + H_2O] +1	783.2
M-[Tyr] + 1	751.8
M-[Tyr + OH] + 1	734.7
M-[Phe + Fatty acid] + 1	697.3
M-[Phe + Fatty acid + OH] + 1	680.5
M-[Phe + Fatty acid + OH + OH] + 1	662.7
M-[Ile + Tyr + H_2O + NH_3] + 1	603.3
M-[Arg + Tyr + (C=O)] + 1	567.6
[Ile + Tyr + Arg + Tyr - (C=O)] + 1	567.6
[Arg + Tyr + Thr + Phe - H_2O] +1	549.4
[Tyr + Thr + Phe + Fatty acid - H_2O] +1	463.9
Tyr + Thr + Phe + Fatty acid – [C=O + OH]	436.6
[Tyr + Thr + Phe + Fatty acid – (C=O+H_2O)] +1	434.2
Arg + Tyr + Ile –[C=O]	404.1
[Arg + Tyr + Thr –(NH_2 + OH)] +1	386.4
[Tyr + Thr + Phe – (C=O + OH + NH)] +1	350.6
[Arg + Tyr] +1	320.7
[Thr + Phe + Fatty acid]+ 1	319.6
[Arg + Tyr –(NH_3)] +1	304.0
[Arg + Tyr –(OH)] +1 //also // [Thr + Phe + Fatty acid – (OH)] + 1	302.9
[Thr + Phe + Fatty acid – H_2O]+ 1	301.3
Arg + Tyr – [C=O]	292.2
Thr + Tyr – [OH]	247.3
Phe + Fatty acid	218.7
Arg + NH	183.7
Tyr-[C=O]	136.3
Phe – [C=O]	120.2
Ile – [H_2] +1	112.2
Phe – [NH + C=O]	104.0
Ile – [C=O]	86.1
Arg-[Guanidine + C=O]	70.1

3.1.6 – N,N-dimethyl Tryptophane metyhl ester (6, new marine natural product)

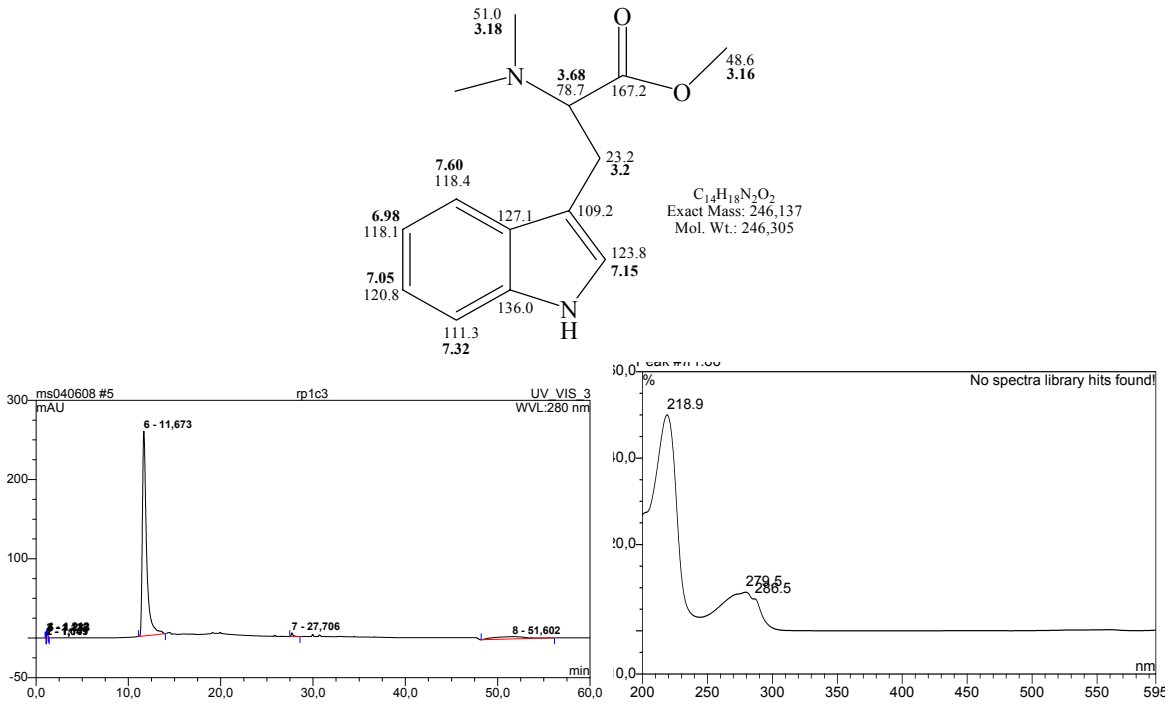

Fig (3.1.39):Compound 6, structure with ^{1}H and ^{13}C- chemical shift values (up), HPLC chromatogram (down left), UV-spectrum (down right).

Yield : 4.6 mg

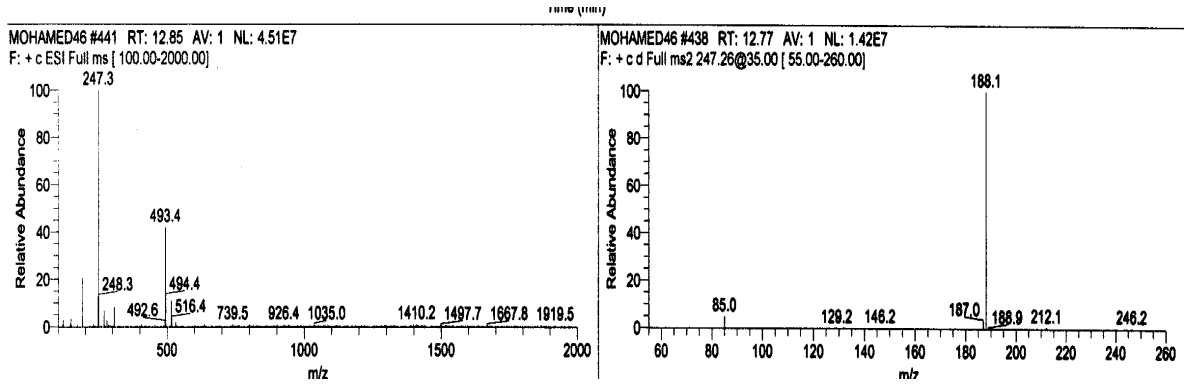

Fig (3.1.40): ESI-MS (left), ESI-MS/MS of compound 6 (right).

Compound **6** [N,N-dimethyl-tryptophan methyl ester] was isolated as a brownish white amorphous powder, with $[\alpha]_D$ of + 20° (*c* 0.25 MeOH). It has UV absorbance of typical indole compounds at λ_{max} 218, 279(sh), 286(sh) nm. ESI-MS showed positive pseudomolecular ion peak *m/z* 247 $[M+1]^+$ and 493 $[2M+1]^+$, 515 $[2M+Na]^+$ and negative pseudomolecular ion peak *m/z* 245.4 $[M-1]^-$, 291.6 $[M + HCOO^-]^-$, 537.8 $[2M + HCOO^-]^-$, suggesting the molecular formula $C_{14}H_{18}N_2O_2$. ^{1}H NMR spectrum showed characteristic proton resonances of tryptophan at δ 3.68 (1H, dd, *J*=10.1,3.8 Hz, H-2), 3.20 (2H, m, H-3), 7.15 (1H, d, *J*=1.2 Hz, H-5), 7.32(1H, d, *J*=8.2 Hz, H-8),7.05(1H, t, *J*=7.3 Hz, H-9), 6.98(1H, t, *J*=7.0 Hz, H-10), 7.6(1H, d, *J*=8.2 Hz, H-11), 10.86 (1H, s, NH), in addition to one methoxy group at δ 3.16 (3H, s) and two N-methyls at δ 3.14 (6H, s). ^{13}C NMR showed the presence of one carboxyl at δ 167.2 (s. C-1), the presence of methoxy carbon and two N-methyls were confirmed by resonances at δc 48.6 ppm and 51.0 ppm respectively. The α- and β-carbon resonances of Trp were evident at 78.7 and 23.2 ppm respectively. COSY spectrum established the connection of H-2 to H-3 and demonstrated the characteristic ABCD spin system of indole moiety. The exchangeable N*H* was confirmed by measuring of the ^{1}HNMR in deuterated methanol. The connection of one methyl to carboxyl and the substitution of the two amino protons with two methyls were confirmed through HMBC correlations between δ_H at 3.16 and δc 167.2 ppm and between δ_H at 3.18 and δc 78.7 ppm respectively as shown in table 3.1.11 and figure 3.1.45. These NMR data and UV-spectrum were identical with those of the terrestrial natural product [N,N-dimethyl-tryptophan methyl ester] which has been previously isolated from the Australian fabaceous plant *Pultenaea altissima* (Fitzgerald 1963). To the best of our knowledge this is the first report of **6** as a marine natural product.

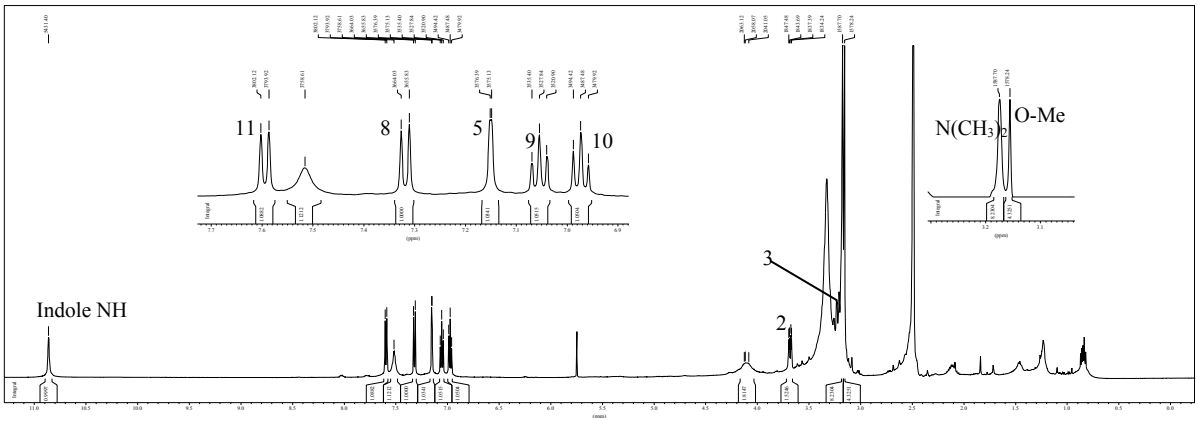

Figure (3.1.41): ^{1}H NMR spectrum of compound 6 meassured in DMSO-d$_6$

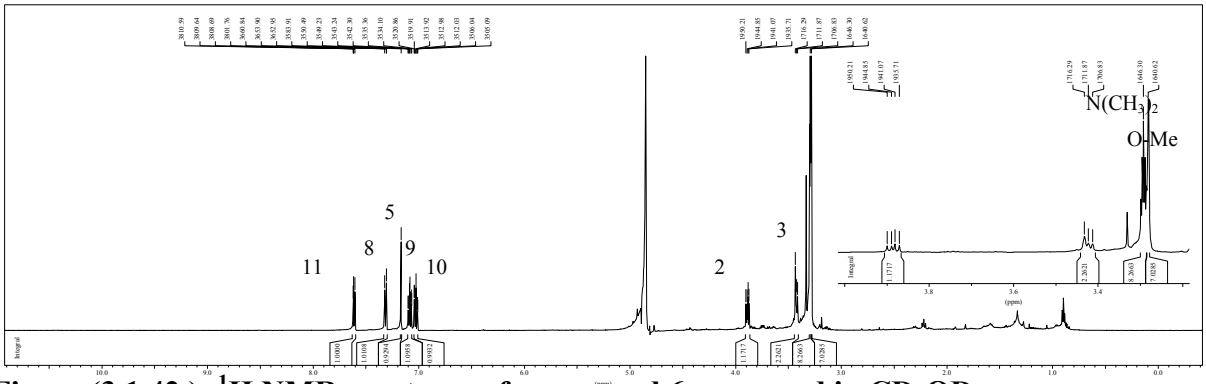

Figure (3.1.42): ^{1}H NMR spectrum of compound 6 measured in CD_3OD

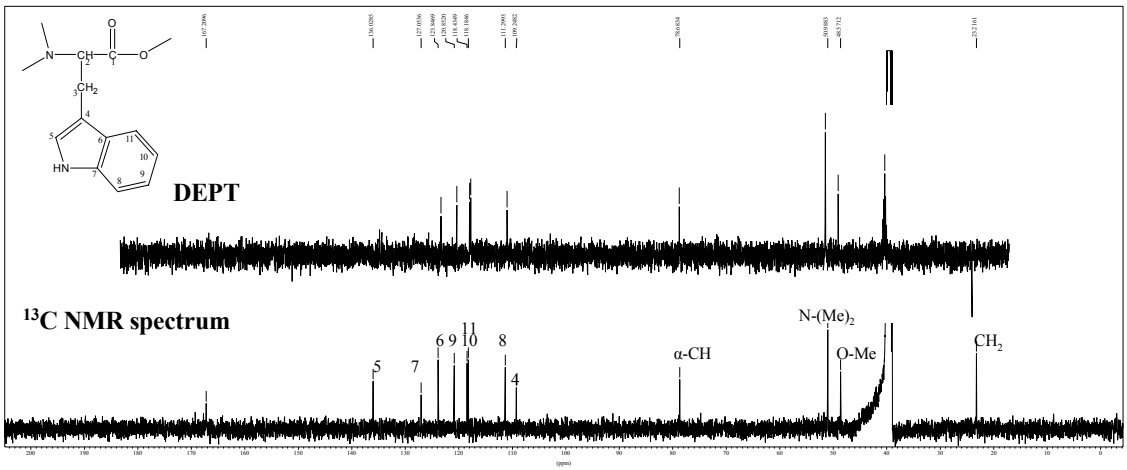

Figure (3.1.43): ^{13}C NMR and DEPT spectra of compound 6

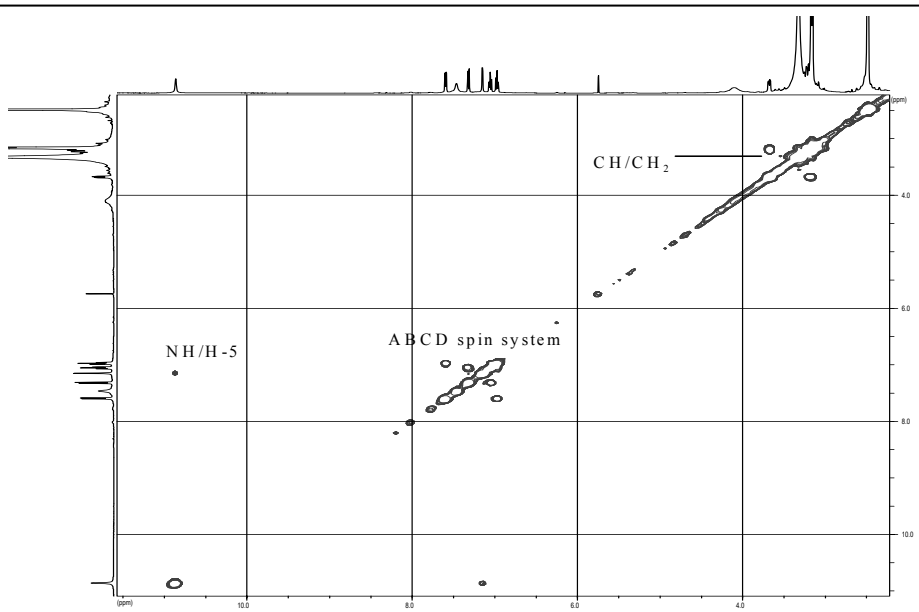

Fig (3.1.44): COSY spectrum of compound 6.

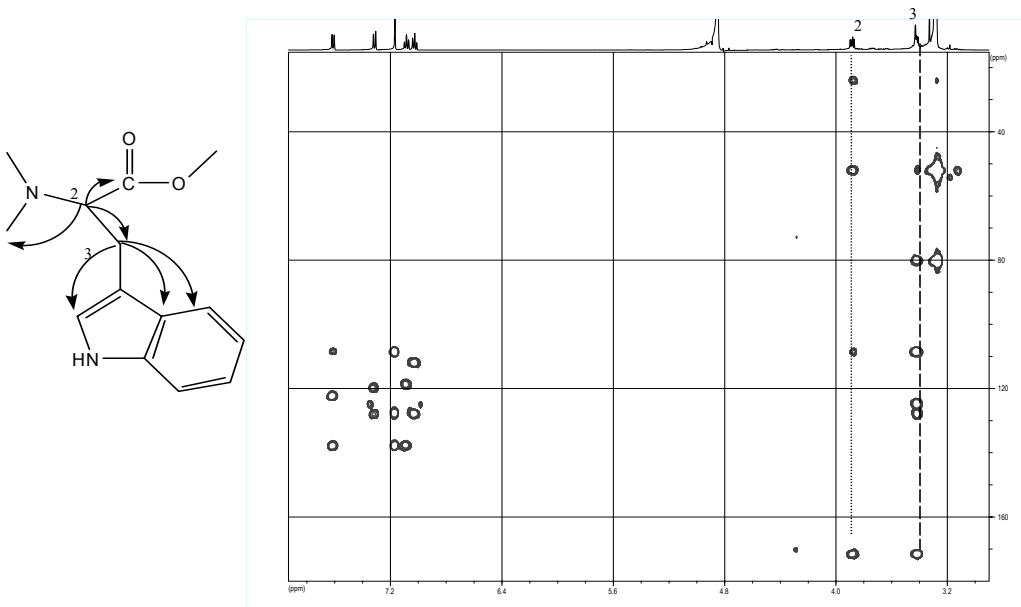

Fig (3.1.45) HMBC of compound 6 [Methanol-d_4]

Table (3.1.11): NMR data of 6 (500 MHz, DMSO-d_6),

Carbon	**^{13}C NMR, ppm**	**^{1}H NMR*, ppm** (Multiplicity, *J*= Hz)	**^{1}H NMR, ppm** (Multiplicity, *J*= Hz)	HMBC H -------C
1	167.2 s			
2	78.7 d	3.86 (dd, *J*=9.1; 5.4)	3.68 (dd, *J*=10.1; 3.8)	C-1, C-4, C-3, $N(CH_3)_2$
3	23.2 t	3.41 (m)	3.20 (m)	C-1, C-2, C-4, C-5, C-6, $N(CH_3)_2$
4	109.2 s			
5	123.8 d	7.16 (s)	7.15 (d, *J*=1.2)	C-4, C-6, C-7
			(NH) 10.86 (s)	C-6
6	127.1 s			
7	136.0 s			
8	111.3 d	7.32 (d, *J*=7.9)	7.32 (d, *J*=8.2)	C-6, C-10
9	120.8 d	7.08 (dt, *J*=1.0,6.9)	7.05 (t, *J*=7.3)	C-7, C-11
10	118.1 d	7.03 (dt, *J*=1.0, 6.9)	6.98 (t, *J*=7.0)	C-6, C-8
11	118.4 d	7.61 (dd, *J*=7.9, 1.0)	7.6 (d, *J*=8.2)	C-4, C-7, C-9
OMe	48.6 q	3.28 (s)	3.16 (s)	
$N-(CH_3)_2$	51.0 q, q	3.28 (s , s)	3.18 (s , s)	C-2, C-3, N-Me

- meassured in (CD_3OD)

3.1.7- β-sitosterol(7, Known compound):

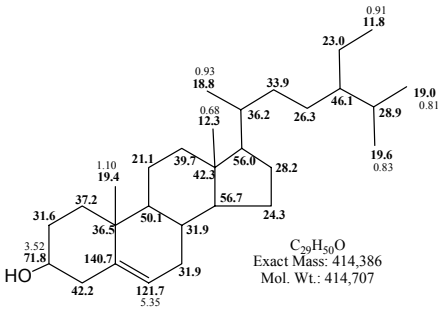

Fig (3.1.46): compound 7

Yield : 15 mg

Compound **7** [β-sitosterol] was isolated from the ether fraction of the total exract as a white amorphous powder, with $[\alpha]_D$ of - 37° (*c* 0.35 $CHCl_3$). EI-MS showed molecular ion peak *m/z* 414 $[M]^+$ and fragment ions at 386, 368, 271, 255, 69, 55, 43 suggesting the molecular formula $C_{29}H_{50}O$. ^1H NMR spectrum showed resonances for six methyl groups at δ 0.68 (3H, s, Me-18), 1.10 (3H, s, Me-19), 0.93 (3H, d, *J*=6.2 Hz, Me-21), 0.81 (3H, d, *J*=7.25 Hz, Me-27), 0.83 (3H, d, *J*=7.57 Hz, Me-26) and 0.86 (3H, t, *J*=7.11 Hz, Me-29). The resonances at δ 5.35 (1H, m, H-6), 3.52 (1H, m, H-3) were indicative for Δ^{5-6} mono hydroxylated steroidal nucleus (Itoh *et al* , 1983).^{13}C NMR showed six methyl signals at δ 11.8, 19.4, 18.8, 19.6, 19.0 and 12.3 for the methyl groups 18, 19, 21, 26, 27 and 29, respectively. ^{13}C NMR spectrum showed one quaternary olefenic carbon resonating at δ 140.7 and one olefenic CH at 121.7 and oxygenated methine at 71.8, in addition to two quaternary aliphatic carbons, 7 aliphatic methines, and 11 aliphatic methylenes (see table 3.1.12). The above NMR data were identical with those of β-sitosterol, which was previously isolated from many other natural sources (Greca *et al* , 1990).

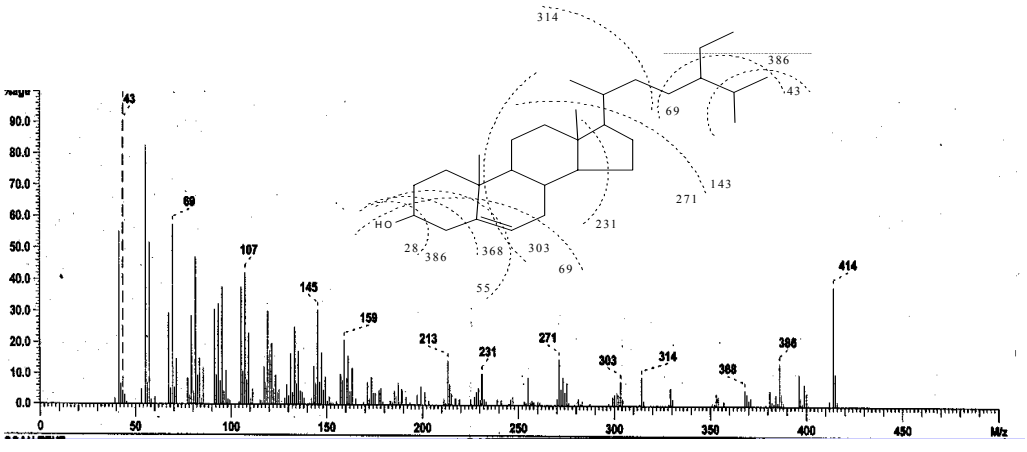

Fig (3.1.47):EI-MS spectrum of compound 7

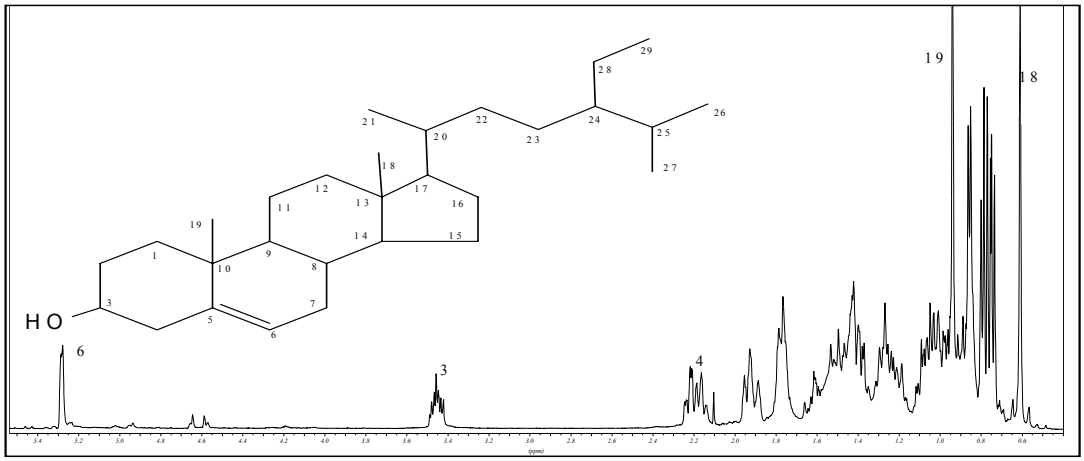

Fig (3.1.48): ^{1}HNMR spectrum of compound 7 ($CDCl_3$)

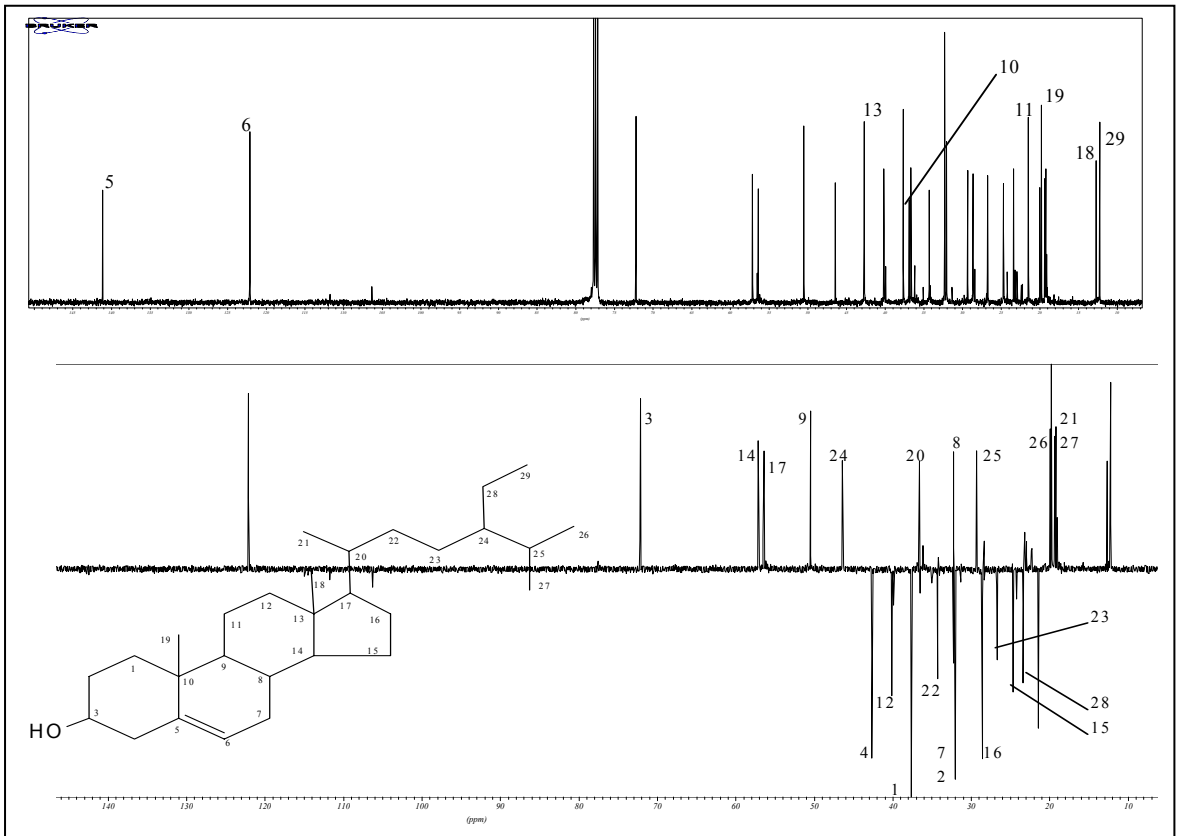

Fig (3.1.49): ^{13}CNMR and DEPT spectra of compound 7 ($CDCl_3$)

Table (3.1.12): ^{1}H, ^{13}C-NMR data of compound 7 in ($CDCl_3$, 500, MHz)

No.	^{13}C (Multiplicity)	^{1}H (Multiplicity, Hz)
1	37.2 t	*
2	31.6 t	*
3	71.8 d	3.52 (m)
4	42.2 t	*
5	140.7 s	-
6	121.7 d	5.35 (m)
7	31.9 t	*
8	31.9 d	*
9	50.1 d	*
10	36.5 s	-
11	21.1 t	*
12	39.7 t	*
13	42.3 s	*
14	56.7 d	*
15	24.3 t	*
16	28.2 t	*
17	56.0 d	*
18	12.3 q	0.68 (s)
19	20.4 q	1.10 (s)
20	36.2 d	*
21	18.8 q	0.93 (d, *J*=6.2 Hz)
22	33.9 t	*
23	26.3 t	*
24	46.1 d	*
25	28.9 d	*
26	19.6 q	0.83 (d, *J*=7.5 Hz)
27	19.0 q	0.81 (d, *J*=7.3 Hz)
28	23.0 t	0.82 (d, 6.6 Hz)
29	11.8 q	0.86 (t, *J*=7.1 Hz)

* not confirmed $\delta_{H,}$ because they are present in the highly overlapping multiplet signals of aliphatic methines and methylenes in the higher field region between 1.00 and 2.28 ppm.

Bioactivity :

Compound **1** (kahalalide F) was reported as the most active kahalalide. Kahalalide F was reported to have a significant biological activity against solid tumour cell lines, human colon and lung cancers and some pathogenic microorganisms that cause the opportunistic infections of HIV/AIDS. Its mode of action and preclinical toxicity have also been studied. It is currently in Phase I and II clinical trials. Kahalalide F displays both *in vitro* and *in vivo* antitumor activity in various solid tumor models, including colon, breast, non–small cell lung, and in particular prostate cancer. *In vitro* antiproliferative studies showed activity among certain prostate cancer cell lines (PC-3, DU-145, T-10, DHM, and RB), but no activity was found against the hormone-sensitive LnCAP. *In vivo* models also confirmed selectivity and sensitivity of the prostate tumor xenograft derived from hormone-independent prostate cancer cell lines, PC-3 and DU-145. Further *in vitro* evaluation showed selective activity but not

restricted to prostate tumor cells. Suares *et al*, 2003 revealed that kahalalide F induces cell death via oncosis preferentially in tumor cells. (Hamann *et al* 1993, Hamann *et al* 1996, García-Rocha et al 1996, Sewell et al 2005, Janmaat et al 2005, Suarez et al 2003, Brown et al 2002, Ciruelos, et al 2002, Rademaker-Lakhai et al 2005). Kahalalide A was reported to have antimalarial and antituberculosis activity (Hamann et al, 1996; Copp 2003 and El-Sayed et al 2000). Furthermore kahalalide E was reported to have selective anti-viral activity against *Herpes simplex* (Hamann et al, 1996).

The cytotoxic activity studies of **1** against three different cell lines (L5178Y, Hela, and PC12) and showed ED_{50} values of **1** as 6.3µg/ml, 6.7µg/ml and >10 µg/ml respectively. The cytotoxicity assays were summerized in Figure (3.1.50). Compounds **1** (kahalalide F), **3** (kahalalide D) and **4** (kahalalide B) showed mild antibacterial activity against *B. subtilis* and *S. cereviisae*. Kahalalide B showed significant cytotoxicity (99 % inhibition) compared to kahalalide D (65.2 % inhibition), kahalalide E (94.8 %), while compound **6** showed no significant activity against L5178Y cancer cell line at concentration of 10µg/ml each, see figure (3.1.51).

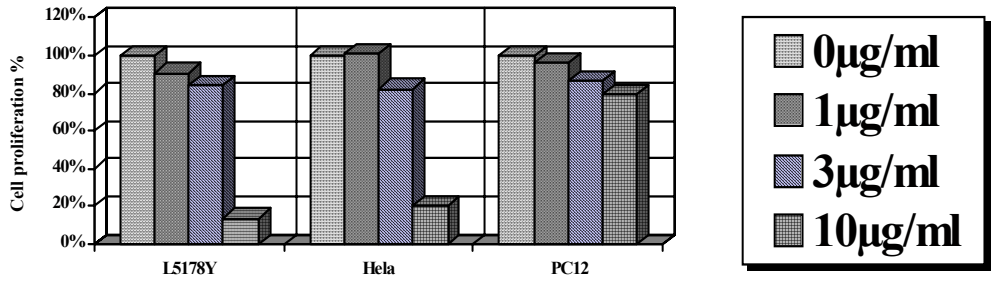

Fig (3.1.50): *In vitro* cytotoxicity assay of kahalalide F against three different cancer cell lines .

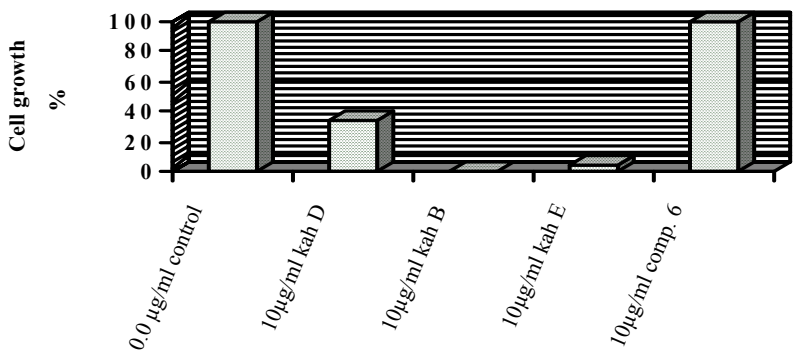

Fig (3.1.51): *In vitro* cytotoxicity assay of compound 2 (kah E), 3 (kah D), 4 (kah B) and 6 (N,N-dimethyl tryptophan methyl ester) against L5178Y cells .

3-2 Natural Products from *Elysia grandifolia*:

Although many natural products were isolated from the genus *Elysia* this is the first report for isolated natural products from *E. grandifolia*. Our interest with this sacoglossan mollusc came up by the strong biological activity of its crude MeOH extract. Organic extracts from the specialist herbivore *E. grndifolia* and its dietary green alga *Bryopsis plumosa* exhibited antimicrobial, cytotoxicity, feeding deterrence and ichthyotoxicity (Padmakumar 1998, Bhosale et al , 1999).

Dereplication procdure using LC-MS was applied for targeting new natural products from *E. grandifolia.* Inspection of the LC-MS chromatograms suggested the presence of kahalalide derivatives giving molecular ion peaks corresponding to kahalalides B, C, D, E, F, G, J, K, O (see figures 2-15 and 2-16). The presence of two unidentified peaks at m/z 1520.2 and 1536.0 aroused our interest to do further chemical work on the mollusc extract.

Chemical investigation of Indian sacoglossan mollusc *E. grandifolia* Kelaart 1858, yielded two known analogues, kahalalide F (53.0 mg) and D (3.4 mg) along with two other new kahalalide derivatives, which we designated as kahalalide R (20 mg) and S (3.4 mg). The structural elucidation of the new kahalalides R and S will be discussed in detail.

3.2.1 Kahalalide R (8, New natural product)

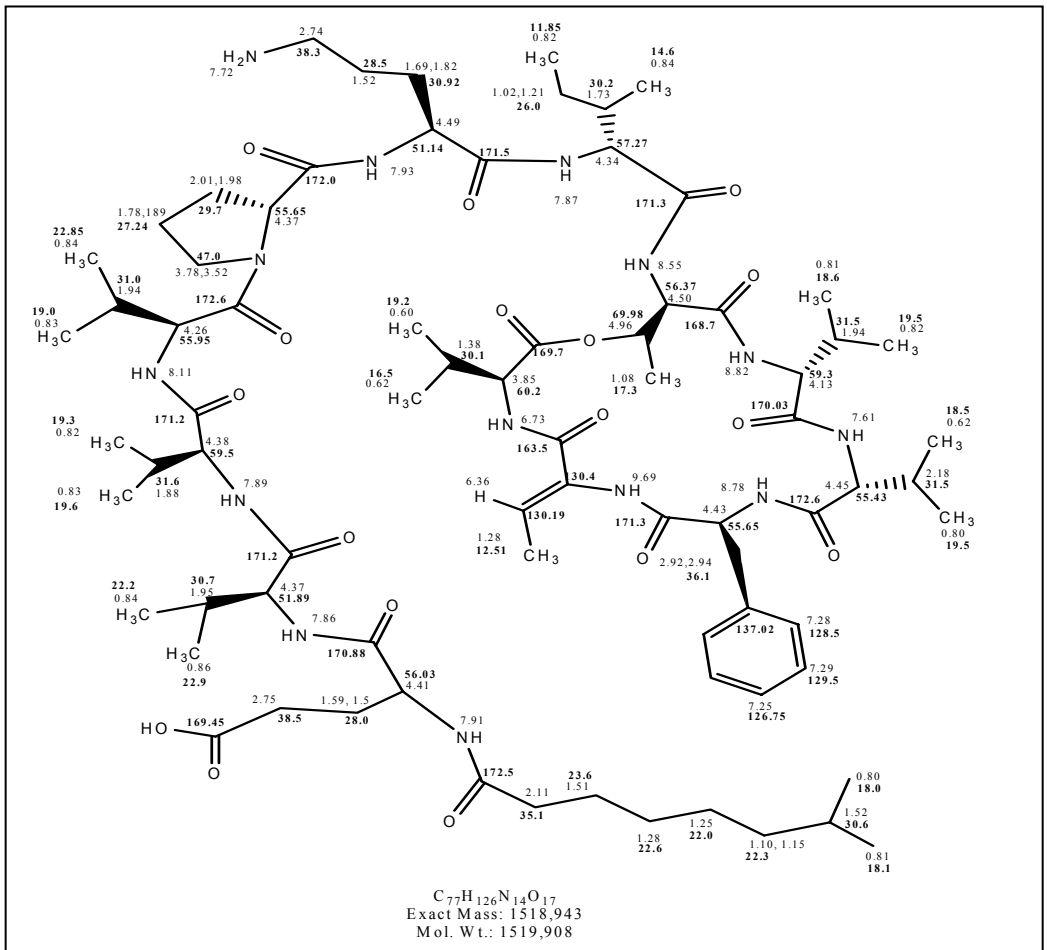

Fig (3.2.1): Compound 8, kahalalide R.

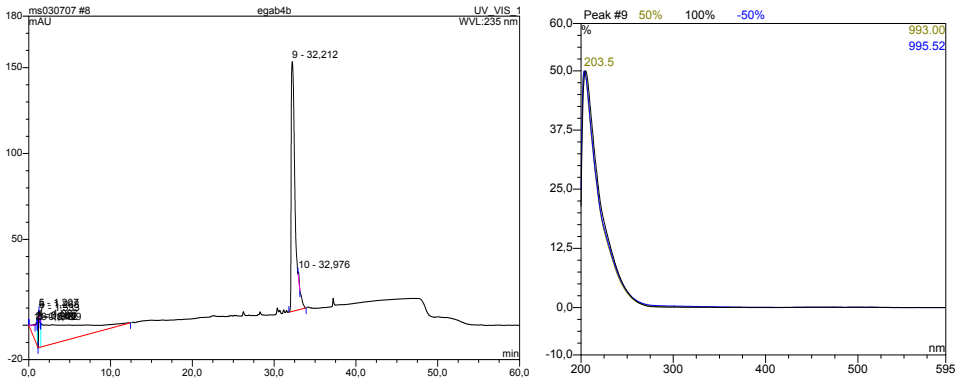

Fig (3.2.2): HPLC chromatogram and UV spectrum of compound 8.

Yield : 20 mg

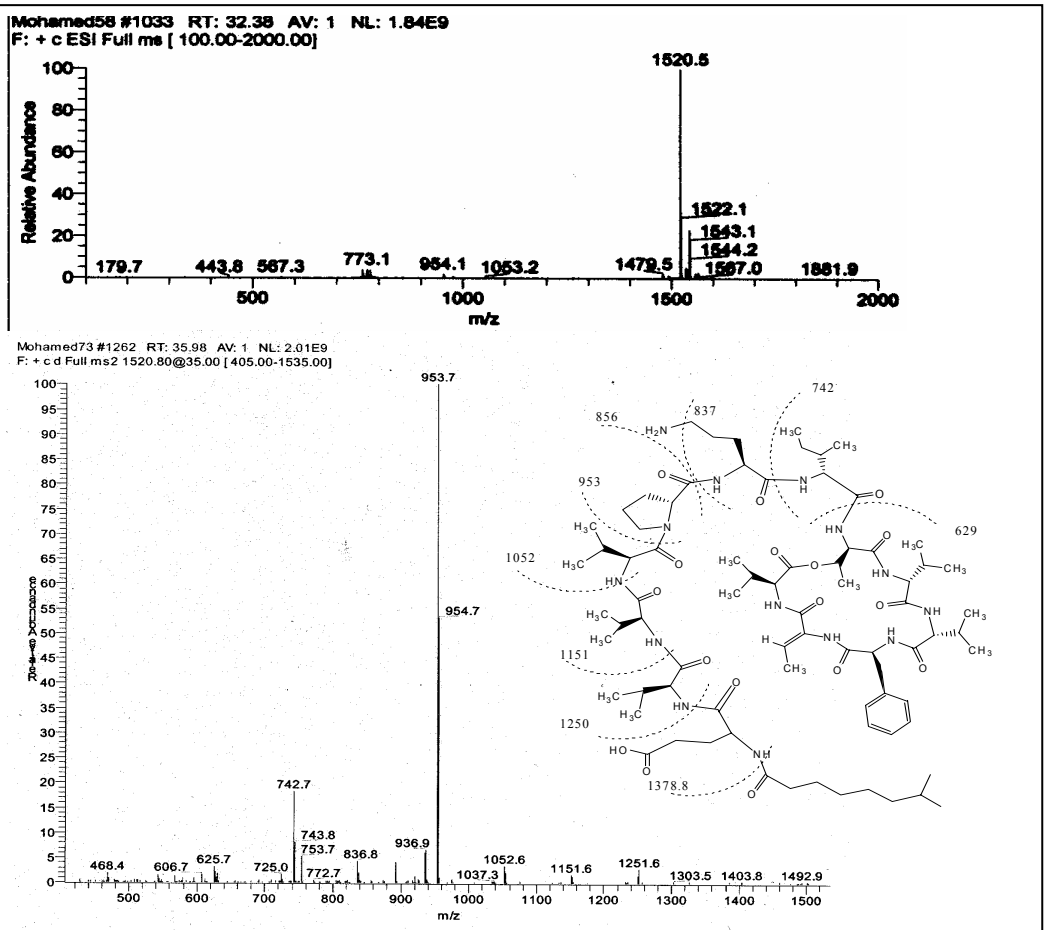

Fig (3.2.3) : ESI-MS (up) and ESI-MS/MS (down) of compound 8

Kahalalide R (compound **8)** was obtained as a white amorphous powder. The reflector mode MALDI-TOF mass spectrum of **8** performed with delayed extraction showed positive monoisotopic ion peaks at *m/z* 1520.2, $[M+H]^+$, 1542.2 $[M+Na]^+$, and 1557.2 $[M+K]^+$. In (+)-ESI-MS, a pseudomolecular ion was detected at *m/z* 1520.8 $[M+H]^+$ that was compatible with the molecular formula $C_{77}H_{127}N_{14}O_{17}$ as established by HRESIMS. The ^1H and ^{13}C NMR data of **8** were comparable to those of kahalalide F (compound **1)**, but had a higher molecular weight of 42 mass units. Inspection of the ^1H and ^{13}C NMR spectra of **8** revealed that kahalalide R shared very similar structural features with kahalalide F. As in **1**, the region between 6.50 and 9.70 ppm of the ^1H spectrum of **8** accounted for a similar number of 14 deshielded amide N*H* resonances. Eleven of those are doublets, one is a singlet at δ 9.69 for the α,β-unsaturated amino acid *Z*-Dhb, and a broad 2H singlet at δ 7.69 for the terminal NH_2 of Orn. Like kahalalide F, compound **8** was also ninhydrin-positive, thus supporting the presence of a free amino group found in Orn. The aromatic region also disclosed the presence of Phe, the only aromatic amino acid in the structure of the new analogue as well as in the known congener (kahalalide F). An apparent difference observed between the ^1H spectrum of

8 and **1**, was the absence of a second methyl triplet at δ 1.02 that suggested the loss of one Ile unit in the structure of the new derivative. Major differences to kahalalide F were more obvious from the ^{13}C NMR and DEPT spectra of **8**. The ^{13}C NMR spectrum displayed 77 carbons signals instead of 75 carbons as in kahalalide F. An additional carbonyl signal was observed between 163.5 and 174.1 ppm. Again, the DEPT spectrum also revealed the presence of 12 regular amino acid residues in the new analogue **8**, as indicated by the 12 α-methine carbon signals between 51.0 and 60.0 ppm. The DEPT spectrum showed 15 instead of 12 methylene carbons and a loss of an oxygenated methine carbon signal in the 65 to 75 ppm region, which further indicated a deficit of one Thr unit that was replaced by another amino acid compared to kahalalide F. Similar to kahalalide F, the sp^2-carbon region of the ^{13}C NMR spectrum of **8** showed evidence for the occurrence of Phe and Dhb. The ^{13}C NMR and DEPT spectral data were in agreement with the molecular formula as determined by HRMS.

The COSY spectrum of **8** revealed 14 spin systems, 12 of which commenced with a deshielded amide N*H* doublet while two other spin systems showed no correlations to any amide N*H* proton and were then allotted to Pro and a saturated fatty acid. The COSY spectrum indicated the presence of 7-methyloctanoic acid (7-Me-Oct). Kahalalide R contained a linear *n*-alkyl side chain that showed an *iso*- type methyl branching at the terminus of the alkyl chain similar to that found in kahalalide F, which could be detected in the COSY spectra of both **8** and **1**. Sequential correlations of the iso-fatty acid (7-Me-Oct) observed from the α-methylene signal at δ 2.11 to the subsequent methylenes at δ 1.51 (H_2-3), 1.28 (H_2-4), 1.25 (H_2-5), and 1.10/1.15 (H_2-6), which then terminated with an aliphatic methine proton at δ 1.52 (H-7) and two methyl functions at δ 0.80 and 0.81. In the ^{13}C and DEPT spectra of the latter, characteristic signals appeared for the terminal carbon atoms, i.e., C_ω, $\delta_{C-8/9}$ 22.5 (2 × q); $C_{\omega-1}$, δ_{C-7} 27.3 (d); and $C_{\omega-2}$, δ_{C-6} 38.3 (t) which were unequivocally assigned by HMQC (see Table 3.2.2).

A TOCSY experiment corroborated the assignments obtained from the COSY spectrum. The TOCSY spectrum unambiguously resolved the amine- and α-proton resonances of each of the different 13 amino acid residues in the structure of the new depsipeptide congener **8**. Kahalalide R (**8**) was thus shown to contain six units of Val, one unit each of Phe, *a*Ile (*allo*-Ile), *a*Thr (*allo*-Thr), Orn, Pro, Glu, also the unusual Dhb, and 7-Me-Oct. In the new analogue, Val and Glu units replaced Thr and Ile previously found in kahalalide F. The TOCSY spectrum allowed the overlapping 12 methyl doublets (J = 6.5 Hz) that belong to the six Val units, which occur between 0.60 and 0.85 ppm, to be explicitly assigned to their

respective spin systems. The presence of Glu also further explains the additional carbonyl signal observed in the ^{13}C NMR spectrum while the extra two methylene carbons could be accounted for by the replacement of the 7-methyl-hexanoic acid (7-Me-Hex) in kahalalide F with 7-methyl-octanoic acid (7-Me-Oct) in compound **8**. Again, two structural regio-isomers of the fatty acid moiety could be identified in the TOCSY spectrum of **8**.

HMBC and ROESY experiments established the connectivity and sequence of the amino acids in the peptide structure of **8** (Figure 3.2.4). The sequence 7-Me-Oct–Glu–Val-6–Val-5–Val-4, which was elucidated as fragment I, was established through the HMBC correlations of N*H* signals at δ 7.93, 7.86, 7.89, and 8.11 for Glu, Val-6, Val-5, and Val-4, respectively, to each of their neighboring vicinal (^2J) carbonyls of 7-Me-Oct, Glu, Val-6, and Val-5 resonating at δ 172.5, 170.9, and 171.2, respectively. Connectivities for fragment II, Pro–Orn–*a*Ile– *a*Thr–Val-3–Val-2–Phe–*Z*-Dhb–Val-1, were similarly determined through HMBC correlations of the N*H* signals at δ 7.93, 7.87, 8.55, 8.82, 7.61, 8.78, 9.69, 6.73, respectively, to their neighboring vicinal carbonyls at δ 172.6, 171.5, 171.3, 168.7, 170.0, 172.6, 171.3, and 163.5, respectively. The cyclization of Val-1 to *a*Thr was confirmed by an HMBC cross peak between the carboxyl signal at δ 169.7 for Val-1 and the β-proton of *a*Thr at δ 4.96, which arises from a characteristic low field acylation shift. This ring closure was corroborated by the ROESY correlation of the β-proton of *a*Thr with the α-proton of Val-1 at δ 3.85. The connectivity of fragment I with II was established through the HMBC correlation of the δ-proton of Pro at δ 3.52 with the carbonyl of Val-4 at 172.6 ppm. This was in agreement with the ROESY cross peak between the δ-proton of Pro at 3.78 ppm and the α-proton of Val-4 at 4.26 ppm.

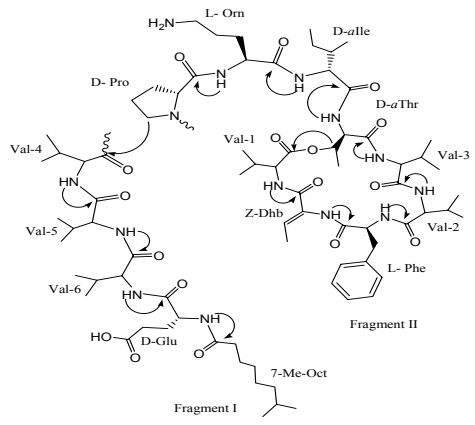

Figure 3.2.4. Key HMBC correlations of kahalalide R (8)

The ROESY spectrum of compound **8** also indicated the *Z* stereochemistry of dehydroaminobutyric acid as shown by the NOE effect of the sharp N*H* singlet at δ 9.69 on the methyl doublet at δ1.28 (*J* = 6.93 Hz). Together with kahalalides F and G, the new analogues kahalalides R (**8**) and S (**9**), are the only derivatives that contain the amino acid *Z*-Dhb. This uncommon amino acid, *Z*-Dhb, was reported as a constituent of peptides isolated from terrestrial blue-green algae (Moore *et al* 1989), and from an herbivorous marine mollusc (Pettit *et al* 1989).

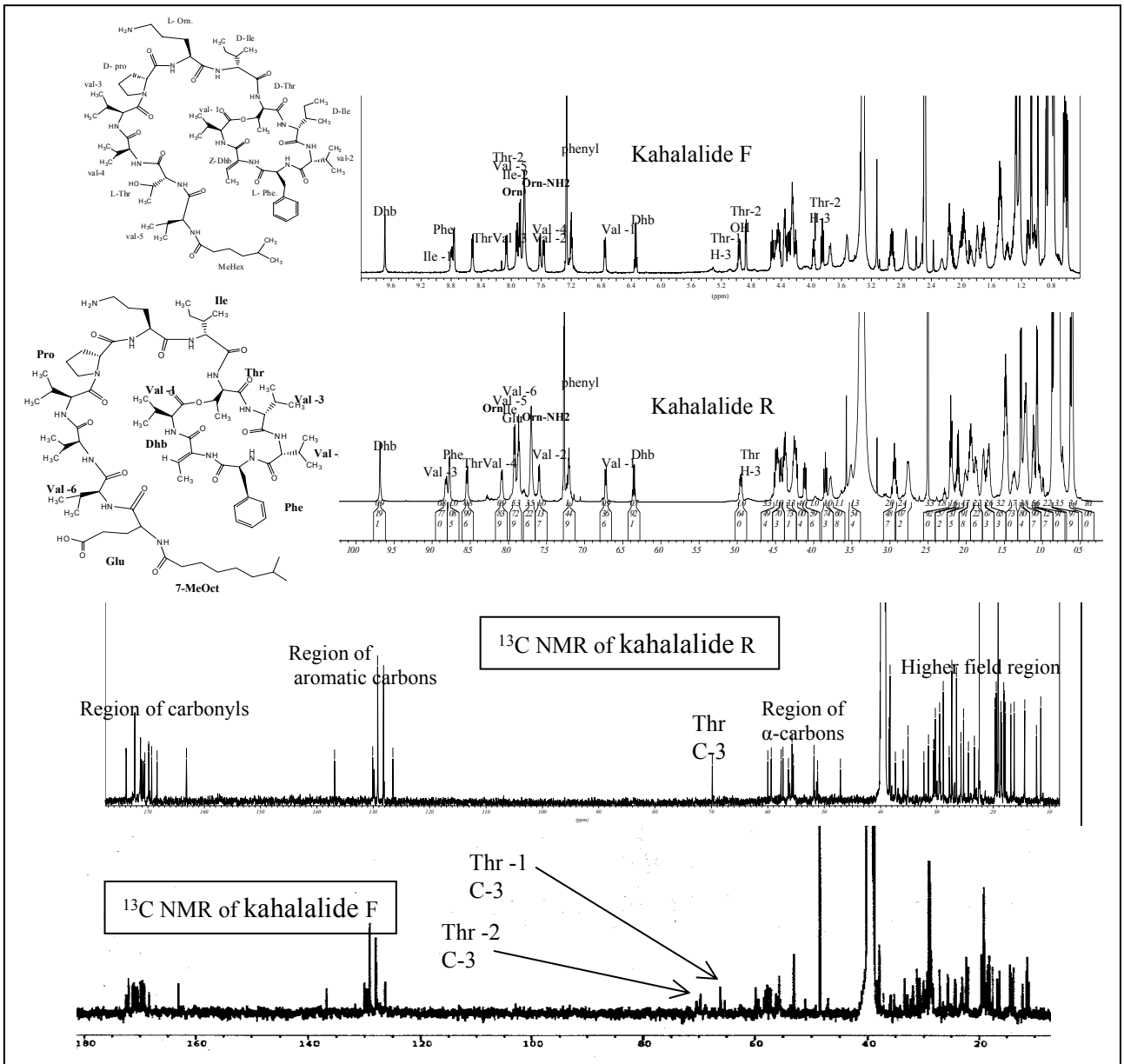

Fig (3.2.5): Comparison between ^{1}H NMR of kahalalide F and R (up) and between ^{13}C NMR of kahalalide R and F (down).

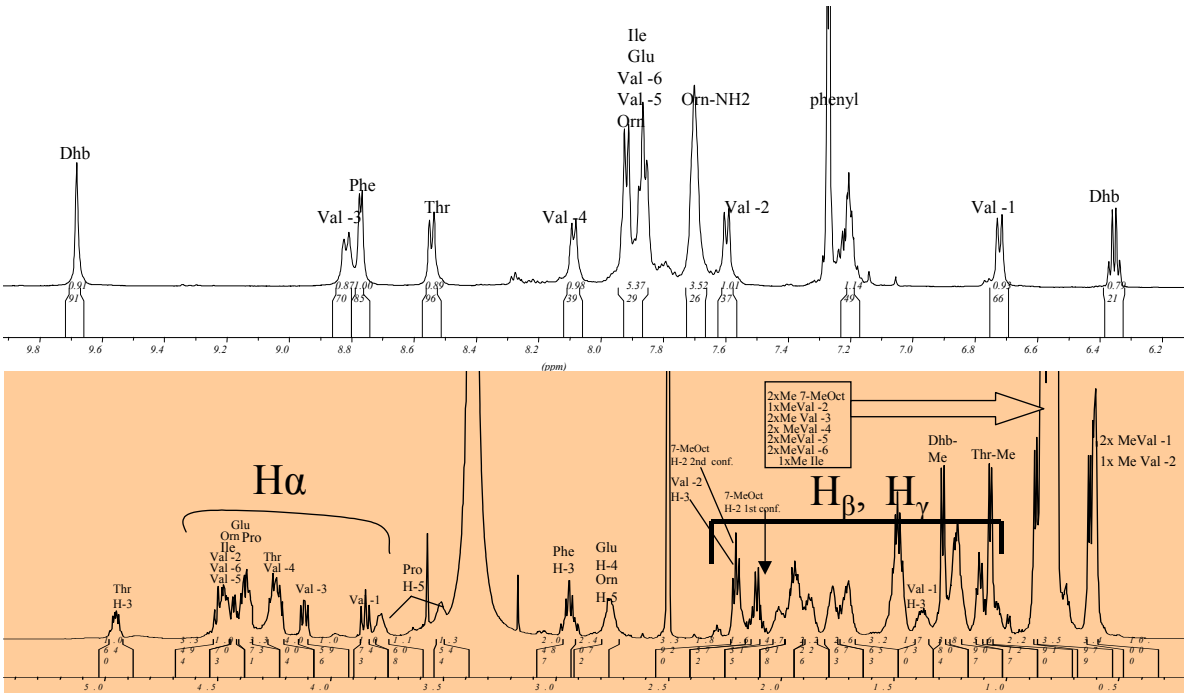

Fig (3.2.6): ^{1}H NMR spectrum of 8, N*H*s and aromatic region (up) and higher field region of α,β,γ and methyl proton signals(down).

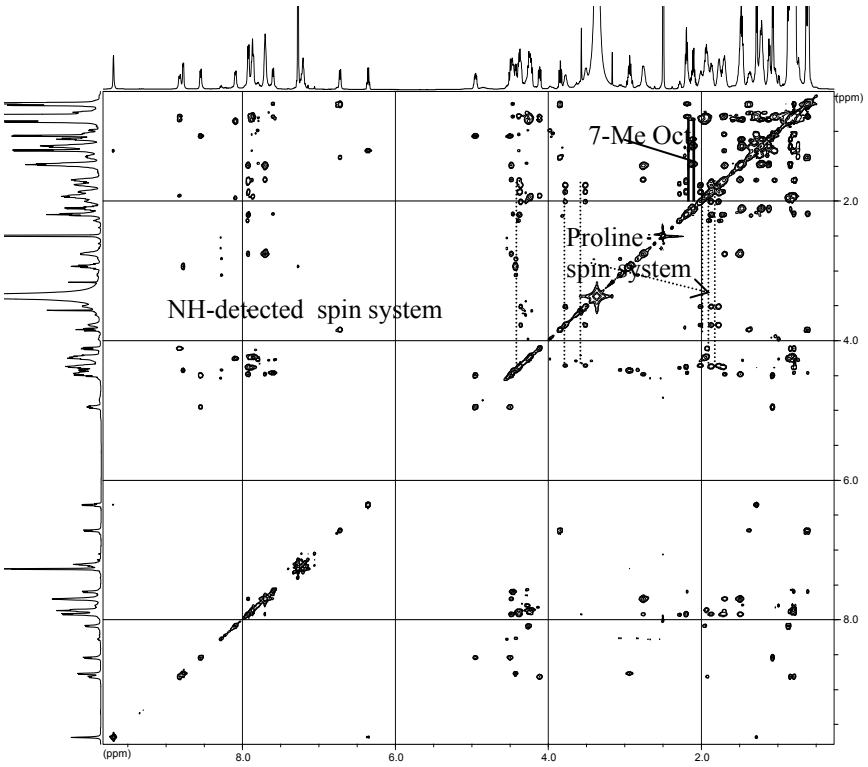

Fig (3.2.7): Total TOCSY spectrum of compound 8 (Kahalalide R).

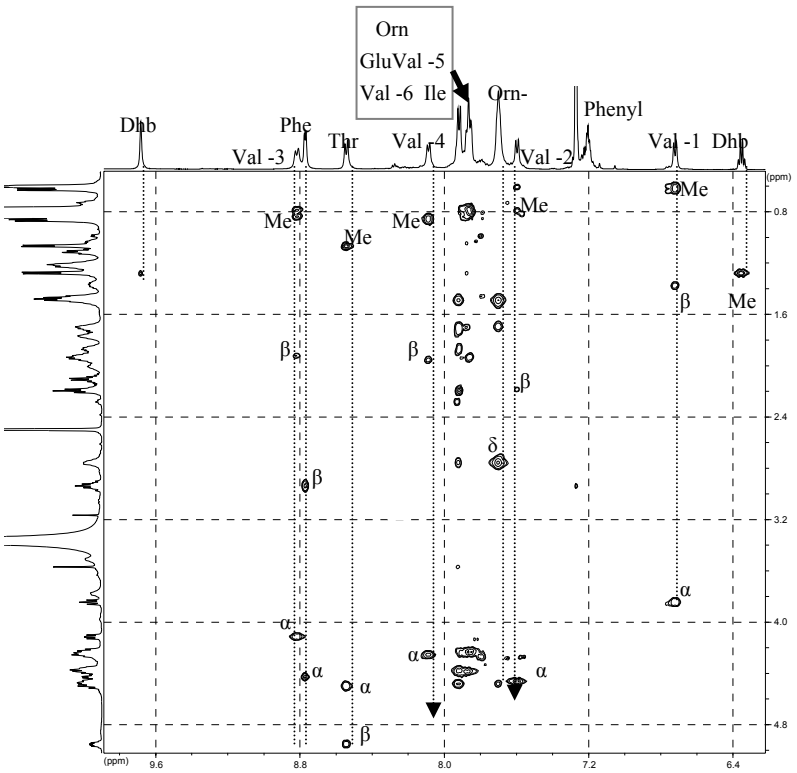

Fig (3.2.8): NH-detected TOCSY correlations of compound 8 (Kahalalide R).

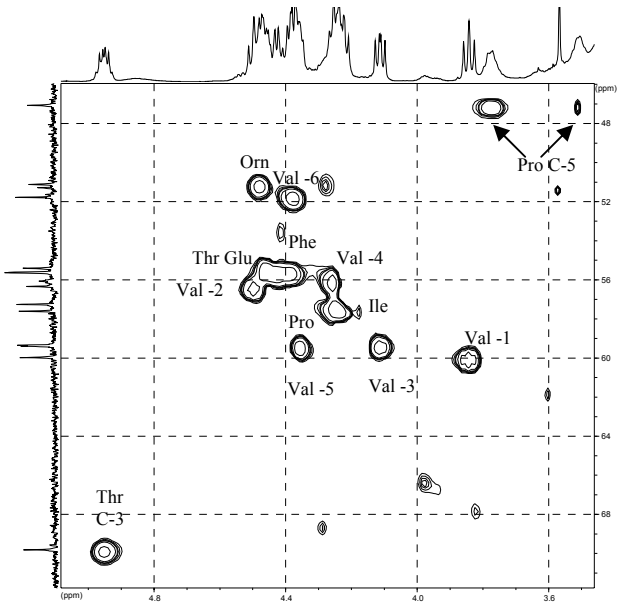

Fig (3.2.9): Part of HMQC spectrum of compound 8 showing H----C direct correlations of α-carbons.

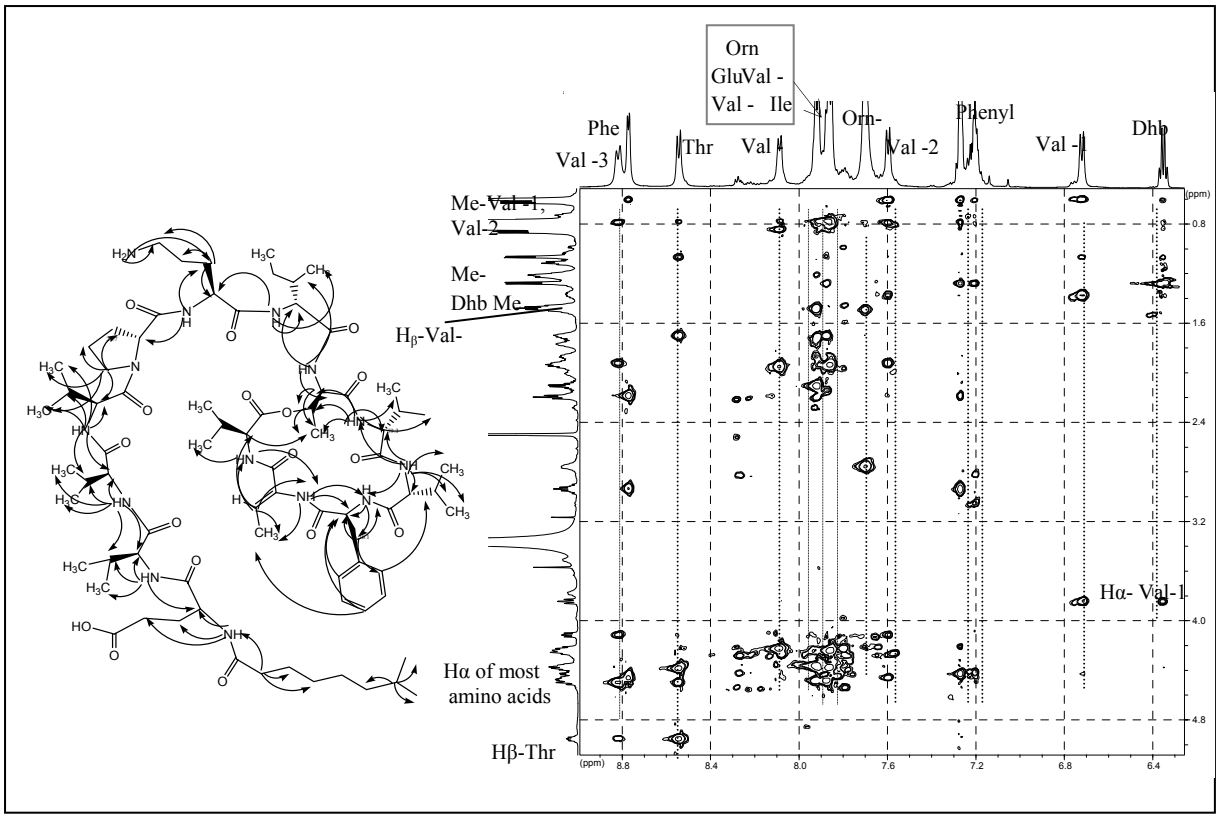

Fig (3.2.10): significant NOEs deduced from the ROESY spectra of compound 8.

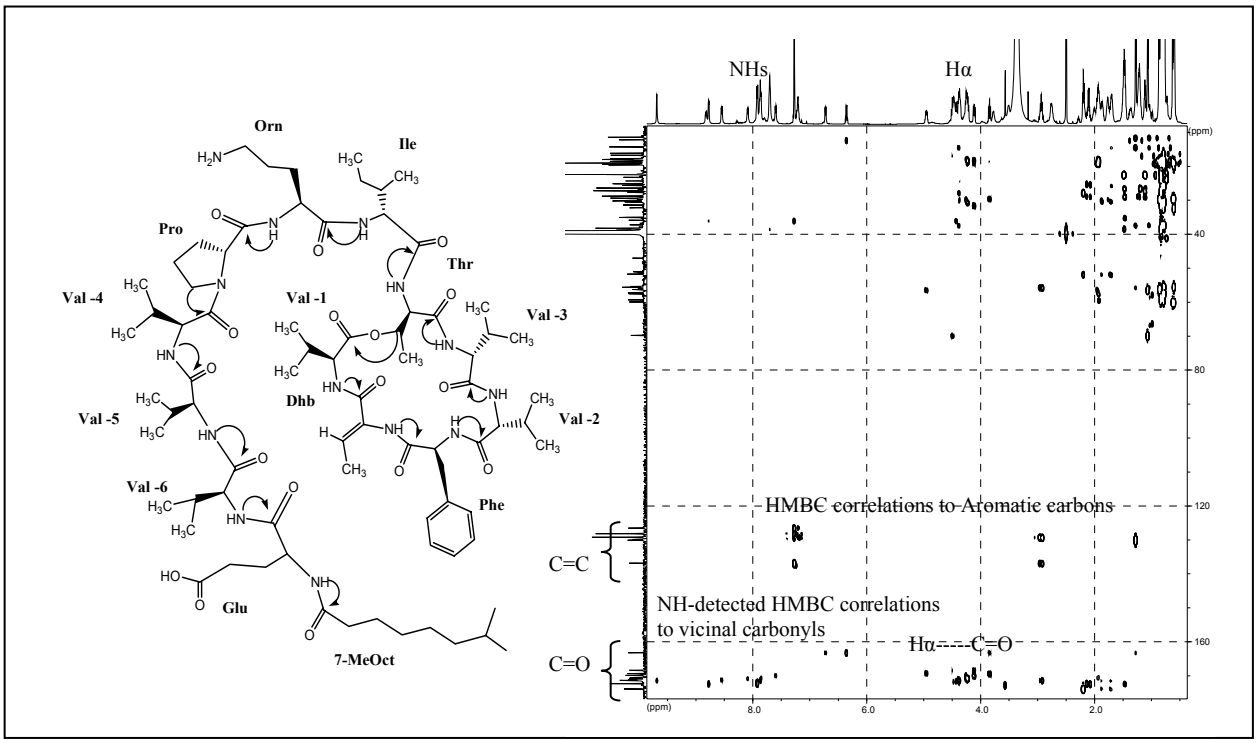

Fig (3.2.11): Total HMBC spectrum of compound 8

The deduced data obtained by 2D NMR (Figure 3.2.4) that determine the amino acid sequence of kahalalide R (**8**) were further confirmed by mass spectrometric methods involving both ESI (Spengler 1999) and MALDI–TOF–PSD (Giorgiani *et al* 2004, Loo and Loo 1997, Puapaiboon *et al* 1999) experiments. Similar results were obtained from the (+) ESI-MS/MS spectrum, where fragment ion peaks were observed at *m/z* 1251.6, 1151.6, 1052.6, 952.9, 742.7 and 629.5 corresponding to $[M–(7\text{-Me-Oct–Glu})]^+$, $[M–(7\text{-Me-Oct–Glu–Val-6})]^+$, $[M–(7\text{Me-Oct–Glu–Val-6–Val-5})]^+$, $[M–(7\text{-Me-Oct–Glu–Val-6–Val-5–Val-4})]^+$, $[M–(7\text{-Me-Oct–Glu–Val-6–Val-5–Val-4–Pro–Orn})]^+$ and $[M–(7\text{-Me-Oct–Glu–Val-6–Val-5–Val-4–Pro–Orn–}a\text{Ile})]^+$, respectively. However, this MS/MS fragmentation of **8** was limited to confirmation of the linear peptide side chain. In contrast, the MALDI–TOF–PSD spectrum established unequivocally the sequence of the depsipeptide, kahalalide R, as shown in Table 3.2.1. The amino acid sequence of the cyclic component was indicated by ion composition peaks at *m/z* 628.4 $[\text{Thr(-H)–Val-1–Dhb–Phe–Val-2–Val-3}]^+$, 330.2 $[\text{Val-1–Dhb–Phe}]^+$ or $[\text{Dhb – Phe – Val-2}]^+$, 247.1 $[\text{Val-2–Phe}]^+$, and 183.1 $[\text{Val-1–Dhb}]^+$. The terminal functional units 7-Me-Oct–Glu were also shown by peaks at *m/z* 270.1 $[\text{7-Me-Oct–Glu}]^+$ and 142.1 $[\text{7-Me-Oct}]^+$. The stereochemistry of the amino acids was determined by Marfey analysis (Marfey 1984), which identified one mole unit each of D-Glu, D-Pro, L-Orn , D-*a*Ile, D-*a*Thr, and L-Phe. For the six Val units, Marfey analysis suggested the presence of both D and L isomers in compound **8**. The stereochemistry of the individual Val units could not, however, be unambiguously determined as there are three moles each of Val in both the cyclic and linear fragments. This is not suprising as the stereochemistry of Val-3 and Val-4 in kahalalide F has been long debated. The overall structure of kahalalide F was initially elucidated by Scheuer's group in 1993 (Hamann and Scheuer 1993), where Val-3 and Val-4 were respectively assigned the L and D stereochemistry (Goetz *et al* 1999). The originally proposed structure (Goetz *et al* 1999) was then synthesized by the groups of Albericio and Giralt (López-Maciá *et al* 2001a), and showed differences in chromatographic and spectroscopic behavior between the synthesized and the natural peptide. They indicated that the stereochemistry of Val-3 and Val-4 should be reversed. Later, Rinehart's group (Bonnard *et al* 2003) confirmed this indication and proved that the stereochemistry of Val-3 and Val-4 plays an important role in the activity of kahalalide F since the depsipeptide with L-Val-3 and D-Val-4 in its structure was not active while the molecule with D-Val-3 and L-Val-4 possesses the activity.

Table 3.2.1 Important MALDI-TOF-PSD fragment ions of Kahalalide R

Ion composition	*m/z*
M–[7-Me-Oct– Glu]$^+$	1250.6
M–[7-Me-Oct–Glu–Val-6]$^+$	1150.7
M–[7-Me-Oct–Glu–Val-6–Val-5]$^+$	1051.6
M–[7-Me-Oct–Glu–Val-6–Val-5–Val-4]$^+$	952.6
M–[7-Me-Oct –Glu–Val-6–Val-5–Val-4–Pro]$^+$	855.5
M–[7-Me-Oct–Glu–Val-6–Val-5–Val-4–Pro–Orn]$^+$	741.4
Cyclo[Thr(-H)–Val-1–Dhb–Phe–Val-2–Val-3]$^+$	628.4
[Val-1–Dhb–Phe]$^+$ or [Dhb–Phe–Val-2]$^+$	330.2
[Val-2–Phe]$^+$	247.1
[Val-1–Dhb]$^+$	183.1
[Pro–Orn]$^+$	212.1
[7-Me-Oct-Glu]$^+$	270.1
[7-Me-Oct]$^+$	142.1

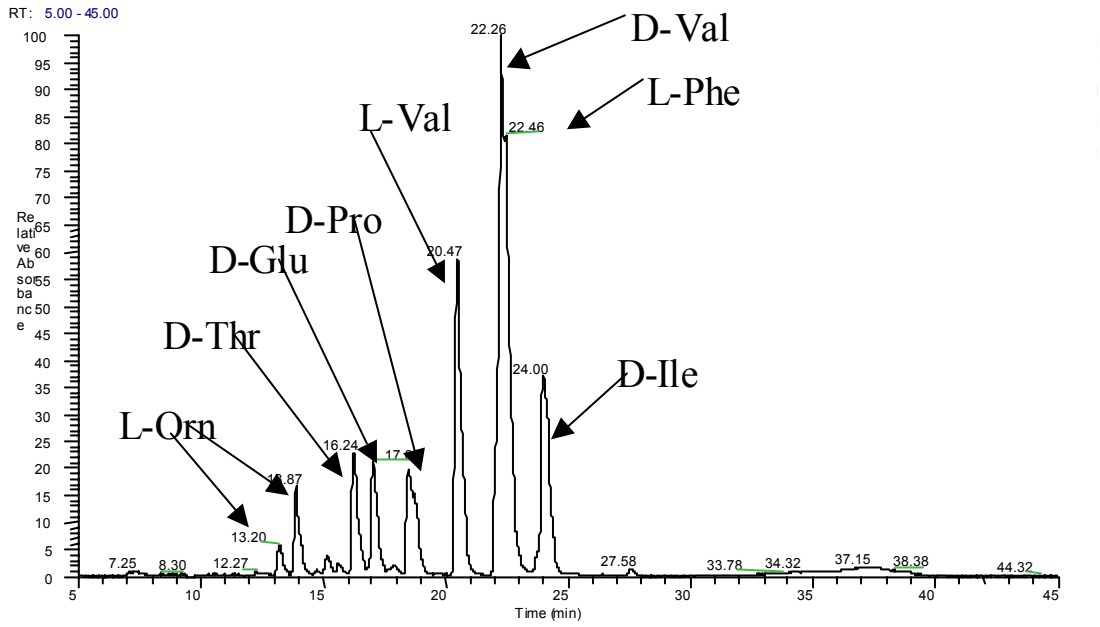

Fig (3.2.12): Marfey analysis result and sterochemical profile of Kahalalide R

Table 3.2.2. ^{1}H and ^{13}C NMR Data of Kahalalide R in DMSO-d_6.

Amino acid	No.	^{13}C (ppm)	^{1}H (ppm)	mult.	Amino acid	No.	^{13}C (ppm)	^{1}H (ppm)	mult.
Val-1	1	169.7	(N*H*) 6.73	(d, *J*=8.5 Hz)	**Pro**	1	172.6		
	2	60.2	3.85	(t, *J*= 9.0 Hz)		2	55.6	4.37	(m)
	3	30.1	1.38	(m)		3	29.7	2.01, 1.98	(m, m)
	4	16.5	0.62	(d, *J*=6.3 Hz)		4	27.2	1.78, 1.89	(m, m)
	5	19.2	0.60	(d, J=6.3 Hz)		5	47.0	3.78, 3.52	(m, m)
(*Z*)-Dhb	1	163.5	(N*H*) 9.69	(s)	**Val-4**	1	172.6	(N*H*) 8.11	(d, *J*=8.5 Hz)
	2	130.4				2	55.9	4.26	(m)
	3	130.2	6.36	(q, *J*=7.0 Hz)		3	31.0	1.94	(m)
	4	12.5	1.28	(d, *J*=7.5 Hz)		4	22.8	0.84	(m)
						5	19.0	0.83	(m)
Phe	1	171.3	(N*H*) 8.78	(d, *J*=5.5 Hz)	**Val-5**	1	171.2	(N*H*) 7.89	(d, *J*=8.5 Hz)
	2	55.65	4.43	(q, *J*=6.5 Hz)		2	59.5	4.38	(m)
	3	36.1	2.94, 2.92	(m, m)		3	31.6	1.88	(m)
	4	137.0				4	19.3	0.82	(m)
	5,5’	128.5	7.28	(m)		5	19.6	0.83	(m)
	6,6’	129.5	7.29	(m)					
	7	126.7	7.25	(m)					
Val-2	1	172.6	7.61 (N*H*)	(d, *J*=8.5 Hz)	**Val-6**	1	171.2	(N*H*) 7.86	(d, *J*=8.5 Hz)
	2	55.4	4.45	(m)		2	51.89	4.37	(m)
	3	31.5	2.18	(m)		3	30.7	1.95	(m)
	4	19.5	0.80	(d, *J*=7.0 Hz)		4	22.2	0.84	(m)
	5	18.5	0.62	(d, *J*=6.5 Hz)		5	22.9	0.86	(m)
Val-3	1	170.0	(N*H*) 8.82	(d, *J*=8.5 Hz)	**Glu**	1	170.9	(N*H*) 7.93	(d, *J*=7.5 Hz)
	2	59.3	4.13	(m)			2nd regio-isomer	(N*H*) 7.91	(d, *J*=7.5 Hz)
	3	31.5	1.94	(m)					
	4	18.6	0.81	(d, *J*=7.0 Hz)		2	56.0	4.41	(m)
	5	19.5	0.82	(d, *J*=6.5 Hz)		3	28.0	1.59, 1.50	(m)
						4	38.5	2.75	(m, m)
						5	169.4	(O*H*) 7.71	(bs)
***a*Thr**	1	168.7	(N*H*) 8.55	(d, *J*=8.0Hz)	**7-Me-Oct**	1	172.5		
	2	56.4	4.50	(t, *J*=7.8 Hz)		2	35.1	2.11	(m)
	3	70.0	4.96	(m)		3	23.6	1.51	(m)
	4	17.3	1.08	(d, *J*=6.5Hz)		4	29.5	1.28	(m)
***a*Ile**	1	171.3	(N*H*) 7.87	(d, *J*=8.2 Hz)		5	29.5	1.25	(m)
	2	57.2	4.34	(m)		6	38.3	1.15, 1.10	(m)
	3	30.2	1.73	(m)		7	27.3	1.52	(m)
	4	14.6	1.21	(m)		8	22.5	0.80	*
	5	26.0	1.02	(t, *J*=6.5 Hz)		9	22.5	0.81	*
	6	11.8	0.82	(d, *J*=6.5 Hz)					
Orn	1	171.5	(N*H*) 7.93	(d, *J*=8.5 Hz)					
	2	51.1	4.49	(m)					
	3	30.9	1.69, 1.82	(m, m)					
	4	28.5	1.52	(m)					
	5	38.3	2.74	(m)					
			(NH_2) 7.72	(bs)					

*Resonance is underneath the methyl signals of Val and *a*Ile.

3.2.2- Kahalalide S (9, New natural product)

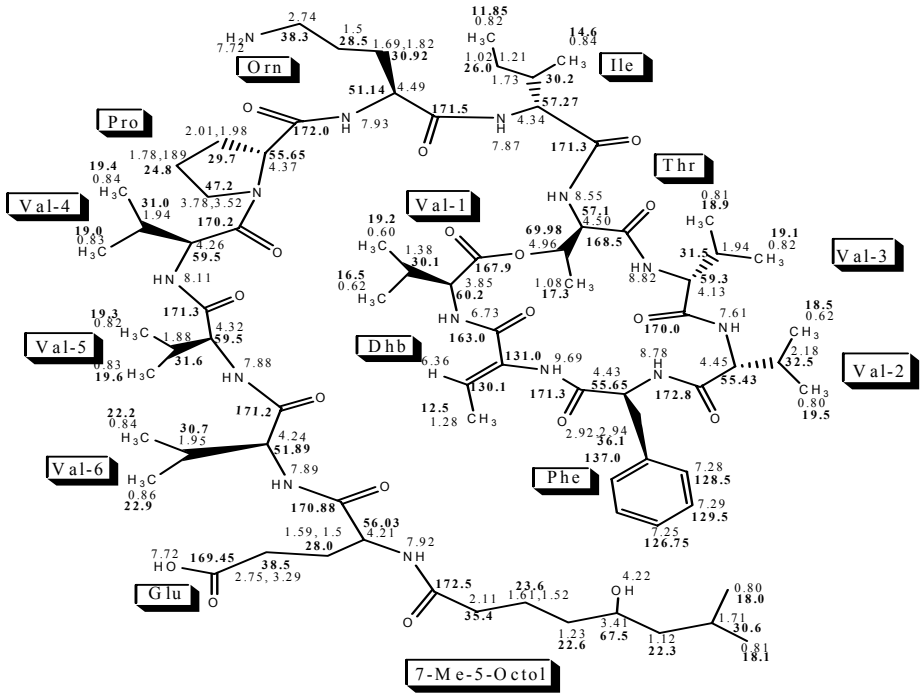

$C_{77}H_{126}N_{14}O_{18}$
Exact Mass: 1534,937
Mol. Wt.: 1535,907

Fig (3.2.13): compound 9, Kahalalide S

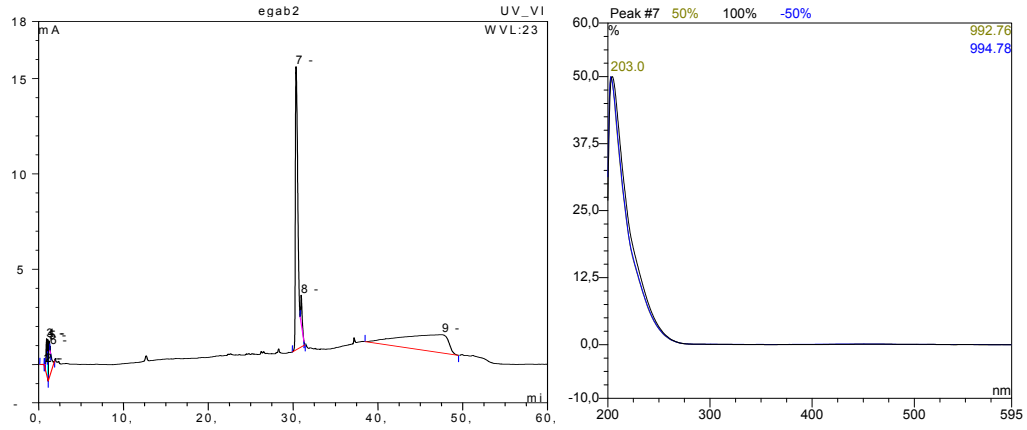

Fig (3.2.14): HPLC chromatogram and the corresponding UV spectrum of compound 9.

Yield: 8 mg

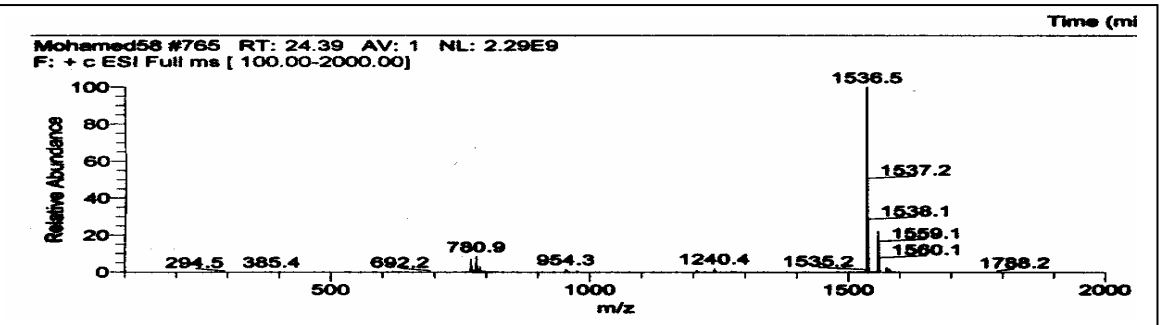

Fig (3.2.15): ESI-MS of compound 9.

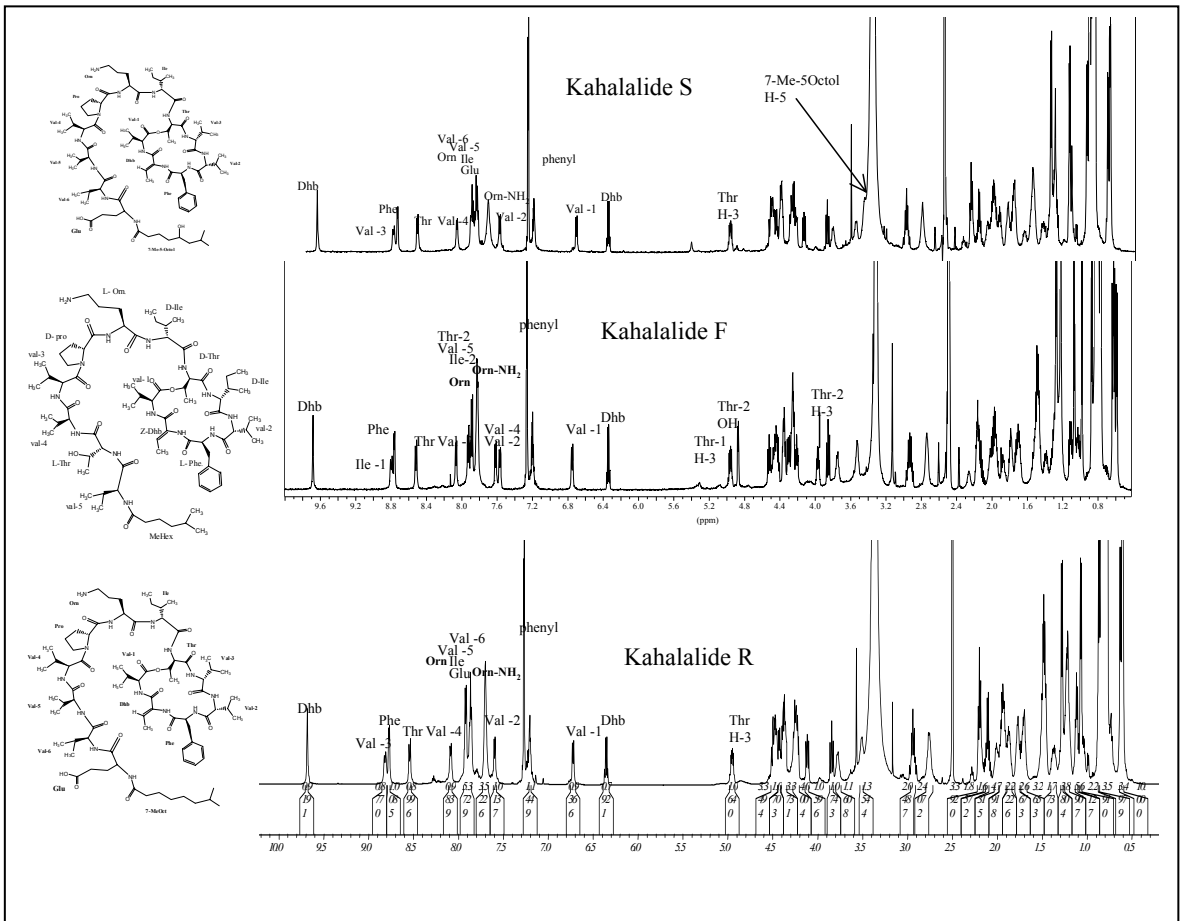

Fig (3.2.16): comparison of ^{1}H NMR spectra of Kahalalides F, R and S.

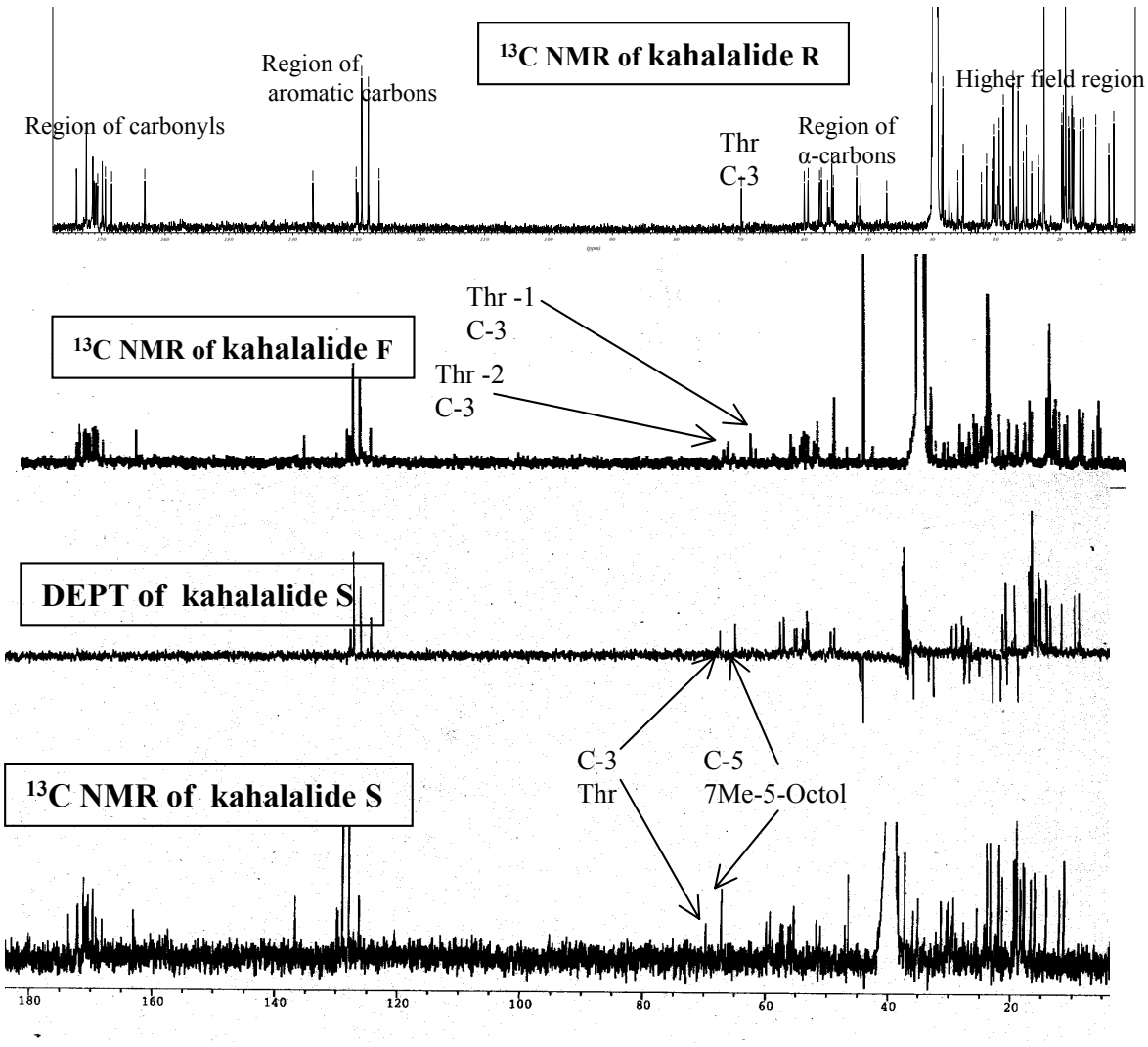

Fig (3.2.17): comparison of ^{13}C NMR spectra of Kahalalides F, R and S.

Kahalalide S (**9**) was obtained as a white amorphous powder. The reflector mode MALDI-TOF mass spectrum of **9** performed with delayed extraction showed positive monoisotopic ion peaks at *m/z* 1536.0, $[M+H]^+$, 1558.0 $[M+Na]^+$, and 1574.0 $[M+K]^+$. In (+)-ESI-MS, a pseudomolecular ion was detected at *m/z* 1535.9 $[M+H]^+$ that was compatible with the molecular formula $C_{77}H_{127}N_{14}O_{18}$ as established by HRESIMS

Kahalalide S differs from kahalalide R by 16 mass unit (one oxygen atom) in the fatty acid, 7-methyl-5-hydroxyoctanoic acid (7Me-5-Octol). It consists of all amino acid residues found in kahalalide R. It is also the fourth kahalalide containing unusual dehydroaminobutyric acid (Dhb), table 3.2.3 shows the structural differences between the four largest kahalalides (F, G, R and S) .

In comparison with kahalalide R, **9** has 16 mass units more, which implied the occurrence of an additional oxygen atom in the molecule. Inspection of the ^{1}H and ^{13}C NMR spectra of **9** revealed that kahalalide S shared very similar structural features with **8** (Table 3.2.5). The amino acid residues of depsipeptide **9** were identical to those of **8**. The only obvious difference was exhibited in the ^{13}C NMR and DEPT spectra of **9** where an extra oxygenated methine carbon was observed at δ 67.5 and the subsequent loss of one methylene carbon in the 20 to 25 ppm region. COSY and TOCSY spectra of **9** revealed changes occurring in the fatty acid residue. Instead of 7-Me-Oct as in **8**, the fatty acid residue in **9** was substituted by 5-hydroxy-7-methyloctanoic acid (7-Me-5-Octol). Sequential COSY correlations were observed between the α-methylene signal at 2.11 ppm to the subsequent methylene signals at δ 1.61, 1.52 (C*H*$_2$-3), 1.25 (C*H*$_2$-4), then to the oxygenated methine at δ_{H-5} 3.41 and further to the methylene proton at δ 1.12 (C*H*$_2$-6), which terminates with an isopropyl unit at δ 1.71 (C*H*-7), 0.80 (C*H*$_3$-8) and 0.81 (C*H*$_3$-9) Table 3.2.5.

HMBC and ROESY spectra of **9** also gave similar results to **8**, indicating an identical amino acid sequence to **8**. The ROESY spectra of **9** also implied the occurrence of *Z*-Dhb in the depsipeptide. The connectivity of 7-Me-5-Octol to Glu was also afforded by the HMBC correlation of the Glu–N*H* resonance at δ 7.92 with the carbonyl signal at δ 172.5, which was assigned to C-1 in 7-Me-5-Octol.

The amino acid sequence of depsipeptide **9** was further confirmed by ESI-MS/MS fragmentation and MALDI–TOF–PSD (Table 3.2.4) experiments, which again confirmed the 2D NMR results. The terminal unit, 7-Me-5-Octol–Glu, was evident from the peak at *m*/*z* 286.2 in the MALDI–TOF–PSD spectrum. Amino acid analysis using Marfey´s method revealed the prevalence of a similar stereochemistry for each of the amino acids as found in **8**. The same problem was encountered in **9** as in **8** regarding the assignment of the stereochemistry of each of the six Val units.

Except for the presence of glutamic acid (Glu) in kahalalides R (**8**) and S (**9**), the new derivatives have a similar set of amino acids to those of kahalalide F (**1**). The new analogues further differ from kahalalide F with regard to the occurrence of octanoic acid instead of hexanoic acid. Kahalalide S (**9**) was found to contain an identical sequence of amino acids along with the unusual amino acid, *Z*-Dhb, as in kahalalide R (**8**) and differed only in the terminal fatty acid function, which was 7-Me-5-Octol instead of 7-Me-Oct. (see tables 3.2.3 and 3.2.5)

Table (3.2.3) Structural differences between the four largest kahalalides, (F, G, R and S) .

Kah	Mol.wt	Mol.formula	Aminoacids								Fatty acid	Structure form
			Dhb	Glu	Ileu	Orn	Phe	Pro	The	Val		
F	1477.9	$C_{75}H_{124}N_{14}O_{16}$	1	0	2	1	1	1	2	5	5-MeHex	cyclic peptide
G	1495.9	$C_{75}H_{126}N_{14}O_{17}$	1	0	2	1	1	1	2	5	5-MeHex	linear peptide
P	1519.9	$C_{77}H_{126}N_{14}O_{17}$	1	1	1	1	1	1	1	6	7-MeOct	cyclic peptide
Q	1535.9	$C_{77}H_{126}N_{14}O_{18}$	1	1	1	1	1	1	1	6	7-Me-5-Octol	cyclic peptide

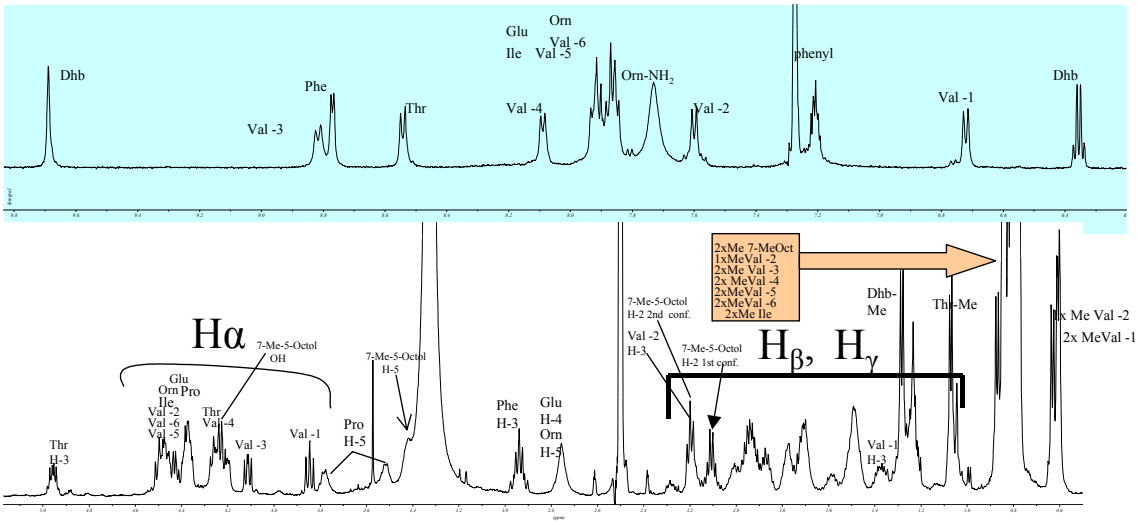

Fig (3.2.18): ^{1}H NMR spectrum of compound 9, NH and aromatic region (up), high field region (down).

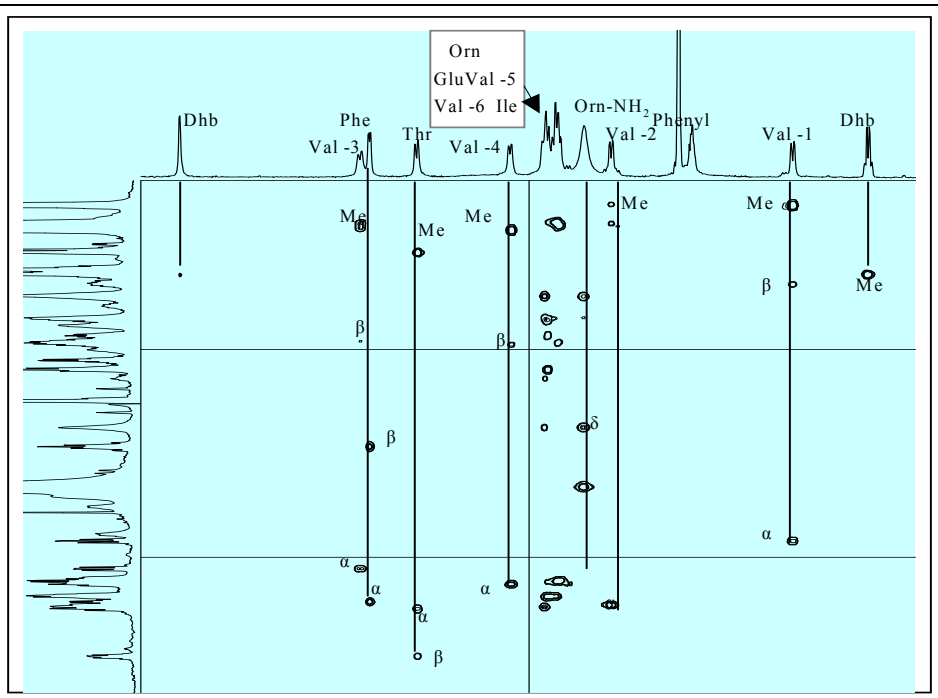

Fig (3.2.19): Part of TOCSY of compound 9 showing NH-detected correlations.

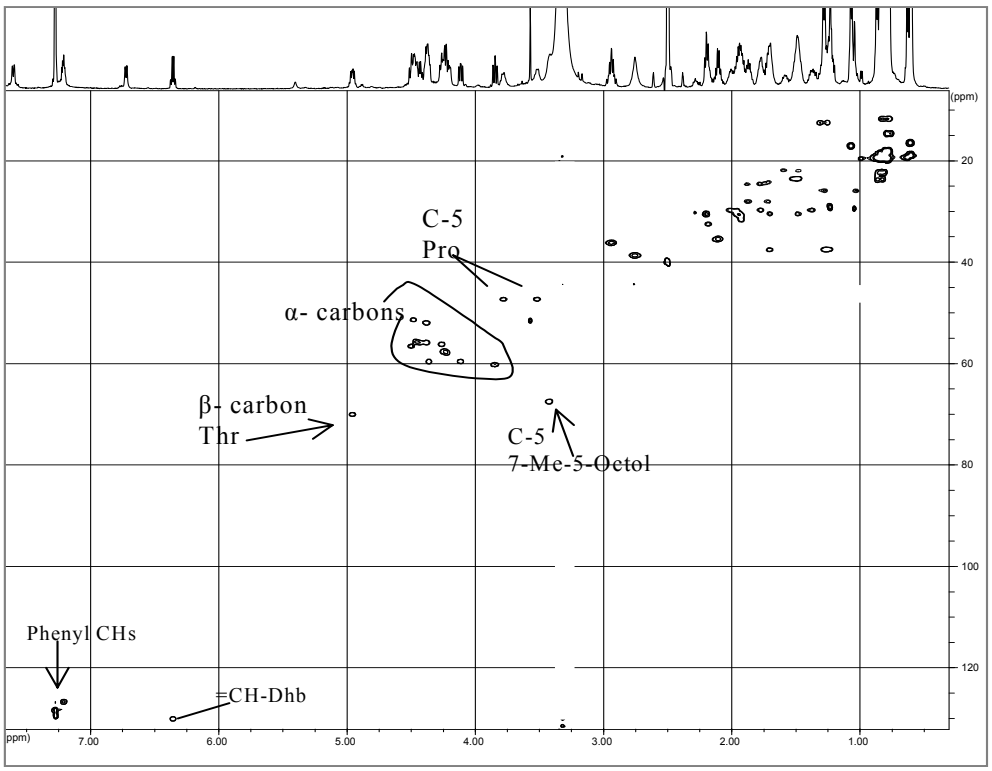

Fig (3.2.20): Total HMQC of compound 9

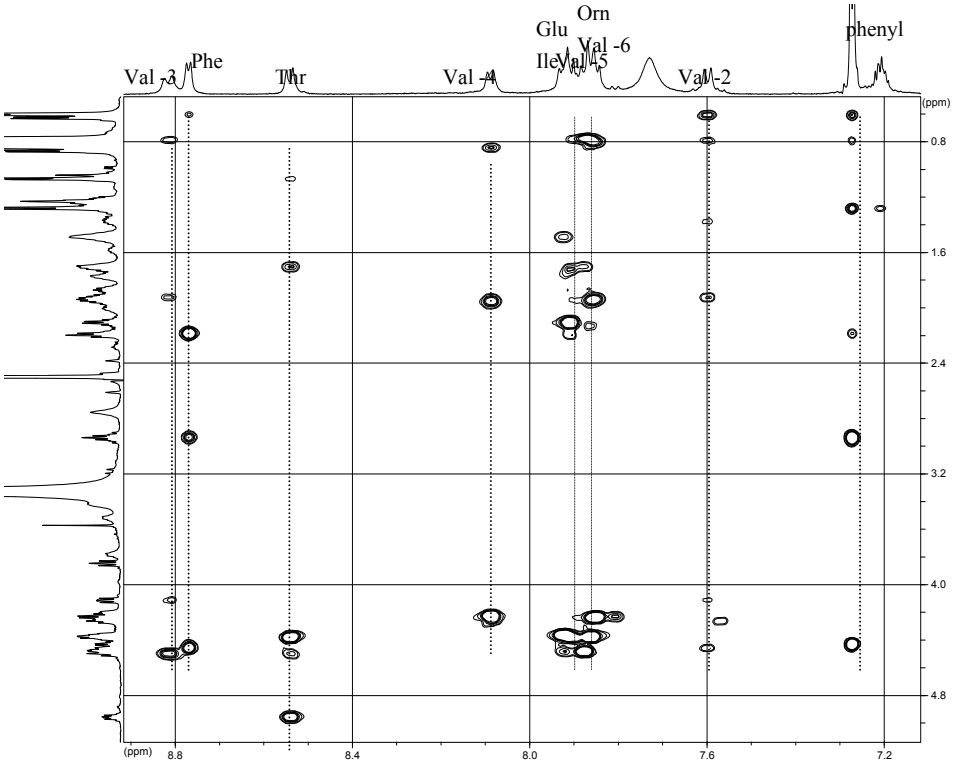

Fig (3.2.21): Part of the ROESY spectrum of compound 9.

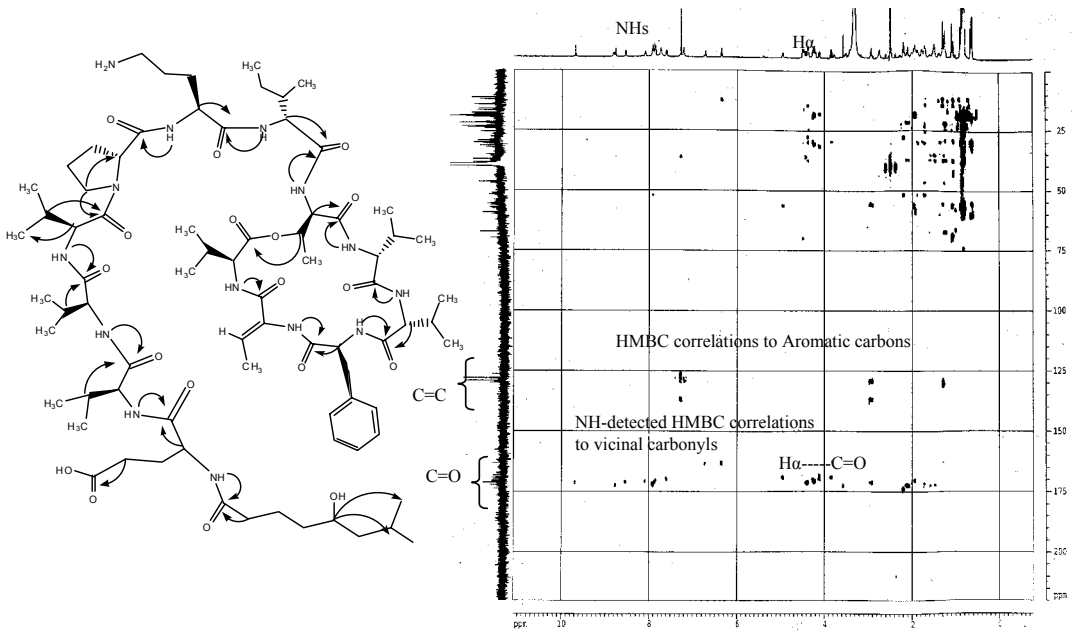

Fig (3.2.22): Total HMBC correlations of compound 9

The sequence of kahalalide S was confirmed using MALDI-TOF-PSD modus, and LC-MS/MS spectra. The reflector mode MALDI-TOF mass spectrum performed with delayed extraction (DE) showed a positive ion signal at *m/z* 1558.0, identified as sodium-ion associated monoisotopic peak $[M+Na]^+$ of kahalalide S, and showed also a positive ion signal at *m/z* 1574.0, $[M+K]^+$ and at *m/z* 1536.0, $[M+1]^+$. MALDI-TOF– PSD spectrum revealed and confirmed the sequence of a depsipeptide, kahalalide S, as shown in table (3.2.4). Similar results were obtained from LC-MS/MS spectrum, where the positive protonated fragment ion peaks could be seen at *m/z* 1379.9, 1250.6, 1151.6, 1052.6, 952.9, 742.7 and 629.5 corresponding to M-[7Me-5-Octol], M-[7Me-5-Octol - Glu], M-[7Me-5-Octol - Glu- Val-6], M-[7Me-5-Octol - Glu- Val-6- Val-5], M-[7Me-5-Octol - Glu- Val-6- Val-5- Val-4], M-[7Me-5-Octol - Glu- Val-6- Val-5- Val-4- Pro- Orn] and M-[7Me-5-Octol - Glu- Val-6- Val-5- Val-4- Pro- Orn- Ileu] respectively, See figure (3.2.23).

Amino acid analysis using Marfey´s method revealed the presence of D-Glu, D-pro, L-Orn, D-aIle, D-athr, L-Phe , D-Val & L-Val,

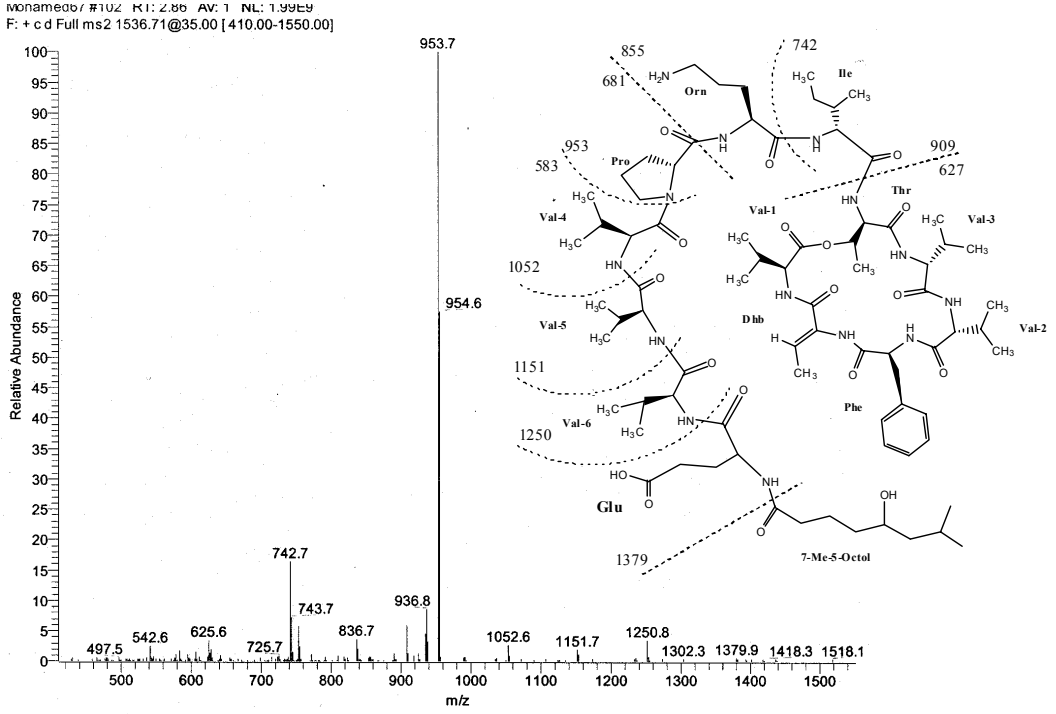

Fig (3.2.23): ESI-MS/MS of compound 9

Table 3.2.4. Important MALDI-TOF-PSD fragment ions of Kahalalide S

Ion composition	***m/z***
M–[7-Me-5-Octol–Glu]$^+$	1250.6
M–[7-Me-5-Octol–Glu–Val-6]$^+$	1150.7
M–[7-Me-5-Octol–Glu–Val-6–Val-5]$^+$	1051.6
M–[7-Me-5-Octol–Glu–Val-6–Val-5–Val-4]$^+$	952.6
M–[7-Me-5-Octol–Glu–Val-6–Val-5–Val-4–Pro]$^+$	855.5
Ile + Cyclo[Thr(-H)–Val-1–Dhb–Phe–Val-2–Val-3]$^+$	741.4
Cyclo[Thr(-H)–Val-1–Dhb–Phe–Val-2–Val-3]$^+$	628.4
[Val-1–Dhb–Phe]$^+$ or [Dhb–Phe–Val-2]$^+$	330.2
[Val-2–Phe]$^+$	247.1
[Val-1–Dhb]$^+$	183.1
[Pro–Orn]$^+$	212.1
[7-Me-5-Octol–Glu]$^+$	286.2

Table 3.2.5 ^{1}H and ^{13}C NMR data of Kahalalide S in DMSO-d_6.

Amino acid	No.	^{13}C (ppm)	^{1}H (ppm)	mult.	Amino acid	No.	^{13}C (ppm)	^{1}H (ppm)	mult.
Val-1	1	167.9	(N*H*) 6.73	(d, *J*=9.0 Hz)	**Pro**	1	172.0		
	2	60.2	3.85	(t, *J*=9.0 Hz)		2	55.6	4.37	(m)
	3	30.1	1.38	(m)		3	29.7	2.01, 1.98	(m, m)
	4	16.5	0.62	(d, *J*=7.0 Hz)		4	24.8	1.78, 1.89	(m, m)
	5	19.2	0.60	(d, *J*=6.0 Hz)		5	47.2	3.78, 3.52	(m, m)
(*Z*)-Dhb	1	163.0	(N*H*) 9.69	(s)	**Val-4**	1	170.2	(N*H*) 8.11	(d, *J*=8.5 Hz)
	2	131.0				2	59.5	4.26	(m)
	3	130.1	6.36	(q, *J*=7.0 Hz)		3	31.0	1.94	(m)
	4	12.5	1.28	(d, *J*=7.5 Hz)		4	19.4	0.84	(m)
						5	19.0	0.83	(m)
Phe	1	171.3	(N*H*) 8.78	(d, *J*=5.5 Hz)	**Val-5**	1	171.3	(N*H*) 7.88	(d, *J*=8.5 Hz)
	2	55.6	4.43	(q, *J*=6.5 Hz)		2	59.5	4.32	(m)
	3	36.1	2.94	(m)		3	31.6	1.88	(m)
	4	137.0				4	19.3	0.82	(m)
	5,5’	128.5	7.28	(m)		5	19.6	0.83	(m)
	6,6’	129.5	7.29	(m)					
	7	126.7	7.25	(m)					
Val-2	1	172.8	(N*H*) 7.61	(d, *J*=8.5 Hz)	**Val-6**	1	171.2	(N*H*) 7.89	(d, *J*=8.5 Hz)
	2	55.4	4.45	(m)		2	51.9	4.24	(m)
	3	32.5	2.18	(m)		3	30.7	1.95	(m)
	4	19.5	0.62	(d, *J*=7.0 Hz)		4	22.2	0.84	(m)
	5	18.5	0.80	(d, *J*=6.5 Hz)		5	22.9	0.86	(m)
Val-3	1	170.0	(N*H*) 8.82	(d, J=8.5 Hz)	**Glu**	1	170.9	(N*H*) 7.92	(d, *J*=7.5 Hz)
	2	59.3	4.13	(m)			2nd	(N*H*) 7.91	(d, *J*=7.5 Hz)
	3	31.5	1.94	(m)			regio-		
	4	18.9	0.81	(d, *J*=7.0 Hz)		2	isomer	4.21	(m)
	5	19.1	0.82	(d, *J*=6.5 Hz)		3	56.0	1.59, 1.50	(m)
						4	28.0	2.75, 3.29	(m)
						5	38.5	(O*H*) 7.72	(bs)
							169.4		
***a*Thr**	1	168.5	(N*H*) 8.55	(d, *J*=8.0 Hz)	**7-Me-5-Octol**	1	172.5		
	2	57.1	4.50	(t, *J*=7.8 Hz)		2	35.4	2.11	(m)
	3	70.0	4.96	(m)		3	23.6	1.61,1.52	(m)
	4	17.3	1.08	(d, *J*=6.5 Hz)		4	22.6	1.25	(m)
***a*Ile**	1	171.3	(N*H*) 7.87	(d, *J*=8.2.Hz)		5	67.5	3.41	(m)
	2	57.27	4.34	(m)				(O*H*) 4.22	(d)
	3	30.2	1.73	(m)		6	38.3	1.12	(m)
	4	14.6	1.21	(m)		7	27.3	1.71	(m)
	5	26.0	1.02	(t, *J*=6.5 Hz)		8	18.0	0.80	*
	6	11.9	0.82	(d, *J*=6.5 Hz)		9	18.1	0.81	*
Orn	1	171.5	(N*H*) 7.93	(d, J=8.5 Hz)					
	2	51.1	4.49	(m)					
	3	30.9	1.69, 1.82	(m, m)					
	4	28.5	1.5	(m)					
	5	38.3	2.74	(m)					
			(NH_2) 7.72	(bs)					

*Resonance is underneath the methyl signals of Val and *a*Ile.

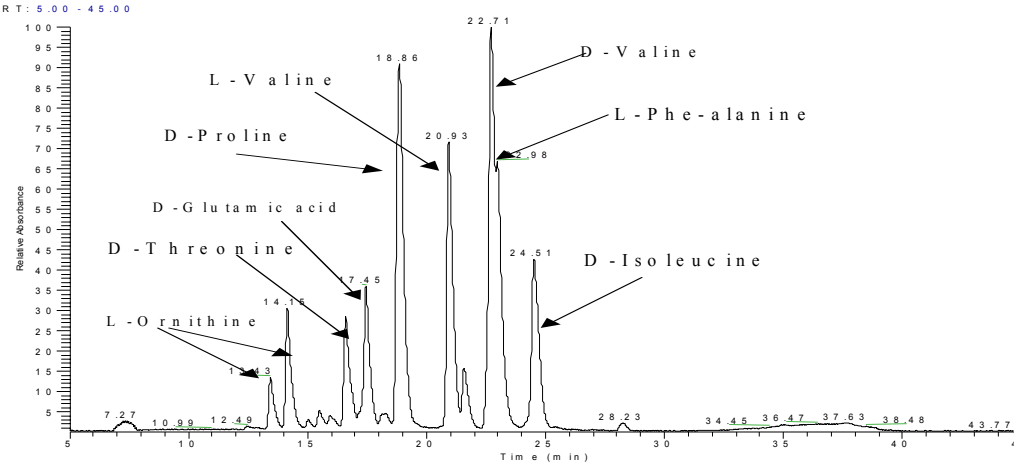

Fig (3.2.24) Marfey analysis results showing the stereochemical profile of amino acids of compound 9.

Table 3.2.6 Marfey´s analysis results of kahalalide F, R and S hydrolysates :

Amino acid-DAA deriv.	L. aIle	D. aIle	L. Phe	L. Val	D. Val	L. Pro	D. Pro	L. aThr	D. aThr	L. Glu	D. Glu	L. Orn*	D. Orn*
Mol. wt (+ve mode)	384.0	384.0	418.0	370.0	370.0	368.1	368.1	372.0	372.0	400.0	400.0	385.1	385.1
Mol. wt (-ve mode)	382.4	382.4	416.5	368.3	368.3	366.3	366.3	370.3	370.3	398.3	398.3	383.5	383.5
Ret.time in minutes	23.48	24.53	22.98	20.97	22.77	18.02	18.68	15.93	16.60	16.61	17.45	13.44 & 14.14	13.54 & 16.40
Occcurence in Kah. F	-	+	+	+	+	-	+	+	+	-	-	+	-
Occcurence in Kah. R	-	+	+	+	+	-	+	-	+	-	+	+	-
Occcurence in Kah. S	-	+	+	+	+	-	+	-	+	-	+	+	-

*it was detected that each Ornithine isomer has two different retention times, because ornithine contains α- and δ-reactive amino groups which called be react with FDAA producing ESI-MS detectable products.

Bioactivity :

Crude aqueous methanol extract obtained from *E. grandifolia* was reported to exhibit significant antifungal activity against *Aspergillus japonica*, *A. fresenii* and *A. niger* (Bhosale et al , 1999). Although many natural products were isolated from genus *Elysia,* this is the first report for isolated natural products from *E. grandifolia*.

The known derivatives, kahalalides B, D, E, F, together with the new congeners, kahalalides R and S, were assayed for their cytoxicity toward L1578Y, HELA, PC12, H4IIE, and MCF7 cancer cell lines. Kahalalides F and R were found to be comparably cytotoxic toward MCF7 cells with IC_{50}-values of 0.22 ± 0.05 µmol/L and 0.14 ± 0.04 µmol/L, respectively. Kahalalide S and E were less cytotoxic in MCF7 cells with IC50-values of 3.55 ± 0.7 µmol/L and 4.5 ± 0.49 µmol/L, respectively (Figure 3.2.25). Kahalalide R was cytotoxic towards the mouse lymphoma L1578Y cell line at an IC_{50} of 4.28 ± 0.03 nmol/mL, which is

almost identical to that of kahalalide F with an IC_{50} of 4.26 ± 0.04 nmol/mL. The kahalalides including kahalalides F and R were found to be inactive toward HELA, H4IIE and PC12 cancer cell lines. This implied the cytotoxic selectivity and specificity of kahalalides F and R.

Statistics

Data are given as mean ± S.E.M. of 3 independent experiments. The significance of changes in the test responses was assessed using a one-way ANOVA followed by LSD test (Analyse-it, Leeds, UK), differences were considered significant at $p<0.05$.

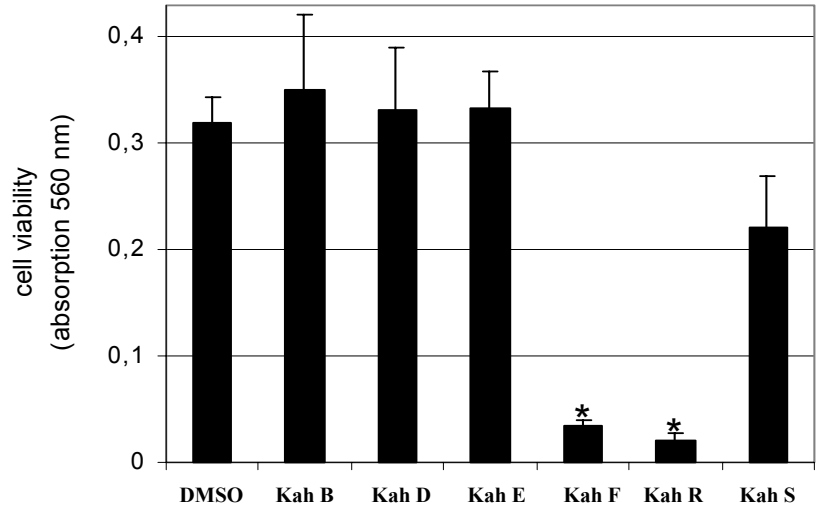

Fig (3.2.25): Cytotoxicity of Kah B, D, E, F, R and S in MCF7 cells

MCF7 cells were incubated with different kahalalides (1 µmol/L) for 24 h, and then MTT reduction as a marker of cell viability was measured. Results are expressed as absorption of reduced MTT (560 nm) ± S.E.M. (n=3), * $p < 0.05$ vs. control (DMSO).

Antimicrobial activity

In an agar diffusion assay, kahalalide R at a disc loading concentration of 5 µg, showed strong antifungal activity against the plant pathogens *Cladosporium herbarum* and *C. cucumerinum* with inhibition zones of 16 and 24 mm, respectively. These results were almost identical to kahalalide F, which exhibited its fungicidal activity with inhibition zones of 17 and 24 mm, respectively, at the same concentration as the latter compound. Using the same concentration, the fungicidal activity of kahalalides F and R were also comparable to that of nystatin showing inhibition zones of 19 and 39 mm, respectively. However, kahalalides F and R did not show a broad spectrum of antibiotic activity as the derivatives did not exhibit any antibacterial activity. Kahalalide S exhibited neither antibacterial nor antifungal activities.

3.3-Natural products from *Pachychalina sp* :

From some of the unidentified marine poriferian *Pachychalina* sp. from the South China Sea, 15 steroids with five different nuclei including 7-en-sterol, 8-en-sterols, Anorsterols, 5-en-sterols and sterols with 4-Me cholestanol nuclei and glycerin-3-heptacosyl ether (Zeng *et al* 1996, Zeng 2000), in addition to methyl-p-hydroxyphenylacetate, thymine, uracil, thimidine and 2´deoxyuridine (Xiao *et al* 1997) have been previously reported.

An unidentified Indonesian *Pachychalina* sp. was chemically investigated in the present study and three compounds were isolated which included two 5α,8α- epidioxysterols (compounds **10** and **11**) and 8-hydroxy-4-quinolone (compound **12**).

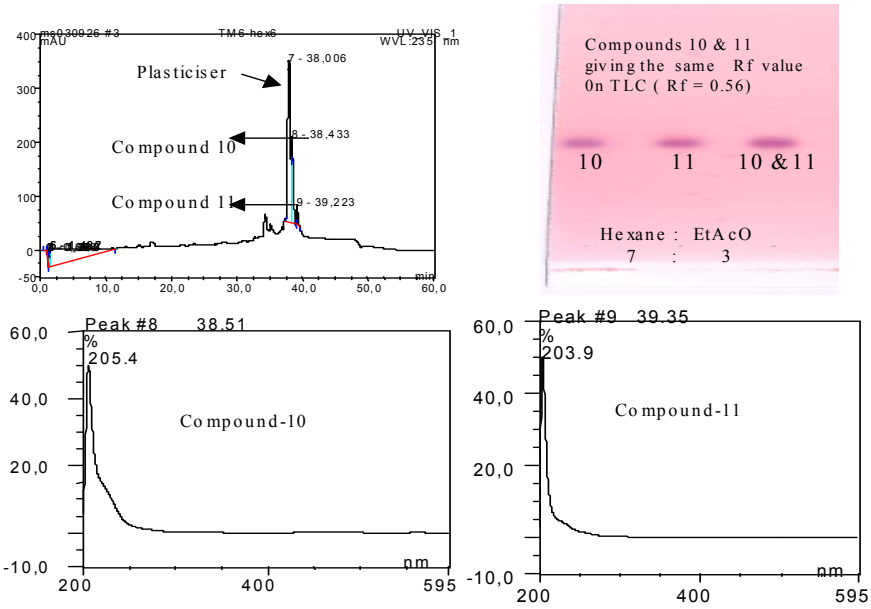

Fig (3.3.1): HPLC chromatogram showing the mixture of compounds 10 & 11 before separation (up-left), TLC of both compound showing the same Rf- value and complete overlapping before separation (up-right), UV-spectrum of compound 10 (down left) and UV-spectrum of compound 11 (down right).

Compounds **10** and **11** are 5α,8α-epidioxysterols. The difference in molecular weight is only 14 mass units which seems to be an additional CH_2 unit in the side chain as explained below. Both compounds show the same Rf value on TLC and the same UV-spectrum. HPLC chromatogram shows slight differences in the relative retention times which were consequently used as the basis for the isolation using semi-preparative HPLC.

3.3.1- 5α,8α-epidioxy-24ξ-methylcholesta-6,22-dien-3β-ol (10, known compound)

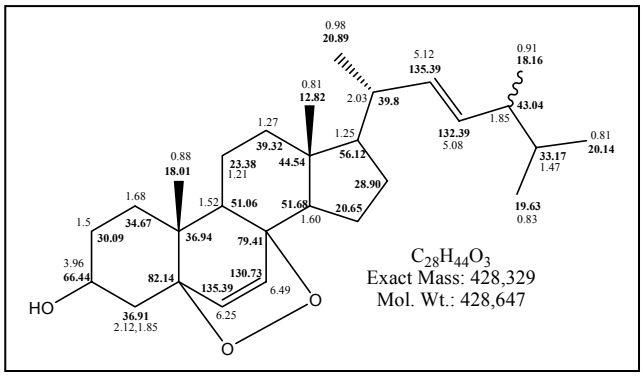

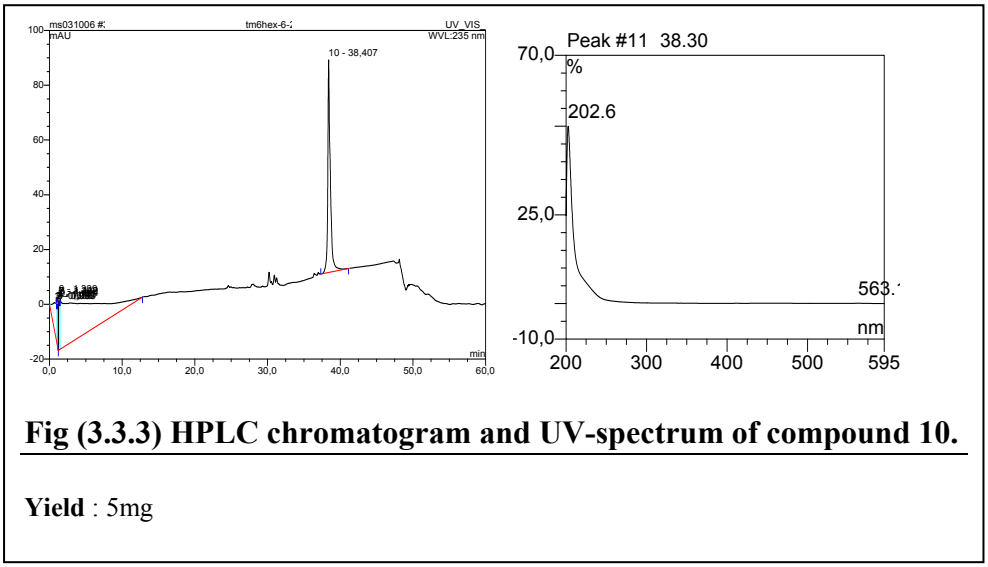

Fig (3.3.3) HPLC chromatogram and UV-spectrum of compound 10.

Yield : 5mg

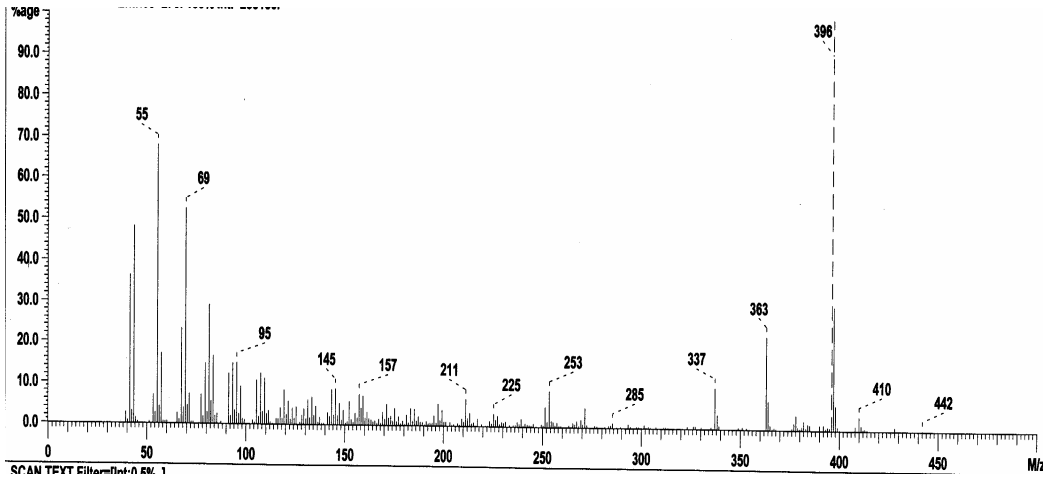

Fig (3.3.4) EI-MS spectrum of compound 10

Compound **10** was isolated as crystalline white needles, with $[\alpha]_D$ of - 5° (*c* 0.35 $CHCl_3$). Compound **10** has UV absorption at λ_{max} 203 nm. EI-MS showed molecular ion peak at *m/z* 428 $[M]^+$ and fragment ions at *m/z* 396 $[M-(O_2)]^+$, 378 $[M-(O_2 + H_2O)]^+$, 363 $[M-(O_2 + H_2O + CH_3)]^+$, 271 [M-($O_2$ + side chain)]$^+$, and 253 [M-(O_2 + side chain + H_2O)]$^+$ suggesting the molecular formula $C_{29}H_{46}O_3$. ^{1}H NMR spectrum showed resonances for six methyl groups at δ 0.81 (3H, s, Me-18), 0.88 (3H, s, Me-19), 0.98 (3H, d, *J*=6.31 Hz, Me-21), 0.81 (3H, d, *J*=6.3 Hz, Me-26), 0.83 (3H, d, *J*=6.93 Hz, Me-27), 0.91 (3H, d, *J*=6.63 Hz, Me-28). The resonances at δ 3.96 (1H, m, H-3), 6.25 (1H, d, *J*=8.83 Hz, H-6) and 6.49 (1H, d, *J*=8.83 Hz, H-7) suggested a Δ^6, mono hydroxylated 5α,8α-epidioxysteroidal compound (Gauvin *et al* , 2000). This was confirmed by the presence of an ion fragment at *m/z* 396 [M-O_2] through the loss of O_2 from the molecular ion, presumably by a retro Diels-Alder fragmentation (Gunatilaka *et al* 1981), and by ^{13}C NMR signals at 82.14 and 79.41 of C-5 and C-8, respectively (Yaoita *et al* 1998 and Yue *et al* 2001). The presence of two olefenic protons at δ 5.08 (1H, ddd, *J*=15.2, 8.83, 2.5 Hz) and 5.12 (1H, ddd, *J*=15.6, 8.81, 2.3Hz) was indicative to Δ^{22} unsaturation and assigned to H-23 and H-22 respectively, which were also confirmed by ^{13}C NMR resonances at 135.39 and 132.39 ppm for C-22 and C-23, respectively. The β-configuration of hydroxy group at position 3, δ_H 3.96 (1H, m, H-3) and δ_C 66.44 ppm (d, C-3) was suggested by comparison with the published data of 3α- and 3β- hydroxy steroids (Eggert *et al* 1976, Wright *et al* 1978, and Gauvin *et al*, 2000). Although the NMR data of the position 24 were compared with those given by (Gunatilaka *et al* 1981) the sterochemistry of this position, is still undetected because the chemical shifts of the side chain carbons were not similar enough to those (meassured in C_6D_6) given by (Gunatilaka *et al* 1981) for 24(*R*) or 24(*S*). Therefore, it preferred not to assign the stereochemistry at C-24 for compound **10**. The position of the double bonds and also the methyl groups were confirmed with 2D-NMR experiments of the compound. The NMR data assigned compound **10** as 5α,8α-epidioxy-24ξ-methylcholesta-6,22-dien-3β-ol, that was previously isolated from some marine sponges (like *Axinella cannabina*, *Tethya aurantia*, and *Raphidostila incisa* (Gunatilaka *et al* 1981).

Table (3.3.1): ^{1}H, ^{13}C-NMR data of compound 10 in ($CDCl_3$, 500, MHz)

No.	^{13}C (Multiplicity)	^{1}H (Multiplicity, Hz)	HMBC correlation H-------C
1	34.67 t	1.68 (m)	
2	30.09 t	1.5 (m)	
3	66.44 d	3.96 (m)	C-5
4	36.91 t	1.85 (m), 2.12 (ddd *J*=13.87, 5.04, 1.89 Hz)	C-3, C-5
5	82.14 s	-	
6	135.39 d	6.25 (d, *J*=8.83 Hz)	C-4, C-5, C-8
7	130.73 d	6.49 (d, *J*=8.83 Hz)	C-5, C-8
8	79.41 s	-	
9	51.06 d	1.52 (t)	C-8, C-10
10	36.94 s	-	
11	23.38 t	1.21 (m)	C-8, C-13
12	39.32 t	1.27 (m)	
13	44.54 s	-	
14	51.68 d	1.6 (m)	C-13, C-8
15	20.65 t		
16	28.90 t		
17	56.12 d	1.25(m)	
18	12.82q	0.81 (s)	C-12, C-13, C-14 ,C-17
19	18.01q	0.88 (s)	C-10, C-9, C-5
20	39.8 d	2.03(m)	
21	20.89	0.98 (d, *J*=6.31 Hz)	C-20
22	135.39 d	5.08 (ddd, *J*=15.2, 8.83, 2.5 Hz)	C-20, C-24
23	132.39 d	5.12 (ddd, *J*=15.6, 8.81, 2.3 Hz)	C-20, C-24
24	43.04 d	1.85 (m)	
25	33.17 d	1.47 (m)	
26	20.14 q	0.81 (d, *J*=6.3 Hz)	C-25, C-24
27	19.63 q	0.83 (d, *J*=6.93 Hz)	C-25
28	18.16 q	0.91 (d, *J*=6.62 Hz)	C-25, C-24

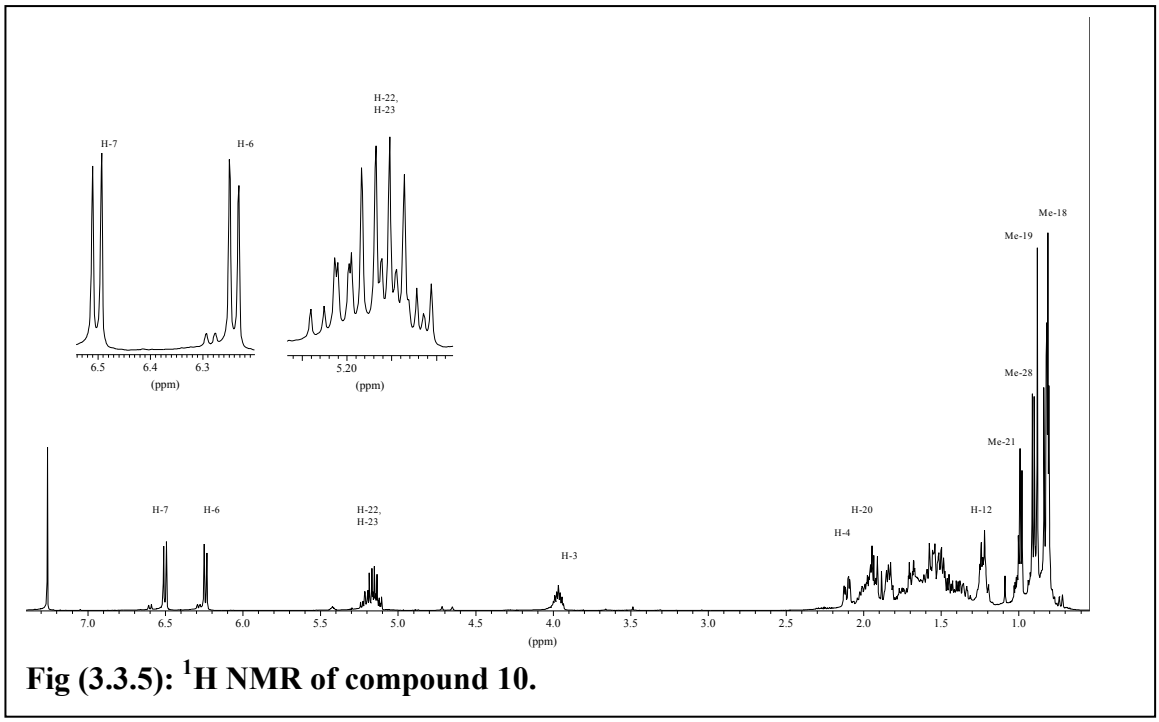

Fig (3.3.5): ^{1}H NMR of compound 10.

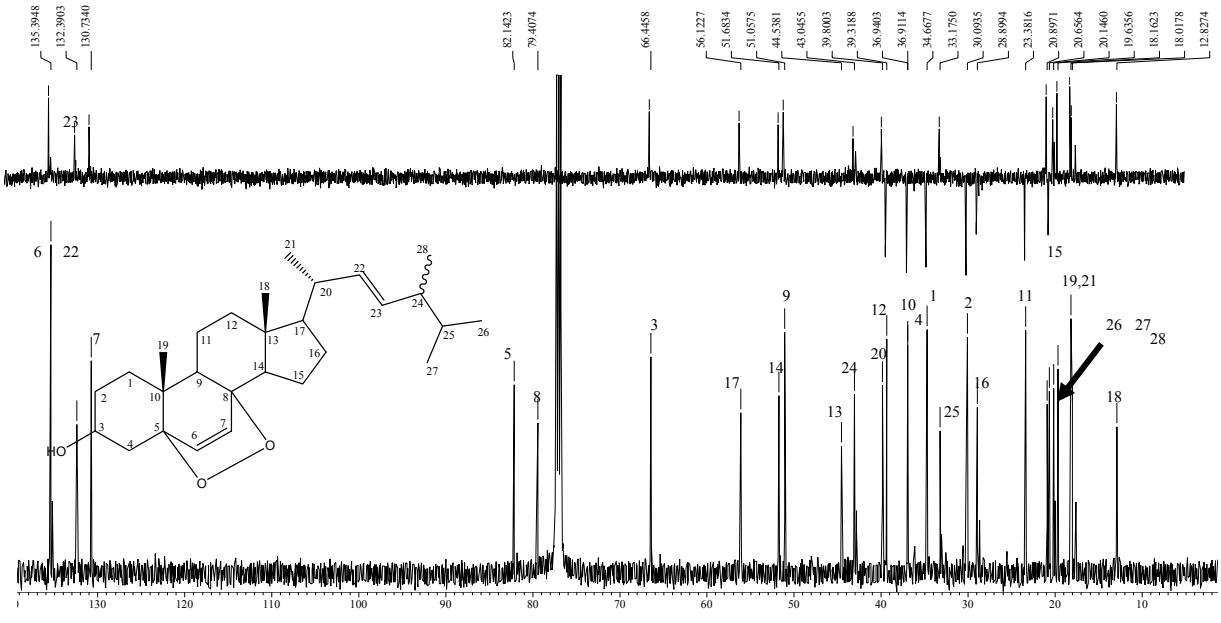

Fig (3.3.6): ^{13}C NMR and DEPT spectra of compound 10.

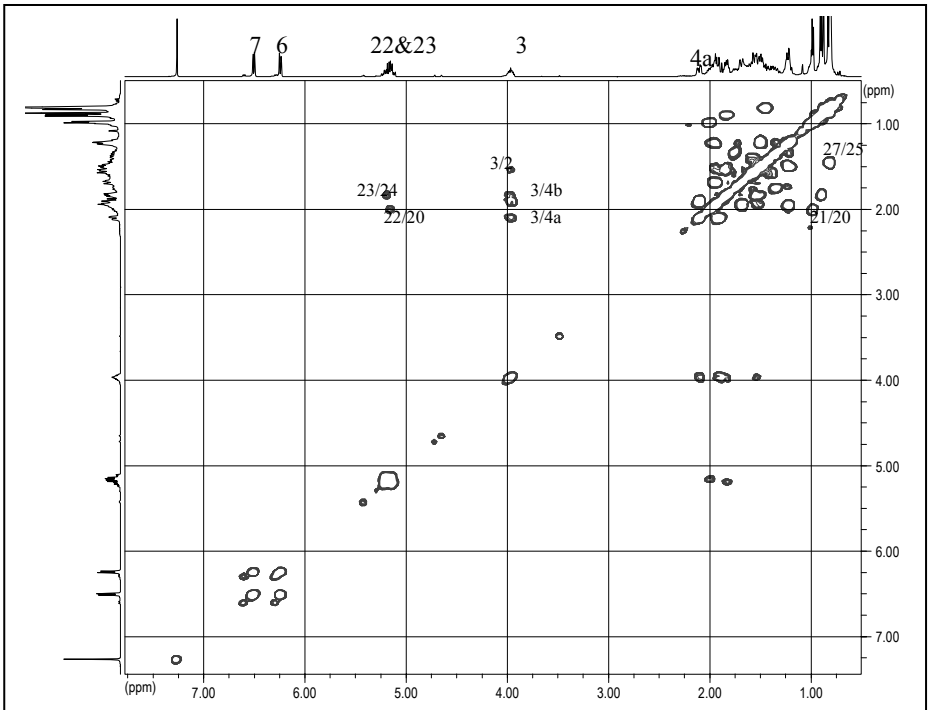

Fig (3.3.8): COSY spectrum of of compound 10

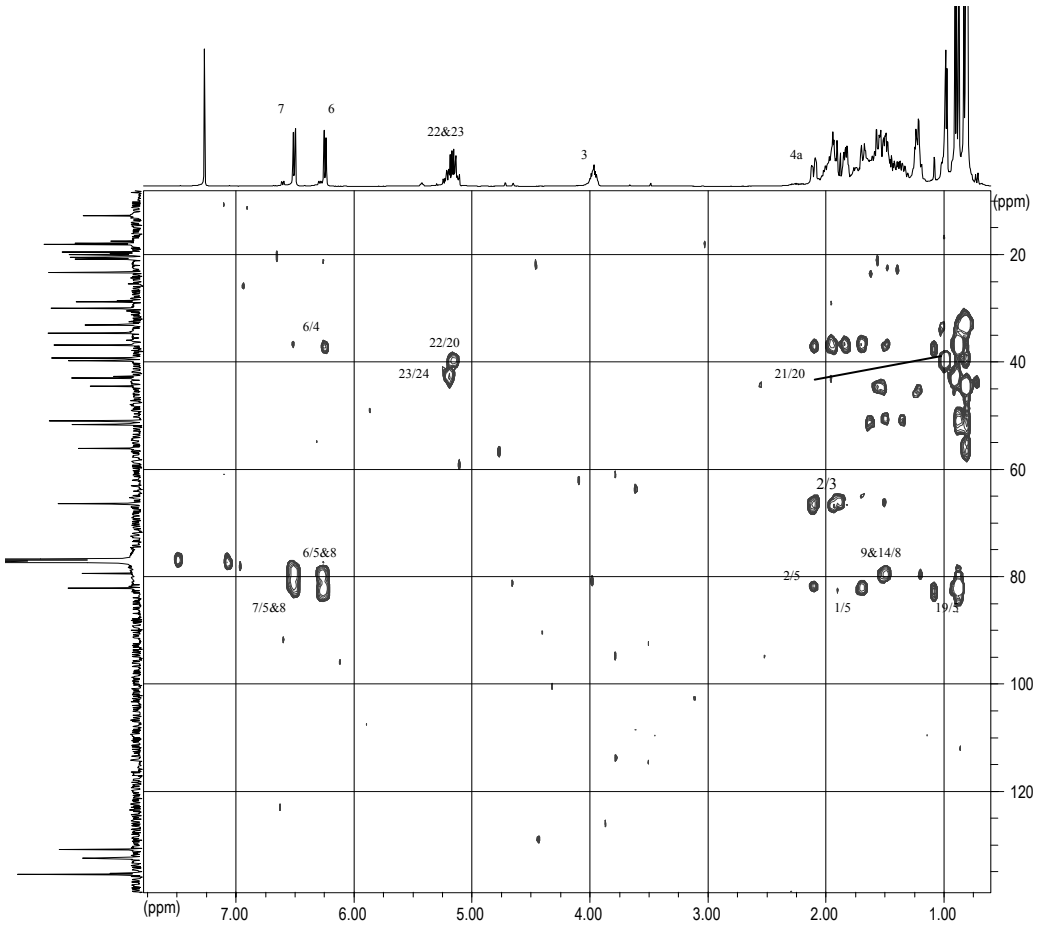

Fig (3.3.9): HMBC spectrum of of compound 10

3.3.2- 5α,8α-epidioxy-24ξ-ethylcholesta-6,22-dien-3β-ol (11, known compound)

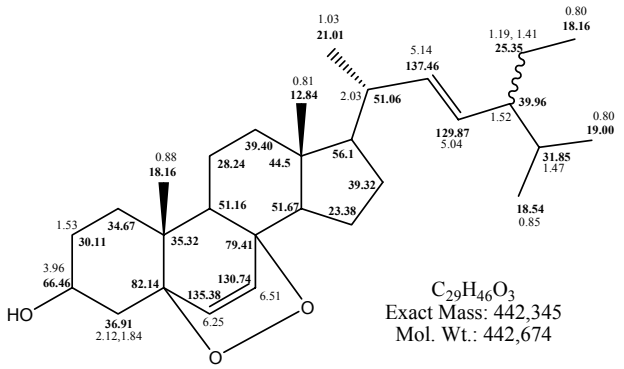

Fig(3.3.10): compound 11.

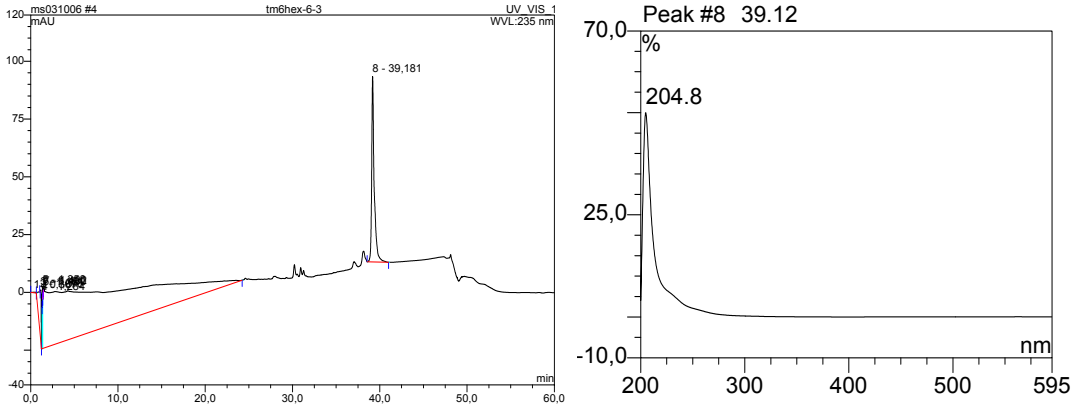

Fig (3.3.11) HPLC chromatogram and UV-spectrum of compound 11.

Yield : 4.5 mg

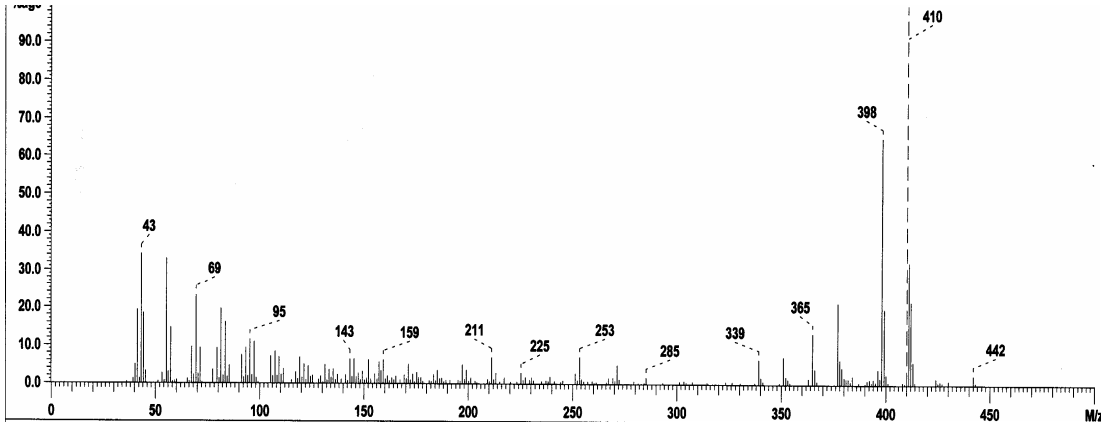

Fig (3.3.12) EI-MS spectrum of compound 11

Compound **11** was also isolated as crystalline white needles, with $[\alpha]_D$ of - 10° (*c* 0.3 $CHCl_3$). Compound **11** has UV absorption at λ_{max} 204 nm. EI-MS showed molecular ion peak at *m/z* 442 $[M]^+$ and fragment ions at *m/z* 410 $[M\text{-}O_2]^+$, 398 $[M\text{-}(C_2H_3O)]^+$, 396 $[M\text{-}(O_2 + CH_2)]^+$, 377 $[M\text{-}(O_2 + H_2O + CH_3)]^+$, 363 $[M\text{-}(O_2 + H_2O + C_2H_5)]^+$, 271 [M-($O_2$ + side chain)]$^+$ and 253 [M-(O_2 + side chain + H_2O)]$^+$. suggesting the molecular formula $C_{29}H_{46}O_3$. ^{1}H NMR spectrum showed resonances for again six methyl groups at δ 0.81 (3H, s, Me-18), 0.89 (3H, s, Me-19), 1.03 (3H, d, *J*=6.41 Hz, Me-21), 0.80 (3H, d, *J*=6.92 Hz, Me-27), 0.85 (3H, d, *J*=6.91 Hz, Me-26), 0.80 (3H, t, *J*=6.3 Hz, Me-29) as found in compound 10. The resonances at δ 3.96 (1H, m, H-3), 6.25 (1H, d, *J*=8.83 Hz, H-6) and 6.51 (1H, d, *J*=8.83 Hz, H-7) suggested a Δ^6, mono hydroxylated 5α,8α-epidioxysteroidal compound (Gauvin *et al* 2000). By comparison between the EIMS spectra of compounds **10** and **11** especially for the most abundant fragment (M-O_2, rel. abundance 100%) for both compounds, compound **11** is 14 mass units larger than **10** which indicated the presence of one additional methylene group in **11**. This CH_2 group is assigned at position 28 as evident from its COSY spectrum. The differences in the NMR data between **10** and **11** are evident only for the side chain as mentioned in table 3.3.2, while the NMR data of the tetracyclic carbon skeleton are superimposible. Compound **11** formed two stereoisomers due to the stereochemistry at position 24 as evident from ^{1}HNMR spectrum where the triplet signal at δ 0.80 of C*H*$_3$-29 showed another set of resonances at the same position with only 1.2 Hz difference in the chemical shift value. Therefore compound **11** was assigned as a racemic mixture of 24(*R*) and 24(*S*) at a ratio of 1:1. This was also confirmed by the corresponding δ_C values of the side chain which showed signals with small intensities compared to those of the tetracyclic part. The NMR data assigned compound **11** as [5α,8α-epidioxy-24ξ-ethylcholesta-6,22-dien-3β-ol], which was also previously isolated from some marine sponges like *Luffariella* sp. (Gauvin *et al* 2000) and *Raphidostila incisa* (Gunatilaka *et al* 1981).

Table (3.3.2): ^{1}H, ^{13}C-NMR data of compound 11 in ($CDCl_3$, 500, MHz)

No.	^{13}C (Multiplicity)	^{1}H (Multiplicity, Hz)	HMBC correlation H-------C
1	34.67 t		
2	30.11 t	1.53 (m)	
3	66.46 d	3.96 (m)	C-5
4	36.91 t	1.85 (m), 2.12 (ddd *J*=13.87, 5.04, 1.89 Hz)	C-3, C-5
5	82.14 s	-	
6	135.38 d	6.25 (d, *J*=8.83 Hz)	C-4, C-5, C-8
7	130.74 d	6.51 (d, *J*=8.83 Hz)	C-5, C-8
8	79.41 s	-	
9	51.16 d		
10	35.32 s	-	
11	28.24 t		
12	39.40 t		
13	44.5 s	-	
14	51.67 d		
15	23.38 t		
16	39.32 t		
17	56.10 d		
18	12.84 q	0.81 (s)	C-12, C-13, C-14 ,C-17
19	18.16 q	0.89 (s)	C-10, C-9, C-5
20	51.06 d	2.03(m)	
21	21.01 q	1.03 (d, *J*=6.31 Hz)	C-20
22	137.46 d	5.14 (ddd, *J*=15.2, 8.83, 2.3 Hz)	C-20, C-24
23	129.87 d	5.04 (ddd, *J*=15.6, 8.81, 2.3 Hz)	C-20, C-24
24	39.96 d	1.52 (m)	
25	31.85 d	1.47 (m)	
26	19.00 q	0.80 (d, *J*=6.93 Hz)	C-25, C-24
27	18.54 q	0.85 (d, *J*=6.93 Hz)	C-25
28	25.35 t	1.19, 1.41 (m,m)	
29	18.16 q	0.80 (m)	C-28

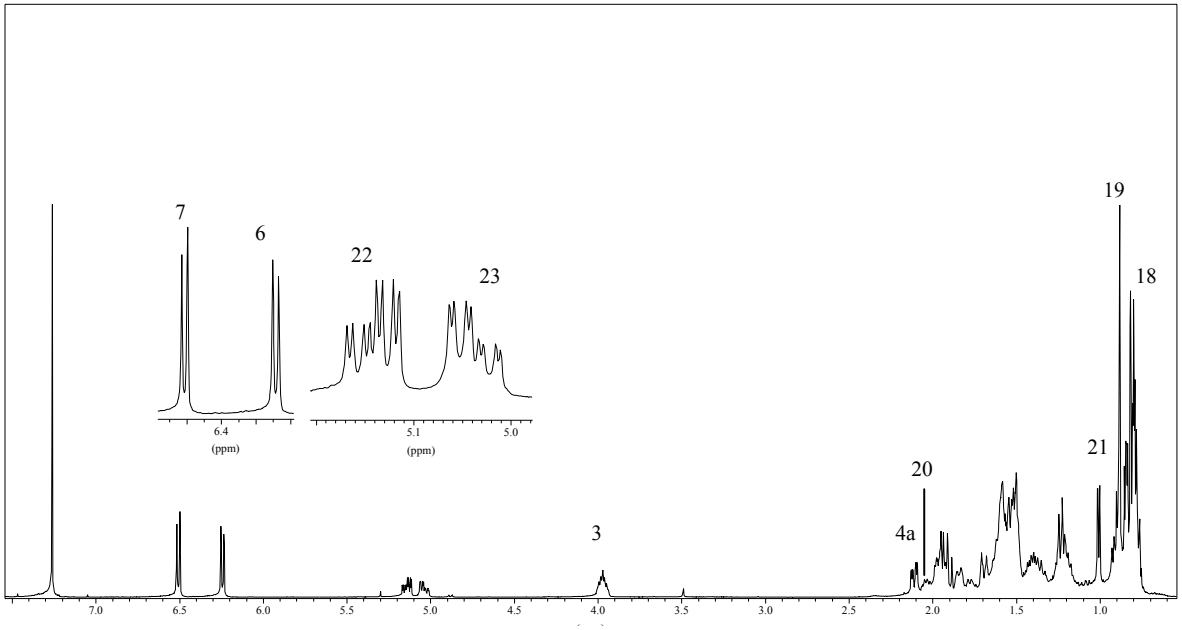

Fig (3.3.13): ^{1}H NMR spectrum of compound 11.

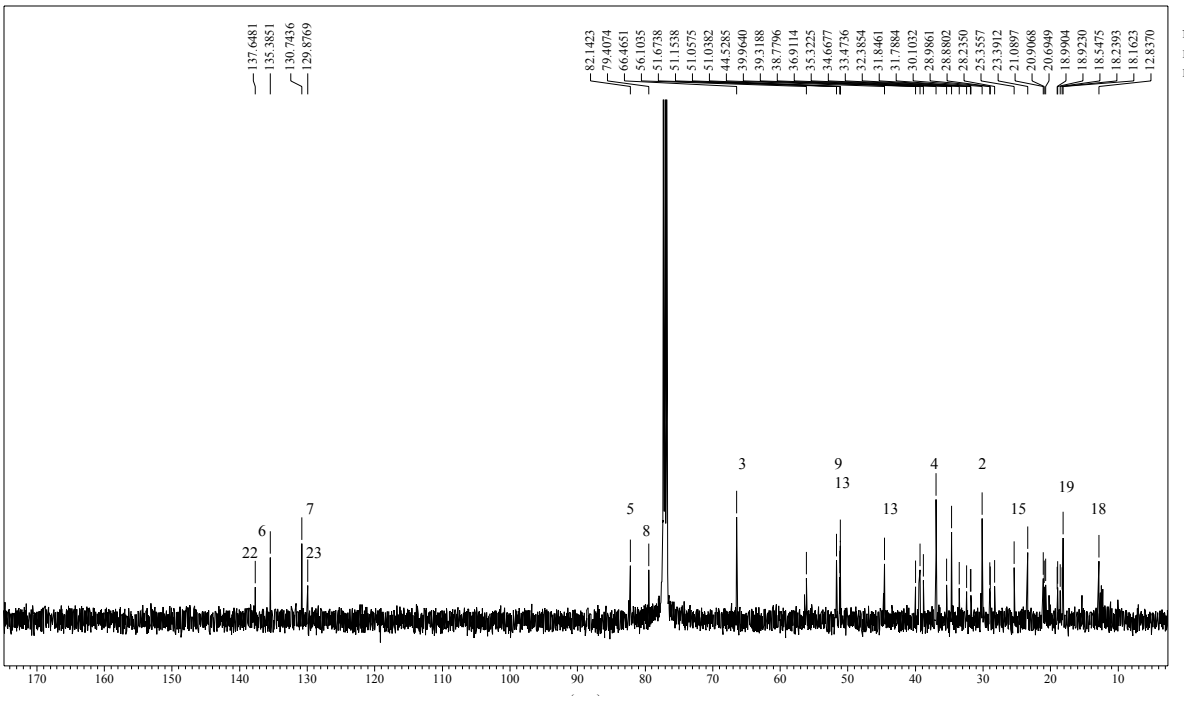

Fig (3.3.14): ^{13}C NMR spectrum of compound 11.

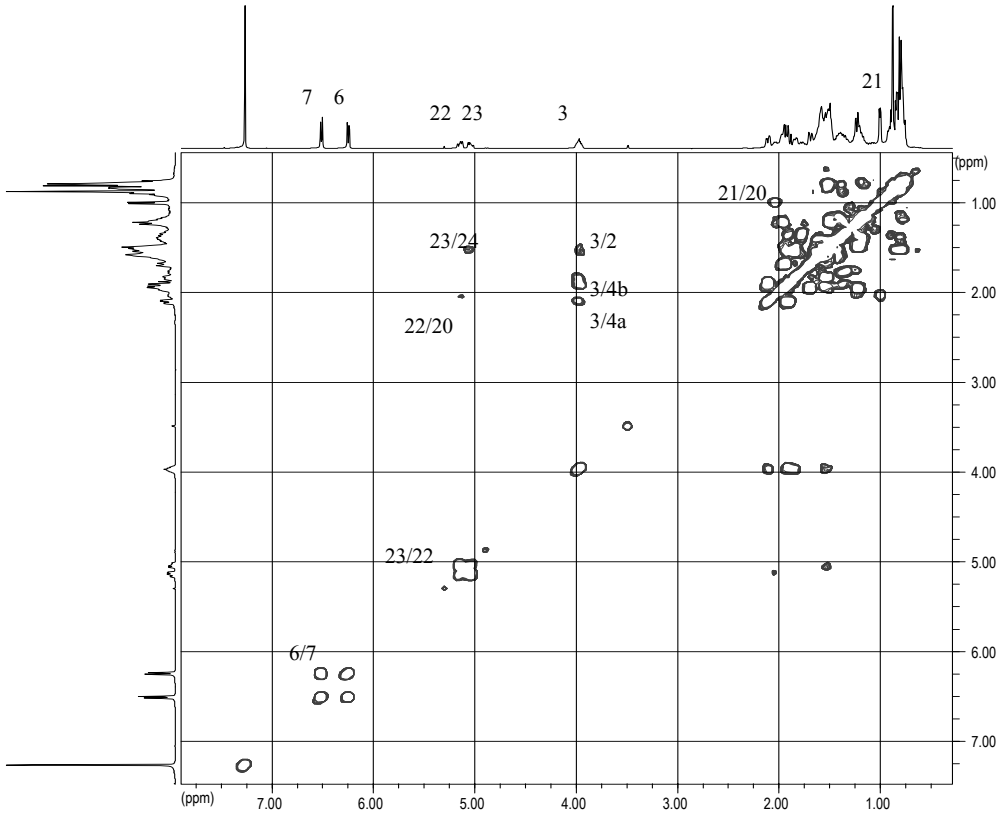

Fig (3.3.15): COSY spectrum of compound 11.

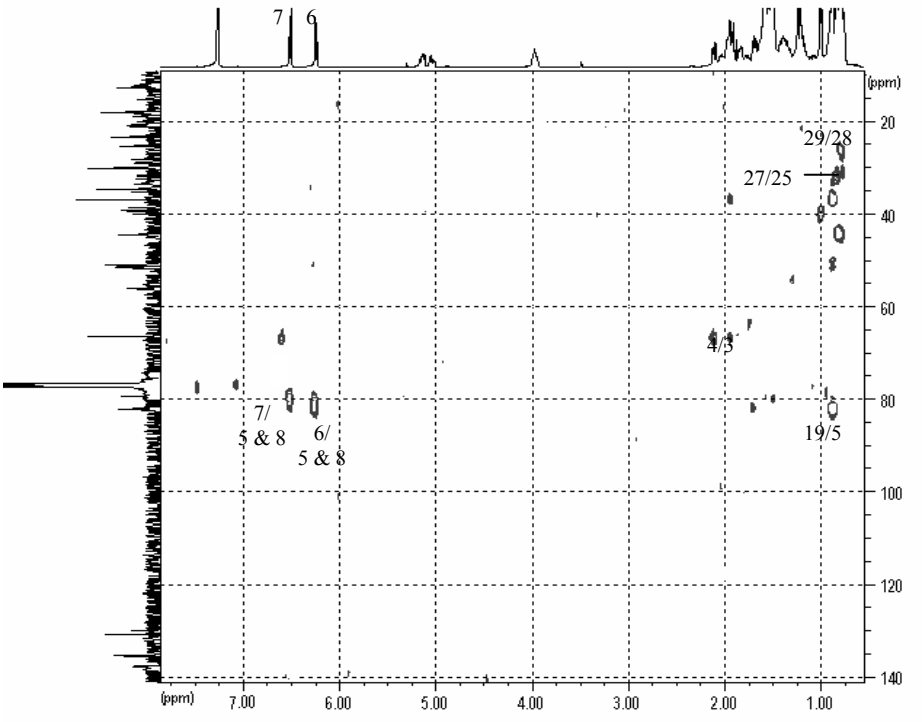

Fig (3.3.16): HMBC spectrum of compound 11.

3.3.3- 8-hydroxy-4-Quinolone (12, known compound)

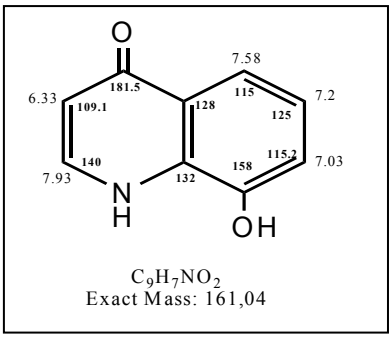

$C_9H_7NO_2$
Exact Mass: 161,04

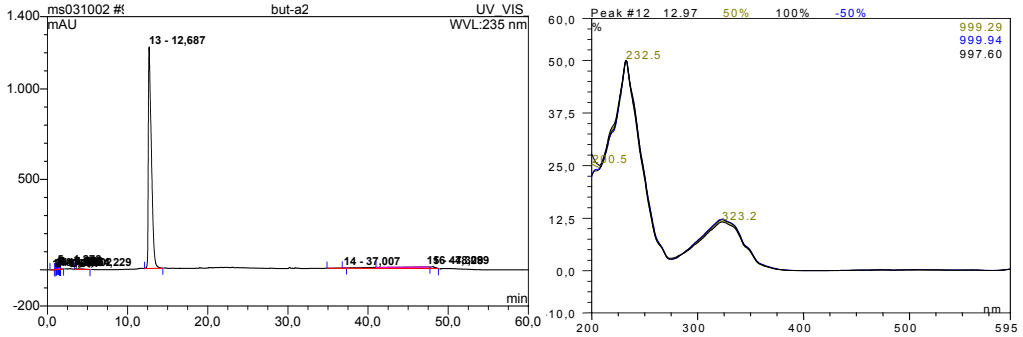

Fig (3.3.17): HPLC chromatogram and UV-spectrum of compound 12.

Yield : 3.8 mg

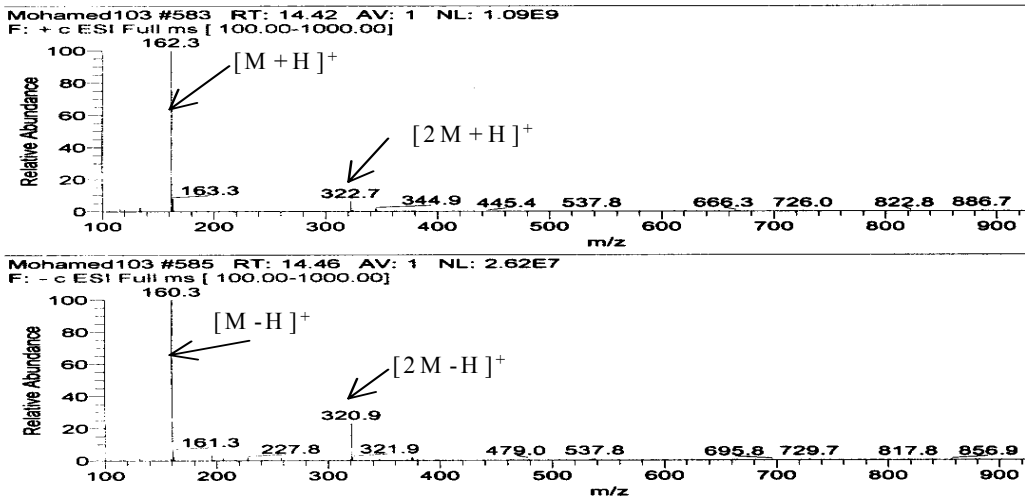

Fig (3.3.18): ESI-MS of compound 12.

Compound **12** [8-hydroxy-4-quinolone] was isolated as a brownish yellow amorphous powder. Compound **12** has UV absorption at λ_{max} (MeOH) 200, 232, 220, 323 and 335 nm. Positive ESI-MS showed molecular ion peak at *m/z* 162 $[M+H]^+$ and negative molecular ion peak at *m/z* 160 $[M-H]^-$ suggesting the molecular formula $C_9H_7NO_2$. ^{1}H NMR spectrum showed resonances for five aromatic protons for two spin systems, 1st spin system composed of two resonances at δ 7.93 (1H, d, *J*= 6.94 Hz) and 6.33 (1H, d, *J*= 6.94 Hz), the 2nd spin system composed of three proton resonances at δ 7.58 (1H, dd, *J*= 7.90, 0.94 Hz), 7.2 (1H, t, *J*= 7.88 Hz) and 7.03(1H, dd, *J*= 7.90, 0.94 Hz). COSY spectrum confirmed the above spin systems. These data sugested the presence of two aromatic rings, the odd numbered MW suggested the occurence of one nitrogen atom while the presence of three nitrogens or more was excluded. The disappearence of the exchangeable protons (N*H* and O*H*) was expected because deuterated methanol was used. By searching in the commercially available computer program „Dictionary of Natural Product (DNP)“ it was suggested that compound **12** is 8-hydroxy-4-quinolone which was isolated previously (Siuda 1974). The NMR data were identical to those of 8-hydroxy-4-quinolone which was previously isolated from the ink glands of the marine giant octopus, *Octopus dofleini martini* (Siuda 1974). The deduced data of compound **12** were confirmed by HMQC and HMBC experiments. The presence of tautomerisation was evident from the presence of four aromatic spin systems (two spin systems for each tautomer) as evident from the ^{1}H NMR and COSY spectra of the same sample in deuterated DMSO as shown in figures (3.3.19 and 3.3.20).

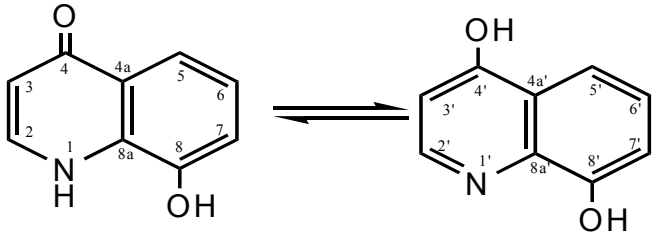

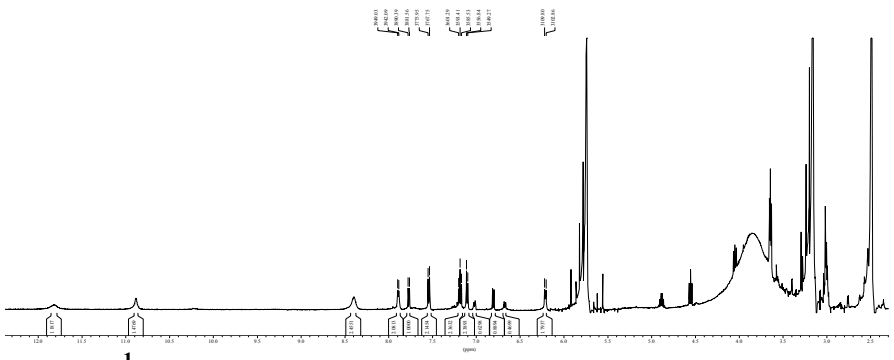

Fig (3.3.19):^{1}H NMR spectrum of compound 12 (measurred in DMSO)

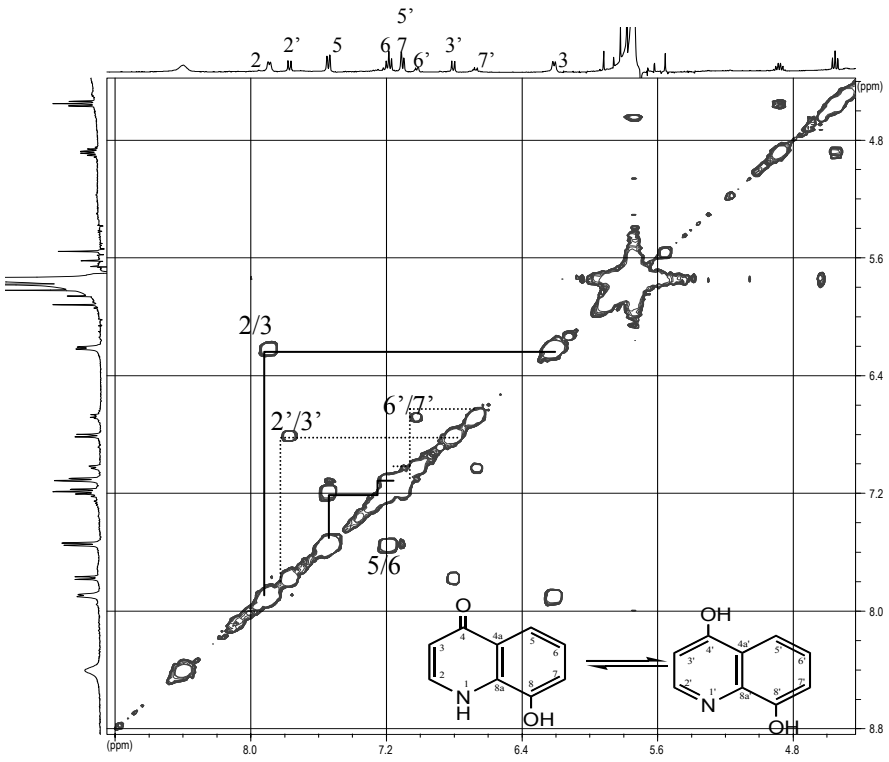

Fig (3.3.20):COSY spectrum of compound 12 (DMSO-d_6)

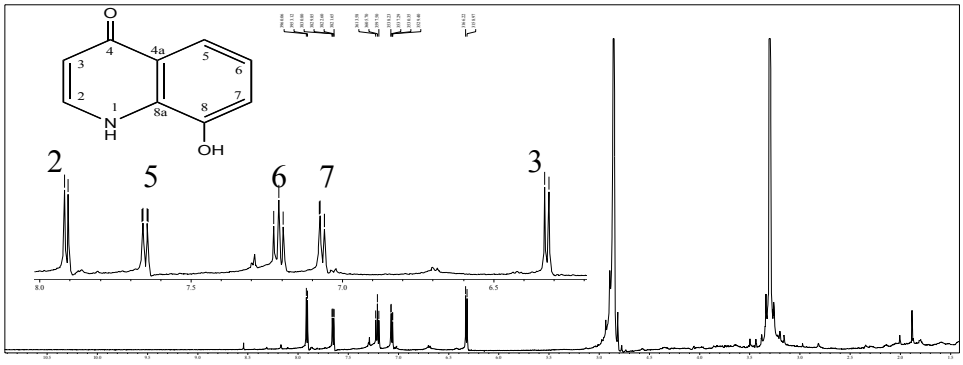

Fig (3.3.21):^{1}H NMR spectrum of compound 12 (methanol-d_4)

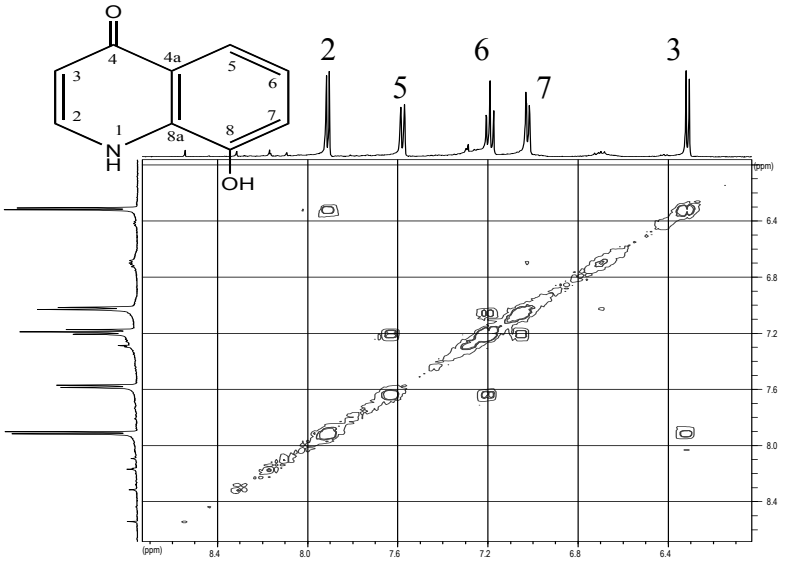

Fig (3.3.22):COSY spectrum of compound 12 (showing H/H correlations)

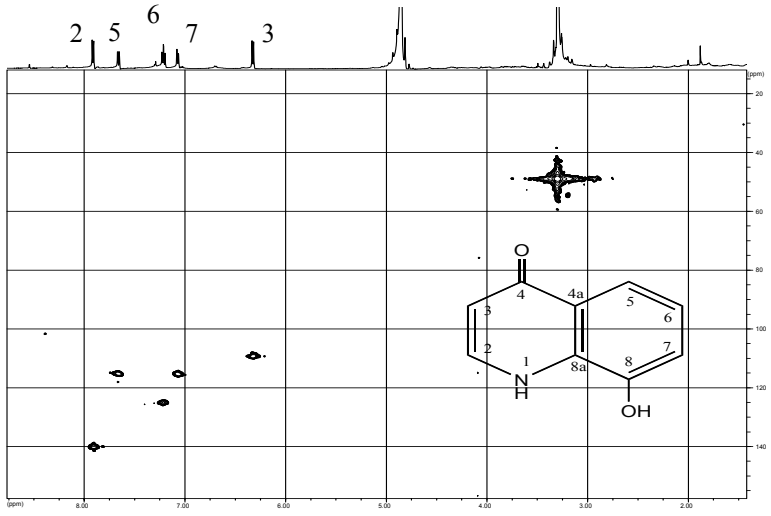

Fig (3.3.23):HMQC spectrum of compound 12 (showing H/C direct correlations)

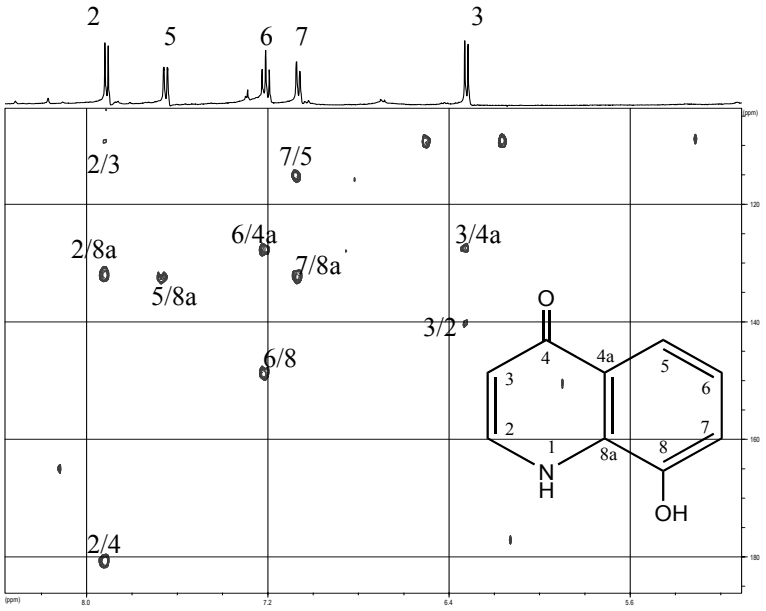

Fig (3.3.24):HMBC spectrum of compound 12 (showing H/C long range correlations)

Bioactivity:

Many of the reported 5α, 8α- epidioxy sterols showed significant biological activity including antimycobacterial activity (Cantrell *et al* 1999), inhibitive activity against the human T-cell leukemia/lymphotropic virus type I (HTLV-I), cytotoxic activity against the human breast cancer cell line (MCF_7 WT) (Gauvin *et al* 2000), and antitumor activity against different tumour cell lines (Bok *et al* 1999). 8-Hydroxy-4-quinolone (compound **12**) was reported to be one of the ink components that is ejected by the giant octopus *Octopus dofleini martini* which was reported to have antipredatory activity (Siuda 1974). Some other quinolone analogues (e.g. 3,8-dihydroxyquinoline) showed mild cytotoxic activity against the growth of several human tumour cell lines(Moon *et al* 1996).

Cytotoxic activity of compounds **10** and **11** showed growth inhibitiory effect of 57.2 % and 38.6 %, respectively at a concentration of 10 µg/mL each against L5178Y cancer cells. Compound **12** showed neither significant antimicrobial activity nor cytotoxic activity in our available test systems.

3.4-Natural products from *Hyrtios erectus*

The secondary metabolites from the genus *Hyrtios* especially *Hertios erectus* (also called *H. erecta*) have been investigated extensively [Kobayashi *et al* 1990; Kobayashi *et al* 1994a; Miyaoka *et al* 2000; Pettit *et al* 1998a; Pettit *et al* 1998b; Pettit *et al* 1998c; Youssef 2005; Youssef *et al* 2005, Youssef *et al* 2002]. Previous chemical investigations of different *Hyrtios* sp. and their associated microorganisms have revealed the presence of numerous structurally unique natural products including scalarane sesterterpenoids, acyclic triterpenoids, indole alkaloids, macrolides and usual- and unusual steroids. Many of these compounds possess important biological activities. The most important metabolites of the genus *Hyrtios* discovered to date include the powerful anticancer agents spongistatins (Pettit *et al* 1993; Pettit *et al* 1994). Which in turn prompted the same authers to exhaustively recollect the same sponge *Hyrtios erecta* (600 kg wet wt.) for further chemical investigations. The later chemical investigations resulted in the isolation of antineoplastic sesterstatins in very minute quantities (Pettit *et al* 1998b, Pettit *et al* 1998c, and Pettit *et al* 2005).

However, in the present study, 210 g. dry weight of *Hyrtios erectus* collected from the Red Sea – Egypt were chemically investigated and nine compounds were isolated. The isolated compounds consisted of 8 known compounds and one new 5-hydroxy-1*H*-indole derivative.

3.4.1- Hyrtiosine A (13, Known compound):

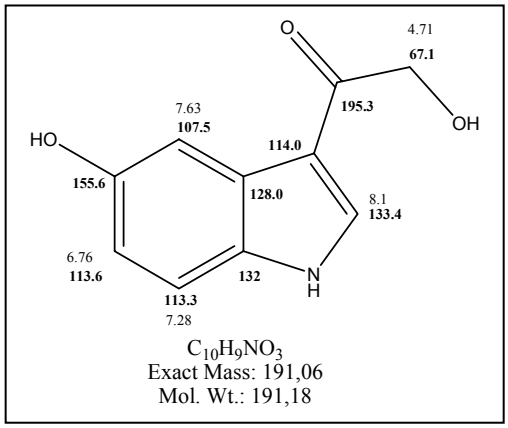

$C_{10}H_9NO_3$
Exact Mass: 191,06
Mol. Wt.: 191,18

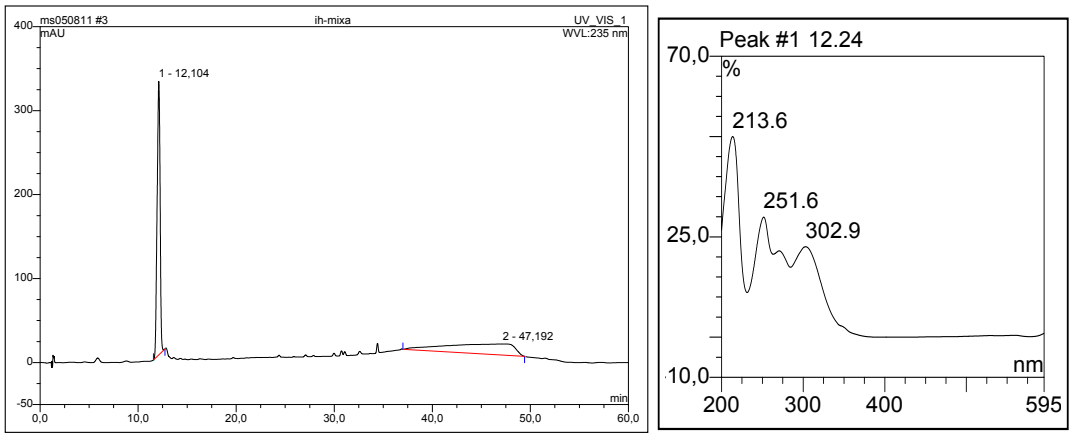

Fig (3.4.1):HPLC chromatogram and UV-spectrum of compound 13.

Yield : 5 mg

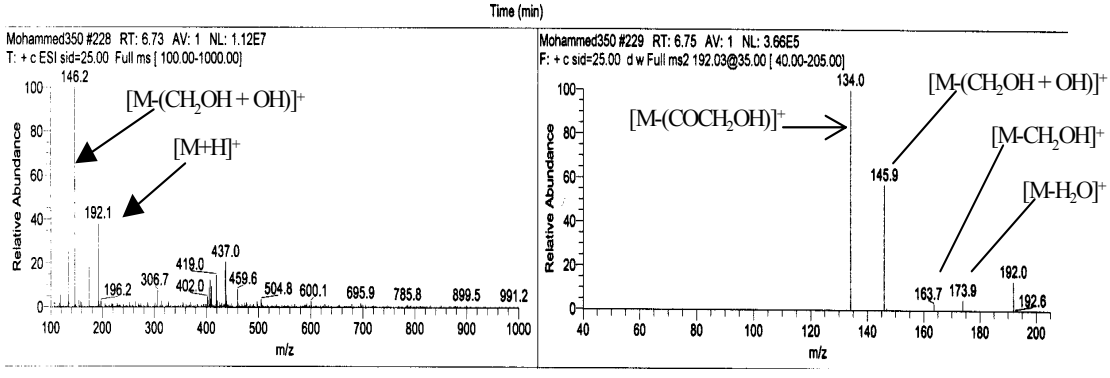

Fig (3.4.2):(+ve) ESI-MS spectrum of compound 13 and its MS/MS spectrum.

Compound **13**, **Hyrtiosine A**, [5-Hydroxy-3-(hydroxyacetyl)-1H-indole] was isolated as brownish transluscent amorphous powder, with slightly offensive characteristic odour. Compound **13** shows positive pseudomolecular ion peak at *m/z* 192 $[M+1]^+$ and negative pseudomolecular ion peak at *m/z* 190 $[M-1]^-$ suggesting the molecular formula $C_{10}H_9NO_3$. The UV (MeOH) absorption maxima of **13** at λ_{max} 213, 251, 271 and 302 nm indicative of a 3-acyl indole chromophore (Kobayashi *et al* 1990). The ^{1}H NMR (CD_3OD) showed 5 proton resonances at δ 8.1 (1H, s ; H-2), 7.63 (1H, d, *J* = 2.21 Hz; H-4), 6.76 (1H, dd, *J* = 2.21,8.83 Hz; H-6), 7.28 (1H, d, *J* = 8.83 Hz; H-7), 4.71 (2H, s ; H-9). The ^{13}C NMR resonances were obtained indirectly from the long range correlations (HMBC spectrum), see table (3.4.1). The HMBC spectrum showed long range correlations between C*H*$_2$-9 and the carbonyl C-8 at 195.3 ppm and C-3 at 114.0 ppm. Indeed, the following HMBC correlations were observed (H/C): H-2/C-3, H-2/C-3a, H-2/C-7a, H-4/C-5, H-4/C-7a, H-4/C-6, H-4/C-3, H-6/C-7a, H-4/C-5, H-7/C-3a, H-7/C-5. The NMR data and the UV absorption maxima identified **13** as Hyrtiosine A that was previously isolated from the same sponge (Kobayashi *et al* 1990) and from *Dragmacidon* sp (Pedpradab *et al* 2004).

Table (3-4.1): NMR data of compound 13 (Methanol-d$_4$, 500 MHz).

No.	^{13}C, (δ = ppm)	^{1}H (δ = ppm), couppling constant (*J*= Hz)	HMBC correlations H→ C
2	133.4	δ 8.1 (1H, s)	3, 3a, 7a
3	114.0		
3a	128		
4	107.5	7.63 (1H, d, *J* = 2.21)	5, 7a, 6, 3
5	155.6		
6	113.6	6.76 (1H, dd, *J* = 2.21& 8.83)	5, 7a
7	113.3	7.28 (1H, d, *J* = 8.83)	5, 3a
7a	132		
8	195.3		
9	67.1	4.71 (2H, s)	8, 3

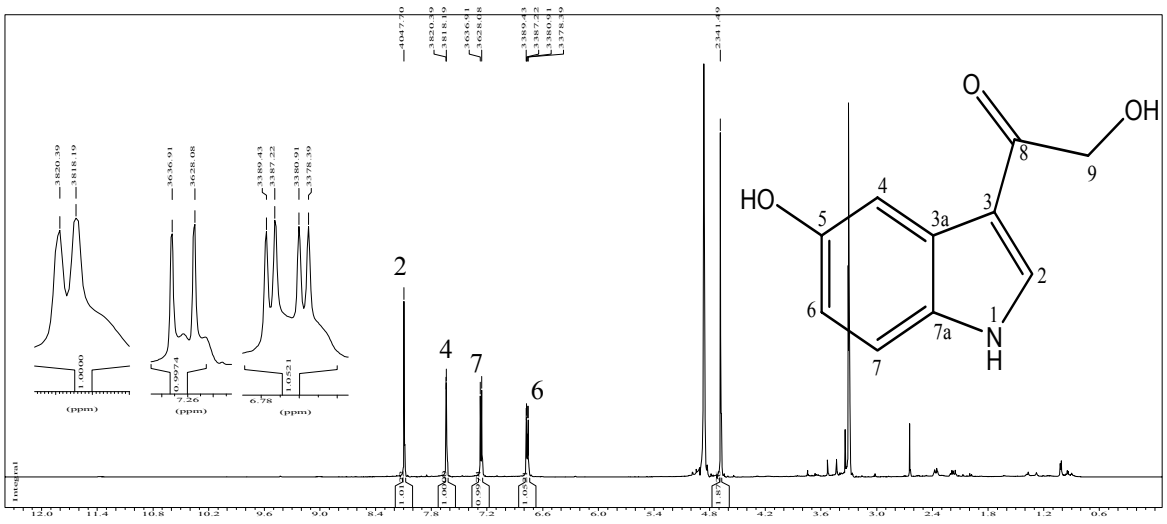

Fig (3.4.3):^{1}H NMR spectrum of compound 13 (CD_3OD).

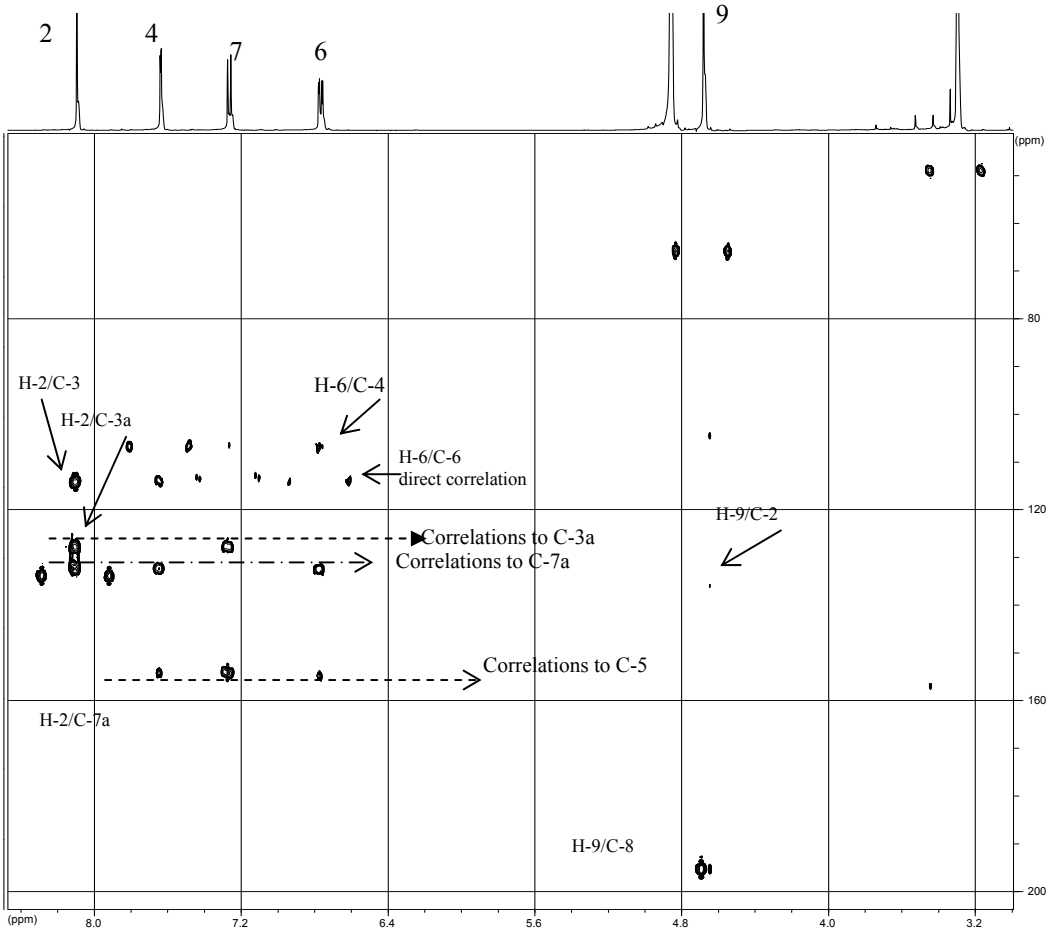

Fig (3.4.4): HMBC spectrum of compound 13 (CD_3OD).

3.4.2- 5-Hydroxy-1*H*-indol-3-carbaldehyde (14, Known compound):

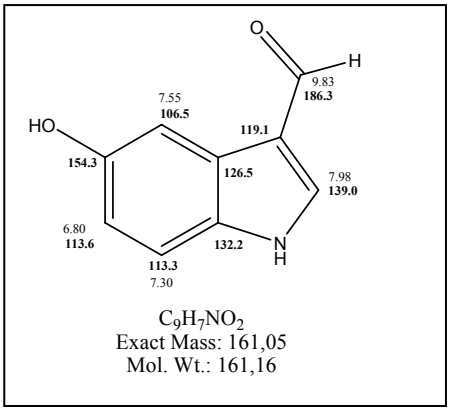

$C_9H_7NO_2$
Exact Mass: 161,05
Mol. Wt.: 161,16

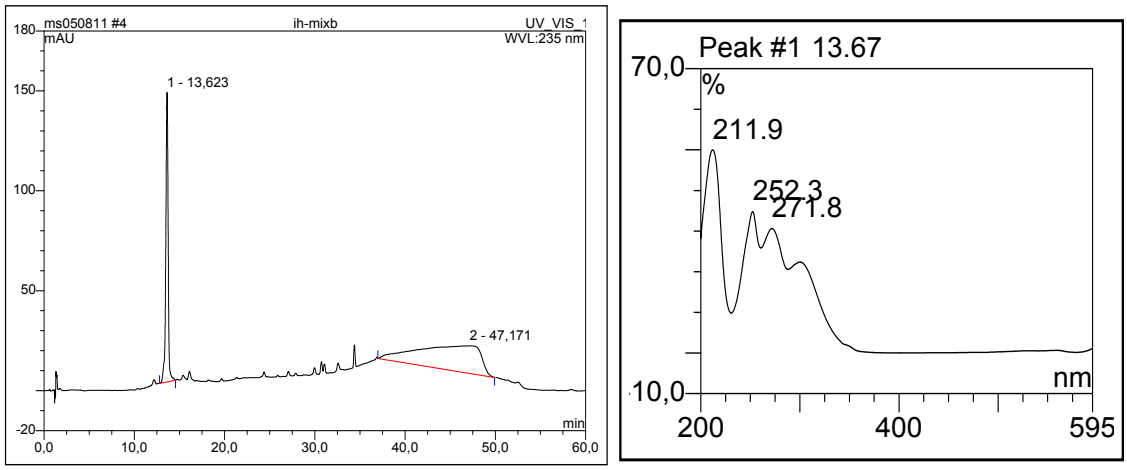

Fig (3.4.5):HPLC chromatogram and UV-spectrum of compound 13.

Yield : 2.5 mg

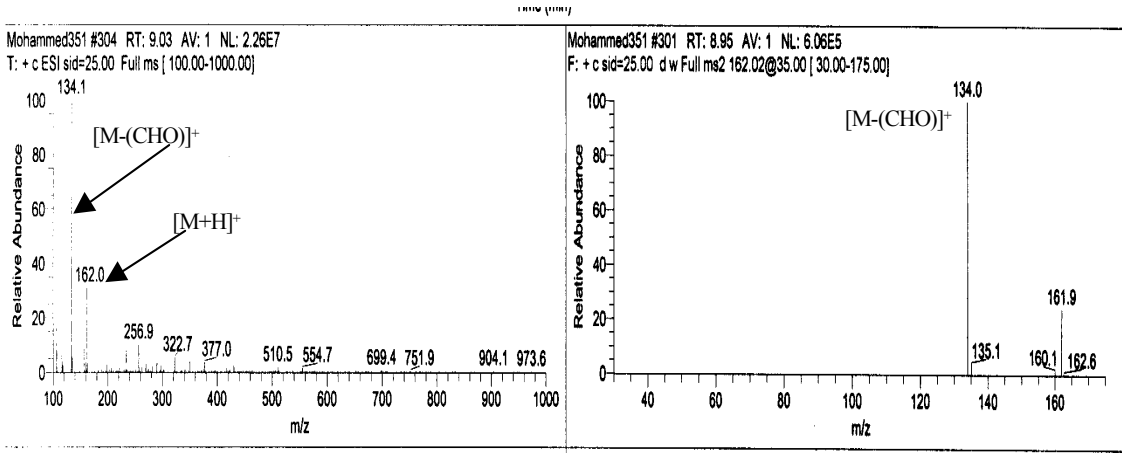

Fig (3.4.6):(+ve) ESI-MS spectrum of compound 14 and its MS/MS spectrum.

Compound **14**, [5-Hydroxy-3-formyl-1*H*-indole] was isolated as a brownish transluscent amorphous powder with characteristic odour. Compound **14** shows a positive pseudomolecular ion peak at *m/z* 162 $[M+1]^+$ and a negative pseudomolecular ion peak at *m/z* 160 $[M-1]^-$ suggesting the molecular formula $C_9H_7NO_2$. The UV (MeOH) absorption maxima of **14** at λ_{max} 211, 252, 271 and 302 nm were indicative of a 3-acyl indole chromophore (Kobayashi *et al* 1990). The ^{1}H NMR (CD_3OD) showed 5 proton resonances at δ 7.98 (1H, s ; H-2), 7.55 (1H, d, *J* = 2.52 Hz; H-4), 6.80 (1H, dd, *J* = 2.52, 8.51 Hz; H-6), 7.3 (1H, d, *J* = 8.51 Hz; H-7) and 9.83 (1H, s ; H-8). The ^{13}C NMR resonances were obtained indirectly from HMBC spectrum, see table 3.4.2 . The following proton-detected long range correlations were observed (H/C): H8/C-3, H-8/C-3a, H-2/C-3, H-2/C-3a, H-2/C-7a, H-4/C-6, H-4/C-7a, H-6/C-7a, H-7/C-3a, H-7/C-5. The NMR data confirmed **14** as 5-hydroxy-3-formyl indole which has been previously isolated from the same sponge (Kobayashi *et al* 1990) and from *Dragmacidon* sp (Pedpradab *et al* 2004).

Table (3.4.2): NMR data of compound 14 (Methanol-d_4, 500 MHz).

No.	**^{13}C, (δ = ppm)**	**^{1}H (δ = ppm), couppling constant (J= Hz)**	**HMBC correlations H→ C**
2	139.0	δ 7.98 (1H, s)	3, 3a, 7a
3	119.1		
3a	126.5		
4	106.5	7.63 (1H, d, *J* = 2.52 Hz)	7a, 6
5	154.3		
6	113.6	6.8 (1H, dd, *J* = 2.52& 8.51 Hz)	7a
7	113.3	7.3 (1H, d, *J* = 8.51 Hz)	5, 3a
7a	132.2		
8	186.3	9.83 (1H, s)	3, 3a

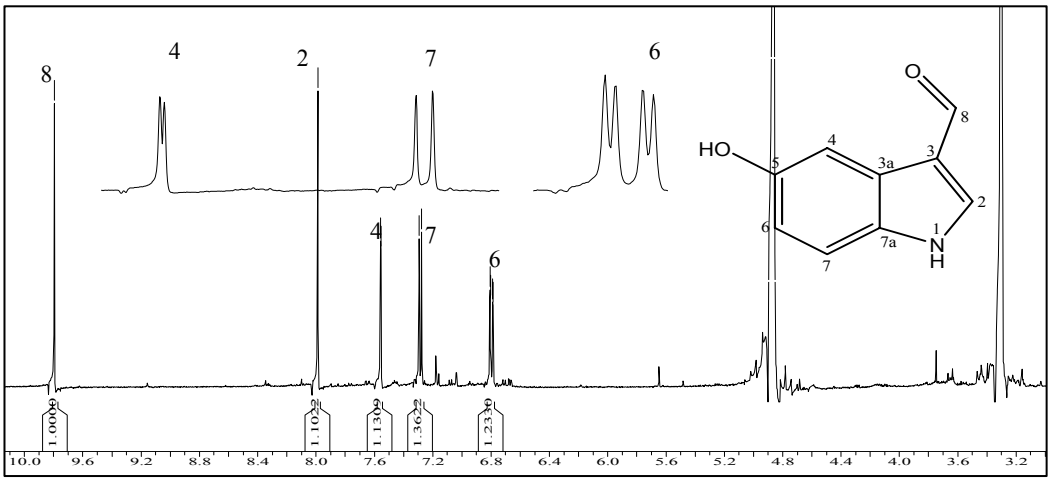

Fig (3.4.7):^{1}H NMR spectrum of compound 14 (CD_3OD).

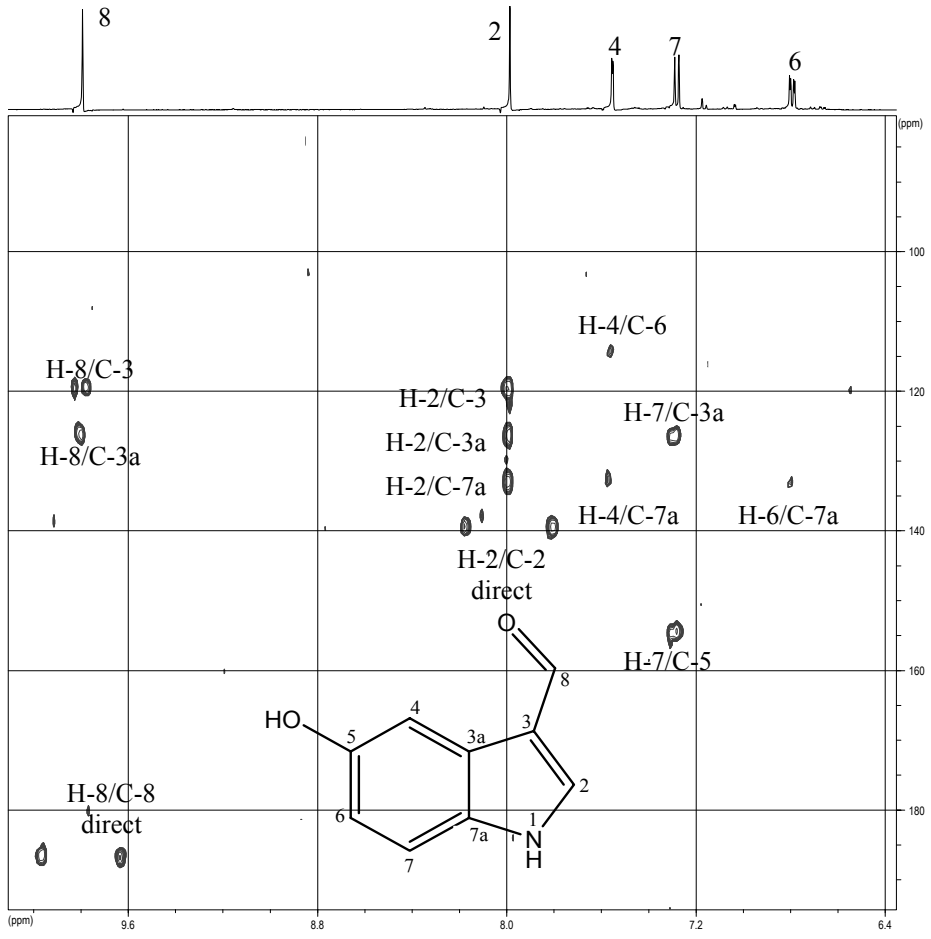

Fig (3.4.8): HMBC spectrum of compound 14 (CD_3OD).

3.4.3- Indol-3 carbaldehyde (15, Known compound, first isolation from genus *Hyrtios*):

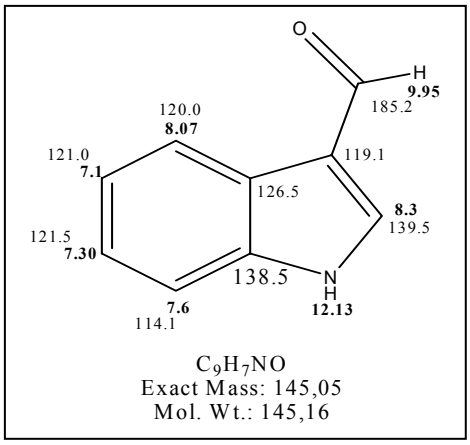

C_9H_7NO
Exact Mass: 145,05
Mol. Wt.: 145,16

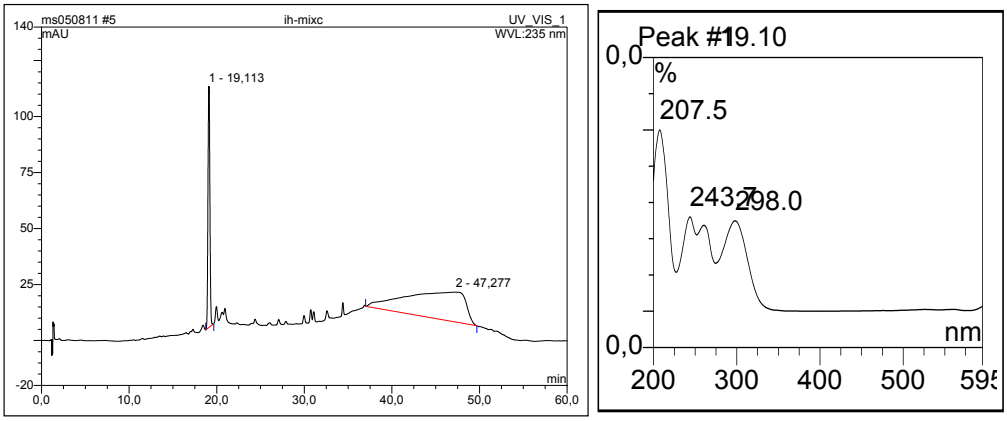

Fig (3.4.9):HPLC chromatogram and UV-spectrum of compound 13.

Yield : 2.3 mg

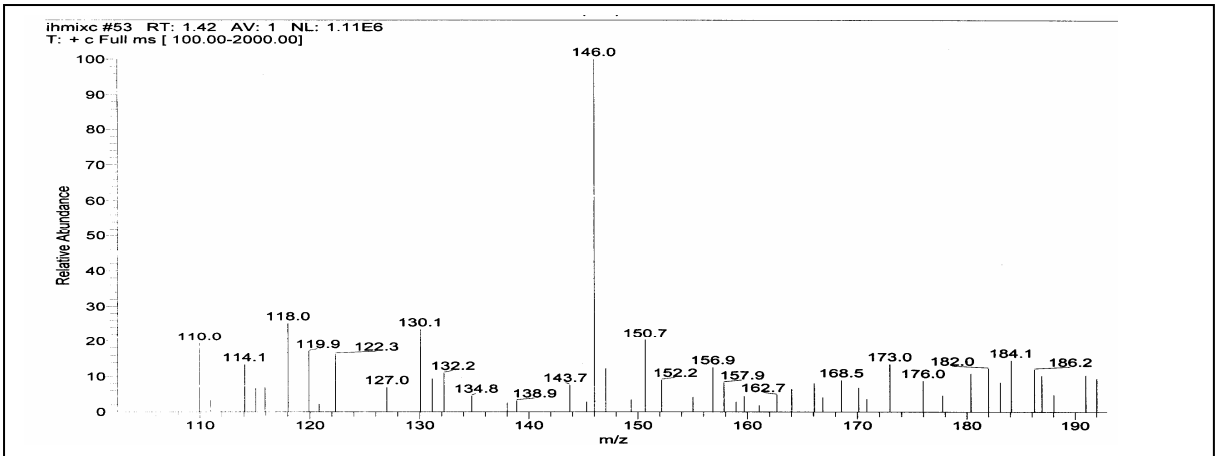

Fig (3.4.10):ESI-MS spectrum of compound 15 [direct injection, +ve mode, $(M+H)^+$].

Compound **15**, [indole-3-carbaldehyde] was isolated as a yellowish white amorphous powder, with slightly offensive characteristic oder. Compound **15** shows positive pseudomolecular ion peak at *m/z* 146 $[M+1]^+$ suggesting the molecular formula C_9H_7NO. The UV (MeOH) absorption maxima of **15** at λ_{max} 206, 243, 255, and 298 nm were indicative of a 3-acyl indole chromophore. The ^1H NMR (DMSO-d_6) showed 7 proton resonances which include the aromatic ABCD spin system at δ 8.07 (1H, d, *J* = 7.4 Hz ; H-4), 7.10 (1H, dt, *J* = 1.21, 7.4 Hz; H-5), 7.30 (1H, dt, *J* = 1.31, 7.4 Hz; H-6) and 7.60 (1H, d, *J* = 7.4 Hz; H-7) in addition to 3 proton resonances at δ 8.30 (1H, s ; H-2) and the aldehydic proton at 9.95 (1H, s; H-8) and the most downfield broad singlet at δ 12.13 (1H, s ; H-1) see table (3.4.3). The HMBC spectrum showed long rang correlation between H-2/C-3, H-2/C-3a, H-2/C-7, H-2/C-7a, H-2/C-8, H-6/C-7, H-6/C-7a, H-4/C-6, H-4/C-7a, H-4/C-3a, H-4/C-3, H-5/C-7, H-5/C-3a, H-7/C-3a, H-7/C-5. The NMR data were identical to those of indole 3-carbaldehyde (Aldrich, 1990, Hiort, 2002) but this is the first isolation of **15** from genus *Hyrtios*.

Table (3.4.3): NMR data of compound 15 (DMSO-d_6).

No.	^{13}C, (δ = ppm), multiplicity	^1H (δ = ppm), couppling constant (J= Hz)	HMBC correlations H→ C
1	-	12.13 (1H, s)	
2	139.5	8.30 (1H, s)	3, 3a, 7, 7a, 8
3	119.1, s	-	
3a	126.5 , s	-	
4	120.0, d	8.07 (1H, d, *J* = 7.4 Hz ; H-4)	3, 3a, 7, 7a, 6
5	121.0	7.10 (1H, dt, *J* = 1.21, 7.4 Hz)	3a, 7
6	121.5	7.30 (1H, dt, *J* = 1.31, 7.4 Hz)	4, 7, 7a
7	114.1	7.60 (1H, d, *J* = 7.4 Hz; H-7)	5, 3a
7a	138.5	-	
8	185.2	9.95 (1H, s)	3, 3a

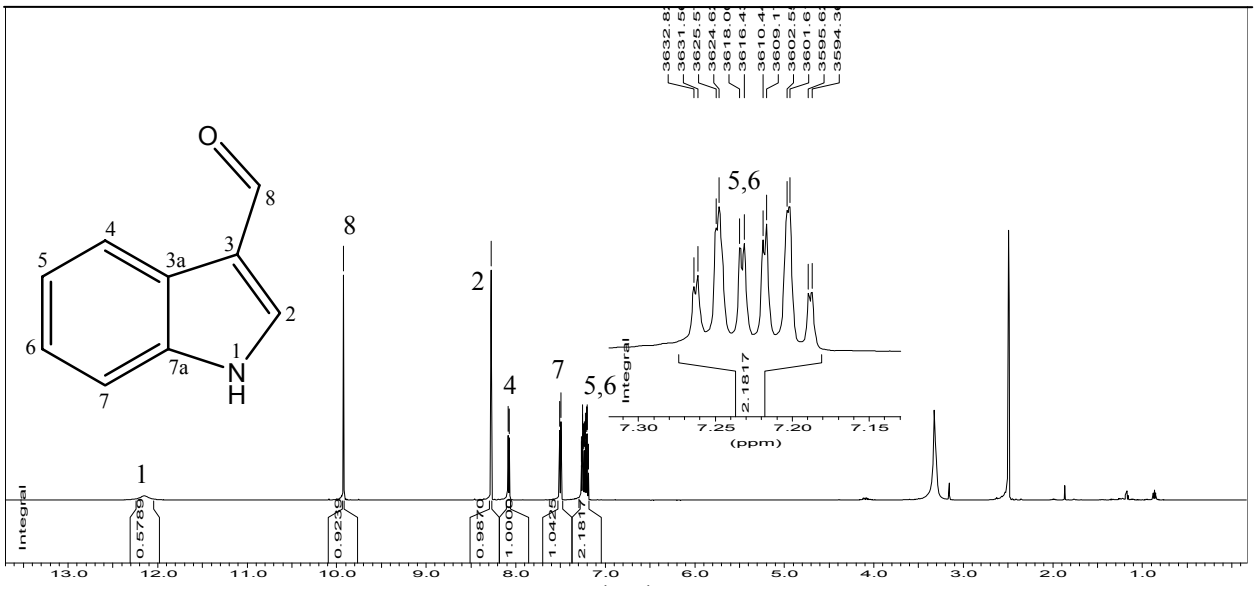

Fig (3.4.11):^{1}H NMR spectrum of compound 15 (DMSO-d_6).

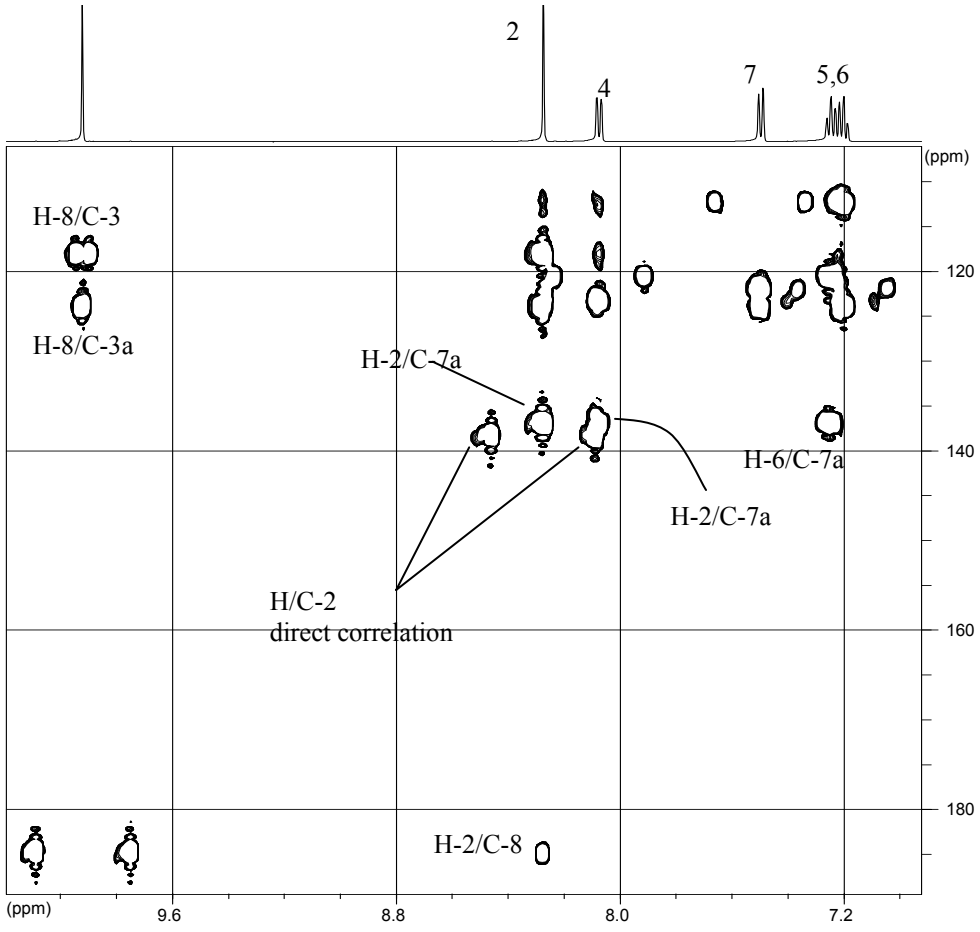

Fig (3.4.12):HMBC spectrum of compound 15 (DMSO-d_6).

3.4.4. 5-Deoxyhyrtiosine A (16, Known compound, first isolation from genus *Hyrtios*):

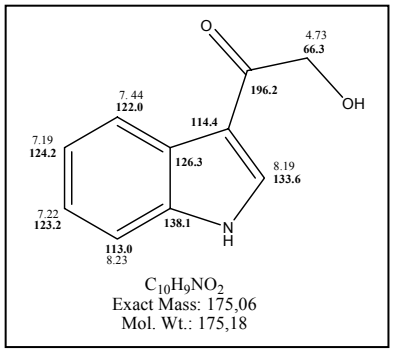

$C_{10}H_9NO_2$
Exact Mass: 175,06
Mol. Wt.: 175,18

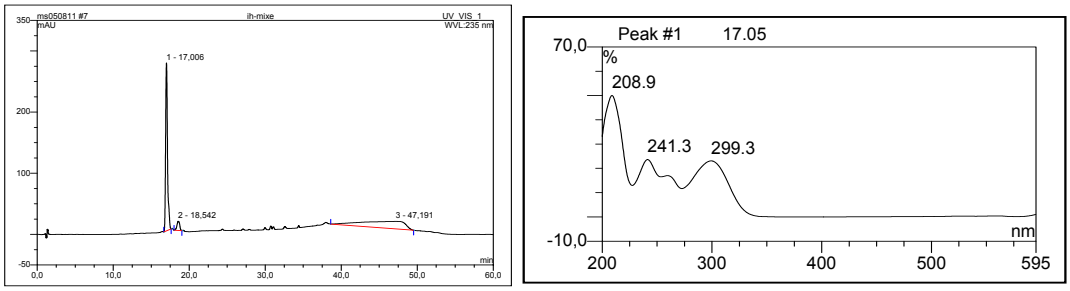

Fig (3.4.13):HPLC chromatogram and UV-spectrum of compound 16.

Yield : 2 mg

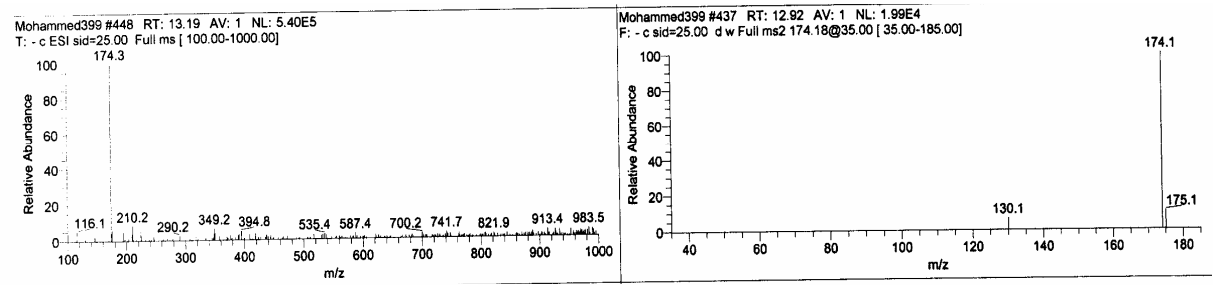

Fig (3.4.14): (-ve) ESI-MS spectrum of compound 16 and its ESI-MS/MS spectrum.

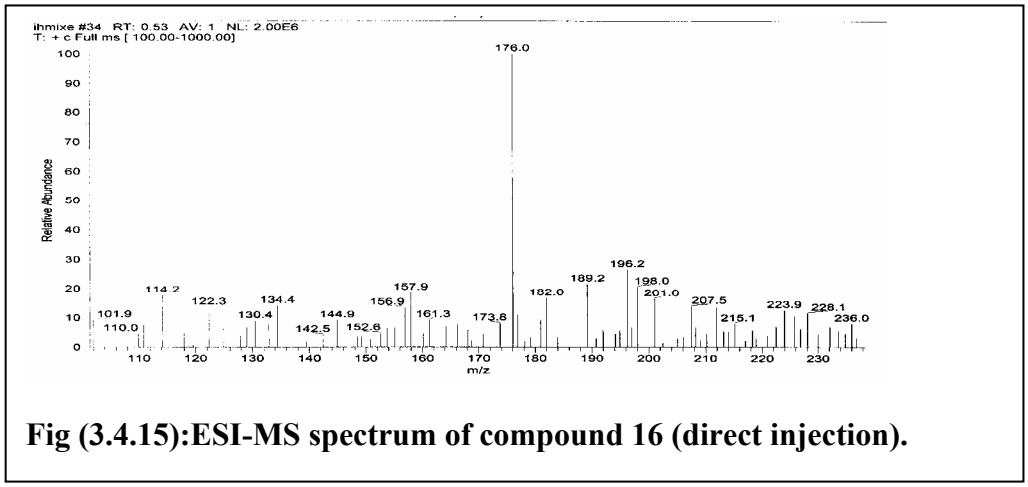

Fig (3.4.15):ESI-MS spectrum of compound 16 (direct injection).

Compound **16**, 5-deoxyhyrtiosine A, [3-(hydroxyacetyl)-1*H*-indole] was isolated as colourless amorphous powder. Compound **16** shows positive pseudomolecular ion peak at *m/z* 176 $[M+1]^+$ and negative pseudomolecular ion peak at *m/z* 174 $[M-1]^-$ suggesting the molecular formula $C_{10}H_9NO_2$, which seems to be smaller than hyrtiosine A (compound **13**) by only 16 mass units (one oxygene atom). The UV (MeOH) absorption maxima of **16** at λ_{max} 209, 241, 261 and 299 nm were indicative of a 3-acyl indole chromophore. The ^{1}H NMR (CD_3OD) showed 5 aromatic proton resonances (instead of 4 aromatic protons as in hyrtiosine A) which included an aromatic ABCD spin system at δ 8.23 (1H, dd, *J* = 6.94, 1.26 Hz; H-4), 7.19 (1H, dt, *J* = 6.94, 1.26 Hz; H-5), 7.22 (1H, dt, *J* = 6.94, 1.26 Hz; H-6) and 7.44 (1H, dd, *J* = 6.94, 1.26 Hz; H-7) and one proton resonance at δ 8.19 (1H, s ; H-2) in addition to the most upfield singlet at δ 4.73 (1H, s ; H-9), see table (3.4.4). The ^{1}HNMR confirmed the loss of a 5-hydroxyl group (compared to Hyrtiosine A). HMBC spectrum showed long range correlations between H-2/C-3, H-2/C-3a, H-2/C-7a, H-6/C-7, H-6/C-4, H-6/C-7a, H-4/C-6, H-5/C-7, H-5/C-3a, H-4/C-7a, H-4/C-3a, H-7/C-5, H-9/C-3, H-9/C-8, see table (3.4.4) and figure (3.4.17). The NMR data and the UV absorption maxima were identical to those of 3-(hydroxyacetyl)-1*H*-indole which has been previously isolated from the Bermudian sponge *Tedania ignis* and their associated bacterium, *Micrococcus* sp. and the red alga (Dillman and Cardellina 1991, Stierle 1988, Bernart and Gerwick 1990, respectively), but this is the first isolation of **16** from genus *Hyrtios*.

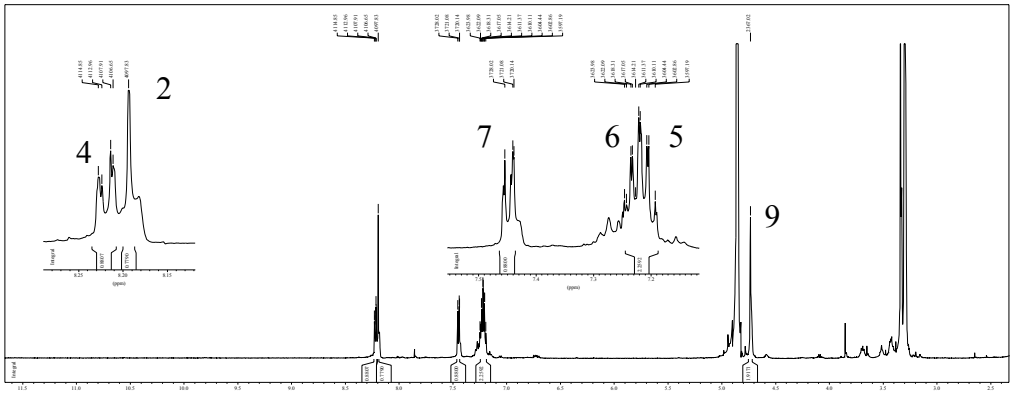

Fig (3.4.16):^{1}H NMR spectrum of compound 16 (CD_3OD)..

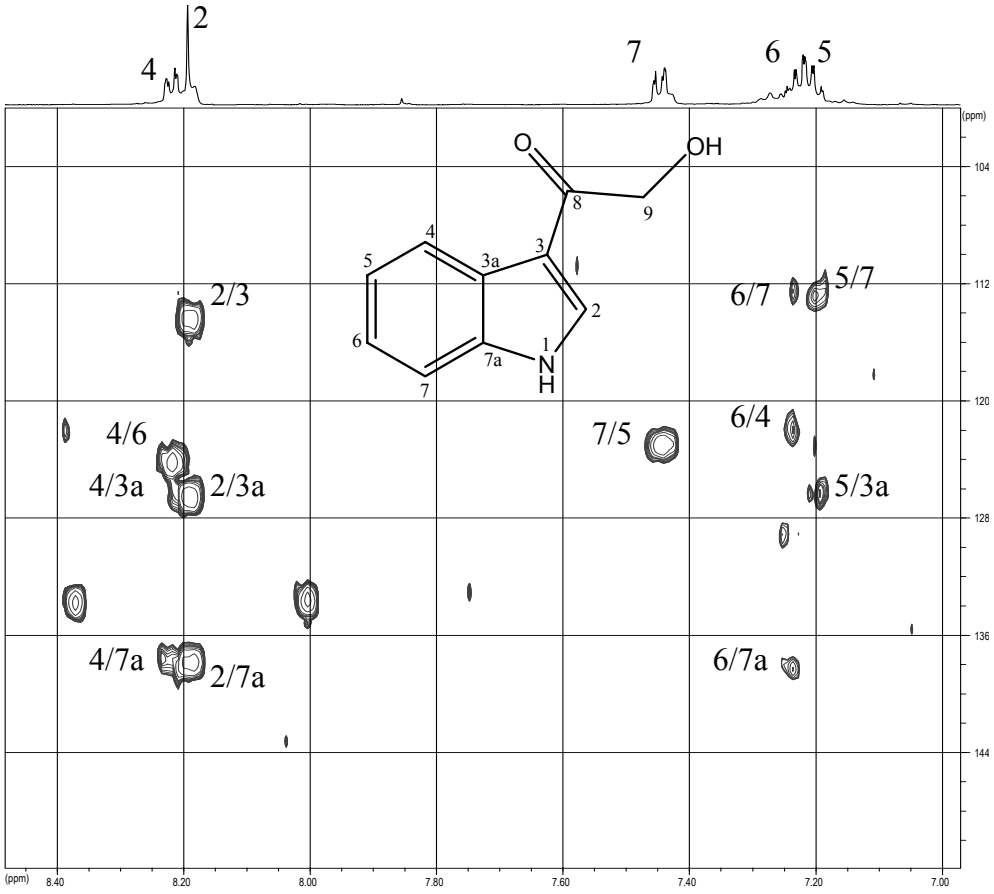

Fig (3.4.17): HMBC spectrum of compound 16(CD_3OD).

Table (3.4.4): NMR data of compound 16 (Methanol-d_4).

No.	^{13}C, (δ = ppm)	^{1}H (δ = ppm), couppling constant (J= Hz)	HMBC correlations H→ C
2	133.6	δ 8.19 (1H, s)	3, 3a, 7a
3	114.4		
3a	126.3		
4	122.0	8.23 (1H, dd, *J* = 6.94, 1.26 Hz)	6, 3a, 7a
5	123.2	7.19 (1H, dt, *J* = 6.94, 1.26 Hz)	7, 3a
6	124.2	7.22 (1H, dt, *J* = 6.94, 1.26 Hz)	4, 7a, 7
7	113.0	7.44 (1H, dd, *J* = 6.94, 1.26 Hz)	5
7a	138.1		
8	196.2		
9	66.3	4.73(2H, s)	8, 3

3.4.5- Isohyrtiosine A (17, New compound):

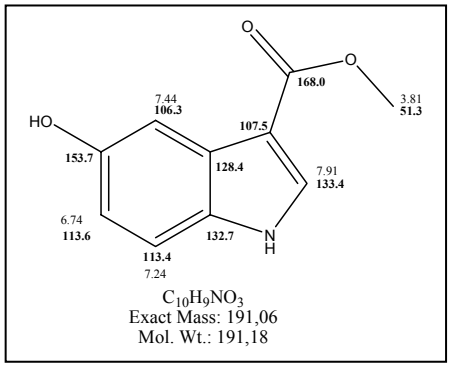

$C_{10}H_9NO_3$
Exact Mass: 191,06
Mol. Wt.: 191,18

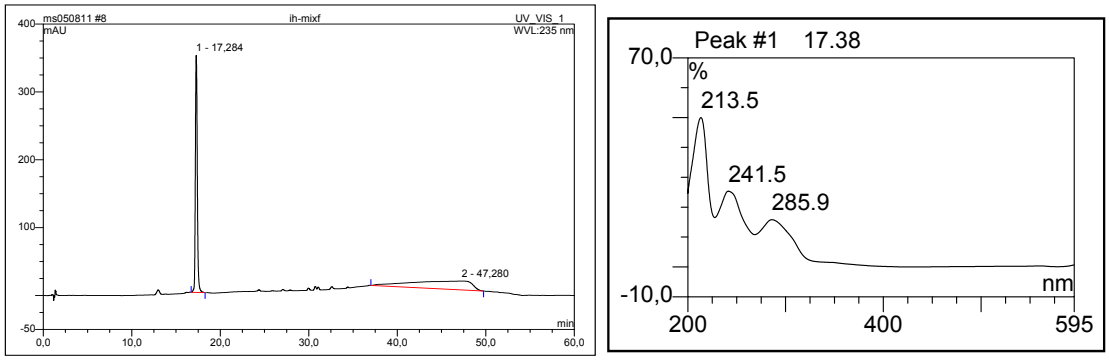

Fig (3.4.18):HPLC chromatogram and UV-spectrum of compound 17.

Yield : 3.0 mg

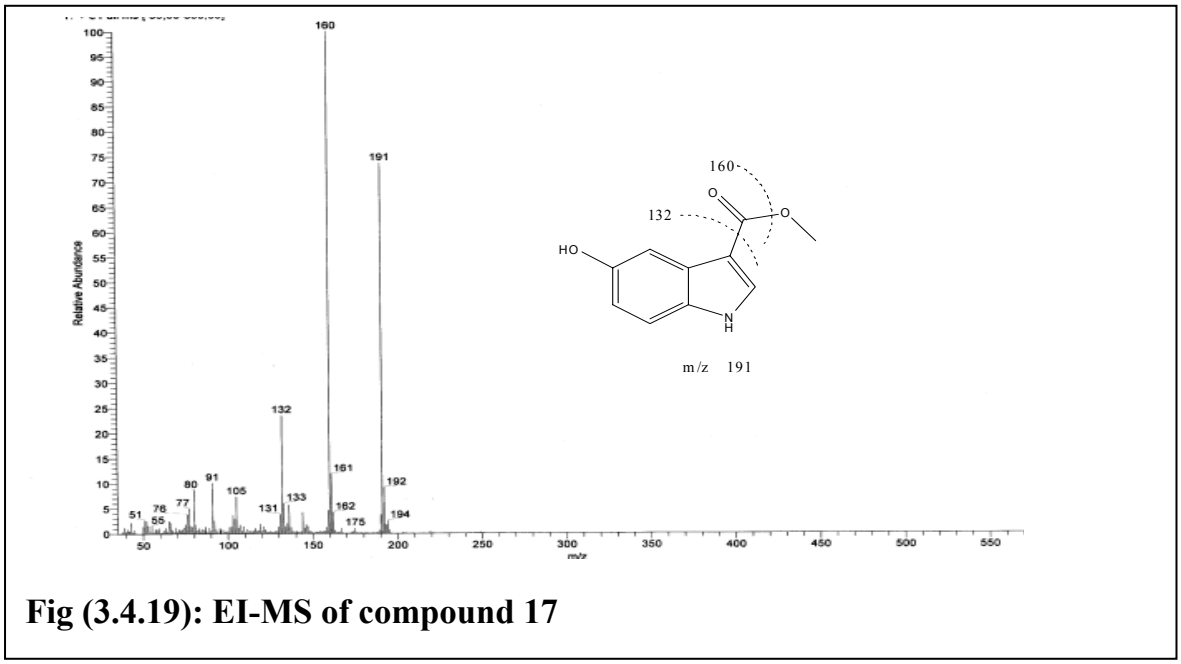

Fig (3.4.19): EI-MS of compound 17

Compound **17**, isohyrtiosine A, [5-hydroxy-1*H*-indole-3-carboxylic acid methyl ester] was isolated as a transluscent needle crystals. Compound **17** shows positive pseudomolecular ion peak at *m/z* 192 $[M+1]^+$ and negative pseudomolecular ion peak at *m/z* 190 $[M-1]^+$ and EI-MS of 17 showed molecular ion peak of *m/z* 191 $[M]^+$ suggesting the molecular formula $C_{10}H_9NO_3$. The UV (MeOH) spectrum of **13** showed an absorption maxima 213, 241 and 286 nm, (slightly deviated from those of **13** „Hyrtiosine A"). The ^{1}H NMR (CD_3OD) showed 5 proton resonances at δ 7.91 (1H, s ; H-2), 7.44 (1H, d, *J* = 2.21 Hz; H-4), 6.74 (1H, dd, *J* = 2.21,8.83 Hz; H-6), 7.24 (1H, d, *J* = 8.83 Hz; H-7), 3.81(2H, s ; H-9). Although the molecular weight is identical to that of hyrtiosine A, the ^{13}C NMR spectrum shows some differences in resonances from those of hyrtiosine A, including the presence of a carboxyl resonance at 168.01 ppm instead of the keto-carbonyl at 195.3 ppm and the methoxy carbon at 51.27 ppm replacing the OCH_2 at 67.1 ppm which were confirmed by its DEPT spectrum. The other ^{13}C NMR resonances seems to be similar to those of hyrtiosine A (compound 13), see table (3.4.5). The attachment of the methoxy group to the carbonyl is also confirmed by HMBC correlation between C*H*$_3$-9 and C-8 at 168.1 ppm. Other HMBC correlations were presented in table 3.4.5 and explained in figure 3.4.22. The NMR data and the UV absorption maxima identified **17** as isohyrtiosine A (5-Hydroxy-1*H*-indole-3-carboxylic acid methyl ester). To the best of our knowledge this is the first report of **17** as a natural product.

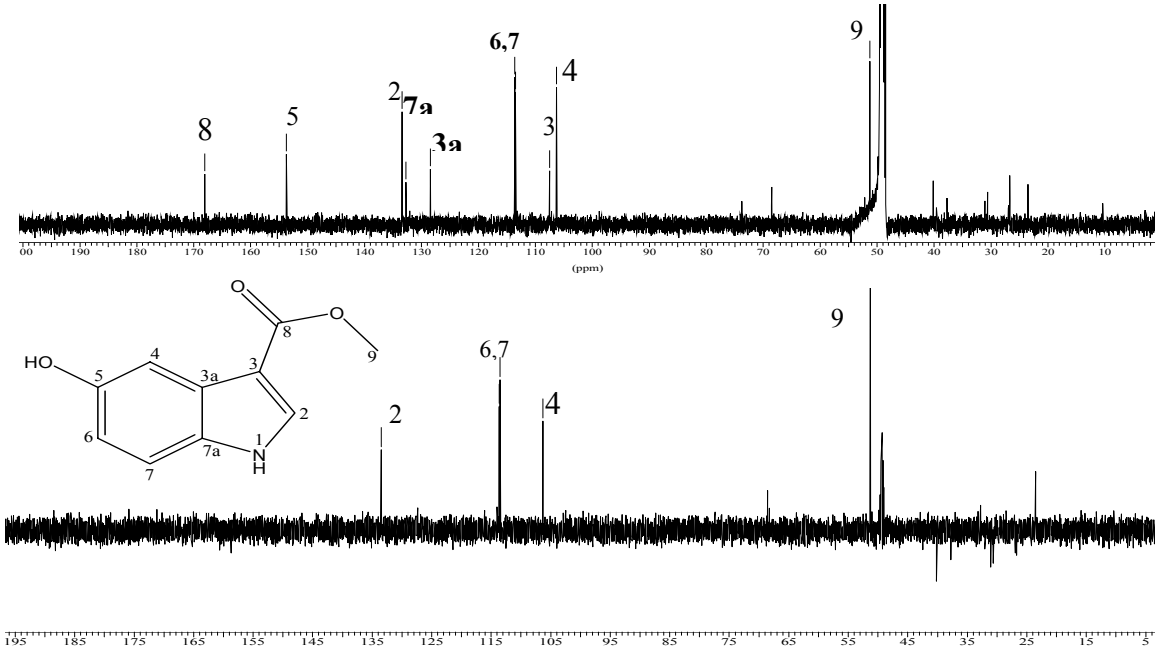

Fig (3.4.20):^{13}C NMR (up) and DEPT (down) spectra of compound 17

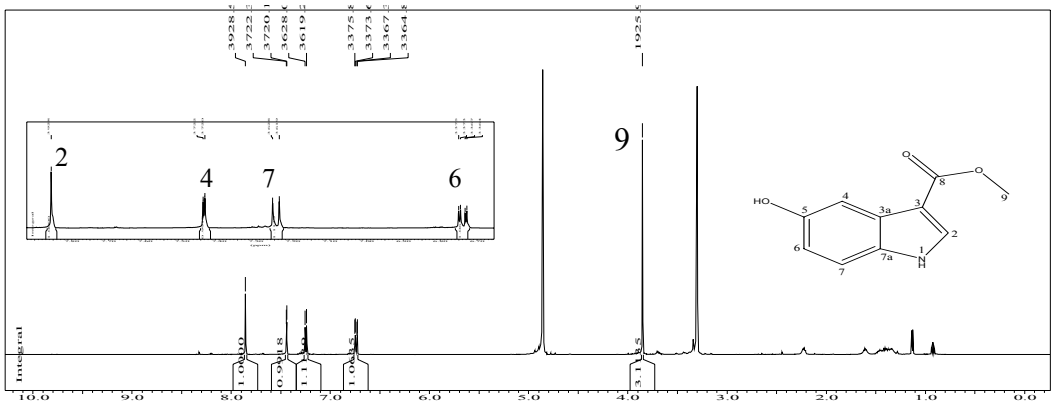

Fig (3.4.21):^{1}H NMR spectrum of compound 17

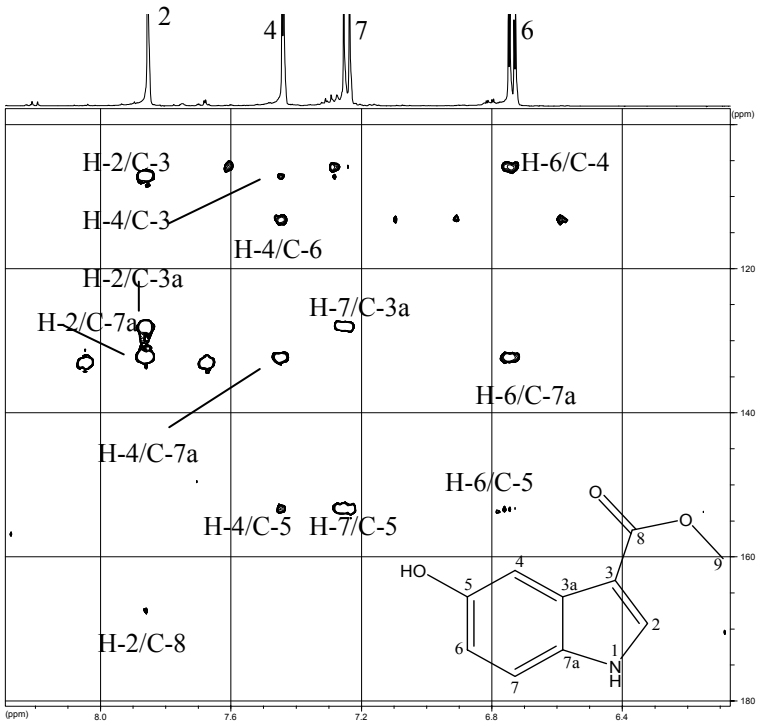

Fig (3.4.22): HMBC spectrum of compound 17

Table (3.4.5): NMR data of cpompound 17 (Methanol-d_4).

No.	^{13}C, (δ = ppm)	^{1}H (δ = ppm), couppling constant (J= Hz)	HMBC correlations (H→ C)
2	133.41	δ 7.91 (1H, s)	3, 3a, 7, 8
3	107.5		
3a	128.4		
4	106.27	7.44 (1H, d, *J* = 2.21 Hz)	3, 5, 7a, 6
5	153.7		
6	113.6	6.74 (1H, dd, *J* = 2.21& 8.82 Hz)	4, 5, 7a
7	113.4	7.24 (1H, d, *J* = 8.82 Hz)	5, 3a
7a	132.7		
8	168.01		
9	51.27	3.81 (3H, s)	8

3.4.6- 16-Hydroxyscalarolide (18, Known compound):

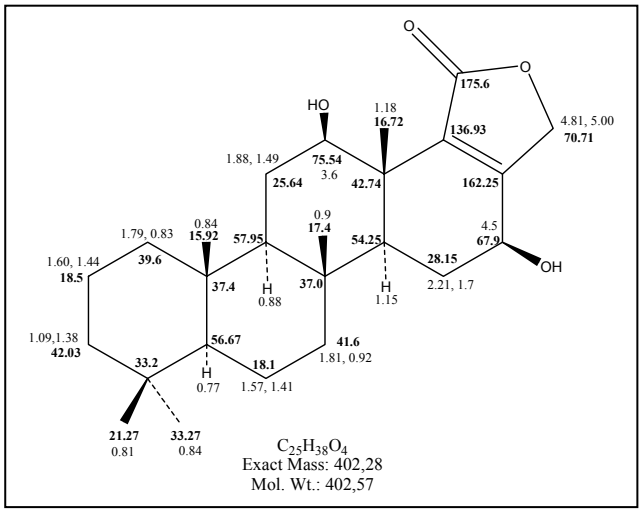

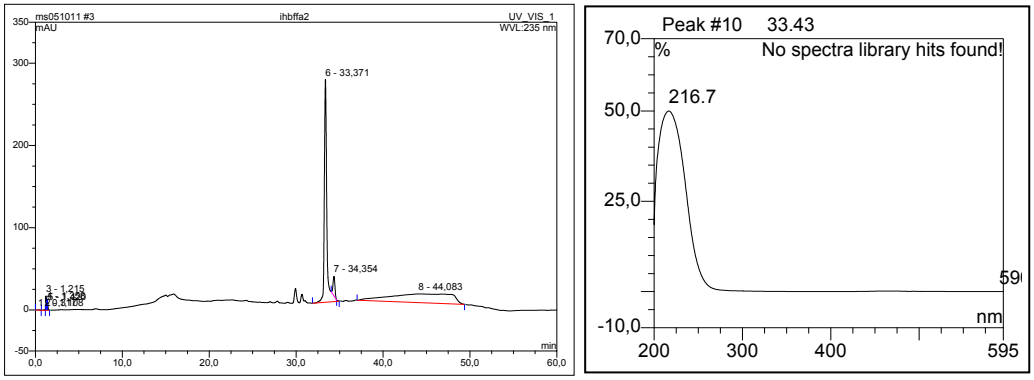

Fig (3.4.23):HPLC chromatogram and UV-spectrum of compound 18.

Yield : 3.5 mg

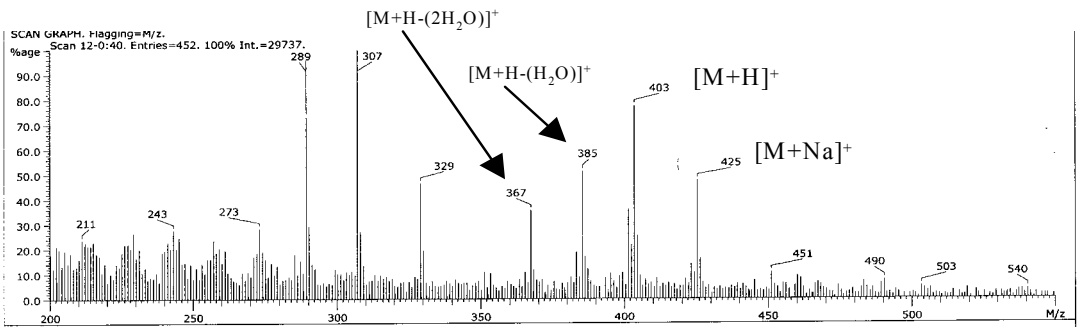

Fig (3.4.24):FAB-MS spectrum of compound 18.

Compound **18** [**16-hydroxyscalarolide**] was isolated as a colourless solid with $[\alpha]_D$ of - 23° (*c* 0.18 $CHCl_3$). Compound **18** has UV absorption at λ_{max} 216 nm and a molecular formula of $C_{25}H_{38}O_4$, as established from its FAB MS and ^{13}C NMR data. FABMS of the compound **18** showed pseudomolecular ion peak *m/z* 425 $[M+ Na]^+$ and pseudomolecular ion peak *m/z* 403 $[M+ H]^+$ suggesting the molecular formula $C_{25}H_{38}O_4$.

^1H NMR spectrum (Table 3.4.6) displayed resonances for 38 protons including five singlets assigned to five methyl groups at δ 0.81, 0.84, 0.9, 0.84, and 1.18, eight methylenes, and five sp^3 methines. The ^{13}C NMR spectrum revealed signals for 25 carbons including five methyls, eight methylenes, two downfield sp^3 methines, three upfield sp^3 methines, and four sp^3 quaternary carbons and three sp^2 quaternary carbons. Analysis of the $^1H,^1H$-COSY led to the assembly of the following structural fragments: C-1 to C-3; C-5 to C-7; C-9 to C-12 with a hydroxyl group at C-12; and C-14 to C-16 with an hydroxyl group at C-16. The proton signals at 4.81(H-24a) and 5.00 (H-24b) ($J_{24a/b}$ = 17.97 Hz) together with the carbon resonances at 70.71 (CH_2, C-24), 162.25 (qC, C-17), 136.93 (qC, C-18), and 175.6 (qC, C-25) were representative of an α,β-unsaturated butenolide moiety (Youssef *et al* 2005, Pettit *et al* 1998b, Miyaoka *et al* 2000). This was supported by interpretation of the HMBC spectrum (Table 3.4.6), which indicated that C-16 and C-24 were connected to the sp^2 quaternary carbon C-17, with these situated, along with C-18 and C-25, in the α,β-unsaturated-γ-lactone ring (Youssef *et al* 2005, Pettit *et al* 1998b, Miyaoka *et al* 2000). Connectivities of the five ring systems of **18**, as well as the assignments of all quaternary carbons, were supported unequivocally by HMBC data. In addition, the placements of the OHs at C-12 and C-16, were secured from HMBC correlations of H-11/C-12, H-16/C-17, and H-16/C-18. Moreover, COSY coss-peaks of H-12/H-11a, H-12/H-11b, H-16/H-15a, and H-16/H-15b supported these assignments. The partial structures and the above α,β-unsaturated-γ-lactone (C-17, C-18, C-24 and C-25) were found to be connected through quaternary carbons based on HMBC data; also observed were the cross-peak: Me-20/C-3, C-5, C-19; Me-19/C-3, C-5, C-20; Me-22/C-1, C-5, C-9; Me-21/C-7, C-9, C-14; Me-23/C-12, C-14, C-18, and H-16/C-14, C-17, C-18, so that the tetracarbocyclic scalarane skeleton could be constructed. The planar structure of **18** was thus determined. All trans junctions of the tetracyclic rings (A, B, C, and D) were demonstrated from ^{13}C NMR chemical shifts of methyl groups (δ_C 15.92, 16.7, 17.4, 21.27, and 33.27), (Miyaoka *et al* 2000). The NMR spectra of **18** were closely related to those of known scalarane sesterterpenoids [(scalarolide, seterstatins 1-7, and 16-hydroxyscalarolide), (Walker *et al* 1980, Pettit *et al* 1998b, Pettit *et al* 1998c and Pettit *et al* 2005, Youssef *et al* 2005, Miyaoka *et al* 2000)]. Compound 18 seems to be identical with the 16-

hydroxyscalarolide see the comparative NMR data, table 3.4.6. The planar structure of **18** was supported by COSY, and HMBC spectra. The equatorial geometry of OH at C-12 was established from the large coupling constant of H-12 (J = 11.04 Hz), (Youssef *et al* 2005, Pettit *et al* 1998b). Similarly, the β-configuration of the hydroxyl at C-16 was established from the coupling constant (J = 9.45 Hz) (Youssef *et al* 2005, Pettit *et al* 1998b). From the above discussion, compound **18** was assigned as 16-hydroxyscalarolide and its spectral data is identical with those of 16-hydroxyscalarolide isolated from the Okinawan sponge *H. erectus* (Miyaoka *et al* 2000).

Table (3.4.6): NMR data of compound 18 ($CDCl_3$, 500 MHz)

	16-Hydroxyscalarolide (Miyaoka et al 2000)		**compound 18**		
No.	^{13}C (mult.)	^{1}H [mult., J (Hz)]	^{13}C (mult.)	^{1}H [mult., J (Hz)]	HMBC
1	39.7 (CH_2)	0.78 (1H, m), 1.72 (1H, br d, 13.0)	39.6, CH_2	1.79, m, 0.83, m	C-10
2	18.2 (CH_2)	1.42 (1H, m),1.62 (1H, m)	18.5, CH_2	1.60, m, 1.44, m	C-4, C-10
3	42.0 (CH_2)	1.09 (1H, m), 1.38 (1H, m)	42.0, CH_2	1.09, m, 1.38, ddd (13.5, 13.5, 4.0)	C-4
4	33.3 (C)		33.2, qC		
5	56.7 (CH)	0.75 (1H, m)	56.67, CH	0.77, m	C-4
6	18.6 (CH_2)	1.40 (1H, m), 1.58 (1H, m)	18.1, CH_2	1.57, m, 1.41, m	
7	41.7 (CH_2)	0.92 (1H, m), 1.80 (1H, td, 3.3, 12.4)	41.6, CH_2	1.81, m, 0.92, m	C-8
8	37.0 (C)		37.0, qC		
9	58.0 (CH)	0.88 (1H, m)	58.0, CH	0.88, m	C-10, C-12
10	37.4 (C)		37.4, qC		
11	25.7 (CH_2)	1.49 (1H, dd, 2.1, 13.2), 1.88 (1H, m)	25.7, CH_2	1.49, ddd (11.5, 4.2, 1.8) 1.88, m	C-12
12	75.5(CH)	3.64 (1H, dd, 4.5, 10.9)	75.5, CH	3.60, dd (11.5, 4.4)	C-13
12-OH		5.75 , s		5.75, s	
13	42.8 (C)		42.8, qC		
14	54.3 (CH)	1.14 (1H, m)	54.25, CH	1.15, m	C-8, C-13, C-16
15	28.2 (CH_2)	1.66 (1H, dd, 2.1, 12.4), 2.23 (1H, dd, 6.7, 12.5)	28.2, CH_2	1.7, m; 2.21, dd (11.7, 7.1)	C-16
16	67.9 (CH)	4.50 (1H, m)	67.9, CH	4.50, dd (9.45, 6.93)	C-17, C-18
17	162.3 (C)		162.25, qC		
18	136.93 (C)		136.93, qC		
19	21.3 (CH_3)	0.81 (3H, s)	21.27, CH_3	0.81, s	C-4,C-3, C-5, C-20
20	33.3 (CH_3)	0.84 (3H, s)	33.27, CH_3	0.84, s	C-4, C-3, C-5, C-19
21	17.4 (CH_3)	0.90 (3H, s)	17.4, CH_3	0.9, s	C-8, C-14, C-9, C-7
22	15.9 (CH_3)	0.84 (3H, s)	15.92, CH_3	0.84, s	C-1, C-10, C-9
23	16.7 (CH_3)	1.19 (3H, s)	16.72, CH_3	1.18, s	C-12, C-13, C-18,C-14
24	70.7 (CH_2)	4.81 (1H, d, 17.8), 4.99 (1H, d, 17.8)	70.7, CH_2	4.81, dd (17.87, 1.27) 5.0, d (17.97)	C-17, C-18, C-25
25	175.6 (C)		175.6, qC		

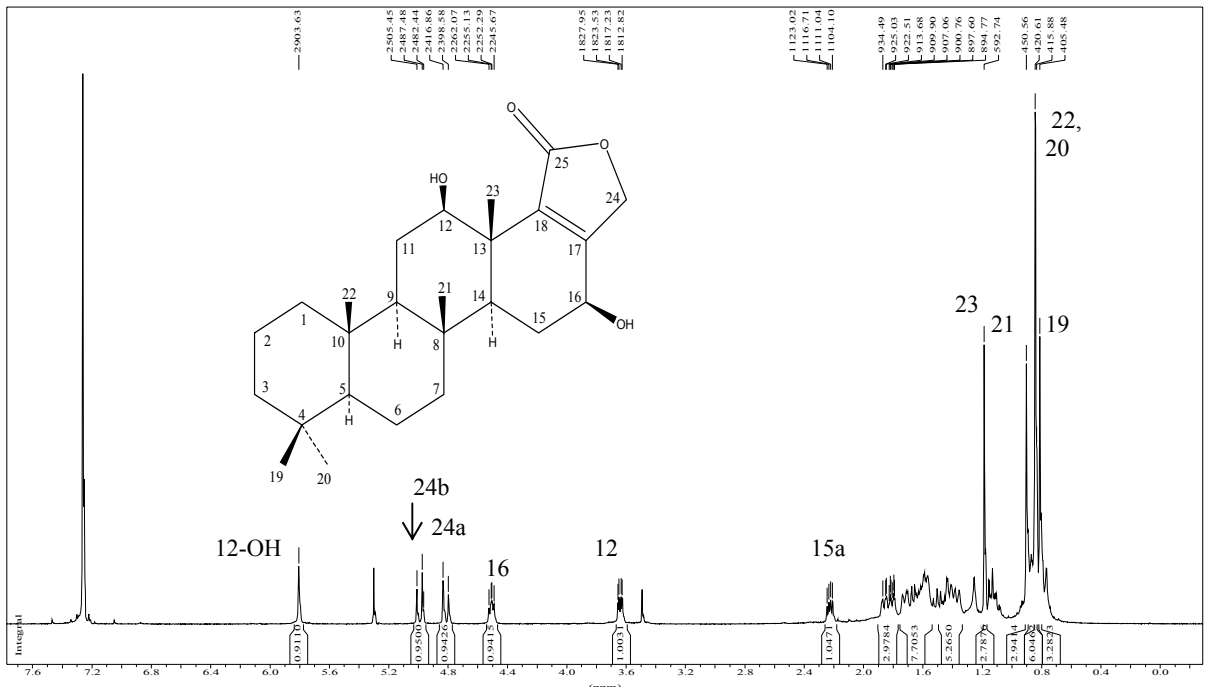

Fig(3.4.25): ^{1}H NMR spectrum of compound 18

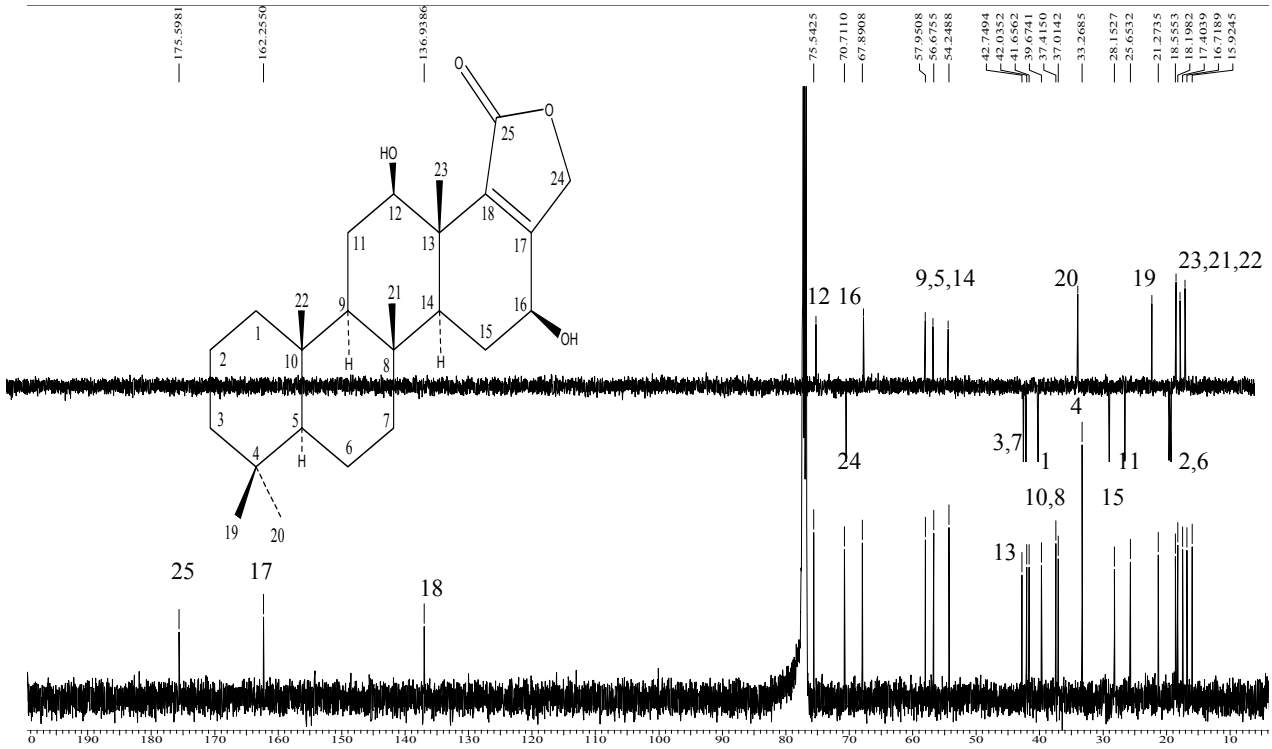

Fig(3.4.26): ^{13}C NMR and DEPT spectra of compound 18

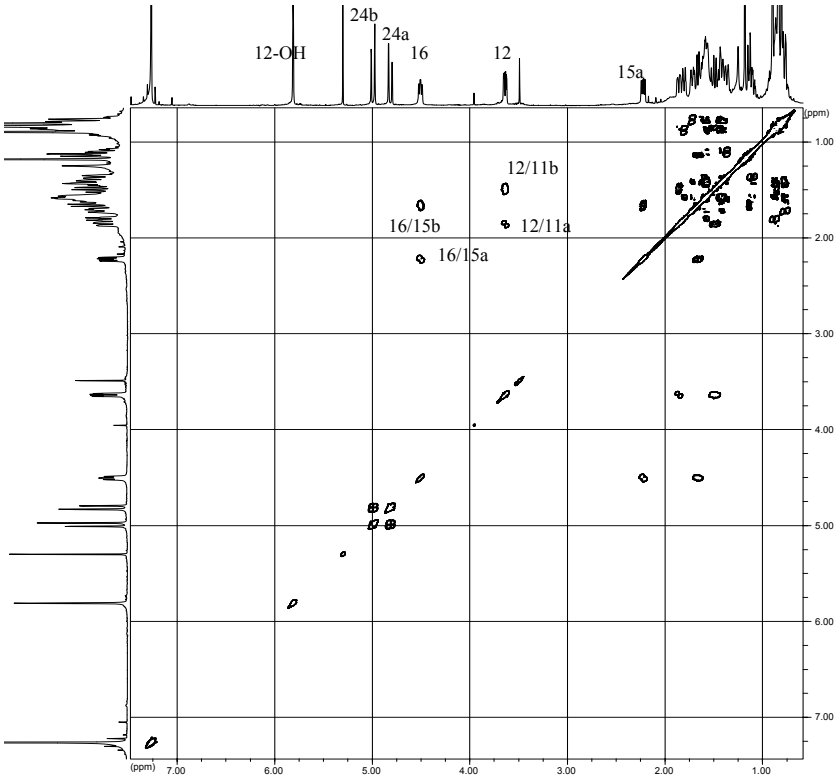

Fig(3.4.27): H-H COSY spectrum of compound 18

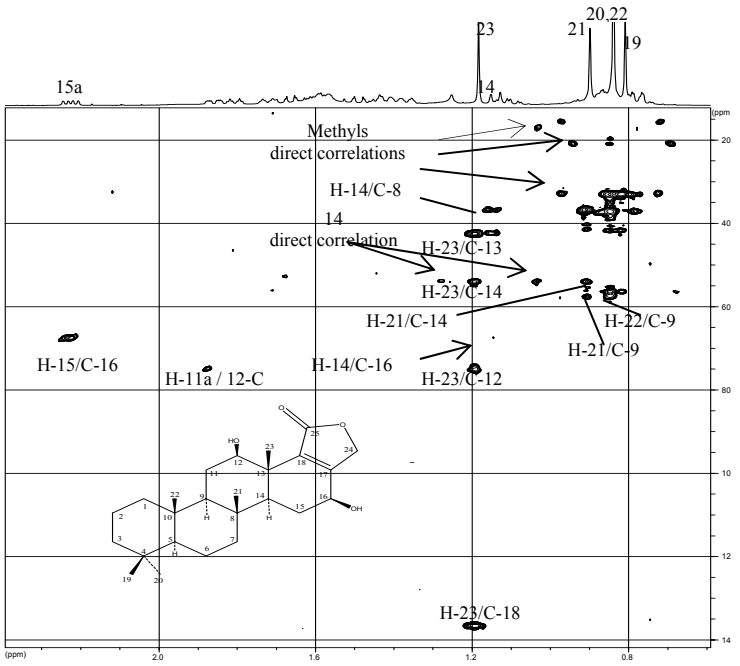

Fig(3.4.28): Part of HMBC spectrum of compound 18 showing H/C direct and H/C long correlations of the methyl groups.

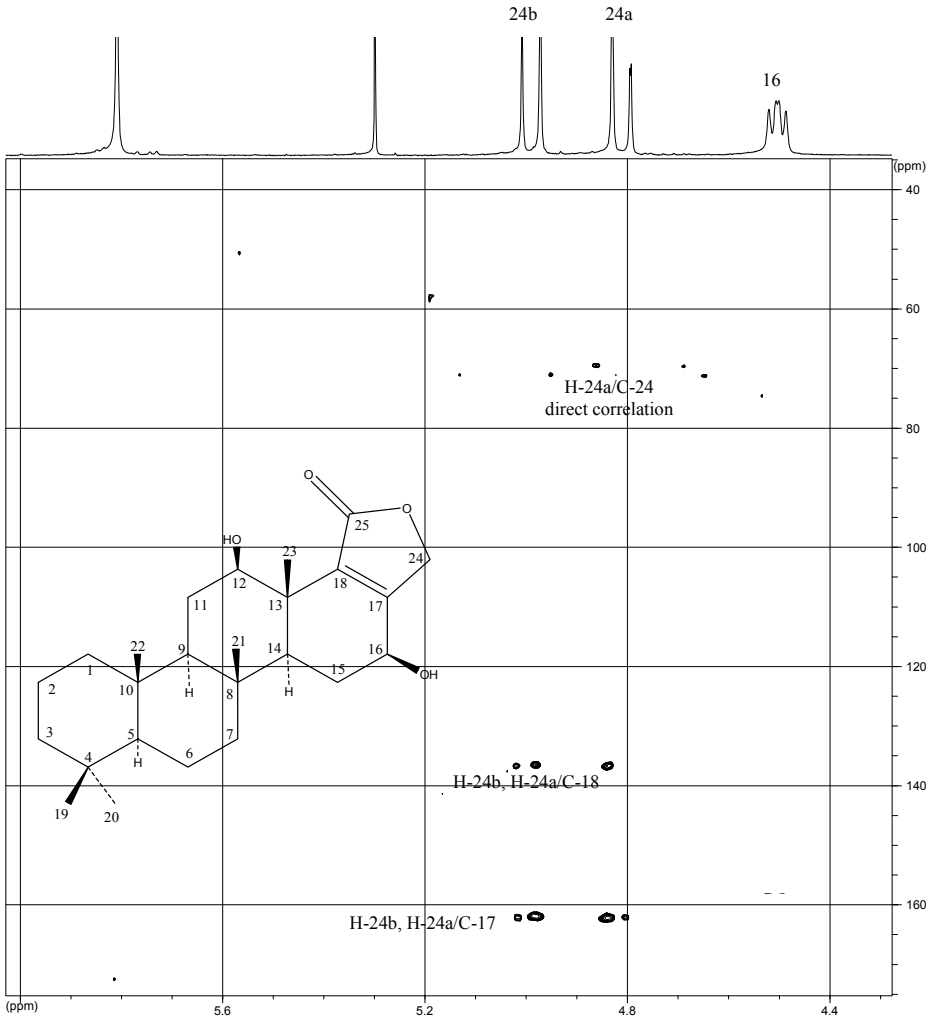

Fig(3.4.29): Part of HMBC spectrum of compound 18 showing H/C direct and H/C long correlations of the methylene group (CH_2-24).

3.4.7- Scalarolide (19, Known compound):

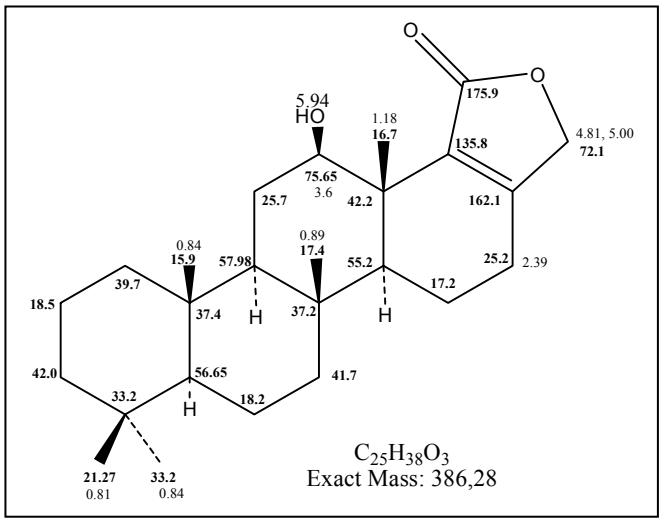

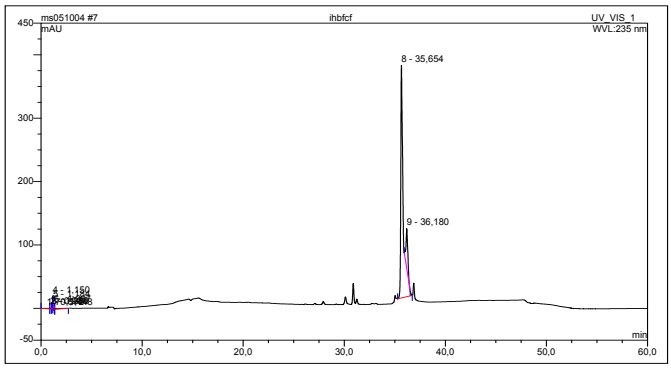

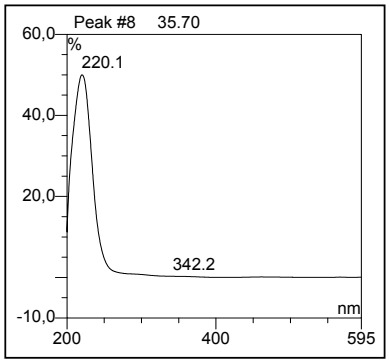

Fig (3.4.30):HPLC chromatogram and UV-spectrum of compound 19.

Yield : 5 mg

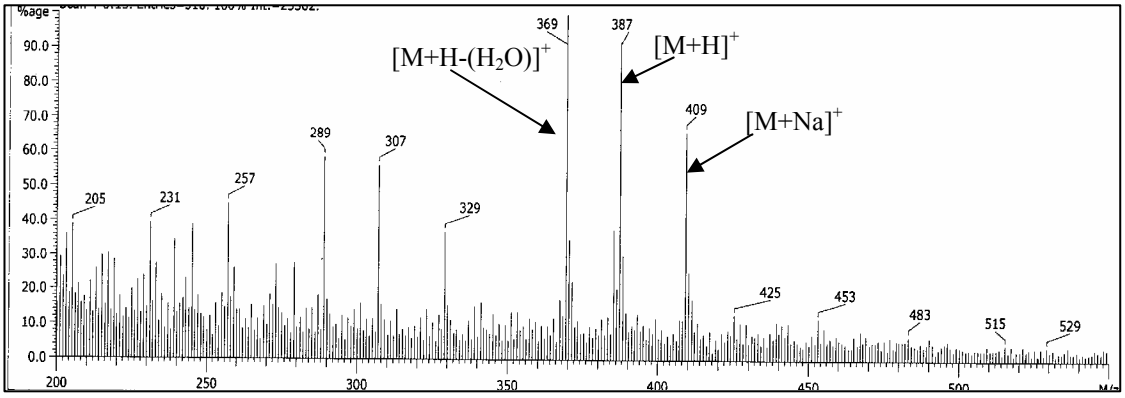

Fig (3.4.31):FAB-MS spectrum of compound 19.

Compound **19** [**scalarolide**] was isolated as a brownish white amorphous solid with $[\alpha]_D$ of + 23° (*c* 0.2 $CHCl_3$). Compound **19** has a UV absorption at λ_{max} 220 nm and a molecular formula of $C_{25}H_{38}O_3$, as established from its FAB MS and ^{13}C NMR data. FAB MS of compound **19** showed pseudomolecular ion peak *m/z* 409 $[M+ Na]^+$ and pseudomolecular ion peak *m/z* 387 $[M+ H]^+$ suggesting the molecular formula $C_{25}H_{38}O_3$.

^1H NMR spectrum (Table 3.4.7) displayed resonances for five methyls at δ 0.81, 0.85, 0.89, 0.85, and 1.13, one downfield sp^3 methine at δ 3.67 (dd, *J*=11.0, 4.4 Hz) and downfield methylene at δ 4.69 (1H, d, *J*=16.8 Hz) and 4.68 (1H, d, *J*=17.3 Hz) and one O*H* broad singlet at δ 5.94. The ^{13}C NMR spectrum revealed signals for 25 carbons including five methyls, eight upfield methylenes, one downfield methylene at δ 72.1 three upfield sp^3 methines, one downfield sp^3 methine (oxygenated carbon) at δ 75.6, and four sp^3 quaternary carbons and three sp^2 quaternary carbons. The presence of five singlet methyl signals at δ 0.81 (3H), 0.85 (6H), 0.89 (3H), and 1.13 (3H) suggested the pentacyclic scalarin derivative (Walker *et al* 1980), the presence of α,β-unsaturated-γ-lactone was evident from the ^{13}C chemical shift of carbons resonating at δ 72.1, 162.1, 135.8 and 175.9 corresponding to C-24, C-17, C-18, and C-25 respectively which also confirmed by HMBC correlations between the methylene protons at δ 4.69 (2H, d, *J*=16.8 Hz; d, *J*=17.3 Hz) and three downfield sp^2 quaternary carbons resonating at δ 162.1, 135.8 and 175.9. The HMBC correlation (^3J coupling) between the methyl proton at δ 1.13 (3H, s, CH_3-23) and the sp^2 Quaternary carbon resonating at δ 135.8 and an oxygenated sp^3 methine carbon at 75.5 (C-12) further indicaterd that the compound **19** seems to be very similar to compound **18** except the loss of one oxygenated methine carbon (C-16) and consequently the presence of one upfield methine carbon more than those present in compound **18**. Compound **19** is smaller than **18** by 16 mass unit which could be demonstrated by the loss of an oxygen atom from position C-16 as demonstrated above. The ^1H and ^{13}C NMR data of Compound **19** was found to be identical with those of scalarolide that isolated before (Walker *et al* 1980) from the sponge *Spongia idia* .

Table (3.4.7): NMR data of compound 19 ($CDCl_3$, 500 MHz)

	scalarolide (Walker *et al* 1980)		**compound 19**		
No.	^{13}C (mult.)	^{1}H [mult., J (Hz)]	^{13}C (mult.)	^{1}H [mult., J (Hz)]	HMBC
1	39.6 (CH_2)		39.7 (CH_2)		
2	18.5 (CH_2)		18.5 (CH_2)		
3	42.0 (CH_2)		42.0 (CH_2)		
4	33.2 (C)		33.2 (C)		
5	56.6 (CH)		56.6 (CH)		
6	18.1 (CH_2)		18.2 (CH_2)		
7	41.7 (CH_2)		41.7 (CH_2)		
8	37.2 (C)		37.2 (C)		
9	57.9 (CH)		57.9 (CH)		
10	37.3 (C)		37.4 (C)		
11	25.7 (CH_2)		25.7 (CH_2)		
12	75.5(CH)	3.64 (1H, dd, 4.5, 10.9)	75.6 (CH)	3.64 (1H, dd, 4.5, 10.9)	C-13
12-OH		5.75 , s		5.75 , s	
13	42.1 (C)		42.2 (C)		
14	55.1 (CH)		55.2 (CH)		
15	17.1 (CH_2)		17.2 (CH_2)		
16	25.2 (CH_2)	2.39 (1H, m)	25.2 (CH_2)	2.39 (1H, m)	C-18
17	162.0 (C)		162.1 (C)		
18	135.8 (C)		135.8 (C)		
19	21.2 (CH_3)	0.81 (3H, s)	21.2 (CH_3)	0.81 (3H, s)	C-4,C-3, C-5, C-20
20	33.2 (CH_3)	0.85 (3H, s)	33.2 (CH_3)	0.85 (3H, s)	C-4, C-3, C-5, C-19
21	16.3 (CH_3)	0.89 (3H, s)	16.4 (CH_3)	0.89 (3H, s)	C-8, C-14, C-9, C-7
22	15.9 (CH_3)	0.85 (3H, s)	15.9 (CH_3)	0.85 (3H, s)	C-1, C-10, C-9
23	16.6 (CH_3)	1.13 (3H, s)	16.7 (CH_3)	1.13 (3H, s)	C-12, C-13, C-18,C-14
24	72.0 (CH_2)	4.69 m	72.1 (CH_2)	4.68 (d, *J*=17.3 Hz), 4.69 (d, *J*=16.8 Hz)	C-17, C-18, C-25
25	175.9 (C)		175.9 (C)		

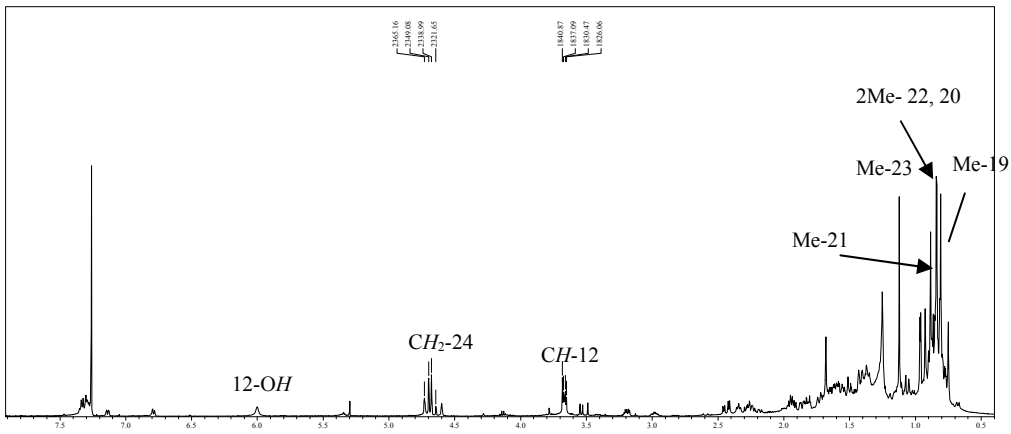

Fig (3.4.32) ^{1}H NMR spectrum of compound 19

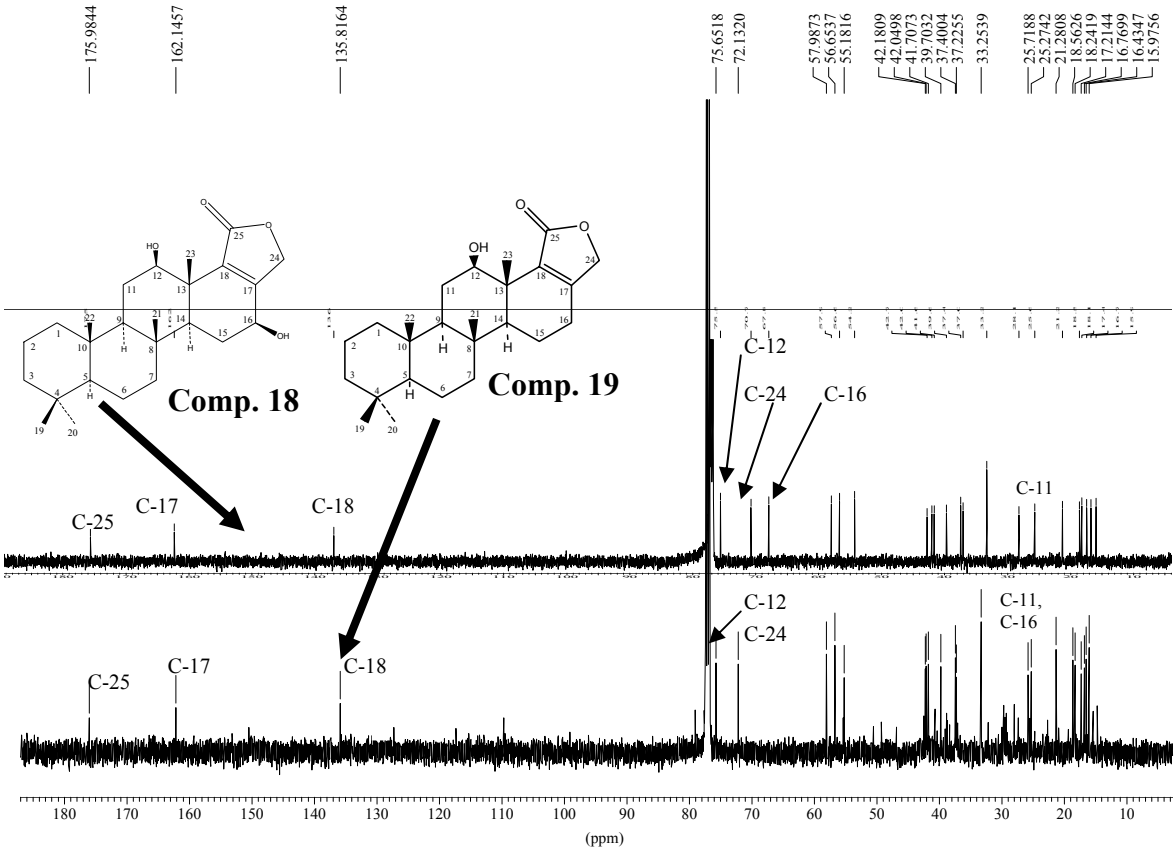

Fig (3.4.33):comparison between ^{13}C NMR spectra of compounds 18 and 19.

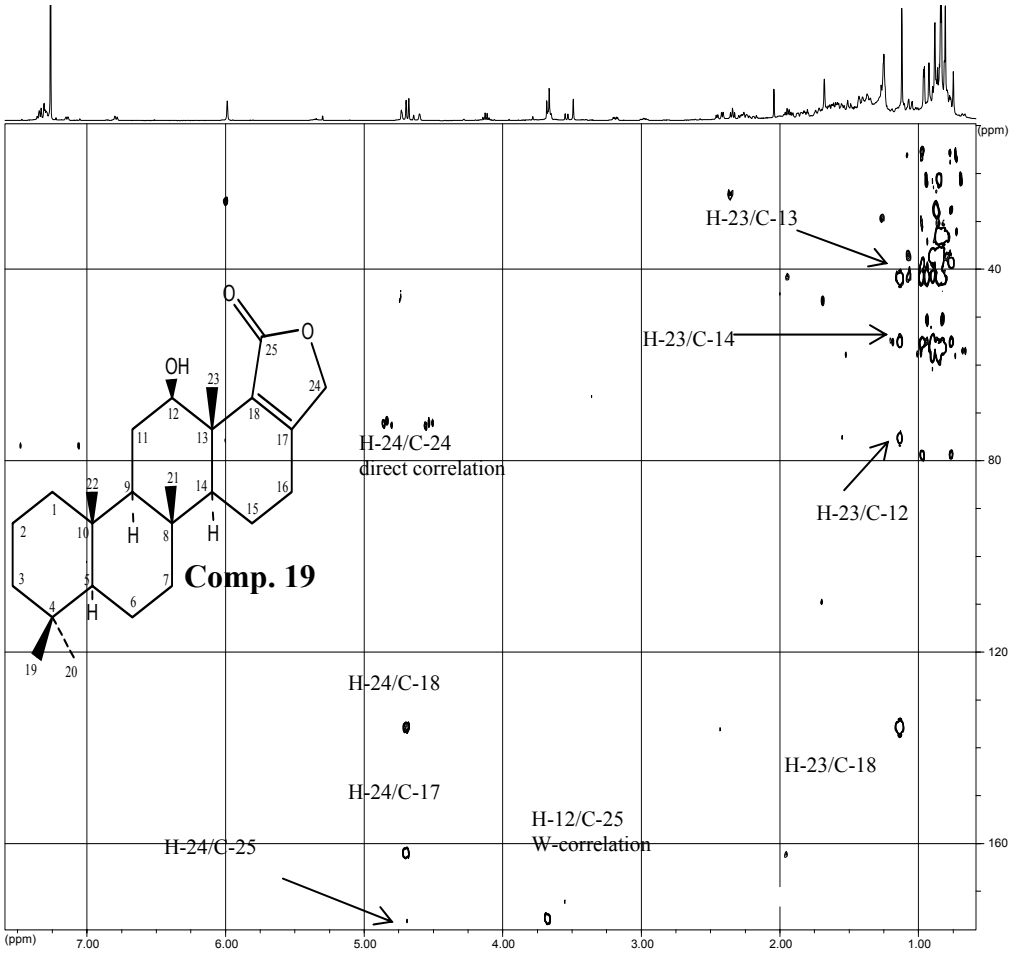

Fig (3.4.34):HMBC spectrum of compounds 19.

3.4.8- 12-O-deacetyl-12-epi-scalarin (20, Known compound):

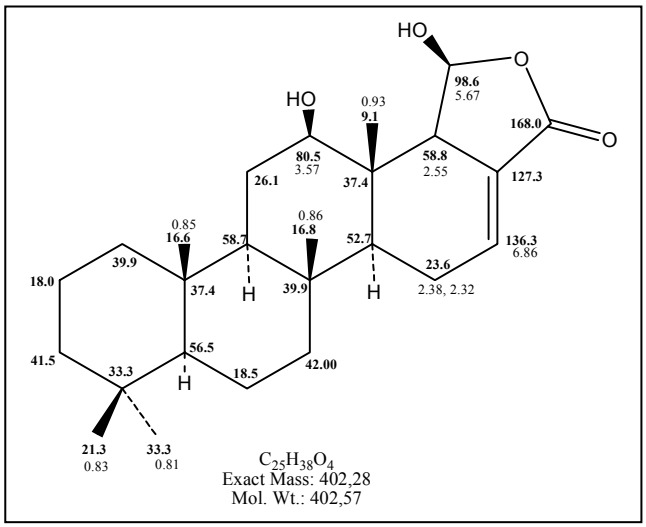

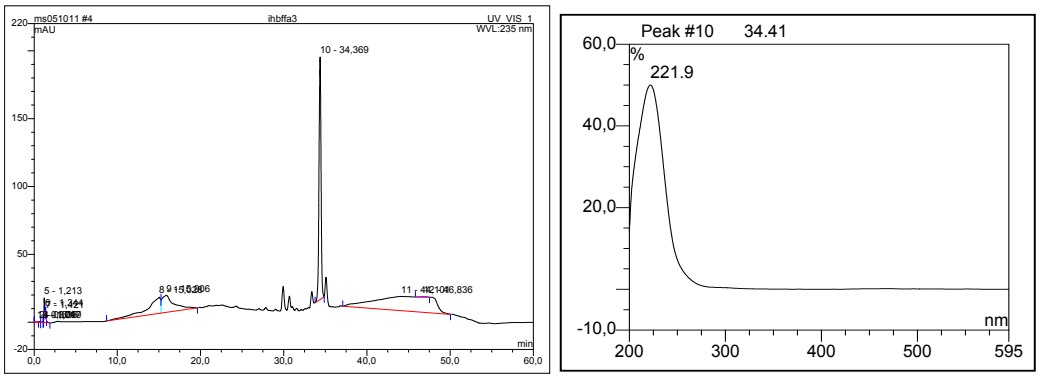

Fig (3.4.35):HPLC chromatogram and UV-spectrum of compound 20.

Yield : 1.5 mg

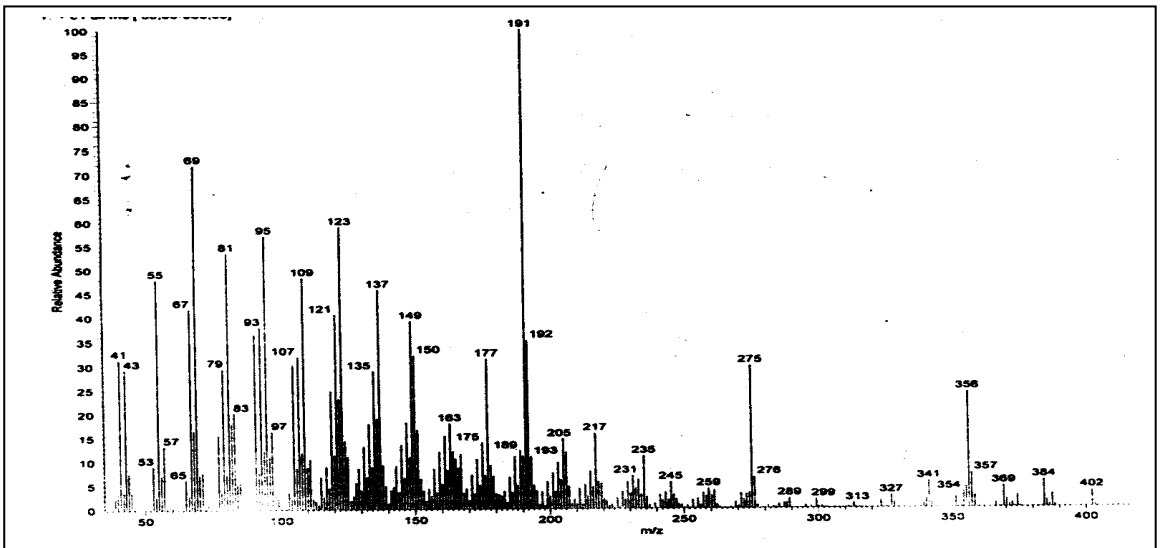

Fig (3.4.36):FAB-MS spectrum of compound 20.

Compound **20** [**12-O-deacetyl-12-epi-scalarin**] was isolated as a white solid with $[\alpha]_D$ of - 15° (*c* 0.1 $CHCl_3$). Compound **20** has a UV absorption at λ_{max} 221 nm and a molecular formula of $C_{25}H_{38}O_4$, as established from its EIMS and ^{13}C NMR data. EIMS of the compound **20** showed molecular ion peak *m/z* 402 $[M]^+$, *m/z* 384 $[M\text{-}H_2O]^+$, *m/z* 356 $[M\text{-}CH_2O_2]^+$, and *m/z* 191 [rings A+B+ 4(CH_3)]$^+$suggesting the molecular formula $C_{25}H_{38}O_4$.

The ^1H and ^{13}C NMR spectra measured in $CDCl_3$ (Table 3.4.8) suggested the scaralane-type sesterterpenoid. ^1H NMR spectrum displayed five singlets assigned to five methyl groups at δ 0.81, 0.83, 0.85, 0.86 and 0.93. One olefinic proton at δ 6.86 (1H, q, 3.1 Hz, H-16), 2 oxygenated methines at δ 5.67 (1H, d, 6.6Hz, H-19) and 3.57 (1H, d, 4.4, 11.7 Hz, H-12) were also observed. The carbon signals in the low-field region at 98.6 (d, C-19), 127.3 (s, C-17), 136.3 (d, C-16), and 168.0 (s, C-20) were reminiscent of those of scalarin (Tsukamoto *et al* 2003). H-12 was assigned as axial on the basis of the coupling constant of 11.7 Hz between H-11 and H-12. The Mol Wt of **20** is identical with that of **18** (both are 402 mass units), showing the same formula ($C_{25}H_{38}O_4$), the bresence of one olefenic proton resonating at 6.86 ppm indicated that the presence of double bond in the lactone ring should be different from that of compound **18** and more likely to be between C-16 and C-17 (instead of C-17 and C-18 as in compound **18**). This was confirmed by the coupling constant of H-16 (q, *J*= 3.1 Hz) due to the adjacent methylene at δ 2.38 and 2.32. furthremore the assignment at the position 18 as methine (δ 2.55, br s) was evident from the adjacent doublet (H-19, d, *J* = 6.6 Hz). The NMR data of **20** were similar to those of 12-*epi*-scalarin (Tsukamoto *et al* 2003 and Cimino *et al* 1977)) and suggested that **20** was a deacetyl derivative of 12-epi scalarin and identical with the previously published 12-*O*-deacetyl-12-*epi*-scalarin which isolated from *Spongia* sp. (Tsukamoto *et al* 2003).

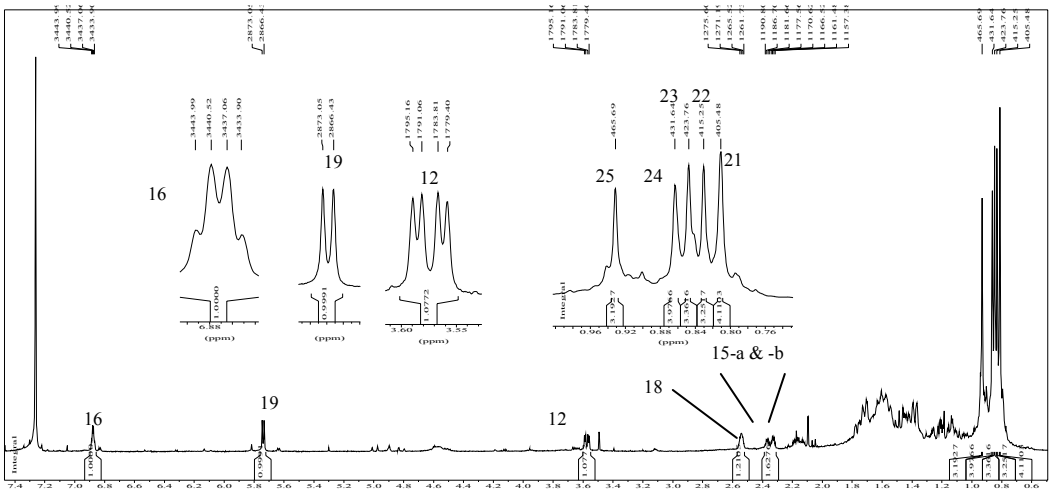

Fig (3.4.37):^{1}HNMR spectrum of compound 20.

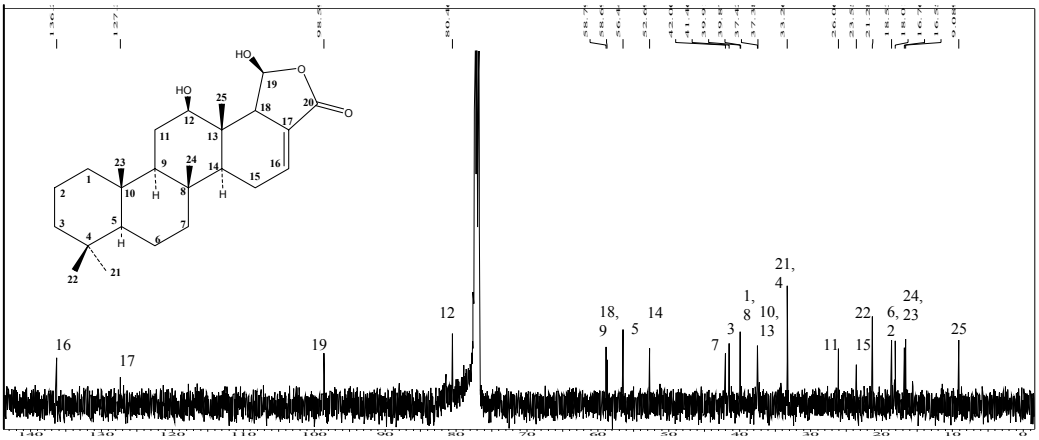

Fig (3.4.38):^{13}CNMR spectrum of compound 20.

Table (3.4.8): NMR data of compound 20 ($CDCl_3$, 500 MHz)

	12-O-deacetyl-12-epi-scalarin (Tsukamoto *et al* 2003) ($DMSO-d_6$)		compound 21 ($CDCl_3$)	
No.	^{13}C (mult.)	^{1}H [mult., J (Hz)]	^{13}C (mult.)	^{1}H [mult., J (Hz)]
1	40.2 (CH_2)	0.80 (1H, m), 1.62 (1H, m)	39.9 (CH_2)	*
2	18.2 (CH_2)	1.57 (1H, m), 1.63 (1H, m)	18.0 (CH_2)	*
3	41.3 (CH_2)	1.10 (1H, m), 1.33 (1H, m)	41.5 (CH_2)	*
4	33.5 (C)		33.3 (C)	
5	56.5 (CH)	0.79 (1H, m)	56.5 (CH)	*
6	18.7 (CH_2)	1.38 (1H, m), 1.46 (1H, m)	18.5 (CH_2)	*
7	42.2 (CH_2)	0.88 (1H, m), 1.63 (1H, td, 3.3, 12.4)	42.0 (CH_2)	*
8	37.5 (C)		39.9 (C)	
9	58.7 (CH)	0.80 (1H, m)	58.7 (CH)	*
10	37.4 (C)		37.4 (C)	
11	27.4 (CH_2)	1.30 (1H, dd, 2.1, 13.2), 1.55(1H, m)	26.1 (CH_2)	*
12	78.6(CH)	3.39 (1H, dd, 4.4, 12.0)	80.5(CH)	3.57 (1H, dd, 4.4, 11.7)
13	37.4 (C)		37.4 (C)	
14	52.9 (CH)	1.20 (1H, m)	52.7 (CH)	*
15	24.1 (CH_2)	2.12 (1H,m), 2.25 (1H, m)	23.6 (CH_2)	2.38 (1H,m), 2.32 (1H, m)
16	135.7(CH)	6.67 (1H, q, 2.9)	136.3(CH)	6.86 (1H, q, 3.1)
17	128.9 (C)		127.3 (C)	
18	58.1 (CH)	2.40 br s	58.8 (CH)	2.55 br s
19	100.5(CH)	5.72 (1H,t 5.9)	98.6(CH)	5.67 (1H,d, 6.6)
20	167.5 (C)		168.0 (C)	
21	33.7 (CH_3)	0.63 (3H, s)	33.3 (CH_3)	0.81 (3H, s)
22	21.7 (CH_3)	0.77 (3H, s)	21.3 (CH_3)	0.83 (3H, s)
23	16.4 (CH_3)	0.80 (3H, s)	16.6 (CH_3)	0.85 (3H, s)
24	16.8 (CH_3)	0.81 (3H, s)	16.8 (CH_3)	0.86 (3H, s)
25	9.8 (CH_3)	0.83 (3H, s)	9.1 (CH_3)	0.93 (3H, s)
* chemical shifts can not be precisely characterized from ^{1}HNMR spectrum.				

3.4.9- 7-dehydrocholesterol peroxide (21, Known compound):

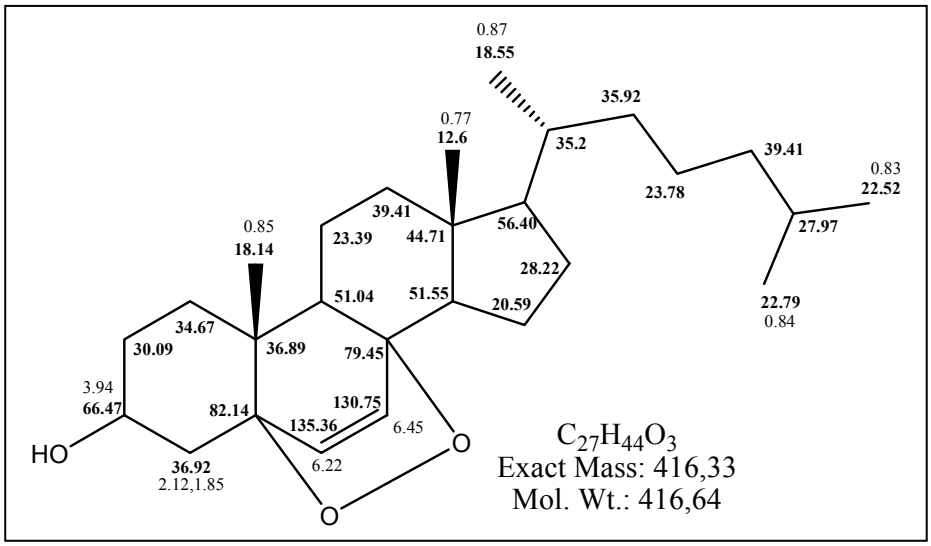

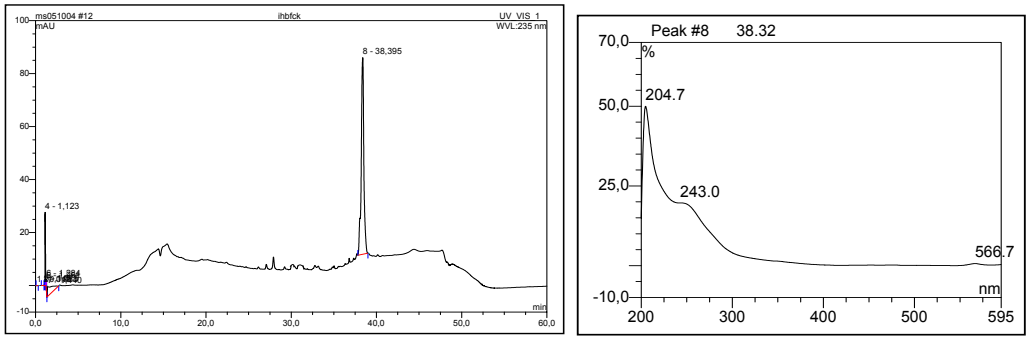

Fig (3.4.39):HPLC chromatogram and UV-spectrum of compound 21

Yield : 4 mg

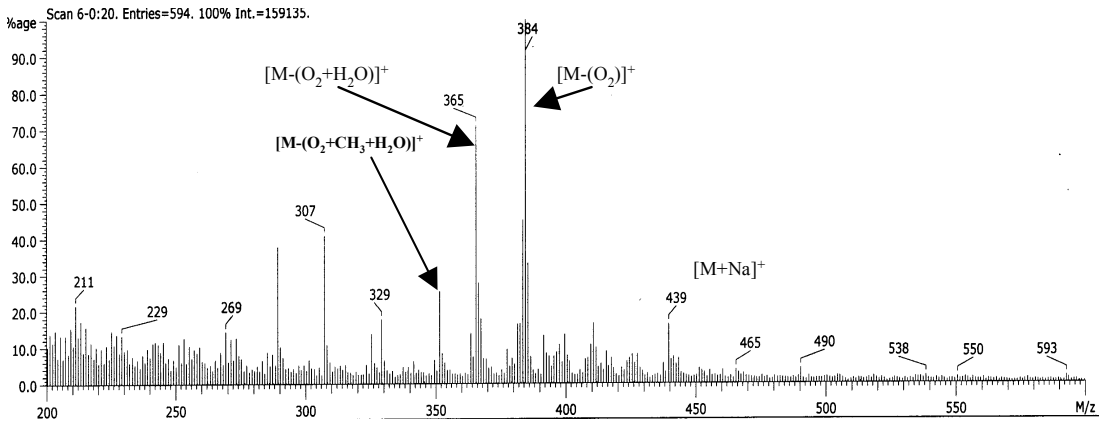

Fig (3.4.40):FAB-MS spectrum of compound 21.

Compound **21** [5α,8α-epidioxy-cholesta-6-en-3β-ol] was isolated as a white needle crystals. Compound **21** has a UV absorption at λ_{max} 204 and 243 nm. FAB-MS showed pseudomolecular ion peak *m/z* 439 $[M+Na]^+$ and characteristic fragment ions of typical 5α,8α-epidioxy-cholesta-6-en-3β-ol (Gauvin *et al*, 2000) suggesting the molecular formula $C_{27}H_{44}O_3$. ^{1}H NMR spectrum showed resonances for five methyl groups at δ 0.77 (3H, s, Me-18), 0.85 (3H, s, Me-19), 0.87 (3H, d, *J*=6.5 Hz, Me-21), 0.83 (3H, d, *J*=6.6 Hz, Me-26), and 0.84 (3H, d, *J*=6.6 Hz, Me-27). The resonances at δ 3.94 (1H, m, H-3), 6.22 (1H, d, *J*=8.5 Hz, H-6) and 6.45 (1H, d, *J*=8.5 Hz, H-7) suggested Δ^6, mono hydroxylated 5α,8α-epidioxysteroidal compound (Gauvin *et al* , 2000). This was confirmed by the presence of a fragment ion at *m/z* 384 (rel. int., 100 %) $[M-O_2]$ through the loss of O_2 from the molecular ion, presumably by a retro Diels-Alder fragmentation (Gunatilaka 1981), and by ^{13}C NMR signals at 82.14 and 79.41 of C-5 and C-8 respectively (Yaoita *et al* 1998, and Yue *et al* 2001). The β-configuration of hydroxy group at position 3, δ 3.96 (1H, m, H-3) and 66.44 ppm (d, C-3) was suggested by comparison with the published data of [5α,8α-epidioxy-cholesta-6-en-3β-ol] (Gauvin *et al*, 2000). From the above discussion, compound **21** was assigned as 5α,8α-epidioxy-cholesta-6-en-3β-ol.

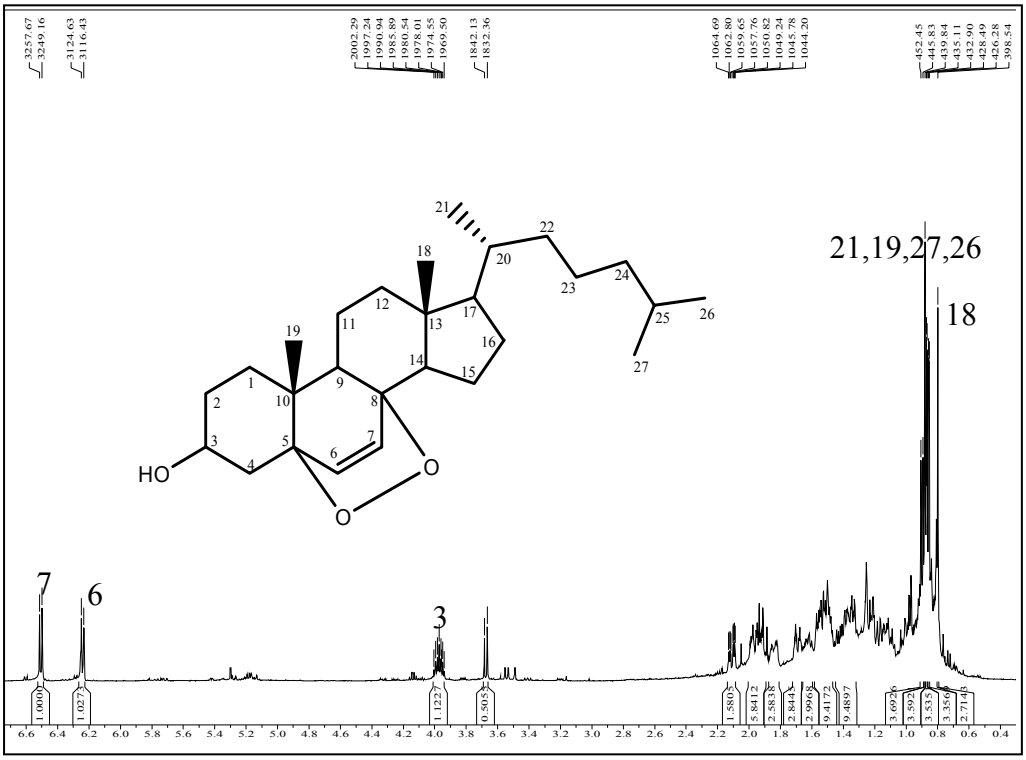

Fig(3.4.41): ^{1}H NMR spectrum of compound 21

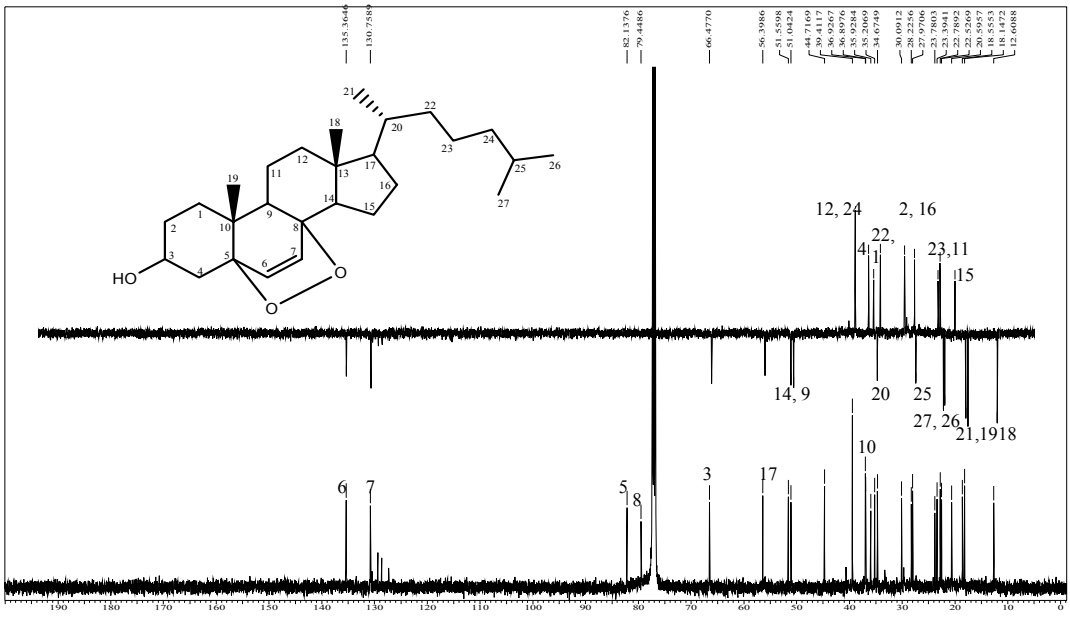

Fig(3.4.42): ^{13}C NMR and DEPT spectra of compound 21

Table (3.4.9): ^{1}H, ^{13}C-NMR data of compound 21 in ($CDCl_3$, 500, MHz)

	5α,8α-epidioxy-cholesta-6-en-3β-ol. (Guavin *et al* , 2000)		Compound 20	
No.	**^{13}C (Multiplicity)**	**^{1}H (Multiplicity, Hz)**	**^{13}C (Multiplicity)**	**^{1}H (Multiplicity, Hz)**
1	34.74 t		34.67 t	
2	30.16 t		30.09 t	
3	66.52 d	3.94 (m)	66.48 d	3.94 (m)
4	37.00 t		36.93 t	
5	82.24 s		82.14 s	
6	135.46 d	6.22 (d, *J*=8.5 Hz)	135.36 d	6.22 (d, *J*=8.51 Hz)
7	130.83 d	6.45 (d, *J*=8.5 Hz)	130.75 d	6.45 (d, *J*=8.51 Hz)
8	79.54 s		79.45 s	
9	51.10 d		51.04 d	
10	37.00 s		36.90 s	
11	23.46 t		23.39 t	
12	39.49 t		39.41 t	
13	44.80 s		44.72 s	
14	51.63 d		51.56 d	
15	20.68 t		20.59 t	
16	28.32 t		28.22 t	
17	56.46 d		56.40 d	
18	12.69q	0.77 (s)	12.61q	0.77 (s)
19	18.24q	0.85 (s)	18.15q	0.85 (s)
20	35.29d		35.21d	
21	18.64q	0.87 (d, *J*=6.5 Hz)	18.55 q	0.87 (d, *J*=6.62 Hz)
22	36.00 t		35.93 t	
23	23.86 t		23.78 t	
24	39.49 t		39.41 t	
25	28.06 d		27.97 d	
26	22.62 q	0.83 (d, *J*=6.6 Hz)	22.53 q	0.83 (d, *J*=6.62 Hz)
27	22.89 q	0.84 (d, *J*=6.6 Hz)	22.79 q	0.84 (d, *J*=6.62Hz)

Bioactivity:

Many scalarane-type sesterterpenoids have been isolated from marine sponges belonging to the order Dictyoceratida. Scalarane-type sesterterpenes display a variety of biological activities such as cytotoxic, antimicrobial**,** antifeedant, antimycobacterial, ichthyotoxic, anti-inflammatory, and platelet-aggregation inhibitory effects, as well as nerve growth factor synthesis-stimulating action (Youssef *et al*, 2005).

The isolated compounds from the *Hyrtios erectus* were tested for cytotoxic activity against L5178Y cells and the results wer summarised in table (3.4.10). Compounds **14**, **16**, **18** showed mild antimicrobial activity against *Bcillus subtilis* and *Saccharomyces cereviisae*.

Table (3.4.10): cytotoxic activity of compounds 13-18 and 21 against L5178Y cells.

Compound	**Cell growth % (conc. of 3µg/ml)**	**Cell growth % (conc. of 10µg/ml)**	**Cell growth % (-ve control)**
13	98.1	92.4	100
14	100	96.6	100
15	95.5	80.5	100
16	119	94.5	100
17	95.8	64	100
18	59.5	44.7	100
21	86.4	77	100

3.5. Natural products from *Petrosia nigricans*

Marine sponges of the genus *Petrosia* are known as a source of diverse bioactive natural products. Sponge species of genus *Petrosia* are rich in polyacetylenic compounds (Faulkner 1998, Faulkner 2002, Watanabe *et al* 2005), unusual bioactive steroids and steroidal sulphates acting as anti-HIV, antivirals, and anti-inflammatory (Goud *et al* 2003, Giner *et al* 1999, Reddy *et al* 1999, Shatz *et al* 2000, Sun *et al* 1992, Qureshi and Faulkner 1999).

Many alkaloidal natural products were isolated from genus *Petrosia* belonging to various subclasses, examples are bioactive manzamines (Crews *et al* 1994, Yousaf *et al* 2002), mimosamycins (Kobayashi *et al* 1994, Kobayashi *et al* 1992), cardioactive pentacyclic hydroquinones (Gorshkova *et al* 1999), dihydroisoquinolines (Ramesh *et al* 1999), pentacyclic pyridoacridines (Skyler *et al* 2002, Molinski *et al* 1988), isoquinoline quinones (Venkateswarlu *et al* 1993), 3-alkylpyridinium polymers (Sepcic *et al* 1997), bis-quinolizidine alkaloid (Braekman *et al* 1982, Braekman et al 1984), and dihydrotubastrines – phenethylguanidine (Sperry and Crews 1998). *Petrosia*–derived fungal strain *Penicillium brevicompactum* was reported to produce cyclodepsipeptides (Bringmann et al 2004).

However, this is the first report of *Petrosia nigricans*-derived natural products. An Indonesian *Petrosia sp.* (*Petrosia nigricans,* family Petrosiidae) was chemically investigated and several compounds were isolated. These compounds can be divided into the following chemical classes:

1- steroidal compounds (24ξ-ethyl-cholesta-5-en-3β-ol, 24ξ-ethyl-cholesta-8(9)-en-3β-ol, 5α,8α-epidioxy-24ξ-ethyl-cholesta-6-en-3β-ol)
2- phenylacetic acid derivatives (phenylacetic acid, p-hydroxyphenylacetic acid, p-hydroxyphenylacetic acid methylester, p-hydroxyphenylacetic acid ethylester, p-hydroxyphenylacetic acid butylester*)
3- primary metabolites (adenosine, nicotinamide)
4- cerebrosides. (petrocerebroside 1*, petrocerebroside 2*).
5- purine derivatives (Nigricine 1*, Nigricine 2*, Nigricine 3*, Nigricine 4*)
6- indole alkaloid *

(* = new natural products).

3.5.1- 24ξ-Ethyl-cholesta-5-en-3β-ol (22, known compound)

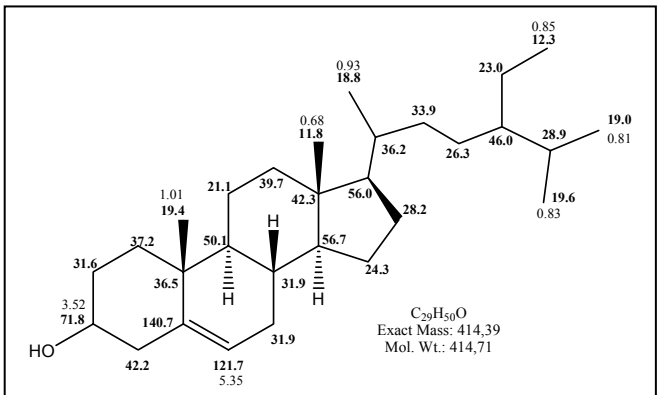

Yield : 2g

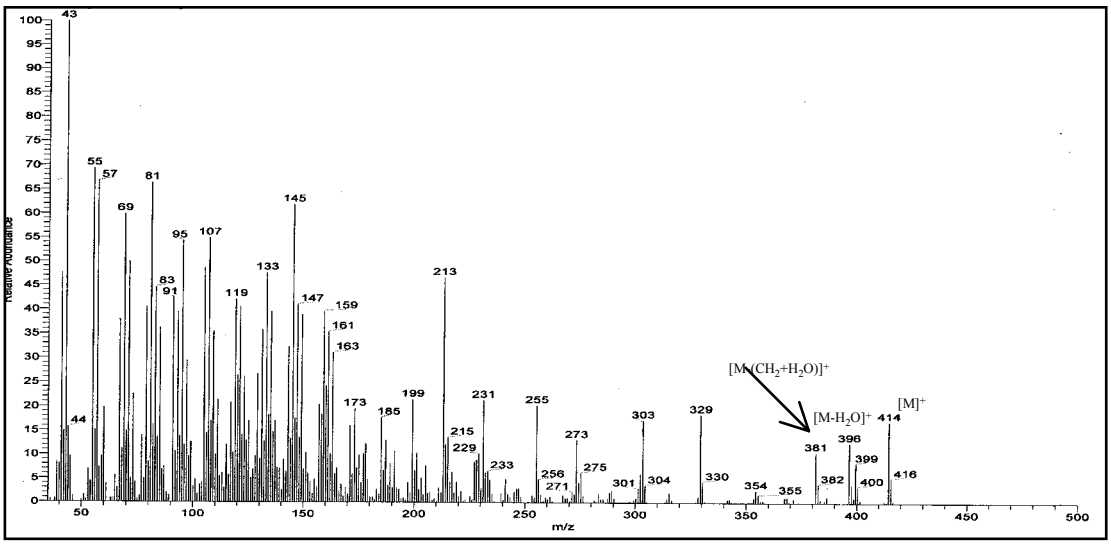

Fig (3.5.1):EI-MS spectrum of compound 22

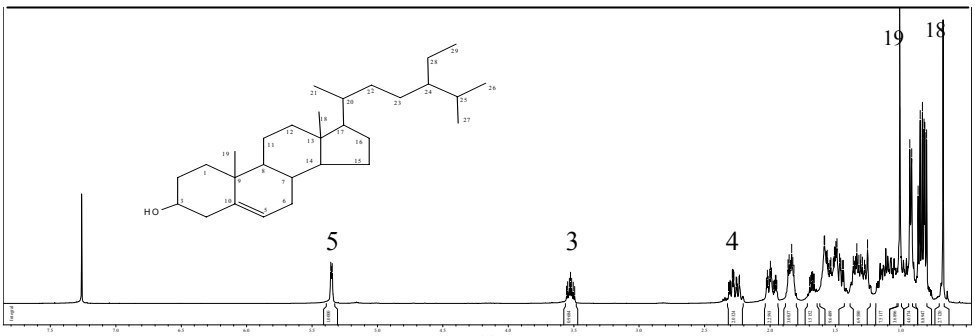

Fig (3.5.2): ^{1}HNMR spectrum of compound 22 (in $CDCl_3$)

Compound **22** [24ξ-ethyl-cholesta-5-en-3β-ol] was isolated as a white amorphous powder, with $[\alpha]_D$ of - 17° (*c* 0.1.2 $CHCl_3$). EI-MS showed molecular ion peak *m/z* 414 $[M]^+$ and fragment ions at 396 $[M-(H_2O)]^+$, 382 $[M-(CH_2 + H_2O)]^+$, 368 $[M-C_2H_5OH]^+$, 273 [M-side chain]$^+$, 255 [M- (side chain+H_2O)]$^+$, suggesting the molecular formula $C_{29}H_{50}O$. ^1H NMR spectrum showed resonances for six methyl groups at δ 0.68 (3H, s, Me-18), 1.01 (3H, s, Me-19), 0.93 (3H, d, *J*=6.94 Hz, Me-21), 0.81 (3H, d, *J*=6.93 Hz, Me-27), 0.83 (3H, d, *J*=6.94 Hz, Me-26), 0.85 (3H, t, *J*=7.56 Hz, Me-29). The resonances at δ 5.35 (1H, m, H-6), 3.52 (1H, m, H-3) were indicative for Δ^{5-6} mono hydroxylated steroidal nucleus (Itoh et al , 1983).^{13}C NMR showed six methyl signals at δ 12.3, 11.8, 19.4, 18.8, 19.6 and 19.0 for the methyl groups 29,18, 19, 21, 26, and 27, respectively. ^{13}C NMR spectrum showed one sp^2 quaternary olefenic carbon resonance at δ 140.7 and one sp^2 methine at 121.7, and an oxygenated methine at 71.8. In addition, ^{13}C NMR spectrum shows 7 sp^3 methines, and 11 aliphatic methylenes (see table 3.5.1). The above EI-MS, and NMR data were identical with that of 24ξ-ethyl-cholesta-5-en-3β-ol (Wright *et al* 1978, Younus *et al* 1974). Compound **22** was also isolated from *Petrosia* (*Strongylophora*) *durissima* (Shen and Prakash 2000).

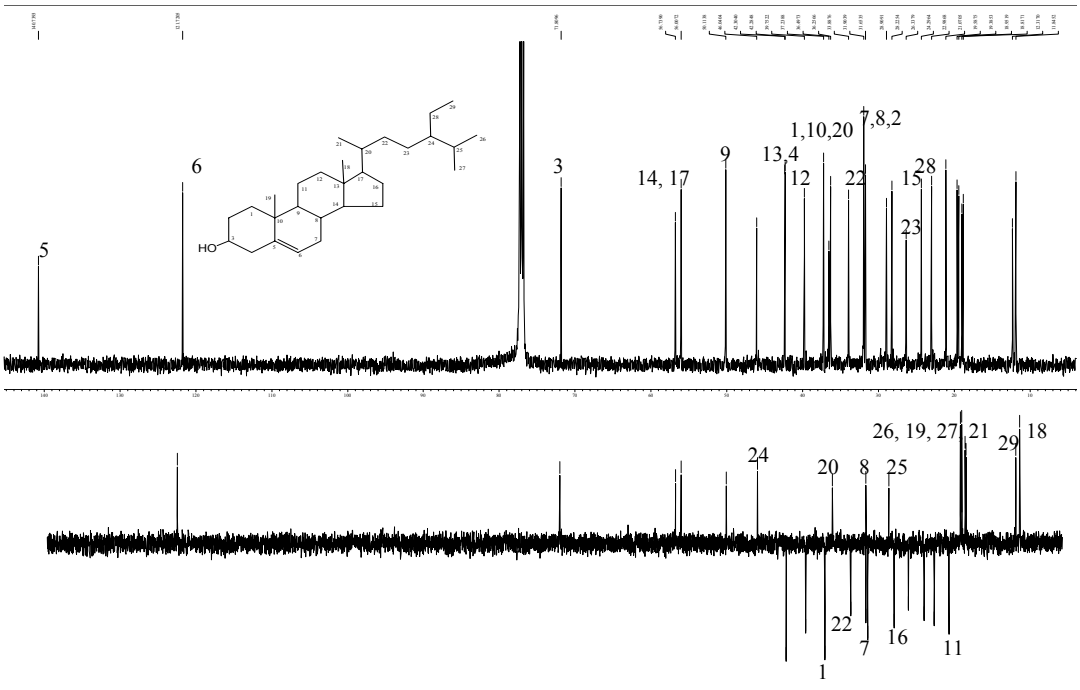

Fig (3.5.3): ^{13}CNMR and DEPT spectra of compound 22 (in $CDCl_3$)

3.5.2- 4α-Methyl-5α-cholesta-8-en-3β-ol (23, known compound)

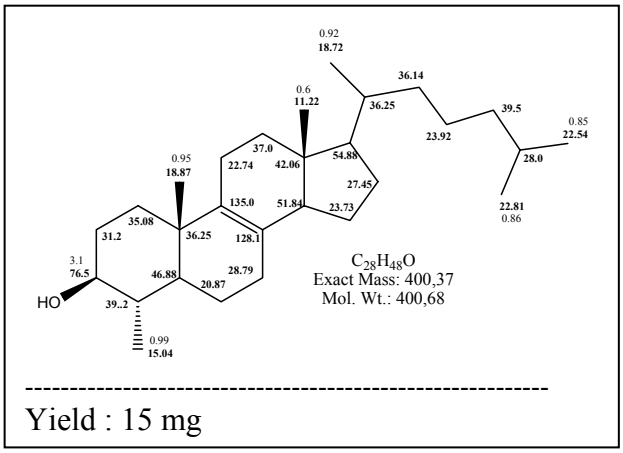

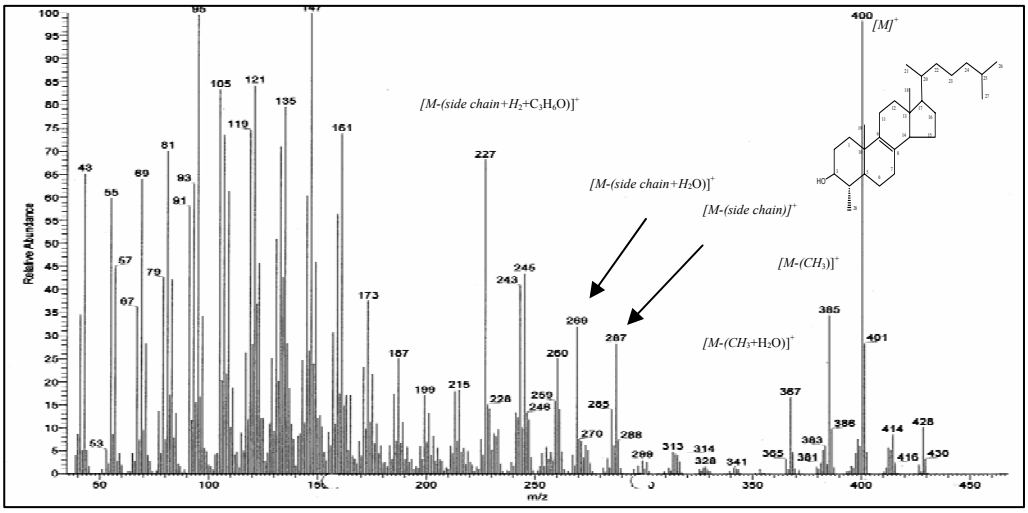

Fig (3.5.4): ES-MS spectrum of compound 23

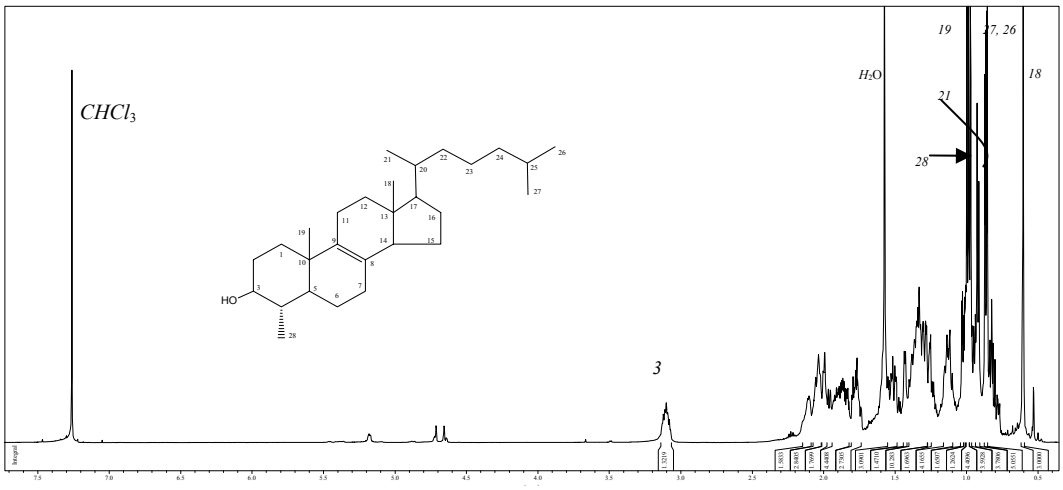

Fig (3.5.5): ^{1}HNMR spectrum of compound 23 (in $CDCl_3$)

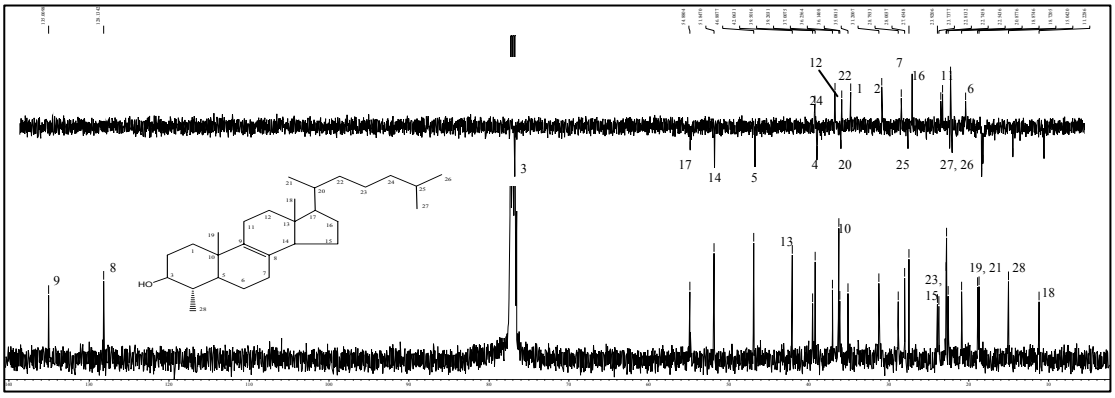

Fig (3.5.6): ^{13}CNMR and DEPT spectra of compound 23 (in $CDCl_3$)

Compound **23** [4α-methyl-5α-cholesta-8-en-3β-ol] was isolated as white amorphous powder, with $[\alpha]_D$ of + 44° (*c* 0.5 $CHCl_3$). EI-MS showed molecular ion peak *m/z* 400 $[M]^+$ and characteristic fragment ions at 385 [M-CH_3], 367 [M- (CH_3+H_2O)], 287 [M-(side chain)], 269 [M-(side chain+H_2O)], 227 [M-(side chain+C_3H_6O+H_2)] suggesting the molecular formula $C_{28}H_{48}O$. ^{1}H NMR spectrum showed resonances for six methyl groups at δ 0.6 (3H, s, Me-18), 0.95 (3H, s, Me-19), 0.92 (3H, d, *J*=6.31 Hz, Me-21), 0.86 (3H, d, *J*=6.6 Hz, Me-27), 0.85 (3H, d, *J*=6.61 Hz, Me-26), 0.99 (3H, t, *J*=6.31 Hz, Me-28). The presence of the typical 3β- hydroxyl group was indicated by the methine signal at δ 3.1. Furthermore, appearance of the methine signal as a triple doublet with coupling constant of *J*=4.7, 9.9, 11.1 Hz indicated that the methine proton is axial and is coupled to three adjacent hydrogens as in other 4α-methylsterols (König *et al*, 1998 & Gunasekera *et al*, 1989). The two axial–axial couplings of 9.9 and 11.1 Hz confirmed the α-equatorial nature of the 4-methyl group. The ^{13}C-NMR spectrum revealed only two singlets in the olefenic region (δ128.1 and 135.0) indicating the presence of tetrasubstituted double bond (Gunasekera *et al*, 1989). The mass spectrum showed the characteristic peak at *m/z* 287 (M-side chain). The above NMR and MS data confirmed compound **23** as 4α-methyl-5α-cholesta-8-en-3β-ol. The structure of **23** was confirmed by comparing its spectral data with the literature data reported for the same compound isolated from *Agelas oroides* and *Agelas flabelliformis* (König *et al*, 1998 & Gunasekera *et al*, 1989 respectively).

3.5.3. 5α,8α-Epidioxy-24ξ-ethyl-cholesta-6-en-3β-ol (24, known compound)

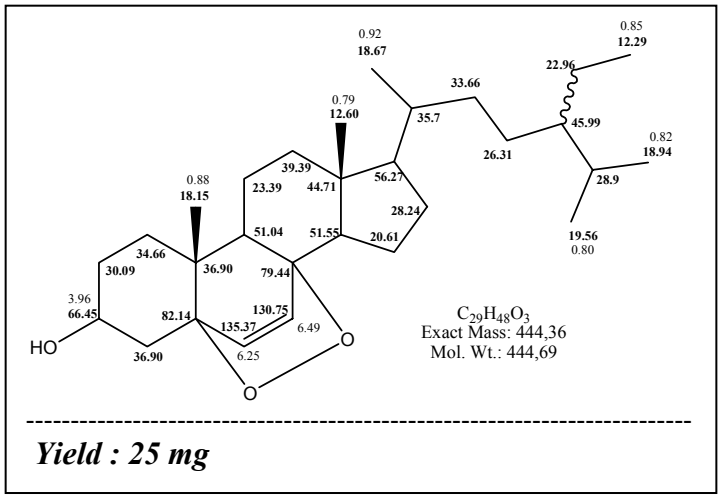

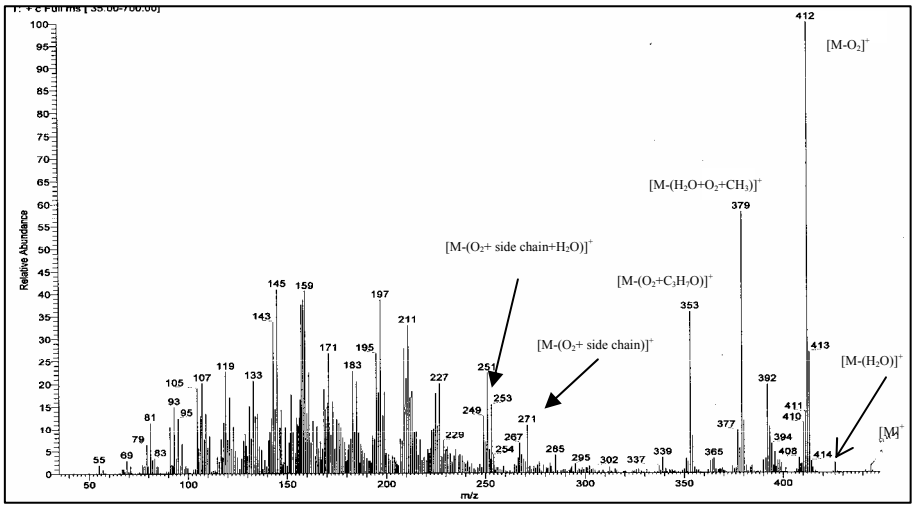

Fig (3.5.7):EI-MS spectrum of compound 24

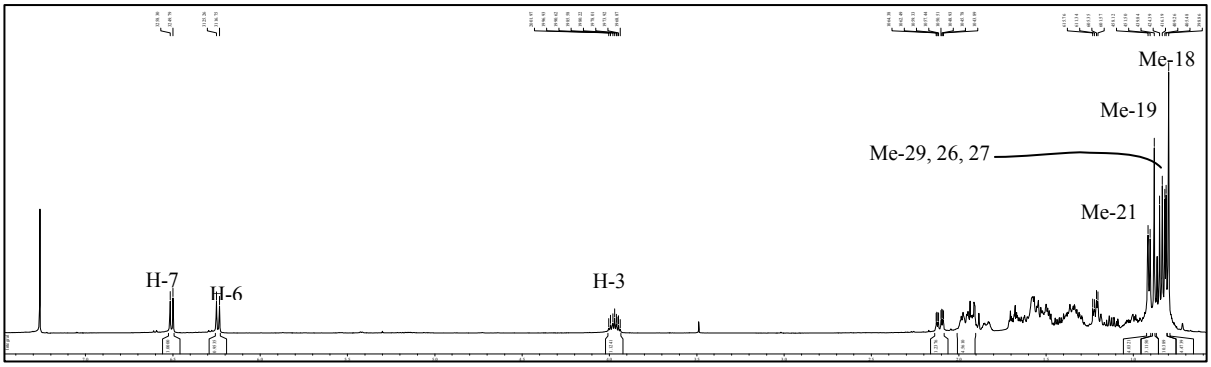

Fig (3.5.8): ^{1}HNMR spectrum of compound 24 (in $CDCl_3$)

Compound **24** [5α,8α-epidioxy-24ξ-ethyl-cholesta-6-en-3β-ol] was isolated as white needle crystals with $[\alpha]_D$ of + 4° (*c* 0.70 $CHCl_3$). EI-MS showed molecular ion peak *m/z* 444 $[M]^+$ and characteristic fragment ion peaks at *m/z* 426 $[M-H_2O]$, 412 $[M-O_2]$, 379 $[M-(H_2O,+O_2+CH_3)]$, 353 $[M-(O_2+ C_3H_7O)]$, 271 [M-(side chain $+O_2$)] and 253 [M-(side chain + O_2+ H_2O)] suggesting the molecular formula $C_{29}H_{48}O_3$. ^{1}H NMR spectrum showed resonances for six methyl groups at δ 0.79(3H, s, Me-18), 0.88 (3H, s, Me-19), 0.92 (3H, d, *J*=6.7 Hz, Me-21), 0.80 (3H, d, *J*=6.6 Hz, Me-27), 0.82 (3H, d, *J*=6.90 Hz, Me-26), 0.85 (3H, t, *J*=7.5 Hz, Me-29). The resonances at δ 3.96 (1H, m, H-3), 6.25 (1H, d, *J*=8.51 Hz, H-6) and 6.49 (1H, d, *J*=8.51 Hz, H-7) suggested a Δ^6 mono hydroxylated 5α,8α-epidioxysteroidal compound (Gauvin *et al* , 2000). This was confirmed by the presence of an ion fragment at *m/z* 412 $[M-O_2]$ through loss of O_2, presumably by a retro Diels-Alder fragmentation (Gunatilaka 1981), and by ^{13}C NMR signals at 82.14 and 79.41 of C-5 and C-8, respectively (Yaoita *et al* 1998, and Yue *et al* 2001). The β-configuration of hydroxyl group at position 3, δ 3.96 (1H, m, H-3) and 66.44 ppm (d, C-3) was suggested by comparison with the published data of 3α- and 3β-hydroxy steroids (Eggert *et al* 1976, Wright *et al* 1978, and Gauvin *et al*, 2000). Although the NMR data of the position 24 were in comparison with those reported by Wright *et al* 1978 and Gauvin *et al*, 2000, the sterochemistry at this position is still undetected because the chemical shifts of the side chain carbons which were not similar enough to those given for 24*R* or 24*S*.

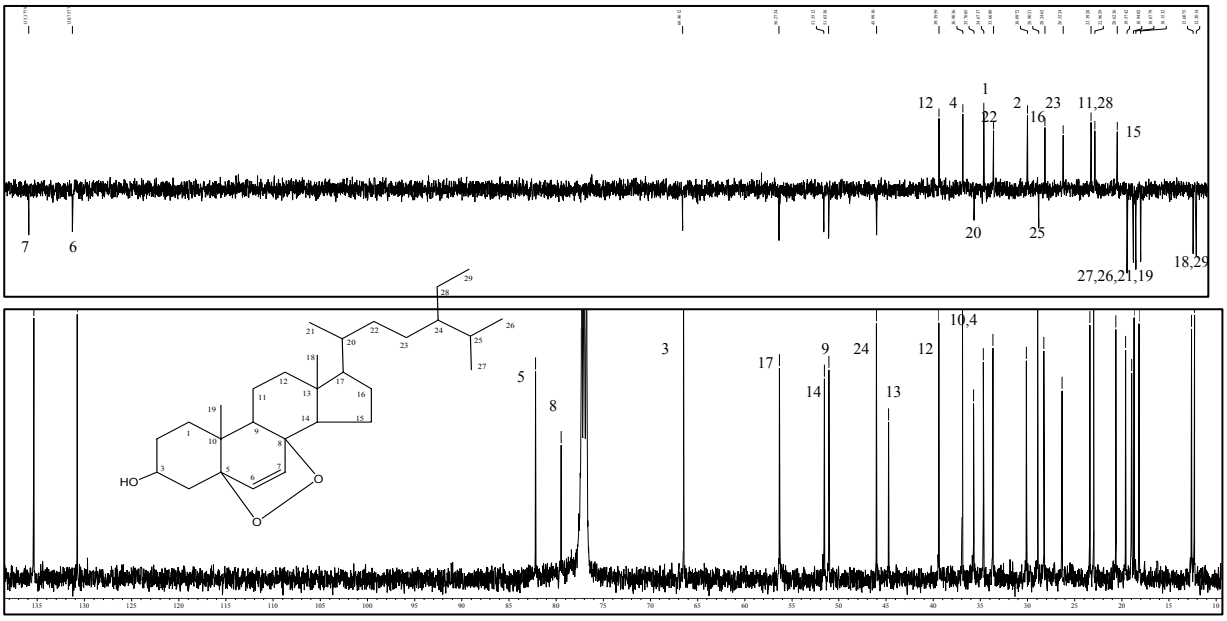

Fig (3.5.9): ^{13}CNMR and DEPT spectra of compound 24 (in $CDCl_3$)

Table (3.5.1): ^{1}H- and ^{13}C-NMR data of compounds 22, 23 and 24 in ($CDCl_3$, 500, MHz)

	Compound 22		Compound 23		Compound 24	
No.	**^{13}C (Multi-plicity)**	**^{1}H (Multiplicity, Hz)**	**^{13}C (Multi-plicity)**	**^{1}H (Multiplicity, Hz)**	**^{13}C (Multi-plicity)**	**^{1}H (Multiplicity, Hz)**
1	37.2 t		35.08 t		34.66 t	
2	31.6 t		31.2 t		30.09 t	
3	71.8 d	3.52 (m)	76.5 d	3.1 (ddd, *J*=4.7, 9.9, 11.1)	66.45 d	3.96 (m)
4	42.2 t		39.50 d		36.90 t	
5	140.7 s		46.88 d		82.14 s	
6	121.7 d	5.35 (m)	20.87 t		135.37 d	6.25 (d, *J*=8.51)
7	31.9 t		28.79 t		130.75 d	6.49 (d, *J*=8.51)
8	31.9 d		128.1 s		79.44 s	
9	50.1 d		135.0 s		51.03 d	
10	36.5 s		36.25 s		36.90 s	
11	21.1 t		22.74 t		23.39 t	
12	39.7 t		37.0 t		39.39 t	
13	42.3 s		42.06 s		44.71 s	
14	56.7 d		51.84 d		51.55 d	
15	24.3 t		23.73 t		20.61 t	
16	28.2 t		27.45 t		28.24 t	
17	56.0 d		54.88 d		56.27 d	
18	11.8 q	0.68 (s)	11.22 q	0.6 (s)	12.60q	0.79 (s)
19	20.4 q	1.01 (s)	18.87 q	0.95 (s)	18.15q	0.88 (s)
20	36.2 d		36.25 d		35.70 d	
21	18.8 q	0.93 (d, *J*=6.94 Hz)	18.72 q	0.92 (d, *J*=6.31)	18.67 q	0.92 (d, *J*=6.7 Hz)
22	33.9 t		36.14 t		33.66 t	
23	26.3 t		23.92 t		26.31 t	
24	46.0 d		39.5 t		45.99 d	
25	28.9 d		28.0 d		28.89 d	
26	19.6 q	0.83 (d, *J*=6.94 Hz)	22.54 q	0.85 (d, *J*=6.61)	18.94 q	0.82 (d, *J*=6.9 Hz)
27	19.0 q	0.81 (d, *J*= 6.93Hz)	22.81 q	0.86 (d, *J*=6.61 Hz)	19.56 q	0.80 (d, *J*=6.6 Hz)
28	23.0 t		15.04 q	0.99 (d, *J*=6.31)	22.96 t	
29	12.3 q	0.86 (t, *J* = 6.94 Hz)			12.29 q	0.85 (t, *J*=7.5Hz)

3.5.4- Phenylacetic acid (25, known compound)

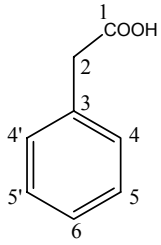

$C_8H_8O_2$
Exact Mass: 136,05
Mol. Wt.: 136,15

δ_{H-2} 3.65 (2H, s)
$\delta_{H(4,5,6,4',5')}$ 7.3 (5H, m)

Yield : 6.0 mg

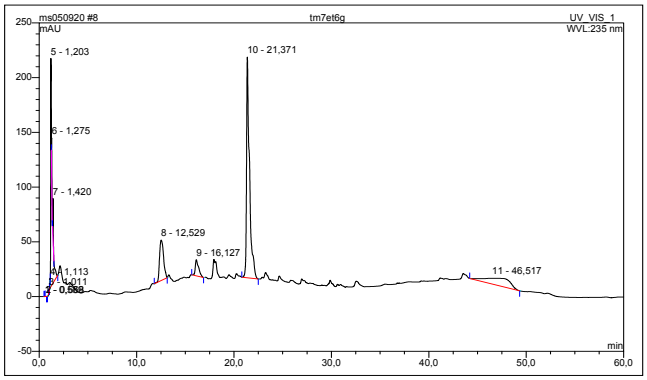

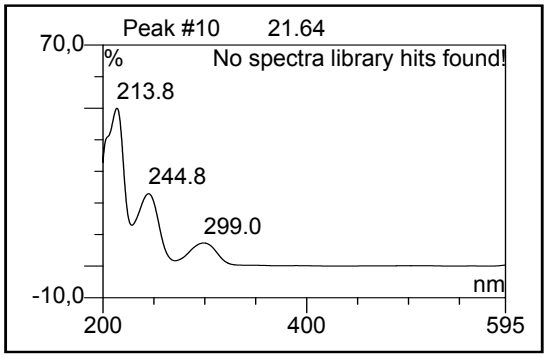

Fig (3.5.10): HPLC chromatogram and UV spectrum of compound 25

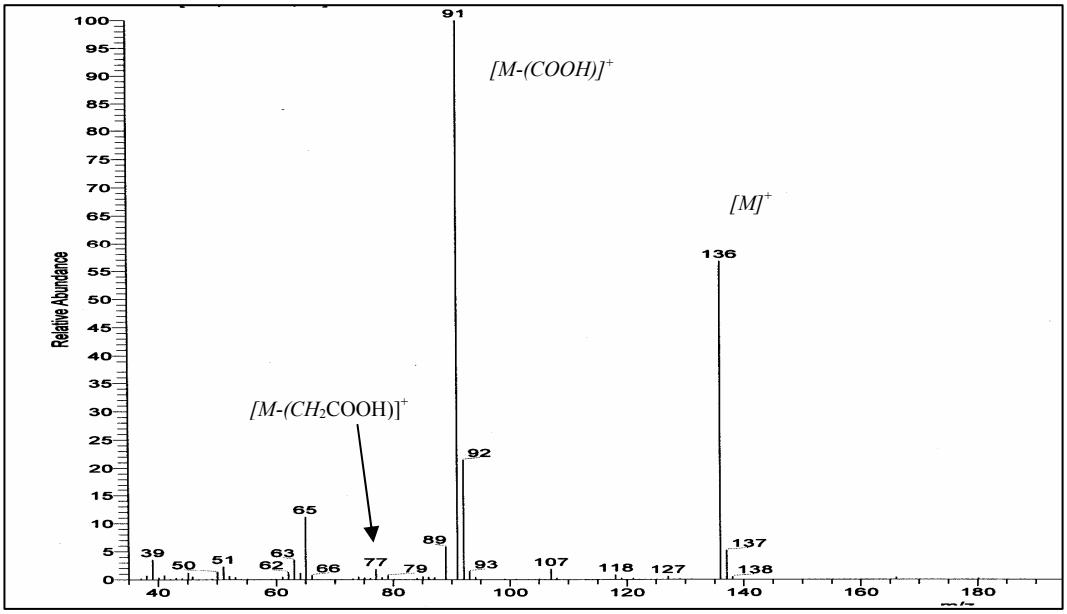

Fig (3.5.11):EI-MS spectrum of compound 25

Compound **25** [phenylacetic acid] was isolated as a white amorphous powder, UV absorption at λ_{max} 213, 244, 299 nm. EI-MS showed molecular ion peak at m/z 136 $[M]^+$, and fragment ion peaks at m/z 91 $[M\text{-}COOH]^+$, 77 $[M\text{-}CH_2COOH]^+$, (see figure 3.5.22) suggesting the molecular formula $C_8H_8O_2$. A deceptively simple ^1H NMR spectrum (meassured in $CDCl_3$) showed two sets of protons resonating at δ 3.65 (2H, s) suggesting the presence of lower field methylene group (i.e., attached to aromatic spin system), and at δ 7.3 (5H, m) suggesting monosubstituted phenyl group. The above NMR data together with the EI-MS fragments confirmed compound **25** to be phenylacetic acid. ^1H-NMR and ^{13}C-NMR of **25** is identical with those reported for phenylacetic acid (Aldrich, 1993, **2**/981).

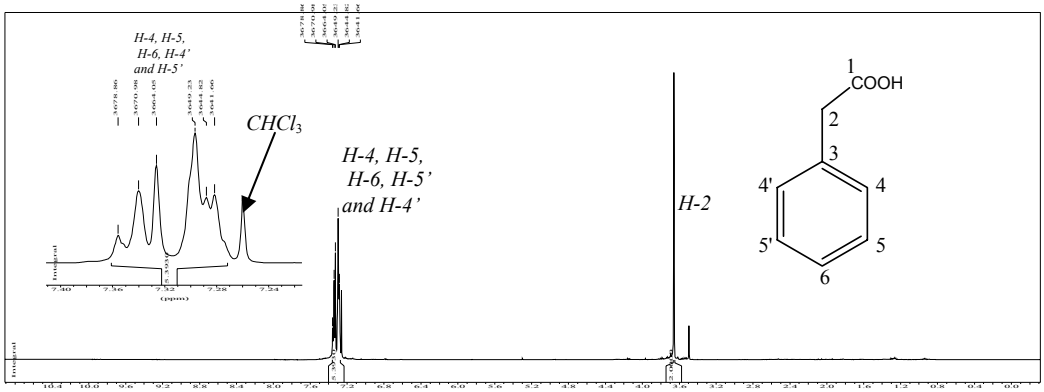

Fig (3.5.12):^{1}HNMR spectrum of compound 25

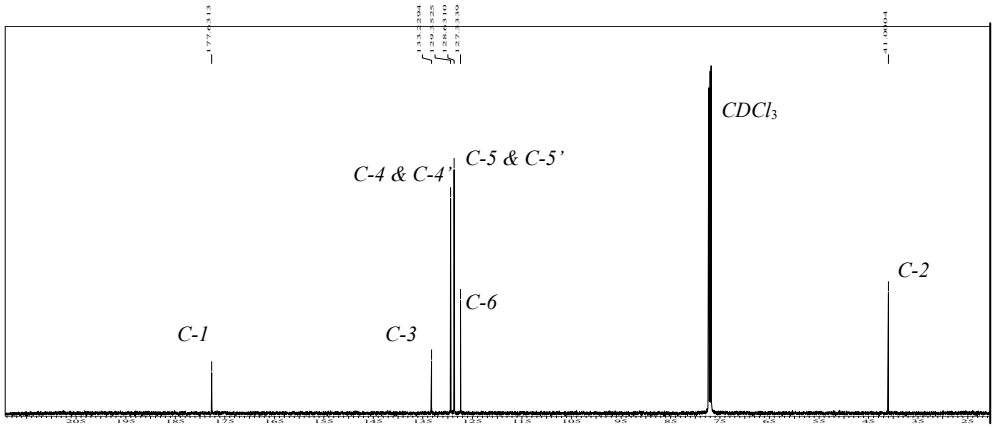

Fig (3.5.13):^{13}CNMR spectrum of compound 25

3.5.5- *p*-Hydroxyphenylacetic acid (26, known compound)

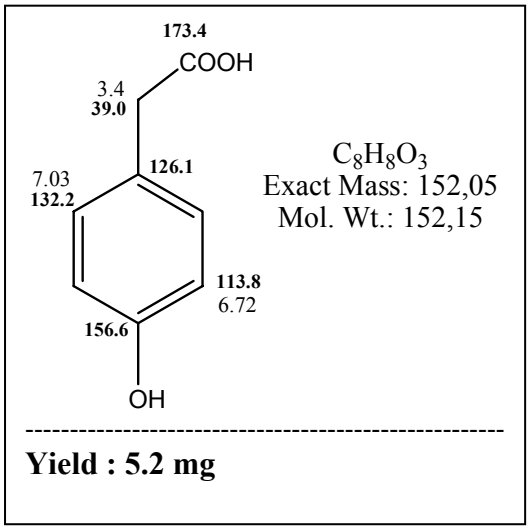

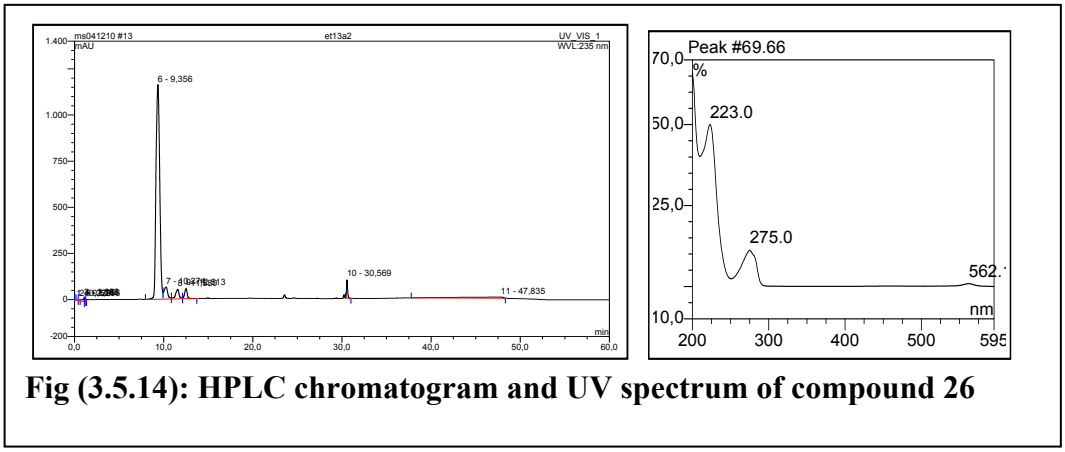

Fig (3.5.14): HPLC chromatogram and UV spectrum of compound 26

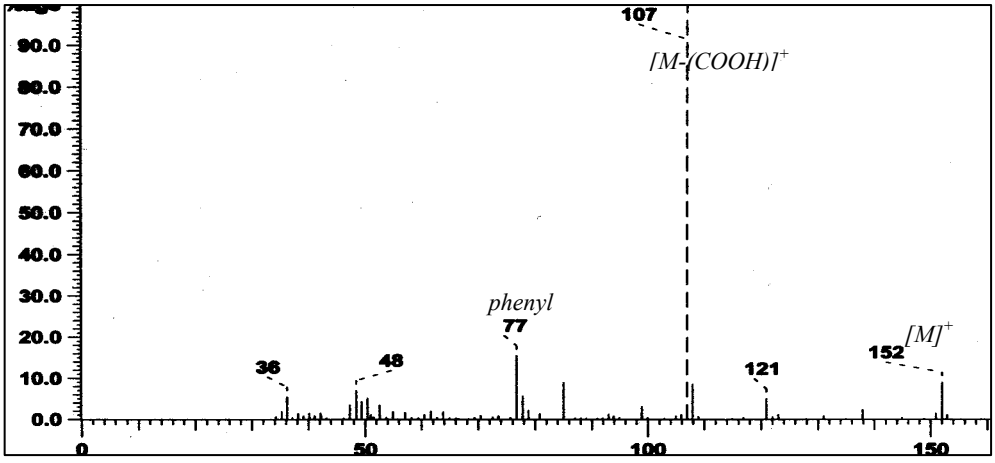

Fig (3.5.15):EI-MS spectrum of compound 26

Compound **26** [p-hydroxyphenylacetic acid] was isolated as a white amorphous powder, UV absorption at λ_{max} 201, 223, 275 nm. EI-MS showed molecular ion peak m/z 152 $[M]^+$, and fragment ion peaks at m/z 107 $[M\text{-}COOH]^+$, 77 $[M\text{-}(CH_2COOH+OH)]^+$, (see figure 3.5.26) suggesting the molecular formula $C_8H_8O_3$. The difference between **25** and **26** is only 16 mass units which indicates the presence of one oxygen atom in **26** more than **25**. Comparable to compound **25**, ^{1}H NMR spectrum of **26** in DMSO-d_6 showed three proton resonances at δ 3.38 (2H, s) suggesting the presence of lower field methylene group, attached to an aromatic spin system and at δ 7.03 (2H, d, J=8.52 Hz, H-4& H-4') and δ 6.72 (2H, d, J=8.2 Hz, H-5& H-5'), suggesting p-disubstituted phenyl group instead of 5 proton resonances overlaping at δ7.3 in ^{1}HNMR of compound **25.** The NMR data together with the ESI-MS fragments suggested compound **26** to be p-hydroxyphenylacetic acid, which was confirmed by HMBC correlations (see figure 3.5.17). The CH_2 at 3.38 showed HMBC correlations to C-1, C-3, C-4 and C-4` at δ 173.4, 126.1, and 132.2, while H-4 and H-4` at δ 7.03 showed HMBC correlations to C-2, C-5, and C-6 at δ 39.0, 113.8, and 156.6, respectively. The NMR data of **26** are identical to those of p-hydroxyphenylacetic acid (Aldrich, 1993, **2**/1018). p-Hydroxyphenylacetic has been previously isolated from many terresterial biological sources [e.g. Mellilotus officinalis and Taraxacum officinale (DNP 2005)].

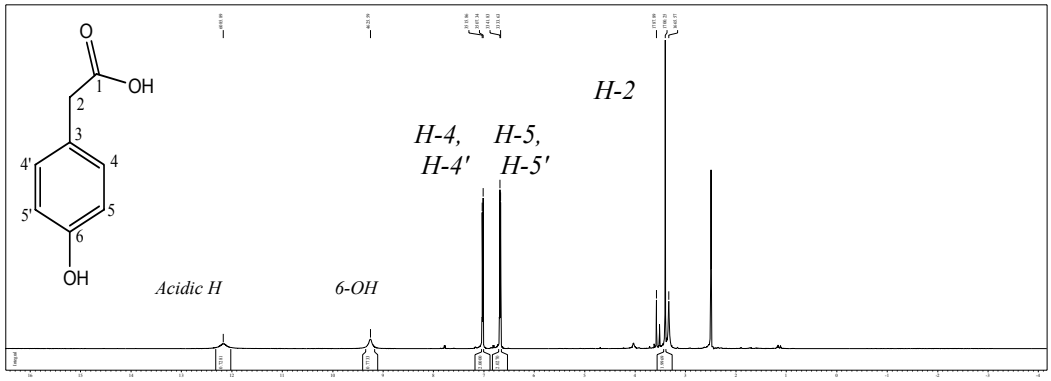

Fig (3.5.16):^{1}HNMR spectrum of compound 26

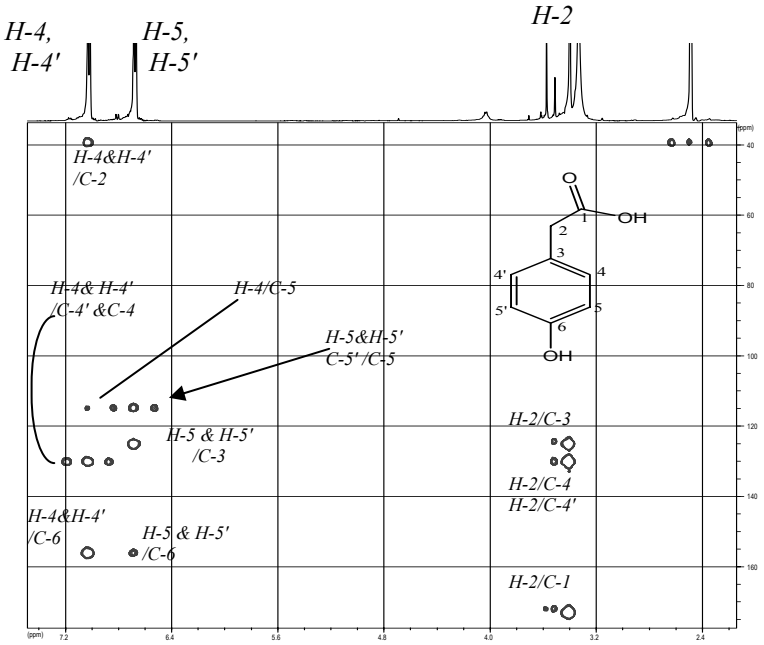

Fig (3.5.17): HMBC spectrum of compound 26

3.5.6- Methyl 2-(4-hydroxyphenyl)acetate (27, known compound)

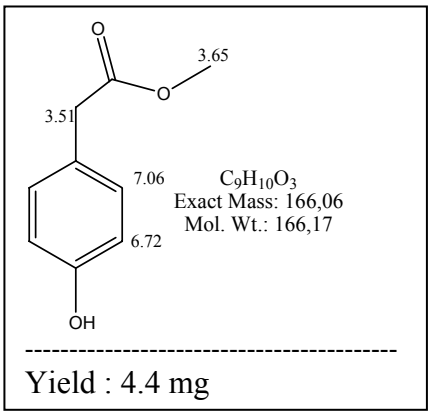

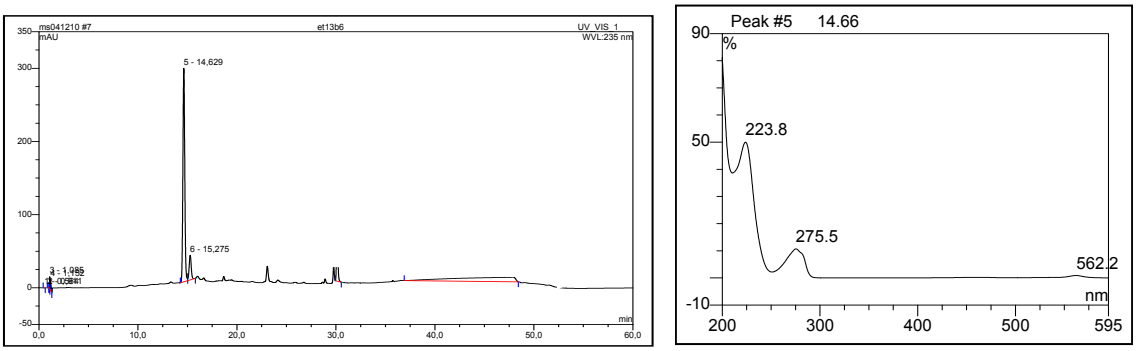

Fig (3.5.18): HPLC chromatogram and UV spectrum of compound 27

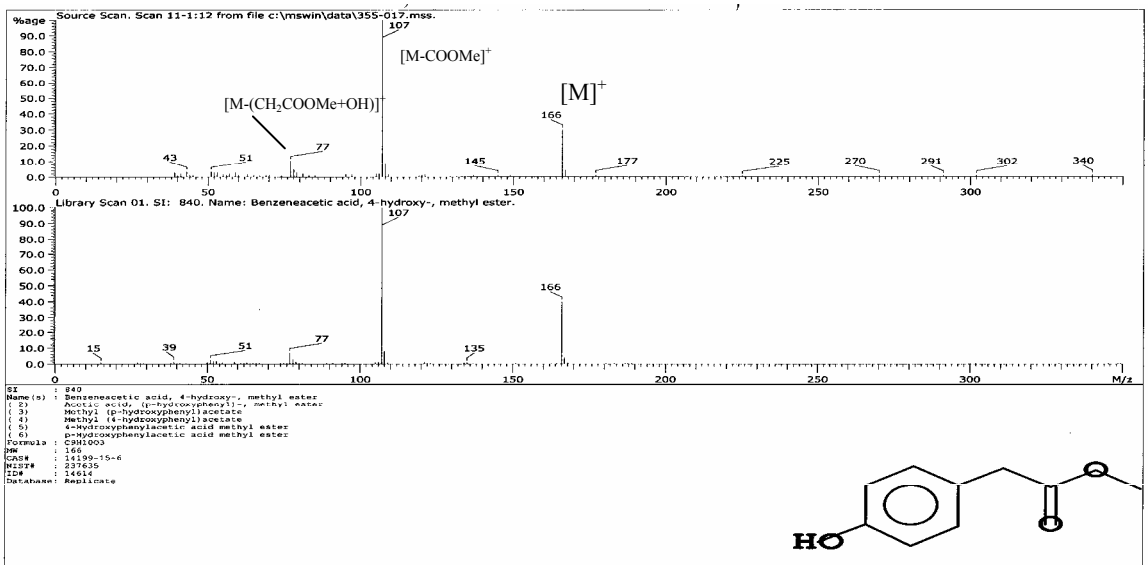

Fig (3.5.19):EI-MS spectrum of compound 27 (up) compared with standared *p*-hydroxy-phenylacetic acid methyl ester (down).

Compound **27** [methyl 2-(4-hydroxyphenyl)acetate] was isolated as a white amorphous powder, UV absorption at λ_{max} 201, 223, 275 nm. EI-MS showed molecular ion peak at m/z 166 $[M]^+$, and fragment ion peaks at m/z 107 $[M\text{-}COOMe]^+$, 77 $[M\text{-}(CH_2COOMe+O)]^+$, (see figure 3.5.30) suggesting the molecular formula $C_9H_{10}O_3$. It is clear that compound **27** is 14 mass units larger than compound **26** which indicates the presence of one CH_2 group or exactly, the replacement of the carboxylic proton with methyl group as evident from the ^1H NMR spectrum. The ^1H NMR spectrum in methanol-d_4 of **27** showed the same set of proton resonances as compound **26**, in addition to the presence of a methoxy proton at 3.65 ppm which indicated the methyl ester of compound **26**. Compared to the authentic sample of methyl 2-(4-hydroxyphenyl)acetate, compound **27** showed the same molecular ion peak as well as the same fragmentation pattern (as shown in figure 3.5.19). From NMR data and EIMS compound **27** was assigned as methyl 2-(4-hydroxyphenyl)acetate which was previously isolated from many biological sources [like Fusarium oxysporum (Kachlicki P., et al . (1997)]

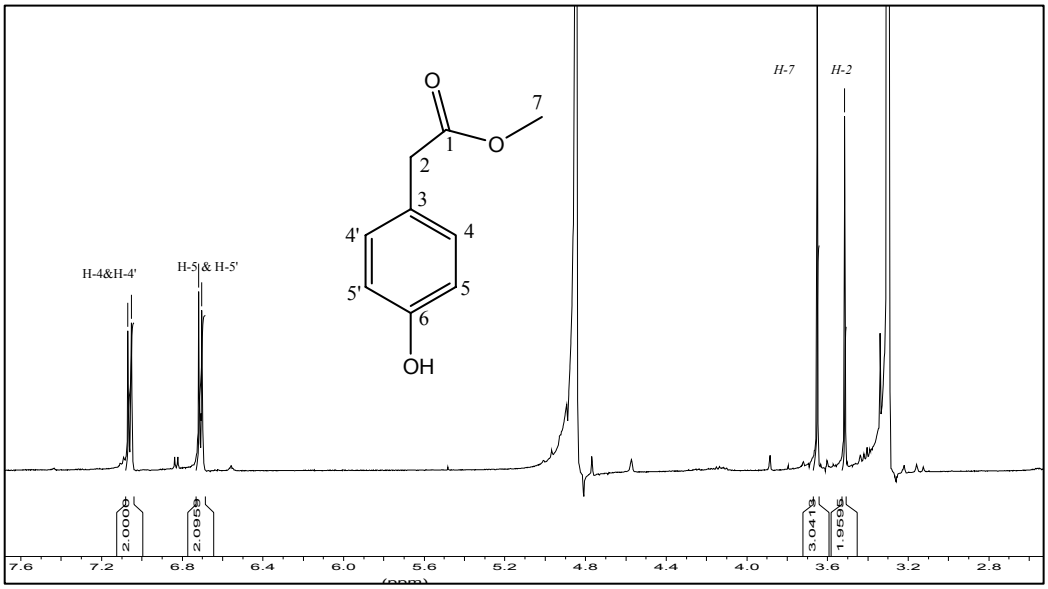

Fig (3.5.20):^{1}HNMR spectrum of compound 27

3.5.7 Ethyl 2-(4-hydroxyphenyl)acetate (28, known compound)

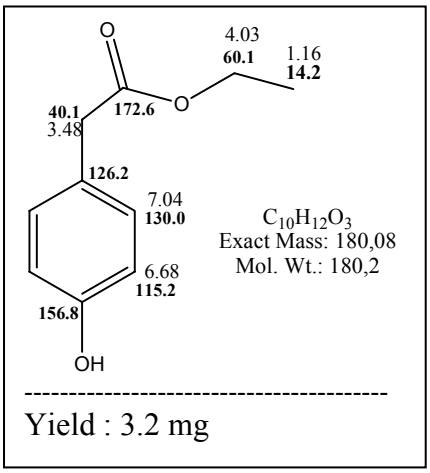

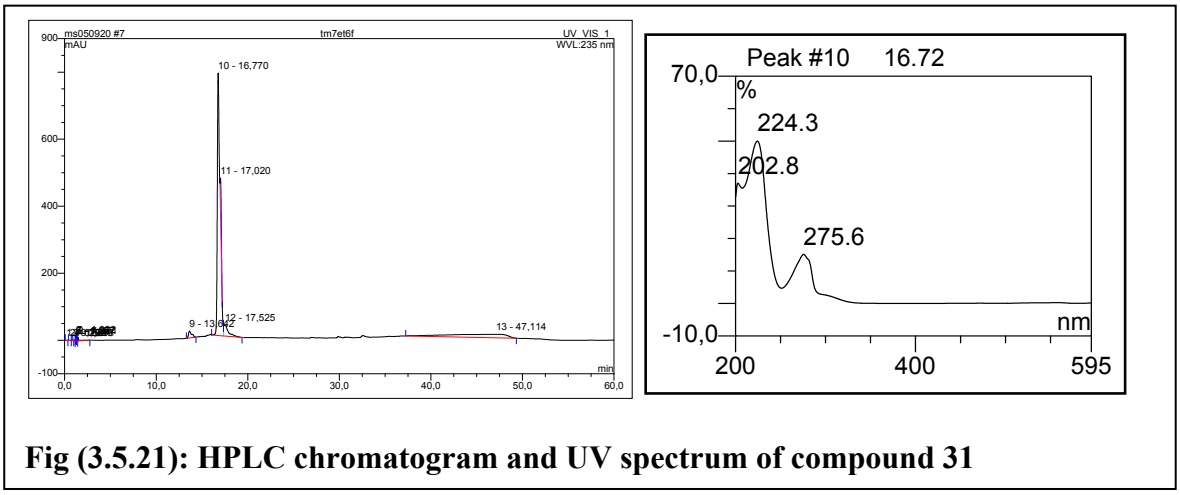

Fig (3.5.21): HPLC chromatogram and UV spectrum of compound 31

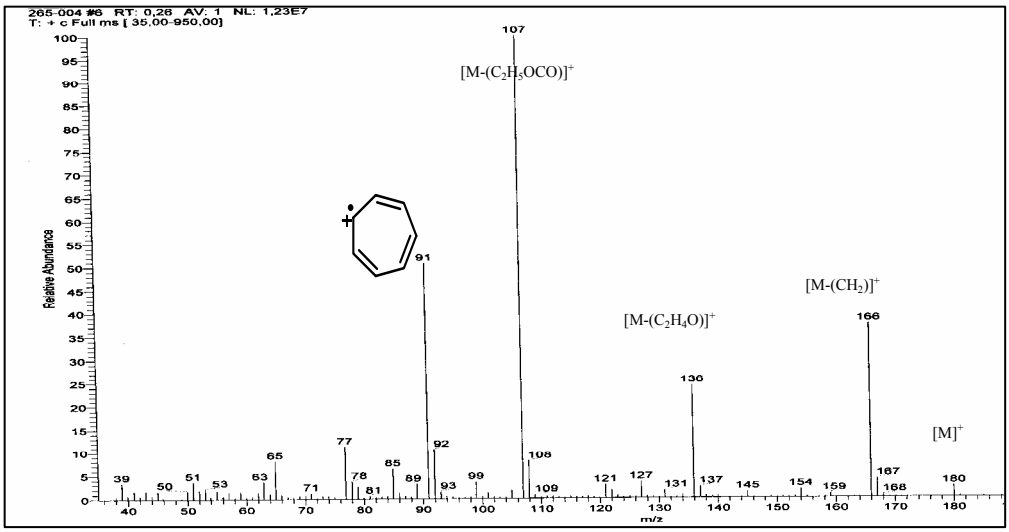

Fig (3.5.22):EI-MS spectrum of compound 28

Compound **28** [ethyl 2-(4-hydroxyphenyl)acetate] was isolated as white amorphous powder, UV absorption at λ_{max} 202, 224, 275 nm. EI-MS showed molecular ion peak m/z 180 $[M]^+$, and fragment ion peaks at 136 $[M\text{-}C_2H_4O]^+$, 107 $[M\text{-}COOC_2H_5]^+$, 91 $[M\text{-}(COOEt+O)]^+$, (see figure 3.5.33) suggesting the molecular formula $C_{10}H_{12}O_3$. Compound **28** is 14 mass units more than compound **27** which indicates the presence of one CH_2 group or exactly elongation of one carbon in the alkoxy group of **27** as evident from the NMR data. The ^1H NMR spectrum in DMSO-d_6 of **28** showed proton resonances of ethoxy group at δ 4.03 (2H, q, J=6.93 Hz, H-7) and 1.16 (3H, t, J=6.93 Hz, H-8) instead of a methoxy proton at 3.65 ppm as in compound **27.** The other proton resonances of **28** are the same as those of **27.** The methylene CH_2-7 at δ 4.03 of **28** showed an HMBC correlations to C-8 and C-1 at δ 14.2 and 172.0, respectively. The other HMBC correlations were identical with those of compound **26,** see figure (3.5.24). p-Hydroxyphenylacetic acid ethylester is a synthetic product (Bhawal et al 1991, Meltzer et al 1957). However, according to our knowledge, it is the first report of p-hydroxyphenylacetic acid ethylester as natural product.

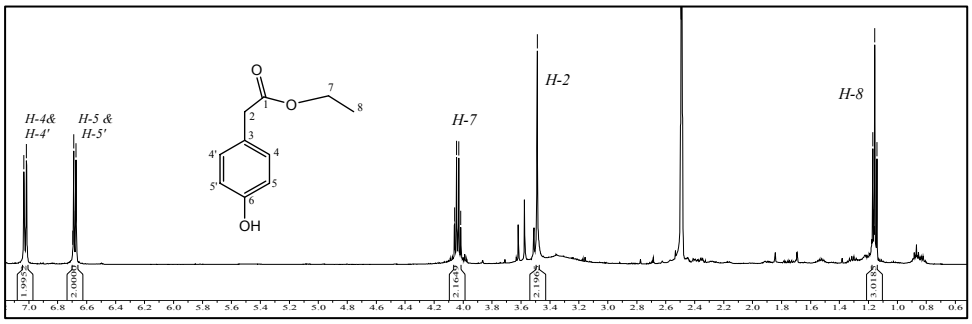

Fig (3.5.23):^{1}HNMR spectrum of compound 28

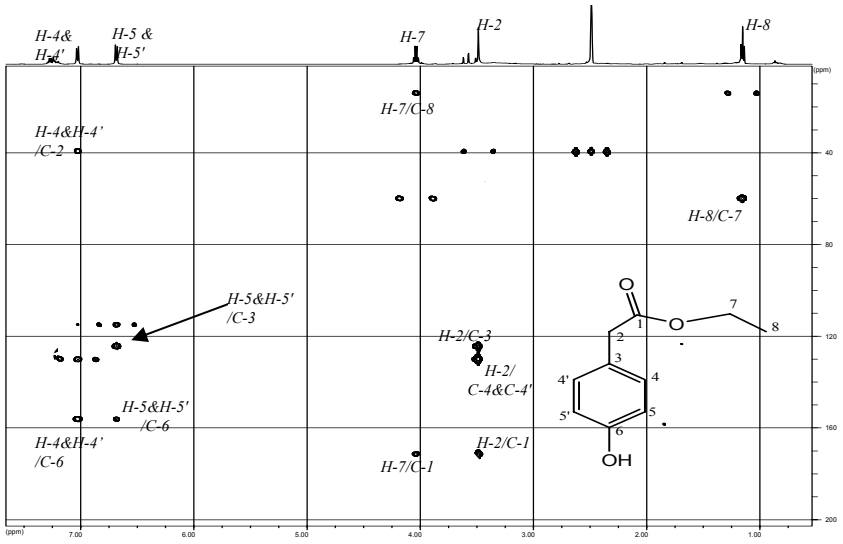

Fig (3.5.24): HMBC spectrum of compound 28

3.5.8 - Butyl 2-(4-hydroxyphenyl)acetate (29, new compound)

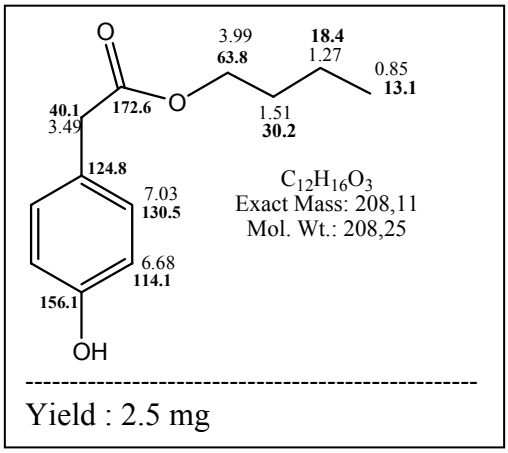

Yield : 2.5 mg

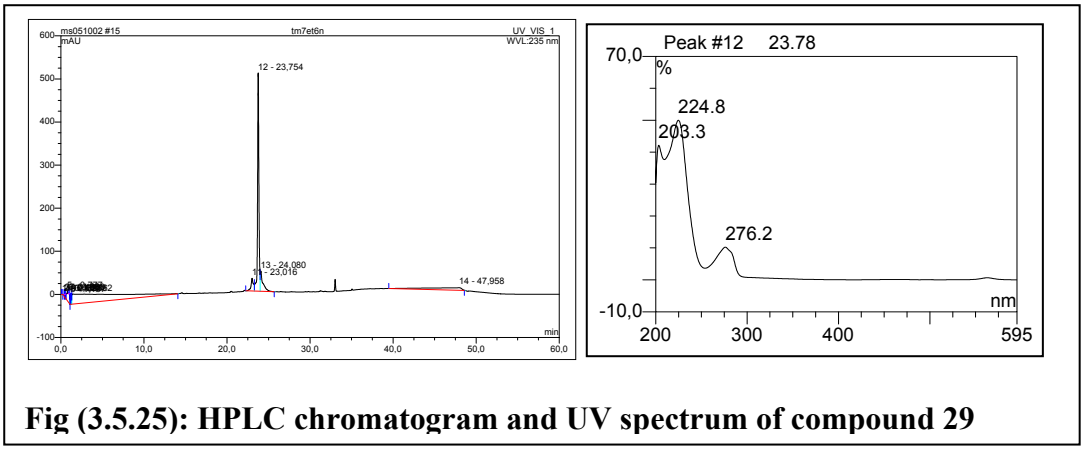

Fig (3.5.25): HPLC chromatogram and UV spectrum of compound 29

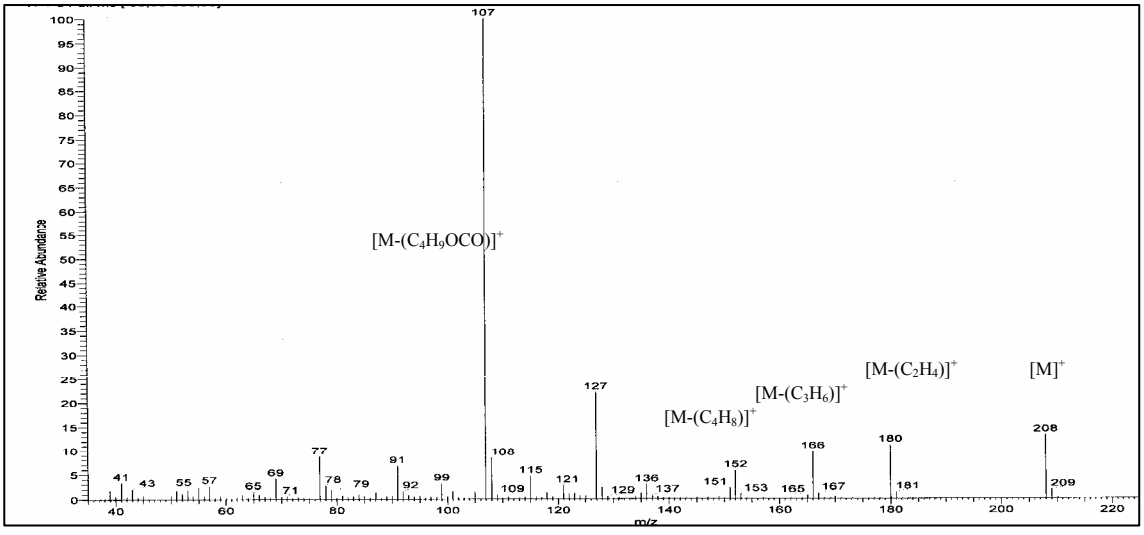

Fig (3.5.26):EI-MS spectrum of compound 29

Compound **29** [butyl 2-(4-hydroxyphenyl)acetate] was isolated as white amorphous powder, UV absorption at λ_{max} 203, 225, 276 nm. EI-MS showed molecular ion peak m/z 208 $[M]^+$, and fragment ion peaks at 180 $[M\text{-}C_2H_4]^+$, 166 $[M\text{-}C_3H_6]^+$, 152 $[M\text{-}C_4H_8]^+$, 136 $[M\text{-}C_4H_8O]^+$, 107 $[M\text{-}COOC_4H_9]^+$, and 91 $[M\text{-}(COOC_4H_9+O)]^+$, (see figure 3.5.37) suggesting the molecular formula $C_{12}H_{16}O_3$. The difference between compounds **28** and **29** is only 28 mass units which suggested the elongation of the alkoxy group with C_2H_4 unit as evident from the NMR spectra of **29**. ^{1}H NMR spectrum in DMSO-d_6 showed the presence of four sequentially correlated proton resonances (integrated as 2:2:2:3) at δ 3.99 (2H, triplet, J=6.63 Hz, H-7), 1.51 (2H, quintet, J=7.23 Hz, H-8), 1.27 (2H, sextet, J=7.56 Hz, H-9) and 0.85 (3H, t, J=6.93 Hz, H-8). This indicated the presence of a butoxy group instead of a methoxy group as in compound **27** and ethoxy group as in compound **28**. The other proton resonances of **29** are the same as those of **27** and **28**. The NMR data together with the ESI-MS fragments suggested compound **29** to be butyl-2-(4-hydroxyphenyl)acetate, which was further confirmed by HMBC correlations as shown in figure 3.5.28. To the best of our knowledge this is the first report of a butyl-2-(4-hydroxyphenyl) acetate as a natural product.

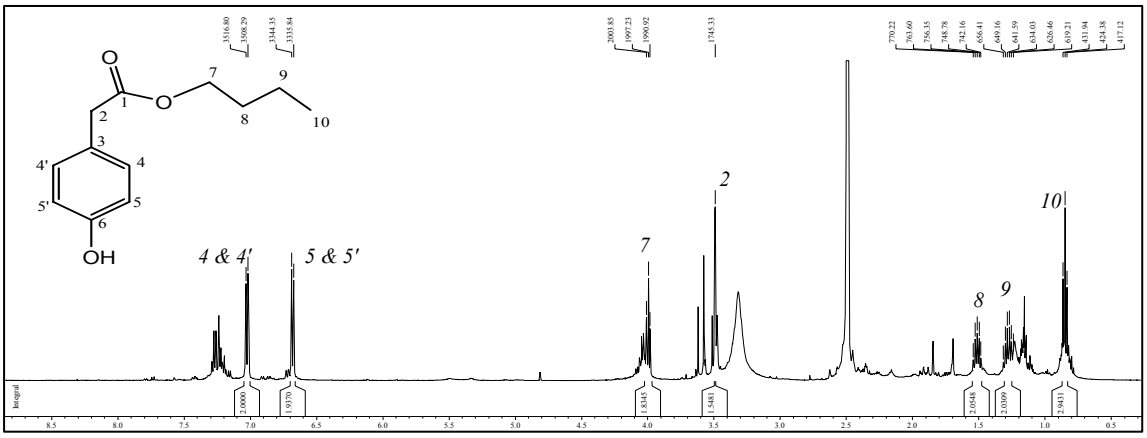

Fig (3.5.27):^{1}HNMR spectrum of compound 29

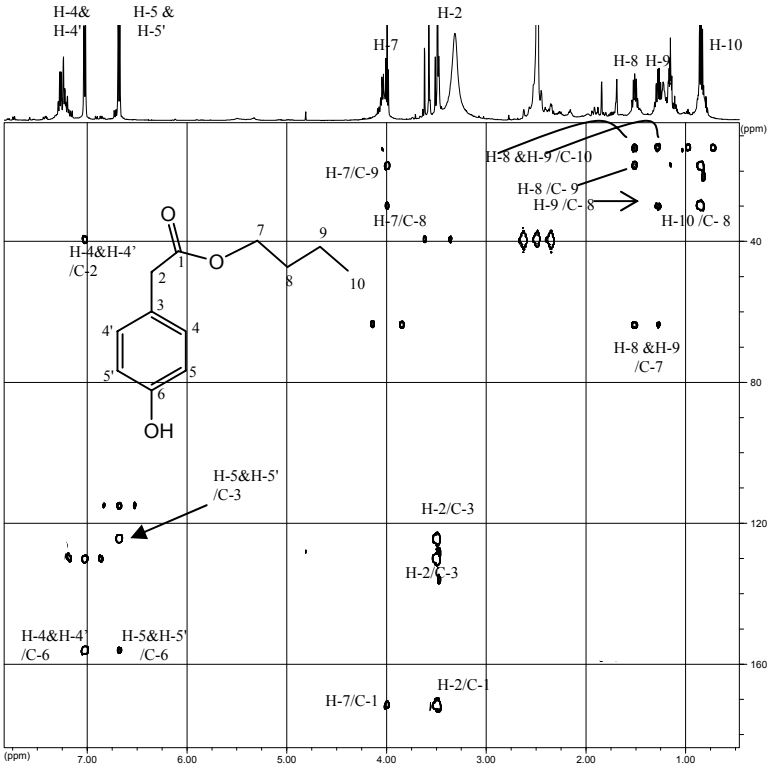

Fig (3.5.28):HMBC spectrum of compound 29

Table (3.5.2): NMR data of compounds 25, 26, 27, 28 and 29

	Compound 25		*Compound 26*		*Compound 27*	*Compound 28*		*Compound 29*	
No.	**^{13}C (ppm)**	**^{1}H (ppm) (Multiplicity, Hz)**	**^{13}C (ppm)**	**^{1}H (ppm) (Multiplicity, Hz)**	**^{1}H (ppm) (Multiplicity, Hz)**	**^{13}C (ppm)**	**^{1}H (ppm) (Multiplicity, Hz)**	**^{13}C (ppm)**	**^{1}H (ppm) (Multiplicity, Hz)**
1	177.6	-	173.4	-	-	172.0	-	172.6	-
2	41.0	3.65 (2H, s)	39.0	3.38 (s)	3.51 (s)	40.1	3.48 (s)	40.1	3.49 (s)
3	133.2	-	126.1	-	-	124.3	-	124.8	-
4, 4'	129.3	7.3 (5H, m)	132.2	7.03 (d,*J*=8.52)	7.06 (d, *J*=8.5)	130.0	7.04(d, *J*=8.5)	130.5	7.03 (d, *J*=8.51)
5, 5'	128.6		113.85	6.72 (d,*J*=8.2)	6.72 (d,*J*=8.5)	115.1	6.68 (d,*J*=8.5)	114.1	6.68 (d,*J*=8.51)
6	127.3		156.6	-	-	156.8	-	156.1	-
7					3.65 (s)	60.1	4.03 (q,*J*=6.93)	63.8	3.99 (t,*J*=6.93)
8						14.2	1.16 (t,*J*=6.93)	30.2	1.51 (t,*J*=6.93)
9								18.4	1.27 (t,*J*=6.93)
10								13.1	0.85 (t,**J**=6.93)

3.5.9 - Adenosine (30, known compound)

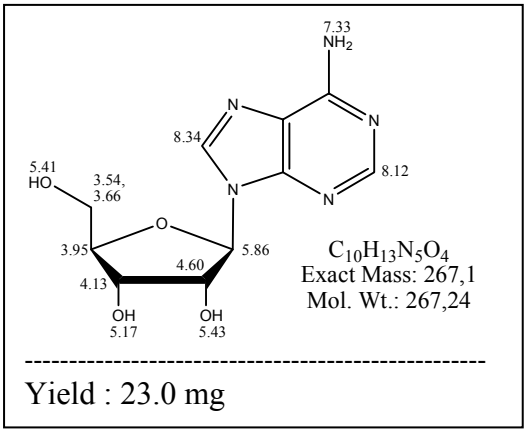

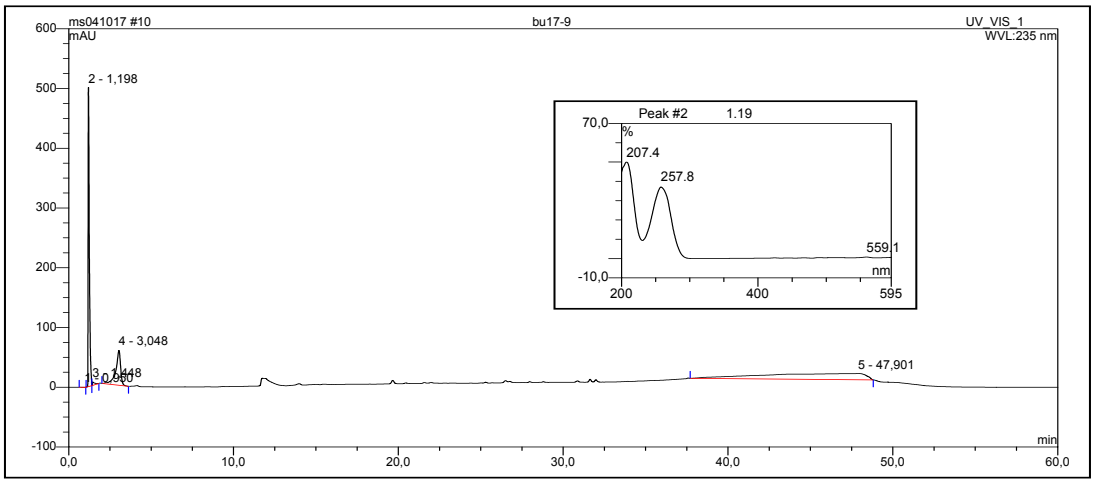

Fig (3.5.29): HPLC chromatogram and UV spectrum of compound 30

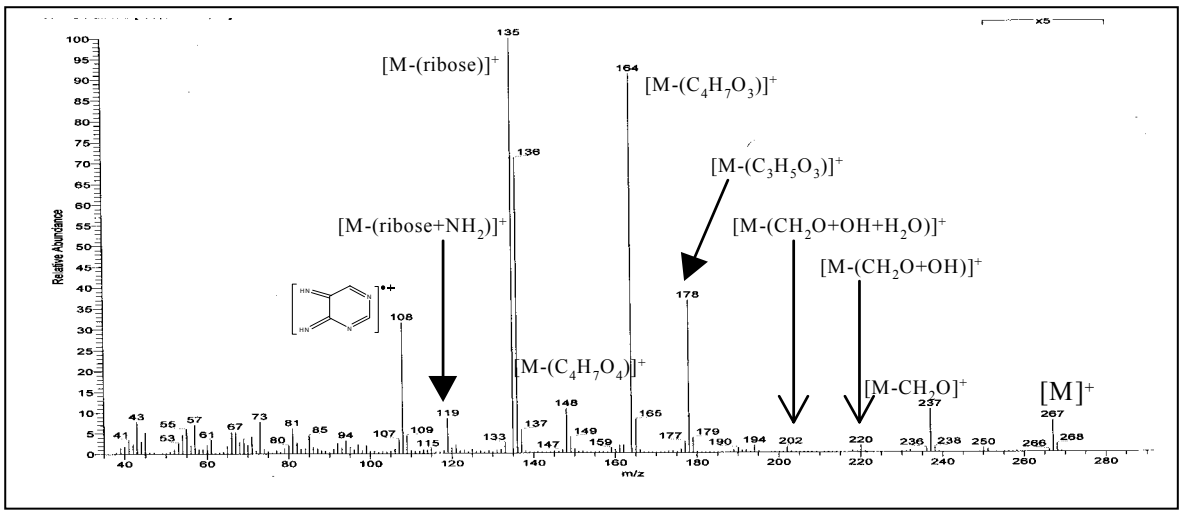

Fig (3.5. 30):EI-MS spectrum of compound 30

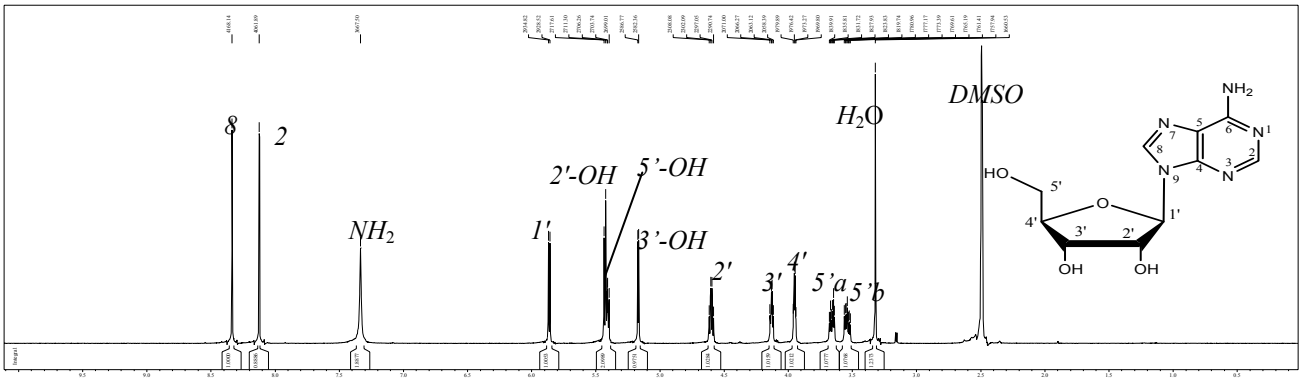

Fig (3.5. 31):[1]HNMR spectrum of compound 30

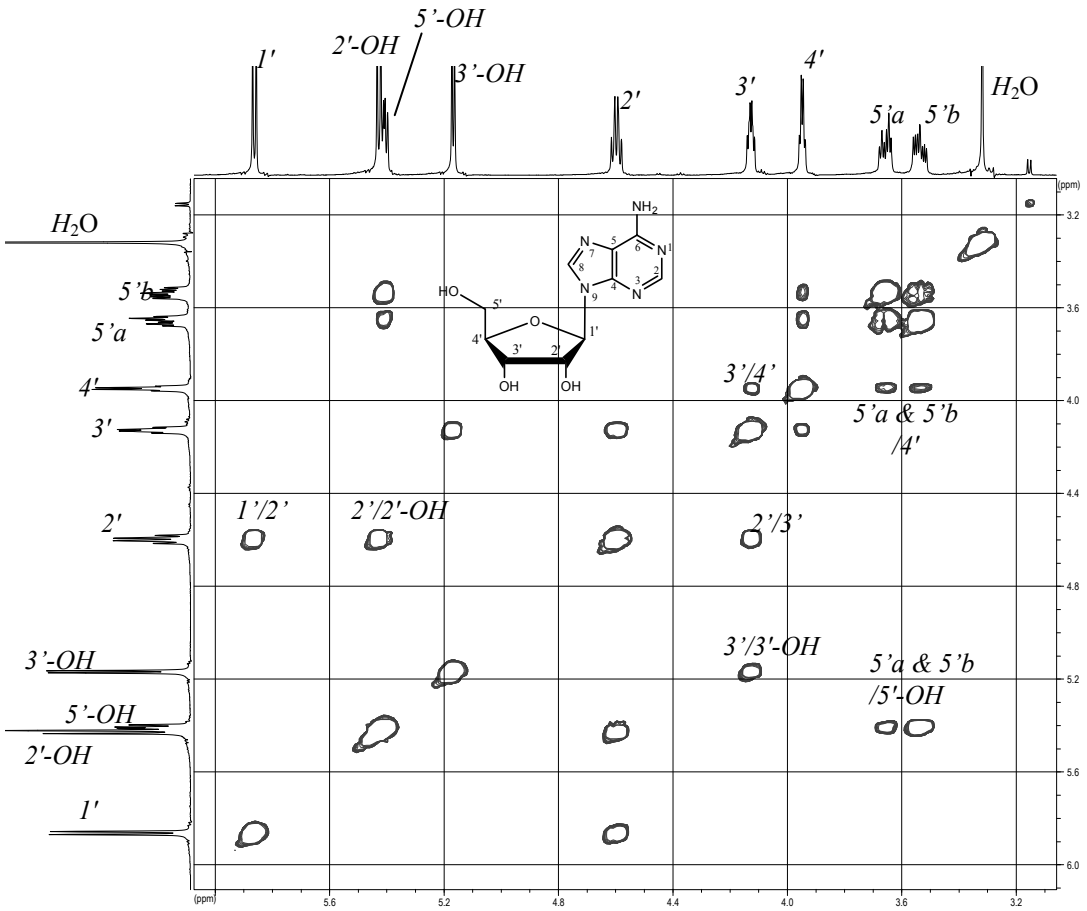

Fig (3.5.32):COSY spectrum of compound 30

Compound **30** was isolated as brownish-white amorphous powder, UV absorption at λ_{max} 207, 257 nm of a very polar peak in HPLC chromatogram suggested the nucleoside nature of the compound. EI-MS showed molecular ion peak at m/z 267 $[M]^+$, and fragment ion peaks at 237 $[M\text{-}CH_2O]^+$, 220 $[M\text{-}CH_2O\text{+}OH]^+$, 202 $[M\text{-}CH_2O\text{+}OH\text{+}H_2O]^+$, 178 $[M\text{-}C_3H_5O_3]^+$, 164 $[M\text{-}C_4H_7O_3]^+$, 148 $[M\text{-}C_4H_7O_4]^+$, 135 [M-(ribose)]$^+$, and 119 [M-(ribose+NH_2)]$^+$, (see figure 3.5.41) suggesting the molecular formula $C_{10}H_{13}N_5O_4$. ^{1}H NMR spectrum which was meassured in DMSO-d_6 showed resonances at δ 8.12 (s, H-2), 8.34 (s, H-8), 7.33 (s, 6-NH_2) suggesting the presence of 9H-purin-6-ylamine moiety. The existence of a ribosyl moiety in this compound was evident by a number of protons resonating between δ 3.54 and 5.86 (table 3.5.4). Furthermore, the presence of hydroxyl functional groups at the positions 2', 3', 5' were determined by resonances at δ 5.43(d, J=6.3) 2'-OH, 5.17 (d, J=4.41) 3'-OH, 5.41 (dd, J=7.25, 4.73) 5'-OH as shown in ^{1}H-NMR and confirmed by its COSY spectrum (figure3.5.31 & 3.5.32). The above NMR data together with the EI-MS fragments confirmed compound **30** to be adenosine.

Table 3.5.3 ^{1}H-NMR data of Compound 30:

No.	^{1}H (ppm) (Multiplicity, Hz)
2	8.12 (s)
8	8.34 (s)
6-NH_2	7.33 (s)
1'	5.86 (d, *J* =6.3)
2'	4.60 (dd, *J*=11.35, 6.3)
2'-OH	5.43(d, *J* =6.3)
3'	4.13 (dd, *J* =7.88, 4.73)
3'-OH	5.17 (d, *J* =4.41)
4'	3.95 (dd, *J* =6.62, 3.47)
5'a	3.54 (ddd, *J* =3.47, 7.25, 11.67)
5'b	3.66 (ddd, *J* =4.09, 8.19, 11.98)
5'-OH	5.41 (dd, *J* =7.25, 4.73)

3.5.10 Nicotinamide (31, known compound)

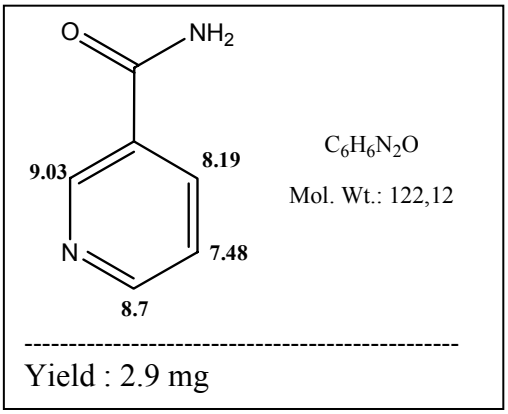

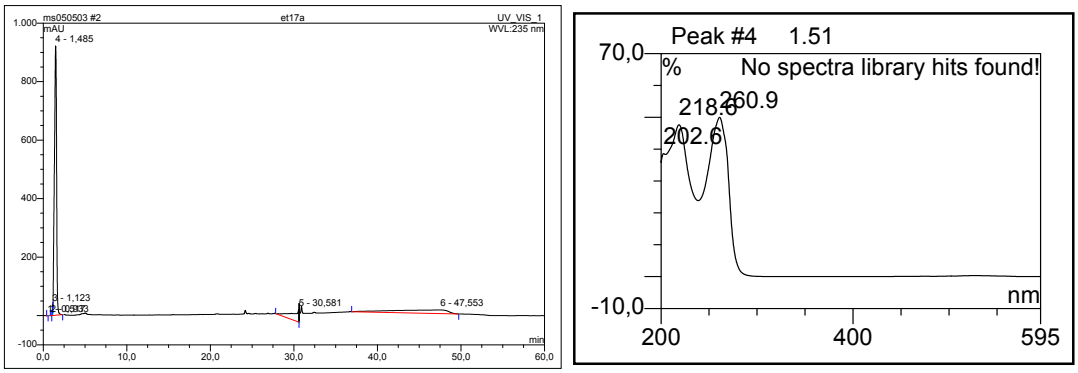

Fig (3.5.33): HPLC chromatogram and UV spectrum of compound 31

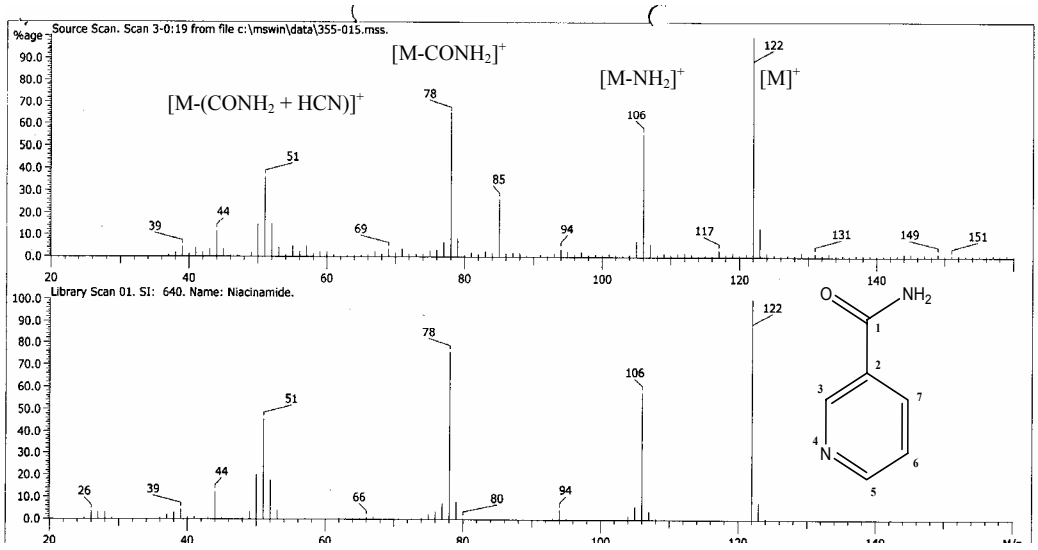

Fig (3.5.34):EI-MS spectrum of compound 31 (up) compared to authentic sample of nicotinamide (down)

Compound **31** was isolated as white amorphous powder. It has UV absorption at λ_{max} 202, 218, 260 nm. EI-MS showed molecular ion peak at m/z 122 $[M]^+$, and showed the same fragmention pattern of authentic sample of nicotinamide where it displays a fragment ion peaks at m/z 106 $[M\text{-}NH_2]^+$, 78 $[M\text{-}CONH_2]^+$, and 51 $[M\text{- }CONH_2\text{+}HCN]^+$, (see figure 3.5.34) suggesting the molecular formula $C_6H_6N_2O$. ^1H NMR spectrum (meassured in DMSO-d_6) showed resonances at δ 9.03 (br s, H-3), 8.7 (br s, H-5), 7.48 (dd, J=7.88, 4.73), 8.19 (d, J=7.88 H-4). The ^1H NMR spectrum of compound **31** is identical with those of nicotinamide (Aldrich 1993, pp 3/338).

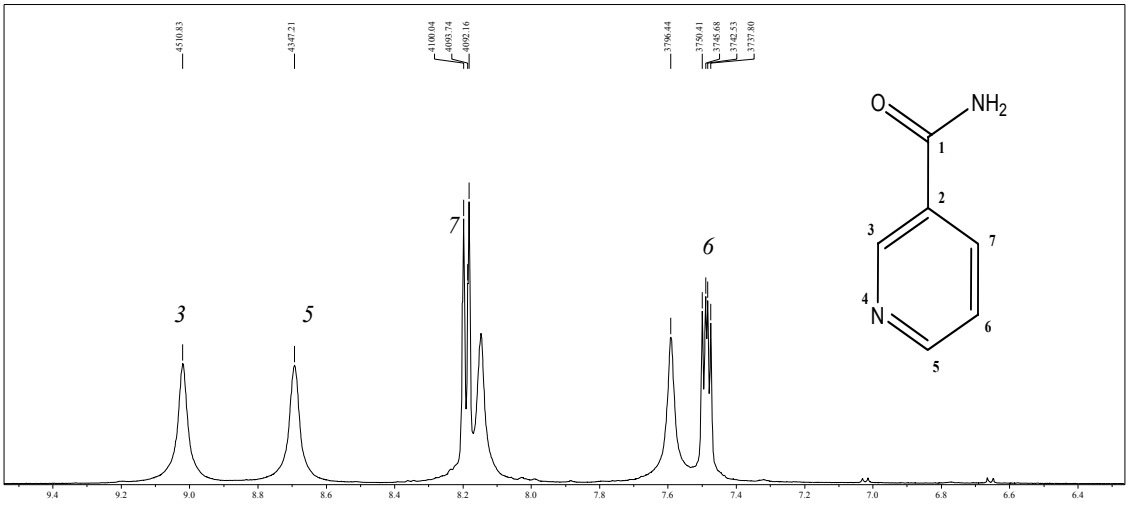

Fig (3.5.35):^{1}HNMR spectrum of compound 31

3.5.11 and 12 Petrocerebrosides 1 and 2 (32 & 33, new compounds)

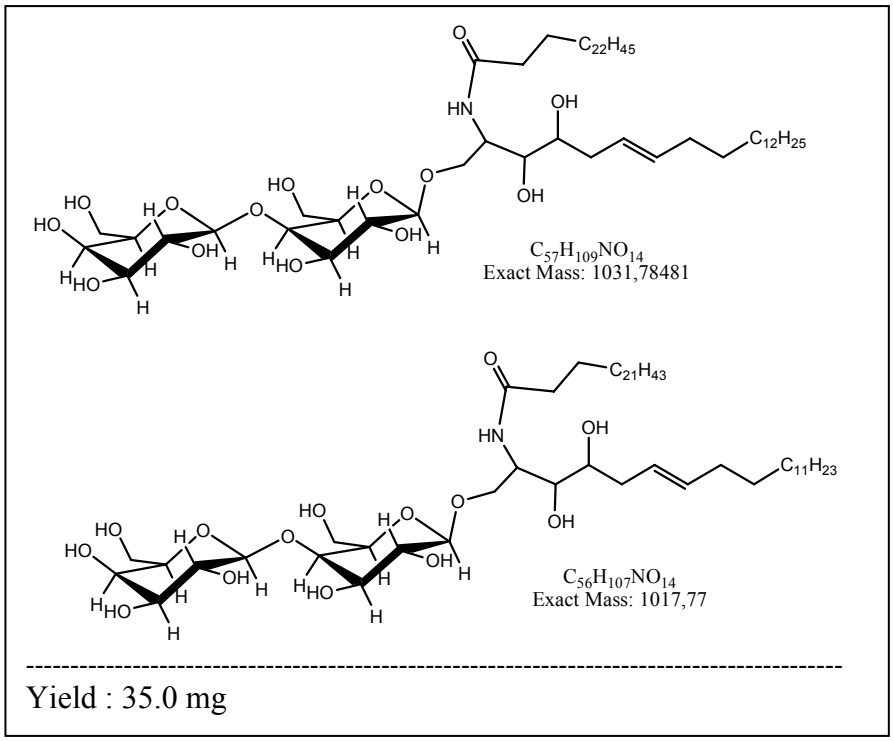

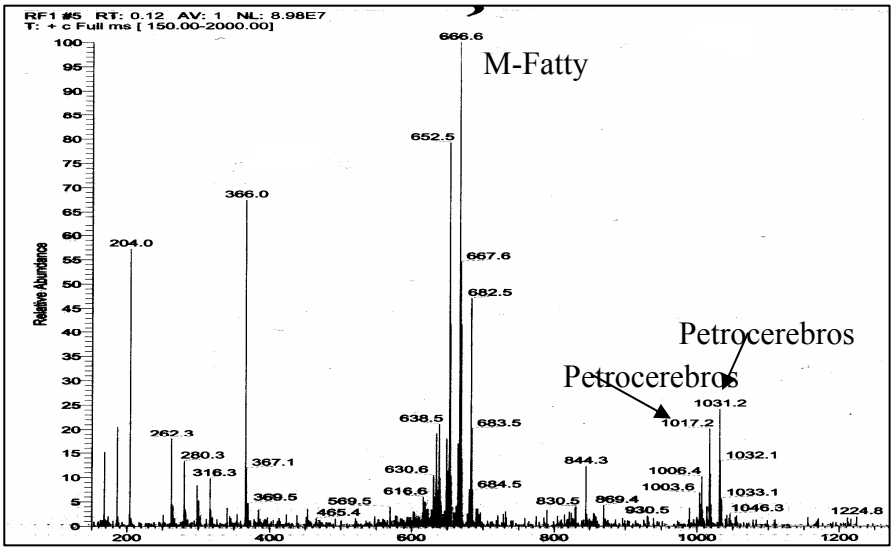

Fig (3.5.36):EI-MS spectrum of compounds 32 and 33

Cerebrosides are glycolipids composed of a long chain aminoalcohol, known as a sphingoid base (sphingosines), a fatty acid residue linked to its amino group (the resulting amide is called ceramide), and a carbohydrate chain attached to the primary hydroxyl group of the ceramide. The scientific interest in cerebrosides has recently increased on account of the role they play as therapeutical immunomodulating agents (Costantino et al 2004, 2003, 1994). Sphingolipids have come to be used as functional foodstuffs and sphingomyelin isolated from

bovine milk has been found to have significant effects in colon cancer prevention. Sphingoid bases isolated from plants and fungi have been shown to induce apoptosis in the caco-2 cell-line. The ingestive cerebrocides from maize and Saccharomyces kluyveri prevent aberrant crypt foci in mice adminstrated with N,N-dimethylhydrazine (Tanji 2004).

Compound **32** and **33** were obtained as mixture [in a ratio of 5:4, respectively as evident from the fatty acid ratios (see figure 3.5.4)] and as an amorphous powder. The molecular formulas were deduced as $C_{57}H_{109}NO_{14}$ and $C_{56}H_{107}NO_{14}$ based on a molecular ion peak $[M+H]^+$ 1032.1 and $[M]^+$ 1031.2 for petrocerebroside 1 and $[M+H]^+$ 1018.1 and $[M]^+$ 1017.2 for petrocerebroside 2 as obtained from the ESI-MS of the sample. The difference between both cerebroside derivatives is only 14 mass unit which suggested an additional methylene group in petrocerebroside 1 when compared to petrocerebroside 2. The position of this CH_2 group was deduced to be in the long chain fatty acid part of the compound as shown below. The structure elucidation of petrocerebrosides 1 and 2 were obtained using extensive ^1H NMR, ^{13}C NMR, DEPT, and 2D NMR experiments, as well as by acid hydrolysis. GC analysis determined the absolute configuration of the sugar moieties. GC-MS was done to analyze the molecular weights both the free fatty acid and sphingosine base after acid hydrolysis.

The cerebroside nature of the petrocerebrosides 1 and 2 were established from the ^1H NMR which showed a triplet-like signal at δ 0.82 for the terminal methyl units and broad singlet at δ 1.20 for long chain $(CH_2)_n$ group for both fatty acids and long chain bases. The presence of several doublets in the region between 3.35-5.30 ppm indicated the occurrence of the sugar moieties. Two coupling sp^2 methines at δ 5.41 and 5.34 showed the presence of only one double bond. Two doublets at 7.42 and 7.70 ppm exhibited the presence of two amide NHs belonging to two different compounds. ^{13}C NMR showed two resonances at δ 172.3 and 170.15 indicating two amide carbonyls for petrocerebroside 1 and 2, respectively. Two resonances at δ 131.5 and 128.1 were assigned for two sp^2 methine carbons, while two sp^3 methines resonating at 101.2 and 98.9 indicated the presence of anomeric carbons for two monosaccharides.

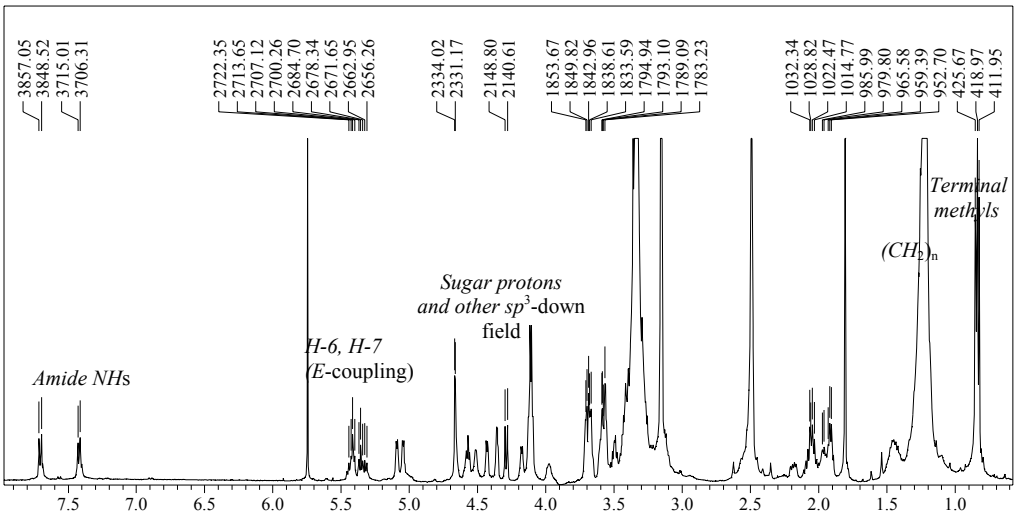

Fig (3.5.37):[1]HNMR spectrum of compound 32 and 33

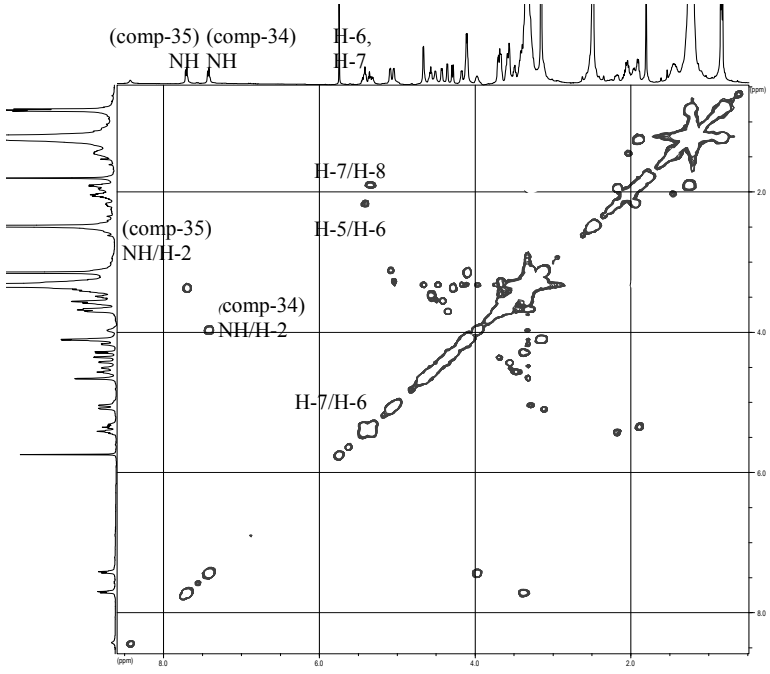

Fig (3.5.38):COSY spectrum of compound 32 and 33

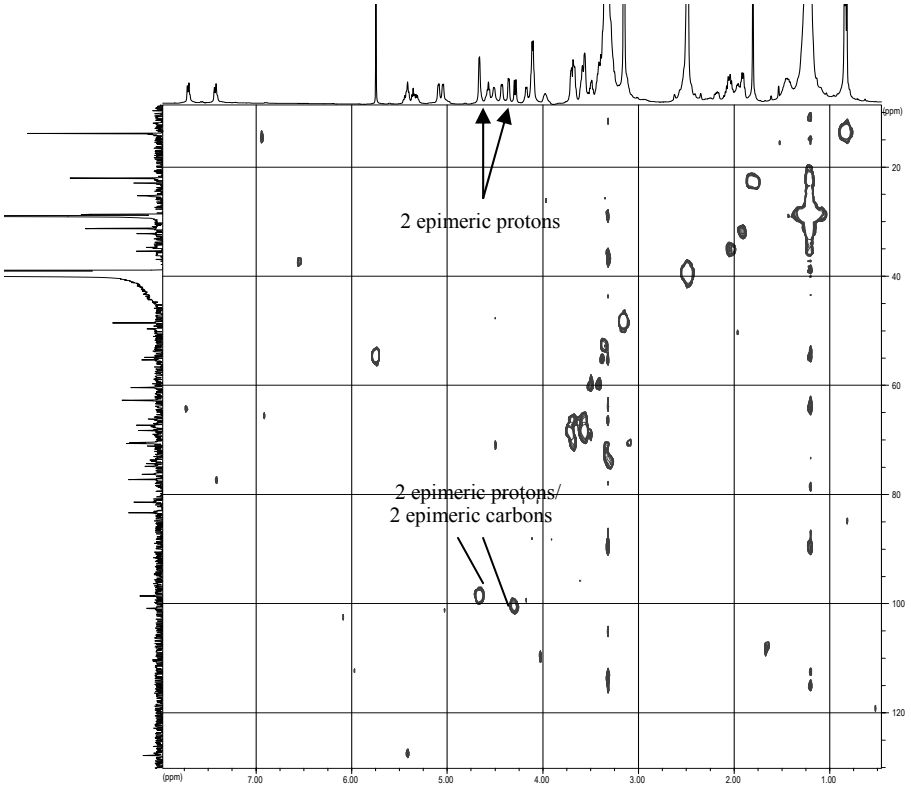

Fig (3.5.39):HMQC spectrum of compound 32 and 33

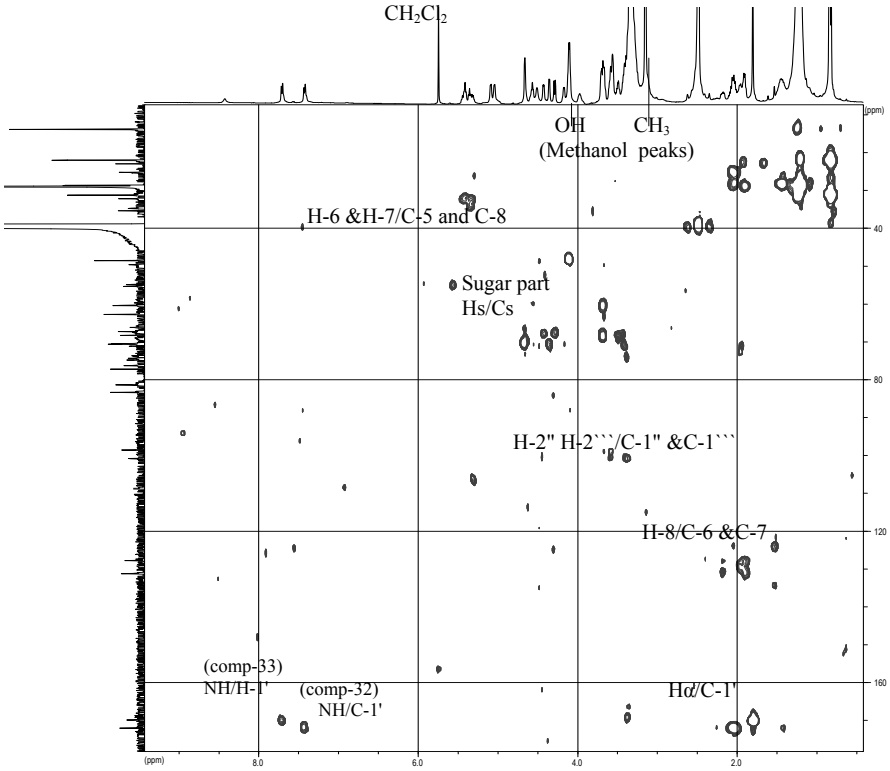

Fig (3.5.40):HMBC spectrum of compound 32 and 33

The sample was hydrolysed using 6N HCl and heated over a hot plate under reflux for 7 hours, then cooled with cold water stream. The hydrolysate were extracted with n-hexane to obtain the fatty acid part which was then examined by GC-MS (figures 3.5.41, 42a &42b) where mixture of two long chain fatty acids (pentacosanoic acid $C_{25}H_{50}O_2$, m/z 382 and tetracosanoic acid $C_{24}H_{48}O_2$, m/z 368) were detected. The aqueous part were purified over a Sephadex column chromatography and the Molish-positive fraction were separated and utilised for determination of the absolute streochemistry of the monosaccharide units. The absolute streochemistry of the monosuccharide units were established through butanolysis, silylation, then GC analysis in comparison with authentic monosaccharides. This experiment revealed that both sugar units are D-galactoses.

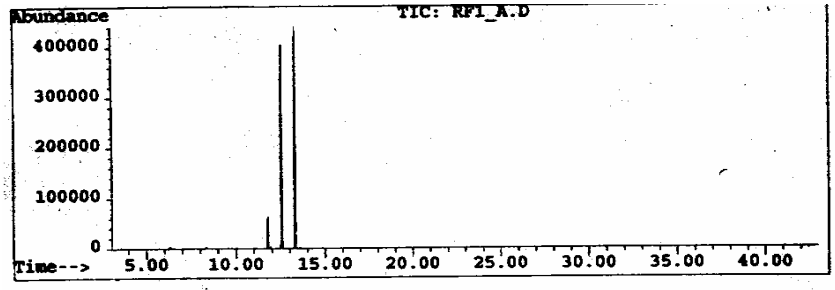

Retention Time	Area	Area %	Ratio %
Total Ion Chromatogram			
11.784	1341259	7.291	13.551
12.568	7156718	38.904	72.304
13.329	9898027	53.805	100.000

Fig (3.5.41):GC-chromatogram of the fatty acid-containig fraction of compound 32 and 33 hydrolysate

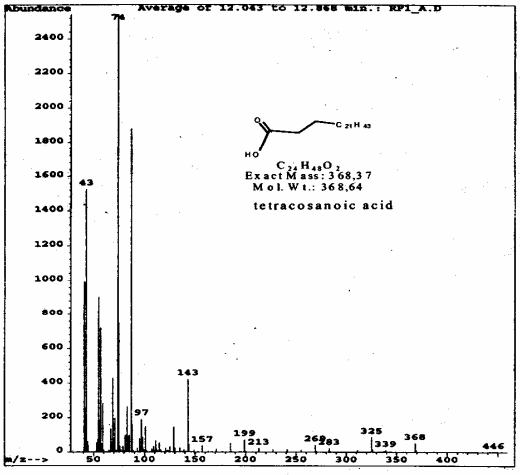

Fig (3.5.42a):GC-MS of tetracosanoic acid

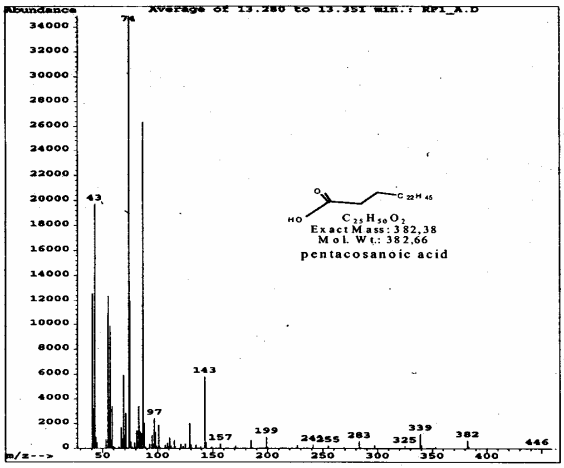

Fig (3.5.42b):GC-MS of pentacosanoic acid

Deduced NMR data of both fatty acid and sphingosine moieties were confirmed after methanolysis. ^{1}H NMR of the fatty acid mixture showed a singlet resonating at δ 3.66 indicating a methoxy group of the derivatised fatty acid. A triplet at δ 0.88 indicated the terminal methyl, a triplet at 2.3 ppm was assigned for the α-CH_2, and the multiplet at 1.61 ppm represented the β-CH_2. This data were confirmed by ^{13}C NMR spectrum where characteristic signals of the long chain fatty acid methyl esters were obtained as shown below (figures 3.5.43 and 44).

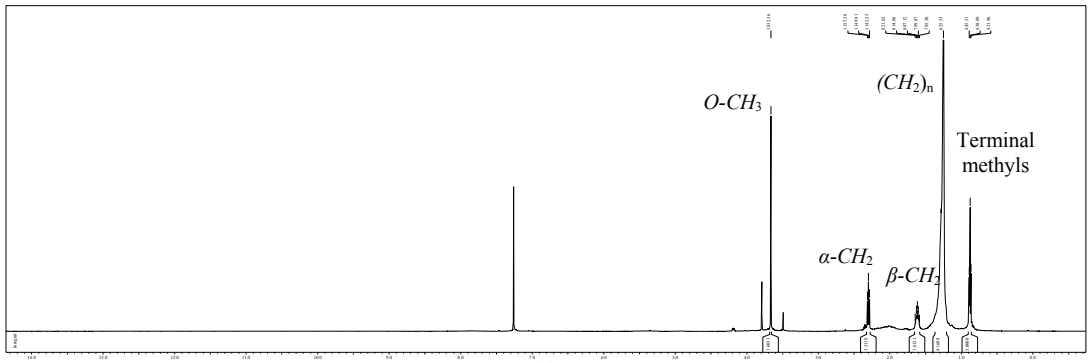

Fig (3.5.43):^{1}HNMR spectrum of fatty acid mixture of compound 32 and 33 hydrolysates.

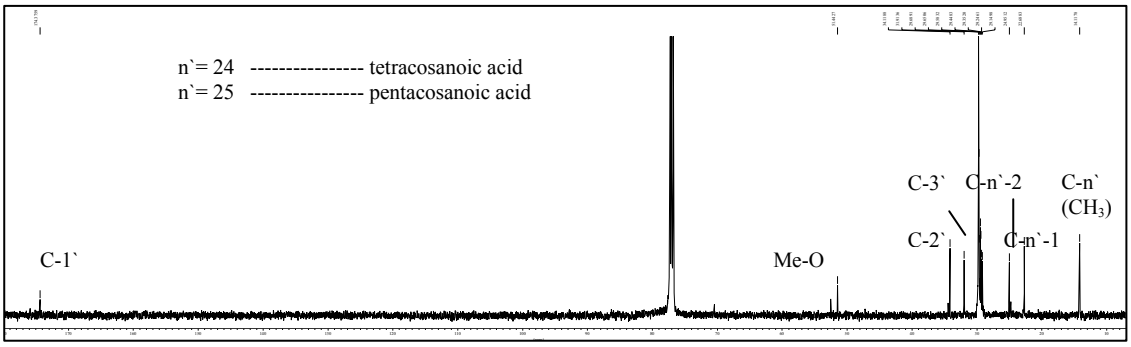

Fig (3.5.44):^{1}HNMR spectrum of fatty acid mixture of compound 32 and 33 hydrolysates.

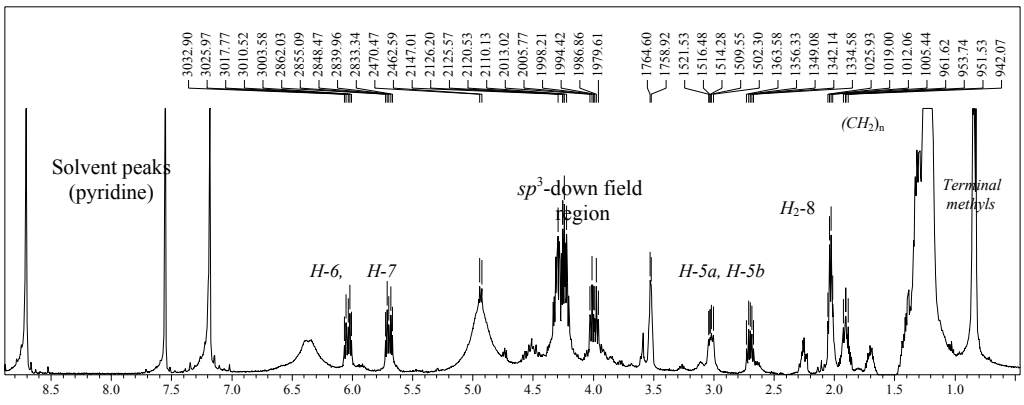

Fig (3.5.45):^{1}HNMR spectrum of sphingosine part of compound 32 and 33

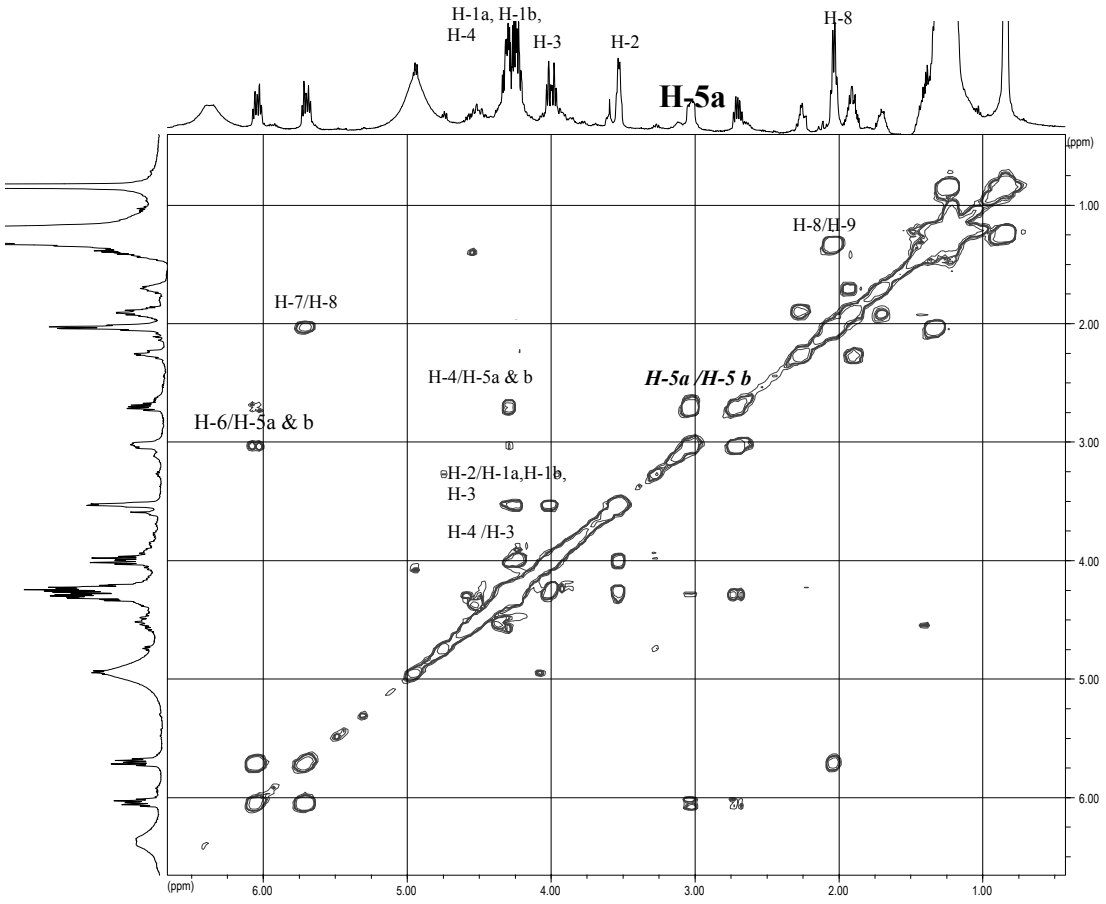

Fig (3.5.46):COSY spectrum of sphingosine part of compound 32 and 33

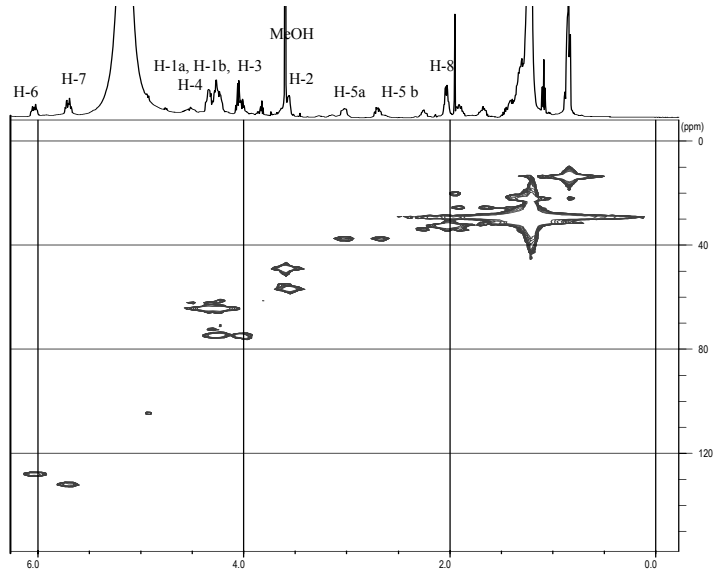

Fig (3.5.47):HMQC spectrum of sphingosine part of compound 32 and 33

Table 3.5.4 NMR data of compound 32 and 33, in addition to free fatty acids and sphingosine

	Compounds 35 &36 (DMSO-d_6)		**Fatty acid ($CDCl_3$)**		**Sphingosine (Pyridine-d_5)**	
No.	**^{13}C (ppm)**	**^{1}H (ppm) (Multiplicity, Hz)**	**^{13}C (ppm)**	**^{1}H (ppm) (Multiplicity, Hz)**	**^{13}C (ppm)**	**^{1}H (ppm) (Multiplicity, Hz)**
1	63.5	4.20 and 4.35 (m & m)			65.0	4.25 & 4.35 (m & m)
****2**	55.2 54.5	3.90 (m) 3.4 (m)			58.0	3.6 (m)
****NHs**	- -	(d, 9.3 Hz) 7.72 (d, 8.2 Hz)				
3	75.0	3.55 (m)			75.0	4.04 (m)
4	74.1	3.43 (m)			74.2	4.25 (m)
5	33.0	2.40 & 1.9 (m &m)			38.2	3.05 (m) & 2.72 (ddd, 14.8, 8.0, 6.8)
6	128.1	5.45 (ddd, 6.4, 8.2, 15.1 Hz)			128.1	6.05(ddd, 15.13, 6.95, 8.19)
7	131.5	5.71 (ddd, 6.6, 8.5, 15.1 Hz)			132.5	5.71 (ddd, 15.13, 6.5, 6.6)
8	34.3	1.9 (m)			34.3	1.99 (m)
9-19	33.0-29.0	1.2 (br s)			33.0-29.0	1.26 (br s)
20	14.29	0.85 (t, 6.9 Hz)			14.2	0.82 (t, 6.9)
****1´**	172.2 170.0	-	174.4			
2´	35.8	2.3 (m)	34.1	2.3 (t, 7.6)		
3´	31.7	1.6 (m)	31.9	1.6 (m)		
***4´-(n-1)´**	30.0 – 22.5	1.2 (br s)	30.0 – 22.7	1.3 (br s)		
n´	14.29	0.85 (t, 6.9 Hz)	14.1	0.88 (t, 7.0)		
1´´	102.0	4.3 (d, 8.5 Hz)				
2´´	71.0	3.5 (m)				
3´´	69.5	3.63 (m)				
4´´	83.2	3.7 (m)				
5´´	68.4	3.4(m)				
6´´	63.5	3.32 &3.25 (m &m)				
1´´´	99.0	4.7 (d, 4.2 Hz)				
2´´´	70.5	3.2(m)				
3´´´	69.2	3.60 (m)				
4´´´	80.7	3.28 (m)				
5´´´	68.2	3.4(m)				
6´´´	62.2	3.30 &3.4 (m &m)				

* n =25 for petrocerebroside 1
n =24 for petrocerebroside 2

** these pairs of NMR values were assigned for both compounds and can be interchanged, These differences attributed mainly to the differences in stereochemistry of the three chiral centers in each cerebroside at C-2, C-3 and C-4.

New purine derivatives isolated from Petrosia nigricans:

Marine organisms particularly sponges have proven to be an exceptionally rich source of modified nucleosides. The isolation of spongouridine and spongothymidine from *Cryptotethia crypta* (Bregman and Feeney 1950) served as models for the development of adenine arabinoside (ARA-A) for treatment of *Herpes simplex* infection and cytosine arabinoside (ARA-C) for the treatment of leukemia (Lindsay *et al* 1999). Subsequent development of antiviral analogues demonstrated the potential medicinal importance of these compounds such as antifungal phidolopine which was isolated from the bryozoan *Phidolopora pacifica* (Ayer *et al* 1984), the hypotensive doridosine which was obtained from the sponge *Tedania digitata* (Cook *et al* 1980) , and the cytotoxic mycalisines which was found from the sponge *Mycale sp.* (Kato *et al* 1985). Many other purines and nucleosides isolated from marine organisms particularly sponges, display potant bioactivities, such as the marine derived 1,3-dimethylisoguanine from *Amphimedon viridis* which showed activity against an ovarian cancer cell line (IC_{50}, 2.1 µg/mL) (Mitchell *et al* 1997) and 3,7-dimethylisoguanine from a Caribbean sponge *Agelas lonigssima*, which displayed mild antibacterial activities (Cafieri *et al* 1995). Investigation of ethylacetate fraction of the Indonesian sponge *Petrosia nigricans*, led to the isolation of four new purine derivatives nigricines **1** to **4**. Their structures were elucidated by extensive spectroscopic analysis, 2D-NMR experiments, EI/MS, ESI/MS, and HRMS.

3.5.13. Nigricine 1 (34 , new compounds)

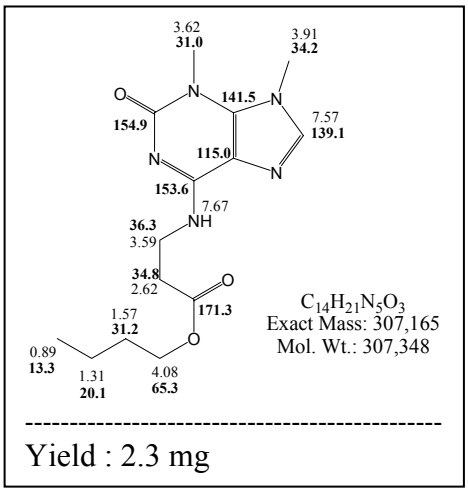

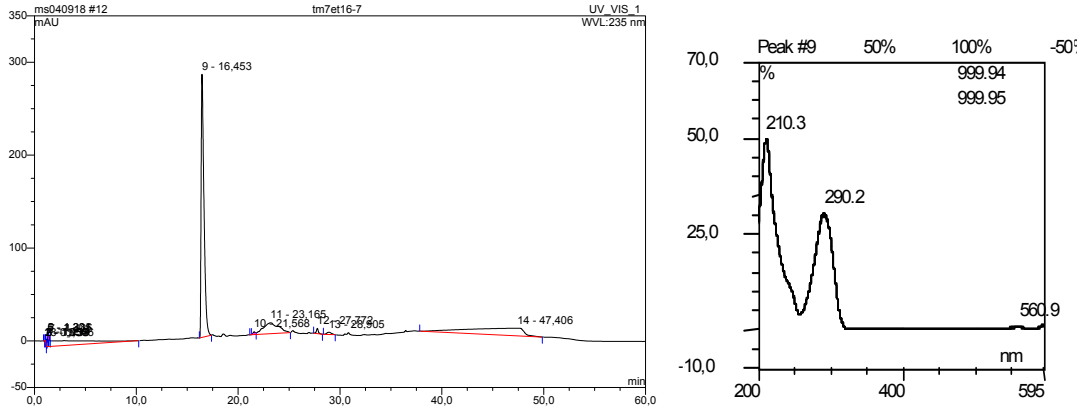

Fig (3.5.48): HPLC chromatogram and UV spectrum of compound 34

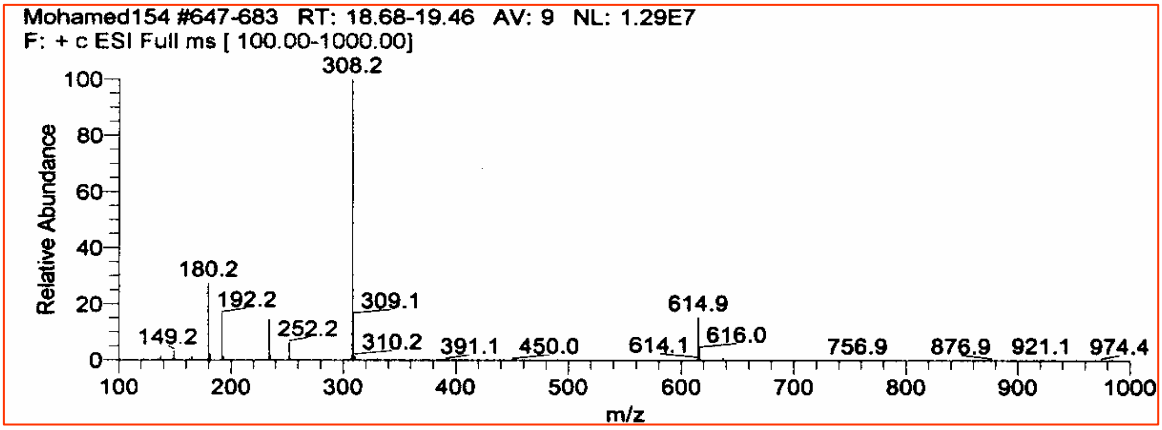

Fig (3.5.49):ESI-MS spectrum of compound 34

Compound **34**, is the key structure for this group of purine derivatives. The HRESIMS$^+$ was in agreement with the molecular formula of $C_{14}H_{21}N_5O_3$ (measured, *m/z* 308.170, [M+H]) with 7 degrees of unsaturation. The UV spectrum of **34** showed absorption λ_{max} (MeOH) at 210 and 290 nm. Simple ^{1}H NMR spectrum (figure 3.5.51) showed an exchangeable triplet signal at δ 7.73 ppm for an N*H*, in addition to signals at δ 7.61 (1H, s , H-8), 4.17 (2H, t , C*H*$_2$), 1.67 (2H, m , C*H*$_2$), 1.4 (2H, m , C*H*$_2$), 0.95 (3H, t , C*H*$_3$), 3.80 (3H, t , N-3 C*H*$_3$), 4.05 (3H, t , C*H*$_3$). The basic structure of the purine skeleton was evident through interpretation of ^{1}H NMR and ^{13}C NMR as well as comparison with those of the literatures of Lindsay *et al* 1999, Mitchell et al 1997, Lindsay et al 1999, Capon et al 2000, Yagi et al 1994.

The NMR measurement of compound **34** in deuterated methanol indicated the presence of only one exchangeable triplet signal at 7.73 ppm for 6-N*H* suggesting a 6-derivatized adenine structure, the methyl signals at δ 31.4 and 34.8 showed a characteristic ^{13}C chemical shifts for NC*H*$_3$ resonances and excluding those of OC*H*$_3$, often found between 50-60 ppm, the confirmation of the positions of both methyl groups were obtained from HMBC correlation of both methyl groups to a quaternary carbon at δ 143.1 (C-4), one of them, N(3)-C*H*$_3$, showed further HMBC correlation to carbonyl at 159.0 ppm (C-2), while the other, N(9)-C*H*$_3$, showed an additional HMBC correlation to the methine carbon at δ 140.6 (C-8). Furthermore, ROESY experiment showed a correlation through space between both methyl signals, thus, the existence of N(7)-C*H*$_3$ was excluded. The methine proton signal, H-8, showed HMBC correlations to both quaternary carbon at 143.1 (C-4) , and 115.0 (C-5). The remaining carbon in the purine skeleton, C-6, was established through HMBC correlation of the N*H* proton signal at δ 7.73 to a quaternary carbon signal at 157.7 ppm (C-6). The position of β-propionyl side chain was confirmed by sequential COSY correlation between the proton signals at δ 7.73, 3.80, and 2.72 of 6-N*H*, β-C*H*$_2$, and α-C*H*$_2$ of propionyl group, and compared with chemical shifts of the same substructure of the previously described marine derived purine compound, erinacean **(5)**, which was obtained from the antarctic sponge *Isodictya erinacea* (Moon et al 1997). In addition, HMBC experiment showed a correlation of both α- and β- C*H*$_2$ groups to the carboxyl at 173.0 ppm. The attachment of this group to the purine skeleton was evident through HMBC correlation betwwen β-C*H*$_2$ proton signal and the quaternary carbon at 157.7 ppm (C-6). The last substructure (alkoxy group) was confirmed through a sequential COSY correlations between 4 aliphatic proton signals at δ 4.17 (2H, t. C*H*$_2$), 1.67 (2H, m. C*H*$_2$), 1.4 (2H, m. C*H*$_2$) and 0.95 (3H, t. C*H*$_3$), the

connection of this substructure to the purine skeleton was established through HMBC correlation between α-CH_2 at δ 4.17 and the carboxyl at 173.0 ppm.

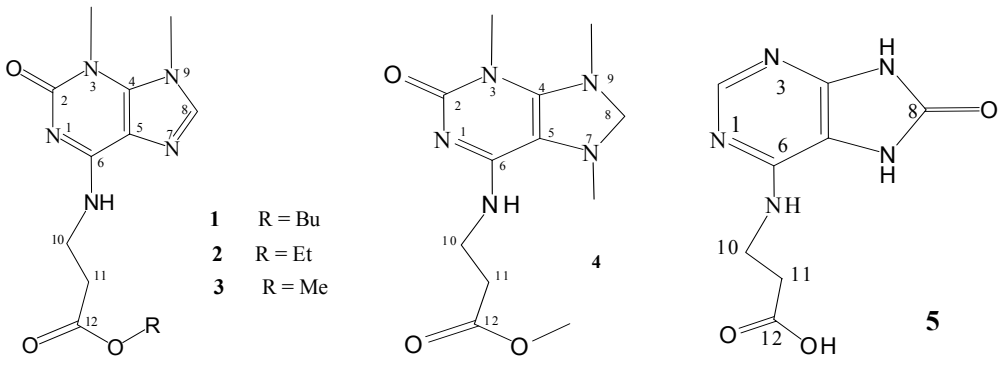

New compounds, nigricines 1 to 4, as well as the known analogue erinacean (5)

LC/MS of compound **34** showed a positve pseudomolecular ion peak at *m/z* 308(M+1), and at *m/z* 615 (19 % , 2M+1) and a characteristic fragment ion at *m/z* 234 [M-alkoxy group] and 192 [M-(alkoxy group+NCO)] indicating the loss of NCO fragment due to retro Diels-Alder cleavage of N-1/C-6 and C-2/N-3 bonds which is a characteristic fragmentation pattern for 2-oxopurines (Cafieri *et al* 1995). The presence of a fragment ion peak at *m/z* 180 indicated 3,9-dimethyl isoguanine skeleton after loss of the side chain (*m/z* 138). Both MS fragmentaion pattern and NMR spectra corroborate with the structure proposal and established the identity of **34** as butyl 3-(3,9- dihydro-3,9-dimethyl –2-oxo-2*H*-purin-6-ylamino) propanoate. To the best of my knowledge this is the first report of **34** as a natural product and also as far as I know this is the first report of an 2-oxo-3,9-dimethylpurin-6-ylamino derivative, which we assign the trivial name nigricine 1.

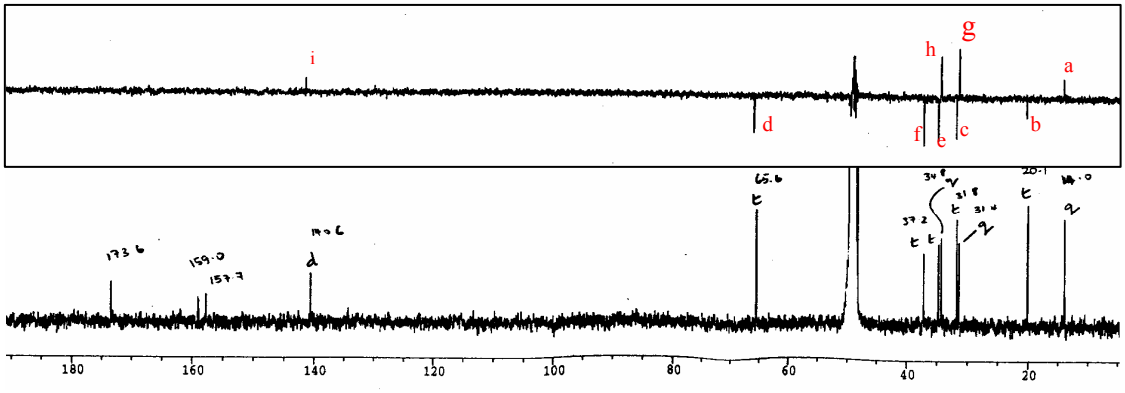

Fig (3.5.50):^{13}CNMR and DEPT spectra of compound 34

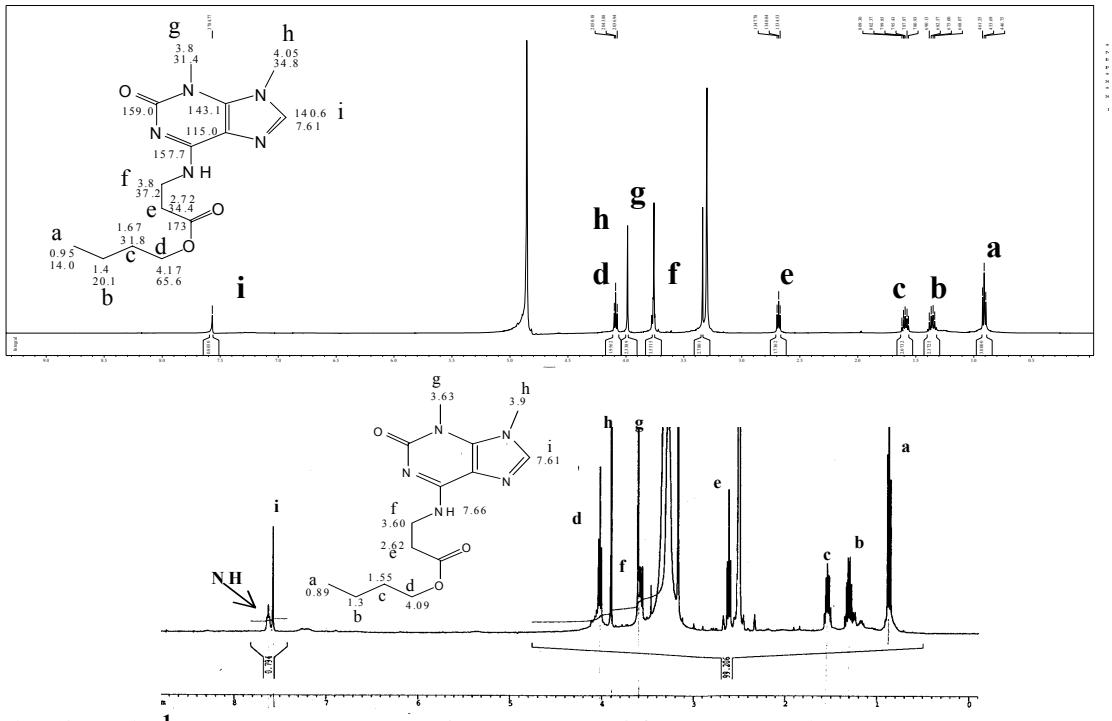

Fig (3.5.51):^{1}HNMR spectrum of compound 34 measured in methanol-d_4 (up) and DMSO-d_6 (down).

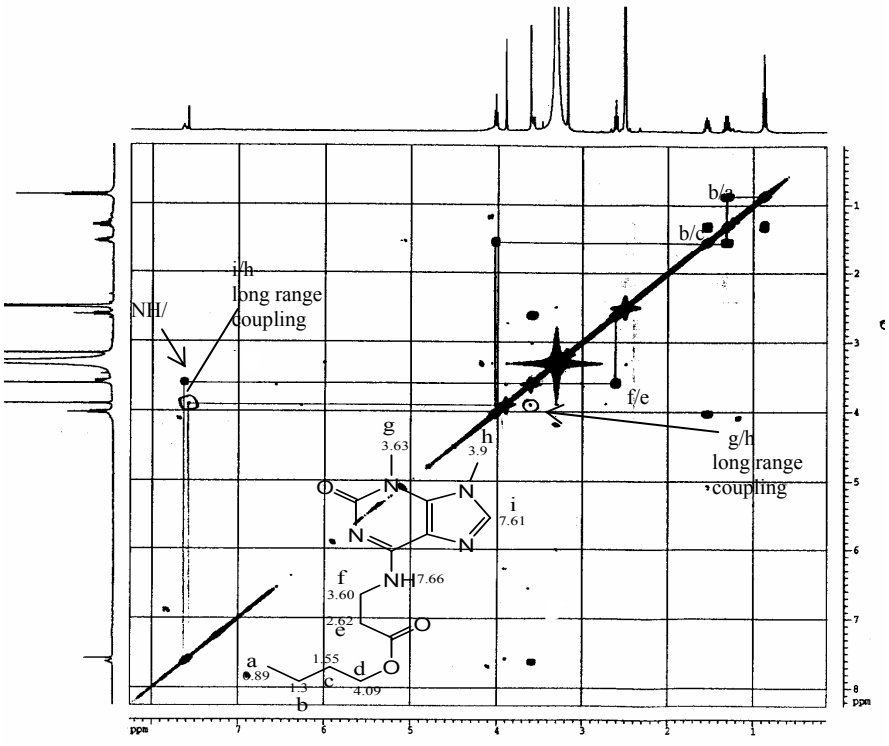

Fig (3.5.52):COSY spectrum of compound 34

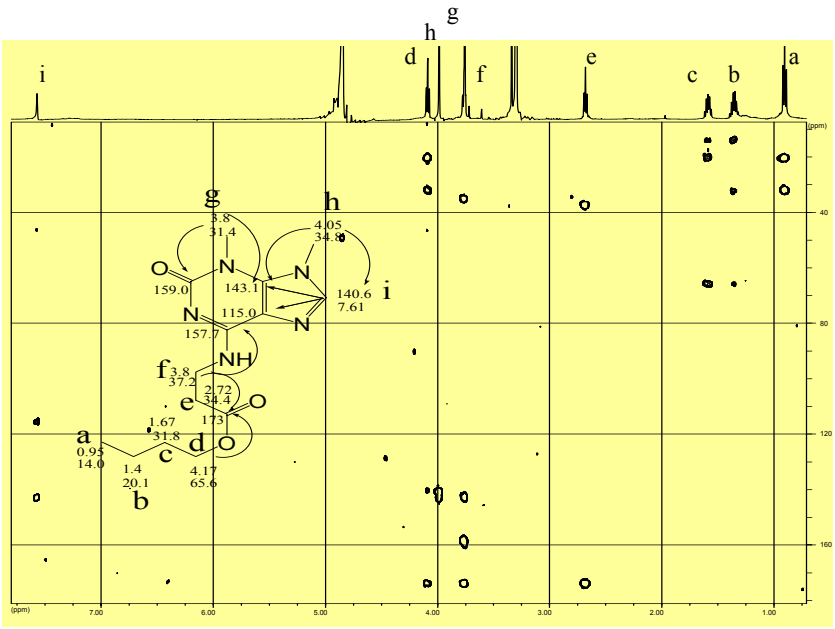

Fig (3.5.53):total HMBC spectrum of compound 34

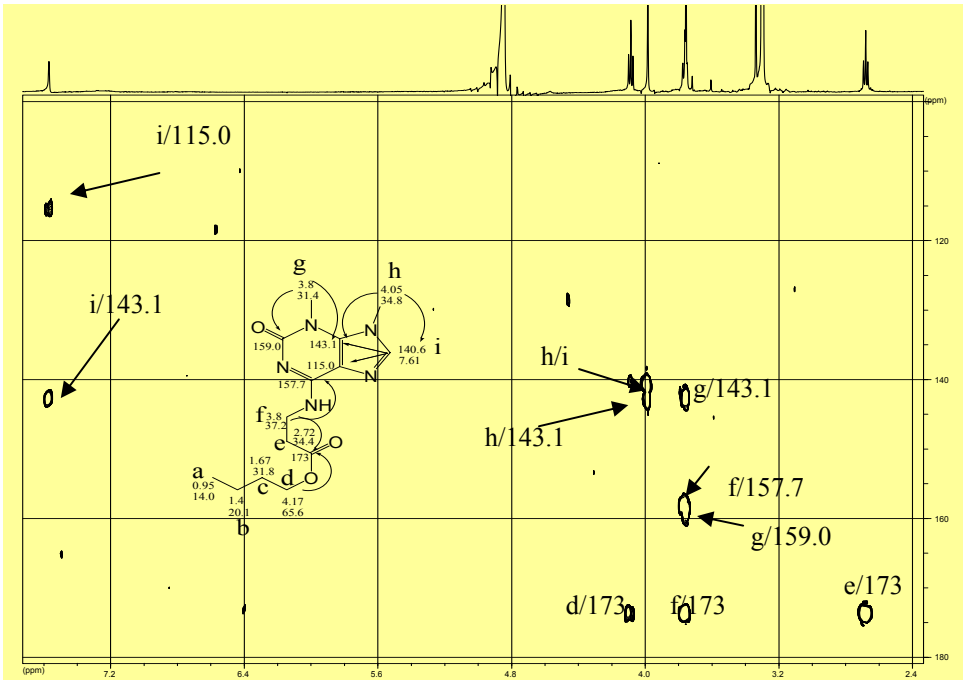

Fig (3.5.54):part of HMBC spectrum of compound 34

Table 3.5.5. ^{1}H and ^{13}C NMR Data of compound 34 (Nigricine **1) (**500 MHz)

Position	^{13}C δ ,m (DMSO-d_6)	^{1}H δ,m, *j*(Hz) (DMSO-d_6)	^{13}C δ ,m (CD_3OD)	^{1}H δ,m, *j*(Hz) (CD_3OD)	HMBC (H--------- C)
2	154.9	-	158.9	-	
N(3)-CH_3	31.0	3.62	31.4	3.80 (s)	C-2, C-4
4	141.5	-	142.5	-	
5	115.0	-	115.4	-	
6	153.6	-	157.6	-	
6-NH	-	7.67 (t,5.8)	-	-	C-6
8	139.1	7.57	140.6	7.61 (s)	C-4, C-5
N(9)-CH_3	34.2	3.91	34.5	4.02 (s)	C-8, C-4
10	36.3	3.59 (dt,6.30&5.8)	37.2	3.81 (t,6.30)	C-6, C-12, C-11
11	34.8	2.62 (t,6.30)	34.8	2.72 (t,6.31)	C-12, C-10
12	171.3	-	173.5	-	
13	65.3	4.08 (t,6.30)	65.4	4.17 (t,6.94)	C-12, C-15, C-14
14	31.2	1.57 (tt,6.93&6.94)	31.8	1.67, (tt,6.93&6.94)	C-13, C-15, C-16
15	20.1	1.31(tt,6.93&6.94)	20.6	1.40 (qt,6.93&6.94)	C-13, C-14, C-16
16	13.3	0.89 (t,6.94)	13.9	0.95 (t,6.94)	C-14, C-15

3.5.14 – Nigricine 2 (35, new compounds)

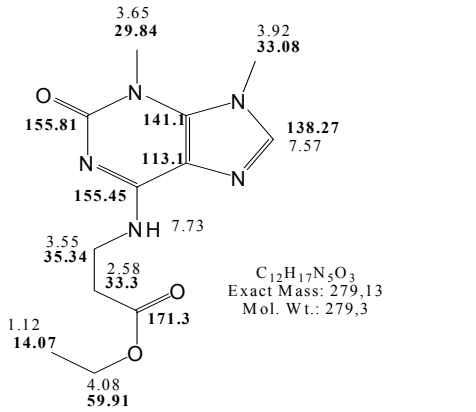

Yield : 6.1 mg

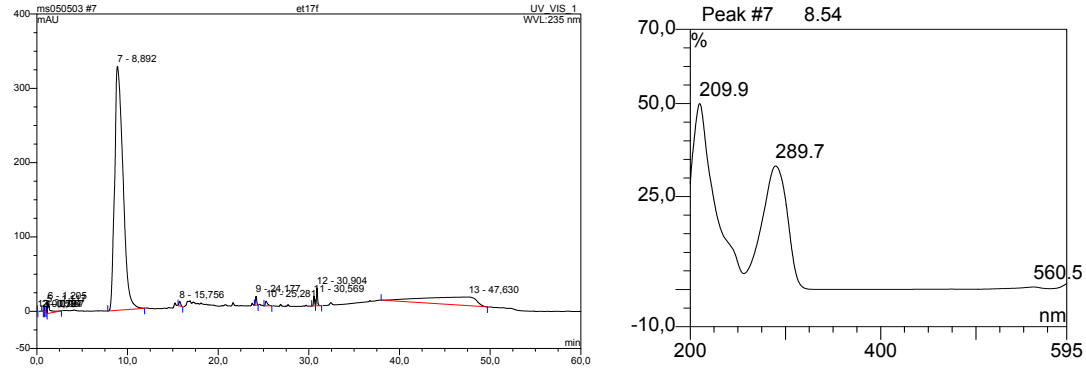

Fig (3.5.55): HPLC chromatogram and UV spectrum of compound 35

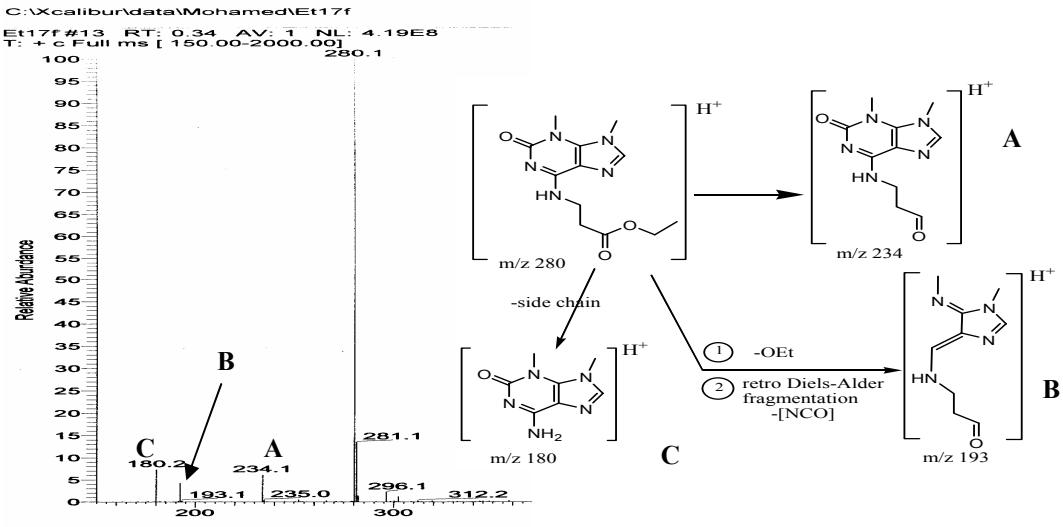

Fig (3.5.56):ESI-MS spectrum of compound 35

Compound **35**, showed molecular formula $C_{12}H_{17}N_5O_3$ through HRESIMS-TOF analysis (measured, *m/z* 280.139, $[M+H]^+$) with 7 degrees of unsaturation. The UV spectrum of **35** showed absorption λ_{max} (MeOH) at 210 and 290 nm indicating the same chromophoric functionalities as **34**. The difference in molecular weight between **34** and **35** was only 28 mass units indicating a loss of C_2H_4 group from the alkoxy group as evident from its ^{1}HNMR spectrum. ESI/MS spectrum showed pseudomolecular ion peak at *m/z* 280.1 (M+H) and at *m/z* 559 (2M+H) and at *m/z* 838 (3M+H). Tandem MS fragmentation spectrum showed a retro Diels-Alder fragment ion peak at *m/z* 192 $[M-(\text{ethoxy group} +OCN)]^+$ which confirmed the loss of an OCN group suggesting 2-oxopurine derivative (Cafieri *et al* 1995), and also exhibited a molecular ion fragment at *m/z* 234 indicating the loss of an alkoxy group.The ^{1}H NMR and ^{13}C NMR spectra showed signals at chemical shift the same as those of nigricine **1** with the exception of loss of 2 C*H*$_2$ chemical shifts from the terminal alkoxy group.

The proton signals for 6-N*H* exhibited HMBC correlations to the adjacent quaternary carbon signals at 155.45 and 113.1 ppm and also HMBC correlation to the β-methylene carbon of propionc acid moiety at 35.34 ppm. The aromatic proton signal, H-8, at 7.57 ppm showed HMBC correlation to N(9)-Me carbon signal at 33.08, quaternary aromatic carbon signals at 113.1 and 141.1 ppm of C-5 and C-4 respectively. N(3)-Me proton signal exhibited HMBC correlation to the carbonyl (C-2) at 155.81 ppm. The connection of the ethoxy group was established through HMBC correaltion between C*H*$_2$ proton signal to the carboxyl at δ 171.3. Both MS fragmentaion pattern and NMR spectra confirmed the proposed structure and established the identity of **35** as ethyl 3-(3,9- dihydro-3,9-dimethyl –2-oxo-2H-purin-6-ylamino) propanoate and was assigned the trivial name nigricine 2.

Table 3.5.6. NMR Data of compound 38 (Ashourine 2) [500 MHz]

Position	^{13}C δ ,m (DMSO-d_6)	^{1}H δ,m, *j*(Hz) (DMSO-d_6)	HMBC (H-------- C)
2	155.8	-	
N(3)-CH_3	29.84	3.65 (s)	C-2, C-4
4	141.1	-	
5	113.1	-	
6	155.45	-	
6-NH	-	7.73 (t,5.68)	C-6, C-5, C-10
8	138.27	7.57 (s)	C-4, C-5, N(9)-CH_3
N(9)-CH_3	33.08	3.91 (s)	C-8, C-4
10	35.34	3.56 (dt,6.63&5.8)	C-6, C-12, C-11
11	33.56	2.58 (t,7.25)	C-12, C-10
12	171.3	-	
13	59.91	4.08 (q,7.25)	C-12, C-14
14	14.07	1.12 (t,7.25)	C-13

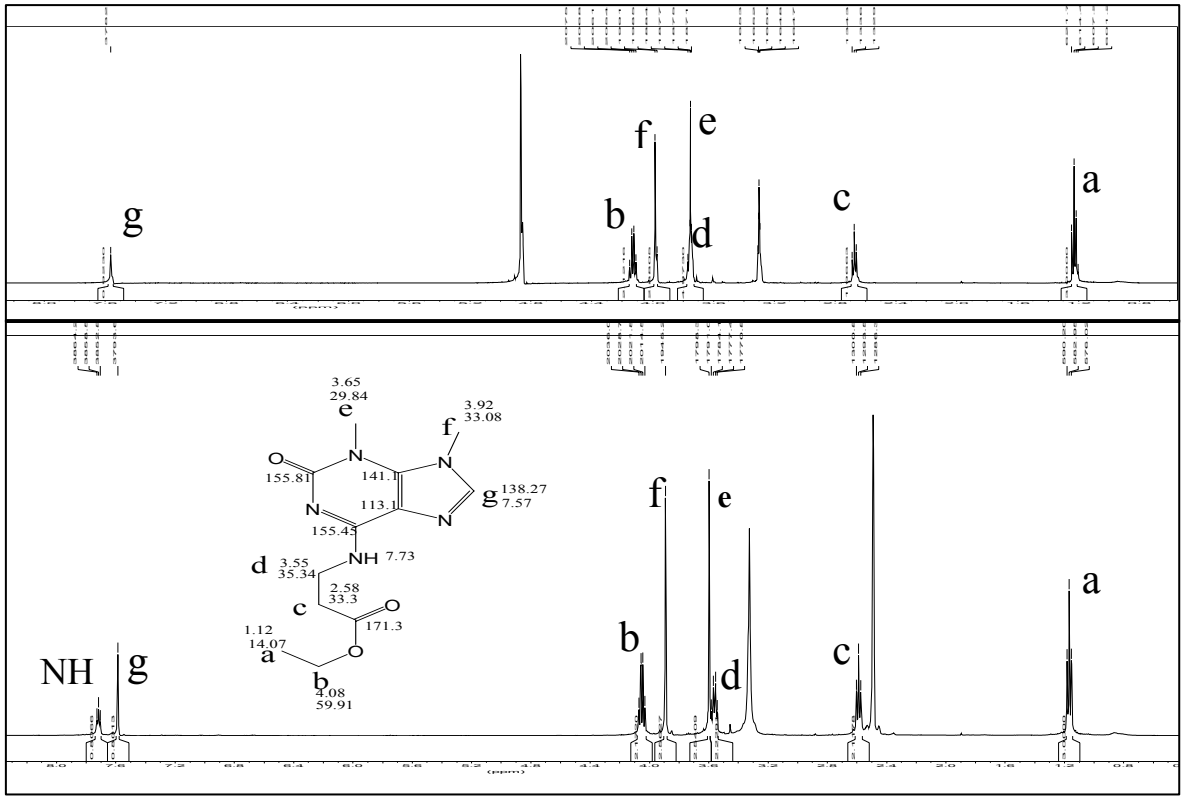

Fig (3.5.57):[1]HNMR spectrum of compound 35

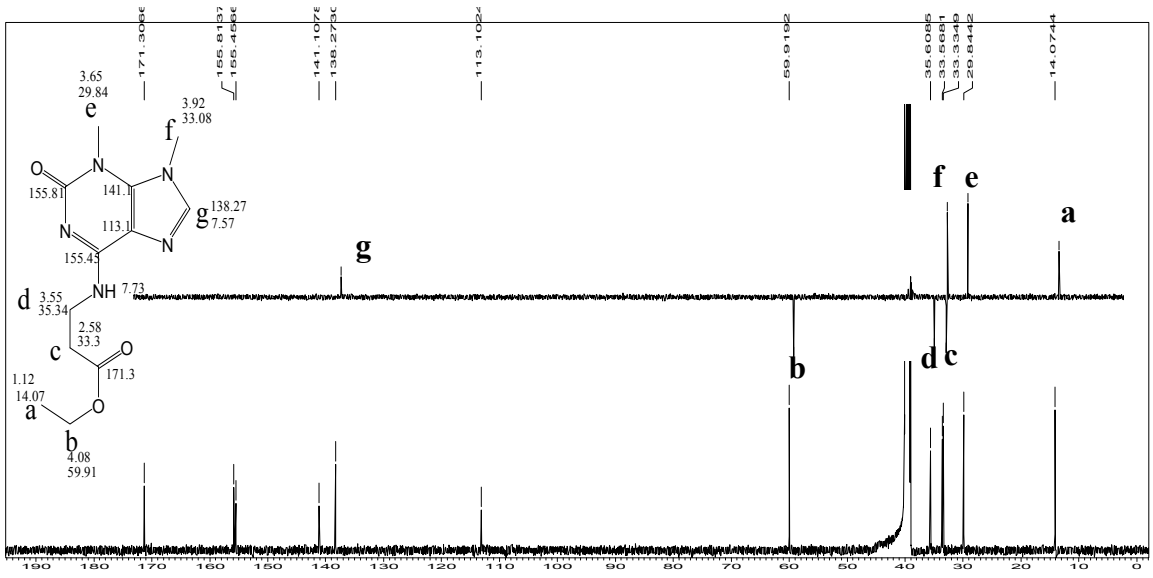

Fig (3.5.58):[13]CNMR and DEPT spectra of compound 35

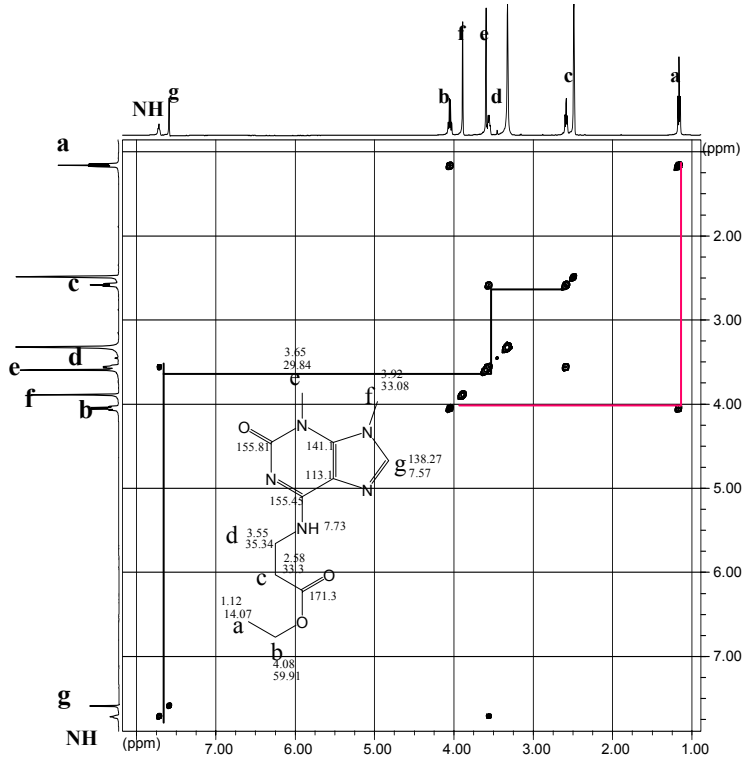

Fig (3.5.59):COSY spectrum of compound 35

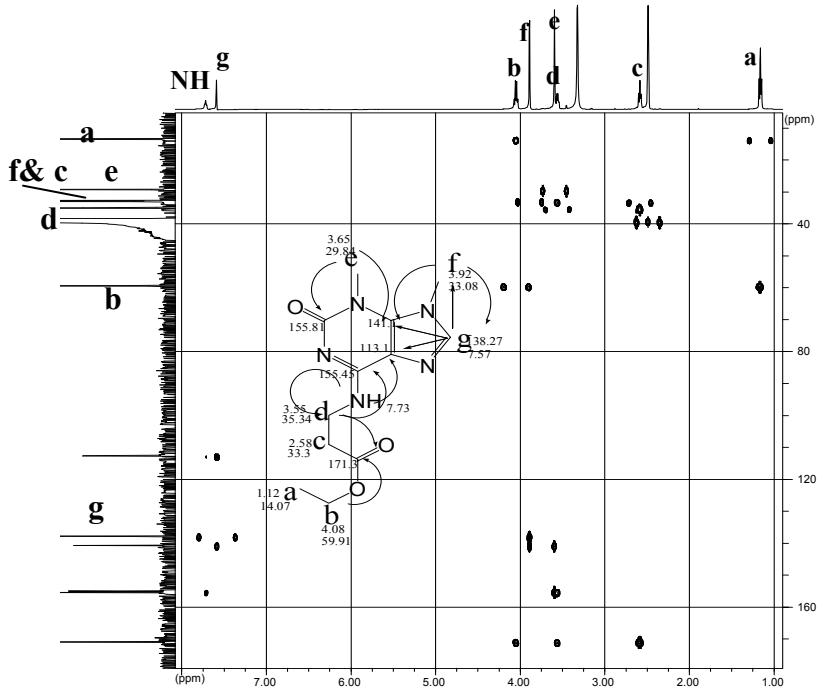

Fig (3.5.60):HMBC spectrum of compound 35

3.5.15 – Nigricine 3, (36 , new compounds)

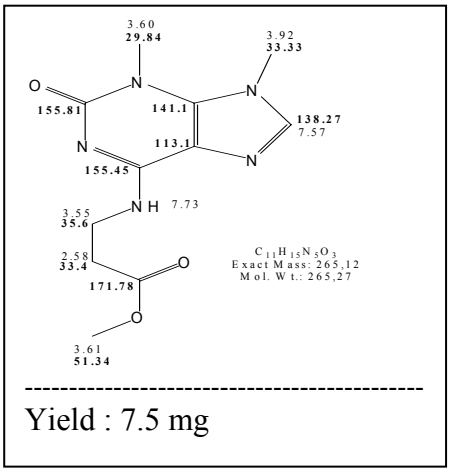

Yield : 7.5 mg

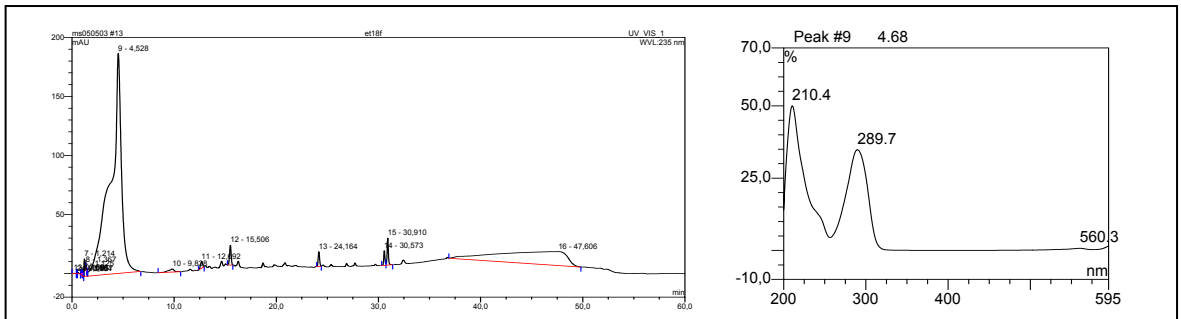

Fig (3.5.61): HPLC chromatogram and UV spectrum of compound 36

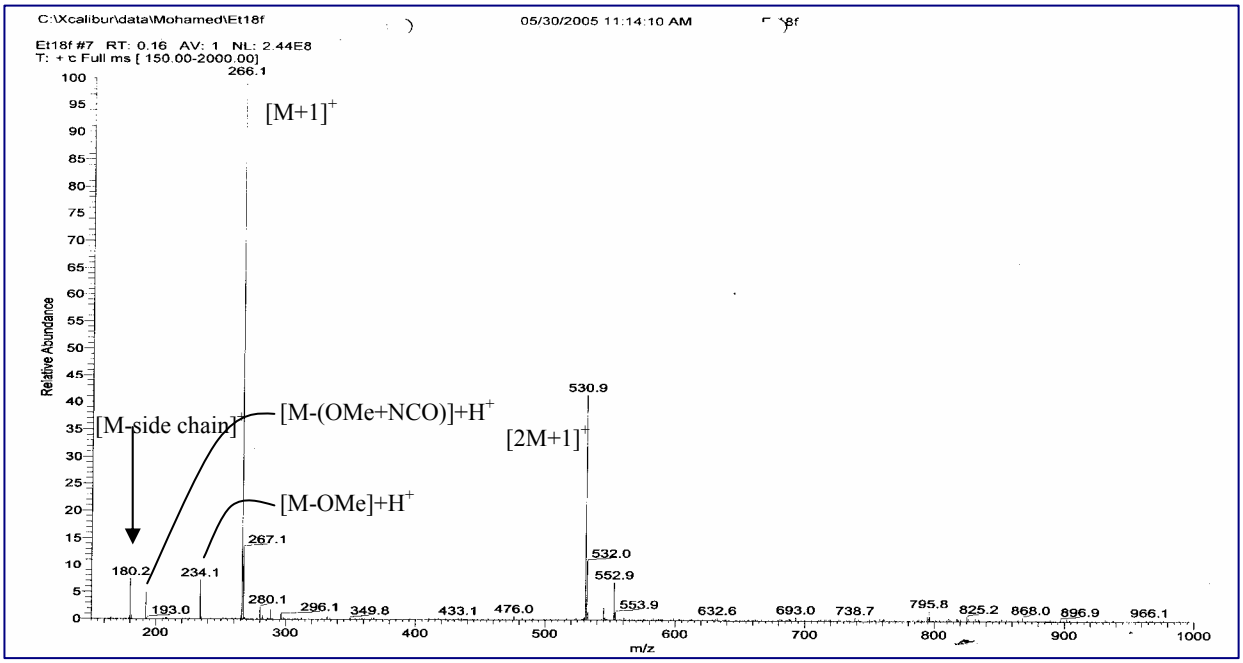

Fig (3.5.62):ESI-MS spectrum of compound 36

Compound **36**, has the molecular formula $C_{11}H_{15}N_5O_3$ based on HRESIMS-TOF (measured, *m/z* 266.123 [M+H]) with 7 degrees of unsaturation. The UV spectrum of **36** showed UV λ_{max}(MeOH) absorption at 210 and 290 nm indicating the same chromophoric functionalities as **34** and **35**. The difference in molecular weight between **34** and **36** was only 32 mass units indicating a loss of C_3H_6 group from the alkoxy group as evident from its ^{1}H NMR spectrum. ESI/MS spectrum showed pseudomolecular ion peak at *m/z* 266.1 (M+H), 531 (2M+H) and 796 (3M+H). Tandem MS fragmentation spectrum showed a retro Diels-Alder fragment ion peak at *m/z* 192 which confirmed a loss of OCN group indicating 2-oxopurine derivative (Cook *et al* 1980, Mitchell *et al* 1997, Lin *et al* 1996), and also exhibited a molecular ion fragment at *m/z* 234 indicating the loss of a methoxy group.

The ^{1}H NMR spectrum of **36** (see figure 3.5.63) showed four singlets at δ 7.57 (8-C*H*), 3.60 (N(3)-CH_3), 3.92 (N(9)-CH_3), and 3.61 (O-CH_3), in addition to a triplet signal at δ 2.58 for the α-CH_2 of the propionic acid moiety, multiplet at 3.55 ppm for the β-CH_2 of the propionic acid and an exchangeable triplet signal at 7.73 ppm for 6-N*H*. DEPT experiment of **36** deduced a downfield methyl carbon signal at 51.34 ppm and absence of the upfieled methyl carbon signals which were established for **34** and **35**. The attachment of the methyl group directly to the carboxyl of propionic acid part was confirmed through HMBC correlation between the methyl proton signal and the carboxyl resonance at 171.78 ppm. Additional HMBC correlations were assigned in figure 3.5.66 and presented in table 3.5.7. Compound 36 was then elucidated as methyl-(3,9-dihydro-3,9-dimethyl-2-oxo-2H-purin-6-ylamino) propanoate and was named nigricine 3.

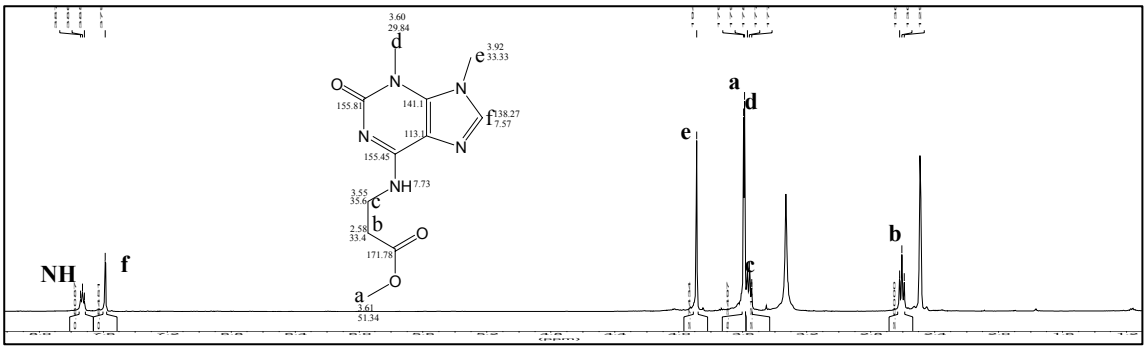

Fig (3.5.63):^{1}HNMR spectrum of compound 36

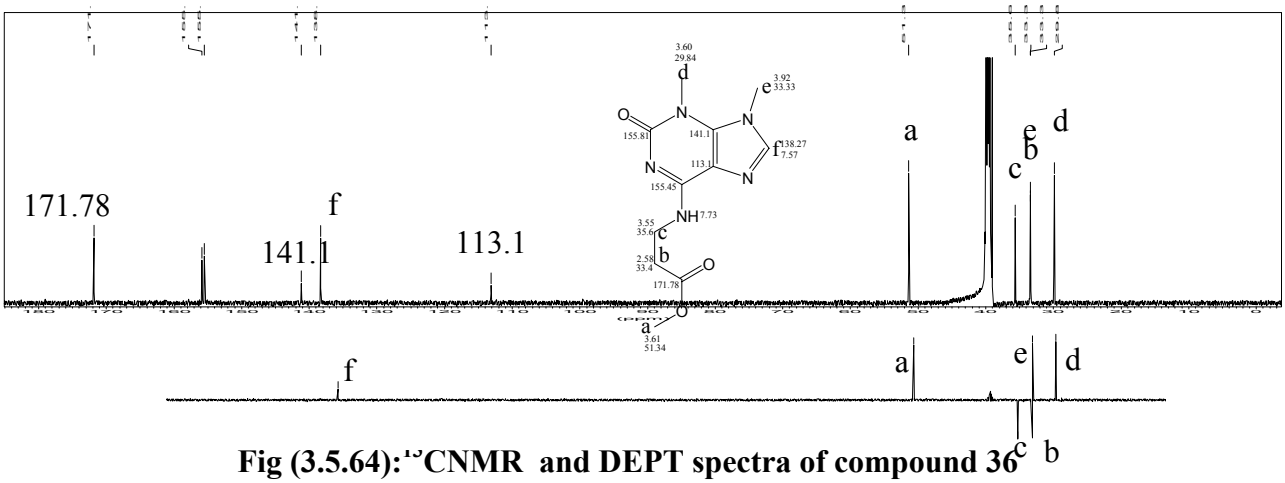

Fig (3.5.64):¹³CNMR and DEPT spectra of compound 36

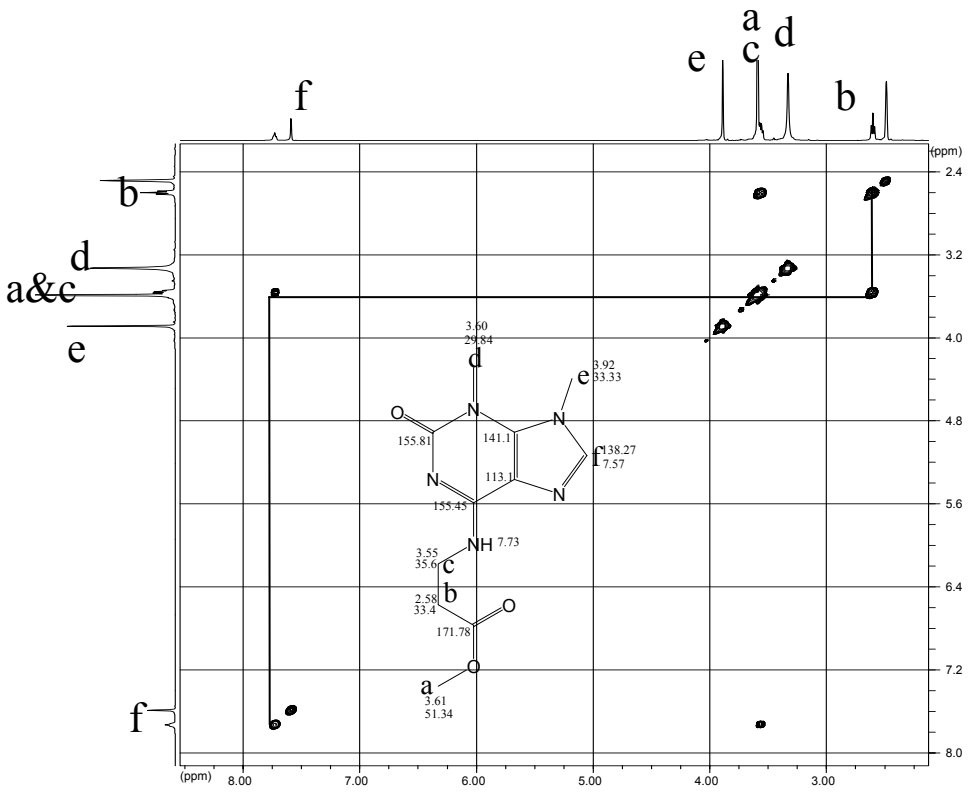

Fig (3.5.65):COSY spectrum of compound 36

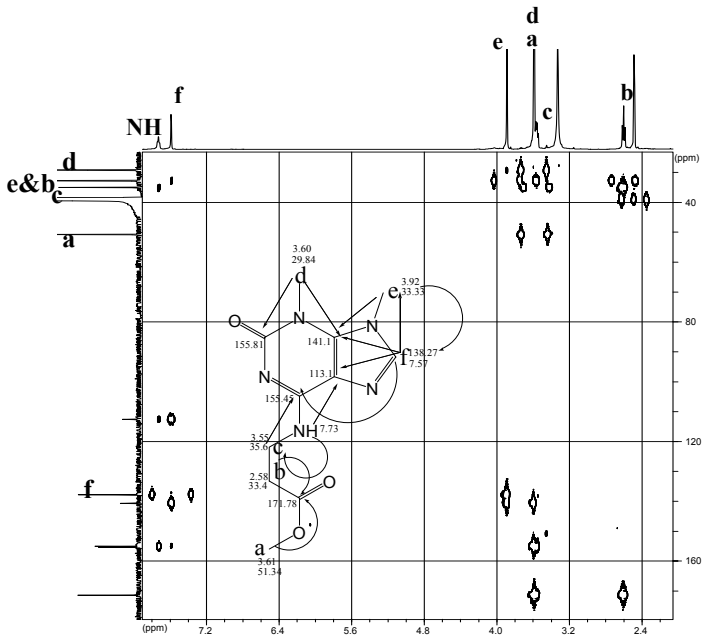

Fig (3.5.66): HMBC spectrum of compound 36

Table 3.5.7. NMR Data of compound 36 (Ashourine 3) [500 MHz]

Position	^{13}C δ ,m (DMSO-d_6)	^{1}H δ,m, *j*(Hz) (DMSO-d_6)	HMBC
2	155.81	-	
N(3)-CH_3	29.84	3.60 (s)	C-2, C-4
4	141.1	-	
5	113.1	-	
6	155.45	-	
6-NH	-	7.73 (t,5.36)	C-6, C-5, C-10
8	138.27	7.57 (s)	C-4, C-5, N(9)-CH_3, C-6
N(9)-CH_3	33.33	3.93 (s)	C-8, C-4
10	35.6	3.57 (dt,6.94&6.0)	C-6, C-12, C-11
11	33.4	2.58 (t,6.94)	C-12, C-10
12	171.78	-	
13	51.34	3.91 (s)	C-12

3.5.16 – Nigricine 4 (37, new compounds)

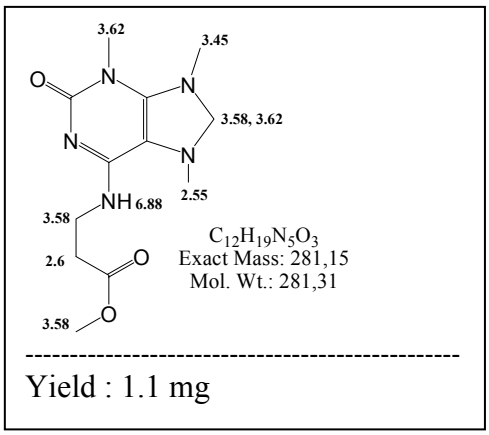

$C_{12}H_{19}N_5O_3$
Exact Mass: 281,15
Mol. Wt.: 281,31

Yield : 1.1 mg

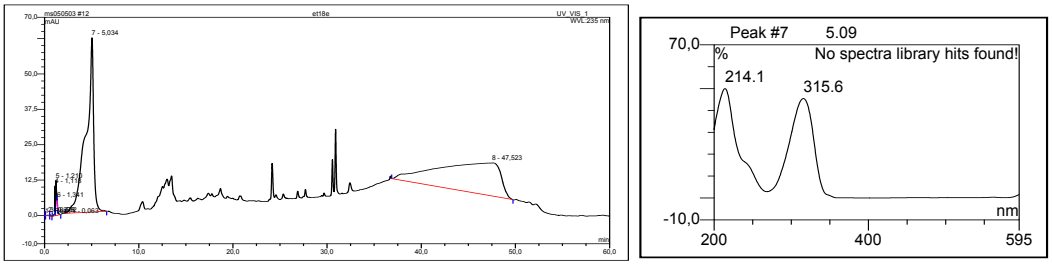

Fig (3.5.67): HPLC chromatogram and UV spectrum of compound 37

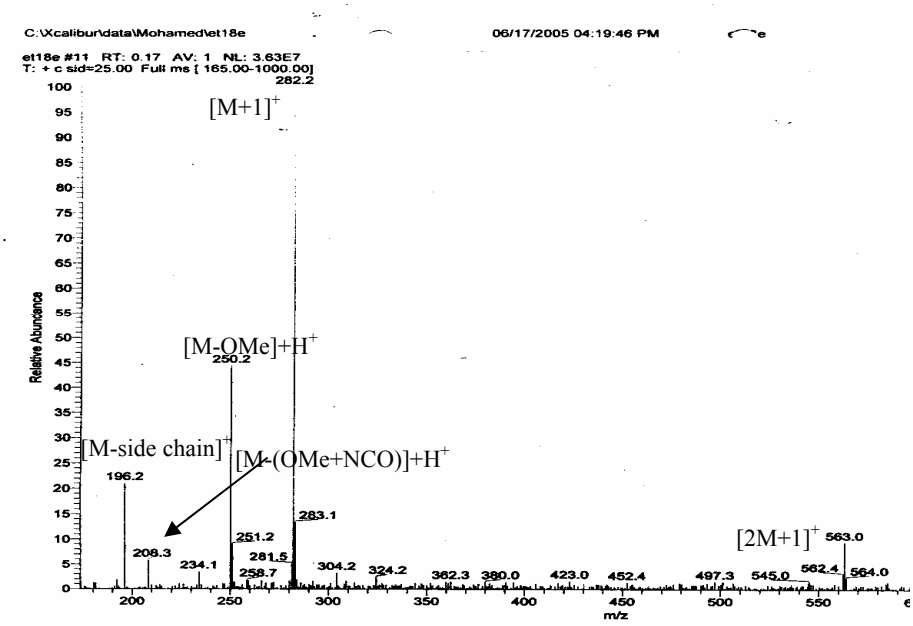

Fig (3.5.68):ESI-MS spectrum of compound 37

Compound **37**, was assigned molecular formula $C_{12}H_{19}N_5O_3$ based on ESIMS analysis with 6 degrees of unsaturation. ESI/MS spectrum showed positive pseudomolecular ion peaks at *m/z* 282.1 (M+H), 280 (M-H) and 563 (2M+H). Similar to the previous congeners, MS fragmentation showed a fragment ion peak at *m/z* 250.2, $[M-(OMe)]^+$ and a characteristic

fragment ion peak at *m/z* 208, $[M-(OMe+NCO)]^+$ which confirmed the loss of OCN group indicating 2-oxopurine derivative (Cook *et al* 1980, Mitchell *et al* 1997, Lin *et al* 1996), and also exhibited a fragment ion peak at *m/z* 196.2 (24 %) indicating the loss of the side chain. This fragmentation pattern is typical as those of **36** (nigricine **3),** [figures 3.5.62 & 3.5.68] with the exception of a loss of one double bond and addition of one methyl group at position 7.

The UV spectrum of **37** showed bands at λ_{max} (MeOH) 214 and 315 nm indicating the same chromophoric functionalities as **34, 35,** and **36**. The difference in molecular weight between **36** and **37** was 16 mass units. The additional substituent was deduced to be away from the alkoxy group, because the methoxy group is still present at δ 3.58 as evident from its ^{1}H NMR spectra. The additional methyl singlet at δ 2.55 indicated an additional N-methyl function [N(7)-CH_3]. Disappearence of the sharp singlet at 7.57 ppm and presence of two coupled protons at 3.58 and 3.62 ppm indicated the saturation at position 8. The presence of a triplet signal at 6.88 ppm (J=5.7Hz) ensures the presence of NH which showed a COSY correlation to adjacent ethylenes at δ 3.58 (2H, m) and δ 2.6 (2H, t, J= 6.6 Hz). The NH signal was shifted upfield indicating the shielding effect of the new methyl group at position 7. From the above NMR data, MS fragmentation pattern and other spectral data, compound **37** was elucidated as methyl-(3,7,8,9-tetrahydro-3,7,9-trimethyl-2-oxo-2*H*-purin-6-ylamino) propanoate and assigned the trivial name nigricine **4**.

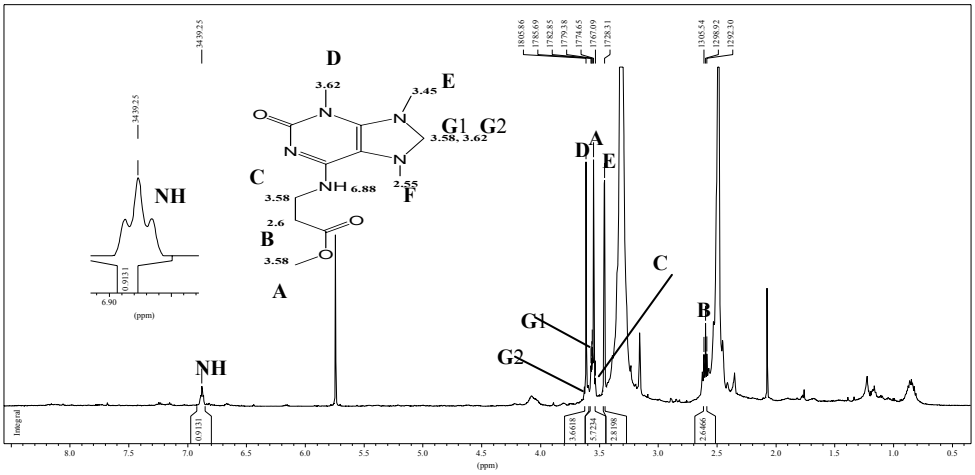

Fig (3.5.69) total ^{1}HNMR spectrum of compound 37

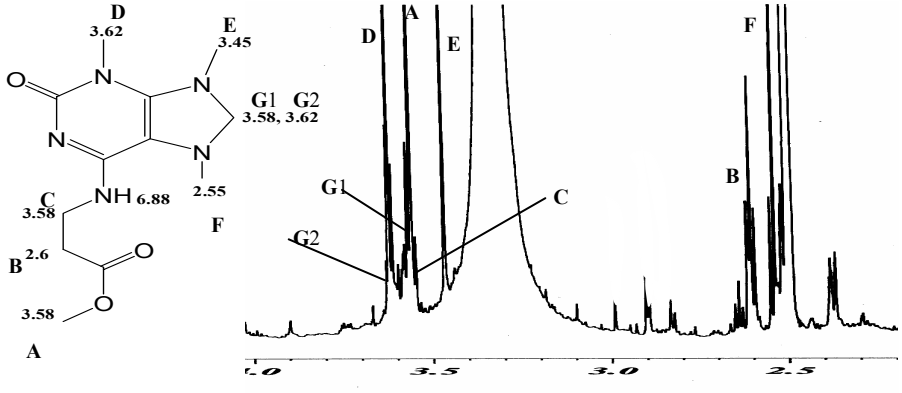

Fig (3.5.70): part of ^{1}HNMR spectrum of compound 37

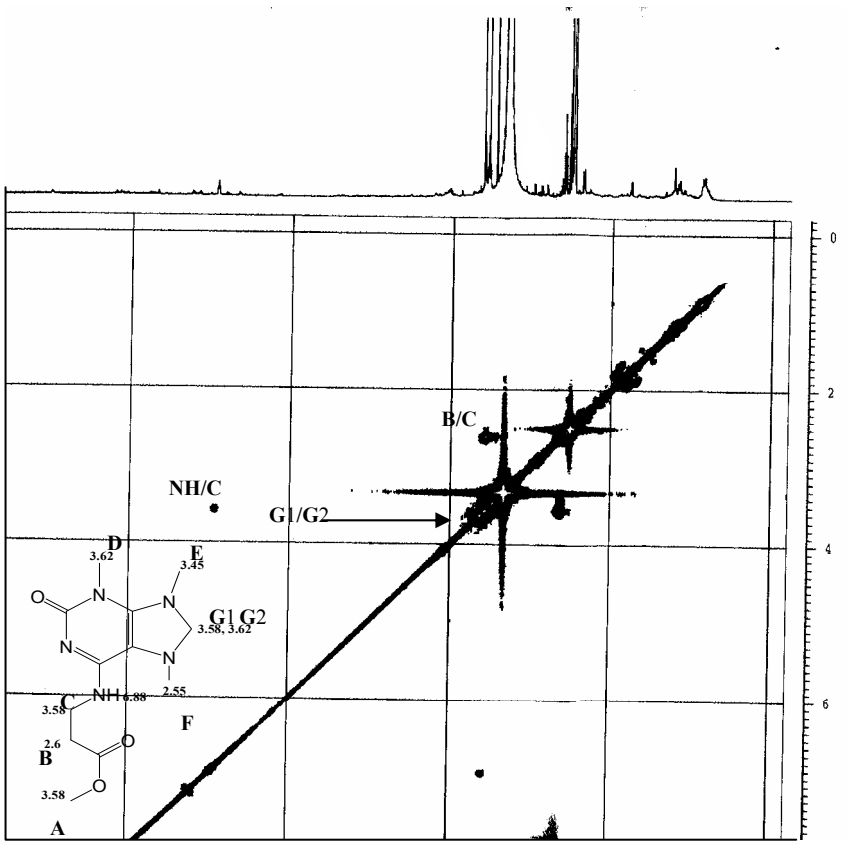

Fig (3.5.71) COSY spectrum of compound 37

3.5.17. Nigricinol [4-((1H-Indol-3-yl)methyl)-2-amino-5-(1H-indol-3-yl)-3H-pyrrol-3-one] (38, new compounds)

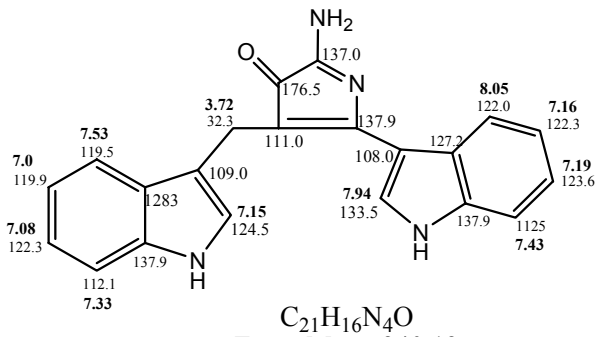

$C_{21}H_{16}N_4O$
Exact Mass: 340,13

Yield : 3.2 mg

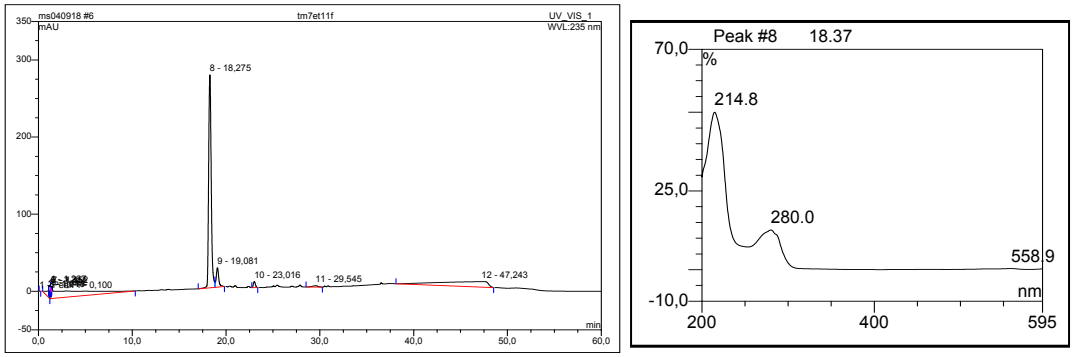

Fig (3.5.72): HPLC chromatogram and UV spectrum of compound 38

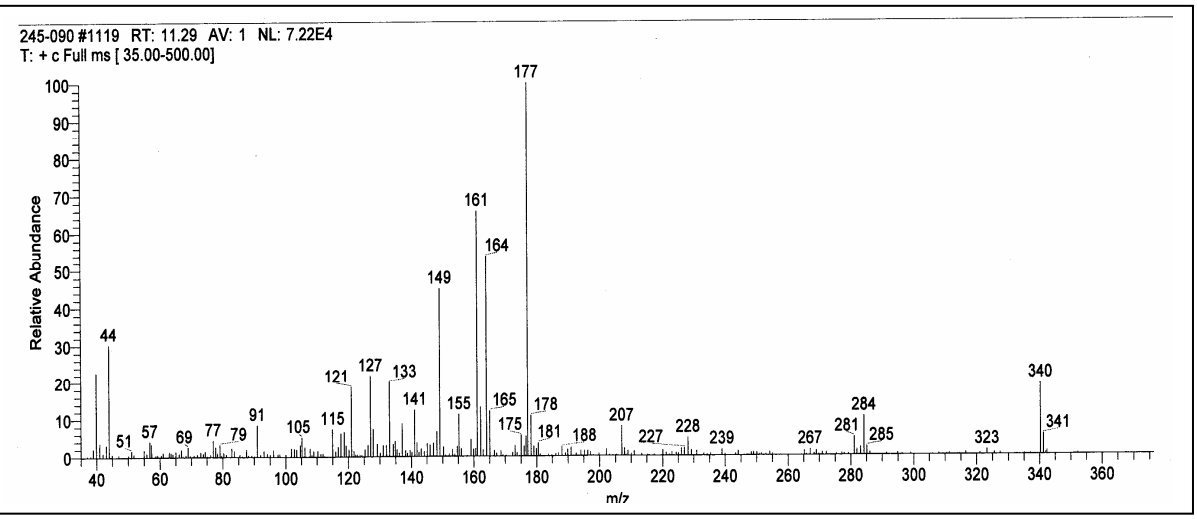

Fig (3.5.73):GC-MS spectrum of compound 38

Compound **38** was isolated as brownish white amorphous powder. It has UV absorbance of typical indole compound at λ_{max} 214 and 280 nm. ESI-MS showed

pseudomolecular ion peak *m/z* 339.1 [M-H] while GC-MS showed a molecular ion peak at *m/z* 340 $[M]^+$ and fragment ion peaks at *m/z* 284 $[M-(COCNH_2)]^+$, 207 [M-(indolyl group + NH_2)]$^+$ and 177 [M-(3-indolylmethylene group + O + NH_2)]$^+$, suggesting the molecular formula $C_{14}H_{18}N_2O_2$. ^{1}H NMR spectrum showed characteristic spin systems for two indole groups. The first indole group showed an ABCD spin system at δ 7.55 (d, *J*=7.56 Hz), 7.00 (dt, *J*=1.2,6.9 Hz), 7.08 (dt, *J*=1.2, 6.9 Hz), 7.33 (d, *J*=8.2 Hz) for H-4', H-5', H-6', and H-7', respectively. Furthermore, the H-2' resonance at δ 7.15 (s) exhibited a COSY correlation to an exchangeable N*H* signal at 10.9 ppm. Another indole group showed an ABCD spin system as shown by ^{1}H signals at 8.05 (dd, *J*=6.3, 1.2 Hz), 7.16 (dt, *J*=1.2, 6.9 Hz), 7.19 (dt, *J*=1.2, 6.9 Hz), 7.43 (dd, *J*=6.9, 1.2 Hz) for H-4", H-5", H-6", and H-7", respectively. The H-2" signal at δ 7.94 (s) exhibited a COSY correlation to another exchangeable N*H* resonance at 11.8 ppm. The first 3-indolyl group is attached to a methylene group resonating at δ 3.72 (s) which displays an HMBC correlations to carbons at δ124.5, 109.0, and 128.0 of C-2', C-3', and C-3a', respectively. The methylene protons also exhibited an additional HMBC correlations with two carbons resonating at 176.5 ppm (C-3) and 110.0 ppm (C-4). The H-2" methine singlet showed HMBC correlations to carbons resonating at δ 108.0, 127.2, and 137.9 for C-3", C-3a", and C-7a", respectively. The NMR data and mass fragmentation pattern confirmed **38** to be 4-((1H-indol-3-yl)methyl)-2-amino-5-(1H-indol-3-yl)-3H-pyrrol-3-one and was assigned as nigricinol.

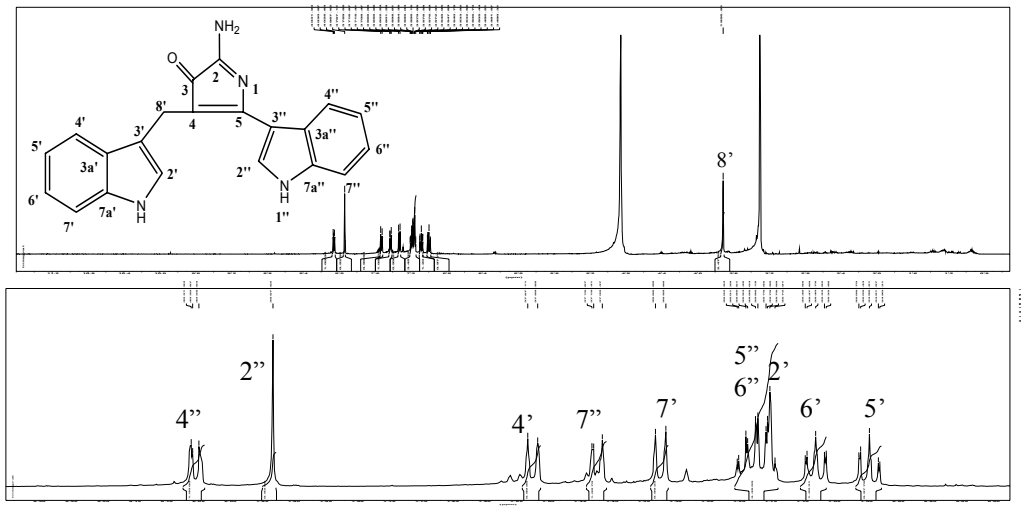

Fig (3.5.74):total ^{1}HNMR spectrum of compound 38 (up) and part of ^{1}HNMR showing an aromatic region (down).

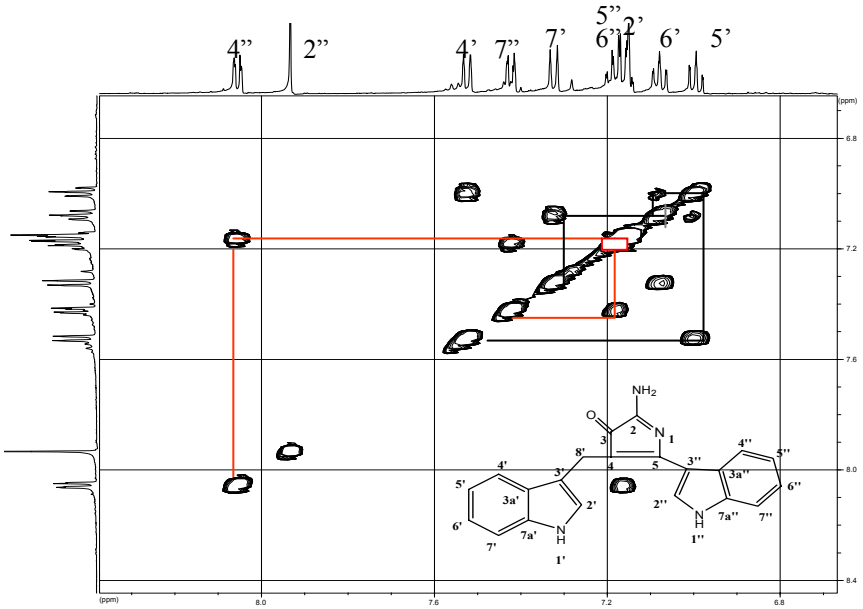

Fig (3.5.75):Part of COSY spectrum of compound 38

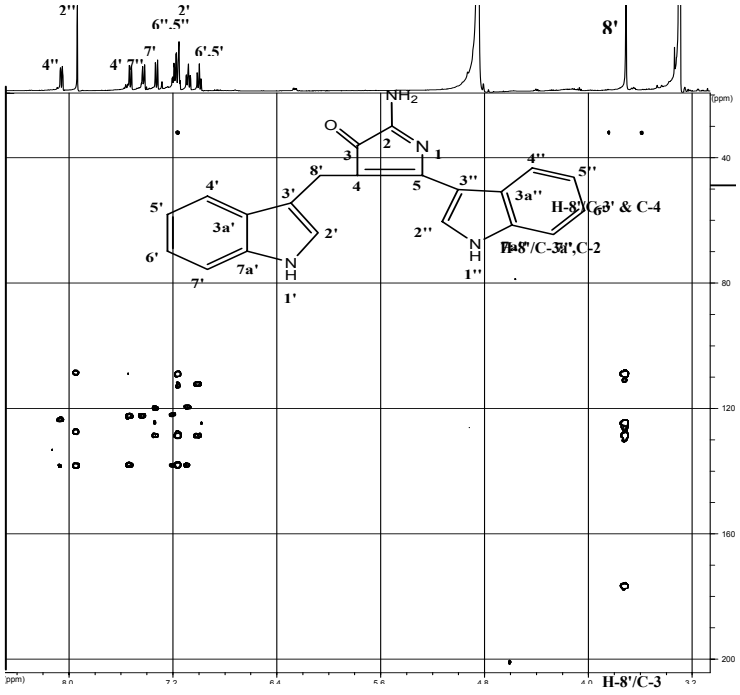

Fig (3.5.76):Total HMBC spectrum of compound 38

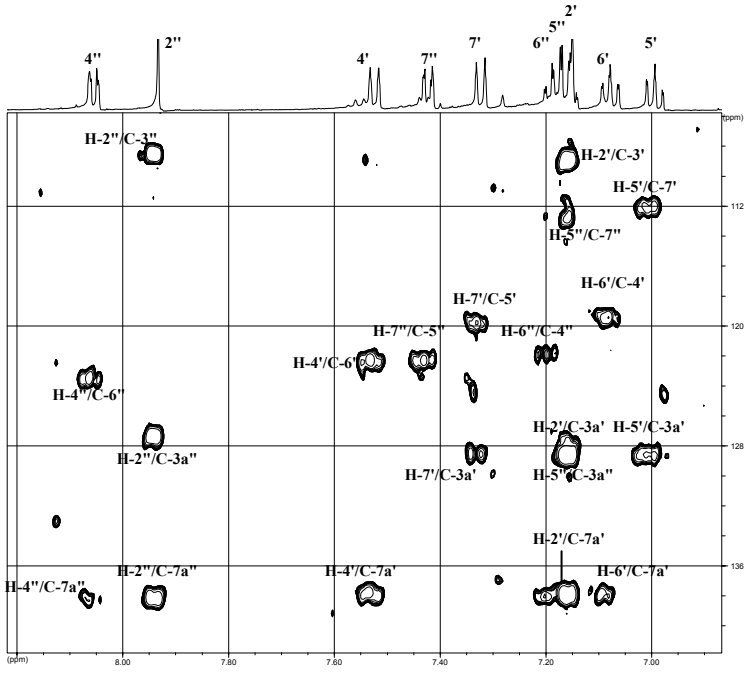

Fig (3.5.77):part of HMBC spectrum of compound 38

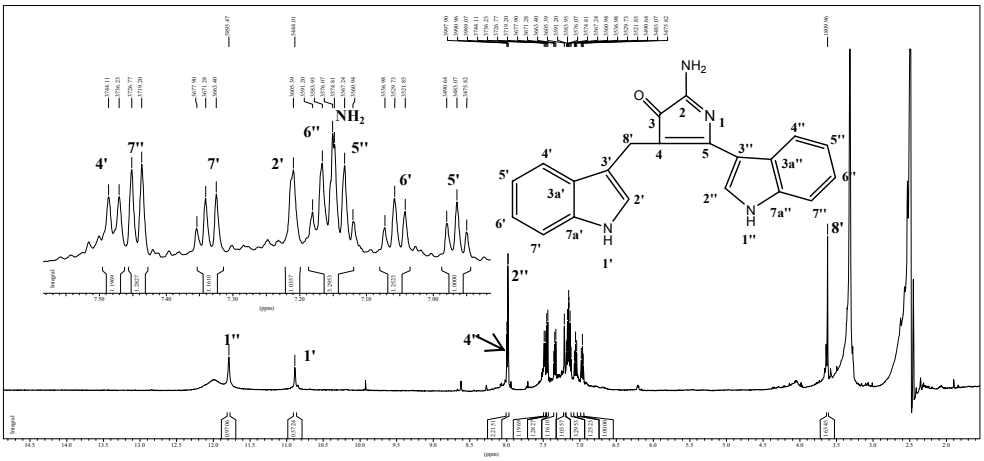

Fig (3.5.78):^{1}HNMR spectrum of compound 38 (measured in DMSO-d_6)

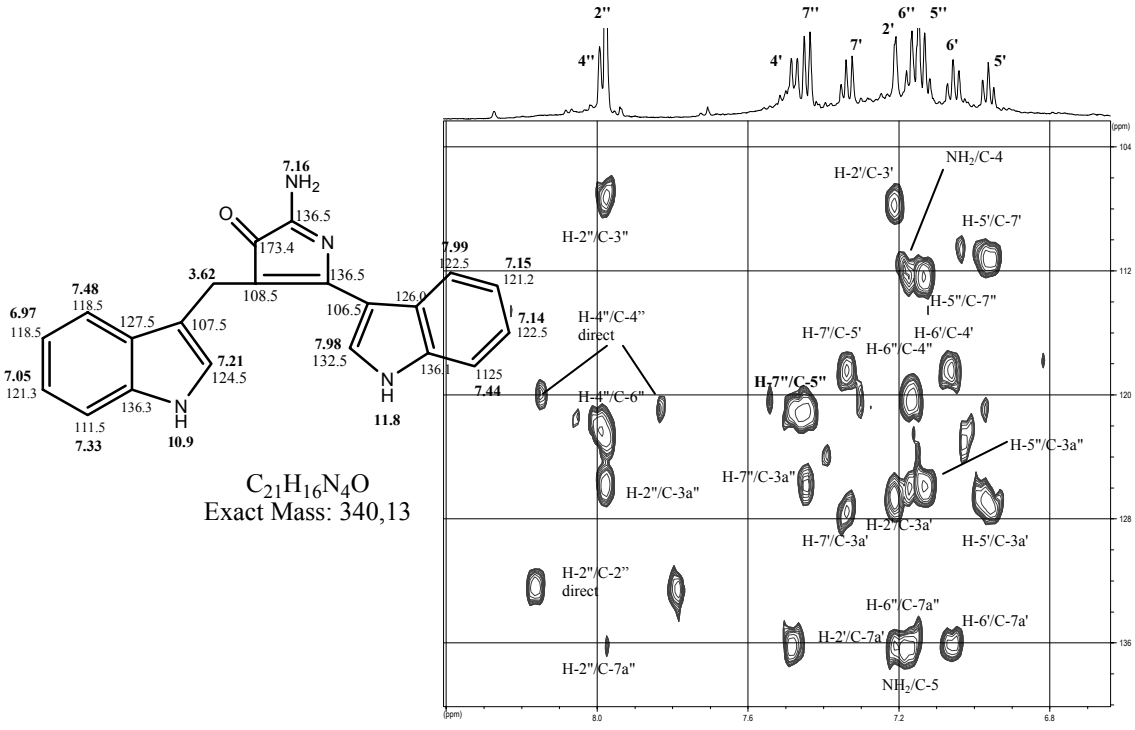

Fig (3.5.79):part of HMBC spectrum of compound 38

Table (3.5.9): NMR data of 38 (500 MHz, Methanol-d_4),

Carbon	^{13}C NMR, ppm	^{1}H NMR, ppm (Multiplicity, *J*= Hz)	^{1}H NMR*, ppm (Multiplicity, *J*= Hz)
2	137.0		(NH_2), 7.15 br s
3	176.5		
4	111.0		
5	137.9		
1'			10.9 (s)
2'	124.5 d	7.15 (s)	7.15 (s)
3'	109.0 s		
3a'	128.3 s		
4'	119.5 d	7.55 (d, *J*=7.56)	7.48 (d, *J*=7.9)
5'	119.9 d	7.00 (dt, *J*=1.2,6.9)	6.97 (t, *J*=8.2)
6'	122.3 d	7.08 (dt, *J*=1.2, 6.9)	7.05 (t, *J*=7.9)
7'	112.0 d	7.33 (d, *J*=8.2)	7.33 (d, *J*=7.8)
7a'	137.9 s		
8'	32.3 t	3.72 (s)	3.62 (s)
1"			11.8 (s)
2"	133.5 d	7.94 (s)	7.98 (s)
3"	108.0 s		
3a"	127.2 s		
4"	122.0 d	8.05 (dd, *J*=6.3, 1.2)	7.99 (dd, *J*=7.00)
5"	122.3 d	7.16 (dt, *J*=1.2, 6.9)	7.15 (t, *J*=7.3)
6"	123.6 d	7.19 (dt, *J*=1.2, 6.9)	7.14 (t, *J*=7.00)
7"	112.5 d	7.43 (dd, *J*=6.9, 1.2)	7.44 (dd, *J*=7.5)
7a"	137.9 s		
* meassured in DMSO-d_6			

Biological activity :

None of the isolated compounds from *Petrosia nigricans* showed significant antimicrobial activity against *B.subtilis, S. cerevisae*, *C. herbarum,* and *C. cucumerinum*.

All purine derivatives (nigricines **1** to **4**) showed no cytotoxic activity against L5178Y cell line, while nigricinol (compound **38**) showed 68.1 % cytotoxic activity at a concentration of 10 µg/ml.

3-6- Natural Products from *Callyspongia biru*

Sponges belonging to the genus C*allyspongia* are extensively investigated for bioactive natural products. Many new bioactive natural products have been isolated from different *Callyspongia sp*., these natural products includes unusual steroids (Theobald *et al* 1978, Agrawal and Garg 1997); acetylene derivatives (Youssef *et al* 2003, Nakao *et al* 2002 and Youssef *et al* 2000); uncommon fatty acids (Carballeira and Pagan 2001, Toth and Schmitz 1994); diterpenes (Garg and Agrawal 1995) and triterpenes (Fukami *et al* 1997). Cyclic peptides have also been described from the genus C*allyspongia* which includes phoriospongins A and B from *C. bilamellata* (Capon *et al* 2002), callynormine A from *C. abnormis* (Berer *et al* 2004) and callyaerins from *C. aerizusa* (Min, et al., 2001). Many natural product-producing fungi have been isolated from some *Callyspongia* sp., and cultivated on artificial media for production of natural products [spiciferone derivatives, macrolides, anthraquinones, and benzofuran have been isolated from *C. aerizusa*–derived fungi (Edrada *et al* 2000, Jadulco *et al* 2001, Jadulco *et al* 2002)]. The most attractive compound, that was isolated from *Callyspongia* sp., is callystatin A. Callystatin A is a potant cytotoxic polyketide isolated from Nagasakian marine sponge, *Callyspongia truncata* (Kobayashi *et al* 1997a), and due to the biological importance many studies have been carried out to synthesize this natural product (Murakami *et al* 1997, Lautens and Stammers 2002, Enders *et al* 2002, Vicario *et al* 2002).

Methanol extract of an Indonesian sponge *Callyspongia biru* was investigated in the present study and five compounds were elucidated. These compounds includes indole-3-carbaldehyde, *p*- hydroxyphenylacetic acid, *p*-hydroxyphenylacetic acid methylester, which have been described earlier (see compounds **15**, **26,** and **27**) in the present study, in addition to indole-3-acetic acid, and 2`-deoxythymidine.

3.6.1- Indole-3-acetic acid (39, known compound)

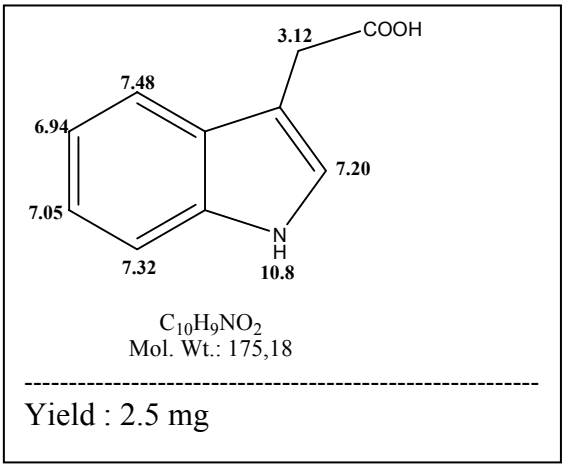

$C_{10}H_9NO_2$
Mol. Wt.: 175,18

Yield : 2.5 mg

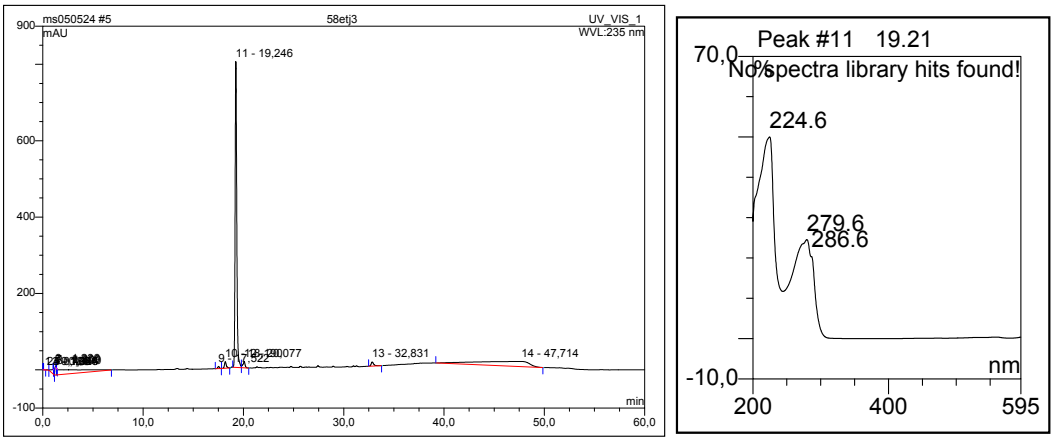

Fig (3.6.1) HPLC chromatogram and UV spectrum of compound 39

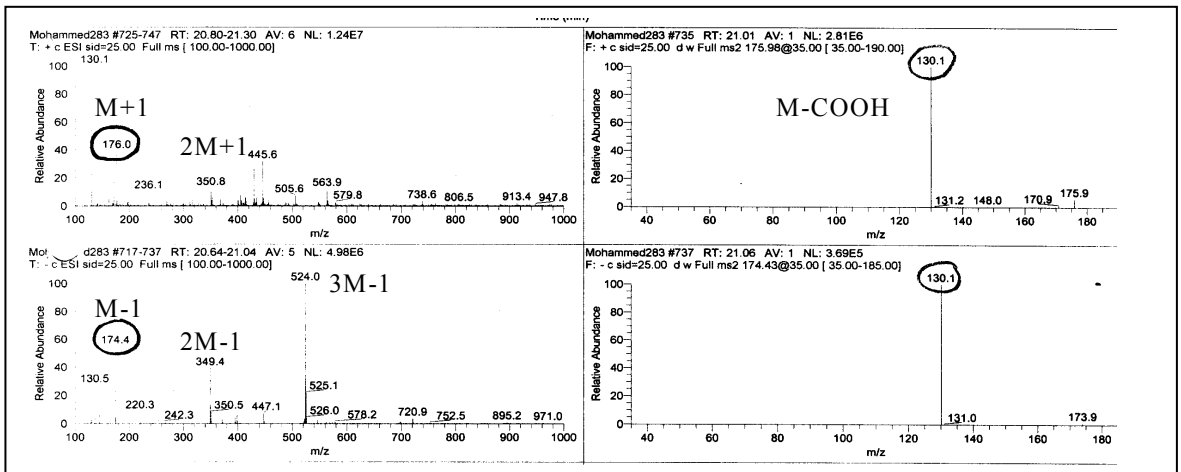

Fig (3.6.2) ESI-MS spectrum of compound 39

Compound **39**, [indole-3-acetic acid] was isolated as yellowish white amorphous powder. Compound **39** shows pseudomolecular ion peak at *m/z* 176 $[M+H]^+$ and in the negative mode at *m/z* 174 [M-H], 349 [2M-H], and 524 [3M-H] suggesting the molecular formula $C_{10}H_9NO_2$. The UV λ_{max} (MeOH) absorption of **39** was at 224, 279, 286 nm and were indicative of an indole chromophore. The ^1H NMR (measured in DMSO-d_6) showed 7 proton resonances that included an aromatic ABCD spin system at δ 7.48 (1H, d, *J* = 7.5 Hz, H-4), 6.94 (1H, t, *J* = 7.3 Hz, H-5), 7.05 (1H, t, *J* = 7.4 Hz, H-6), 7.32 (1H, d, *J* = 8.2 Hz, H-7). In addition to three proton resonances at δ 7.20 (1H, s , H-2), a most downfield broad singlet at δ 10.8 (1H, s , H-1) and singlet proton signal at δ 3.12 (2H, s , C*H*$_2$-8) were also observed. The NMR data and the UV absorption maxima were identical to those of indole-3-acetic acid (Aldrich, 1990 and Hiort, 2002).

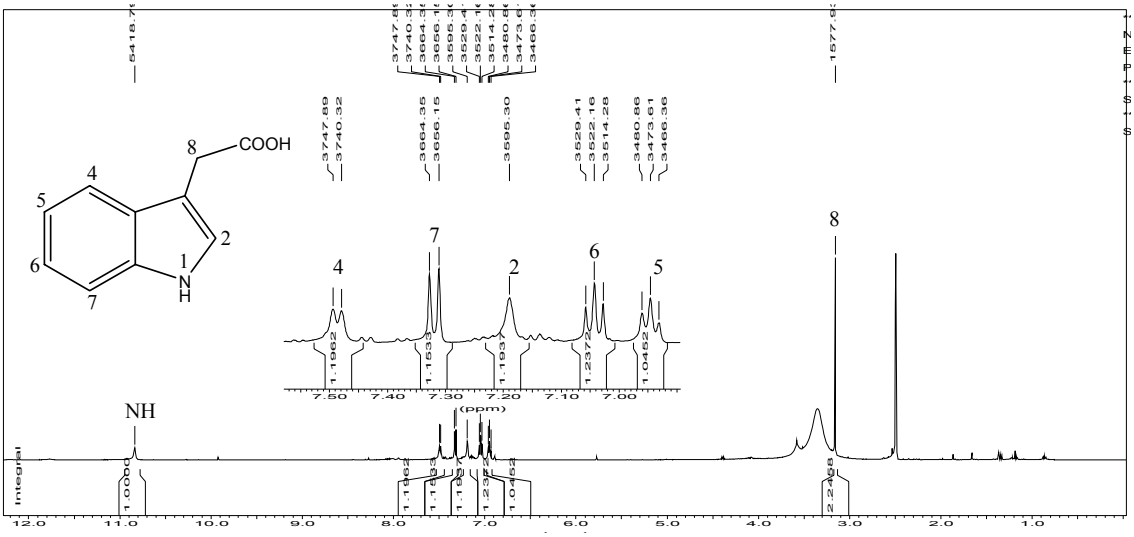

Fig (3.6.3) ^{1}HNMR spectrum of compound 39

3.6.1- 2'-Deoxythymidine (40, Known compound)

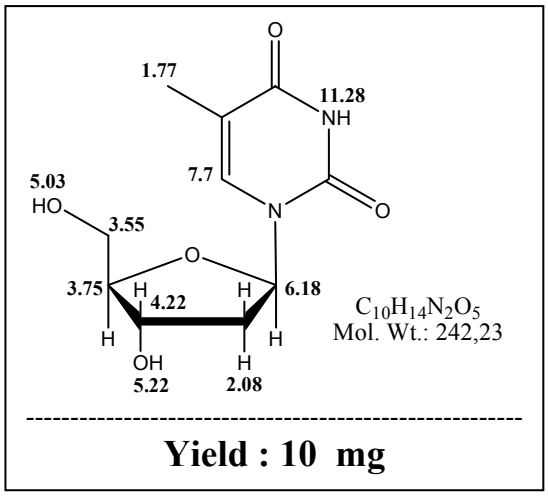

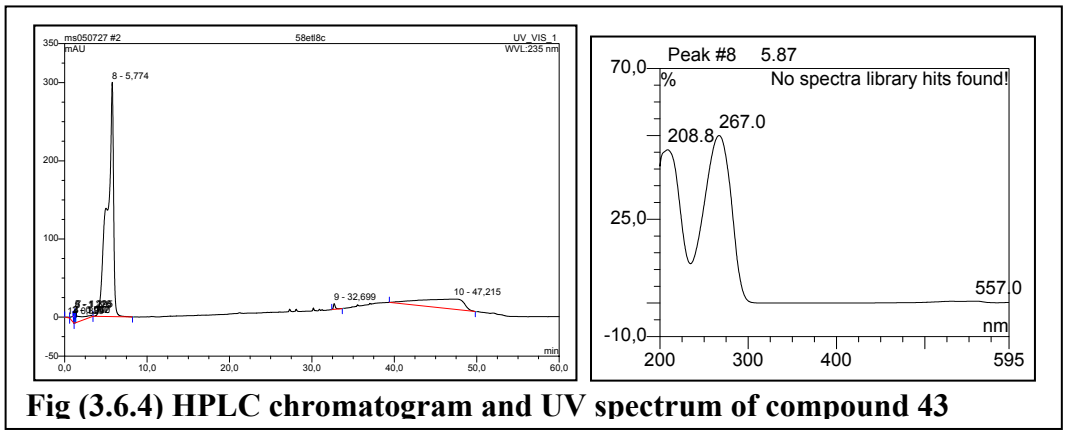

Fig (3.6.4) HPLC chromatogram and UV spectrum of compound 43

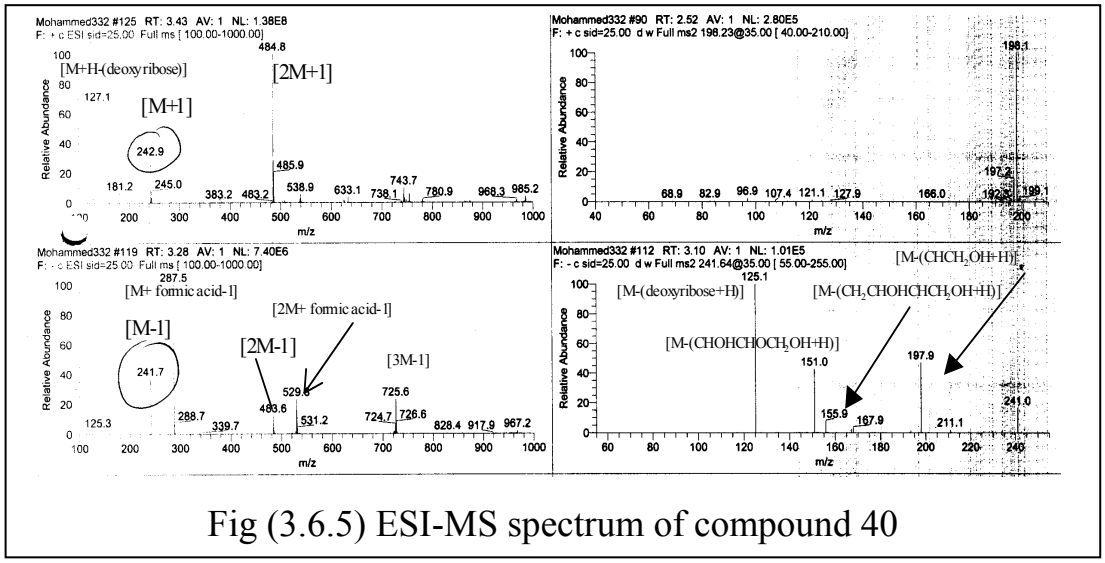

Fig (3.6.5) ESI-MS spectrum of compound 40

Compound **40**, [2'-deoxythymidine] was isolated as white amorphous powder. It showed pseudomolecular ion peaks at *m/z* 243 [M+H], 486 [2M+H], 241 [M-H], 287 [M+formic acid-H], 483 [2M-H], 529 [2M+formic acid -H], and 725 [3M-H] suggesting the

molecular formula $C_{10}H_{14}N_2O_5$. The UV λ_{max} (MeOH) of **40** at 208, and 267 nm was deduced for a nucleoside nature of the compound. Molecular ion fragmentation pattern confirmed the presence of thymine-2‘-deoxyribose (see figure 3.6.5). ^{1}H NMR spectrum showed a broad singlet at 11.28 (1H, s, 3-NH), 7.7 (1H, s, H-6), 6.18 (1H, t, *J* = 7.0 Hz, H-1'), 2.08 (2H, m, H-2'), 4.22 (1H, br s, H-3'), 3.75 (1H, dd, *J* = 6.6& 3.1 Hz, H-4'), 3.55 (2H, m, H-5'), 1.77 (3H, s, H_3-7). The ^{1}H NMR data were identical with those of thymine-2‘-deoxyribose (Aldrich 1992). From the above NMR data, mass fragmentation patterns, and UV spectrum, compound **40** was concluded to be thymine 2′-deoxyribose.

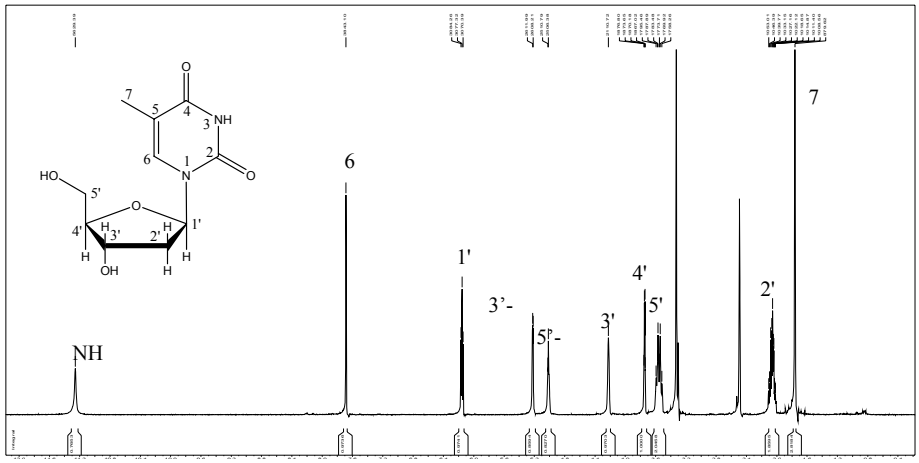

Fig (3.6.6) ^{1}HNMR spectrum of compound 40

Biological activity:

Total methanol extract, ethylacetate- and butanol-fractions along with n.butanol subfractions were tested for cytotoxic activity using the brine shrimp assay. The butanol subfraction (but-V) showed strong cytotoxic activity against the brine shrimp (*Artemia salina* Leach). This fraction was further chromatographed and purified to gave (But-Ve3) which seems to be alkylpyridinium compound. Howevere the structure elucidation of the compound is still under revision.

Deoxythymidine (compound **40**) showed cytotoxic activity 76.2 % and 41.7 % against L5178Y mouse lymphoma cell line at concentrations 3 and 10 µg/ml respectively.

IV- Discussion

The main target of the medicinal chemist is concerned about the exploration of new effective and less toxic medicaments. However, the main objective of the pharmacognosist or phytochemist is the presentation of this effective medicament from the natural sources. The essential topics that the phytochemist will be dealing with through the achievement of this task includes isolation, chracterisation, structure elucidation, and biological evaluation of the targeted natural products (Exarchou, *et al*, 2005; Lambert, *et al*, 2005).

Concerning the above mentioned topics many problems will be faced. However, the employment of the new technology in the field of natural product chemistry solved many of these problems. All parts of the process leading to an elucidated structure have experienced an immense speed-up in the past fifty years. Separation technology, analytical and spectroscopic methods have improved steadily and with good fortune, a chemist might be able to go from a crude extract to a full set of 2D NMR spectra in one day (Steinbeck 2004). It should be borne in mind that the above mentioned tasks (isolation, characterisation, structure elucidation, and biological evaluation) are only a part of the whole process of new drug discovery. Scheme 1 (Giersiefen et al., 2003), summarizes the whole drug discovery process.

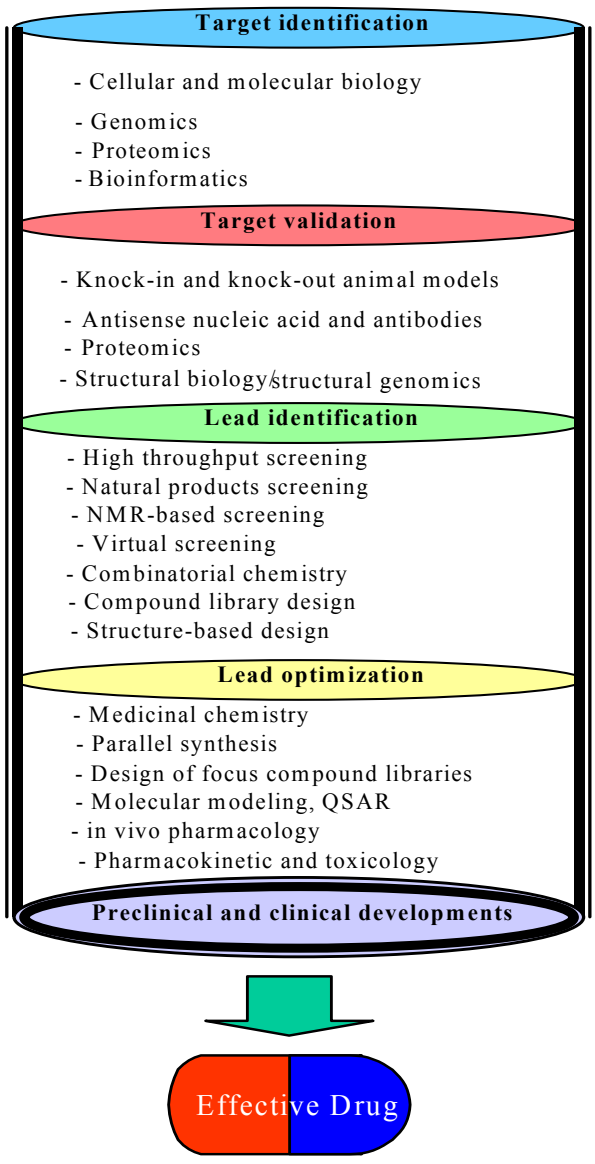

Scheme (1) phase of drug discovery process (Giersiefen *et al*., 2003)

4-1 Isolation, characterisation, structure elucidation, and biological evaluation of natural products:

4.1.1 Isolation of natural products:

Unlike the medicinal chemist, who usually concentrates on a series of synthetic compounds of known chemical and physical properties and hence is able to master the limited number of separation techniques applicable to the specific chemotype, the natural product chemist must be prepared to deal with molecules of the whole spectrum of bioactive metabolites. These can vary in hydro- and lipophilicity, charge, solubility, and size. (McAlpine and Hochlowski 1994). In general, the more hydrophilic metabolites may be candidates for ion exchange chromatography, reversed phase silica gel chromtography, or size exclusion chromatography on polysaccharide resins. The more lipophilic metabolites can be further purified by chromatography on normal phase silica gel, florisil, alumina, or lipophilic size exclusion resins such as sephadex LH-20. They may be also candidates for a variety of high-speed countercurrent techniques or chromatography on polyresins (McAlpine and Hochlowski1994). However, this branch of the main task of the natural product chemist was advanced to large extent. The production of many new packing materials, new isolation instruments with high degree of resolution and detection facilitated the chemist´s duty in this branch of the task. Some problems are still unresolved, for example, separation of individual pure compounds from mixture of cerebrosides, many trials were applied for achievement of this goal but unfortunately, all failed. The sphingolipids (cerebrosides) are easy to be separated as a mixture of closely similar chemical constituents from natural sources. However, they are very difficult to be separated from each other or in another word they are very difficult to be separated and purified to analytical purity. The difficulty arises probably from their chromatographic properties being overshadowed by the polar nature of the glycoside, thus making these metabolites difficult to separate to analytical purity (Jenkins 1999). Furthermore, the fact that, these metabolites are present oftenly as a series of very similar chemical nature, where the difference in most cases is one or two methylene groups, thus many of the published cerebrosides were reported as a groups of mixed compounds (e.g., Jenkins 1999& Inagaki 2003). However, HPLC in reversed-phase mode is now the standard method for separation of molecular species of cerebroside mixture, often after benzoylation so that the lipids can be detected by sensitive UV spectroscopy. Mass spectrometric methods are now being used increasingly for charaterization purposes of such sphingolipids (Christie, 2003)

4.1.2 Characterisation of natural products:

This branch of the task is the first step in structure elucidation. Therefore it is very important for the natural product chemist, he has to spend his effort and time to drive the structure proposal in the right direction. In contrast, the medicinal chemist, who is dealing with the synthetic chemicals, has no need to spend his time and effort here because he knew previously what type of chemicals he is dealing with. In the fact, there are many simple and general chemical tests that are widely available and more applicable since a long time, for example, Molish's test for carbohydrates, Mayer`s and Dragendorf`s reagents for alkaloids, alkali solution (e.g.NaOH, and KOH) for both anthraquinones and phenolic compounds. However, these reagents were intended to dissolve a small part of the problem. The phytochemist can not decide precisely and also confirm the structure using these simple reagents. These reagents tells us about the general chemical class to which the isolated compound may be related. But in most cases they give no idea about the subchemical class rather than the smallest details of the structure. Metabolite profiling is not an easy task to perform since natural products display a very important structural diversity. For each compound, the order of the atoms and stereochemical orientations have to be elucidated *de novo* in a complex manner and the compounds can not simply be sequenced as it is the case for genes or proteins. Consequently a single analytical technique does not exist, which is capable of profiling all secondary metabolites in the biological source (Wolfender, et al 2005). However, the employment of advanced analytical and spectroscopic methods like UV- and IR- spectroscopy solved such problems to a large extent, where they can give a good idea about the different substructures and/or functional groups of the structure. The hyphenated techniques coupled to HPLC give not only ideas about the details of functional groups, but also play an important role in what is called „Dereplication process" in order to avoid the tedious isolation of known compounds, and directed the chemist´s effort toward the targted isolation of constituents presenting novel or unusual spectroscopic features (Wolfender, *et al* 2005).

In the present study, a lot of chemical compounds that share the same chromophoric functions were examined by the hyphenated technique HPLC-UV-photodiode array detection (LC/UV-DAD). This examination showed that, all chemicals having the same chromophoric functions will show the same UV spectrum with the same absorption maxima even though they are different in their additional non-chromophoric functions and their molecular weights.

- Kahalalide F, (compound **1**, *m/z* 1478), R (**8**, *m/z* 1520) and S (**9**, *m/z*1536), all having the same chromophoric function and therefore showing the same UV spectrum and having approximately the same absorption maximum at ~ 203 nm.
- Kahalalide E (**2**, *m/z* 836), Kahalalide D (**2**, *m/z* 596), N,N-dimethyl tryptophan methylester. (**6**, *m/z* 246), indole-3-acetic acid (**39**, *m/z* 175), all having the same chromophoric function (tryptophan amino acid) and therefore showing the same UV spectrum and having approximately the same absorption maxima at ~ 220, 279 sh and 285 sh nm.
- A group of 3-acyl indole derivatives, e.g., hyrtiosine A (**13**, *m/z* 191), 5-hydroxy-1H-indole-3-carbaldehyde (**14**, *m/z* 161),), indole-3-carbaldehyde (**15**, *m/z* 145) and 5-deoxyhyrtiosine A (**16**, *m/z* 175) all having the same chromophoric function (3-acyl indole) and therefore showing the same UV spectrum and having approximately the same absorption maxima at ~ 210, 250, 275 and 300 nm. The same UV spectrum was obtained for the new indole derivative, isohyrtiosine A (**17**, *m/z* 191) with a little deviation in the UV-absorption maxima. Isohyrtiosine A showed an absorption maxima at 214, 241 and 286 nm due to the presence of carboxyl group instead of a ketonic group.
- New purine derivatives, nigricines 1-3 (**34**, *m/z* 307), (**35**, *m/z* 279), (**36**, *m/z* 265), all having the same chromophoric function (2-oxo-purine) and therefore showing the same UV spectrum and having approximately the same absorption maxima at ~ 210 and 290 nm. The same UV spectrum was obtained for both nigricine 4 (**37**, *m/z* 281), and adenosine (**30**, *m/z* 267), with a little deviations in the UV-absorption maxima. Ashourine 4 showed an absorption maxima at 214 and 315 nm due to N(7)-methylation and loss of one double bond at position 8, while adenosine showed an absorption maxima at 207 and 257 nm because it has no 2-oxo- group.
- *p*-Hydroxyphenyl acetic acid, and its methyl-, ethyl- and butylesters, [(**26**, *m/z* 152) (**27**, *m/z* 166) (**28**, *m/z* 180) and (**29**, *m/z* 208)] all having the same chromophoric function (4-hydroxyphenyl) and therefore showing the same UV spectrum and having approximately the same absorption maxima at ~ 202, 224 and 275 nm.

However, the compounds that have no chromophoric functions can not be characterised by LC-UV hyphenated technique.

Also, NMR spectroscopy play a significant role in characterisation of natural products:

The peptide nature of isolated kahalalides (compounds **1-5**, **8**& **9**) was suggested by:

1) From ^{1}HNMR, the presense of amide N*H*s resonating in the downfield region between 7.0-9.0 ppm, α-protons resonating arround 4.0 ppm and the C*H*$_3$ groups resonating in the higher field region arround 1.0 ppm.
2) From ^{13}C NMR, The presence of amide carbonyls resonating arround 170 ppm, α- carbons (sp^3 methines) resonating between 50-60 ppm and methyl carbons in the higher region.
3) From a COSY, each amino acid could be distinguished by a sequential correlations beginning from the amide NH, through α-, β-, γ- to the methyl protons which could be confirmed by the total correlation spectroscopy (TOCSY).

- The cerebroside nature of compounds 32 and 33 (petrocerebrosides 1 and 2) were established from the ^{1}HNMR which showed a triplet-like signal at δ 0.82 (terminal methyls) and broad singlet at δ 1.2 (long chain $(CH_2)_n$ groups for both fatty acids and long chain bases), the presence of several doublets in the region between 4.2-5.3 ppm indicated the presence of many OHs (of the sugar parts), the presence of multiplet signals between 3.35 and 5.0 ppm indicated the presence of sugar CHs. In addition to one amide N*H* in the lower field region rather than the sp^2 methines in aromatic region between 5.0 – 9.0 ppm region. This suggestion cauld be supported by the presence of amide carbonyl signal in ^{13}CNMR at approximately 170.0 ppm.
- The steroidal nature of the isolated steroidal compounds and also the scalarane type sesterterpenoids could be suggested from ^{1}HNMR by the presence of a characteristic methyl around 1.0 ppm and presence of overlaping methylenes and sp^3 methines in the higher field region between 1.0 and 2.0 ppm, which was supported by a characteristic ^{13}C-NMR spectrum.
- *p*-Disubstituted phenyl group could be distinguished from ^{1}HNMR by the presence of two doublets inter-correlated at approximately 6.8 and 7.2 ppm (especially for 4-hydroxy-1-substituted phenyl group), for example, tyrosine-containig natural products (kahalalide B, compound 4), and *p*-hydroxyphenylacetic acid and its derivatives (compounds 26, 27, 28 and 29).
- 3-Substituted-indole could be easily distinguished from ^{1}HNMR by the presence of ABCD spin system in the aromatic reagion (approximately between 7.00 and 8.2 ppm) for proton resonances of H-4, H-5, H-6 and H-7, in addition to a relatively sharp singlet or in rare cases doublet with small coupling constant of H-2 between 7.0 and 8.0 ppm. Furthermore the sharp singlet in the down field region between 10.0 and 12.5 ppm indicating the indole NH. The present examples are compounds 2, 3, 6, 15, 16, 38, and 39. In contrast 5-hydroxy-3-substituted indole displays an ABM spin system

(approximately between 6.80 and 8.0 ppm) for proton resonances of H-4, H-6 and H-7 instead of the above ABCD spin system (see ^{1}H NMR of compounds 13, 14 and 17).

Mass fragmentation pattern, could play a significant role in characterisation of natural products:

- Comparison of the MS fragmentation of the isolated compound with those of the known authentic samples may be enough not only for characterisation of substructures but also for full structure elucidation of the compounds (e.g. compounds 27 and 31).
- MS fragmentation pattern may be helpful in characterisation of some substructures which seem difficult to be distinguished by other means, rather than they are also helpful in establishing the relation between the closely related natural products, for example, the characteristic loss of 42 mass unit through retro Diels-Alder fragmentation from the new purines, nigricines 1-4, (compounds 34-37) indicated the presence of 2-oxo-purine derivatives and consequently the loss of NCO fragment, thus, the closed relation between them could be established.
- MS fragmentation mechanisms (e.g. tandem ESI/MS and MALDI-TOF-PSD) are described as the methods of choice in characterisation and confirmation of the amino acid sequence of the isolated peptides, for example, kahalalides F, E, D, B, C, R and S (compounds 1, 2, 3, 4, 5, 8 and 9 respectively).

4.1.3 Structure Elucidation of Natural Products:

After the characterisation of the isolated natural product and determination of the subchemical class to which the compound is related, the phytochemist has to demonstrate unambigiously the small details of the substructures and consequently the elucidation of the complete structure. Structure elucidation of the isolated new natural product is still the bottleneck of the objective achievement. Actually, the new technology in the field of NMR spectroscopy (including 1D- and 2D- NMR experiments) and mass spectrometry facilitated the chemist´s effort in this part of the whole task. Furthermore, the presence of commercial and non commercial computer-assisted structure elucidation (CASE) programs even though they are not widely available and less applicable nowadays but may be the method of choice in the near future. It is important to say that the interaction between a spectroscopist and a CASE system will remain important in order to generate the correct structure rapidly. Therefore CASE will complement the skills of the spectroscopist, not replace them. The use of CASE system is likely to increase in the near future, and this will enable the bottleneck so often caused by structure elucidation to be removed from the natural product drug discovery process (Jaspers 1999).

4.1.4 Biological evaluation of natural products:

In general, drug discovery strategies can be trivially separated into three categories:

1. Chemically driven, finding biological activities for purified compounds.
2. Biologically driven, bioassay-guided approach begining with crude extracts.
3. Combination of chemically and biologically driven approaches (vide infra). (McConnell *et al.* 1994)

Beginning in the 1970´s through today, the majority of the academic-based research efforts has become essentially „biologically driven“ i.e., the object of the search has shifted to discover natural products with biological activity. The biological activities include exploring their potential as agrochemicals (Crawley 1988) and pharmaceuticals, as well as their possible chemical ecological roles (Bakus et al. 1986; Hay and Fenical 1988).

Drug discovery in industry has evolved to the use of specific assays with target receptors and enzymes involved in the pathogenesis of disease rather than cellular or tissue assays (Johnson and Hertzberg 1989), and has benefitted immensely from breakthroughs in receptor technology (Hall 1989; Reuben and Wittcoff 1989). These assays reflect new opportunities due to the recent identification of previously unrecognized biomolecular targets for therapy (Larson and Fischer 1989). More specifically, this approach for most disease areas is characterized in industry by:

1. Essentially exclusive reliance on biological activity of crude extracts in numerous target-specific assays, i.e., enzyme assays and receptor-binding assays, for selection of crude extracts and bioassay-guided fractionation of the crude extracts (prioritization criteria emphasize selectivity and potency).
2. High volume, automated screening, i.e., thousands of samples per year for smaller companies and thousands per week for larger companies.
3. The use of „functional“ or whole-cell assays to confirm activity in a particular disease state and to further prioritize samples for fractionation.
4. The use of genetically engineered microorganisms, enzymes, and receptors.

Because of low correlation between cytotoxity and antitumor activity, a number of programs have utilized *in vivo* tumor models directly for drug discovery (Johnson and Hertzberg 1989). From 1958 through 1985, National Cancer Institute (NCI) used in vivo L1210 and P-388 murine leukemia assays as primary screens (Suffness *et al*. 1989; Boyd *et al*. 1988) and was successful primarily in identifying compounds possessing clinical activity against leukemias and lymphomas. Unfortunately, they were not very successful in finding

compounds active against slow growing tumours in humans. Further, these *in vivo* assays were expensive, time consuming, and relatively insensitive (Suffness *et al*. 1989). In other disease areas it was shown that activity in *in vitro* antiviral assays does not translate well to *in vivo* activity, e.g., using *Herpes simplex.* In contrast, reasonable correlations exist between *in vitro* and *in vivo* antifungal activity, e. g., using *Candida albicans*.(McConnell *et al*., 1994).

General or non-specific cytotoxic assays could be insufficient to prove or disprove the activity. For example, the known antitumour drug candidate (kahalalide F, compound **1**) shows no cytotoxic activity against *Artemia salina* using brine shrimp assay even though it has potent antitumour activity.

Using bioactivity guided isolation, it should be borne in mind that the active substance may be present at very low concentration in the total extract and/or subfractions otherwise many active compounds will be rejected at an early stage because of lack of significant activity. Firn and Jones 1996, mentioned some limitations that affect the biological activity studies of the secondary metabolites and consequently minimize the chance of detecting high biologically active compounds, specially for commercial use, for example:

- The high selectivity required for a biologically active substance means that many active compounds will be rejected at an early stage because of lack of specificity.
- Some active compounds are unstable and are either lost during isolation or are unsuitable for use .
- Some compounds have already been isolated (and possibly patented before).
- The type of biological activity found is not meaningful in terms of the particular usage sought.
- The screening process is inappropriate.
- Some forms of biological activity are dependent on the presence of other compounds (synergists) which are lost during the purification processes before the substance is bioassayed.

4.1.5 Technology of HPLC:

High performance liquid chromatography (HPLC) including both normal and reversed phases (RP) is now a well-developed and widely used technique for separation of complex mixtures (Exarchou, *et al,* 2005). HPLC is now available in many forms of hyphenated systems such as LC-UV, LC-mass spectroscopy (LC-MS, LC-MS-MS) and LC-NMR which has been successfully and practically achieved in the last decade. (Wolfender, et al 2005, and Exarchou, *et al*, 2005). With the aid of the modern HPLC-coupled spectroscopic techniques

such as HPLC-UV, HPLC-MS as well as HPLC-NMR, the main constituents of plants that are frequently used in traditional Chinese medicine have been characterized and identified. As well as compared with reference compounds (Zschocke *et al* 2005; Albert 2002; Wilson, *et al* 1999).

Analytical HPLC that is coupled to a UV detector is ideal for detection of most natural products that possess chromophoric functions in their structures. However, in some cases, HPLC-UV hyphenated systems fail to detect the important biological substances such as purine derivatives, nucleotides and other similar small biologically active metabolites, the presence of acidified water as a part of the mobile phase make the nitrogenous compounds protonated (in other word, highly polar according to the affinity of that compounds to accept protons), which in turn elute the compounds very rapidly and in some cases can not be detected with the UV-detector). This problem prompted some analytical chemists (e.g. Nordström *et al* 2004) to derivatise such basic compounds to be more hydrophobic, consequently improve their retentions on reversed phase materials and enhance their ESI response in the case of LC-MS analysis. The use of o*rtho*-phosphoric acid in maintainence of the mobile phase-pH around 2 give a good compound-separation, allowing the UV-detector to impart sharp peaks with high resolution, but it is not compatible with all possible analytes. In some cases of poly-nitrogenous compounds (new purine derivatives and known compound adenosine in the present study), phosphorylated H_2O (pH 2) rendered the compounds very polar, providing very short retention time and consequently masking their detection by UV detector. The following example will explain the effect of *o*-phosphoric acid in masking peaks of purine derivatives during HPLC analysis.

From the above example, it was clear that, low concentrated analyte couldn`t be detected by elution of the sample with eluant composed of pH 2 aqueous solution as in fig **4**.**1**.**A.** In contrast, the same sample concentration could be easily detected (fig **4**.**1**.**B**) through elution with mobile phase composed of neutral H_2O (free of phosphoric acid). Furthermore, high concentrated sample (fig **4**.**1**.**C**) provides a broad peak with relatively low resolution and short retention time by elution with mobile phase that composed of pH 2 water. while sharp peak with high resolution separation and relatively delayed retention time could be obtained through elution with mobile phase composed of neutral water (fig **4**.**1**.**D**).

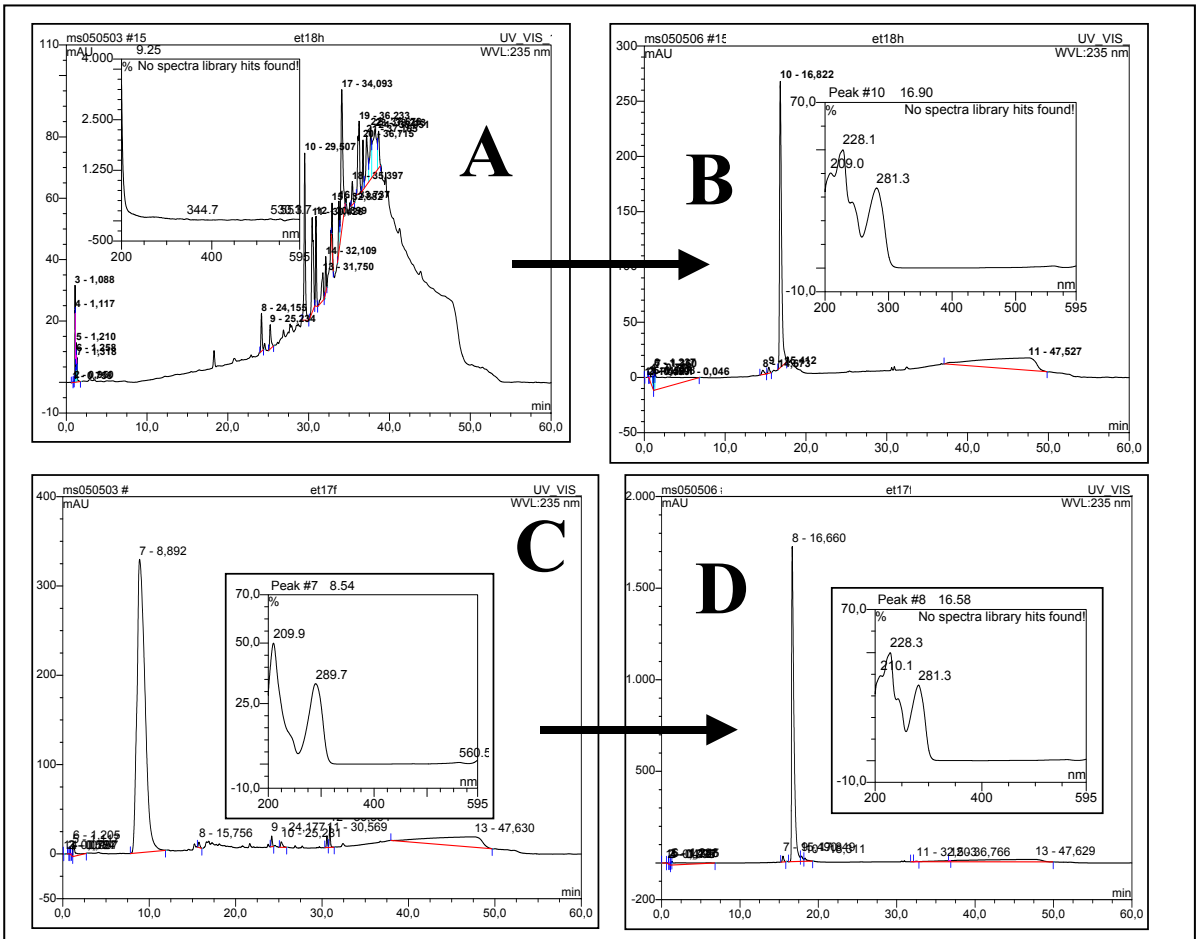

Fig(4.1) different HPLC chromatograms of a new purine derivative (compound **35**, ashourine 2); **A**: diluted solution, the chromatogram was obtained after running in HPLC using acidic aqueous solvent (pH 2); **B**: the same sample of **A**, the chromatogram was obtained after running in HPLC using neutral water (pH 7); **C**: concentrated solution, the chromatogram was obtained after running in HPLC using acidic aqueous solvent (pH 2); **D**: the same sample of **C**, the chromatogram was obtained after running in HPLC using neutral water (pH 7).

This problem during analysis by HPLC hyphenated systems confirmed that some of the important bioactive natural products may be undetected even though they have adequate chromophoric functionalities especially when present at low concentrations (as the case during an early stage of their isolation from biological sources).

The same problem would be faced during LC-MS analysis of such compounds. Two major problems are associated with LC-MS analysis. First, no universal LC column packing material can be used for all possible kinds of analytes. Second, no eluent system is compatible with both all possible analytes and ESI. A compromise has to be made at some level

regarding the packing material, eluent system, or analyte response. Positive ESI is an excellent interface for reversed-phase chromatography. The solvents used, acidic acetonitrile/MeOH-H_2O mixtures, are suitable for the desolvation process. However, many biologically important compounds do not separate readily on reversed-phase packing material due to their high polarity. The need for acetate or formate buffers or ion pairing reagents often hampers the ESI response (Nordström *et al* 2004). During the LC-MS analysis of the new purine derivatives (compounds nigricines **1-4**), adenosine (compound **30**) and nicotinamide (compound **31**), it was noted that, only the more hydrophobic compound, nigricine **1**, could be measured by LC-MS while the sensitivity was decreased as the side chain (alkoxy group) was decreased. Adenosine and nicotinamide couldn`t be analysed in the same condition.

Hyphenated HPLC systems play a significant role in comparison the components of biological extracts or mixtures of substances and a previously known compounds. Thus, the tedious isolation of known compounds can be avoided and a targeted isolation of constituents presenting novel or unusual spectroscopic features can be undertaken. (Wolfender, *et al* 2005).

Furthermore, HPLC-UV-MS hyphenated system is the method of choice for detection the absolute configuration of amino acids and thus helps in the unambiguous structure elucidation of new peptides not only by indication of certain amino acids of which the peptide composed but also by detection and confirmation of stereochemistry of the amino acid. HPLC analysis of the kahalalide hydrolysates after derivatisation by Marfey`s reagent, N-(5-flouro-2,4-dinitrophenyl)-L-alanine amide (FDAA), and comparison of their retention times and molecular weights with those of authentic diastereoisomer amino acids which were treated in the same manner confirmed the stereochemistry of the kahalalide amino acids (see figures **3.1.11-3.1.15**). Due to some of an expected negative effects of factors such as concentration of the sample, or minute changes in the solvent gradient or in the pH of the mobile phase that could affect the retention times, peak enrichment technique was applied to give unambiguous streochemistry determinations. This procedure was made by co-elution of the kahalalide hydrolysates together with the expected standard amino acids at the same time. Complete overlapping of both standard and test amino acid peaks indicated complete stereoidentity (see figures **3.1.11**).

LC-ESI/MS/MS hyphenated systems supported online amino acid sequencing of a mixture of peptides without separation and purification which in turn avoid the cost of

expensive adsorbents and eluents, and save the time and effort that may be lost during isolation of known peptides, and for cheking whether a compound that is intended to be isolated is a genuine new peptide (Bringmann and Lang 2003). The same advantages could be obtained by online LC-NMR analysis (Wolfender, et al 2005).

4.2. Isolated compounds from genus *Elysia* (sacoglossan mollusc):

Genus *Elysia* is known as a rich source of bioactive natural products such as diterpenoids (Paul and Van Alstyne 1988) polypropionates (Gavagnin, *et al* 1994, Cueto *et al* 2005) and depsipeptides (Hamann and Scheuer 1993, Hamann *et al* 1996, Goetz *et al* 1997, Horgen *et al* 2000, Dmitrenok *et al* 2006). *Elysia*-derived depsipeptides known as kahalalides consist of 3 to 13 amino acid units, ranging from a C_{31} tripeptide to a C_{75} tridecapeptide, with cyclic and linear components, the latter terminating in a saturated fatty acid moiety. Ten of these derivatives are cyclic depsipeptides, kahalalides A to F, K, O, P,and Q while three analogues, kahalalides G, H, and J are linear peptides. Kahalalide F and its linear analogue kahalalide G as well as the two new kahalalides R and S are the only congeners that feature the unusual amino acid, *Z*-dehydroaminobutyric acid (*Z*-Dhb). The methanol extract of *Elysia grandifolia* showed a promising biological activity such as antimicrobial, cytotoxicity, feeding deterrence and icthyotoxicity (Padmakumar 1998, Bhosale et al, 1999). These bioactivities attracted our attention to investigate the methanol extract of the mollusc. The investigation which was guided by online LC-MS analysis resulted in the detection of many known kahalalides [kahalalides B, C, D, E, F, G, J, K, O (see figures 2-15 and 2-16)] with regard to their molecular weights and amino acid sequences through interpretation of ESI-MS fragmentation patterns. The presence of two unidentified peaks at m/z 1520.2 and 1536.0 aroused our interest to do further chemical work on the mollusc extract. A steady continuous effort led to the isolation characterisation, and full structure elucidation of two new depsipeptides, kahalalides R and S.

4.2.1 Which of the following organism is actually responsible for kahalalides production? The animal sacoglossan mollusc (*Elysia* sp.), the plant *Bryopsis* sp (algal diet of the mollusc), or the procaryotic symbiont bacterium (*Vibrio* sp.) ?

The green algal diet, *Bryopsis* sp., has been found to yield kahalalides A, B, F, G, K, P, and Q. Kahalalides A-K were isolated from the molluscan *E. rufescens*, while kahalalide O was isolated from *E. ornata*. In the present study, the corresponding molecular ion peaks of kahalalides B, C, D, E, F, G, J, K, O as well as the new congeners R and S have been characterized from online LC-ESI-MS analysis of the methanol extract. Furthermore , kahalalide F was produced by a symbiont bacterium *Vibrio* sp. associated with both the specialist herbivore mollusc *Elysia* sp and their algal diet *Bryopsis* sp (Ashour *et al* 2006).

The existence of the kahalalides in the extracts of these taxonomic unrelated groups of organisms (animal, plant and procaryote) led the question: which of these organisms is actually responsible for kahalalides production?

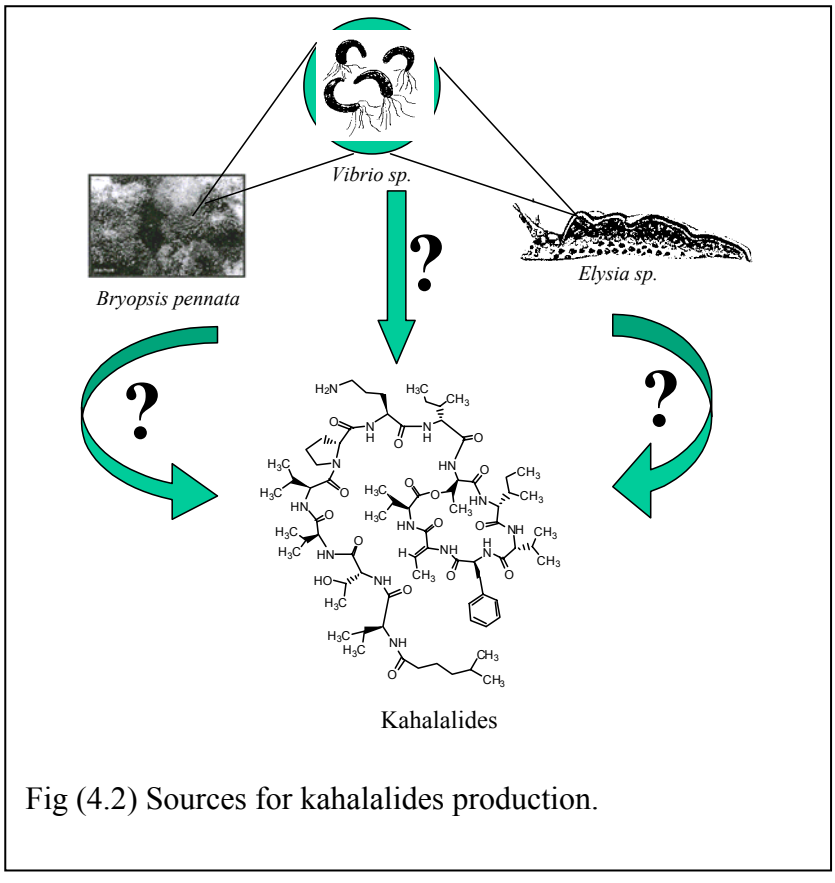

Fig (4.2) Sources for kahalalides production.

- kahalalides, especially the major one (kahalalide F) play an important ecological role, since it was reported that they show significant antipredatory effects against fish predation (Becerro *et al* 2001). Thus, these compounds increase the fitness of the mollusc even though they play no role in primary metabolism.

- Hamann and Scheuer 1993, stated that the herbivorous sacoglossan mollusc *E. rufescens* has the ability to sequester from their algal diet „*Bryopsis sp*“ functioning chloroblasts, which then perhaps may participate in the biosynthesis of secondary metabolites (Hamann and Scheuer 1993).
- It was hypothesized that *E. rufescens* acquires Kahalalide F–producing *Vibrio* from the surface of the algal diet *Bryopsis* sp and maintain these microbes as symbionts (Ashour *et al* 2006).
- According to the natural product definitions (Bennett 1995 and Firn 2004) it is considered that kahalalides are actually secondary metabolites or true natural products since they are not active participants in primary metabolism and have no function in growth. Consequently their production is restricted to certain closely related taxonomic groups of living organisms. Therefore it is not accepted that the above mentioned organisms of completely different taxonomic groups (animal, plant and procaryotic members) are responsible for production of one chemical class of closely related secondary metabolites.

This discussion led to the following conclusion:

1- Kahalalides may be procaryotic products, produced by *Vibrio* bacterium and accomulated in both algae and mollusc. (the most likely scenario, but needs further confirmation).

2- Kahalalides may be plant products, since their production by *Vibrio* sp is still unconfirmed (there is no true publication that describe the natural production of the kahalalides by procaryotic organisms)

3- Kahalalides may be procaryotic products, produced by *Vibrio* bacterium, and their production by plant, *Bryopsis* sp, may be attributed to a possible spontaneous transplantation of a responsible gene from the bacterium to the plant

4- It is not accepted that kahalalides are actually animal products because of their production by another completely unrelated organisms, and the presence of kahalalides in the animal extract may be attributed to accomulation of the secondary metabolites by contineous intake of the algal diet *Bryopsis* sp.

5- It is possible that kahalalides are plant or bacterial products liable to modification through the molluscan metabolism.

6- The isolation of β-sitosterol (compound **7**) and a previously known plant secondary metabolite (N,N-dimethyltryptophan methylester, compound **6**) from the animal extract may confirm the plant responsibility for the production of the kahalalides.

However, this interesting point needs further study and explanation from the biosynthetically oriented chemists.

4.2.2 The possible biosynthetic pathway of kahalalides:

In spite of the long debating discussion about the producing organisms, the kahalalides are considered as non-ribosomal depsipeptides (Marahiel et al 1997). The possible biosynthetic pathway of kahalalides (as depispeptide natural products) was obtained from the references (Marahiel et al 1997 and Schwarzer et al 2003). The kahalalide biosynthesis may be supported by large multifunctional enzymes called non-ribosomal peptide synthetases. The depsipeptides are assembled from diverse groups of precursors including pseudo-, non proteinogenic, hydroxy, N-methylated, and D-amino acids. These peptides then undergo further modifications that lead to additional structural diversity. A typical enzyme module - concerning the depsipeptide biosynthesis – consists mainly of three steps as shown in figure 4.2

a) Adenylation domain (A): responsible for amino acid activation .
b) Thiolation domain (T) or peptide carrier protein (PCP): responsible for thioestrification of the activated amino acids by the attachment to the cofactor, phosphopantotheiene.
c) Condensation domain (C): responsible for the peptide bond formation to elongate the growing peptide chain.

The modification (e.g. epimerization, cyclization, N-methylation, reduction and/or oxidation) of the peptidyl substrate during this process takes place according to special considerations regarding the essential properties of the individual species.

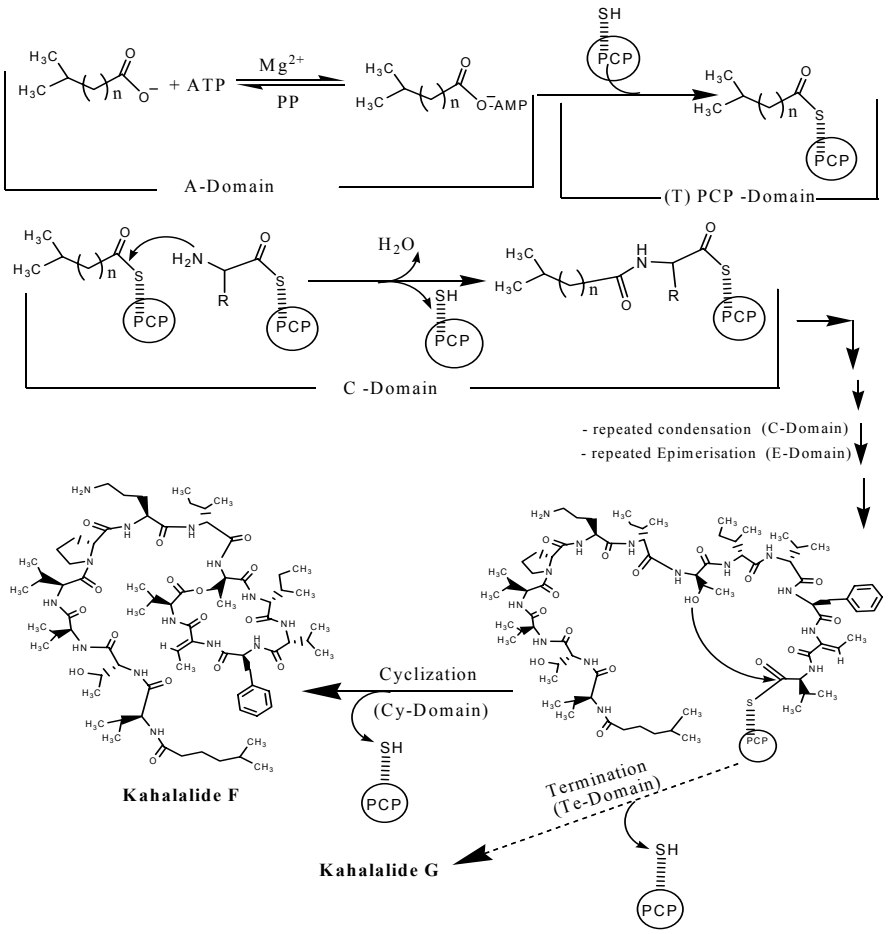

Scheme (4.2) Possible biosynthetic pathway of kahalalide F (modified from Schwarzer *et al* 2003)

4.2.3 Structure-activity relationship:

In an agar diffusion assay, kahalalide R at a disc loading concentration of 5 µg, showed strong antifungal activity against the plant pathogens *Cladosporium herbarum* and *C. cucumerinum* with inhibition zones of 16 and 24 mm, respectively. These results were almost identical to those of kahalalide F, which exhibited its fungicidal activity with inhibition zones of 17 and 24 mm, respectively, at the same concentration as kahalalide R. Using the same concentration, the fungicidal activity of kahalalides F and R were also comparable to that of nystatin showing inhibition zones of 19 and 39 mm, respectively. other kahalalides exhibited neither antibacterial nor antifungal activities.

The known derivatives, kahalalides B, D, E, F, together with the new congeners, kahalalides R and S were assayed for their cytoxicity toward L1578Y, HELA, PC12, H4IIE,

and MCF7 cancer cell lines. Kahalalides F and R were found to be comparably cytotoxic toward MCF7 cells with IC_{50}-values of 0.22 ± 0.05 µmol/L and 0.14 ± 0.04 µmol/L, respectively. Kahalalide S and E were less cytotoxic in MCF7 cells with IC_{50}-values of 3.55 ± 0.7 µmol/L and 4.5 ± 0.49 µmol/L, respectively. Kahalalide R was cytotoxic towards the mouse lymphoma L1578Y cell line at an IC_{50} of 4.28 ± 0.03 nmol/mL, which is almost identical to that of kahalalide F with an IC_{50} of 4.26 ± 0.04 nmol/mL. The kahalalides including kahalalides F and R were found to be inactive toward HELA, H4IIE and PC12 cancer cell lines. This implied the cytotoxic selectivity and specificity of kahalalides F and R. Furthermore the depsipeptide, kahalalide G, (linear analogue of kahalalide F) lack the antitumour activity (Hamann *et al* 1996). This overview indicated that :

1) the presence of the sequential fragment [Val-1-Dhb-Phe-Val-2-Ile-1-Thr-1] with lactone bond is essential for the antitumour activity.
2) The activity is not affected by substitution of Ile-1 with Valine (as in kahalalide R)
3) Opening of the lactone ring results in loss of the activity (as in kahalalide G)
4) The presence of terminal fatty acid (5-MeHex or 7-MeHex) is also responsible for the activity
5) Hydroxylation at position 5 of the fatty acid (7-MeHex) is responsible for decreasing the activity (as in kahalalide S)
6) The activity is not affected by substitution of The -2 and Val-5 of kahalalide F with Val and Glu respectively (as in kahalalide R).
7) The streochemistry of individual valines is responsible for the biological activity.

4.3 Isolated compounds from unknown *Pachychalina* sp:

4.3.1 Epidioxy Sterols

Chemical investigation of unknown Indonesian sponge *Pachychalina sp* led to isolation and structure elucidation of two 5α, 8α- epidioxy sterols (compounds **10** and **11**), as well as of the previously known *Octopus* derived natural product, 8-hydroxy-4-quinolone (compound **12**)

Many of the reported 5α, 8α- epidioxy sterols showed significant biological activity including antimycobacterial activity (Cantrell *et al* 1999), inhibitory activity against the human T-cell leukemia/lymphotropic virus type I (HTLV-I) and cytotoxic activity against the human breast cancer cell line (MCF_7 WT) (Gauvin *et al* 2000), and antitumor activity against different tumour cell lines (Bok *et al* 1999). 8-Hydroxy-4-quinolone (compound **12**) was reported to be one of the ink components that is ejected by the giant octopus *Octopus dofleini*

martini which was reported to have antipreditory activity (Siuda 1974). Some other quinolone analogues (e.g. 3,8-dihydroxyquinoline) showed mild cytotoxic activity against the growth of several human tumour cell lines(Moon *et al* 1996).
Cytotoxicity study of compounds **10** and **11** showed activity with growth inhibitory activity of 57.2 % and 38.6 % for compounds **10** and **11** respectively at concentration of 10µg/ml each against L5178Y cancer cells. Compound **12** showed no significant antimicrobial activity.

Biosynthetic pathway of 5α, 8α- epidioxy sterols:

Steroids are formed biosynthetically from active isoprene, isopentenyl pyrophosphate, (see figure 4.3) which involve the same pathway as those for terpenoid biocynthesis. The triterpenoid squalene is an intermediate in the steroid biosynthesis (Dewick, 1997). Oxidation of $\Delta^{5,7}$ steroid results in formation of 5-, 8- epidioxysterol, this oxidation can be produced spontaneously or enzymatically (Gunatilaka *et al* 1981)

Until recently, reservation has been expressed that naturally isolated ergosterol peroxides may be an artefact (Gunatilaka *et al* 1981). However White and co-workers (Bates *et al* 1976) investigated the conversion of ergosterol into its epidioxide in two unrelated fungi and demonstrated that both chemical (photooxidation) and enzymatic pathways are operative. Gunatilaka *et al* 1981 suggested that the peroxidation of ergosterol and semilar $\Delta^{5,7}$ sterols is a biological process and is aided by peroxidases. This suggestion was confirmed by the recent isolation of polyketide peroxides from a number of marine sponges (Stierle and Faulkner 1980). Gauvin *et al* 2000 considered that these peroxides may be biosynthetic precursors for $\Delta^{4,7}$-3,6-diketones where both chemical groups were isolated together from the marine sponge *Raphidostila incisa*. Furtheremore, Serebryakov *et al* 1970 isolated such epidioxy sterols from fungi in the absence of oxygen. However, these epidioxysterols and their analogues were previously isolated from many unrelated sponge species for example *Axinella cannabina* (Fattorusso *et al* 1974), *Tethya aurantia* (Sheikh and Djerassi 1974), *Raphidostila incisa* (Malorni *et al* 1978), *Thalysias juniperina* (Gunatilaka *et al* 1981), *Haliclona rubens* (Calderon *et al* 1982), *Hyrtios sp*.(Koch *et al* 1983), *Axinissa sp*.(Iguchi *et al* 1993),and *Dysidea. fragilis*. (Elenkov et al 1994).

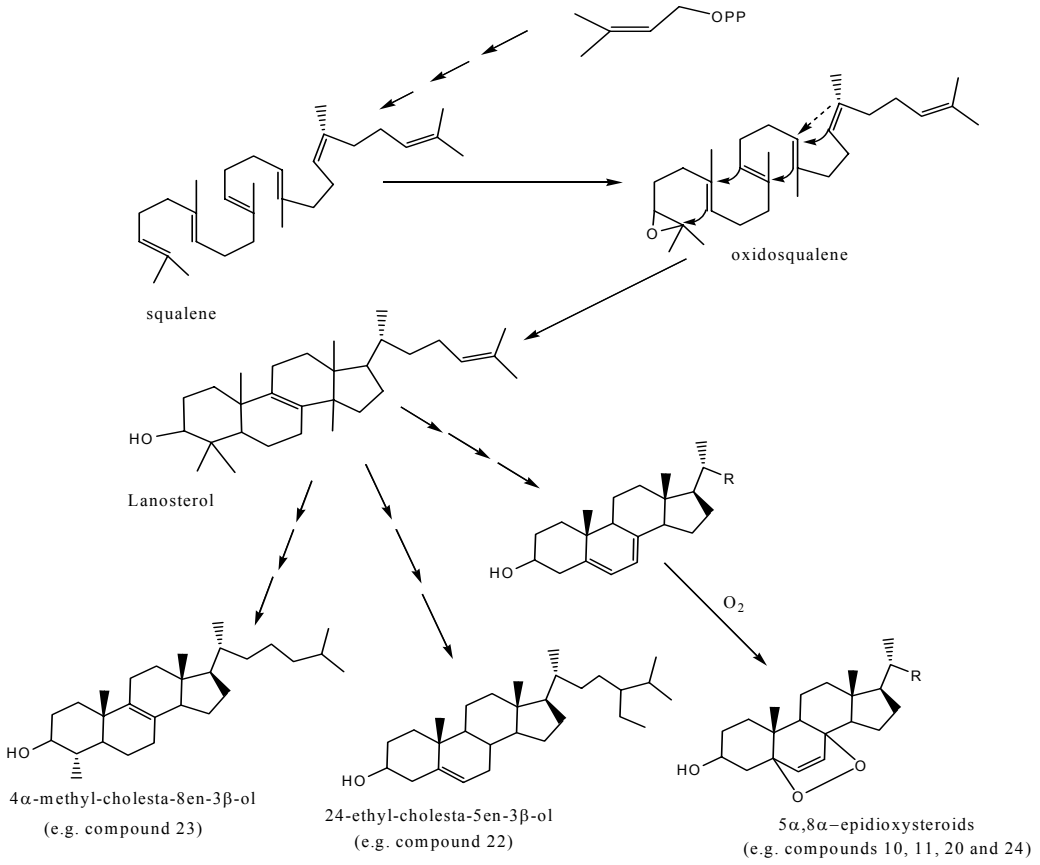

Scheme (4.3) The biosynthetic pathway of steroids

The possible biosynthetic pathway of 8-hydroxyquinolin-4-one from *Pachychalina sp*. may include acetylation and cyclization of *o*-aminobenzoyl CoA as explained in (scheme 4.4)

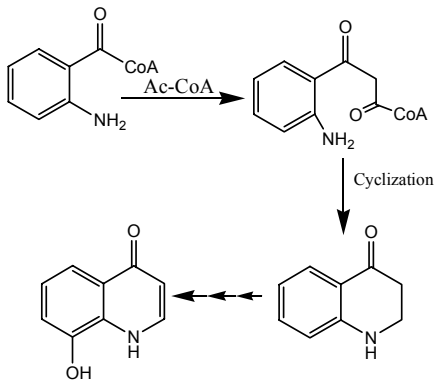

Scheme (4.4) Biosynthesis of 8-hydroxy-quinolin-4-one (modified from Torssell 1997)

4.4 Isolated compounds from *Hyrtios erectus* :

Marine sponges of the genus *Hyrtios* (family Thorectidae, order Dictyoceratida) have proven to be a rich source of secondary metabolites, including terpenoids, macrolides, and tryptamine-derived alkaloids. The most important metabolites of the genus *Hyrtios* discovered to date include the powerful anticancer agents spongiastatins 1-3 that were discovered by the Pettit group in 1993 and 1994, (Youssef 2005).

In the present study, 210 g dry weight of *Hyrtios erectus* collected from the Red Sea – Egypt were chemically investigated and nine compounds were structurally elucidated including 8 known compounds and one new 5-hydroxy-1*H*-indole derivative.

4.4.1 Exessive harvesting of the wild-type living organisms:

The potent antitumour activity of spongiastatins 1-3 from *H. erectus* (Pettit *et al* 1993; Pettit *et al* 1994) prompted the same authers to exhaustively recollect the wild-type of the same sponge *Hyrtios erecta* (600 kg wet wt.) for further chemical investigations. The later chemical investigations resulted in the isolation of antineoplastic sesterstatins 1, 2 and 3 in very minute concentrations 3 x 10^{-7} %; 3 x 10^{-7} % and 5 x 10^{-7} % respectively (Pettit *et al* 1998b), sesterstatins 4 and 5 in concentrations of 1 x 10^{-6} % and 4 x 10^{-5} % respectively (Pettit *et al* 1998c) and sesterstatin 6 in concentration of 8.3 x 10^{-7} % (Pettit *et al* 2005).

Concerning this point (excessive harvesting of a wild–type living organisms), I think that, we should be aware of the ecological problems that might occur as a result of such irresponsible collections. Otherwise a big environmental problem takes place, in this case, we have to balance the advantages against the disadvantages of such exhaustive re-collections. In order to overcome this problem, I predict the same as Prof. Dr. Faulkner (Faulkner 2000a) he also predict a great impact of chemical and biological researches including genetic engineering concerning to different forms of marine living forms ranging from marine invertebrates to the marine-derived microorganisms, Faulkner also expect that, in the near future we will be able to transfer biosynthetic genes from one marine organism to another and imagine the marine natural product chemist of 2025 still involved in structural elucidation, but considerable effort to the genetic engineering required to produce unique metabolites by fermentation of genetically modified microbes. This will accomplish the goal of having the marine organisms provide the inspiration for new compounds while avoiding their excessive harvesting.

4.4.2. Biosynthesis of scalaran-type sesterterpenoids:

Tetracyclic sesterterpenes with a scalarane skeleton occur frequently as metabolites of sponges of the family Thorectidae (order dictyoceratida) which includes the genera *Hyrtios*, *Cacospongia* and *Ircinia* (Faulkner, 1997). Sesterterpenoids are composed of a C_{25} backbone. Sesterterpenoid is built-up of 5 isoprene units. Their biocynthetic pathway involves enzymatic cyclization of all-trans pentaprenyl methyl ether (which is a detoxification product of isoprenic alcohol) as illustrated in (scheme 4.5) to form scalarane derivative (tetracyclopentaprenyl methyl ether). The conversion is aided by cyclase enzymes (Renoux and Rohmer, 1986)

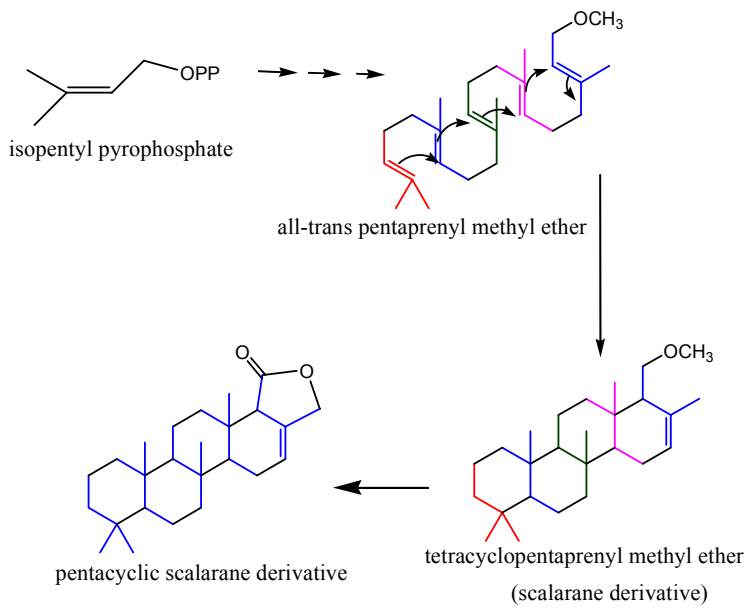

Scheme (4.5) Scalarane biosynthesis. (Renoux and Rohmer, 1986)

Although the origin of scalarane-type sesterterpenes is still highly obscure, and since in most of sponges up to one third of the volume is occupied by symbiotic microbes and various detritus filtered off by invertebrate Renoux and Rohmer 1986, suggested that the scalarane-type sesterterpenes which are restricted to a few sponges, (dictyoceratidae family) might be in fact microbial metabolites. The authors (Renoux and Rohmer 1986) exhibited the conversion of all-*trans* pentaprenyl methyl ether to tetracyclopentaprenyl methyl ether through incubation of the former with cell-free extract of the protozoan ciliate (*Tetrahymena pyriformis*).

4.4.3. The pharmacological activity of scalaran-type sesterterpenoids:

Many scalarane-type sesterterpenoids have been isolated from marine sponges belonging to the order Dictyoceratida. Scalarane-type sesterterpenes display a variety of biological activities such as cytotoxic, antimicrobial**,** antifeedant, antimycobacterial, ichthyotoxic, anti-inflammatory, and platelet-aggregation inhibitory effects, as well as nerve growth factor synthesis-stimulating action (Youssef *et al*, 2005). The most important scalarane derivatives are spongiastatins1-3 which displayed a potent antineoplastic effect. (Youssef 2005). However compound **18** (16-hydroxyscalarolide) showed cytotoxic activity 59.5 and 44.7 % at concentrations 3.0 µg and 10.0 µg respectively against L5178Y cells.

4.4.4. Indole derivatives from *Hyrtios erectus* :

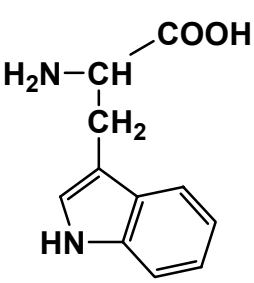

Tryptophan

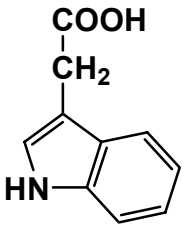

Indol-3-acetic acid

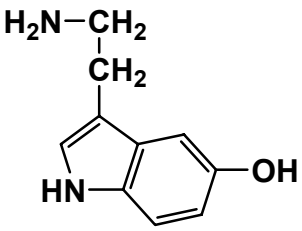

Serotonin

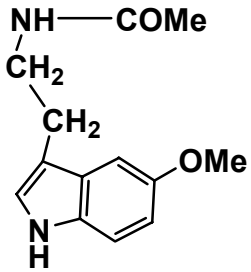

Melatonin

During the 1930's the essential aminoacid tryptophan was discovered as well as the plant growth hormone indole acetic acid (Kogl 1933). Tryptophan is a constituent of most proteins, and serves in man and animal as a biosynthetic precursor for a wide variety of tryptamine and other indole derived metabolites, several of them of paramount physiological importance. Tryptophan is ingested during the animal–diet or vegetarian-protein-diet where it is converted to biologically active derivatives e.g. serotonin and melatonin. Melatonin is thought to control the day and night rhythms, while serotonin is an important neurotransmitter acting at the nerve cells to promote feeling of well being, calm, personal security, relaxation, confidence and concentration. Serotonin neural circuits also help counterbalance the tendency of brain dopamine and noradrenaline circuits to encourage over-arousal, fear, anger, tension, aggression, violence, obsessive-compulsive actions, over-eating (especially carbohydrates), anxiety and sleeping. Serotonin itself can not penetrate the blood brain barrier, but its precursor tryptophan can penetrate it. The typical diet provide about 1-1.5 g. tryptophan daily, this amount is sufficient to maintain the brain essential requirement of serotonin.

The sponge *Hyrtios erectus* is known as rich source of tryptamine derived natural products. Hyrtiosine A, hyrtiosine B, 5-hydroxy-3-formyl-1*H*-indole (Kobayashi *et al* 1990), hyrtiosulawesine, 1,6-dihydroxy-1,2,3,4-tetrahydro-β-carboline, serotonin, 6-hydroxy-1-methyl-1,2,3,4-tetrahydro-β-carboline, 5-hydroxy-3-(2-hydroxyethyl)-indole, 6-hydroxy-3,4-dihydro-1-oxo-β-carboline (Salmoun et al 2002), and hyrtioerectines A-C (Youssef 2005) were previously isolated from *Hyrtios* sp.

In the present study, five indole derivatives were isolated (compounds **13-17**). Isohertiosine A, compound **17,** is new, its molecular formula is the same as hyrtiosine A. The difference has been assigned as a methoxy group attached to the carbonyl in **17** instead of hydroxymethylene group in hyrtiosine A (compound **13**). The known compounds **15** and **16** were not previously reported for *H. erectus*. Some of 5-hydroxy indole derivatives have been reported to exert cytotoxic activity against tumour cell models (Youssef 2005). However, the indole derivative of such basic structure are known to exert their biological effects on CNS. Compound **17** (isohyrtiosine A) showed growth inhibition activity 64 % at concentrations 10.0 µg/ml against L5178Y cells while other compound has no effect at concentrations up to 10 µg/ml.

4.4.5 Biosynthetic pathway of indole derivatives from *Hyrtios erectus*

The possible biosynthetic pathway of *Hyrtios*-derived indole includes hydroxylation at position 5, then decarboxylation leading to the formation of the intermediate 5-hydroxtryptamin (serotonin) which has been already isolated before from the same sponge (Salmoun et al 2002).

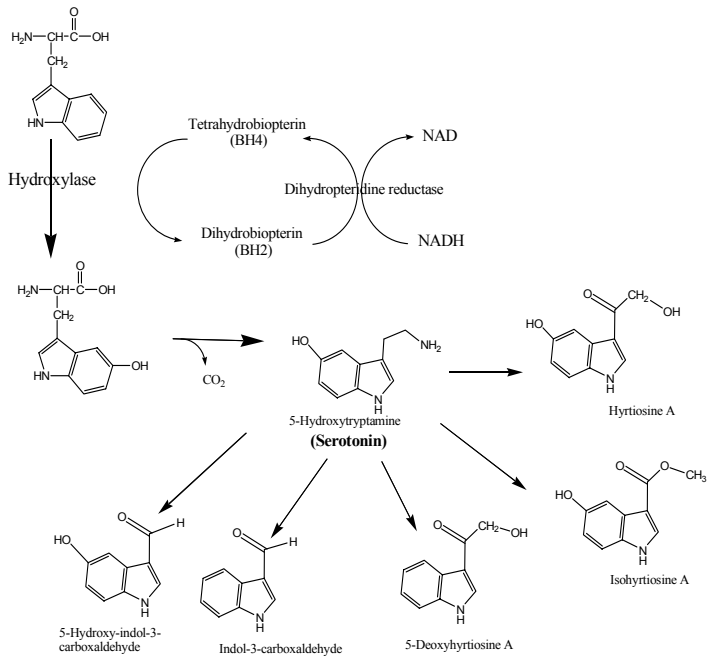

Scheme (4.6) Possible biosynthetic pathway of 3-acyl-indole derivatives

4.5 Isolated compounds from *Petrosia nigricans* :

The total methanol extract of *Petrosia nigricans* yielded 17 compounds, (compounds **22-38**) belonging to different chemical classes which included steroids, aromatic acid derivatives, new cerebrosides, new purine derivatives and new indole derivative, in additon to adenosine and nicotinamide. Although there are a lot of new active metabolites isolated from genus *Petrosia*, this is the first report of isolated compounds from *Petrosia nigricans*. None of the isolated compounds from *Petrosia nigricans* showed significant antimicrobial activity against *B. subtilis, S. cerevisae*, *C. herbarum* and *C. cucumerinum*. All purine derivatives (nigricines 1 to 4) showed no cytotoxic activity against L5178Y cell line, while nigricinol (compound **38**) showed 68.1 % cytotoxic activity at conc. 10 µg/ml.

4.5.1 Biosynthetic pathway of aromatic acids:

Although the isolated aromatic acids are described as catabolic products (waste) of aromatic amines and amino acids metabolism (O'connor *et al* 2001), they exhibit a significant ecological role. For example, p-hydroxybenzaldehyde, which is common in marine sponges, exhibited a significant antipredetory activity against the major predator *Perknaster fuscus* of antarctic sponges (Moon *et al* 1998). However, the following scheme demonstrates the possible biosynthetic pathway of aromatic acids.

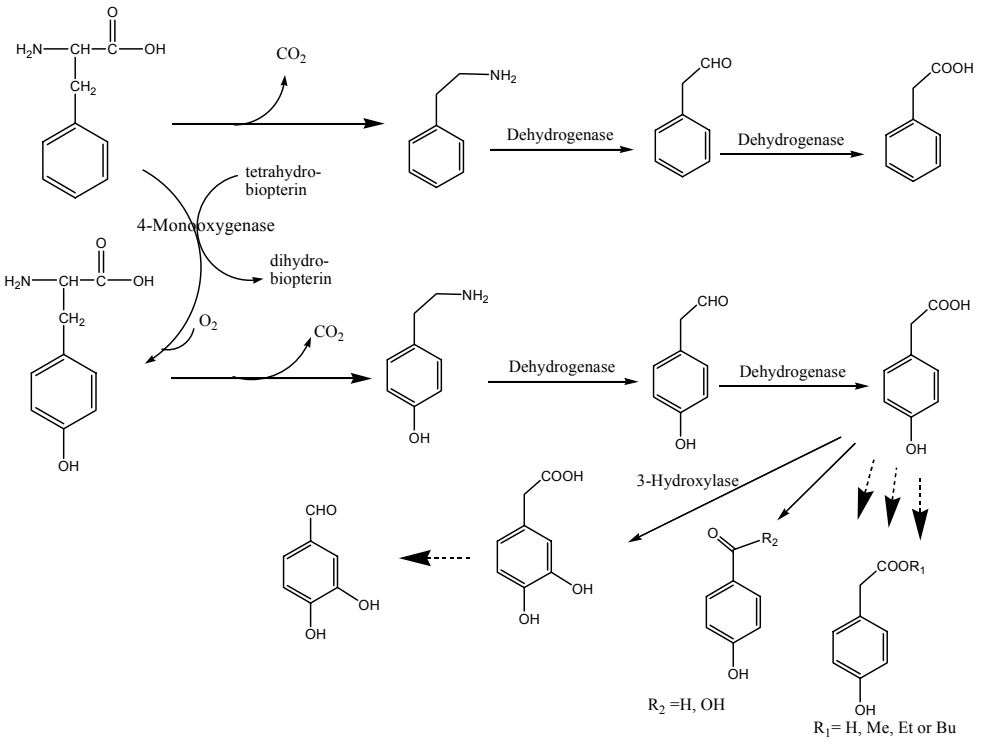

Scheme (4.7) Biosynthetic pathway of aromatic acids and aldehydes. (chosen from O'connor *et al* 2001, Cuskey and Olsen 1988)

4.5.2 Cerebrosides from *Petrosia nigricans*:

Cerebroside is the principal glycosphingolipid in the brain tissue, hence the trivial name „cerebroside", which was first conferred on it in 1874, although it was much later before it was properly characterized. In fact, glycosphingolipids are found in all nervous tissues, but they can amount to 2% of the dry weight of grey matter and 12% of white matter. Cerebroside are found at low levels in animal tissues, such as spleen and erythrocytes, skin lipids as well as in nervous tissues. Cerebrosides containing α-D-galactose are not found in humans, but are known to occur in a marine sponge, they are potent stimulators of mammalian immune systems (Christie, 2003). In the present study cerebroside mixture were separated from total methanol extract of the sponge *Petrosia nigricans*, after many trials using different methods of separation, a mixture of two cerebrosides were separated and elucidated as petrocerebrosides1 and 2.

4.5.3 Biosynthesis of cerebrosides

The basic mechanism for the biosynthesis of sphinganine involves condensation of acyl-coenzyme A with serine, catalysed by the enzyme serine acyltransferase as illustrated, to

form 3-keto-sphinganine. The keto group is then reduced to hydroxyl by a specific reductase. The free sphinganine is rapidly acylated to form a dihydroceramide, by a dihydroceramide synthase, which can utilize a range of acyl-CoAs. Insertion of the trans-double bond in position 4 to produce sphingosine occurs only after the sphinganine has been esterified in this way to form a ceramide. The biosynthesis of cerebrosides takes place through direct transfer of the carbohydrate moiety from a sugar-nucleotide, eg uridine-5-diphosphate (UDP)-galactose, UDP-glucose, etc, to the ceramide unit. During the transfer, which is catalysed by a glycosyl-transferase, inversion of the glycosidic bond occurs (from α to β).

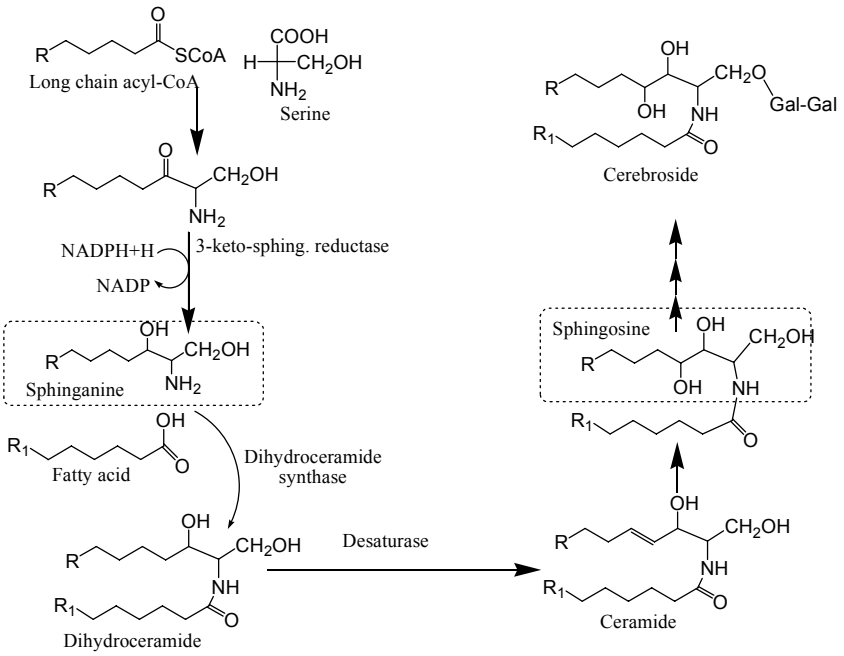

Scheme (4.8) Biosynthesis of cerebrosides (Christie, 2003)

4.5.4 New purine derivatives from *Petrosia nigricans*:

Marine organisms, particularely sponges, have proven to be an exceptionally rich source of modified nucleosides. The isolation of spongouridine and spongothymidine from *Cryptotethia crypta* (Bregmann, and Feeney 1950) which served as models for the development of adenine arabinoside (ARA-A) for treatment of *Herpes simplex* infection and cytosine arabinoside (ARA-C) for the treatment of leukemia (Lindsay *et al* 1999), and subsequent development of antiviral analogues demonstrated the potential medicinal importance of these compounds such as antifungal phidolopine which was isolated from the bryozoan *Phidolopora pacifica* (Ayer *et al* 1984), the hypotensive doridosine which was isolated from the sponge *Tedania digitata* (Cook *et al* 1980), and the cytotoxic mycalisines which were obtained from the sponge *Mycale sp.* (Kato *et al* 1985). Many other purines and

nucleosides isolated from marine organisms particularly sponges display potant bioactivities, such as the marine derived 1,3-dimethylisoguanine from *Amphimedon viridis* which showed activity against an ovarian cancer cell line (IC_{50}, 2.1 µg/mL) (Mitchell *et al* 1997); 3,7-dimethylisoguanine from a Caribbean sponge *Agelas longssima*, which displayed mild antibacterial activities (Cafieri *et al* 1995). Figure 4.3 shows the structure of some purine and pyrimidine derivatives that used as antiviral agents (Baba 2005).

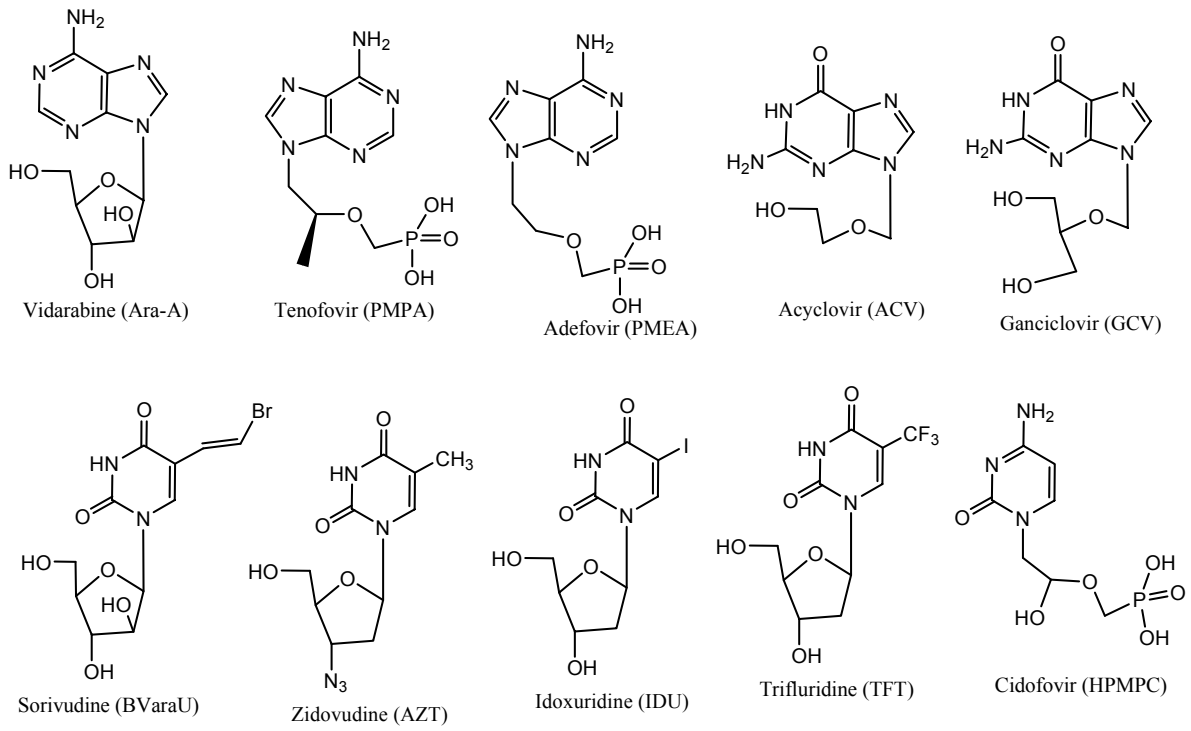

Fig (4.3) Purine and pyrimidine derivatives used as antiviral agents (Baba 2005).

In the present study, investigation of ethylacetate fraction of the Indonesian sponge *Petrosia nigricans*, which was collected from Pulau Baranglompo - Indonesia led to the isolation of four new purine derivatives nigricines 1-4. Their structures were elucidated by extensive spectroscopic analysis, 2D-NMR experiments, EI/MS, ESI/MS and HRMS. Erinacean is a related purine derivatives with unusual 6-β-alanine amino acid was isolated before from the antarctic sponge *Isodictya erinacea* (Moon et al 1997). To the best of our knowledge, Purine derivatives with alkyl 3-(3,9-dihydro-3,9-dimethyl–2-oxo-2*H*-purin-6-ylamino) propanoate were not reported neither as a synthetic nor as a natural product.

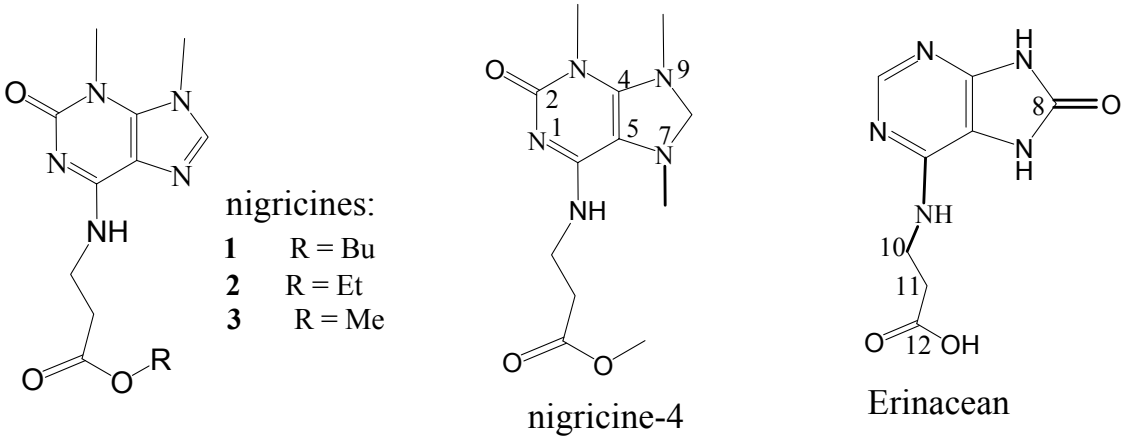

Fig (4.4) Nigricines 1-4 as well as the related compound erinacean

4.5.5 The possible biosynthetic pathway of nigricines 1-4:

Synthesis of the purine ring is a central metabolic function of all cells. The products, AMP and GMP, provide purine bases for DNA and RNA, as well as for a number of essential coenzymes (NAD, NADP, FAD and Coenzyme A) and signaling molecules (e.g. cAMP). The purine pathway also functions in pathways that are different and distinct from these „housekeeping roles." It is employed in specialized tissues to assimilate and detoxify NH_3 (Smith and Atkins 2002). The proposed biosynthetic pathway of nigricines 1-4 seems to follow the same biosynthetic pathway of the normal adenylated nucleotides until the formation of adenylsuccinate then the later substance (adenylsuccinate) is more likely to be used in *de novo* nigricines biosynthesis via a lateral pathway as explained in scheme (4.9).

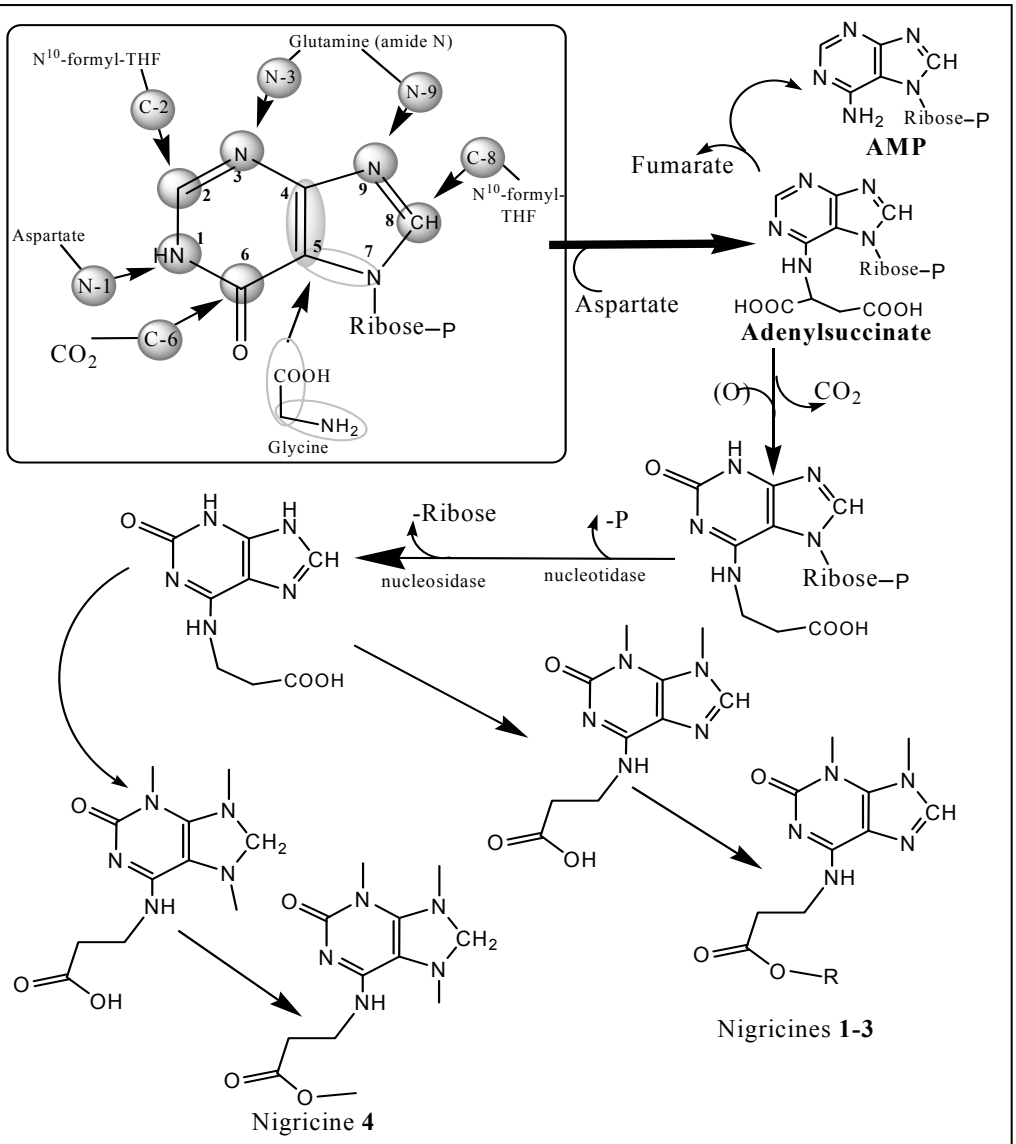

Scheme (4.9) Possible biosynthetic pathway of new purine derivatives from *Petrosia nigricans* (modified from Smith and Atkins 2002)

4.6 Isolated compounds from *Callyspongia biru*:

Sponges belonging to the genus C*allyspongia* are extensively investigated for bioactive natural products. Many new bioactive natural products have been isolated from different *Callyspongia sp*., these natural products include unusual steroids (Agrawal and Garg 1997); acetylene derivatives (Youssef *et al* 2003); uncommon fatty acids (Carballeira and Pagan 2001); diterpenes (Garg and Agrawal 1995); triterpenes (Fukami *et al* 1997); many cyclic peptides have been isolated from the genus C*allyspongia* [phoriospongins A and B from *C. bilamellata* (Capon *et al* 2002), Callynormine A from *C. abnormis* (Berer *et al* 2004) and callyaerins from *C. aerizusa* (Min, et al., 2001)]. Many natural product-producing fungi

have been isolated from some *Callyspongia* sp., and cultivated on artificial media for production of natural products [spiciferone derivatives, macrolides, anthraquinones and benzofuran have been isolated from *C. aerizusa* –derived fungi (Edrada *et al* 2000, Jadulco *et al* 2001, Jadulco *et al* 2002)]. The most attractive compound, that was isolated from *Callyspongia sp*., is callystatin A. Callystatin A is a potant cytotoxic polyketide isolated from Nagasakian marine sponge, *Callyspongia truncata* (Kobayashi *et al* 1997). Methanol extract of Indonesian sponge *Callyspongia biru* was investigated and p-hydroxyphenylacetic acid, p-hydroxyphenylacetic acid methylester, indole-3-carbaldehyde, indole-3-acetic acid, and 2‘-deoxythymidine were isolated. Deoxythymidine (compound **40**) showed cytotoxic activity 76.2 % and 41.7 % against L5178Y mouse lymphoma cell line at concentrations 10 and 3 µg/ml respectively.

V- Summary

The modern techniques as well as the advanced instruments that employed in the discovery programms of bioactive natural product facilitated the task of the natural product chemists and permitted them to detect, target, isolate and elucidate the structure of the pharmacologically active natural product in significantly short times compared with that done in the not too distant past. The targeted natural product may show novel or unusual spectroscopic features and/or promising biological activities. These methodologies are now applicable to achieve the task without the need of tedious isolation procedures of known compounds. The application of these new methodolgies resulted in saving the time, efforts and economy during the processing of the bioactive natural product drug discovery programs. The present study deals with the application of the modern techniques including NMR, MS, and hyphenated HPLC systems as very efficient and applicable tools in the achievement of the above mentioned aim. The biological materials that were employed in this study included six different soft bodied marine animals which were collected from four different geographical zones. The study resulted in isolation, purification, and structure elucidation of 40 compounds. Some of them showed a very promising biological activity and recommended as drug candidates in the near future.

1- The mollusc *Elysia rufescens*

The sacoglossan molluscs *Elysia rufescens* were collected from the black point „Kahala“ in Oahu Island in Hawaii. The animal extract provided 5 known kahalalides (kahalalides B, C, D, E and F) in addition to β-sitosterol and a previously known fabaceous secondary metabolite, N,N-dimethyl-tryptophan methylester.

2- The mollusc *Elysia grandifolia*

The sacoglossan molluscs *Elysia grandifolia* were collected from the Gulf of Mannar and Palk Bay, Rameswaram, India. The hyphenated system (LCMS) detected the molecular ion peaks that corresponding to kahalalides B, C, D, E, F, G, J, K, O as well as two new molecular ion peaks (corresponding to kahalalides R and S) in the total methanol extract. The isolation process was directed to target the new ones, and resulted in structure elucidation of them in addition to another two known kahalalides (kahlalaides D and F).

3- The Indonesian sponge *Pachychalina sp.*

The hithertho new sponge species, *Pachychalina sp*, was collected from Pulau Baranglompo, Indonesia. Chemical investigation of the methanol extract of the sponge led to isolation of two 5α, 8α-epidioxysteroids, as well as the previously known compound, 8-hydroxy-4-quinolone, which was reported as an ink component that is ejected by the giant octopus „*Octopus dofleini martini*".

4- The Indonesian sponge *Petrosia nigricans*

The Indonesian sponge *Petrosia nigricans* was collected from Pulau Baranglompo, Indonesia. Seventeen compounds were isolated from the total methanol extract. These compounds included 10 known natural products, 2 new cerebrosides, one bis-indole derivative and four new 2-oxo-purine derivatives.

5- The Indonesian sponge *Callyspongia biru*

The Indonesian sponge *Callyspongia biru* was collected from Taka Bako, Indonesia. The total methanol extract of the sponge provided five known compounds (indol-3-carbaldehyde, indol-3-acetic acid, *p*- hydroxyphenylacetic acid, *p*-hydroxyphenylacetic acid methylester, and 2`-deoxythymidine).

6- The Red Sea sponge *Hyrtios erectus*

The Red Sea sponge *Hyrtios erectus* was collected from El-Quseir, in the Red sea , Egypt. The total methanol extract of the sponge provided nine compounds including one epidioxycholesterol derivative, three scalaran-type sesterterpenes, four known indole derivatives and one new 5-hydroxy-indole derivative.

References

Agrawal S., Garg H.S., (1997) Indian J. Chem. Sect. B 36 343-346

Albert K., (2002), In : On-line LC-NMR and related techniques (edited by Klaus Albert), John Wiley.

Aldrich library of ^{13}C and ^{1}H Ft NMR spectra (1992) Sigma-Aldrich.

Aldrich Library of ^{13}C and ^{1}H FT NMR spectra (1993) 1st edition, (ed., Pouchert C J and Behnke J)

Ashcroft, A. E., (2005) *Nat Prod Rep*., 22, 452-464.

Ashcroft, A.E. (1997) : In ("*Ionization Methods in Organic Mass Spectrometry*", The Royal Society of Chemistry, UK, and references cited therein, and availableat websites, **http://WWW.astbury.leedsac.uk/Facil/Mstut/mstutorial.htm**, and **http://www.jeol.com/ms/docs/ionize.html** .

Ashour M., Edrada R, Ebel R., Wray V., Wätjen W., Padmakumar K., Müller W. E. G., Lin W. H. and Proksch P. (2006) *J. Nat. Prod*., 69, 1547.

Ayer S.W., Andersen R.J., Cun-Heng H., Clardy J. (1984) *J. Org. Chem*. 49, 3869-3870.

Baba M. (2005) *Uiusu*, Jun;55(1):69-75.

Bakus G. J., Targett N.M., Schulte B., (1986) *J. Chem Ecol*. 12, 951-987.

Barnes R.D. (1986) In : *Invertebrate Zoology* 5th edition, Saunders College publishing New York.

Bates M.L., Reid W.W., White J.D., (1976) *J. Chem. Soc., Chem. Commun*. 44-45.

Becerro M.A., Goetz G., Paul V.J., and Scheuer P.J. (2001), *J. Chem. Ecol*., 27, 2287-2299.

Bennett J.W. (1995) *Can. J. Bot*. 73 : S917-S924.

Bennett J.W., and Bentley R. (1989) *Adv. Appl. Microbiol*., 34, 1-34.

Berer N., Rudi A., Goldberg I., Benayahu Y., and Kashman Yoel (2004) *Org. Lett*., 6, 2543-2545.

Bernart M., Gerwick WM. (1990) *Phytochemistry*, 29, 3697

Bhawal B.M., et al (1991) synthesis 112-114.

Bletsos I.V.;Hercules D.M.; vanLeyen D.; Hagenhoff B., Niehuis E.; Benninghoven A. (1991) *Anal. Chem*., 63, 1951.

Bohsale S. H. Jagtap T.G., and Naik C.G. (1999): *Mycopathologia* 147, 133-138.

Bok J.W., Lermer L., Chilton J., Klingeman H. G. and Towers G. Neil (1999) *Phytochemistry*, 51, 891-898.

Bonnard, I.; Manzanares, I.; Rinehart, K. L. (2003) *J. Nat. Prod.* 66, 1466-1470.

Bourel-Bonnet L., Rao K.V., Hamann M.T., and Ganesan A., (2005), *J. Med. Chem.*, 48, 1330-1335.

Bourguet-kondracki M.-L. and Kornprobst,J. –M. (2005) In: Marine Pharmacology: potentialities in the treatment of infectious diseases, Osteoporosis and Alzheimer's Disease. [book series : Advances in Biochemical Engineering/Biotechnology, 97, 2005, SpringerLink Berlin / Heidelberg, Book : marine biotechnology II].

Boyd M.R., Schoemacker R.H., Cragg G.M., and Sffness M., (1988) in *pharmaceuticals and the sea* (Jefford C.W., Reinhart K.L., and Shield L.S., eds.), pp. 27-44, Technomic Publishing Company, Lancaster, PA.

Boyd R.M. (1989) *Principles Practices Oncol.* 3, 1-12.

Braekman J.C., Daloze D. Macedo D., Abreu P. (1982) *Tetrahedron Lett*. 23, 4277-4280

Braekman J.C., Daloze D., Defay N., Zimmermann D. (1984) *Bull. Soc. Chim. Belg* 93, 941-944.

Bratt K. (2000) , In :*Secondary Plant metabolites as Defense against Herbivores and Oxidative Stress*, (a Thesis presented by Katharina Bratt 2000) , Department of organic chemistry, Institute of chemistry, university of Uppsala, sweden.

Bregman W., Feeney R.J. (1950) *J. Am. Chem. Soc*. 72, 2809- 2810.

Bregmann W., and Feeney R., (1951), *J. Org. Chem*., 16, 981-987.

Bringmann G., Lang G., Steffens S., Schaumann K. (2004) *J. Nat. Prod*. 67, 311-315 .

Brown A.P.; Morrissy R.L.; Faircloth G.T.; Levine B.S. (2002) *Cancer Chemother. Pharmacol*., 50, 333-340

Bu´Lock J.D., (1980). *Mycotoxins as secondary metabolites*, In: *the Biosynthesis of mycotoxins* (Steyn, P.S. ed.) Academic Press. New york. p 1-16.

Burlingame A.L., Baillie T.A., Russell D.H. (1992) *Anal. Chem.,* 64, 467R.

Cafieri F., Ernesto F., Mangoni A., Tagliatela-Scafeti O. (1995) *Tetrahedron Lett*. 36, 7893-7896.

Calderon J.S., Quijano L., Gomez F., Acosta F. and Rios T. (1982) *Rev. Latinoam. Quim*. 13, 49.

Cantrell C.L., Rajab M. S., Franzblau S.G., Fronczek F.R. and Fischer N.H.(1999*) Planta Medica*, 65 732-734.

Capon R.,J., Ford J., Lacey E., Gill J.H., Heiland K., Friedel T., (2002) *J. Nat. Prod*. 65, 358-363

Capon R.J., Rooney F., Murray L.M. (2000) *J. Nat Prod*. 63, 261-262.

Carballeira N.M., Pagan M. (2001) *J. Nat. Prod.* 64, 620-623

Carlson C. & Hoff P.J., 1999 (Aug 15) photos of *Elysia rufescens*. [Message in] Sea Slug Forum. Australian Museum, Sydney. Available from http://www.seaslugforum.net/find.cfm?id=1189

Chaurand P., Luetzenkirchen F., Spengler B. *J. Am. Soc. Mass Spectrom.* (1999), 10, 91-103.

Cimino G., De Stefano S., Minale L., Trivellone E. (1977) *J. Chem. Soc., Perkin Trans. 1* 1587-1593.

Ciruelos C.; Trigo T.; Pardo J.; Paz-Ares L.; Estaun N.; Cuadra C.; Domínguez M.; Marín A.; Jimeno J.; Izquierdo M (2002) . *Eur. J. Cancer*, *38*, Suppl. 7, S33.

Clardy J. and Walsh C., (2004) *Nature*,432, 829-837 and litratures therein.

Constantino V., Fattorusso E., Imperatore C., and Mangoni A.(2003) *J. Org. Chem.* 68, 1433-1437 .

Constantino V., Fattorusso E., Imperatore C., and Mangoni A.(2004) *J. Org. Chem.* 69, 1174-1179 .

Constantino V., Fattorusso E., Mangoni A., Aknin M. and Gaydou E.M.(1994) *Liebigs Ann. Chem.* 1181-1185 .

Cook A.F., Bartlett R.T., Gregson R.P., Quinn R.J. (1980) *J. Org. Chem*. 45, 4020-4025.

Copp B. R. (2003), Nat. Prod. Rep. 6, 535-557.

Corely D.G., and Durley R.C. (1994) *J.Nat. Prod*. 57, 1484.

Cotter R.J. (1980) *Anal.Chem*., 52, 1589A.

Cragg GM., Newmann DJ.; and Snader K.M. (1997) *J. Nat. Prod*., 60 , 52.

Crawley L.S. (1988) : In *pharmaceuticals and the sea* (Jefford, C.W., Reinhart, K.L., and Shield, L.S., eds.), pp. 101-107, technomic publishing company, Lancaster, PA.

Crews P., Cheng X.C., Adamczeski M., Rodriguez J., Jaspars M., Schmitz F.J., Traeger S.C., Pordesimo E.O., (1994) *Tetrahedron* 50, 13567-13574

Cristie W.W. (2003) In: Lipid Analysis (3rd edition). Oily Press, Bridgwater. Available at http://www.lipidlibrary.co.uk/Lipids/cmh/index.htm

Cueto M.; D'Croz L.; Mate J. L.; San-Martin A.; Darias J. (2005) *Org. Lett.*, *7*, 415-418.

Cuskey S M and Olsen R H (1988) *J. Bacteriology,* 170, 393-399

Davies J. (1985) *Recombinent DNA and the production of small molecules*. In : *Microbiology*. (Leive L., Washington A.S.M. eds.) D.C. pp. 364-366.

Dewick P.M.(1997) In: Medicinal natural products, a biosynthetic approach, third avenue, New York, USA, 153-173.

Dillman R.L., Cardellina J.H.(1991) *J. Nat. Prod*. 54, 1056-1061.

Dmitrenok A., Iwashita T, Nakajima T., Sakamoto B., Namikoshi M., Nagai H (2006) *Tetrahedron*, 62, 1301-1308.

DNP (2005), from DNP „Dictionary of natural products“ on CD-Rom version 13:2, Copyright ©1982-2005 Chapman & Hall/CRC.

Edrada R.A., Wray V., Berg A., Grafe U., Sudarsono Brauers G., Proksch P. (2000*) Z. Naturforsch. C Biosci*. 55, 218-221

Eggenberger U., and Bodenhausen, G. (1989), 61, 2298.

Eggert H., Vanantwerp C., Bhacca N., Djerassi C. (1976) *J. Org. Chem.* 41, 71-78.

Elenkov I., Milkova T., Andreev S. and Popov S. (1994) Comp. Biochem Phsiol. 107B, 547.

El-Sayed K.A., Bartyzel P., Shen X., Perry T.L., Zjawiony J.K., Hamann M.T., (2000), *Tetrahedron* 56, 949-953.

Enders D., Vicario J.L., Job A., Wolberg M .M.,Ÿller M., (2002) *Chem. Eur. J.* 8, 4272-4284

Evans J.N.S. (1995) In : Biomolecular NMR spectroscopy, Oxford University Press.

Exarchou V., Krucker M., Beek T.A., Vervoort J.,Gerothanassis I. P., and Alert K. (2005) *Magn. Reson. Chem*. 43, 681-687.and references therein.

Fattorusso E., Magno S., Santacroce C. and Sica D.(1974) *Gazz. Chim. Ital.* 104, 409

Faulkner D. J. (1997). *Nat. Prod. Rep.* 14. 259-302, and previous reviews of this series.

Faulkner D. J. (1998) *Nat. Prod. Rep.,* 15, 113-158, and earlier reviews cited therein.

Faulkner D. J. (2002) *Nat. Prod. Rep.,* 19, 1-48, and earlier reviews cited therein.

Faulkner D. J., (2000a) *Nat. Prod. Rep*., 17, 1-6.

Faulkner D.J., (2000b) Antonie van Leeuwenhoek 77: 135-145.

Fenn J. B., (2003) *Angew. Chem. Int. Ed*., 42, 3871-3894.

Fenn J., (1984) *J. Phys. Chem*., 88, 4451.

Firn R.D. (2004) natural products- module 867. *Lectures 1-9,* available at world web: www.users.york.ac.uk/~drf1/867_1.htm

Firn R.D. and Jones C.G , (2003) *Nat. Prod. Rep*., 20, 382-391.

Firn R.D., (2003) *Biodiversity and Conservation*, 12, 207.

Firn R.D., and Jones C.G. (1998). *Nature*, 393, 617.

Firn R.D., and Jones C.G. (1999) *Nature*, 400: 13-14.

Firn R.D., and Jones C.G. (2000) *Mol. Microbiol*., 37, 989.

Firn R.D., and Jones, C.G. (1996) : An explanation of secondary product "redundancy". In *Recent Advances in Phytochemistry*. Romeo J.T., Saunders J.A., and Barbosa P. (eds). New York: Plenum Press, pp. 295-312.

Fitzgerald J.S. (1963), Aust. J. Chem., 16, 246.

Fleming I.D., Nisbet L.J. Brewer S.J. (1982). In *Bioactive Microbial products : Search and discovery*. (J.D. Bu`lock, N.J.Nisbet, D. J. winstanley , eds.,) Academic press, london, pp107-130.

Fukami A., Ikeda Y., Kondo S., Naganawa H., Takeuchi T., Furuya S., Hirabayashi Y., Shimoike K., Hosaka S., (1997) *Tetrahedron Lett*. 38, 1201-1202

García-Rocha, M.; Bonay, P.; Avila, J. (1996) *Cancer Lett.* 43-50.

Garg H.S., Agrawal S., (1995) *Tetrahedron Lett.* 36, 9035-9038

Gates P., (2005a), available at web page , http://www.chm.bris.ac.uk/ms/theory/maldi-ionization.html .

Gates P., (2005b), available at web page , http://www.chm.bris.ac.uk/ms/theory/cid-fragmentation.html .

Gauvin A., Smadja J., Aknin M., Faure R., and Gaydou E-M. (2000) *Can J. Chem.* 78, 986-992.

Gavagnin M., Spinella A., Castelluccio F and Cimino G. (1994), *J.Nat. Prod*., 57, 298-304.

George J.D., and George J.J. (1979) In : *Marine Life an Illustrated Encyclopedia of Invertebrates in the Sea* , John Wiley Sons, New York U.S.A.

Gerrit J., Johannis P. and Johannis V. (1977) *Carbohydrate Research*. 62, 349-357.

Gerwick W.H. and Bernart M.W. (1992) *Pharmaceutical and bioactive natural products* In : *Marine biotechnology* 1. (Attaway D.H. and Zaborsky O.R. eds) Plenum Press, New York.

Giersiefen H., Hilgenfeld R., Hillish A.(2003): Natural products for lead identification: nature is a valuable resource for providing tools, In: modern methods of drug discovery (ed, Hillish A., Hilgenfeld R) .

Giner J.L., Gunasekera S.P., Pomponi S.A., (1999) *Steroids* 64, 820-824

Giorgiani F.; Cappiello A.; Beranova- Giorgiani S.; Palma P.; Trufelli H.; Desiderio D. M. (2004) *Anal. Chem*., *76*, 7028-7038.

Goetz G.; Yoshida W. Y.; Scheuer P. J. (1999) *Tetrahedron*, *55*, 7739-7746.

GoetzG.; NakaoY.; Scheuer P. J. (1997**)** *J. Nat. Prod*., 60, 562-567. ,

Gorshkova I.A., Gorshkov B.A., Fedoreev S.A., Shestak O.P., Novikov V.L., Stonik V.A., (1999) *Comp. Biochem. Physiol. C Comp. Pharmaco* 122, 93-99 .

Goud T.V., Reddy N.S., Swamy N.R., Ram T.S., Venkateswarlu Y. (2003) *Biol. Pharm. Bull.* 26, 1498-1501

Gullo, V.P. (1994) : In *The Discovery of natural products with therapeutic potential* (Gullo, V. P. ed.), Butterworth-Heinemann press.

Gunasekera S.P., Cranick S., Longly R.E., (1989) *J. Nat. Prod*., 52, 757-761

Gunatilaka A., Gopichand Y., Schmitz F. and Djerassi C. (1981) *J. Org. Chem.* 46, 3860-3866.

Gunatilaka A.A.L., Kingston D.G.I. and Johnson R.K *Pure & Appl. Chem*., 1994, 66, Nos 10/11, pp. 2219-2222.

Hall M.J. (1989) *biotechnology* 7, 427-430.]

Hamann M. T.; Scheuer P. J. (1993) *J. Am. Chem. Soc. 115*, 5825-5826.

Hamann M.T.; Otto C.S.; & Scheuer P. J., Dunbar D.C. (1996) *J.Org.Chem.*.61,6594-6600.

Harborne J.B. : In *Introduction to Ecological Biochemistry*. Academic Press, 1988.

Harborne J.B., (1986) *Nat. Prod. Rep*. 3, 323-344.

Haslam E.(1986) Secondary Metabolism , fact or fiction. *Nat. Prod. Rep*., 3, 217 – 249.

Hay M.E., and Fenical W. (1988) *Annu. Rev. Ecol. Syst.* 19, 111-145.

Hensens O. D, (1994) : In *The Discovery of natural products with therapeutic potential*, (Gullo, V. P., ed.) Butterworth-Heinemann press. pp390.

Hill R.T., Hamann M.T., Enticknap J., and Rao K.V. (2005) Kahalalide-producing bacteria and methods of identifying kahalalide-producing bacteria and preparing kahalalides.. PCT Int. Appl., 41 pp. CODEN: PIXXD2 WO 2005042720.

Hiort J. (2002) Neue Naturstoffe aus Schwamm-assoziierten Pilzen des mittelmeeres-Isolierung strukturaufklärung und biologischen aktivität., (Heinrich-Heine Universität. 2002).

Ho C.S., Lam C.W.K., Chan M.H.M., Cheung R.C.K., Law L.K., Lit L.C.W., Ng K.F., Suen M.W.M., and Tai H.L.; (2003), *Clin. Biochem. Rev*., 24, 4.

Hooper J.N.A., and van Soest R.W.M. (2002) In : *Systema Porifera : A Guide to the Classification of Sponges*, Kluwer Academic/Plenum publishers, New York.

Horgen F. D.; de los Santos D.B.; Goetz G.; Sakamoto B.; Kan Y.;Nagai H.; Scheuer P. J (2000) *J. Nat.Prod*., 63, 152-154

Hunter I.S. (1992) Tibtech, 10, 144-146.

Hussar D.A. (2006): *Nursing* 2006, 36, 54-55

Iguchi K., Shimura H., Yang Z., and Yamada Y. (1993) *Steroid*, 58, 410

Inagaki M., Nakamura K., Kawatake S., Higuchi R. (2003) *Eur. J. Chem.* 325-331

Ireland C. M., Copp B.R., Foster M.P., McDonald L.A., Radisky D.C., Swersey J.C., In : *Marine Biotechnology*,(Attaway,D.H., Zaborsky, O.R., eds) Plenum Press, New York, 1993; Vol. 1, Chapter 1 pp 1-43.

Itoh T., Sica D., and Djerassi C. (1983) *J.Chem. Soc. Perkin Trans* 1, 147-153.

Jadulco R., Brauers G., Edrada R.A., Ebel R., Wray V., Sudarsono., Proksch P., (2002) *J. Nat. Prod.* 65, 730-733

Jadulco R., Proksch P., Wray V., Sudarsono Berg A., Graefe U., (2001) *J. Nat. Prod.* 64, 527-530

Janmaat M. L; Rodriguez J. A; Jimeno J.; Kruty F. A.; Giaccone G. (2005) *Mol Pharmacol*., *68*, 502-510.

Janmaat ML,Rodriguez JA, Jimeno J, Kruty FA, Giaccone G., (2005) *Mol Pharmacol*. 68(2):502-10.

Jaspars M. (1999) *Nat. Prod. Rep.* 16, 241-248.

Jenkins K.M., Jinsen P.R., Fenical W. (1999) *Tetrahedron Lett.*, 40, 7637-40.

Jensen K.R. (1992) Anatomy of some Indo-Pacific Elysiidae (Opisthobranchia: Sacoglossa (=Ascoglossa), with a discussion of the generic division and phylogeny. Journal of Molluscan Studies, 58(3): 257-296.

Jimeno J. M.; Lopez-Martin J. A.; Casado A. R.; Izquierdo M. A.; Scheuer P. J.; Rinehart K. (2004) *Anti-Cancer Drugs*, 15, 321-329.

Johnson R.K., and Hertzberg R.P.(1989) in *Annual Reorts in Medicinal Chemistry*, vol. 25 (Bristol, J.A., ed.), pp.129-140, Academic Press, san diego, CA.

Jones C.G., and Firn R.D. (1991) On the evolution of plant secondary metabolite chemical diversity. *Phil Trans Roy Soc B*, **333**: 273-280.

Kachlicki P., et al . (1997) *Proc. Eur. Fusarium semin., 5th* , 853-855.

Kan Y.; Fujita T.; Sakamoto B.; Hokama Y.; Nagai H.; (1999) *J. Nat.Prod*., 62, 1169-1172.

Karas M.; Hillencamp F. (1988) *Anal. Chem*., 6, 2301.

Karas M.; Hillencamp F., Beavis R.C., Chait B.T. (1991) *Anal. Chem*., 63, 1193.

Kato Y., Fusetani N., Matsunaga S., Hashimoto K. (1985) *Tetrahedron Lett*. 26, 3483-3486.

Kay, E.A. (1979)- Hawaiian Marine Shells,reef and shore fauna of Hawaii, section 4 : Mollusca. Bernice P. Bishop Museum Special Publication 64(4),xviii +653 pp.

Kelaart E.F. (1858). Description of new and little known species of Ceylon nudibranchiate molluscs and zoophytes. *Journal of the Ceylon Branch of the Royal Asiatic Society*, columbo, 3(1): 84-139.

Knox J.P.; Dodge A.D. (1985), *Phytochemistry* 24, 889.

Kobayashi J., Murayama T., Ishibashi M., Kosuge s., Takamatsu M., Ohizumi Y., Kobayashi H., Ohta T., Nozoe S., Sasaki T. (1990) *Tetrahedron Lett.* 46, 7699-7702.

Kobayashi M., Higuchi K., Murakami N., Tajima H., Aoki S., (1997) *Tetrahedron Lett.* 38, 2859-2862

Kobayashi M., Okamoto T., Hayashi K., Yokoyama N., Sasaki T., Kitagawa I. (1994a) *Chem. Pharm. Bull.* 42, 265-270.

Kobayashi M., Rao S.R., Chavakula R., Sarma N.S., (1992) *J. Chem. Res. Synop*. 282-283 .

Kobayashi M., Rao S.R., Chavakula R., Sarma N.S., (1994) *J. Chem. Res. Synop*. 282-283

Koch P., Djerassi C., Lakshmi V., Schmitz F. J. (1983) *Helv. Chim Acta*, 66 2431.

Kogl F., Haagen-Smit A. J., Erxleben . (1933) Z. *Physiol***,** *21*4, 241.

König G.M., Wright A.D., Linden A (1998) *Planta medica* 64, 443-447.

Kreuter M. H., Robitzki A., Chang S., Steffen R., Michaelis M., Klijajic Z., Bachmann M., Schröder H. C. and Müller W.E.G (1992) *Comp. Biochem. Physiol*., 101C, 183-187.

Lambert M.; Staerk D; Hansen S H.; Jaroszewski J W. *Magn.Reson. Chem*. (2005), 43, 771-775 and references therein.

Larson E.R., and Fischer P.H. (1989) in *Annual Reorts in Medicinal Chemistry*, vol. 24 (Allen. R., ed.), pp.121-128, Academic Press, san diego, CA.

Lautens M., Stammers T.A., (2002) *Synthesis* 1993-2012

Leontein K., Lindberg B. and Lönngren J. (1977): *Carbohydrate Research*. 62, 359-362.

Lin Y.L., Lee H.P., OU J.C., Kuo Y.H. (1996) *Heterocycles* 43, 781-786.

Lindsay B.S., Almeida A.M.P., Smith C. J., Berlink R.G.S., Da Rocha R.M., Irland C.M. (1999a) *J. Nat Prod*. 62, 1573-1575.

Lindsay B.S., Battershill C.N., Copp B.R. (1999b) *J. Nat Prod*. 62, 638-639.

Loo J. A.; Loo R. R. O. (1997) In Electrospray Ionization Mass Spectrometry of Peptides and Proteins, edited by Cole, R. B., John Wiley & Sons, Inc. New York.

López-Maciá A.; Jiménez J. C.; Royo M.; Giralt E.; Albericio F (2001a). *J. Am. Chem. Soc.*, *123*, 11398-11401.

López-Maciá A.; Jiménez J. C.; Royo M.; Giralt E.; Albericio F (2001b). *Tetrahedron Lett.*, *41*, 9765-9769.

Luckner M.,(1990). Secondary metabolism in plants and animals. Third edition, Springer Verlag, Berlin.

Malorni L., Minale L. and Riccio R. (1978) *Nouv. J. Chim*. 2, 351

Mann J. (1987) : In *Secondary Metabolism*. Clarendon Press, Oxford.

Mann J. (1994) : In *Chemical Aspects of Biosynthesis*, Oxford University Press.

Marahiel M.A., stachelhaus T. and Mootz H.D.(1997) *Chem. Rev.,* 97, 2651-2673

Marfey P. (1984) *Carlsberg Res. Commun*. *49*, 591-596.

Martin J.F., and Demain A.L. (1978) *Fungal development and metabolite formation*. In : *The Filamentous Fungi. Vol. III. Developmental mycology*. (Smith J.E. and Berry D.R. eds.) Halstead Press, New York.

Mayer A.M.S., and Hamann M.T., (2004) Mar. Biotechnol. 6, 37-52.

McAlpine J.B., and Hochlowski J.E., (1994) : *In The Discovery of natural products with therapeutic potential* (Gullo, V. P., edit.) 1994, Butterworth-Heinemann press. pp349.

McConnell O. J., Longley R.E., and Koehn F. E., (1994) : In *The Discovery of natural products with therapeutic potential* (Gullo, V. P. ed.), Butterworth-Heinemann press, pp109-172.

Meltzer R.I. et al (1957) *J.Org. Chem*. 22, 1577-1581.

Meyer B.N, Ferrigni N.R.,Putnam J.E., Jacobsen L.B., Nichols D.E., and McLaughlin J.L. (1982) : *Planta Medica*, 45, 31-34.

Min C., Lin W.H., Edrada R.A., Ebel R., TeusherF., Wray V., Nimtz M., and Proksch P. (2001): Poster.

Mitchell S.S., Whitehill A.B., Trapido-Rosenthal H.G., Ireland C.M. (1997) *J. Nat Prod*. 60, 727-728.

Miyaoka H., Nishijima S., Mitome H., Yamada Y. (2000) *J. Nat. Prod*.63, 1369-1372.

Molinski T.F., Fahy E., Faulkner D.J., Van Duyne G.D., Clardy J. (1988) *J. Org. Chem.* 53, 1340-1341 .

Moon B., Baker B.J., McClintock J.B. (1997) *J. Nat Prod*. 61, 116-118.

Moon S.S., et al (1996) *J.Nat Prod.* 59, 777-779.

Moore R.E, Bornemann V., Niemczura W.P., Gregson J.M., Chen J., Norton T.R., Patterson G.M.L., Helms G.L.J., (1989) *J. Am. Chem. Soc*., 111, 6128-6132.

Mosmann, T. (1983) *J. Immunol. Methods*. *65*, 55-63.

Müller H., Brackhagen O., Brunne N., Henkel T., and Reichel F. (2000) : Natural products in drug discovery, ernst Schering research foundation workshop 32: *The role of natural product in drug discovery*, Springer-Verlag, Germany, 205-216.

Murakami N., Wang W.Q., Aoki M., Tsutsui Y., Higuchi K., Aoki S., Kobayashi M., (1997) *Tetrahedron Lett*. 38, 5533-5536

Nakao Y., Uehara T., Matsunaga S., Fusetani N., Van Soest R.W.M. (2002) *J. Nat. Prod.* 65, 922-924

Nelson T.C. (1961) *Proceeding of the National Academy of Research Council Supplement*. (1961) .p. 891.

Neudrt R. and Penk M. (1996) *J. Chem. Inf. Comput. Sci*. 36, 244-248.

Newmann D.J. and Cragg GM., (2004) *J. Nat. Prod.* 67, 1216-1238.

Newmann DJ., Cragg GM., and Snader K.M. (2000) *Nat. Prod. Rep*. 17, 215-234]

Nisbet L.J. (1992) In: *Secondary Metabolites: Their Function and Evolution*. (D.J. Chadwick, J.Whelan, eds,.) John Wiley, Chichester, P299.

Nordström A., Tarkowski P., Tarkowska D., Dolezal K., Astot C., Sandberg G., Moritz T. (2004), *Analytical Chem.* 76, 2869-2877.

O'connor K. E., Witholt B., Duetz W. (2001) *J. Bacteriol*. 183, 928-933

Ojima N., Masuda K., Tanaka K., Nishimura O. (2005) *J. Mass Spectrom.*, 40, 380-388.

Padmakumar K. (1998) *Phuket Marine Biological Center Special Publication*., *18*, 187.

Paul v.J., and Van Alstyne K.L (1988), *J.Exp.Mar.Biol.Ecol*., 119, 15-29.

Pearse V., Pearse J., Buchsbaum M. and Buchsbaum R. (1987) In : *Living Invertebrates*, Blackwell Scientific Publications, California.

Pease W.H. (1871). Descriptions of Nudibranchiate Mollusca inhabiting Polynesia. American Journal of Conchology,6(4): 299-305.

Pechenik J.A. (2000) In : *Biology of the Invertebrates*, 4th McGraw-Hill companies.

Pedpradab S., Ederada R., Ebel R., Wray V., Proksch P. (2004) *J. Nat. Prod*.67, 2113-2116.

Pettit G.R., Cichacz Z.A., Gao F., Herald C.L., Boyd M.R., Schmidt j.M., Hooper J.N.A. (1993) *J. Org. Chem*. 58. 1302-1304.

Pettit G.R., Cichacz Z.A., Herald C.L., Gao F., Boyd M.R., Schmidt j.M., Hamel J., Bai R. (1994) *J. Chem. Soc. Chem. Commun.* 1605-1606.

Pettit G.R., Cichacz Z.A., Tan R., Herald D.L., Melody N., Hoard M.S., Doubek D.L., Hooper J.N.A. (1998a) *Collect. Czech. Chem. Commun*. 63, 1671-1677

Pettit G.R., Cichacz Z.A., Tan R., Hoard M.S., Melody N., Pettit R.K. (1998b) *J. Nat. Prod*.61, 13-16.

Pettit G.R., Kamano Y., Herald C.L., Dufresne C., Cerny R.L., Herald D.L. Schmidt T.M., Kizu H.J.(1989), *J. Am. Chem. Soc*., 111, 5015-5017.

Pettit G.R., Tan R., Cichacz Z.A. (2005) *J. Nat. Prod*.68, 1253-1255.

Pettit G.R., Tan R., Melody N., Cichacz Z.A., Herald D.L., Hoard M.S., Pettit R.K., Chapuis J.C. (1998c) *Bioorg. Chem. Lett*. 8, 2093-2098.

Proksch P., Ebel R., Edrada R.A., Wray V., Steube K., (2003) : *In Bioactive Natural Products from Marine Invertebrates and Associated Fungi., Prog. Mol. Subcell. Biol*., 37, 117-142.

Proksch P., Edrada R.A. and Ebel R. (2002). *App. Microbiol.and Biotech*., 59, 125-134.

Puapaiboon U.; Tylor R.T.; Jainhuknan J. (1999) *Rapid Commun. Mass Spectrom. 13*, 516-520.

Qureshi A., Faulkner D.J., (1999) *Tetrahedron* 55, 8323-8330 .

Rademaker-Lakhai J M., Horenblas S., Meinhardt W., Stokvis E., de Reijke T M., Jimeno J M., Lopez-Lazaro L., Lopez-Martin J A., Beijnen J H. and Schellens JH. (2005) *Clinical Cancer Research*, 11, 1854-1862

Ramesh P., Reddy N.S., Venkateswarlu Y. (1999) *J. Nat. Prod*. 62, 780-781 .

Reddy N.S., Ramesh P., Venkateswarlu Y. (1999) *Nat. Prod. Lett.* 14, 131-134 CA133:28562 A .

Reddy N.S., Ramesh P., Venkateswarlu Y., (2000) *Nat. Prod. Lett.* 14, 131-134 .

Renoux J-M., Rohmer M., (1986) *Eur. J. Biochem*. 155, 125-132

Reuben B.G., and Wittcoff, H.A. (1989) *Pharmaceutical Chemicals in Perspective*,John Wiley & Sons, New York.

Rodricks J.V. (1992) : In *Calculated Risks.* Cambridge university press, cambridge, p. 256.

Rosenthal G.A.and Janzen D.H. (1979) : In *Herbivores*. Academic press. New York.

Rudman W.B., 1999 (Aug 10). Comment on Elysia rufescens from Hawaii by Juan Lucas Cervera. [Message in] Sea Slug Forum. Australian Museum, Sydney. Available from http://www.seaslugforum.net/find.cfm?id=1165

Rudman W.B., 1999 (November 4) Elysia ornata (Swainson, 1840). [In] Sea Slug Forum. Australian Museum, Sydney. Available from http://www.seaslugforum.net/factsheet.cfm?base=elysorna

Rudman W.B., 2001 (November 19) Elysia grandifolia Kelaart, 1858. [In] Sea Slug Forum. Australian Museum, Sydney. Available from http://www.seaslugforum.net/factsheet.cfm?base=elysgran

Rycroft D.S., (1988) *In : Natural Product Chemistry III* ; Atta-ur-Rahman A., Le Quesne P. W., Springer –Verlag Berlin Heidelberg, pp. 43.

Salmoun M, Devijver C, Daloze D., Braekman J-C, van Soest R.W.M (2002) *J. Nat. Prod. 65,* 1173-1176.

Schwarzer D., Finking R. and Marahiel M.A. (2003) *Nat. Prod. Rep.,* 20, 275-287.

Seal A.N., Partley J.E., Haig T. and An M. (2004) *J.Chem., Ecol*., 30, 1647-1662.

Seigler D.S (1998) : In *Plant Secondary Metabolism*. Kluwer Academic Publisher. London. 759 P.

Sepcic K., Batista U., Vacelet J., Macek P., Turk T. (1997) *Comp. Biochem. Physiol. C Comp. Pharmaco* 117, 47-53 .

Serebryakov E., Simolon A., Kucherov B. (1970) *Tetrahedron*, 26, 5215

Sewell J.M., Mayer I, Langdon SP, Smyth JF, Jodrell DI, Guichard SM. (2005) *Eur J Cancer*. 41(11):1637-44.

Shamma M.,1989 : *In Studies in Natural products chemistry* , *Volume 5, Structural elucidation* (Part B) , (Atta-ur-Rahman, A., edit.), Elsevier Science Publishers B.V., 1989., pp V.

Shatz M., Yosief T., Kashman Y., (2000) *J. Nat. Prod.* 63, 1554-1556 .

Sheikh Y.M., and Djerassi C. (1974) *Tetrahedron*, 30, 4095.

Shen Y-C ., Prakash C.V.S. (2000) *J. Nat. Prod.* 63, 1686-1688 .

Silverstein R.M.; Bassler G.C.; Morrill T.C. (1991) : In *Spectrometric identification of organic compounds*, John Wiley & Sons pub., Chpt 2.

Siuda J.F. (1974) *J. Nat. Prod.* (*Lloydia*) 37, 501- 503.

Skyler D., Heathcock C.H. (2002) *J. Nat. Prod.* 65, 1573-1581 .

Smith P.M.C., and Atkins C.A. (2002) *Plant Physiology*, 128, 793-802.

Spengler B. (1997) *J. Mass Spectrom. 32*, 1019-1036.

Sperry S., Crews P. (1998) *J. Nat. Prod*. 61, 859-861 .

Steinbeck C. (2004) *Nat. Prod. Rep*., 21, 512-518

Stierle A A.(1988) Investigation of Biologically Active Metabolites from Symbiotic Microorganisms, Ph.D. Dissertation, Montana state University, Bozeman (1988).

Suarez Y, Gonzalez L, Cuadrado A, Berciano M, Lafarga M, Munoz A. (2003) *Mol Cancer Ther.* , 2(9):863-72.

Suckau D., and Cornett D.S., *Analusis Magazine*, 1998,26, M18-M21.

Suffness M., Newman D.J., and Snader K.(1989) : In *Bioorganic Marine Chemistry*, vol.3 (Scheuer, P.J., ed.), pp. 131-168, Springer-Verlag, New York.

Sun H.H., Cross S.S., Gunasekra M., Koehn F.E., (1991) *Tetrahedron* 47, 1185-1190 .

Sun H.H., Cross S.S., Koehn F., Gunasekera M. (1992) *US Pat. Appl.* 0 0, CA116(21):207800v

Swain T. (1977) *Ann. Rev. Plant. Physiol*., 28, 479-501.

Tanaka K., (2003) *Angew. Chem. Int. Ed*., 42, 3861-3870.

Tanji M., Namimatsu K., Kinoshita M., Motoshima H., Oda Y., and Ohnishi M. (2004) *Biosci. Biotechnol. Biochem*., 68 (10), 2205-2208.

Theobald N., Shoolery J.N., Djerassi C., Erdman T.R., Scheuer P.J., (1978) J. Am. Chem. Soc. 100 5574-5575

Torssell K.B.G. (1997) : In *Natural Product Chemistry. A mechanistic ,biosynthetic and ecological approach.* Apotekarsocieteten-Swedish Pharmaceutical Press.

Toth S.I., Schmitz FJ. (1994) *J. Nat. Prod.* 57, 123-127

Tsukamoto S., Miura S., van Soest R.W.M., Ohta T.(2003) J. Nat Prod. , 66, 438-440.

Turner W.B. (1971) : In *Fungal Metabolites* . Academic Press. London.446 p.

Venkateswarlu Y., Reddy M.V.R., Srinivas K.V.N.S., Rao J.V. (1993) *Indian J. Chem. Sect. B* 32, 704.

Vicario J.L., Job A., Wolberg M. M.,Ÿller M., Enders D., (2002) *Org. Lett.* 4, 1023-1026

Vining L.C. (1992) *Gene*, 115, 135-140.

Walker R.P., Thompson J.E., Faulkner, D.J. (1980), *J. Org. Chem*. 45, 4976-4979.

Watanabe K., Tsuda Y., Hamada M., Omori M., Mori G., Iguchi K., Naoki H., Fujita T., Van Soest R.W.M. (2005) *J. Nat. Prod.* 68, 1001-1005

Webb AG. (2005) *Magn.Reson. Chem*. 43, 688-696 and references therein.

Whitehead R. (1999) *Annu. Rep. Prog. Chem*., Sect. B.95, 183-205.

Will M., Fachinger W., and Richert J.R. (1996), *J.Chem.Inf. Comput. Sci.,* 36, 221.

Wilm M., Mann M. (1996) *Anal. Chem*.; 68, 1.

Wilson, I.D., Morgan, E.D., Lafont, R., Shockcor, J.P., Lindon, J.C., Nicholson, J.K. and Wright B., (1999) *Chromatographia*, 49 374.

Wolfender JL., Queiroz EF.; Hostettmann K. (2005) *Magn.Reson. Chem*. 43, 697-709 and references therein.

Woodruff H.B., Hernandez S., Stapley E.D. (1979) *Hindustan Antibiotic Bulletin* 21:71-84.

Woodruff H.B., MacDaniel A.E. (1958) : In *Antibiotic approach in strategy of chemotherapy*. Society of general microbiology symposium 8: 29-48.

Wright J., Mcinnes A., Shimizu S., Smith D. and Walter J. (1978) *Can J. Chem.* 56, 1898-1903.

Xiao D., Deng S. and Wu H. (1997) *Tianran Chanwu Yanjiu Yu Kaifa,* 9, 1-4; C.A. 130: 107540f.

Xu F.and Alexander AJ. (2005) *Magn.Reson. Chem*. 43, 776-782 and references therein.

Yagi H., Matsunaga S., Fusetani N. (1994) *J. Nat Prod*. 57, 837-838.

Yang l., Andersen R.J., (2002) *J. Nat. Prod.* 65, 1924-1926 .

Yaoita Y, Amemiya K., Ohnuma H., Furumura K., Masaki A., Matsuki T., Kikuchi M., (1998) *Chem. Parm. Bull.* 44 , 944-950.

Younus M.S. and Djerassi C. (1974) *Tetrahedron* 30, 4095-4103 .

Yousaf M., El Sayed K.A., Rao K.V., Lim C.W., Hu J.F., Kelly M., Franzblau S.G., Zhang F.Q., Peraud O., Hill R.T., Hamann M.T. (2002) *Tetrahedron* 58, 7397-7402 .

Youssef D.T. (2005) *J.Nat. Prod*.68, 1416-1419.

Youssef D.T. A., Shaala L. A., Emara S. (2005) *J. Nat. Prod.,* 68 (12), 1782 –1784

Youssef D.T., Yamaki R.K., Kelly M., Scheuer P. J.(2002) *J. Nat. Prod*.65, 2-6.

Youssef D.T.A. Yoshida W.Y., Kelly M., Scheuer P.J., (2000) *J. Nat. Prod.* 63, 1406-1410

Youssef D.T.A., Van Soest R.W.M., Fusetani N. (2003) *J. Nat. Prod.* 66, 861-862

Yue J-M., Chen S-N., Lin S-W., Sun H-D., (2001). *Phytochemistry* 56, 801-806.

Zeng Z. (2000) *Redai Haiyang,* 19, 86-89; C.A. 133: 278967s.

Zeng Z., Zeng L. and Su J. (1996) *Zhongshan Daxue Xuebao, Ziran Kexueban,* 35, 52-57; C.A. 125: 190994x.

Zschocke S., Klaiber I., Bauer R., Vogler B. (2005) *Molecular Diversity* 9: 33–39

List of Abbreviations

$[\alpha]^{D}$:	specific rotation at the sodium D-line
br :	broad signal
CI :	chemical ionization
COSY :	correlation spectroscopy
d :	doublet
dd :	double of doublets
ddd :	double double of doublets
DEPT :	distortionless enhancement by polarization transfer
ED :	effective dose
EI :	electron impact
ESI :	electro spray ionization
eV :	electronvolt
FAB :	fast atom bombardment
HMBC :	heteronuclear multiple bond connectivity
HMQC :	heteronuclear multiple quantum coherence
HPLC :	high performance liquid chromatography
Hz :	herz
LC :	lethal concentration
LC-MS:	Liquid chromatography-mass spectrometer
m :	multiplett
MALDI-TOF-PSDMS:	Matrix-assisted laser dessorption ionization-time of flight-post source decay mass spectrometer
MeOD :	deuterated methanol
MeOH :	methanol
mg :	milligram
mL :	millilitre
MS :	mass spectroscopy
m/z :	mass per charge
µg :	microgram
µL :	microliter
NMR :	nuclear magnetic resonance
ppm :	part per million
Prep. HPLC :	preparative HPLC
q :	quartet
ROESY :	rotating frame overhauser enhancement spectroscopy
RP-18 :	reversed phase C-18
s :	singlett
t :	triplett
TFA :	trifluoroacetic acid
TLC :	thin layer chromatography
UV :	ultra-violet
VLC :	vacuum liquid chromatography

Publication

Ashour M., Edrada R, Ebel R., Wray V., Wätjen W., Padmakumar K., Müller W. E. G., Lin W. H. and Proksch P. (2006): „Kahalalide Derivatives from the Indian Sacoglossan Mollusc *Elysia grandifolia*“ , *J. Nat. Prod.,* 69, 1547.

Biographic data

Name:	Mohamed Abdelghaffar Ali Ashour
Date of birth:	18. December 1969
Place of birth:	El-Sharkiya, Egypt
Nationality:	Egyptian
Civil status:	Married, two children
Address:	Universitätsstrasse 1, 40225 Düsseldorf
Home Address:	Al-azhar University, Cairo, Egypt
Educational Background:	
1975 – 1987:	Grade School - Higher School, Belbies Schools for Al-Azhar Sciences, Belbies, Egypt.
1987 – 1992:	Bachelor of Science degree in Pharmacy, Al-Azhar University, Cairo, Egypt.
1994 – 1999:	Master of Science degree in Pharmacy, Al-Azhar University, Egypt
Thesis:	Pharmacognostical Studies of some *Sophora* sp., belonging to family *Fabaceae*
2002-2002:	ZMP certificate of German language, Goethe Institut, Cairo, Egypt.
2003 – present:	Ph.D. candidate, Institute of Pharmaceutical Biology, HHU, Düsseldorf, Germany.
Employment Record:	
1994 – 1999:	Demonstrator, Faculty of Pharmacy, Al-Azhar Univeristy, Cairo, Egypt.
1999 – present:	Assistant Lecturer, Pharmacognosy Department, Faculty of Pharmacy, Al-Azhar University, Cairo, Egypt.